NASA CR71497

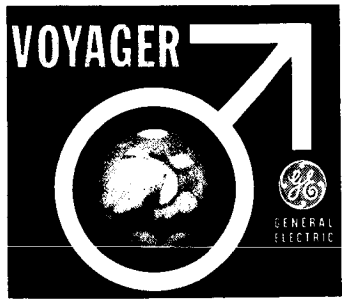
MISSILE AND SPACE DIVISION

VOYAGER SPACECRAFT SYSTEM

PHASE IA TASK B PRELIMINARY DESIGN

SPACECRAFT FUNCTIONAL DESCRIPTION

VOLUME A (BOOK 1 OF 2)



N66-21089 (ACCESSION NUMBER) (THRU) 1
410 (PAGES) (CODE)
CR 71497 (NASA CR OR TMX OR AD NUMBER) 31 (CATEGORY)

GPO PRICE $ _____

CFSTI PRICE(S) $ _____

Hard copy (HC) 7.10

Microfiche (MF) 2.00

ff 653 July 65

GENERAL ELECTRIC

NASA CR71497

DIN 65SD4514
31 January 1966

VOYAGER SPACECRAFT SYSTEM

PHASE IA TASK B PRELIMINARY DESIGN

SPACECRAFT FUNCTIONAL DESCRIPTION

VOLUME A (BOOK 1 OF 2)

PREPARED UNDER CONTRACT 951112
under NAS 7-100

CALIFORNIA INSTITUTE OF TECHNOLOGY

JET PROPULSION LABORATORY

4800 OAK GROVE DRIVE

PASADENA, CALIFORNIA

GENERAL ELECTRIC

MISSILE AND SPACE DIVISION
Valley Forge Space Technology Center
P.O. Box 8555 • Philadelphia 1, Penna.

TABLE OF CONTENTS

Section	Title	CII No.
I	Mission Objectives and Design Criteria	VC211SR101
II	Design Characteristics and Restraints	VC220SR101
III	System Functional Descriptions	
	Trajectory and Guidance Analysis	VC220FD101
	Component Design Parameters	VC220FD103
	Launch Vehicle Interface	VC220FD105
	Flight Capsule Interface	VC220FD106
	MOS/DSN Interface Requirements	VC220FD107
	Experiment Interface	VC220FD108
	Telemetry Data Criteria	VC220FD109
	Accuracy Analyses	VC220FD111
	Flight Sequence	VC220FD112
	Layout and Configuration	VC220FD113
IV	Subsystem Functional Descriptions	
	Telecommunication Subsystem	VC233FD101
	Radio Subsystem	VC233FD102
	Flight Command Subsystem	VC233FD103
	Telemetry Subsystem	VC233FD106
	Data Storage Subsystem	VC233FD107
	Guidance and Control Subsystem	VC234FD101
	Attitude Control Subsystem	VC234FD102
	Attitude Control Cold Gas Jet Subsystem	VC234FD104
	Autopilot	VC234FD105
	Engineering Mechanics	
	Temperature Control Subsystem	VC235FD101
	Spacecraft Structure	VC235FD102
	Pyrotechnic Subsystem	VC235FD104
	Electronic Packaging	VC235FD106
	Spacecraft Harnessing	VC235FD107
	High Gain Antenna Actuation Subsystem	VC235FD109
	Solar Array Structure	VC235FD110
	Power Subsystem	VC236FD101
	Computer and Sequencer Subsystem	VC237FD101
	Midcourse and Orbit Adjust Propulsion Subsystem Functional Description	VC238FD101
	Retropropulsion Functional Description	VC238FD102
V	Implementation Plan	VC200VP

SUMMARY OF PHASE IA TASK B REPORT

VOLUME A - SPACECRAFT FUNCTIONAL DESCRIPTION (2 Books)

Section

I	Mission Objectives and Design Criteria
II	Design Characteristics and Restraints
III	System Functional Descriptions
IV	Subsystem Functional Descriptions
V	Implementation Plan

VOLUME B - OSE FUNCTIONAL DESCRIPTION

I	OSE Objectives and Design Criteria
II	Design Characteristics and Restraints
III	STC System Level Functional Description
IV	STC and Subsystem OSE Equipment Groups Functional Descriptions
V	LCE Design Characteristics and Restraints
VI	LCE System Level Functional Description
VII	LCE Hardware Functional Description
VIII	AHSE Design Characteristics and Restraints
IX	AHSE System Level Functional Description
X	AHSE Hardware Functional Description
XI	MDE Requirements and Functional Description

VOLUME C - PROGRAM SYSTEM ANALYSIS

I	Introduction
II	Selection of Preferred System
III	Configurations
IV	Propulsion
V	Guidance and Control

CII CROSS REFERENCE BETWEEN TASK A AND TASK B INFORMATION*

Title	Task A CII No.	Task B CII No.
Mission Objectives and Design Criteria	VB211SR101	VC211SR101
Design Characteristics and Restraints	VB220SR101	VC220SR101
Trajectory and Guidance Analysis	VB220FD101	VC220FD101
Component Design Parameters	VB220FD103	VC220FD103
Launch Vehicle Interface	VB220FD105	VC220FD105
Flight Capsule Interface	VB220FD106	VC220FD106
MOS/DSN Interface Requirements	VB220FD107	VC220FD107
Experiment Interface	VB220FD108	VC220FD108
Telemetry Data Criteria	VB220FD109	VC220FD109
Accuracy Analyses	VB220FD111	VC220FD111
Flight Sequence	VB220FD112	VC220FD112
Layout and Configuration	VB220FD113	VC220FD113
Telecommunication Subsystem	VB233FD101	VC233FD101
Radio Subsystem	VB233FD102	VC233FD102
Flight Command Subsystem	VB233FD103	VC233FD103
Telemetry Subsystem	VB233FD106	VC233FD106
Data Storage Subsystem	VB233FD107	VC233FD107
Guidance and Control Subsystem	VB234FD101	VC234FD101
Attitude Control Subsystem	VB234FD102	VC234FD102
Attitude Control Cold Gas Jet Subsystem	VB234FD104	VC234FD104
Autopilot	VB234FD105	VC234FD105
Temperature Control	VB235FD101	VC235FD101
Spacecraft Structure	VB235FD102	VC235FD102
Structural Design Criteria	VB235FD103	VC235FD103
Pyrotechnic Subsystem	VB235FD104	VC235FD104
Electronic Packaging	VB235FD106	VC235FD106
Spacecraft Harness	----------	VC235FD107
High Gain Antenna Actuation Subsystem	VB235FD109	VC235FD109
Solar Array Structure	VB235FD110	VC235FD110
Power Subsystem	VB236FD101	VC236FD101
Computer and Sequencer Subsystem	VB234FD107	VC237FD101
Midcourse and Orbit Adjust Subsystem Functional Description	VB238FD101	VC238FD101
Retropropulsion Functional Description	VB238FD101	VC238FD102
Implementation Plan	----------	VC200VP

*This information provides a cross reference between Task A and Task B CII's to facilitate the location of similar information in the two reports.

INTRODUCTION

This volume contains a functional description of the 1971 VOYAGER Flight Spacecraft concept selected as the preferred design. The functional descriptions are divided into the following sections:

I Mission Objectives and Design Criteria
II Design Characteristics and Restraints
III System Functional Descriptions
IV Subsystem Functional Descriptions
V Implementation Plan

In many areas, the Spacecraft design is essentially the same as that described in the Task A final report. Where changes were made because of the change to Saturn V or for other reasons, the rationale supporting the choice of the preferred approach is included in the appropriate functional description.

We have used the same approach to systems engineering and configuration documentation methods in Phase IA Task B as were used in the Task A work in order to make this report compatible with the earlier work. As discussed in the Configuration Management Plan, we have planned a program for an orderly transition to documentation specified for VOYAGER beginning with Phase IB. As a part of that plan, we are suggesting that agreement be reached with JPL, during Phase IB, as to the extent and type of documentation (e.g., functional flow diagrams, requirements allocations, etc.) that would best meet JPL's intent and needs.

Inputs from several subcontractors are included in this volume. The companies and areas to which they contributed are:

Motorola Incorporated	-	Radio, Command
Texas Instruments Inc.	-	Telemetry, Data Storage
Honeywell Incorporated	-	Guidance and Control
Ryan Aeronautical Company	-	Solar Array Structure
Aerojet General Corporation	-	Midcourse and Retropropulsion
Thiokol Chemical Corporation	-	Midcourse and Retropropulsion
The Marquardt Corporation	-	Midcourse Propulsion
Bell Aerosystems	-	Midcourse Propulsion
Rocket Research Corporation	-	Midcourse Propulsion
Thomson Ramo Woolridge	-	Midcourse Propulsion
Rocketdyne	-	Midcourse and Retropropulsion

CII VC211SR101

MISSION OBJECTIVES AND DESIGN CRITERIA

SECTION

1 INTRODUCTION
2 MISSION OBJECTIVES
3 MISSION CONSTRAINTS
4 DESIGN CRITERIA
5 COMPETING CHARACTERISTICS

MISSION OBJECTIVES AND DESIGN CRITERIA

1.0 INTRODUCTION. The purpose of this document is briefly to restate the broad scope and intent of the VOYAGER Program as understood by General Electric from study of the "VOYAGER 1971 Preliminary Mission Description", dated 15 October 1965, with particular emphasis on the 1971 Mars Spacecraft System portion of the Program. This document will also indicate in general terms how this understanding of Program objectives influenced the preferred spacecraft system selection described later in this report.

2.0 MISSION OBJECTIVES. The broad objective of the VOYAGER Program is to provide a basic capability for scientific exploration of nearby planets of the solar system with instrumented, unmanned spacecraft able to fly-by, orbit, and/or land on these planets. The primary emphasis of this endeavor will be the discovery and characterization of extraterrestrial life, with the goal of applying this knowledge to a better understanding of terrestrial life. A further objective will be the extension of man's knowledge in other disciplines, including physics, chemistry, geology and meteorology, and others; again with the goal of application of such new knowledge.

The VOYAGER Program is currently planned to begin with the flight of an unmanned scientific probe to orbit and land on the planet Mars, selected as the currently most promising harbor of extraterrestrial life within this solar system. The first Mars flight will undertake a study of the preconditions for life as we know it and provide the first opportunity for direct surface measurements; both of which achievements will provide the basis for more sophisticated and definitive life detection experiments in later opportunities.

The more specific objectives of the initial VOYAGER Mars mission are considered, in order of priority, to be as follows:

- Successful insertion of a Planetary Vehicle, composed of a Mars orbiter and an atmospheric entry capsule, into a useful orbit about Mars, with sufficient data return to verify this achievement.
- Successful separation, entry, and data return from a Flight Capsule to provide the basis for development for later flights of capsules with more sophisticated capability.
- Return of a large quantity of scientific data about Mars environment and surface, including television pictures, from the Mars orbiter.
- Development of a basic capability and experience with both flight and ground systems to conduct further scientific planetary missions.
- Return of scientific and engineering observations in interplanetary space during the transit to Mars.

3.0 MISSION CONSTRAINTS.

3.1 Planetary Quarantine. The probability that Mars will be contaminated prior to the calender year 2021 as a result of any single launch shall be less than 10^{-4}. Consideration shall be given to the implications of this constraint upon the upper stage of the Launch Vehicle

and adapters, Flight Capsule sterility, Planetary Vehicle orbits and aiming point, and all emissions and ejecta from the Flight Spacecraft. An apportionment of this 10^{-4} probability among the flight systems shall be made to assure compliance of the Space Vehicle with this overall constraint.

3.2. Schedule. Because of the constraint placed upon the schedule by the immovable Mars launch opportunities, the program schedule shall be devised to provide a minimum risk within available funding of being able to launch during each selected Mars opportunity. The implications of this restraint upon the state-of-the art employed in the Planetary Vehicle design, as well as the uncertainties in development, fabrication, test and launching the Space Vehicle shall all be considered.

3.3 Reliability. Because of the high cost of each Space Vehicle and the long time duration required to complete a Mars mission, great emphasis must be placed upon the attainment of the highest long-life reliability possible within the state of the art. Particular emphasis shall be placed on simple and conservative design and a complete and integrated program of component, subsystem, and system testing to increase reliability and assure mission success.

Wherever possible, the VOYAGER design shall take advantage of flight equipment and techniques developed on similar programs. Parts, materials, and processes which cannot demonstrate a history of reliability shall not be used unless they are clearly necessary to meet minimum system performance criteria.

Within the weight restraint, functional redundancy shall be used to provide full capability of critical spacecraft functions to the greatest extent possible; useful, but possibly degraded, performance shall be provided for all critical spacecraft functions. It shall be the clear goal of the Flight Spacecraft design to assure that no single failure of an electronic piece part or critical component will cause destruction of the Flight Spacecraft or complete loss of mission capability.

All scientific instruments shall be designed to be as functionally independent of one another as is practical so as to increase the assurance that a failure in one instrument or in equipment common to several instruments shall have a minimum effect on the total amount of data received. Failure isolation shall be provided for each science instrument to eliminate the adverse effect of instrument failure on the remainder of the Spacecraft System.

3.4 Flexibility. After the initial Mars mission, it is anticipated that the VOYAGER Program may include not only additional flights to Mars, but also the other planets, specifically including Venus. This was kept in mind as the preferred-system-selection tradeoffs were made. As a specific example, the selection of a deployed high-gain antenna for the 1971 Spacecraft System in lieu of a steered but non-deployed alternate not only provides certain advantages for the Mars mission, but also entails less spacecraft design change in this area when adapting the Spacecraft System to Venus missions, if this should later be desired.

3.5 Launch Constraints. One Space Vehicle will be launched from launch complex 39 at the Kennedy Space Center during each selected Mars opportunity. This Space Vehicle is

composed of a Saturn-5 Launch Vehicle and two identical Planetary Vehicles, each containing a Flight Spacecraft and a Flight Capsule. The launch period for the 1971 VOYAGER Mars mission will not be less than 45 days, each of which will have a minimum firing window of not less than two hours with launch azimuths between 60° E of North and 115° E of North. After separation from the launch Vehicle, the Planetary Vehicles shall execute inflight maneuvers to separate the Mars encounter dates by not less than ten days. The total weight of each Planetary Vehicle and its adapter shall not be more than 22,000 pounds, to be apportioned between the Capsule System and the Spacecraft System by JPL.

3.6 Communications. The design of the Planetary Vehicle shall be compatible with the DSN, using DSIF receiving antennas operating at S-band; 210-foot transmitting and receiving antennas will be available for the late transit period and for Mars orbital operations.

4.0 DESIGN CRITERIA. The Flight Spacecraft for the 1971 VOYAGER Mars opportunity is designed to the criteria described below.

4.1 Design Approach. The Flight Spacecraft is a fully attitude-stabilized device using the Sun and Canopus as celestial references. The Flight Spacecraft operation is fully automatic on a nominal mission sequence (i.e., in the absence of in-flight equipment failure) except for the insertion by ground command of the information needed to perform thrusting maneuvers to correct the interplanetary trajectory to the desired aim point and/or improve the Mars orbit achieved to the design nominals, and any instrument calibrations requiring ground command. Performance of all trajectory corrections is automatic, with ground inhibit, after reception of the needed maneuver commands. The orbit-insertion maneuver does not require ground command if the aim point and time of arrival are within design nominals. The capsule separation maneuver is automatic, after ground enable, and does not require transmission of quantitative commands for its execution if the Planetary Vehicle is in a design-nominal Mars orbit.

4.2 Functional Requirements. The major functions performed by the Flight Spacecraft are:

a. Maintenance of a two-way communications link with earth, using fixed and steerable antennas for transmission of telemetry data, command reception, and angle, doppler and range tracking.

b. Support to the Flight Capsule by providing transportation to Mars orbit, and supplying power, telemetry, and command handling until separation; and a high-data-rate telemetry relay link between separation and impact, including provision of a VHF receiving antenna.

c. Execution of propulsive maneuvers to correct the interplanetary trajectory to conform to a preselected aim point and arrival time.

d. Insertion of the Planetary Vehicle into a specified Mars orbit.

e. Execution of propulsive maneuvers to adjust the Mars orbital parameters to within preselected design nominal values.

f. Orientation of the Flight Capsule to the specified celestial separation coordinates, and initiation of the separation sequence.

g. Support to the Flight Spacecraft science payload by supplying physical support and fixed orientation, power, commands, data storage and a telemetry link to earth.

h. Measurement and transmission to earth of Flight Spacecraft engineering data.

5.0 COMPETING CHARACTERISTICS. For the VOYAGER Flight Spacecraft the relative priorities of mission characteristics, in order of decreasing importance, are as follows:

a. The overall reliability of the Planetary Vehicle, as measured by the probability of successfully performing, in at least a degraded mode, all of the functions listed in Section 4.2 of this document.

b. The performance of all Spacecraft-System minimum requirements defined for the VOYAGER Mars Mission.

c. Minimization of the cost of the Flight Spacecraft, both for the initial Mars opportunity and the cost of subsequent modifications required for later VOYAGER missions. The first of these objectives shall take reasonable priority over the second.

d. Maximization of the contribution of the initial VOYAGER Mars Flight Spacecraft to subsequent VOYAGER Missions. This contribution is of two forms: first, return of spacecraft engineering data which will permit needed design refinements or fault correction to be incorporated into future vehicles; and, second, a basic design that is easily modified for later opportunities, including such altered requirements as increased Flight Capsule weight and/or missions to targets other than Mars.

e. Increased spacecraft performance (e.g., telemetry data rate) for the initial VOYAGER Mars opportunity.

CII VC220SR101

DESIGN CHARACTERISTICS AND CONSTRAINTS

SECTION

1	GENERAL DESCRIPTION
2	SELECTION OF PREFERRED SYSTEM
3	TRAJECTORIES
4	SPACECRAFT CONFIGURATION AND STRUCTURE
5	SPACECRAFT FUNCTIONAL RELATIONSHIPS
6	TELECOMMUNICATIONS
7	COMPUTER AND SEQUENCER
8	POWER
9	GUIDANCE AND CONTROL
10	PROPULSION
11	THERMAL CONTROL
12	PYROTECHNICS
13	CABLING
14	DESIGN STANDARDS
15	ENVIRONMENTAL CONSTRAINTS
16	RELIABILITY
17	PLANETARY QUARANTINE

DESIGN CHARACTERISTICS AND CONSTRAINTS

1.0 GENERAL DESCRIPTION

1.1 Planetary Vehicle. The Planetary Vehicle comprises one Flight Capsule mounted to one Flight Spacecraft. Two identical Planetary Vehicles are launched together on a single Saturn-V Launch Vehicle. The Planetary Vehicles interface with the Launch Vehicle through identical Planetary-Vehicle adapters which attach to points on the nose fairing. A general arrangement of the major elements of the Space Vehicle is shown in Figure 1-1.

1.2 Flight Spacecraft. The Flight Spacecraft comprises a spacecraft bus, a spacecraft science payload and a spacecraft propulsion sybsystem. The spacecraft bus combines an electronic equipment compartment, a cylindrical midsection and a fixed solar array. The primary structure houses the retro-propulsion unit and supports a variety of functional elements. The Flight-Spacecraft configuration is shown in Figure 1-2.

Sixteen equipment bays make up the electronic packaging section in which standardized modular assemblies are housed. Environmental control is provided by radiator plates and thermally-controlled louvers. A portion of the spacecraft science payload will be located in this section.

The selected solid-propellant orbit-insertion motor, tanks and ancillary equipment and the midcourse/orbit-adjust units occupy the interior of the spacecraft bus. The midcourse/orbit-adjust assemblies are located around the orbit insertion motor.

Two major articulated elements, the High-Gain Antenna (HGA) and the Planetary Scan Package (PSP), are mounted to the solar-array structure. The HGA has a 7 1/2-foot diameter parabolic reflector which is deployed after transfer-orbit injection. The antenna is provided with two degrees of freedom which provide full Earth coverage during the mission. The PSP is designed to provide required fields of view for the science payload with the largest anticipated (20-foot diameter) Flight Capsule attached. Once deployed, the PSP will track the planet, utilizing two periodically-stepped gimbals and a servo-driven third gimbal.

A fixed medium-gain antenna is mounted on a blank panel of the solar-array structure. This backup to the HGA can provide approximately half of the primary data rate for as long as three weeks after encounter. The 400-mc relay antenna is a fixed turnstile-over-ground-plane located in the vicinity of the +X-axis. Communication with the Flight Capsule will be maintained by having the Spacecraft hold the separation attitude until capsule impact.

The Planetary Vehicle Adapter is attached at the periphery of the solar-array structure. Separation is attained through gas-operated, piston-latch mechanisms which provide minimum tip-off rates and reliable operation.

The preferred Spacecraft System design is fully automatic on a nominal mission, in accordance with the JPL spacecraft specification. That is, if the Spacecraft were to be injected by the Saturn V on a perfect Mars approach trajectory, it could, in the absence of component failures, complete its scientific mission without intervention by ground command, except for

the ground-enable specified before Flight-Capsule separation. For a mission in which trajectory corrections are required, the needed data about orientation and magnitude of velocity changes required are stored in the spacecraft by ground command several hours before the maneuver is to be performed. Thereafter, the maneuver, including return to celestial references, is performed automatically by the Spacecraft, which is monitored on the ground so that the maneuver sequence may be interrupted at any point by ground command. The Spacecraft is also automatic to a large degree in the sense of protecting itself from catastrophic failure due to the malfunction of components. For example, failure of a midcourse engine to fire, results in automatic shutdown of the opposing mate, avoiding uncontrollable tumbling of the Spacecraft.

In the design of the system, a deliberate effort has been made to favor control-and-sequencing techniques that permit automatic operation over as wide a range of nominal orbits as reasonably possible without command updating of the stored sequence of events. For example, while it would be possible to store all planet limb crossing times in the Computer and Sequencer for the selected orbit, in the preferred design this information is computed from the PSP motions. Not only does this save many words of core storage, but it accommodates a larger variation in orbital parameters without any need for ground-command updating of the stored program. Similarly, Earth occultation is sensed by a Mars detector, bore-sighted with the high-gain antenna, with similar benefit to stored program size and automatic operation over a range of orbits. These various techniques (storage, computing and sensing) are combined in the preferred design to provide a high degree of automatic control with very modest complexity of the flight hardware.

1.3 Flight Capsule. The Flight Capsule is designed to carry out the primary function of conducting atmospheric and planetological experiments after release from the orbiting spacecraft. Upon entry, the capsule will gather vital atmospheric information so that an analysis of constituents and a state parameter profile may be obtained. Television pictures during descent are planned. The capsule will be sufficiently instrumented so that a reconstruction of its entry trajectory and vehicle motion is possible.

The Flight-Spacecraft/Flight-Capsule physical interface is a bolted field joint of mating flanges located at the forward end of each Spacecraft. On the capsule side, the flange is the terminus of an adapter section which is connected to the lower half of a two-piece biological canister. The capsule is attached to the canister at the vehicle base; this joint serving as the normal separation plane. Separation of the upper portion of the biological canister takes place before Mars orbit insertion.

The tenuous Martian atmosphere dictates the use of high-drag aerodynamic shapes, as characterized by the blunted 60-degree, half-angle cone configuration. Capsule base diameter has been taken to be 12 feet.

The one overriding constraint on the Planetary Vehicle is the necessity of ensuring that Mars is not contaminated by earth-borne microorganisms before the calendar year 2021 with a probability of 10^{-4} per single launch.

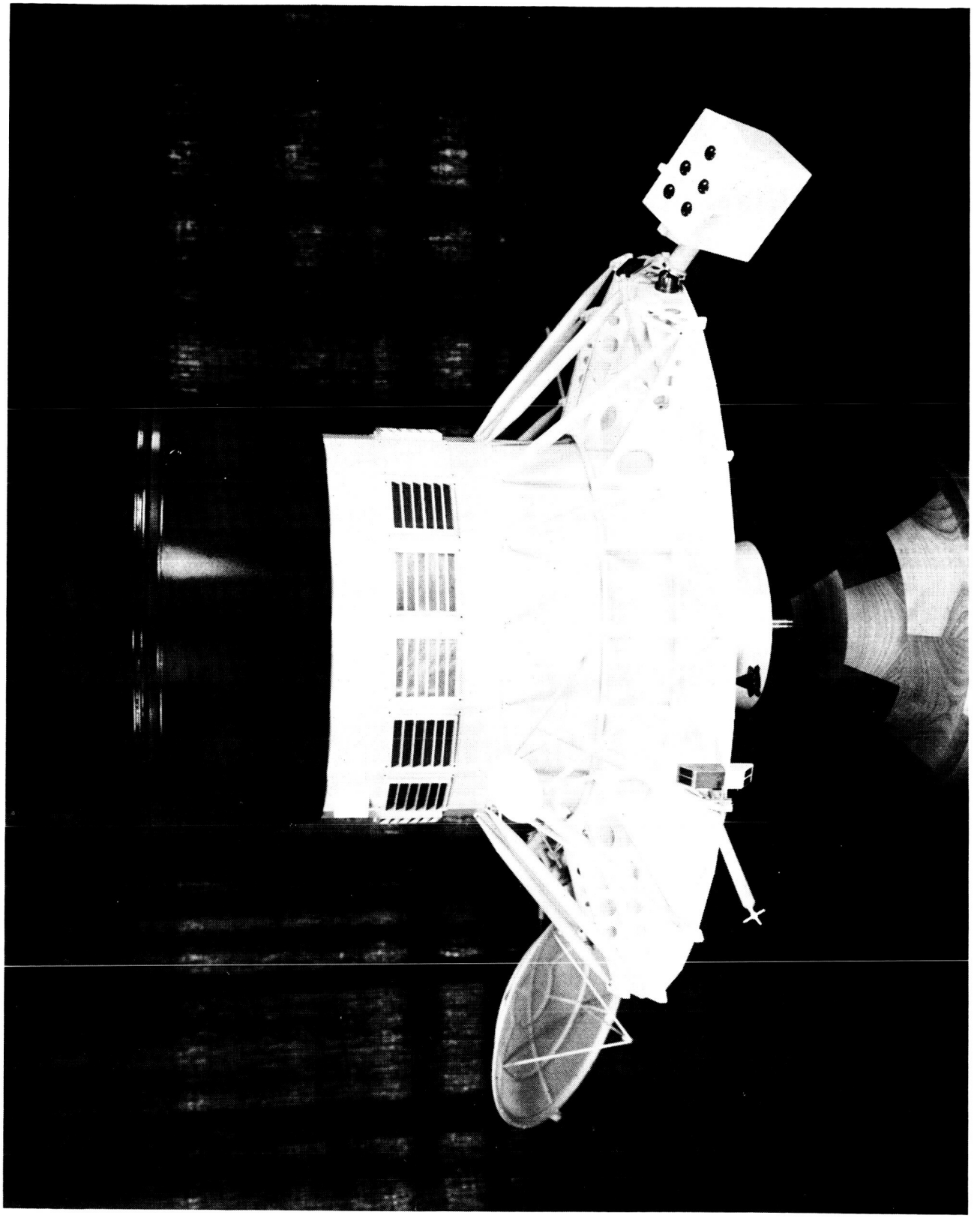


Figure 1-1a. General Electric VOYAGER Spacecraft Preferred Design

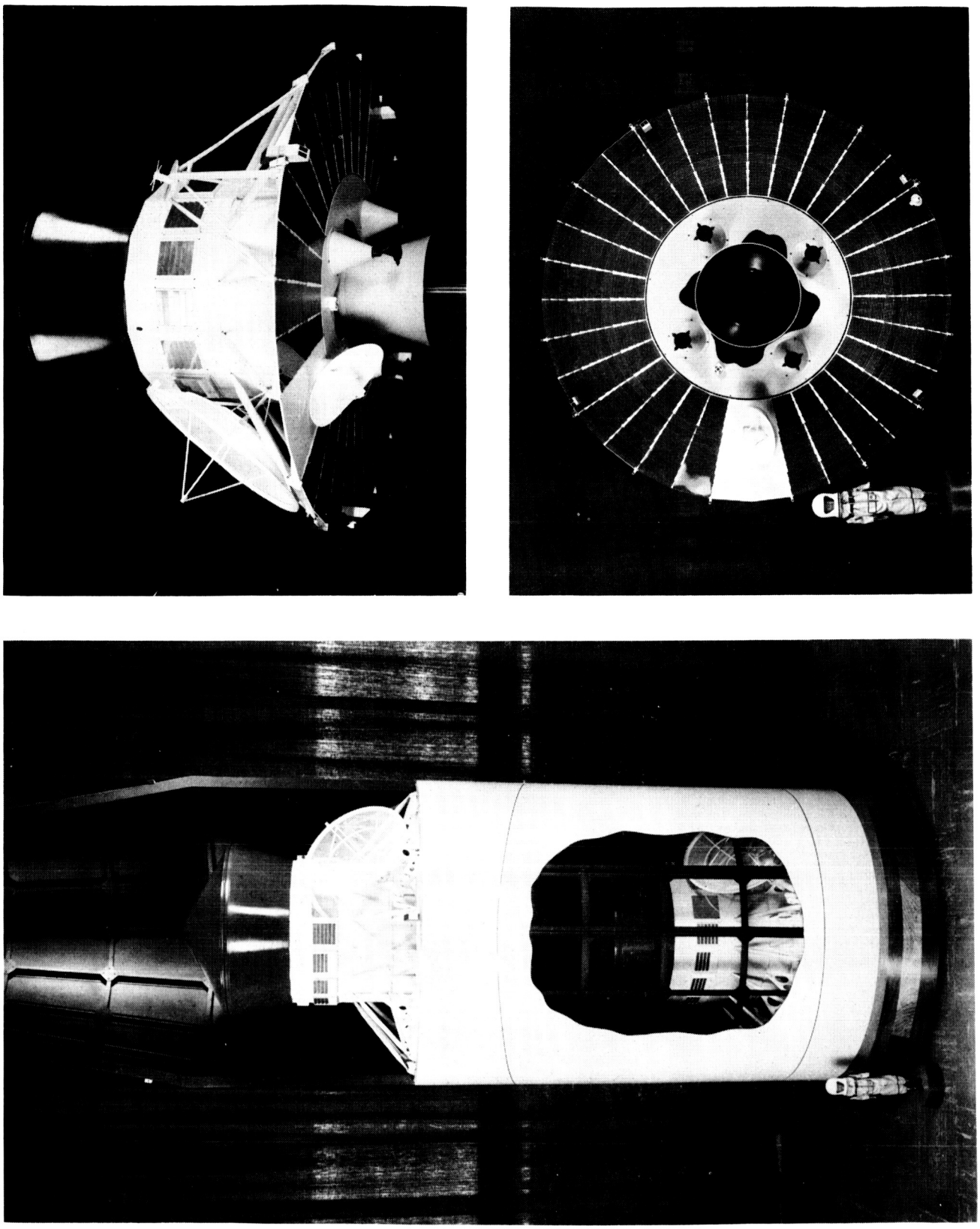


Figure 1-1b. General Electric VOYAGER Spacecraft Preferred Design

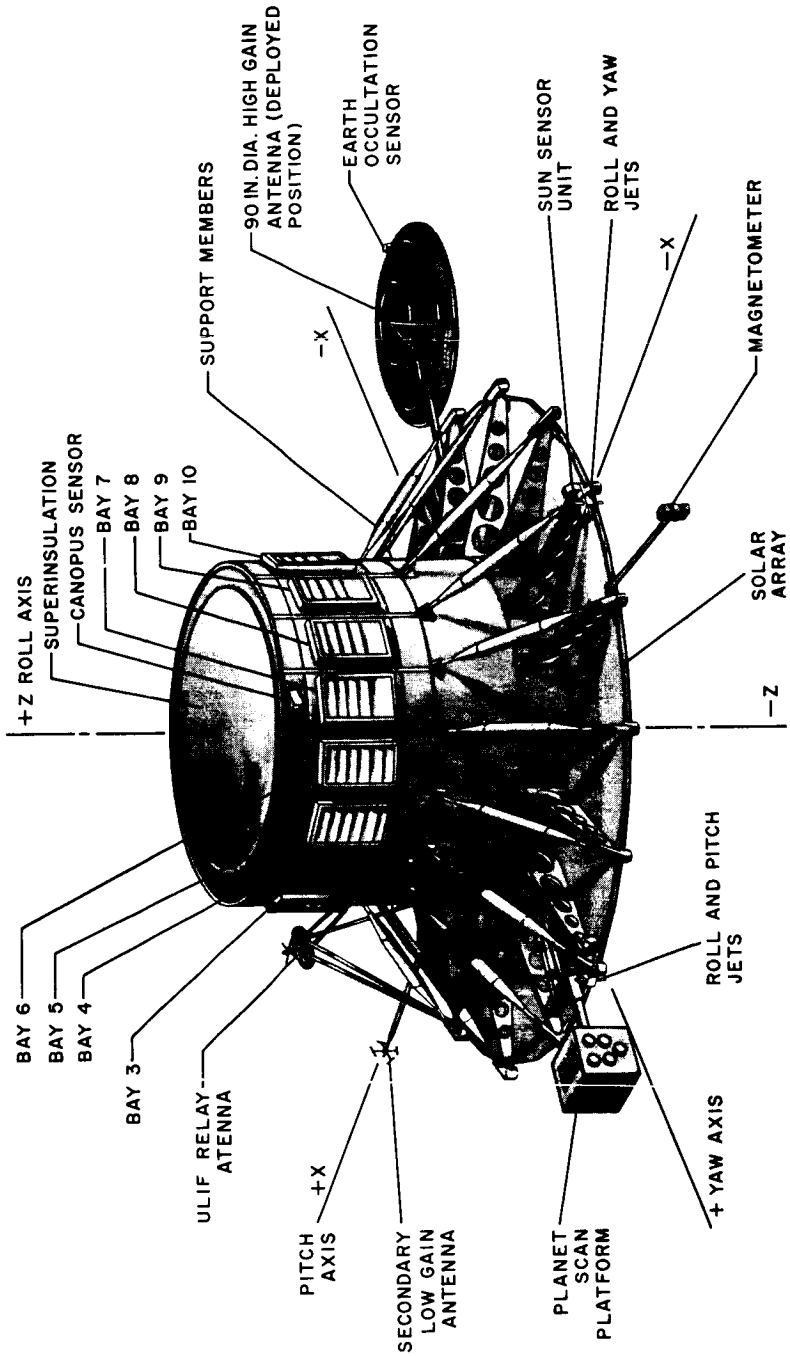


Figure 1-2. Spacecraft Equipment Arrangement

The Flight Capsule constrains the selection of the Mars orbit and release point by limiting the choice to those which concurrently satisfy tolerable entry conditions, landing near the terminator, and acceptable communication distances. The selected 1 x 10,000 km orbit and release point (true anomaly of 230 degrees) ensures entry angle-of-attack below 36 degrees and required de-orbit velocities below 240 m/sec. Landing at the evening terminator is planned, with a maximum communication distance of approximately 1800 km.

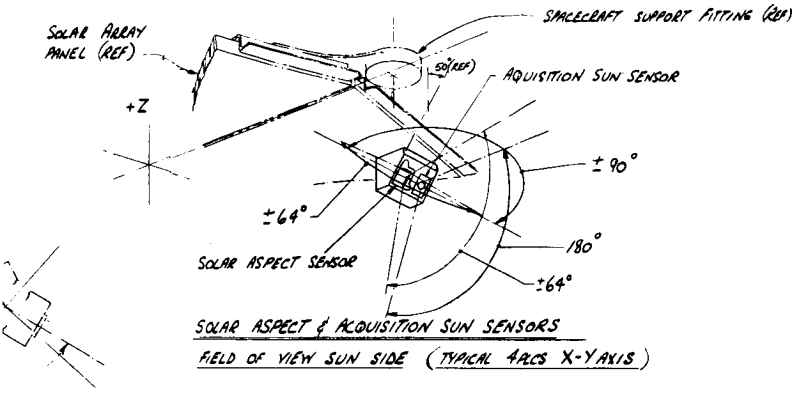
2.0 SELECTION OF PREFERRED DESIGN. This section discusses the factors considered in selecting the preferred system configuration, which includes the following features:

- Capsule located on shaded side
- Single PSP, mounted at the edge of the solar array, with two Canopus trackers providing full planet-viewing capability over the Mission life
- Propulsion system along longitudinal axis, nozzle sun-pointing
- Modular assembly concept
- Toroidal electronic equipment compartment, with 16 bays
- Fixed solar array, with 16 structural panels and a 32-side electrical arrangement
- Solar-aspect sensor for attitude verification
- Deployable and steerable high-gain antenna

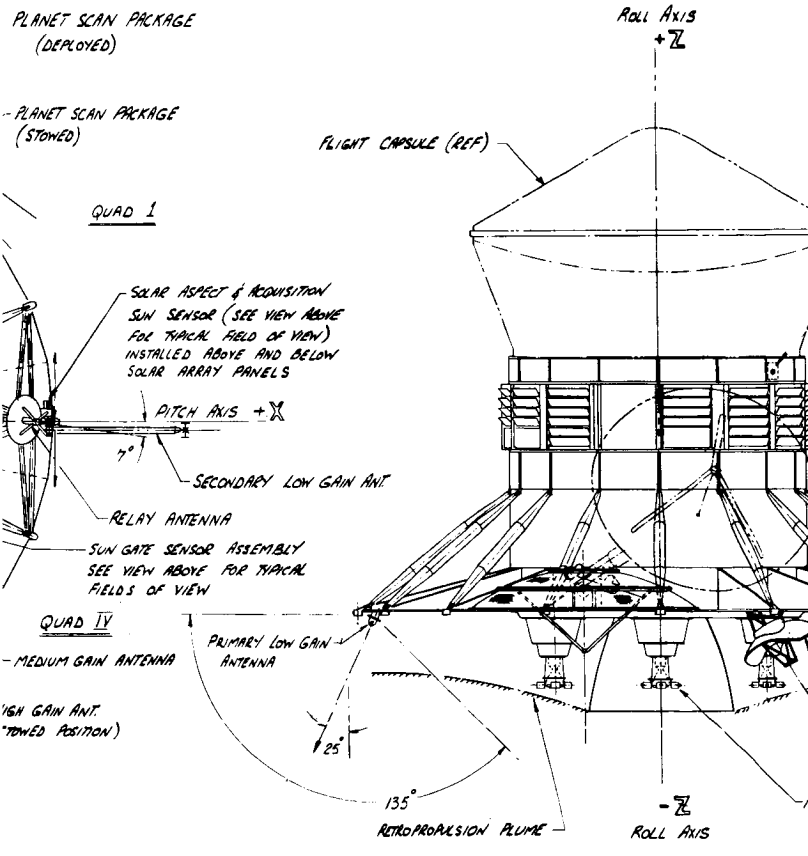
These configuration guidelines were used in developing the spacecraft configuration best suited to the various propulsion subsystems under consideration. After suitable spacecraft configurations had been conceived for each propulsion candidate, they were evaluated against the Mission Restraints and Competing Characteristics, the preferred system selection being a solid-propellant orbit-injection engine and four monopropellant engines for midcourse and orbit adjust. Figure 2-1 shows the preferred design selected. Since the propulsion decision is covered in detail in Volume C of this report, it is not discussed here.

2.1 Capsule Placement. The first configuration question that had to be decided was whether to put the Flight Capsule on the sunlit side, or the shaded side, of the Spacecraft. Two factors favor keeping the capsule on the shaded side of the Spacecraft, as in the Task A preferred design. First, from the spacecraft viewpoint it is desirable to keep the capsule on the shaded side to avoid having to deploy the solar array out beyond the shadow cast by the Flight-Capsule dynamic envelope, specified as 20 feet in diameter. Such a deployment not only adds complexity and risk of failure to the Spacecraft, but also increases the already large spacecraft inertias, with corresponding penalty in control-gas weight. Second, from the capsule thermal-control standpoint, placement on the shaded side assures a simple and reliable design. All that is required is to minimize heat leaks from the capsule and to supply the losses with heater power from the Spacecraft. Then, during maneuvers the insulation employed will prevent excessive heat rise in the capsule when it is exposed to the sun.

A sunlit-side capsule position requires capsule thermal-control coatings that are stable in the space environment, and careful balance of absorbing and radiating surfaces to assure a stable capsule temperature. During maneuvers, thermal control of the capsule might require either

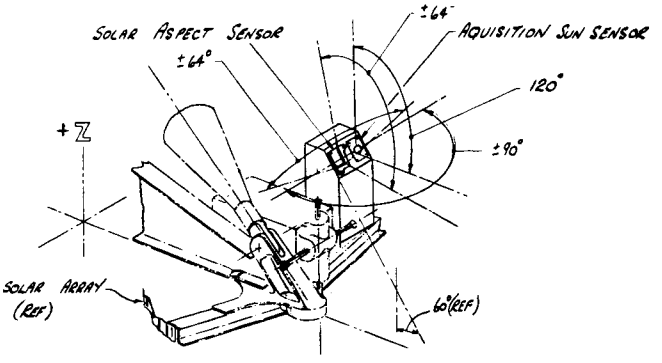


SOLAR ASPECT & ACQUISITION SUN SENSORS
FIELD OF VIEW SUN SIDE (TYPICAL 4 PLCS X-Y AXIS)



SIDE VIEW OF SPACECRAFT
LOOKING ALONG 'Y' AXIS

TO SUN



SOLAR ASPECT & ACQUISITION SUN SENSOR FIELD OF VIEW TYPICAL 4 PLACES ON X-Y AXIS

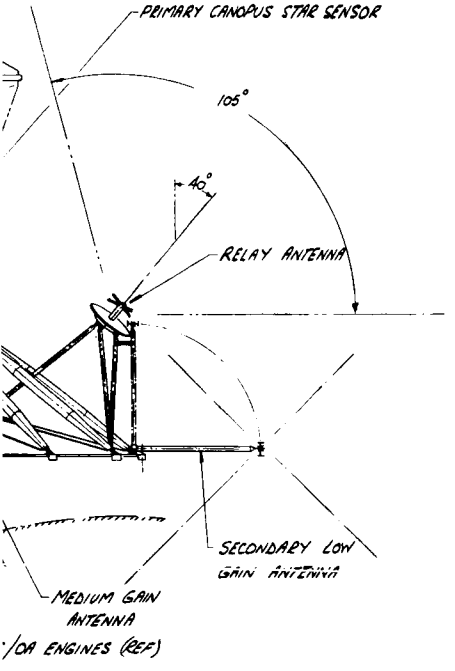
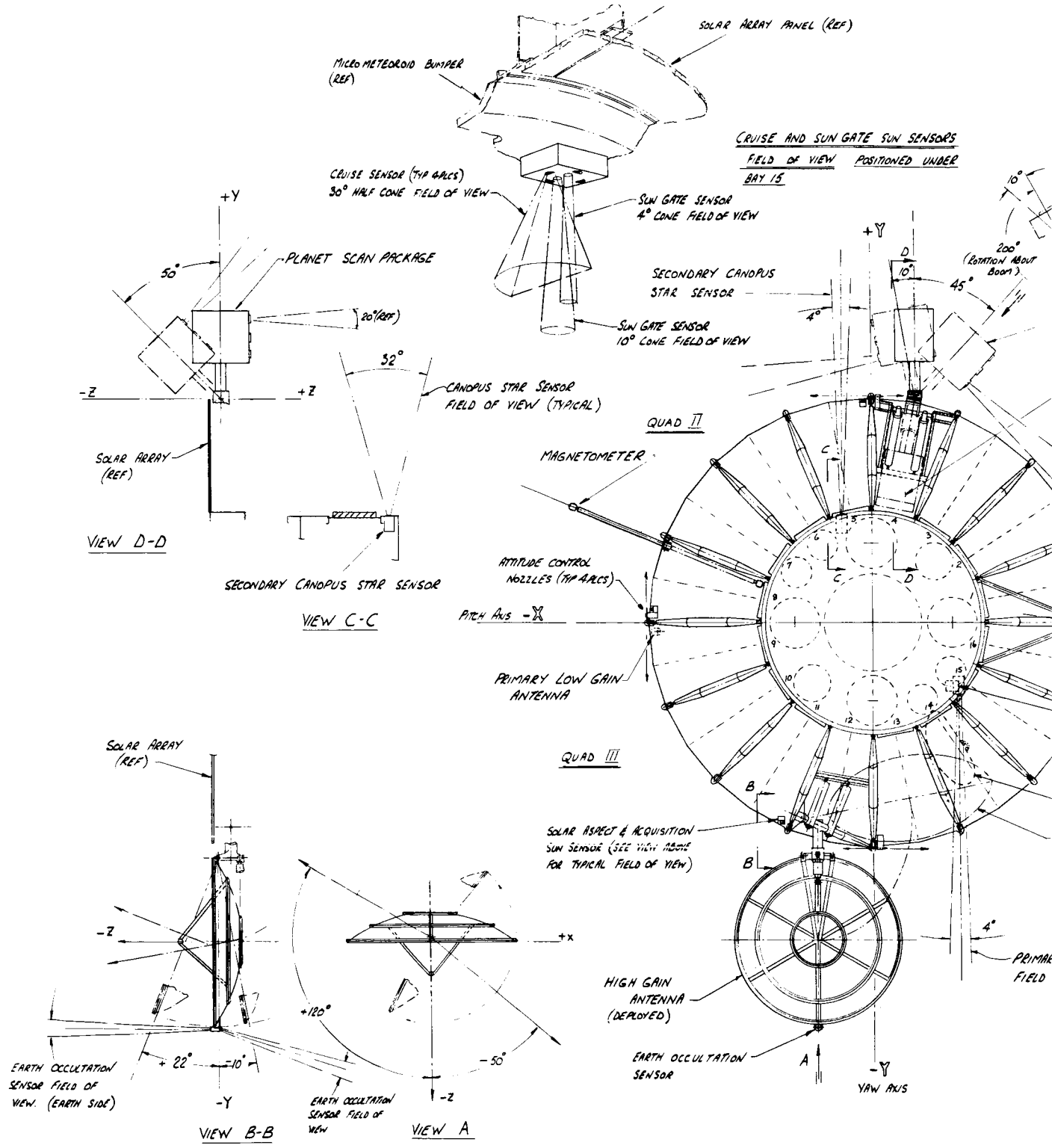


Figure 2-1. Spacecraft Fields of View



HIGH GAIN ANTENNA MOTIONS

thermal-control louvers to minimize heat loss from a shaded capsule, or else the drawing of large amounts of heater power from the spacecraft batteries. Neither alternative is attractive. However, before placement on the shaded side could be selected for the preferred design it was necessary to meet the requirement that the PSP be able to view Mars over the orbiter lifetime with the Flight Capsule in place.

2.2 PSP Location and Viewing. To achieve a flexible spacecraft to accommodate future mission variations, it was decided to consider only those configurations which would permit a full view of Mars, day or night, even though the spacecraft specification called for only daylight-plus-near-terminator viewing. It was further decided that the preferred design concept selected must be compatible with an orbit of any inclination or any eccentricity. It was considered, however, that physical relocation of the PSP to different positions around the spacecraft periphery for different opportunities, involving different orbit geometries, would be acceptable. Several methods of achieving this system goal were considered:

- Long PSP arm with capsule on shaded side
- Capsule on sunlit side, short PSP boom
- Sun-Mars Spacecraft reference coordinates in orbit
- Dual PSP's or dual Canopus trackers

2.2.1 Long Booms. The preferred design in the Task A study took advantage of the necessary absence of the capsule during the orbiting phase of the mission to mount the PSP on a relatively short boom attached to the spacecraft body and looking through the space where the lander had been carried. Application of this approach to the Task B system was precluded by the requirement that the Spacecraft complete its mission successfully with the lander attached. It was immediately evident that a single PSP mounted to a Sun-Canopus-oriented Spacecraft would require a very long boom in order to view the planet over the entire 180-day orbiter mission. Seasonal progression and orbit precession move the PSP scanning plane, which is parallel to the orbit plane, until it intersects the capsule profile, unless the PSP boom is very long. This is shown in Figure 2-2(B). Such a long boom was rejected at once because of the problems of boom stowage, structural dynamics and unfavorable mass properties. A first effort to solve this problem was to consider putting the capsule on the sunlit side of the Spacecraft to avoid long booms for seeing the daylight side of Mars. This did alleviate the situation, as shown in Figure 2-2(A). However, the necessity to deploy the solar array completely, together with the still unfavorable mass properties, suggested a search for better solutions to the PSP-viewing problem.

2.2.2 Sun-Mars Orientation. One concept considered in solving the PSP-viewing problem was the use of a Sun-Mars orientation for the orbit phase of the mission. In this concept, the Spacecraft would roll around the Sun-line to keep the PSP always on the Mars side of the Spacecraft, the PSP requiring only a single motion to track the Mars local vertical. However, the high-gain antenna would have to rotate at orbital rate to track the Earth; and the Canopus tracker would have to be located outboard of the tracking gimbal to provide a fixed celestial reference in order that the antenna angle be stepped as in the Task A design. This concept has many attractive features, including:

- Fewest possible number of gimbals to achieve Sun-Mars-Earth pointing: four, as opposed to five in the Task A design. (Two of these can be servo-controlled, and two periodically-stepped.)

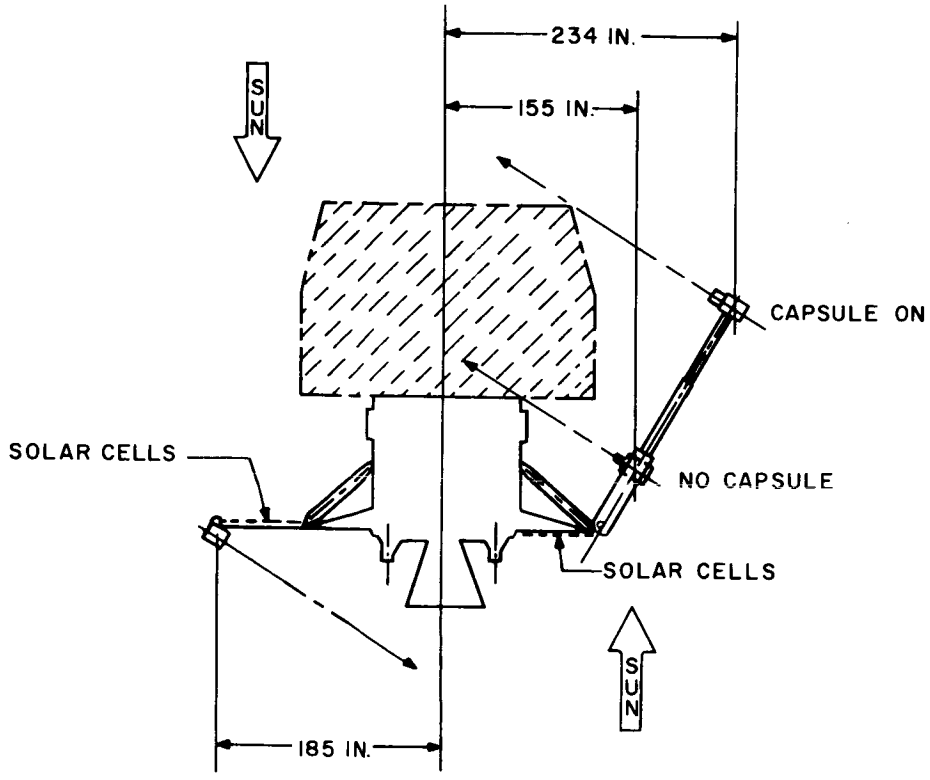


Figure 2-2. Planetary Scan Platform Boom Arrangement

- Short PSP boom.
- Ability to handle any arbitrary orbit without spacecraft modification.
- Ability to maintain positive attitude stability during Sun or Canopus occulation without using gyros.
- Possibility for simple and positive on-board attitude verification before maneuvers, using the antenna-Canopus gimbal and the PSP gimbal to provide turn measurements.

This concept was considered briefly and dropped for three reasons. First, it is a radical departure from the JPL spacecraft specification requirement for Sun-Canopus orientation, which is a flight-proven interplanetary control concept. Second, in this concept the PSP rotates about the local vertical - a nuisance for image-forming science instruments and a major defect if line-scan instruments are contemplated. This problem is solvable, but not without detailed integration with JPL on science requirements. Third, since no simple back-up mode for the constantly rotating antenna gimbal was identified, a failure of this gimbal would be a near-catastrophic mission failure, high-rate telemetry return being possible for only a small fraction of each orbit.

2.2.3 Two Canopus Trackers. It was also seen that two PSP's could be mounted on the top (+Y) and bottom (-Y) edges of the solar array. Then, as the changing geometry required one PSP to look through the capsule location, the other PSP would be in a position to view Mars and continue the observations. This concept had the obvious disadvantage of excessive weight and complexity. However, it was shortly recognized that this concept was equivalent

to having one PSP and two Canopus trackers, and rolling the Spacecraft as required to avoid any need for the PSP to view through the capsule position. It can be shown that only one 180-degree rotation of the Spacecraft is required to maintain PSP viewing capability for a six-month mission. For the preferred orbit (1000K x 10,000 km and 60 degrees inclination) a location near the +Y axis at the edge of the fixed solar array would provide the required field-of-view for the PSP with a short boom, even with the largest lander still in place. View A of Figure 2-3 shows in perspective the surface generated during a 180-day mission by the PSP boom which is erected normal to the orbit plane. Views B and C show the situation at 92 days where further rotation of the boom would move the line-of-sight of the planet-scanning science into the capsule, and how a 180-degree rotation of the spacecraft would permit the PSP to continue to maintain a clear view of the planet. A second Canopus tracker is provided on the Spacecraft to look along the +Y axis in order to provide roll reference during this phase of the orbiting mission.

In conclusion, the PSP location near the +Y axis with a short boom and with three degrees of freedom (gimbals C, D and E, as in the Task A study), with a second Canopus tracker on the +Y axis, was selected as the preferred arrangement for this Task B study. After this solution to the PSP viewing problem was found, the decision to adopt a preferred configuration with the capsule on the shaded side was immediate.

2.3 Propulsion System Placement. After the capsule and PSP locations had been selected, the next major element to place was the Propulsion system. This logically fits along the vehicle longitudinal axis, with the exhaust nozzle pointing away from the Capsule. The location has the advantages of being able easily to accommodate the axial center-of-gravity movements associated with use of propellant and separation of the capsule, plus the feature that the thrust loading associated with the orbit-insertion maneuver is in the same direction as the major launch loads, permitting the same structure to fulfill both requirements. After some brief consideration had been given to transverse engine locations, only disadvantages were found for such an arrangement. Therefore, location of propulsion engines on the longitudinal axis of the Planetary Vehicle was promptly adopted.

A related configuration guideline adopted was that the structural arrangement should permit functional modularity. This means, for example, that it should be possible to assemble, test, sterilize (if necessary), and install the Attitude Control cold-gas-jet subsystems as a unit. In a similar manner, it was a configuration objective to provide a capability for handling the electronic bays and Midcourse Propulsion system (as applicable) as separate modules in assembly and test.

2.4 Electronic Compartment. The next major element of the Spacecraft considered for placement was the electronic equipment. A very obvious arrangement is the use of a torus around the propulsion system, as in the Task A design.

This arrangement has the advantages of minimizing Spacecraft length, of providing ready access to all electronic compartments and including a large thermal radiating area close to the equipment to be cooled. The use of a compact box arrangement might save some weight in harnessing, but the balance of advantages lies with the torus arrangement. Therefore, this was adopted for the preferred design.

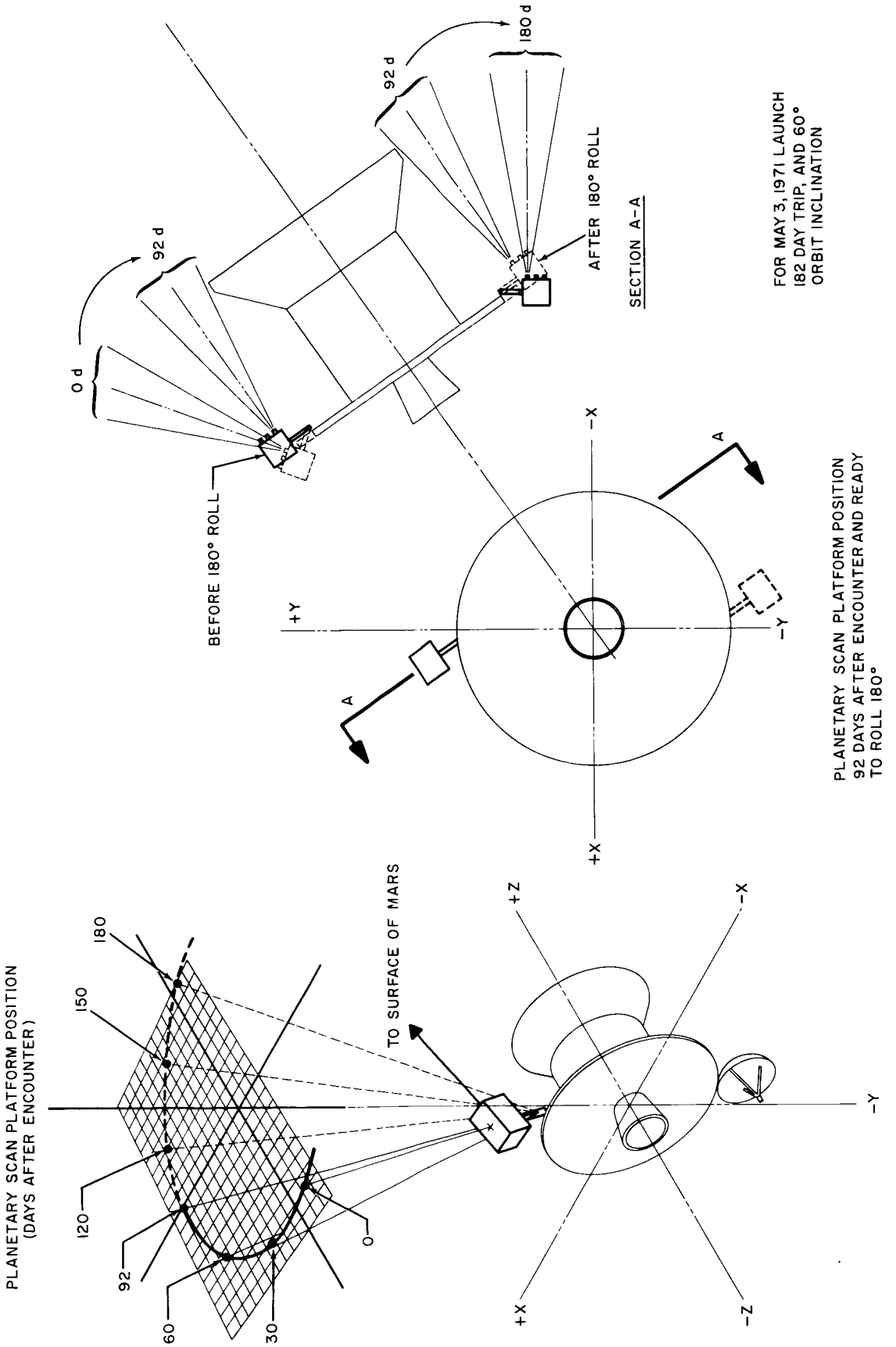


Figure 2-3. Canopus Tracker Boom Arrangement

A study was made of the relative merits of having the electronic equipment compartments structurally integrated as opposed to their being carried on the outside of a self-sufficient structure. The advantage of the latter approach is that removal of compartments and/or components is easier for the non-integrated approach. However, this approach was dropped because it involves both a significant weight penalty and a thermal-control problem. The next step was to move the electronics inside the spacecraft skin line, using the radiating coverplate of the equipment bay as a shear panel to carry spacecraft loads. The individual bay chassis were supported from the radiator-plate/shear-panel in this concept, preserving most of the ease of access of the first approach. However, after the dynamics of this arrangement had been studied, it appeared that the natural frequency of the equipment support could not easily be made high enough to assure a good environment for the electronics. Hence, it was considered necessary to bolt each bay chassis to the longerons to achieve the desired dynamic stiffness. The resulting packaging concept is virtually identical to that of the preferred design of Task A.

2.5 Number Of Sides. A related problem is selection of the number of sides for the spacecraft. The nominal diameter at which the electronic torus would be located is about ten feet for all propulsion system alternatives; further, a structure of this diameter is needed to meet the 120-inch Flight-Capsule interface diameter specified. To carry over the 12-sided configuration of Task A to this greater diameter would make each electronic chassis too long to provide adequate dynamic stiffness. Hence, it was deemed necessary to split each chassis and provide a support point to a longeron in the middle of the span. This effectively makes 24 equipment bays, which can be treated as a circle (i.e., with uniform loading) better if considered as a 24-sided figure than as a center-supported 12-sided figure. On the other hand, the use of bays of the same size as in the Task A study yields a 16-sided spacecraft. The choice of number of sides was essentially a choice between these two alternatives. Since each of these had certain advantages, the study was carried to the point of preliminary packaging layouts and harnessing studies, which led to the conclusion that a reasonable packaging arrangement could be developed for either alternative. While excessive mixing of subsystems with 24 sides was not found to be a problem, several subsystems were divided among many bays, making subsystems testing more complex. Other main disadvantages of the 24-sided configuration are: about a 50% increase in the number of system connectors (from 112 to 171); an increase in the number of thermal-control shutter assemblies; and a need to integrate thermally two bays with a common radiator plate to provide adequate dissipation of the heat from the 50-watt power amplifiers. The advantages of the 24-sided configuration include: lighter, more easily handled, bay assemblies; shorter and stiffer electronic chassis; and better structural load paths. The 24-bay arrangement required more fastners to hold the electronics in place, but permitted easier replacement of any single bay. Because of the larger number of system connectors and thermal control assemblies required by the 24-bay arrangement, and considering the importance of reliability to the VOYAGER Program, the system preference came out in favor of the 16 electronic bays.

Another aspect of the number of sides to the spacecraft that had to be considered was the optimum number of panels for the solar array. Layouts of array panels were made for 16- , 24- , and 32-panel configurations. The objective in these layouts was to obtain balanced string lengths, uniform solar-cell submodule size, and maximum cell area within the available envelope. The 16-panel configuration evinced a serious loss of area in comparison with

the 24- and 32-panel arrangements because the area loss for the fewer-sided figure made impossible the inclusion of as many submodules as needed while maintaining uniform string length. The 24- and 32-panel arrangements were similar in number of cells available, the main difference being that the 32-panel arrangement put more cells in each series string, yielding a higher array output voltage. Figure 2-4 illustrates the advantage of a 32-side arrangement over one of 16 sides. Since this 32-sided module arrangement could be structurally designed as a 16-panel configuration, the module arrangement of view A, Figure 2-4 was dropped from consideration, the choice then lying between the arrangement of View B, Figure 2-4 and that of a 24-sided design.

Another major point considered was that the inclusion of a fixed mid-gain (Mariner-C) antenna would eliminate 8.3% of the area (2 panels) in the 24-panel arrangement, but only 6.2% (2 panels) of the 32-sided configuration. Hence more array power would be available with the panel design of View B. This point, together with the electronic-bay packaging considerations, led to the adoption of 16 panels, with cells laid out to provide 32 electrical elements as shown in view B, Figure 2-4.

2.6 Attitude Verification. The performance requirements of the Spacecraft System from the VOYAGER 1971 Preliminary Mission Description include the capability of enabling the Mission Operation System to verify the attitude of the Planetary Vehicle when ready to launch the Flight Capsule. Although it is not specifically required by this document for other maneuvers, the receipt of attitude-verification telemetry from the Planetary Vehicle at the Mission Operations System would enchance confidence in proceeding with propulsive maneuvers.

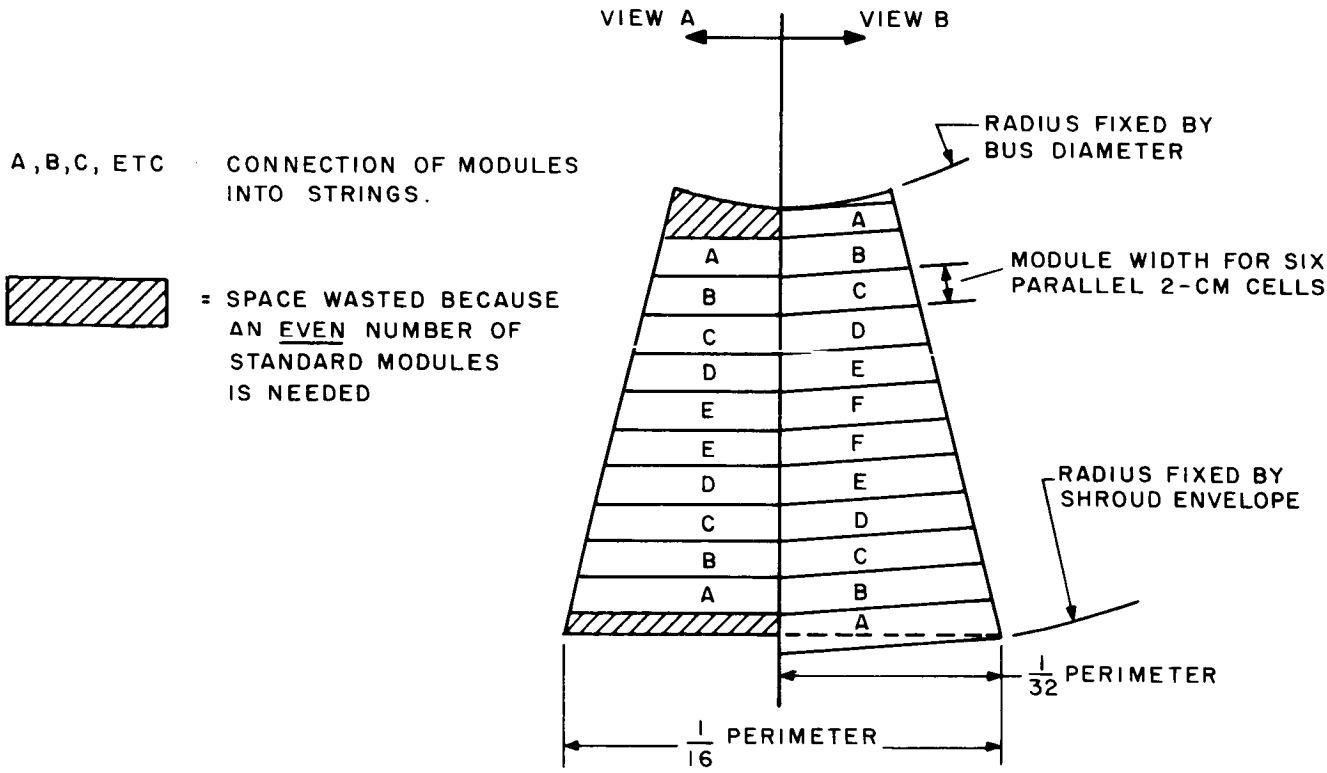


Figure 2-4. Arrangement for 32-Side Spacecraft

Therefore, the ability readily to provide this information for every maneuver without complex operational or hardware penalties was a strong criterion in evaluating methods of attitude verification. Several methods of attitude verification were studied. They include:

- Use of the steerable High Gain Antenna
- Use of attitude-verification gyros
- Pre-maneuver systems confidence check
- Gimbaled Sun and/or Canopus trackers
- Solar-aspect sensor

2.6.1 Use of HGA. In the Task A study attitude-verification was obtained by prepositioning the HGA so that in the maneuver attitude the beam would be received at Earth. If the beam were not received, the vehicle was not at the right attitude, including roll angle, and the maneuver had to be aborted and re-commanded. There are several disadvantages in this approach:

a. There is a risk that the HGA might fail to deploy or point, thus precluding attitude verification even though the trip and at least part of the orbiting mission could be accomplished with the fixed back-up dish.

b. If it fails in maneuver attitude so as to be unable to illuminate Earth in cruise or orbiting attitude, the return of major portions of scientific telemetry expected from the mission would be jeopardized.

c. It offers only a coarse confirmation at best, with no monitoring of the progress of the Planetary Vehicle through the turn sequence.

d. It adds to the command-data load when instructing the Planetary Vehicle to execute a maneuver.

e. It lengthens and complicates the maneuver sequence, since a final roll turn must be added to the two-turn maneuver sequence in order to point the HGA beam to Earth. As the roll turn is being executed, the Planetary Vehicle must maintain thrust-axis orientation by gyro reference, with no way of detecting the error accumulated. Thus, it was deemed worthwhile to seek a better way to obtain attitude telemetry from the Flight Spacecraft.

2.6.2 Additional Gyros. One of the first concepts considered was the use of a second set of gyroscopes in addition to the three integrating rate gyros in the Attitude Control subsystem. Angular displacement information from these gyros, operating independently of the Attitude Control subsystem, would be obtained and telemetered to Earth, thus monitoring the progress and final attitude of a turn sequence. This concept is not particularly attractive, because of the weight and power penalty involved, unless a redundant gyro set has been provided for reliability reasons. In the preferred design recommended, redundant gyros are provided. Use of these gyros for attitude verification was not adopted for several reasons. The most serious defect with this approach is that it provides ambiguous information. That is, if the attitude-verification gyro set does not confirm that the maneuver was properly executed, it may not be easy to determine whether the attitude-control gyros or the verification set are giving erroneous results. The best move would be to abort the maneuver, return to cruise

attitude, and accumulate telemetry data in order to decide which gyro set is reading incorrectly. Although this is acceptable for most maneuvers, it is not possible for one vital maneuver—orbit insertion—because there is only one time interval in the mission when this maneuver can be performed.

In addition to this very serious objection, there are several other disadvantages. If either set of gyros should fail, attitude verification would not be possible, because the redundant gyros would be needed for control purposes. Also, the attitude-verification means is subject to the same systematic errors as is the control system; for example, uncertainty of starting position in the control deadband. Finally, this technique is apt to be less reliable than an alternate method, because both primary and verification sensors are subject to the same design-error failure modes.

2.6.3 Systems Confidence Check. Some enhancement of the confidence is correct maneuvering can be made by executing a systems check prior to each maneuver. The Spacecraft could be commanded to turn away from its celestial references and then turn back to them under gyro control. The error read by the celestial reference at the end of the checkout maneuver would be some measure of the operability of the Planetary Vehicle control system. This concept was not adopted for the preferred design for several reasons:

a. It does not detect any control malfunctions during the actual maneuver.

b. It does not locate systematic but compensating errors in the controls.

c. It requires the addition of significant control-gas weight.

d. It reduces overall mission reliability by adding additional maneuvering events to the flight sequence.

2.6.4 Gimbaled Celestial References. Turns about the Sun-line could be monitored by reading the gimbal angle of a Canopus tracker pivoted to follow that star during roll turns. Similarly, a turn away from the Sun could be monitored by reading the gimbal angle of a pivoted Sun sensor. A combination of these two would permit complete and independent verification of turn accuracy for a spacecraft maneuver. In the Sun/Mars-oriented concept described earlier, both of the gimbals required for this technique are available on the Spacecraft: the Canopus sensor is outboard of the HGA pivot; and a Sun sensor could be installed on the PSP, so that the deployed PSP could track a turn away from the Sun. Hence, this technique was attractive for the Sun/Mars-oriented Spacecraft. However, after that concept was dropped, as previously noted, this idea no longer seemed attractive because it requires extra gimbals and controls.

2.6.5 Solar Aspect Sensor. Since an independent celestial reference and method of determining maneuver attitude was clearly desirable, passive solar sensors were considered. The cruise Sun-sensor system was too specific in purpose and would not readily yield a uniformly accurate signal for any angle. Therefore, a universal, digital Sun-angle sensor was sought. The Adcole "Solar Aspect Sensor" admirably meets this requirement. It is developed, and is being used by GE-MSD for the Gravity Gradient Test Satellite (GGTS) being built at Valley Forge under Air Force contract; and in the NASA Advanced Technology Satellite, for which the attitude-control and monitoring system is under development by GE at Valley Forge.

In the basic sensor, shown in Figure 2-5, sunlight passes through a narrow entrance slit to the interior of a quartz reticle block, and falls on a Gray-coded digital mask on the bottom of the block. Below the mask designed to preclude ambiguous signals is mounted a bank of seven photocells. Individual photocells receive sunlight in accordance with the angular aspect of the sun to the plane of the reticle. The Gray Code is utilized because one and only one bit (i.e., photocell ON or OFF) is changed between any two adjacent numbers. This precludes catastrophic errors in angle determination, possible with conventional binary coding, where several bits must change sign simultaneously, requiring almost perfect synchronization. The binary signal (cells OFF or ON) is available to the spacecraft telemetry system.

Two orthogonal slits are mounted on each sensor to define the solar angle along two axes. The existing sensors have a view-angle of 128 degrees. A seven-bit Gray-code mask provides a discrete digital signal for each increment of one degree; eight bits would double the resolution.

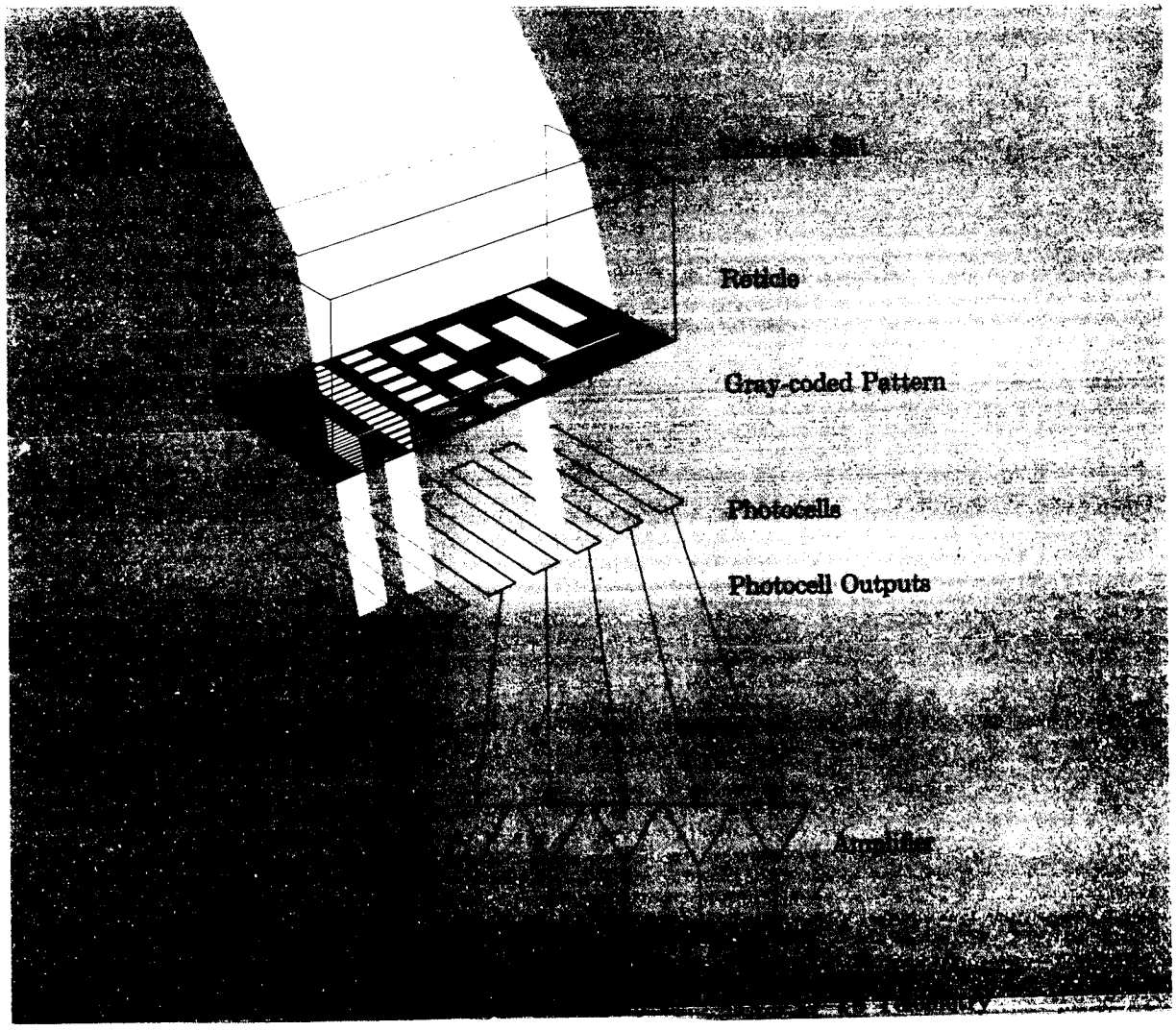


Figure 2-5. Solar Aspect Sensor

The proposed sensor will weigh about five pounds and will consume only one watt. For convenience in packaging and thermal control, and for looking around a large Flight Capsule, eight sensors are mounted in four packages with the cruise Sun-sensors on the outer perimeter of the solar array. Each package contains two sensors mounted back-to-back and looking along the +Z and -Z directions.

This passive sensor, with its easily handled digital output, light weight, low-power requirement, and its ability continuously to monitor the progress of the vehicle in yaw or pitch turns, is selected for the attitude-verification task. Its output will be periodically sampled and transmitted in the maneuver telemetry mode. It could also be used as a back-up for the normal cruise sensor and, with additional circuitry, could provide a solar reference angle to be used to bias the vehicle away from the Sun to point a high-gain antenna with seized gimbals to Earth.

2.7 Deployed Antenna Versus Non-Deployed Antenna. The next major problem considered was whether the HGA should be deployed on a boom, as in the Task A study, or kept non-deployed. A HGA that remains rigidly oriented to the primary Flight Spacecraft structure until after orbit-insertion burn, but is provided with two degrees of freedom to accommodate changes in Earth cone and clock angles throughout the orbiting mission, is termed a non-deployed antenna. If the HGA is to be made capable of continuously pointing toward Earth throughout transit and in maneuver attitudes by the addition of a final roll turn to the maneuver sequence, it must be deployed beyond the shroud envelope and must also have the same two degrees of freedom to accommodate variations in Earth cone and clock angles throughout the mission.

2.7.1 Advantages of Non-Deployed High-Gain Antenna. The non-deployed HGA has several advantages, including:

a. The structure and gimbal mechanism may be lighter than that required for the deployed HGA because the antenna can be rigidly attached at several points on the Flight Spacecraft until after orbit insertion burn, thus distributing acceleration loads to the maximum advantage. An additional weight advantage is realized because there is no deployment mechanism and boom to provide the view angles required by the deployed approach.

b. No additional back-up capability in the form of a fixed Mariner-C antenna is required. The non-deployed HGA would be fixed in encounter position before launch. Unlatching of the structural attachment points and the two-degree-of-freedom gimbal would be accomplished only after orbit insertion. This can be delayed for 10 days after encounter, by which time seasonal progression would have moved the Earth out of the HGA beam. If this release of the non-deployed HGA fails to occur, the mission is unaffected until this time. Furthermore, the failed HGA can be pointed toward Earth by biasing the orientation of the entire orbiting Spacecraft about the Sun-line under gyro control. As the Earth-Sun cone angle changes, the output of the solar array would begin to fall off, but full communication ability could be maintained for two months after seizing of the gimbals.

c. The non-deployed antenna requires less gimbal motion (± 44 degrees) which may eliminate the requirement for a rotating joint in the coaxial antenna feed. If so, this would increase reliability.

d. Overall reliability of a non-deployed HGA is higher than that of one which must be deployed before use, especially if the non-deployed one is launched in encounter position.

2.7.2. Disadvantages of Non-Deployed High-Gain Antenna. The advantages of the non-deployed concept are offset by these factors:

a. This HGA cannot be turned toward Earth for a large part of the trip in cruise attitude; therefore, this convenient way of ensuring high data rates for recorder playback during the entire trip is unavailable, and another means of recorder playback must be found. This would have to be done either by increasing normal cruise data rates through the primary low-gain antenna, or else by not transmitting spacecraft real-time data when it is necessary to play back a recorder containing either maneuver or solar-flare data.

b. It is impossible to support the selected cruise data rate of 116 bps from launch to encounter with 50 watts radiated from the primary low-gain antenna. During late cruise an auxiliary antenna of about 10-db gain, oriented generally toward the earth, would be required. Although this may be a simple fixed antenna, it is almost equivalent to the fixed Mariner-C antenna in terms of weight, orientation, and switching requirements. Hence, we have traded one fixed antenna for another, and the extra antenna is not a very useful backup to the HGA in orbit.

c. The non-deployed HGA cannot be pointed to Earth at most maneuver attitudes even if it were released before orbit insertion. Therefore, the ability to transmit high data rates and to ensure two-way doppler tracking during mid-course engine burn is non-existent.

d. The packaging requirements (i.e., encounter position within shroud envelope) of the non-deployed HGA invariably placed the edge of the parabolic reflector near the lip of the orbit-injection motor so that plume impingement appeared likely. It was not possible to predict with any high degree of precision the thermal effect upon the antenna. Hence, the effect of plume impingement becomes an intangible, but significant, disadvantage of this concept. The packaging requirements also caused a shroud-length and launch-weight penalty. There is no straightforward, structurally and thermally sound configuration that can accommodate both the orbit-injection engine and the non-deployed HGA in encounter position without an increase in spacecraft bus length. This proved to be a significant and almost dominant factor in making the decision.

e. The non-deployed HGA cannot be used to confirm the initial acquisition of the celestial roll reference, Canopus, because it is not released. Even if it were, it could not be pointed far enough to place Earth within the beam for launches that occur during the early portion of the launch window. Moreover, if it were used this way, the advantage in reliability over the deployed HGA would hardly be realized.

f. The packaging requirements for the non-deployed HGA could not be satisfied without shading a portion of the solar-cell array disposed in a disc about the orbit-injection engine nozzle. Since the total available fixed-cell area is just enough for the mission requirements, shading by the HGA means that about 20 to 25% of the array area would have to be provided in deployable solar paddles. This must, necessarily, reduce the attainable reliability of the Planetary Vehicle power supply. This effect offsets the reliability gained from not having to deploy the HGA. This penalty is especially serious if array panels should shade a set of thermal radiation louvers in the launch position. Although the reliability of pointing the HGA beam to Earth is higher for the non-deployed installation than for the deployed one, system considerations indicate that the deployed system has a higher overall probability of mission success. The non-deployed HGA could not be included in the preferred configuration unless it displaced or shaded about 25% of the solar array. Hence, deployable solar paddles must be added in order to satisfy mission power requirements. If just enough area is added, the reliability of attaining the design level of power is now less than for an all-fixed array. To provide the same overall mission reliability in both systems, the probability of deploying several hinged paddles must be equal to the probability of deploying and actuating one (deployable) HGA. This requires the release and actuation system for each hinged paddle to be more reliable than the mechanisms for the deployable HGA. This is, at best, unlikely. Alternately, the equivalent reliability goal could be met by adding paddle area in excess of that lost by shading by the non-deployed HGA. This is an unprofitable way to spend weight. Overall, the Spacecraft with a deployed HGA was regarded as being at least as reliable as one with the non-deployed antenna.

2.7.3 Discussion Of Deployed HGA. The use of a deployed high-gain antenna offers a number of benefits:

a. An easy and reliable means of verifying Canopus acquisition at the start of the mission and after each maneuver.

b. Greatly reduced probability of rocket-exhaust-plume impingement damage.

c. A neat, compact Flight Spacecraft configuration that offsets some of the weight penalty incurred by the deployment function by saving structure length.

d. No solar-panel shading, thus allowing the use of a minimum-risk all-fixed array.

e. Maneuver-attitude verification as a back-up to the passive solar aspect sensor.

f. Increased back-up function in that the fixed Mariner-C antenna, not included with the non-deployed HGA concept, can be used for any HGA failure.

The direct weight penalty for selecting the deployed over the non-deployed HGA is estimated to be 26.5 pounds, of which approximately 22 pounds is for the deployment mechanism, and about 4.5 pounds is for the fixed Mariner-C back-up antenna added to the Flight Spacecraft System. However, this penalty is offset, for most of the spacecraft configurations studied, by permitting a shorter structural arrangement. In addition, any direct weight penalty for

the deployed HGA is further reduced by virtue of the shorter shroud permitted by the compact Spacecraft configuration. This saving in escape weight is as much as 700 pounds in the lower structural shroud.

2.7.4 Compromise Configuration. When consideration was given to the functional capabilities of a deployed HGA that are not realizable with the non-deployed HGA, it was seen that another alternative to deploying versus non-deploying of the 7-1/2-foot HGA is available. A small, deployable, steerable, parabolic antenna of approxiamtely the gain and pattern of the Mariner-C antenna, mounted on the edge of the solar array on a two-degree gimbal, would provide all the transit functions, such as Canopus confirmation and recorder playback, and the other advantages just described, that could be provided by the deployed HGA. The non-deployed, limited-steering, HGA would be mounted in encounter position and could remain in that position from the pad to post-orbit injection. Unfortunately, this compromise concept did not resolve all the disadvantages of non-deployed systems such as solar-panel shading and packaging problems. Since these two problem areas have such a significant effect on overall system effectiveness and mission reliability, and because of the limited time, this concept was rejected.

The conclusion reached was that the use of the deployed high-gain antenna would result in a lighter and more reliable Spacecraft, and in greater operational flexibility. It was, therefore, selected for our preferred system.

2.7.5 Size Of High-Gain Antenna. The diameter of the parabolic reflector is a major configuration factor. A 7-1/2-foot parabolic reflector was selected as the preferred design in the Task A study on the basis of optimization of net gain after pointing losses when using state-of-the-art attitude control. This diameter just clears the bottom of the full lander envelope when deployed from its launch position in the preferred design without increasing the overall length of either the Flight Spacecraft or the Launch Vehicle shroud. Therefore, it was carried over into the Task B design.

3.0 TRAJECTORIES

3.1 Earth-Mars Trajectories. The selection of the Earth-Mars trajectories meets the following requirements:

a. Launch azimuths of between 60 degrees and 115 degrees East of North.

b. Minimum launch period of 45 days.

c. Minimum daily launch window of two hours.

d. Type-I trajectories having a maximum vis-viva energy (C_3) of 25 m^2/sec^2.

e. Hyperbolic excess velocities at Mars less than 4.5 m/sec.

f. Declination of the Earth departure geocentric asymptote greater than |5| degrees.

g. Inclination of the heliocentric transfer plane to the ecliptic plane greater than |0.1| degree.

h. Insertion of the Flight Spacecraft into an areocentric orbit within view of Goldstone.

i. An Earth-orbit coast time of between 2 and 90 minutes.

j. A time-of-arrival separation of the two Planetary Vehicles of at least 10 days.

Further criteria used in the selection of the design trajectories are:

a. A launch period as long as possible consistent with other requirements and criteria.

b. The required Mars arrival separation of 10 days between the two Spacecraft to be obtained by a velocity correction of 100 m/sec for each Spacecraft, applied at the time of the first midcourse trajectory correction.

c. The propagation of injection and maneuver errors to be minimized.

d. The variation in Mars arrival geometry and arrival velocity to minimized.

e. The characteristic of the heliocentric trajectory and the satellite orbit to permit insertion into the satellite orbit with a velocity increment of 1.9 km/sec, the Sun and Canopus occultations during satellite orbit phase to be minimized, and the science-viewing conditions during the satellite orbit phase to be such as to maximize the scientific data value.

The requirements are met and a good compromise is obtained among the various criteria by trajectories having launch dates between 28 April and 28 June, and having an approach velocity for the first Planetary Vehicle to arrive at Mars of 3.5 km/sec. These trajectories result in an arrival date for the first vehicle of between 1 and 17 November 1971, and of between 11 and 27 November for the second vehicle.

3.2 Trajectory Corrections. Each Planetary Vehicle will nominally perform one trajectory correction maneuver within 10 days after launch to correct for injection errors. Combined with this maneuver, each Planetary Vehicle will be given a velocity change sufficient to change its time of arrival at Mars by five days in order to obtain the required 10-days

separation between arrival of the two Planetary Vehicles. The velocity change will vary between approximately 50 m/sec for a 3 May 1971 launch, and 100 m/sec for a 28 June launch; the time-of-arrival adjustment is the predominant component of velocity imparted to the vehicle at the time of the first correction.

The propagation of maneuver errors in both the impact parameter plane and in time of arrival is greatest, and the total maneuver velocity change is highest, for launches during the latter part of the launch period. For this reason, the 28-June-launch/27-November-1971-arrival trajectory is used for determining the maneuver error. For this trajectory, three trajectory corrections including a time-of-flight correction, 2.6-degree (3σ) pointing error, trajectory biasing and one percent (3σ) velocity error, the three sigma value of the semi-major and semi-minor axes of the dispersion ellipse in the impact parameter plane are 83 km and 49 km, respectively; the time of flight error is 25 seconds. This maneuver accuracy is well within the required accuracy of the semi-major axis for the dispersion ellipse of 100 km (3σ) and $\pm$ 1.0 minutes (3σ).

3.3 Satellite Orbit. Except for those relating to the Flight Capsule de-orbit, the constraints and criteria for the selection of the satellite orbit are the same as those defined in the Task A Study Report (VB220FD101). To meet the capsule de-orbit requirements, it is necessary to rotate the natural line of apsides at the time of orbit insertion, utilizing a maximum insertion velocity change of 2.2 per second. A good compromise among all constraints and criteria is an orbit having a periapsis altitude of 1000 km, an apoapsis altitude of 10,000 km, an inclination to the Mars equator of 60 degrees, and a period of seven hours. This 60-degree orbit is the one recommended for the 1971 mission from Planetary Vehicle considerations. However, it was recognized that the Spacecraft design should be flexible enough to accommodate more demanding orbit conditions. Hence, the Spacecraft was designed to accommodate this same orbit at 40 degrees inclination. This lower inclination involves more Sun and Canopus occultations, thus sizing the power system, setting life requirements for gyros, and making the flight sequence more complex.

For the selected capsule de-orbit trajectory, and a capsule impact point 20 degrees from the terminator and separation on the same day as the orbit insertion, the rotation of the line of apsides varies between 11.5 and 34.1 degrees. These conditions will provide a capsule impact within the required 30 degrees from the terminator if the capsule separation is delayed up to 10 days after orbit insertion. The minimum orbit insertion velocity varies between 1.66 and 1.90 km/sec. The selected orbit can be achieved for zero use of midcourse trajectory correction fuel by a fixed impulse propulsion system sized to give 2.2 km/sec if all of the midcourse correction fuel is used. Variations in impulse requirements due to variation in arrival velocity and midcourse trajectory correction fuel use, are eliminated by varying the impact parameter and hence the true anomaly of insertion into the satellite orbit.

The selected orbit provides viewing of Mars between 10 and 50 degrees from the evening terminator at a low altitude (as low as 1000 km) during the early part of the orbit phase, and viewing of the morning terminator at a minimum altitude during the latter part of the six-month orbit phase. Good viewing (Sun-orbiter-Mars angle greater than 150 degrees) for color TV is provided for several months during the middle of the orbit phase. Also,

occultation of Earth is obtained during the first month of the orbit phase, with occultation of the Sun occurring for less than a month of the six-month orbit phase, and occultation of Canopus not occurring until the last month or two of the orbit phase.

For a semi-major axis of the dispersion ellipse of 300 kilometers measured in the impact parameter plane, and a time of arrival uncertainty of ± 1.0 minute due to orbit determination, a semi-major axis of the dispersion ellipse of 100 km and time-of-arrival error of ± 1.0 minute due to trajectory correction maneuver errors, a worst-case heliocentric trajectory, and inclusion of orbit-insertion errors, the 3σ-orbit parameter deviations are as follows:

Periapsis, ± 260 km or 26% from the nominal
Orbit inclination, ± 2 degrees
Line of apsides, 4.3 degrees
Orbital period, ± 1.3 hours

These orbit parameter deviations are well within the required ± 30%, ± 2 degrees, and 10 degrees for periapsis altitude, orbit inclination, and line of apsides, respectively.

3.4 Orbit Trim. The allowed 100-m/sec orbit trim capability is not sufficient to correct an orbit which has a maximum error in each orbit parameter as specified in the Preliminary Mission Description: ± 30% periapsis altitude, ± 5 degrees inclination, and 10 degrees line of apsides. However, it is to be expected that the actual orbit-trim capability will be between 200 and 250 m/sec because the expected velocity requirements for trajectory correction are less than the specified 200 m/sec.

As an example, a 1300 by 12,000-km altitude orbit can be corrected to the nominal orbit in two maneuvers requiring a total velocity increment of 90 m/sec. For the nominal orbit, a line-of-apsides rotation of 10 degrees can be obtained with a velocity increment of 65 m/sec if two maneuvers are made, while the inclination of the orbit plane can be changed by less than four degrees when utilizing the full 100-m/sec specified capability. Combined maneuvers to change the periapsis or apoapsis with changes in line-of-apsides or inclination can be made. Provided that sufficient fuel is available to make the required orbit trim, the deviation of the final orbit from the nominal orbit is within the accuracy of the DSIF orbit determination capability. However, unless the propulsion system is sterilized, orbit trim corrections should be made with the velocity change approximately opposite to the orbit velocity so as to decrease the probability of propulsion products entering the Mars atmosphere and impacting the surface.

3.5 Capsule De-Orbit. The capsule is to be released 20 minutes before firing of the capsule propulsion system, the magnitude of the capsule velocity increment for de-orbit is to be less than 550 m/sec, the minimum time between engine firing and capsule entry is to be greater than 50 minutes, but less than 12 hours, the angle of attack at entry is to be less than 60 degrees, the entry angle is to be between vacuum graze and 20 degrees, separation and de-orbit maneuvers are to be in view of Goldstone, and impact is to be between 15 and 30 degrees of the terminator for a capsule release occurring between 3 and 10 days after orbit injection. For the nominal de-orbit trajectory selected, the engine firing occurs at a true anomaly of 230 degrees, and entry at 330 degrees true anomaly of the satellite orbit. The direction of

the velocity vector for a nominal satellite orbit and a 16-degree entry angle. For these separation conditions the maximum change of the Spacecraft from the Sun-line is 40 degrees; therefore, the Spacecraft can maintain the separation attitude until after capsule impact without requiring an excessive battery capability. Entry will occur at 1.2 hours after engine firing at a velocity of 4.3 km/sec and an angle of attack of less than 50 degrees. The range at entry is 1800 km, and at impact is dependent on the Mars atmospheric profile. The maximum line-of-sight variation between the capsule and orbiter is also dependent upon the atmosphere profile, varying between 37 and 107 degrees for a surface pressure of 4 to 10 mb. Even if the surface pressure were as high as 25 mb, the capsule would remain in view of the orbiter through impact.

Even with a deviation of 19 degrees of the line of apsides from nominal, and orbits ranging from 700 by 8000 to 1300 by 13,000 km altitude, the location of the capsule entry with respect to the terminator can be maintained constant with a constant de-orbit velocity increment. Assuming an orbit determination capability of 5 km (3σ), a pointing error of two degrees, and a velocity error of 3% (3σ), the impact dispersion is only 245 km (3σ) for an atmospheric variation between the VM3 and VM8 atmospheres.

For a separation velocity between the capsule and orbiter of one m/sec and a 20-minute wait between separation and capsule engine firing, the line of sight between capsule and orbiter is only 0.576 degree at the time of engine firing. For the design dimensions of the capsule and orbiter, this results in a 2.2-% probability that large capsule engine pieces, if released, will strike the orbiter. By increasing the period between separation and engine firing to 30 minutes, the line of sight increases to 1.15 degrees and the probability of particle impact becomes only one-ninth of that for a 20-minute wait period.

4.0 SPACECRAFT CONFIGURATION AND STRUCTURE

4.1 Location of Major Spacecraft Elements. Major elements of the Spacecraft influencing the configuration are:

a. The spacecraft science and electronic equipment which is mounted in the 16-bay upper equipment module as shown in Figure 4-1. Total packaging volume is 20.8 cubic feet.

b. A planet-scan platform, mounted on the solar-array support structure and deployed after Mars orbit insertion.

c. A 7.5-foot diameter high-gain communications antenna mounted on the solar-array support structure and deployed after orbit injection with its nodding axis parallel to the X axis, and with a second axis parallel to the Y axis when in the zero-nod position.

d. A medium-gain Mariner C-type fixed antenna mounted on the solar-array support structure so that it can see Earth during the early part of the orbit phase.

e. A fixed primary low-gain antenna mounted off the fixed solar array on the -X axis so that it can radiate a hemispherical pattern with its centerline 25 degrees off the -Z axis. (Note: this antenna is also used for launch signals.)

f. A secondary low-gain antenna on a boom deployed from the solar array along the +X axis.

g. A fixed relay turnstile antenna mounted on the solar-array structure along the +X axis so that it can radiate a pattern with a centerline 40 degrees off the +Z axis.

h. Dual cold-gas reaction jets mounted on the edge of the solar-array structure for pitch, roll and yaw control.

i. A magnetometer mounted at the end of the 3-inch diameter, 5-foot boom deployed off the solar array between the +Y and -X axes.

j. A fixed solid-propellant engine, with thrust-vector control, mounted in the bus structure with its thrust axis along the Z axis.

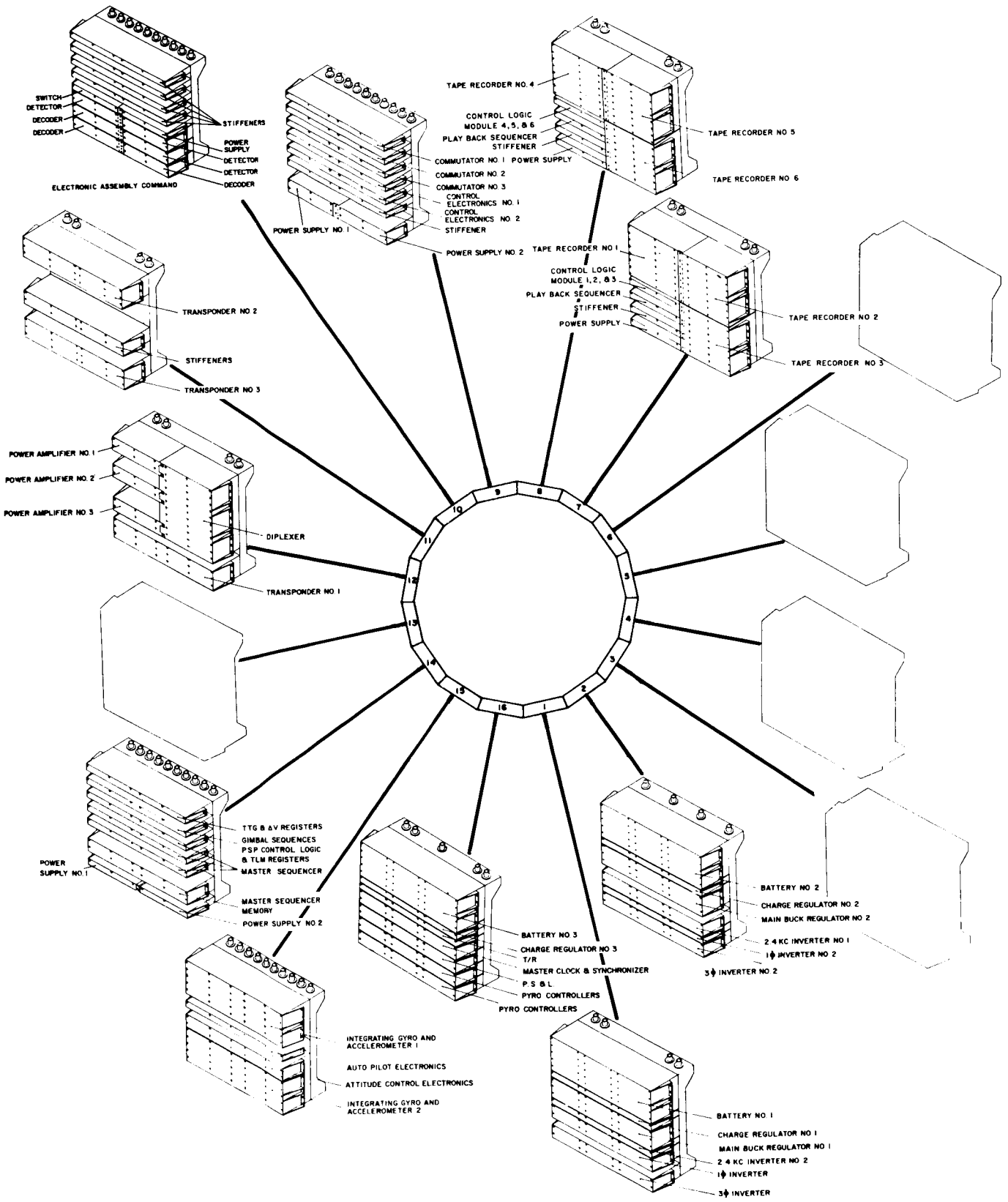
k. Four fixed monopropellant engines with thrust-vector control and tanks mounted in the bus structure with their thrust axes parallel to the Z axis.

l. Attitude Control Sun sensors consisting of one primary assembly and four secondary individual sensors, mounted on the solar-array structure.

m. Two Canopus sensors mounted on the bus structure aligned along the Y axis.

n. Eight solar-aspect sensors mounted on the edge of the solar-array structure.

4.2 Spacecraft and Structure Configuration. The spacecraft structure and the basic arrangement of equipment is shown in Figure 4-2. The Spacecraft Bus structure provides for the overall mounting of equipment, and serves as the load-carrying medium between the capsule and the Launch Vehicle shroud. The bus structural arrangement has been designed as two separate module sections: (a) an upper bus module, Stations 49.25 to 101.25; and (b) a lower


SWITCH DETECTOR
DECODER
DECODER
STIFFENERS
POWER SUPPLY
DETECTOR
DETECTOR
DECODER
ELECTRONIC ASSEMBLY COMMAND
POWER SUPPLY NO. 1
COMMUTATOR NO. 1
COMMUTATOR NO. 2
COMMUTATOR NO. 3
CONTROL ELECTRONICS NO. 1
CONTROL ELECTRONICS NO. 2
STIFFENER
POWER SUPPLY NO. 1
POWER SUPPLY NO. 2
TAPE RECORDER NO. 4
CONTROL LOGIC MODULE 4, 5, & 6
PLAY BACK SEQUENCER
STIFFENER
POWER SUPPLY
TAPE RECORDER NO. 5
TAPE RECORDER NO. 6
TAPE RECORDER NO. 1
CONTROL LOGIC MODULE 1, 2, & 3
PLAY BACK SEQUENCER
STIFFENER
POWER SUPPLY
TAPE RECORDER NO. 2
TAPE RECORDER NO. 3
TRANSPONDER NO. 2
STIFFENERS
TRANSPONDER NO. 3
POWER AMPLIFIER NO. 1
POWER AMPLIFIER NO. 2
POWER AMPLIFIER NO. 3
DIPLEXER
TRANSPONDER NO. 1
TTG & ΔV REGISTERS
GIMBAL SEQUENCES
PSP CONTROL LOGIC & TLM REGISTERS
MASTER SEQUENCER
MASTER SEQUENCER MEMORY
POWER SUPPLY NO. 2
POWER SUPPLY NO. 1
INTEGRATING GYRO AND ACCELEROMETER 1
AUTO PILOT ELECTRONICS
ATTITUDE CONTROL ELECTRONICS
INTEGRATING GYRO AND ACCELEROMETER 2
BATTERY NO. 3
CHARGE REGULATOR NO. 3
T/R
MASTER CLOCK & SYNCHRONIZER
P.S & L
PYRO CONTROLLERS
PYRO CONTROLLERS
BATTERY NO. 2
CHARGE REGULATOR NO. 2
MAIN BUCK REGULATOR NO. 2
2.4 KC INVERTER NO. 1
1φ INVERTER NO. 2
3φ INVERTER NO. 2
BATTERY NO. 1
CHARGE REGULATOR NO. 1
MAIN BUCK REGULATOR NO. 1
2.4 KC INVERTER NO. 2
1φ INVERTER
3φ INVERTER
1
2
3
4
5
6
7
8
9
10
11
12
13
14
15
16

260

3

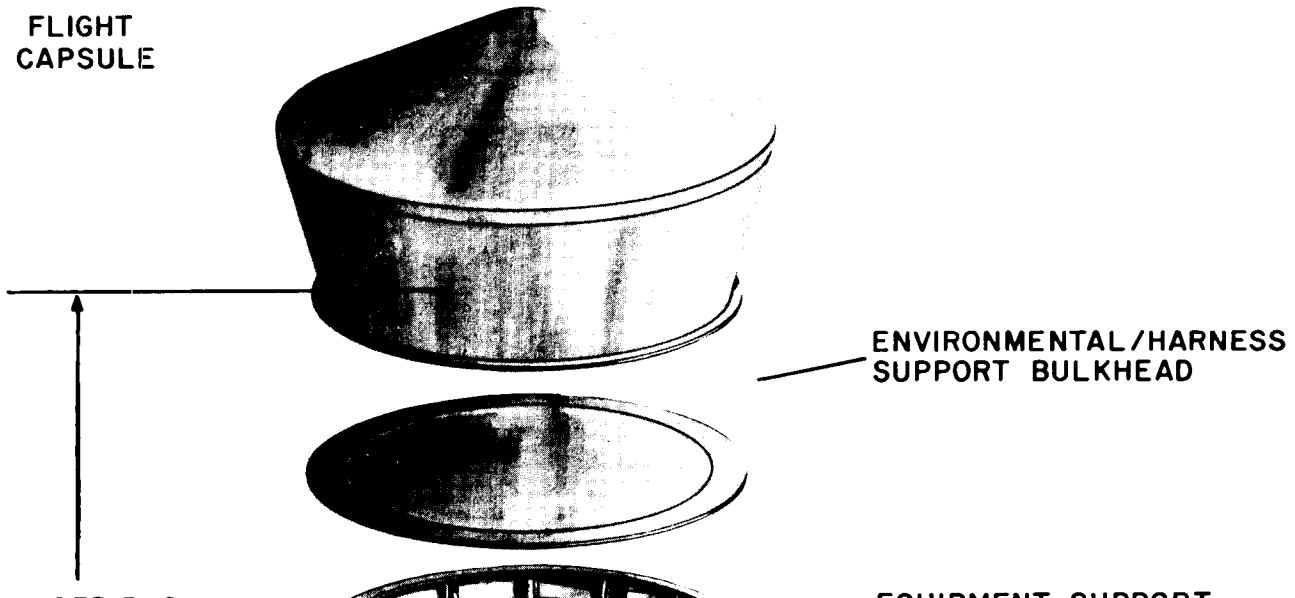
Bay No.	Assembly Function	W
1	1/3 POWER SUBSYSTEM - Battery No. 1; Charge Regulator No. 1; Main Buck Regulator No. 1; 2.4 Kc Inverter No. 2, 3 Φ No. 1	
2	1/3 POWER SUBSYSTEM - Battery No. 2, Charge Regulator No. 2; Main Buck Regulator No. 2; 2.4 Kc Inverter No. 1; 3 Φ Inverter No. 2	
3	SCIENCE ELECTRONICS	
4	SPARE	
5	SCIENCE ELECTRONICS	
6	SCIENCE DAE	
7	1/2 DATA STORAGE SUBSYSTEM 3 ea. Tape Recorders, 3 ea. CLM, 1 ea. PBS	
8	1/2 DATA STORAGE SUBSYSTEM 3 ea. Tape Recorders, 3 ea. CLM, 1 ea. PBS; 1 ea. Power Supply	
9	RADIO SUBSYSTEM	
10	COMMAND SUBSYSTEM Command Detectors, Command Decoders, Command Access Switch, Power Supply	
11	1/2 RADIO SUBSYSTEM Transponders No. 2 and 3	
12	1/2 RADIO SUBSYSTEM 2 ea. TWT's, 1 ea. Solid State Exciter, 1 ea. Diplexer Assembly, 1 ea. Transponder	
13	RELAY RADIO SUBSYSTEM	
14	COMPUTER AND SEQUENCER SUBSYSTEM	
15	GUIDANCE AND CONTROL SUBSYSTEM Integrating Gyro & Accelerometer Package, A/C Electric, Auto Pilot Electr.	
16	1/3 POWER SUBSYSTEM - BATTERY No. 3, Charge Regulator, PS&L, Pyro Controller, Synchronizer, Charge Control	
	Total	

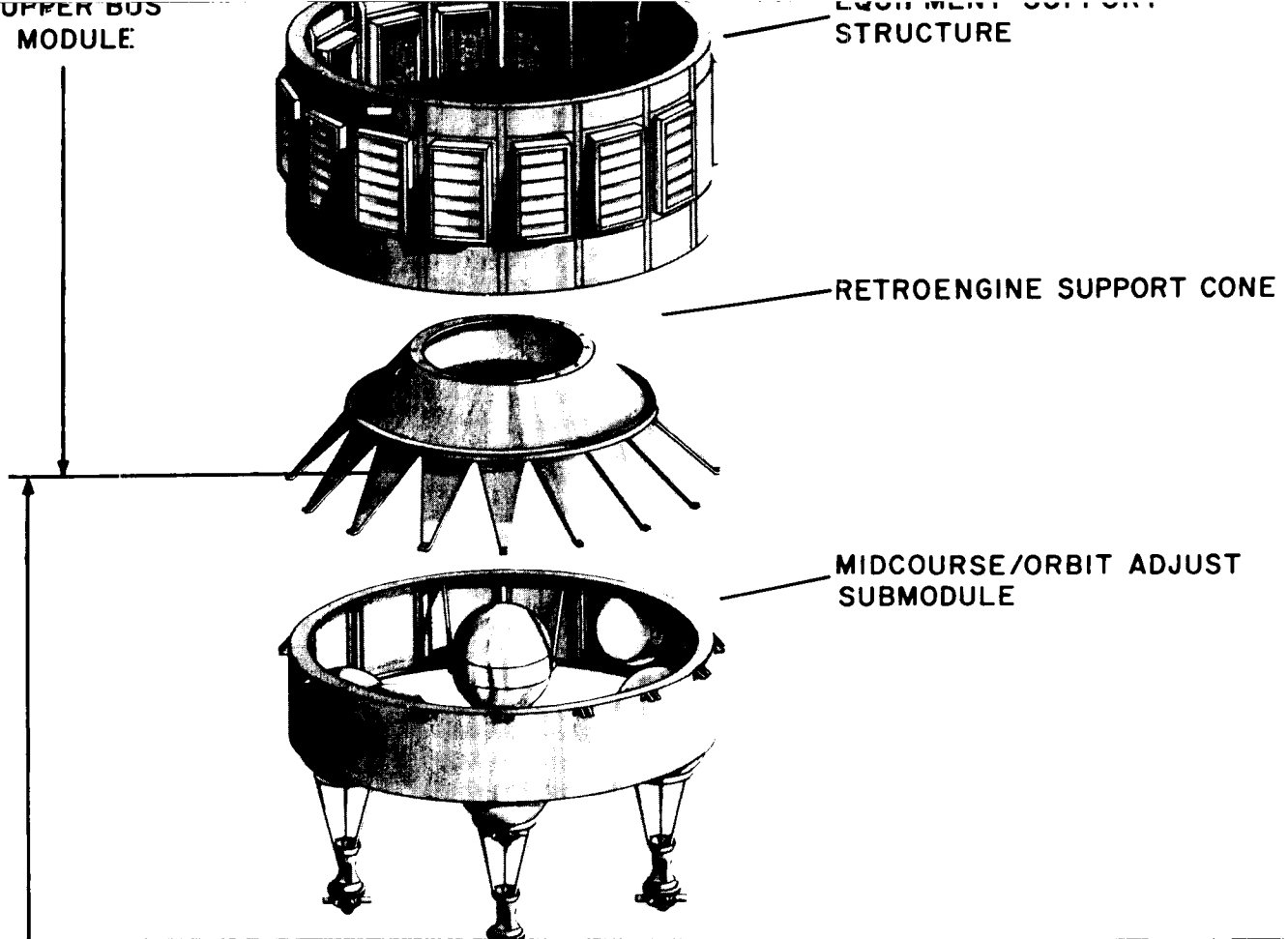
*Weight estimate based on PIR 5200-JHC-008
Weight does not include harness trays, cabli
**Power estimates based on PIR 5200-JHC-00
represents worst case.

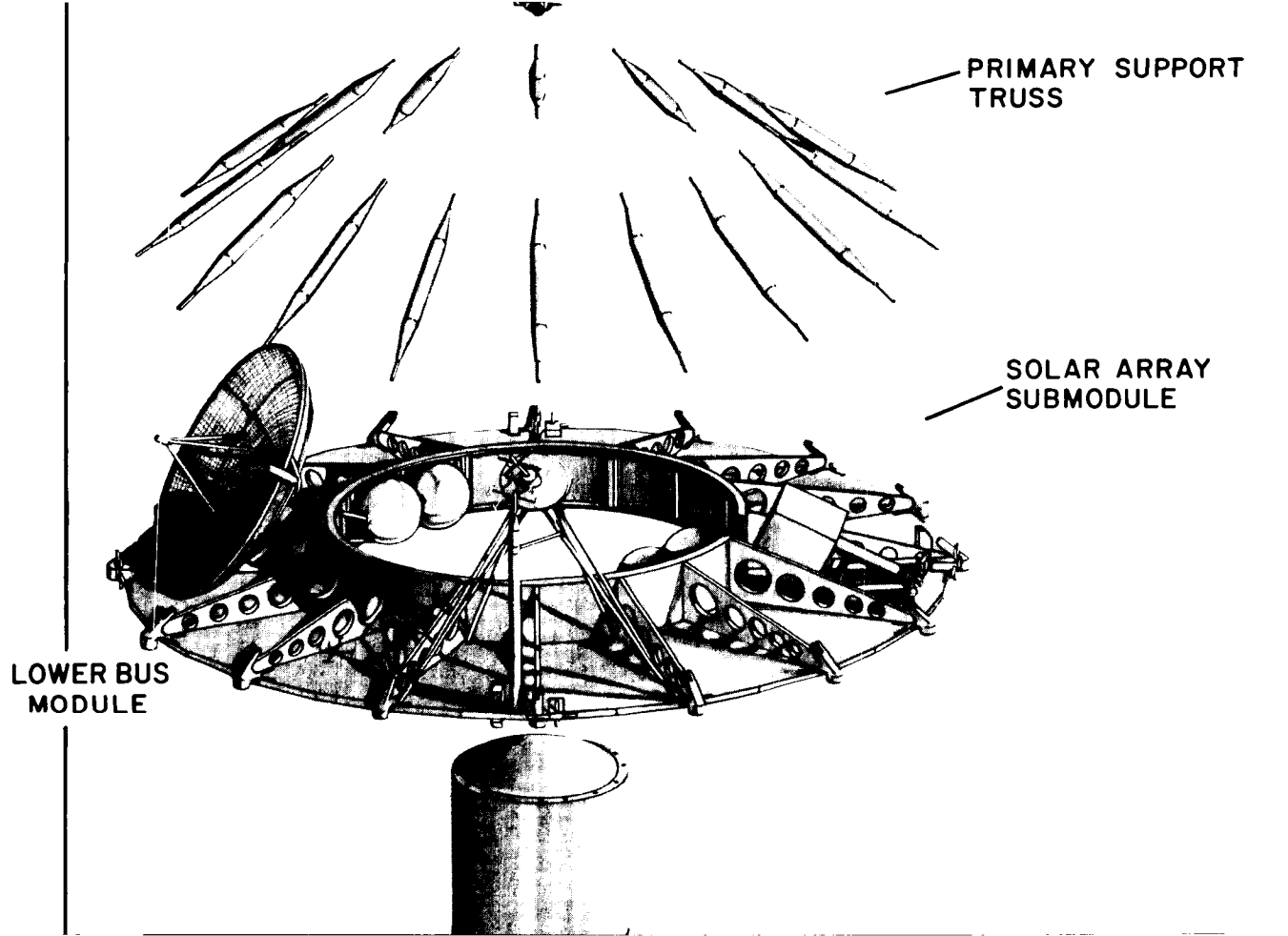
Figure 4-1. Equipment Arrangement Packages within the Equipment Module

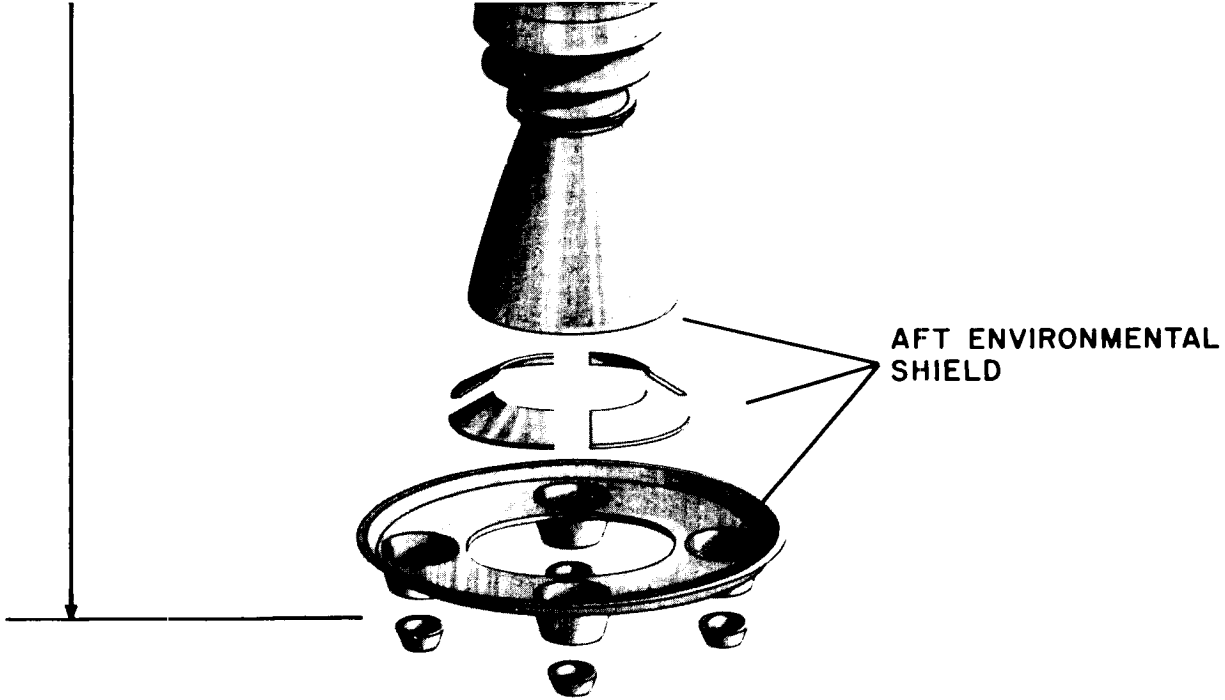
eight* (Est) (lb)	Power** (Est)* (Watts)	No. of System Connections	Volumetric Efficiency %
74	78.5	8-10	60
74	17.3	8-10	60
45	33		
45	33		
55	30	8	
55.5	18	4	92
60.5	12.2	4	92
18	8.2	15-16	28
30	20.2	12	48
26.6	15	4	45
43.3	110	4	79
25	10	4	44
35	30	13	52
28.4	65.8	13	50
68.5	27.3	10	79
683.8	508.3	112	60 Aug.

are later inputs from Subsystem Engineers.
g and other hardware.
, PIR 4428-07 Rev. C and VB236FD101 and


FLIGHT
CAPSULE
ENVIRONMENTAL/HARNESS
SUPPORT BULKHEAD


UPPER BUS MODULE
STRUCTURE
RETROENGINE SUPPORT CONE
MIDCOURSE/ORBIT ADJUST SUBMODULE


PRIMARY SUPPORT TRUSS
SOLAR ARRAY SUBMODULE
LOWER BUS MODULE


AFT ENVIRONMENTAL
SHIELD

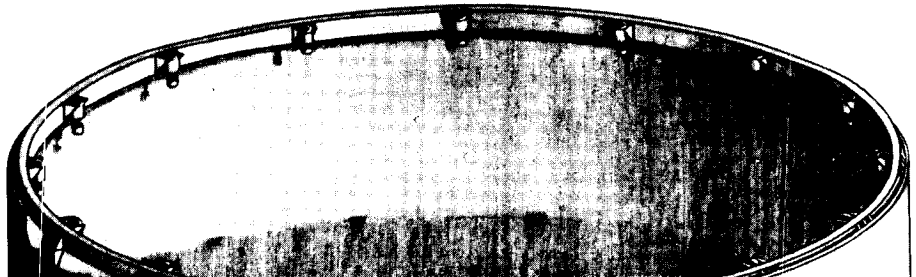

PLANETARY VEHICLE
ADAPTER



Figure 4-2. Spacecraft Structural Breakdown

bus module extending from Station 0.00 to 49.25. The modules are joined by the production break (at station 49.25), consisting of 32 tension bolts (two per longeron) designed to carry axial and shear loads across the joint.

The upper bus module primarily contains the equipment bays, divided into 16 modular packages. In addition, the module serves as the primary mounting support for the forward thrust-cone adapter to the modified Minuteman motor. The structure is designed as a 16-sided polygon in the equipment support bays. It consists of longerons and shear-carrying skin sections, the longerons serving to transmit axial loads through the section and also to provide mounting support for the equipment modules. The equipment modules are designed integrally with the structure to carry primary shear loads through thermal radiating cover plates which provide heat dissipation and thermal control of the components. Thirty-two structural load-carrying doors are provided adjacent to the equipment bays for ready access to the main system harness and connectors.

The lower bus module serves as the mounting structure for the 190-square-foot fixed solar array, the medium-gain and high-gain antennas, the relay antenna and the Planet Scan Platform. The module also shrouds and houses the midcourse propulsion system, and the Attitude Control subsystem together with the associated equipment.

The lower module structure (Stations 0.00 to 49.25) is designed as two separate submodule sections for ease of assembly and installation of equipment. The lower portion, containing the solar array and the antenna supports, provides an integral mounting structure for the Attitude Control subsystem. This arrangement permits modular removal of this subsystem without disassembly of interconnecting plumbing joints and fittings. The upper portion of the module (MC/OA sub-module) provides for mounting and modular installation of the midcourse propulsion system, which may be bench-assembled as a separate unit. The submodular sections are joined by the production joint at Station 19.25.

The lower bus module is constructed as a cylindrical sheet-stringer-stiffened arrangement. Primary shear is transferred through beaded shear panels, and then through the solar array honeycomb panels to the bus-adapter section. Sixteen diagonal truss members provide axial load continuity for the lower bus module between the production break, at station 49.25, and the adapter interface connection, at station 0.00.

The modular arrangement of equipment and structural sections described above offers a high degree of space utilization, placement flexibility and equipment accessibility. Also, it provides parallel flow paths within the production and system-test cycles.

5.0 SPACECRAFT FUNCTIONAL RELATIONSHIPS

5.1 Functional Relationships. The System Functional Diagram (Figure 5-1) portrays the relationships among the various subsystems. Insofar as practical, all system signals which exercise the various subsystems for nominal operation of the Spacecraft are shown. For a more detailed description of the spacecraft events refer to the section on Flight Sequence (VC220FD113).

Primary command source lines are shown. C&S commands which are backed up by the command decoder are indicated by asteriskes.

5.2 Mass Properties. Table 5-1 presents a weight summary of the Planetary Vehicle.

TABLE 5-1. WEIGHT SUMMARY OF THE PLANETARY VEHICLE

Description	Weight (lb)
Power	473.2
Computer and Sequencer	35.0
Guidance and Control	313.5
Radio (Includes Relay)	188.3
Telemetry	16.6
Command	29.9
Data Storage	115.6
Pyrotechnics	11.9
Temperature Control	144.8
Harnesses	117.4
Diagnostic	9.0
Structure	457.0
Science	400.0
Spacecraft Bus	2312.2
Spacecraft Bus Margin	187.2
Total Spacecraft Bus	2500.0
Spacecraft Propulsion	11863.4
Spacecraft Propulsion Margin	3136.6
Total Spacecraft Propulsion	15000.0
Total Flight Spacecraft	17500.0
Flight Capsule (includes Bio-Barrier)	3000.0
Separated Overall Planetary Vehicle	20500.0
Planetary Vehicle Adapter	113.3
Planetary Vehicle Adapter Margin	1386.7
Total Planetary Vehicle Adapter	1500.0
Total Planetary Vehicle Weight	22000.0
Total Margin %	21%

The mass properties of the Planetary Vehicle for the nominal capsule center-of-gravity locations are shown in Table 5-2. A further definition of the mass properties can be found in VC220FD113, Layout and Configuration.

5-3. Electrical Interfaces

5.3.1 Power. The raw power from the photovoltaic solar cells and batteries is converted and distributed as square-wave, 2400-cps, single-phase, 50V rms; and 400-cps, 3-phase, 26V rms power.

Each subsystem using the primary power distribution provides its own transformer-rectifier for converting the a-c power to the required voltages. The Radio Subsystem converts the array/battery raw-bus power to the appropriate voltages for operating the power amplifiers. The array/battery raw-bus power is available also for miscellaneous loads such as solenoid valves and heaters.

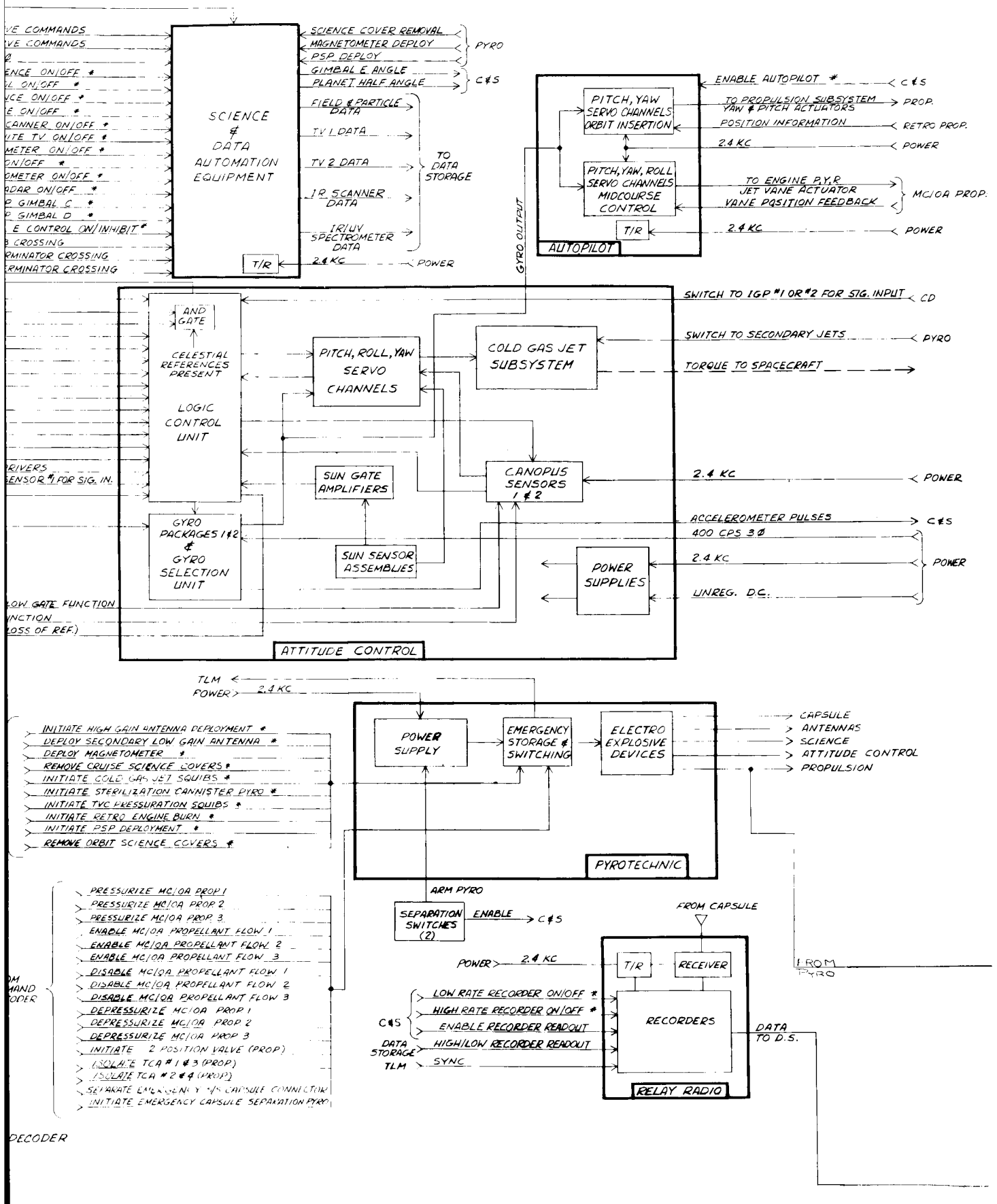
TABLE 5-2. PLANETARY VEHICLE MASS PROPERTIES

Description	Weight (lb)	cg Location			Moments of Inertia* (Slug ft^2)			Products of Inertia* (Slug ft^2)		
		Z*	X	Y	I_{oz}	I_{ox}	I_{oy}	W_{zx}	W_{zy}	W_{xy}
Prior to Orbit Insertion	15780	76.17	0.25	0.06	7577	17064	17198	5.2	59.5	80.3
Prior to Capsule Release	7322	102.47	0.54	0.12	6997	14499	14093	-17.1	54.3	80.2
After Capsule Release	4572	42.47	1.83	2.61	3970	3634	2781	-30.6	-90.0	299.1

*CG location with respect to Station O

5.3.2 Interface Signal Characteristics. These are shown in the VOYAGER Functional Block Diagram, Figure 5-1.

5.3.3 Grounding Nets. Electrically conductive paths among equipment elements such as chassis, housing, structure, earth-ground and circuit-common meet the requirements of the "General Specification for the Performance and Design Requirements for the VOYAGER 1971 Spacecraft System" dated September 17, 1965. The locations of the common tie-points are shown on the following page.


SCIENCE COVER REMOVAL
MAGNETOMETER DEPLOY
PSP DEPLOY
PYRO
GIMBAL & ANGLE
PLANET HALF ANGLE
C&S
SCIENCE & DATA AUTOMATION EQUIPMENT
FIELD & PARTICLE DATA
TV 1 DATA
TV 2 DATA
IR SCANNER DATA
IR/UV SPECTROMETER DATA
TO DATA STORAGE
T/R
2.4 KC
POWER
GYRO OUTPUT
ENABLE AUTOPILOT *
C&S
PITCH, YAW SERVO CHANNELS ORBIT INSERTION
TO PROPULSION SUBSYSTEM YAW & PITCH ACTUATORS
PROP.
POSITION INFORMATION
RETRO PROP.
2.4 KC
POWER
PITCH, YAW, ROLL SERVO CHANNELS MIDCOURSE CONTROL
TO ENGINE P.Y.R
JET VANE ACTUATOR
VANE POSITION FEEDBACK
MC/OA PROP.
T/R
2.4 KC
POWER
AUTOPILOT
SWITCH TO IGP #1 OR #2 FOR STIG. INPUT
CD
AND GATE
CELESTIAL REFERENCES PRESENT
LOGIC CONTROL UNIT
PITCH, ROLL, YAW SERVO CHANNELS
COLD GAS JET SUBSYSTEM
SWITCH TO SECONDARY JETS
PYRO
TORQUE TO SPACECRAFT
SUN GATE AMPLIFIERS
CANOPUS SENSORS 1 & 2
2.4 KC
POWER
ACCELEROMETER PULSES
C&S
400 CPS 3Ø
2.4 KC
POWER
GYRO PACKAGES 1&2 & GYRO SELECTION UNIT
SUN SENSOR ASSEMBLIES
POWER SUPPLIES
UNREG. D.C.
ATTITUDE CONTROL
TLM
POWER
2.4 KC
INITIATE HIGH GAIN ANTENNA DEPLOYMENT *
DEPLOY SECONDARY LOW GAIN ANTENNA *
DEPLOY MAGNETOMETER *
REMOVE CRUISE SCIENCE COVERS *
INITIATE COLD GAS JET SQUIBS *
INITIATE STERILIZATION CANNISTER PYRO *
INITIATE TVC PRESSURATION SQUIBS *
INITIATE RETRO ENGINE BURN *
INITIATE PSP DEPLOYMENT *
REMOVE ORBIT SCIENCE COVERS *
POWER SUPPLY
EMERGENCY STORAGE & SWITCHING
ELECTRO EXPLOSIVE DEVICES
CAPSULE
ANTENNAS
SCIENCE
ATTITUDE CONTROL
PROPULSION
PYROTECHNIC
ARM PYRO
SEPARATION SWITCHES (2)
ENABLE
C&S
FROM CAPSULE
POWER
2.4 KC
T/R
RECEIVER
FROM PYRO
PRESSURIZE MC/OA PROP 1
PRESSURIZE MC/OA PROP 2
PRESSURIZE MC/OA PROP 3
ENABLE MC/OA PROPELLANT FLOW 1
ENABLE MC/OA PROPELLANT FLOW 2
ENABLE MC/OA PROPELLANT FLOW 3
DISABLE MC/OA PROPELLANT FLOW 1
DISABLE MC/OA PROPELLANT FLOW 2
DISABLE MC/OA PROPELLANT FLOW 3
DEPRESSURIZE MC/OA PROP 1
DEPRESSURIZE MC/OA PROP 2
DEPRESSURIZE MC/OA PROP 3
INITIATE 2 POSITION VALVE (PROP)
ISOLATE TCA #1 & 3 (PROP)
ISOLATE TCA #2 & 4 (PROP)
SEPARATE EMERGENCY S/S CAPSULE CONNECTOR
INITIATE EMERGENCY CAPSULE SEPARATION PYRO
DECODER
C&S
LOW RATE RECORDER ON/OFF *
HIGH RATE RECORDER ON/OFF *
ENABLE RECORDER READOUT
HIGH/LOW RECORDER READOUT
DATA STORAGE
TLM
SYNC
RECORDERS
DATA TO D.S.
RELAY RADIO

30 (6)

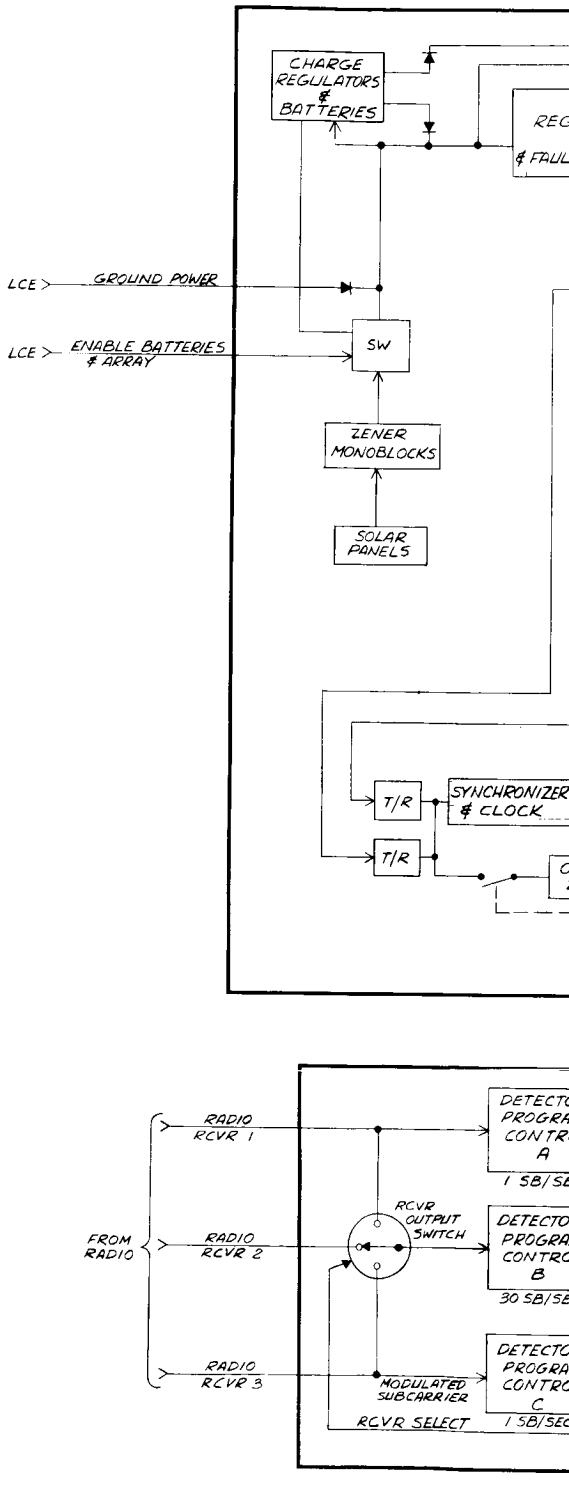
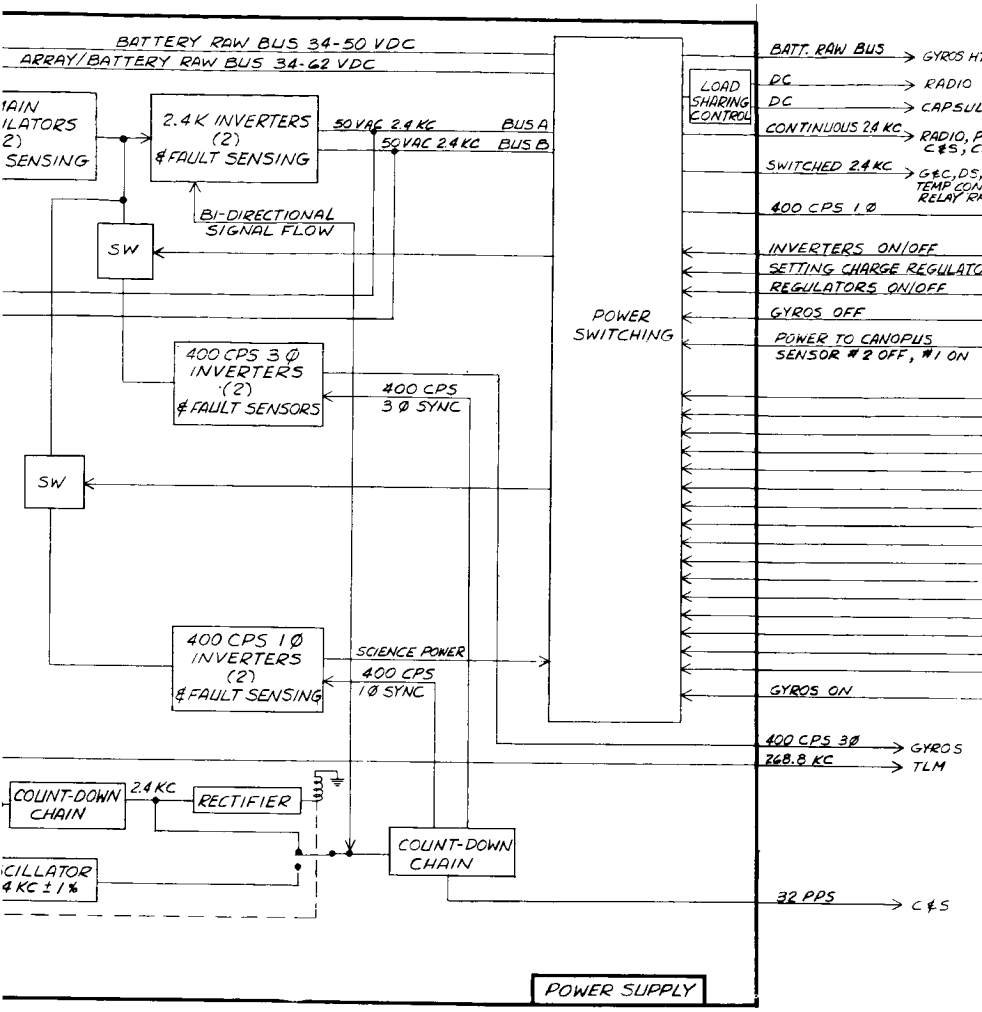
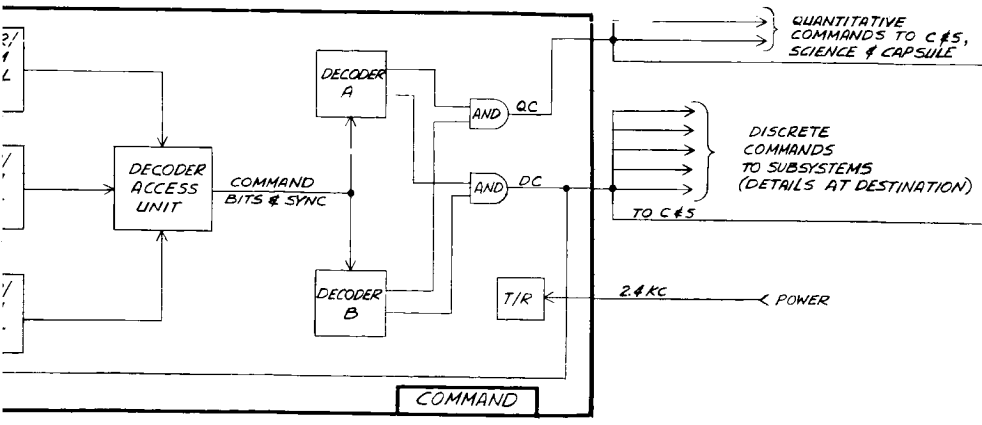


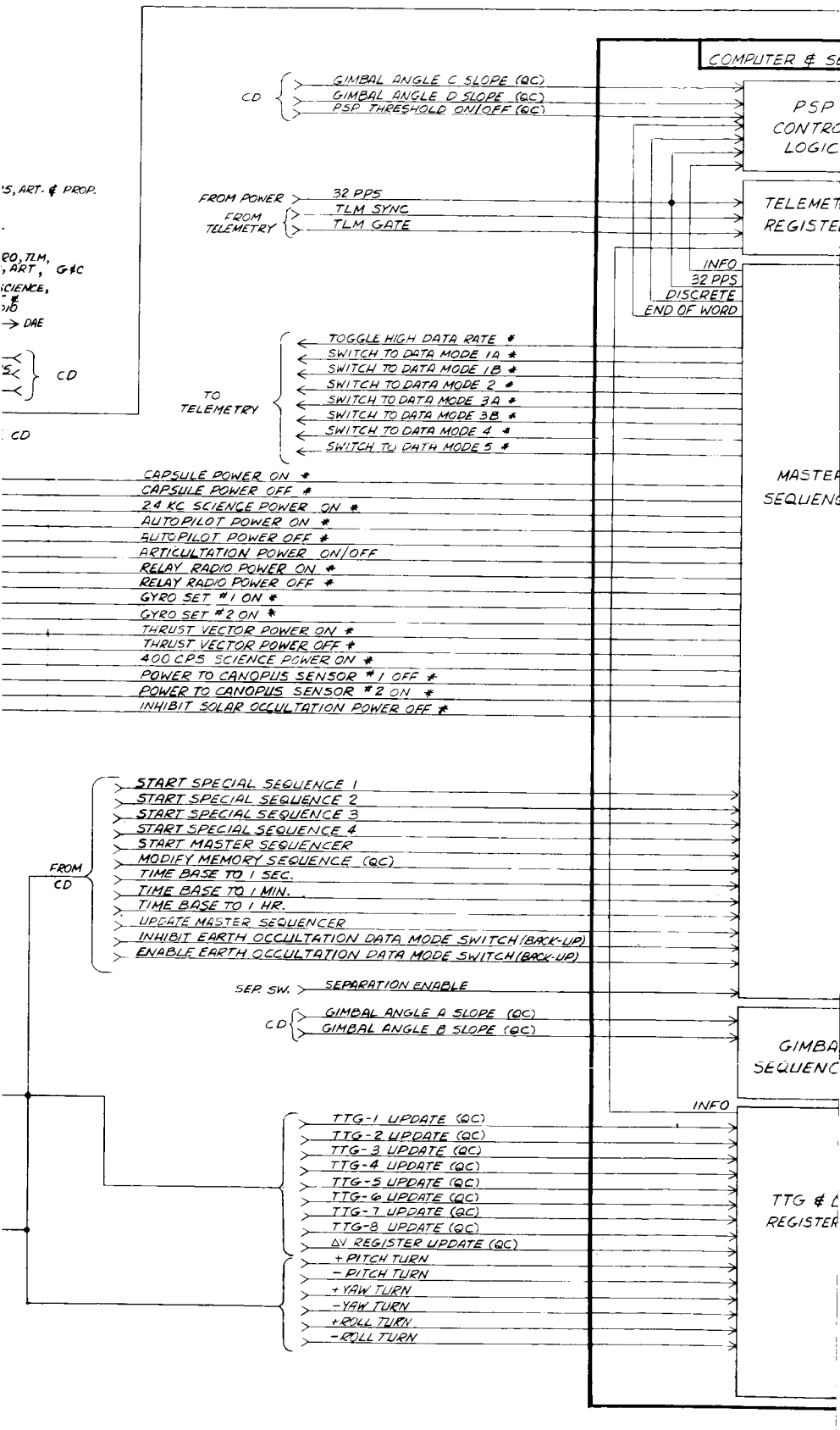
Figure 5-1. VOYAGER Functional Block Diagram (Sheet 1 of 2)



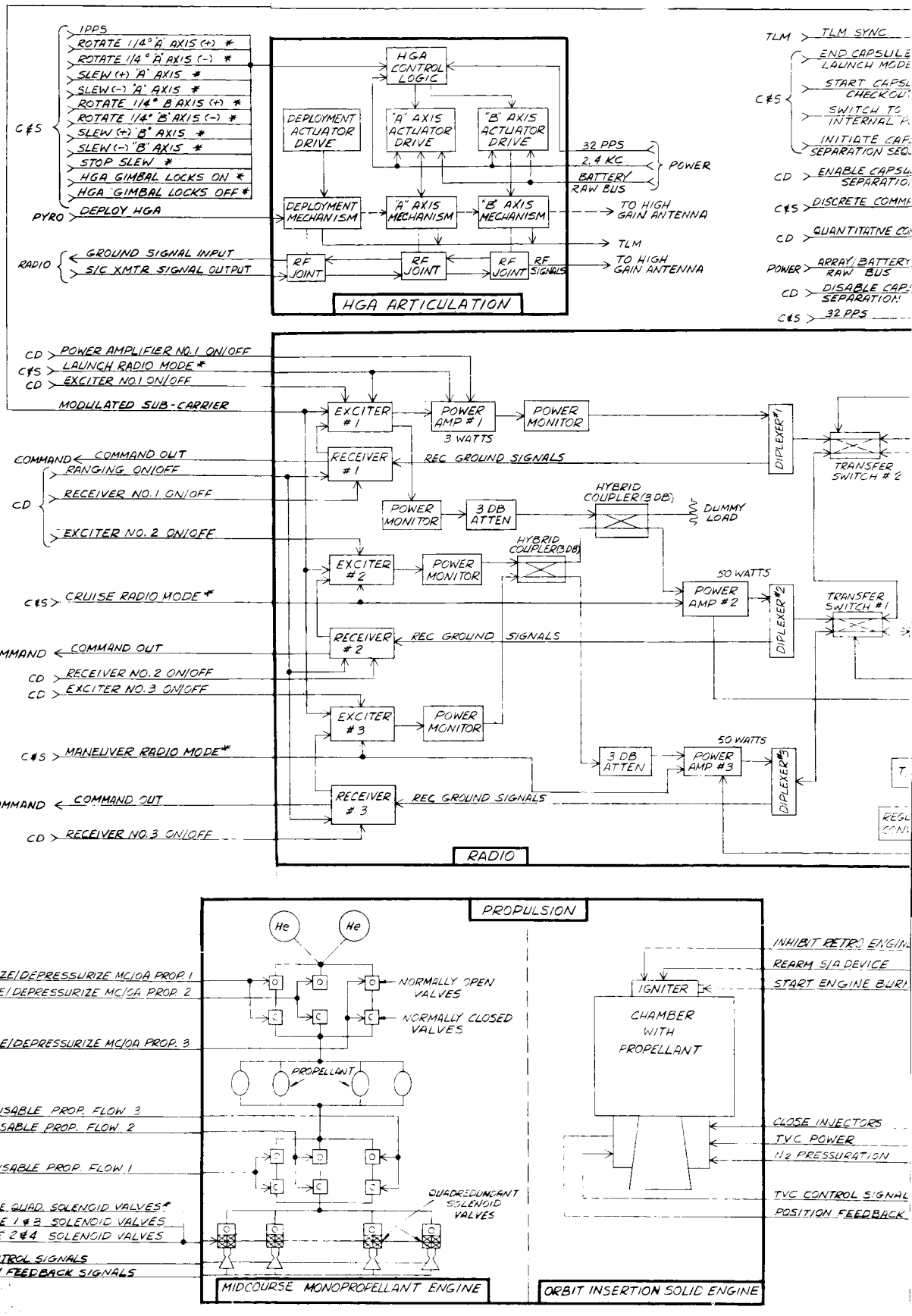


* BACK-UP FROM COMMAND DECODER
(QC) QUANTITATIVE COMMANDS

302


COMPUTER & SE
PSP CONTRO LOGIC
TELEMET REGISTE
MASTE SEQUENC
GIMBA SEQUENC
TTG & REGISTER
CD
GIMBAL ANGLE C SLOPE (QC)
GIMBAL ANGLE D SLOPE (QC)
PSP THRESHOLD ON/OFF (QC)
FROM POWER
32 PPS
FROM TELEMETRY
TLM SYNC
TLM GATE
INFO
32 PPS
DISCRETE
END OF WORD
TO TELEMETRY
TOGGLE HIGH DATA RATE *
SWITCH TO DATA MODE 1A *
SWITCH TO DATA MODE 1B *
SWITCH TO DATA MODE 2 *
SWITCH TO DATA MODE 3A *
SWITCH TO DATA MODE 3B *
SWITCH TO DATA MODE 4 *
SWITCH TO DATA MODE 5 *
CAPSULE POWER ON *
CAPSULE POWER OFF *
2.4 KC SCIENCE POWER ON *
AUTOPILOT POWER ON *
AUTOPILOT POWER OFF *
ARTICULTATION POWER ON/OFF
RELAY RADIO POWER ON *
RELAY RADIO POWER OFF *
GYRO SET #1 ON *
GYRO SET #2 ON *
THRUST VECTOR POWER ON *
THRUST VECTOR POWER OFF *
400 CPS SCIENCE POWER ON *
POWER TO CANOPUS SENSOR #1 OFF *
POWER TO CANOPUS SENSOR #2 ON *
INHIBIT SOLAR OCCULTATION POWER OFF *
FROM CD
START SPECIAL SEQUENCE 1
START SPECIAL SEQUENCE 2
START SPECIAL SEQUENCE 3
START SPECIAL SEQUENCE 4
START MASTER SEQUENCER
MODIFY MEMORY SEQUENCE (QC)
TIME BASE TO 1 SEC.
TIME BASE TO 1 MIN.
TIME BASE TO 1 HR.
UPDATE MASTER SEQUENCER
INHIBIT EARTH OCCULTATION DATA MODE SWITCH (BACK-UP)
ENABLE EARTH OCCULTATION DATA MODE SWITCH (BACK-UP)
SEP. SW.
SEPARATION ENABLE
CD
GIMBAL ANGLE A SLOPE (QC)
GIMBAL ANGLE B SLOPE (QC)
INFO
TTG-1 UPDATE (QC)
TTG-2 UPDATE (QC)
TTG-3 UPDATE (QC)
TTG-4 UPDATE (QC)
TTG-5 UPDATE (QC)
TTG-6 UPDATE (QC)
TTG-7 UPDATE (QC)
TTG-8 UPDATE (QC)
ΔV REGISTER UPDATE (QC)
+ PITCH TURN
- PITCH TURN
+ YAW TURN
- YAW TURN
+ ROLL TURN
- ROLL TURN

C&S
32 PPS
CD
QUANTITATI
C&S
QUANTITATI
POWER
400 CPS
CRUISE SCI
PSP CONTRO
ORBIT SCIE
PSP SCIENC
INFRARED S
BLACK & WH
IR SPECTRO
COLOR TV
UV SPECTR
BISTATIC R
UPDATE PS
UPDATE PS
PSP GIMBAL
PLANET LIM
MORNING TE
EVENING
GYROS OFF
DIGITAL DATA
TELEMETRY
SOLAR ASPECT SENSOR
EARTH OCCULTATION SENSORS
GIMBAL E ANGLE
PLANET HALF ANGLE
SCIENCE
INFO
NO PARITY
TLM REG SYNC
MEMORY INITIATE
ADDRESS WORDS & MEMORY WORDS, 26 BITS
ENABLE PNEUMATIC DRIVERS *
GYRO SET 1 OFF *
GYRO SET 2 OFF *
SWITCH TO CANOPUS #2 FOR SIGNAL INPUT *
SWITCH TO CRUISE MODE *
ALL AXIS TO INERTIAL CONTROL *
ENABLE SUN OCCULTATION MODE *
SWITCH TO ROLL INERTIA MODE *
SUN LOOPS TO MEDIUM GAIN *
SUN LOOPS TO HIGH GAIN *
SELECT CANOPUS #1 FOR INCREMENTING *
SELECT CANOPUS #2 FOR INCREMENTING *
INCREMENT CANOPUS FUNCTION (+) *
INCREMENT CANOPUS FUNCTION (-) *
GYRO TEMP. OVER-RIDE *
CD
DISABLE PNEUMATIC D
SWITCH TO CANOPUS S
ROLL OVER RIDE
GYRO SELECTION UNIT
TO AUTOPILOT
TO ARTICULATION
TO RADIO
CD
ENABLE CANOPUS HIGH/
ENABLE CONE ANGLE FU
GYROS ON
TO RELAY RADIO
32 PPS
TO CAPSULE & DAE
TO PROPULSION
TO CAPSULE
TO PYRO
1 PPS
1 PPS
STEP GIMBALS
TO ARTICULATION
START POS. PITCH TURN *
START NEG. PITCH TURN *
START POS. YAW TURN *
START NEG. YAW TURN *
START POS. ROLL TURN *
START NEG. ROLL TURN *
STOP TURN (S) *
START RETRO ENGINE
STOP MIDCOURSE ENGINE (BACKUP)
START MIDCOURSE ENGINE
PYRO
PROPULSION
T/R
2.4 KC
POWER
* BACK-UP FROM COMMAND


C&S
1PPS
ROTATE 1/4° "A" AXIS (+) *
ROTATE 1/4° "A" AXIS (-) *
SLEW (+) "A" AXIS *
SLEW (-) "A" AXIS *
ROTATE 1/4° B AXIS (+) *
ROTATE 1/4° "B" AXIS (-) *
SLEW (+) "B" AXIS *
SLEW (-) "B" AXIS *
STOP SLEW *
HGA GIMBAL LOCKS ON *
HGA GIMBAL LOCKS OFF *
PYRO
DEPLOY HGA
RADIO
GROUND SIGNAL INPUT
S/C XMTR SIGNAL OUTPUT
HGA CONTROL LOGIC
DEPLOYMENT ACTUATOR DRIVE
"A" AXIS ACTUATOR DRIVE
"B" AXIS ACTUATOR DRIVE
32 PPS
2.4 KC
BATTERY/RAW BUS
POWER
DEPLOYMENT MECHANISM
"A" AXIS MECHANISM
"B" AXIS MECHANISM
TO HIGH GAIN ANTENNA
TLM
RF JOINT
RF JOINT
RF JOINT
RF SIGNALS
TO HIGH GAIN ANTENNA
HGA ARTICULATION
TLM
TLM SYNC
C&S
END CAPSULE LAUNCH MODE
START CAPSU
CHECKOUT
SWITCH TO INTERNAL P
INITIATE CAP
SEPARATION SEQ
CD
ENABLE CAPSU
SEPARATIO
C&S
DISCRETE COMM
CD
QUANTITATIVE CO
POWER
ARRAY/BATTERY RAW BUS
CD
DISABLE CAP
SEPARATION
C&S
32 PPS
CD
POWER AMPLIFIER NO. 1 ON/OFF
C&S
LAUNCH RADIO MODE *
CD
EXCITER NO. 1 ON/OFF
MODULATED SUB-CARRIER
EXCITER #1
POWER AMP #1
3 WATTS
POWER MONITOR
DIPLEXER #1
TRANSFER SWITCH #2
COMMAND
COMMAND OUT
RECEIVER #1
REC GROUND SIGNALS
CD
RANGING ON/OFF
RECEIVER NO. 1 ON/OFF
EXCITER NO. 2 ON/OFF
POWER MONITOR
3 DB ATTEN
HYBRID COUPLER (3 DB)
DUMMY LOAD
EXCITER #2
POWER MONITOR
HYBRID COUPLER (3 DB)
50 WATTS
POWER AMP #2
DIPLEXER #2
TRANSFER SWITCH #1
C&S
CRUISE RADIO MODE *
COMMAND
COMMAND OUT
RECEIVER #2
REC GROUND SIGNALS
CD
RECEIVER NO. 2 ON/OFF
CD
EXCITER NO. 3 ON/OFF
EXCITER #3
POWER MONITOR
50 WATTS
C&S
MANEUVER RADIO MODE *
3 DB ATTEN
POWER AMP #3
DIPLEXER #3
COMMAND
COMMAND OUT
RECEIVER #3
REC GROUND SIGNALS
CD
RECEIVER NO. 3 ON/OFF
RADIO
PROPULSION
He
He
FROM PYRO
PRESSURIZE/DEPRESSURIZE MC/OA PROP. 1
PRESSURIZE/DEPRESSURIZE MC/OA PROP. 2
PRESSURIZE/DEPRESSURIZE MC/OA PROP. 3
NORMALLY OPEN VALVES
NORMALLY CLOSED VALVES
PROPELLANT
ENABLE/DISABLE PROP. FLOW 3
ENABLE/DISABLE PROP. FLOW 2
ENABLE/DISABLE PROP. FLOW 1
QUADREDUNDANT SOLENOID VALVES
C&S
OPEN/CLOSE QUAD. SOLENOID VALVES *
CD
OPEN/CLOSE 1 & 3 SOLENOID VALVES
CD
OPEN/CLOSE 2 & 4 SOLENOID VALVES
AUTOPILOT
VANE CONTROL SIGNALS
POSITION FEEDBACK SIGNALS
MIDCOURSE MONOPROPELLANT ENGINE
IGNITER
CHAMBER WITH PROPELLANT
INHIBIT RETRO ENGIN
REARM S/A DEVICE
START ENGINE BUR
CLOSE INJECTORS
TVC POWER
N2 PRESSURATION
TVC CONTROL SIGNAL
POSITION FEEDBACK
ORBIT INSERTION SOLID ENGINE

	Bay No.
Frame Ground Net & SGP	12
Low Level Signal CGN	9
Radio CGN & SGP	12
Raw Power CGN & SGP	1
Distributed Power CGN & SGP	1
Pyrotechnic CGN & SGP	16
Science Subsystem CGN & SGP	6

5.3.4 Relays Versus Solid-State Switching. Solid-state circuitry is preferred for all power and signal switching unless there is not sufficient life and reliability history for the designer to have confidence in solid-state switching for a particular application.

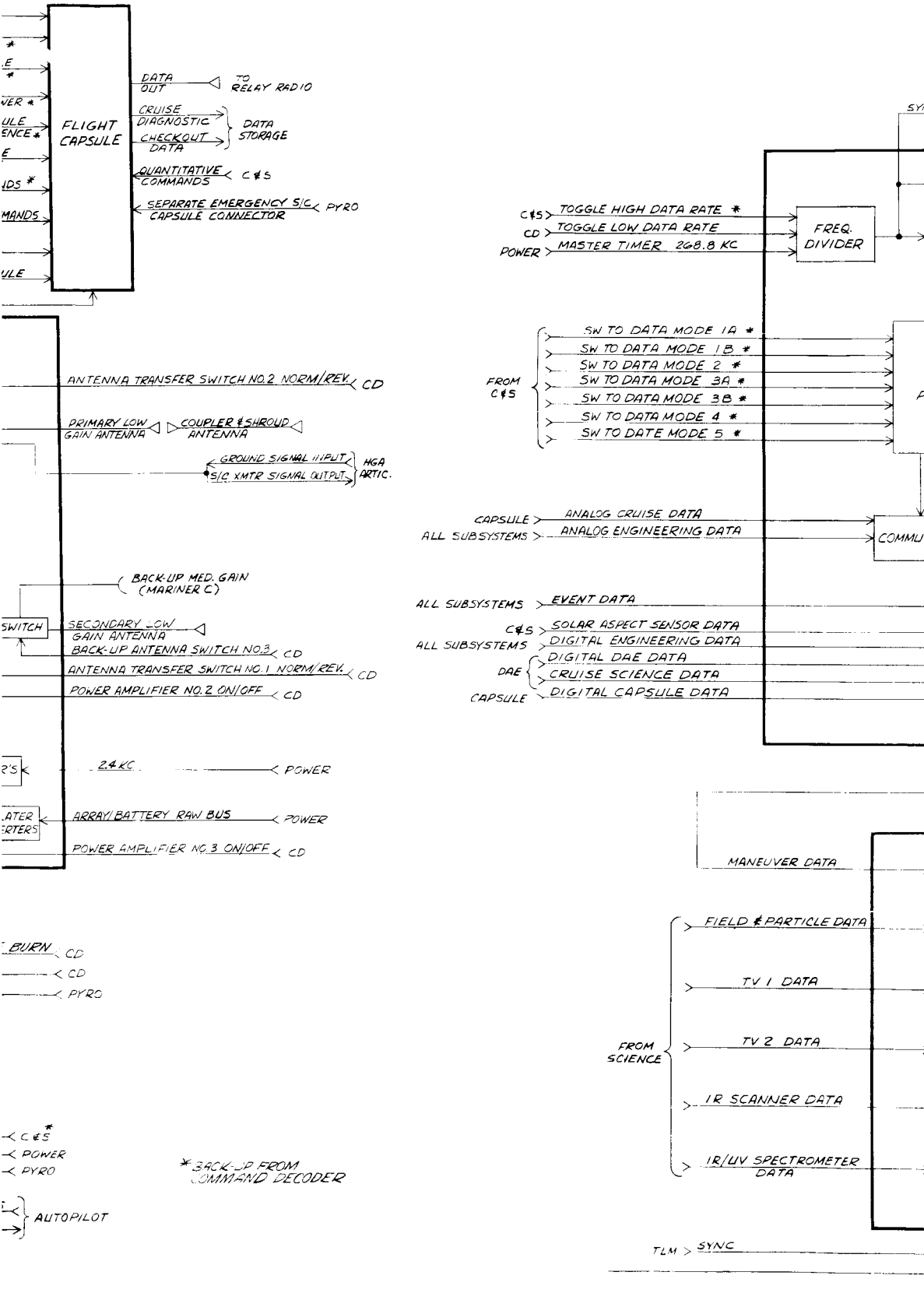
Other examples of circuit applications which may require relays are:

a. High-current switching.
b. Complex switching which requires multiple simultaneous contacts.
c. Where extreme circuit-isolation requirements exist.
d. Where it is easier to use a relay to meet the non-volatile toggle function requirements in case of a momentary loss of power during an inverter switchover.

5.3.5 Conventional Versus Flat Harness. It is planned to use the standard-wire conventional system harness instead of a flat-ribbon-type cable. However, the latter will be further investigated during Phase IB and will be given consideration for a system harness, at least in areas where it can be implemented easily, if there appears to be enough weight-saving and if the state-of-the-art for flat cables and connectors has advanced sufficiently.

5.3.6 Electromagnetic Interference. The design of all spacecraft electronic equipments shall be compatible with the electrical transients and the electromagnetic environment estimated in the VOYAGER Environmental Predictions Document. The electromagnetic radiation generated by any of the spacecraft equipments shall be such that it does not interfere with any other spacecraft equipment. All subsystem and system interface designs shall permit normal operation of interface circuits in the presence of the specified electromagnetic environment with a 6-db minimum performance margin.

6.0 TELECOMMUNICATIONS. The Telecommunications subsystem shall provide telemetry, command and tracking functions compatible with the DSIF stations. Telemetry shall be provided for engineering data to support the operation of the vehicle, to provide diagnostic information and to transmit interplanetary science data throughout the entire mission. Capsule data (about 1 bps) must be transmitted during cruise (100 bps during capsule checkout) and the data stored during capsule orbital descent to impact must be relayed after capsule impact. A data rate capability of 116-1/3 bps is provided during launch and acquisition by a 3-watt transmitter on a fixed primary low-gain antenna coupled to a parasitic antenna on the Launch Vehicle shroud. Real-time interplanetary science data must be transmitted after acquisition at an average rate of at least 29 bps (the design goal of 58 bps is provided) and are time-division-multiplexed with the engineering data. During maneuvers, the data are stored for subsequent transmission. Selected engineering data are transmitted throughout the


FLIGHT CAPSULE
DATA OUT
TO RELAY RADIO
CRUISE DIAGNOSTIC CHECKOUT DATA
DATA STORAGE
QUANTITATIVE COMMANDS
C&S
SEPARATE EMERGENCY S/C CAPSULE CONNECTOR
PYRO
C&S
CD
POWER
TOGGLE HIGH DATA RATE *
TOGGLE LOW DATA RATE
MASTER TIMER 268.8 KC
FREQ. DIVIDER
FROM C&S
SW TO DATA MODE 1A *
SW TO DATA MODE 1B *
SW TO DATA MODE 2 *
SW TO DATA MODE 3A *
SW TO DATA MODE 3B *
SW TO DATA MODE 4 *
SW TO DATE MODE 5 *
ANTENNA TRANSFER SWITCH NO.2 NORM/REV.
CD
PRIMARY LOW GAIN ANTENNA
COUPLER & SHROUD ANTENNA
GROUND SIGNAL INPUT
S/C XMTR SIGNAL OUTPUT
HGA ARTIC.
CAPSULE
ALL SUBSYSTEMS
ANALOG CRUISE DATA
ANALOG ENGINEERING DATA
BACK-UP MED. GAIN (MARINER C)
SWITCH
SECONDARY LOW GAIN ANTENNA
BACK-UP ANTENNA SWITCH NO.3
CD
ANTENNA TRANSFER SWITCH NO.1 NORM/REV.
CD
POWER AMPLIFIER NO.2 ON/OFF
CD
ALL SUBSYSTEMS
EVENT DATA
C&S
SOLAR ASPECT SENSOR DATA
ALL SUBSYSTEMS
DIGITAL ENGINEERING DATA
DAE
DIGITAL DAE DATA
CRUISE SCIENCE DATA
CAPSULE
DIGITAL CAPSULE DATA
2.4 KC
POWER
ARRAY/BATTERY RAW BUS
POWER
POWER AMPLIFIER NO.3 ON/OFF
CD
MANEUVER DATA
BURN
CD
CD
PYRO
FIELD & PARTICLE DATA
TV 1 DATA
FROM SCIENCE
TV 2 DATA
IR SCANNER DATA
IR/UV SPECTROMETER DATA
C&S *
POWER
PYRO
* BACK-UP FROM COMMAND DECODER
AUTOPILOT
TLM
SYNC

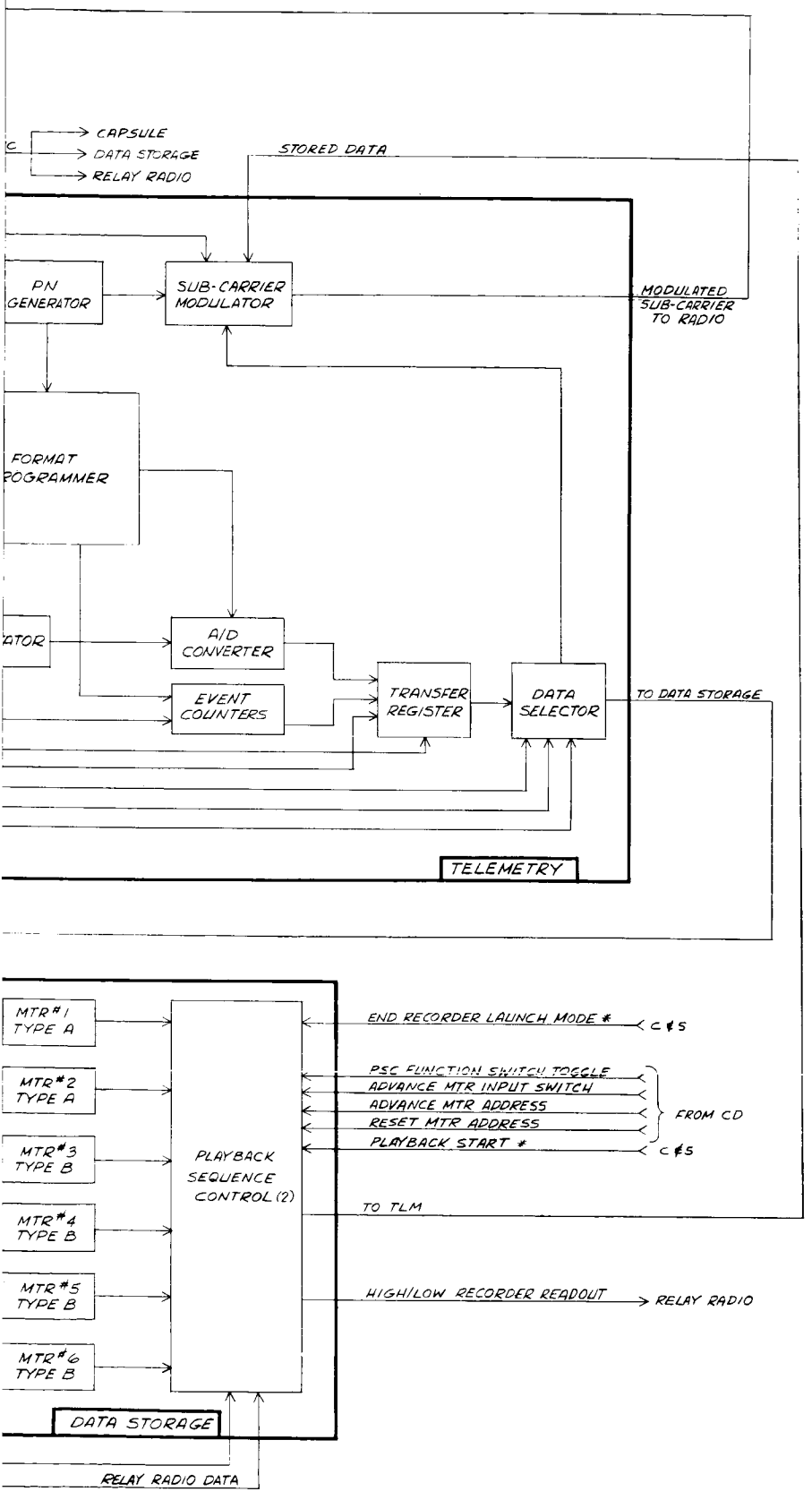


Figure 5-1. VOYAGER Functional Block Diagram (Sheet 2 of 2)

maneuver at 7-7/24 bps by a 50-watt transmitter and a secondary low-gain antenna. After acquisition, transmission is via a second 50-watt transmitter and a steerable 7-1/2 foot parabolic reflector antenna. Any of the three transmitters may drive this high-gain antenna, which also transmits the planet-scan science data which is required to exceed an average rate of 580 bps at the end of the six-month orbital mission. Data rates of 14933-1/3, 7566-2/3 and 3733-1/3 bps are provided for transmitting this science data on a subcarrier separate from that used for engineering-data transmission. The rate of 3733-1/3 bps may be maintained throughout the mission. As a backup to the steerable antenna, a non-deployed, fixed medium-gain antenna yields a high data-rate capability near encounter: 7466-2/3 bps may be maintained for 20 days after encounter, for a typical 1971 encounter, 933-1/3 bps for 120 days.

Data storage by four magnetic tape recorders is provided for the planet-scan science data. A total capacity of 5×10^7 bits is required; a capability of 6×10^8 bits is provided including two additional recorders which are used to store maneuver data and interplanetary science data. Each recorder has 10^8 bits capacity, and can play back at all the high data rates. The planet-scan science recorders accept data at rates up to 50,000 bps. The maneuver recorder accepts a rate of 116-2/3 normally, and the interchangeable interplanetary science recorder accepts up to 15,000 bps during solar flares, or 58 bps during normal orbital operations. During orbital operations, the recorders are readout in cascade at the high rates.

Both the telemetry and the command links employ PSK subcarriers which phase-modulate the carrier. Phase-lock techniques are used to demodulate the carrier and the subcarriers, and the data is matched-filter detected for efficient use of power. PN synchronization is used; each telemetry subcarrier uses the JPL single-channel system; command uses the two-channel system.

Command must be provided through low-gain antennas from launch through end of mission. Command rates of 1/2 and 15 information bits per second are provided. Frequency-addressable receivers are connected to each of the two low-gain antennas; another receiver on a third frequency is connected to the high-gain antenna. Redundant 1/2-bps detectors are connected to the two receivers on the low-gain antennas, while the 15-bps detector may be connected by command to any receiver. Two decoders, which are selected by two bits in the command, are normally connected in series so that a false output from either will not cause a false command. In the event of failure of one decoder, it may be bypassed. The command system provides up to 246 discrete and quantitative commands. The probability of no response of the command system at threshold meets its specification of less than 10^{-4}. Similarly, the bit-error-rate is less than 10^{-5}, and the probability of a false command is less than 10^{-8}.

Both range-rate tracking and turn-around ranging are required. The three command receivers and telemetry exciters in the form of a modified Mark I transponder may all be used for tracking.

A 400-mc antenna is required to support the capsule relay link. A turnstile-above-ground plane with a peak gain of 5-db and a 3-db beamwidth of 90 degrees is used. This antenna is not deployed and is fixed to the Spacecraft so that it views the capsule during de-orbit and

entry and atmospheric descent to impact. A gain margin in excess of 4 db above the specified minimum gain is achieved at impact for the range-of-view angles resulting from descent through atmospheres with surface pressures ranging from 5 to 10 millibars.

7.0 COMPUTER AND SEQUENCER. The Computer and Sequencer (C&S) is a cycled, special-purpose, digital computer, which generates and distributes the necessary on-board commands to make the VOYAGER Spacecraft automatic. Except for permission to separate the capsule, the C&S obviates the need for any ground command provided that (a) the flight is nominal (all systems are functioning as expected), and (b) trajectory corrections, trajectory bias, instrument calibration and updating of time-dependent or trajectory-dependent sequences are not required.

7.1 Sequenced Functions. The entire nominal flight sequence is pad-loaded into the C&S by the Launch Complex Equipment (LCE). The nominal flight sequence includes all of the events in the initial stabilization, cruise, orbit injection, capsule separation, orbit and occulation modes. The sequencing of these events is carried out automatically by the C&S. All elements of contingency modes which can be identified prior to launch are pad-loaded into the C&S by the LCE. Contingency modes include trajectory-adjust, orbit-adjust and back-up modes. In the event the flight is not nominal, the Command Subsystem is used to modify the sequences stored in the C&S. In the event that contingency modes are required, the command subsystem is used to load the missing elements of the required sequence into the C&S. Thereafter, the sequencing of the contingency mode is carried out automatically by the C&S. Certain events controlled by the C&S are based on functions other than time. Some examples are given in the following sections.

7.2 Planetary-Science Sequencing and Canopus-Occultation Sequencing. The sequencing of these events is based on the argument of the Spacecraft. It is assumed here that the Planetary Scan Platform (PSP) is articulated in a manner described in Task A. In that arrangement, the outboard gimbal of the science package rotates the package about the normal to the orbit plane. The gimbal angle of the outboard gimbal is equivalent to the argument of the Spacecraft referenced to the morning terminator. A measure of this gimbal angle is provided to the C&S by the PSP. The sequencing of the planetary science and Canopus occultation is based on discrete values of this angle.

7.3 Limb Sensing. Limb sensing is also based on the output of the outboard PSP gimbal. It is assumed here that this gimbal is controlled by means of a horizon sensor. This horizon sensor can be made to provide an indication of the planet half-angle. The PSP provides this angle to the C&S. When the outboard gimbal angle of the PSP is equal to the planet half-angle, the Spacecraft is at the morning limb. When the complement of the outboard gimbal angle is equal to the planet half-angle, the Spacecraft is at the evening limb. Indications of these limb passages are generated by the C&S and provided to the PSP.

7.4 Maneuver Attitude Verification. The C&S subsystem includes a 4π steradian digital Sun sensor which is used to track maneuver turns. The output of this sensor is telemetered to the ground where it is used to confirm maneuver attitude. Certain events in the Mission are highly repetitive. The control of the high-gain-antenna orientation is an example. Another example might be the control of one or more gimbals in the Planetary Scan platform.

7.5 Antenna Control. The antenna gimbals are corrected 0.25 degree when the accumulated error reaches 0.125 degree. The program for controlling these angles is stored in the C&S. The gimbal-angle time history is approximated by means of connected straight-line segments. The error in the approximation is less than 0.25 degree. The time between 0.25-degree changes in gimbal angle, appropriate to each line, is stored in the C&S. The C&S increments the gimbal angle at the rate appropriate for the current line segment. This rate is changed when a new line segment is encountered.

7.6 Critical Event. Certain C&S controlled events are highly critical to mission success. Among these are maneuver turns, start solid engine, start and stop monopropellant engine, separate capsule. For these events, neither false commands (command at the wrong time) nor false dismissals (no command at the right time) can be tolerated. The C&S control of these events is organized so that the number of piece parts involved in controlling each individual event is minimized and no single piece-part failure can cause either a false command or a false dismissal.

7.7 Semi-Critical Events. The remaining events that are controlled by the C&S have a lesser degree of criticality. If such an event were to be falsely dismissed, there is sufficient time in the sequence to back-up the C&S with the command subsystem. Therefore, for the remaining events controlled by the C&S, the C&S is organized so that no single piece-part failure shall cause false commands.

7.8 Power Interruption. The implementation of the C&S is such that a temporary interruption of power will not cause a catastrophic loss of memory. The transformer-rectifier in the C&S is designed to maintain its output voltage for a sufficient period of time to complete a cycle in the C&S. Between cycles the state of all critical functions is maintained in non-volatile devices. Thus, the consequence of a temporary power outage is that spacecraft time is interrupted for the duration of the outage.

7.9 Flexibility. The C&S is designed to incorporate approximately 20% excess capacity over and above that required to carry out the currently defined mission. This excess capacity is in the form of 20% excess memory as well as 20% excess capacity in output functions.

7.10. Test. The design of the C&S is such that the entire mission sequence can be cycled out in four hours or less. This feature is included to facilitate C&S checkout and systems cycling.

8.0 POWER. Raw power for the Spacecraft and the capsule is provided by a solar array during periods of full or partial solar illumination and by batteries during periods of solar array disorientation or peak power periods in excess of array capability.

The solar array consists of 15 panels which provide an effective solar cell area of 181 square feet capable of supplying 650 watts at the end of the mission. The panels are arranged to form an annular ring about the Spacecraft. Each panel contains four strings of 2 cm x 2 cm N/P silicon solar cells; each string is arranged in a matrix of six cells in parallel by 123 cells in series. Each string is diode-isolated by a zener diode monoblock which limits upper array voltage to 62 volts.

Three batteries provide a total capacity of 3240 watt-hours. Two of the batteries are of the silver-cadmium type rated at 20 ampere-hours each; the third battery is a silver-zinc type rated at 50 ampere-hours. This combination has been selected because the mission needs are characterized by a few, but deep battery discharges, for which the silver-zinc battery is adequate, up to the time of capsule separation; and thereafter, by many, but shallow discharges during Martian solar occultations. The installed capacity permits the full loss of any single battery. Each battery is charged through a separate regulator with options to remove charging or to adjust the charge voltage limit by command.

Power is distributed to the users as unregulated dc or in several forms of regulated ac. The characteristics of the available power from seven bus sources are as given in Table 8-1.

TABLE 8-1. CHARACTERISTICS OF AVAILABLE POWER

Bus	Voltage	Frequency	Regulation (%)		Max Peak Power (watts)	Max Average Power (watts)	Users	Notes
			Steady-State	Transient				
A	32-50 volts	DC	-	-	2000	10	Misc. low duty cycle loads	
B	32-62 volts	DC	-	-	2000	350	Radio, capsule	Capsule receives 200 ω during solar illumination periods only.
C	50 volts RMS	2.4 KC, 1 φ, square wave *	±2	±5	450	300	All other	
D	50 volts RMS	2.4 KC, 1 φ, square wave*	±2	±5	C&D combined	C&D combined	Spacecraft loads	
E	26 volts RMS	400 cps, 3 φ, stepped square wave *	±5	±10	45	30	Gyros	
F	26 volts RMS	400 cps, 3 φ, stepped square wave *	±5	±10	45	30	Gyros	
G	28 volts RMS	400 cps, 1 φ square wave *	±5	±10	15	10	Science	
			*Frequency regulation- Normal: ±0.01% Backup oscillator: ±1% Free run: -4 to -6%					

All a-c buses are supplied from redundant sources with automatic switchover capability in the event of element failure. For the 2.4-kc power, which is the principal source of a-c power, redundant buses are provided, permitting the use of redundant transformer-rectifiers for critical loads.

Power-control switches are generally contained in the power subsystem for those cases where the switching signal is derived externally to the user subsystem. This permits switch elements to be concentrated in one location, permitting optimum design to minimize magnetic effects. Fault protection is provided for the capsule by combining an overcurrent sensor with the capsule power control switch. In other cases, similar protection (fuses) is used depending on load criticality, complexity and reliability.

The power subsystem has circuitry designed to prevent the possibility of a solar-array/battery-sharing mode of operation during times when the array is capable of supplying the total power. This is accomplished by comparing solar-array and battery voltages and accordingly withholding power from specific loads.

The central clock and synchronizer for the Spacecraft is contained in the power subsystem. It provides a 268.8-kc signal to the telemetry subsystem, 2.4-kc and 400-cps signals to the power-system inverters, and a 32-cps signal to the C&S subsystem. Frequency accuracy of one part in a million provides the time base required. An oscillator with ±1% frequency accuracy is provided as a backup. Further backup is available from the free-run capability of the 2.4-kc inverters.

9.0 GUIDANCE AND CONTROL

9.1 Constraints. The Guidance and Control Subsystem shall provide the capability for three-axis control of the Spacecraft to an accuracy of 12 mrad per axis during interplanetary and orbit cruise. The nominal angular rate while in inertial control or locked on to the celestial references shall be 0.007 mrad/sec. The Spacecraft must be capable of being pointed in any arbitrary inertial orientation during capsule separation or trajectory correction maneuvers, and held to less than 2.5 degrees accuracy. The cg offset from the vehicle axis may be 0.5 inch at the end of the orbit-injection engine burn. The velocity uncertainty of propulsion firings shall be less than one percent.

The attitude-control gas supply shall be sufficient for the complete mission even if one solenoid valve should stick in the open position or any other single leakage source should occur. The control system will cause the Spacecraft automatically to reaquire the celestial references if they are lost during the cruise or orbit phases.

9.2 Characteristics. The Guidance and Control Subsystem provides the capability for the following:

a. Automatically acquiring and stabilizing the Spacecraft to the celestial references, Sun and Canopus.

b. Orienting the Spacecraft to a predetermined attitude for trajectory corrections, capsule separation, and areocentric orbit injection.

The following subsystems are provided to fulfill the above functions:

a. Attitude Control
b. Autopilot

9.2.1 Attitude Control Subsystem. Since the attitude-control function is similar to that required for Mariner C, the VOYAGER Attitude Control subsystem is similar to that of the Mariner C, the differences being primarily in redundancy and choice of components for improved or more accurate performance. Provision is also made for maintaining inertial control of only the pitch and yaw axes during Sun occultations, and of the roll axis only, during Canopus occultation.

Attitude during cruise is three-axis stabilized by the processing of signals from the fine Sun sensors and the Canopus sensor, and the turning of the Spacecraft by a dual cold-gas expulsion system. The attitude is maintained to an accuracy of 0.69 degree maximum with respect to each spacecraft axis. The Spacecraft can be stabilized to the Sun in less than 20 minutes and to Canopus in less than 70 minutes; stabilization to the Sun is required before Canopus acquisition can be initiated. Reacquisition of the references and normal spacecraft attitude is automatic whenever the Spacecraft is in normal control.

For maneuvers, the orientation of the Spacecraft is obtained by placing the Attitude Control in the inertial-control mode and torquing the gyros at a fixed rate for a pre-determined time.

The cold-gas expulsion system reacts to the artificial error signal, causing the Spacecraft to turn. The turn rate provided is +3.14 mrad/sec/sec with the addition of two minutes between each turn for settling. The pointing error, including autopilot error, is less than 2.5 degrees for a nominal trajectory correction for capsule separation and for orbit injection. By using temperature-controlled gyros, the three-sigma gyro drift is held to less than 0.25 degree per hour.

For magnetometer calibration and Canopus acquisition, the Spacecraft is made to roll at fixed rates by providing constant artificial rate errors to the attitude-control logic. Observation of a star of proper magnitude removes the error signal during Canopus acquisition.

9.2.2 Autopilot Subsystem. The Autopilot maintains the attitude of the Spacecraft to ± 2.5 degrees (3 σ) during propulsion operation. This error includes those accumulated during turns made to achieve the desired direction. By utilizing velocimeters, the error of velocity changes during trajectory corrections is maintained to less than 1.0% (3 σ) for all velocity increments above 0.2 mrad/sec.

During midcourse-trajectory and orbit-adjust maneuvers, which are performed with four monopropellant engines, the Autopilot controls the vehicle attitude by positioning jet vanes in the engine exhaust, thus obtaining thrust vectoring. During the retro-maneuver, which is achieved with a solid rocket engine, the Autopilot controls the spacecraft pitch and yaw axes by controlling the flow of a secondary injection system, again providing thrust vectoring.

Roll-control during retro-thrusting is achieved by the cold-gas jet system.

The Autopilot subsystem employs the body-mounted rate-integrating gyros for position sensing, and processes this information by means of appropriate amplifiers and compensating networks.

10.0 PROPULSION SUBSYSTEM. The GE-MSD preferred Propulsion subsystem design consists of a monopropellant hydrazine system to perform the Midcourse and Orbit-Adjust (MC/OA) functions, and a solid-propellant rocket system to perform the retro (orbit-insertion) function. The MC/OA system utilizes the Shell-405 spontaneous catalyst to decompose the hydrazine. The retro-system design is based on a modification of the Minuteman Stage-II, Wing-VI configuration.

The Planetary-Vehicle propulsion subsystem weight for the 1971/73 opportunities is calculated as 11,691 pounds (9513 pounds for retro and 2178 pounds for MC/OA).

10.1 Midcourse and Orbit-Adjust Subsystem. The basic design specifications for the MC/OA subsystem are:

a. Impact a total midcourse velocity change of 200 mps in several starts to the Planetary Vehicle.

b. The accuracy of the midcourse changes shall be 1.0 ± 0.07 mps with a desired accuracy of 0.1 ± 0.007 mps.

c. Impart a total orbit-adjust velocity change of 100 mps in several starts to the Planetary Vehicle.

The system is helium-gas pressure-regulated to supply monopropellant hydrazine to the four fixed-thrust decomposers. The pressurant is stored at 3600 psia in two spherical tanks manifolded together and isolated from the downstream section of the system by a set of squib-actuated valves. These valves provide isolation during launch and long coast periods. A regulator reduces gas pressure from storage to tank pressure. Redundancy is provided for this function by a parallel standby regulator that is automatically switched into the circuit if the primary regulator fails in the over-pressure mode.

The propellant is stored in four spherical-ended, cylindrical tanks which are manifolded to a single feed line. Each tank contains a butyl-rubber bladder and standpipe for positive propellant acquisition and slosh control. As with the pressurant, the propellant is isolated from the downstream sections by a set of squib-actuated valves, which provide positive sealing during launch and long coast periods.

Each of the four thrust chamber assemblies mounted parallel to the roll axis, 90 degrees apart, consists of a cavitating venturi, a quad-redundant solenoid valve and a decomposer. The venturi maintains propellant flow-rate constant regardless of dynamic changes downstream. By this method, assurance is gained in the repeatability and uniformity of the start transient and the maintenance of full-flow (constant thrust), should there be a change in the pressure drop downstream of the venturi. Quad-redundant solenoid valves are used to start and stop decomposer operation. This type of valve provides redundancy in the opening and closing operations. The decomposer holds the Shell-405 catalyst which spontaneously decomposes the liquid hydrazine to gases at 150 psia and 1800°F. In the 100:1 area-ratio nozzle, the gases are expanded to produce 100 pounds of thrust under vacuum conditions. Jet vanes, similar to those used on Ranger and Mariner, mounted at the nozzle-exit plane, divert the gas flow, as required, to provide torques about the pitch, yaw and roll axes.

At a significant gain in reliability, pair-out capability has been designed into the decomposers. Under this concept it is possible to sense a malfunction in any one of the decomposers, and terminate its operation and that of the opposite unit without loss of MC/OA capability.

Pressure and temperature sensors and position indicators are provided to monitor system condition and operation via telemetry. Fill, drain, vent and test ports are also provided for ground checkout and test.

10.2 Retropropulsion Subsystem. The VOYAGER orbit-injection maneuver will be performed by a solid-propellant Retropropulsion subsystem. The selected subsystem is a modified Stage II, Wing-VI Minuteman motor, which meets all the mission requirements. Major components include a carboxy-terminated polybutadiene propellant (88% solids with 15% aluminum); a finocyl-grain configuration; a 6V-4A1 titanium-alloy case; a silica-loaded nitrila-rubber internal insulation; a single semi-submerged contoured nozzle with a non-eroding tungsten throat insert and ablative plastic liner; a liquid secondary injection-thrust vector-control system using Freon-114B2 injectant and a gaseous nitrogen pressurant; and a propellant igniter with a safety-and-arming device.

The primary modifications to the existing Minuteman motor that are required include shortening the cylindrical case section from 88.63 to 45 inches, decreasing the propellant burning rate from 0.33 to 0.25 inch per second at 500 psi while increasing the burn time to 90 seconds, decreasing the nozzle throat diameter from 9.63 to 6.78 inches, increasing the nozzle expansion ratio to 70:1, replacing the thrust-vector control hot-gas pressurizing system with cold-gas pressurization, modifying the Freon tank, and providing new igniter squibs.

The Retropropulsion subsystem is 52 inches in diameter and approximately 138.4 inches long, with a total weight of 9513 pounds. It has an effective mass fraction of 0.89, a deliverable effective specific impulse of 292.1 seconds, and imparts a velocity increment of 2.2 km/sec. The velocity increment variability is ±0.34% and the maximum acceleration imparted to the Spacecraft is 2.73g.

11.0 THERMAL CONTROL. Temperature control of the Spacecraft Bus is attained by regulating the quantity of rejected heat from an insulated structure. The regulated heat rejection is accomplished by means of an active control-louver system. All electronic components, propellant and gas tankage, plumbing and structure are thermally integrated within the super-insulation blanket which encloses the structure. Thermal coupling is achieved by promoting radiant interchange as well as conduction heat transfer among all equipments within the bus. To this end, high-emittance surfaces are provided wherever possible for all equipments, and an open structure is maintained between equipment bays and the propellant/gas tankage. In addition, electronic assemblies are packaged and mounted with minimum thermal resistance to the heat-rejection radiator plates. Louver assemblies of two different areas are provided for 14 of the equipment bays. The two areas are required to handle the variation in dissipated heat among the equipments. A single bay, the high-power (TWT) radio-equipment bay, is passively controlled.

Equipments on the outside of the bus structure are thermally controlled by the use of thermal coatings and/or by means of electrical heating. Wherever applicable, the external equipments are conductively tied to the bus structure in order to maintain their operating temperatures within required limits. With some components, such as the Sun Sensors and the cold-gas nozzle/solenoid assemblies, packaging and/or mounting of the equipments takes into consideration the requirement for sufficient thermal mass so that required operating temperatures can be maintained during transient periods of solar shade or eclipse.

The Spacecraft is designed to maintain all component parts within acceptable temperature limits throughout the Mission life-span. The normal operating temperature limits for all bus equipments is 45°F to 90°F. The upper temperature limit may be exceeded somewhat during maneuvers. However, in no case is the maximum operating temperature considered detrimental to equipment performance.

12.0 PYROTECHNICS. The Pyrotechnic subsystem performs such Planetary Vehicle functions as vehicle separation, control of the Propulsion subsystem, emergency separation of the Flight Capsule, initiation of retropropulsion, deployment of booms, antennas and science instrument cover removal. Power to the Pyrotechnic subsystem is blocked by the normally-open contacts of the separation switch. Upon vehicle separation, power is applied to the pyrotechnic controller, which is ready to fire when commanded by the C&S or CD. Completely

redundant firing channels and circuitry are provided in the controller and to each Electro-explosive Device (EED). Each EED contains two bridgewires and will not fire if one amp/one watt is applied to each bridge simultaneously. Each EED is also capable of withstanding a static discharge of 26 kv from a 500-picofarad capacitor applied between pins or between pins and case at all atmospheric pressures. All design requirements are met by the EED firing circuits. The EED's used to initiate retropropulsion have pigtail leads in order to integrate them into the Minuteman safe/arm device with a minimum amount of redevelopment. Redundant devices are used throughout the subsystem except for pin-pullers which utilize two squibs per pin-puller.

13.0 CABLING DESIGN. The VOYAGER Spacecraft system harness consists of rings of cables in two major groupings above and below the electronic bays. In each ring-assembly individual cables interconnect the electronic bays on a functional/point-to-point basis, and separate cables break out of the rings to interconnect the electronic bays to the associated peripheral equipments, solar arrays, sensors, propulsion, guidance, pyro devices and in-flight disconnects. A stiffened-ring harness tray supports the upper cables. The lower cables are attached to existing spacecraft structure for support. Removable outside covers above and below the bays allow access for mating/demating of connectors, attachment of OSE and system test cables, and provide limited capability for rework of the harness in the assembled equipment module.

14.0 DESIGN STANDARDS

14.1 Standard Circuits. Electronic circuit-design standards[1] will be generated by Product Engineering early in the program for use in the design of all spacecraft electronic circuits. These standards will establish circuit design Procedures for circuit synthesis, worst-case and error analyses, testing specifications and documentation. The documentation provides a method for recording the design evolution and analysis for future reference and will be the primary item analytically audited in the technical review of the design.

The use of standard electronic circuits will receive strong consideration in the implementation of spacecraft electronic functions. The standard circuits will be chosen and the necessary work performed in order to specify and detail their characteristics for spacecraft use. Previously used and proven circuits and microcircuits will be given first consideration.

14.2 Packaging. The packages which house the electronic equipment form an integral part of the spacecraft structure, in the 16 trapezoidal bays of the Equipment Module. To facilitate thermal and cg balancing, cabling optimization and functional association of components, the assemblies and subassemblies are of standard size and shape. Any assembly may be located in any equipment bay, and subassemblies are interchangeable within any assembly.

The packaging standards also control parts, materials and methods of assembly. This approach minimizes the number of materials, processes and techniques used in order to eliminate sources of unreliability and allow sharper focus on packaging problems.

---

(1) For a more complete description see the VOYAGER Reliability Program Plan, Phase IB Proposal, Electronic Circuit Standards.

Three standard packaging options will be allowed: low-power, high-power, and microelectronic. In addition, a general Design Constraints Standard will be prepared to control packaging of parts which do not lend themselves to one of the other options. Included in this latter category are r-f components, electromechanical devices and parts having other special geometry requirements.

15.0 ENVIRONMENTAL CONSTRAINTS. The Planetary Vehicles shall be designed to survive and operate as appropriate in the induced and natural environments specified in the VOYAGER Environmental Predictions Document dated 18 October and amended 12 November 1965.

15.1 Magnetic. A special environmental constraint exists as a result of the maximum permissible magnetic field of less than one gamma at the science magnetometer sensor under all normal operating conditions for a demagnetized Spacecraft, and less than 10 gamma after a Planetary Vehicle has been exposed to a magnetic field of 25 oersteds.

The apportionment of magnetic cleanliness to the Planetary Vehicle subsystems will be monitored and controlled at the subassembly level by the GE Magnetic Analysis Computer Program. This program has the capability of operating at the component level, but will probably be used primarily at the subassembly or tray level for the approtionment. It considers the magnetic field of each tray, its location, effects of current loops, effects of perming and deperming, current variations, shielding and magnetic compensations. No single assembly shall contribute more than 20% of the total allowable field at the magnetometer sensor. The stability of the magnetic field at the magnetometer sensor shall be such that neither mode switching nor voltage-and-current changes over the full design range will change the field by more than 0.1 gamma.

15.2 Micrometeoroids. Based upon the micrometeoroid model in the VOYAGER Environmental Predictions Document and the Planetary Vehicle Configuration, Table 15-1 shows the expected number of impacts and their masses, sizes and momentum transfers. Momentum transfer between a hypervelocity meteoroid and a Planetary Vehicle is greater than mass times velocity because of the secondary spray of particles. At a velocity of 42 km/sec, the target momentum is about four times that of the incident particle. The Planetary Vehicle attitude-control subsystem shall be capable of responding to a momentum transfer on the longest moment arm of the vehicle.

TABLE 15-1. EXPECTED IMPACTS AND THEIR MASSES, SIZES, AND MOMENTUM TRANSFERS

Particle Mass M (gm)	Particle Diameter (mm)	No. of impacts of Particles of mass M and greater		Momentum Transfer to Vehicle/Impact, (kgm-m/sec)
		Max. Projected area*	Critical Projected area*	
10^{-6}	0.21	581.00	27.00	0.000168
10^{-5}	0.46	23.00	1.09	0.00168
10^{-4}	0.98	1.04	0.049	0.0168
10^{-3}	2.12	0.0483	0.00226	0.168
10^{-2}	4.57	0.00155	0.000071	1.680

*Maximum projected area includes solar array and high-gain antenna. The critical projected area includes only the electronics, thermal control panels and attitude control fuel tanks

Although surveys have shown that 99 percent of brighter sporadic earth meteors ($M > 10^{-2}$gm) are moving in direct orbits, at fainter magnitudes ($M \approx 10^{-5}$gm) the fraction of meteors having high inclinations becomes very pronounced. Therefore, using Earth-Mars-space meteoroid distributions, it must be recognized that the highly anisotropic meteoroid distributions are likely to exist only for meteoroids producing visual and photographic meteors ($M > 10^{-2}$gm). For fainter or less massive particles, the distribution must be considered to be isotropic from the design point of view.

16.0 RELIABILITY

16.1 Design Approach. The Spacecraft system has been designed consistent with the constraint that no single failure mode of an electronic or electrical part or component shall cause catastrophic loss of the mission. Furthermore, the design attempts to maximize mission success and partial success in the event of non-catastrophic failure.

Within the Computer and Sequencer, nine critical command registers (capsule-release, start-retropropulsion, start-and-stop MC/OA engines, Δ V register and maneuver commands) and the master-sequencer logic incorporate triple-majority logic guarding against both false command and false dismissal. Since both failure modes are considered equally catastrophic, the design makes them equally probable, but extremely remote. Other C&S functions, which can be recommanded via the command subsystem without catastrophe or severe degradation, have been protected against false commanding at the expense of false dismissal. These functions include the master-sequence matrix and memory, and the Planet Scan Platform and gimbal registers. Special attention has been directed towards tracing these critical commands from the C&S through the subsystems to their functional destination to assure that a consistent degree of protection exists everywhere along the way. All non-time-critical C&S commands are backed up via ground command through the command subsystem.

A feature of the four-engine MC/OA subsystem is the ability to perform without significant degradation on a single pair of engines. The failure of any single engine automatically shuts down the opposite one to limit disturbance torques to a value the system can handle.

The cold-gas portion of the Attitude Control subsystem is a completely redundant, cooperative load-sharing design. Two separate assemblies with tank, regulators, solenoids and jets operate in parallel, each assembly providing one-half the thrusting couple to change spacecraft attitude. Dual solenoids operating in series provide redundant protection against gas leakage. Any failure mode of one assembly (except catastrophic explosion of a cold-gas tank) can be compensated for by the other assembly without jeopardizing the ability to complete the mission due to insufficient total impulse remaining. The Attitude Control electronics is triply-redundant, with majority voting on the output to the pneumatic drivers.

Two Canopus sensors are provided, primarily for performance considerations; however, redundancy is thereby provided with degraded performance (relative to high-gain antenna pattern interference) in either late Martian orbital operations or sooner, depending on which sensor fails.

Two gyro packages are provided to assure availability of gyros for maneuver. The Gyro Control Unit controls the switching of power from either three-phase, 400-cps inverter in the power subsystem to either of the gyro packages according to the operational status of the equipment.

The main regulator and the 2400-cps inverters are provided in a redundant, load-sharing configuration. The present design requires dropping the malfunctioning unit(s) from the line; hence, internal switching logic backed up by ground command is provided. Each of the

2400-cps inverters supplies a separate bus to which the loads are connected according to their criticality. For example, some critical loads will be connected to both buses with redundant, load-sharing transformer-rectifier units.

Any two of the three battery-and-associated-charger combinations can fulfill anticipated power requirements while the Spacecraft is off the Sun; the third battery and charger provides redundancy and reduced depth of discharge under normal conditions.

The pyrotechnic subsystem features dual banks (transformer-rectifier + capacitor + SCR switch) each firing one of the redundant pair of bridgewires in each electro-explosive device. Extra protection against false initiation and false dismissal will be afforded to the critical pyro subsystem functions (e.g., initiating retro engine burn).

Redundancy within the telecommunications subsystem is primarily achieved by switching in standby units via ground command. In the Telemetry section, there are redundant power supplies and data paths. The commutator and signal conditioners are connected to telemetry points in a redundant manner. The data-storage recorders are in quad-redundancy for the science data with the capability of time-sharing to receive all data at a reduced rate. High rate down-link transmission is provided by switchable power amplifiers, antennas and exciters. Transmission using the medium-gain antenna (933-1/3 bps) is considered a degraded mode. For up-link command and ranging there are three receivers which are always turned on, each connected to its own antenna. Command-signal detection and decoding in the command section is redundant through three command detectors, program controllers and a redundant power supply which are always on.

In case of severe capsule malfunction, an alternate mission option is available through exercising the emergency capsule separation joint and continuing the mission with the Spacecraft and its experiments alone. Additional details concerning alternate path and redundancy applications have been included in the individual subsystem discussions.

16.2 Apportionment. Numerical reliability design goals for each subsystem were apportioned at the beginning of this study using the scheme described in the Task A study report (VB110VP010), with modification of the complexity and criticality factors according to information gained during Task A. These goals were used by the subsystem design groups, guiding their effort in selecting applications of redundancy and/or alternate paths where adequate reliability could not be achieved through design simplification.

Three basic constraining points were selected around which was built the apportionment: the probability of injecting two Planetary Vehicles into acceptable planetary trajectories was fixed at 0.90; the obtaining of data from at least one spacecraft science payload for one month in orbit was fixed at approximately 0.80; and Launch Vehicle reliability was assumed to be 0.95. The resulting subsystem reliability goals are shown in Table 16-1 for a single spacecraft system. Based on these numbers, the model shown in Table 16-2 corresponds to the functional segments of the mission defined in VOYAGER 1971, "Preliminary Mission Description," October 15, 1965.

TABLE 16-1. PROBABILITY OF SUCCESS ALLOCATIONS

Mission Phase	A	B	C	D	E
Subsystem Time Duration	2 hr	185 days	15 days	3 hrs	30 days
Radio	Spacecraft Design Goal = 0.9737 for Powered Flight Phase. Extreme Envir. Contributes Equivalent Risk of 7 days Orbital Operations (Acceleration Factor of Approx. 850 During Burn)	0.9722	0.9977	0.9996	0.9954
Command		0.9681	0.9974	0.9996	0.9947
DH&S		0.9674	0.9973	0.9996	0.9946
C&S		0.9681	0.9974	0.9996	0.9947
Power		0.9715	0.9976	0.9996	0.9953
Thermal Control		0.9802	0.9984	0.9996	0.9967
G&C - Vehicle		0.9681	0.9965	0.9994	0.9945
G&C - Antenna		0.9908	0.9992	0.9999	0.9985
G&C - Autopilot		0.9857	0.9929	-	0.9962
Propulsion - MC		0.9863	0.9924	-	0.9960
Propulsion Retro		-	0.9944	-	-
Pyro Control		0.9847	0.9942	0.9986	0.9977
Vehicle Mechanisms		0.9886	0.9932		-
Planet Scan Package		-	0.9929	0.9998	0.9858
Single Spacecraft Reliability By Phase	0.9737	0.7594	0.9430	0.9953	0.9421

TABLE 16-2. CUMULATIVE PROBABILITIES OF SUCCESS

Mission Phase	Description	Cumulative Probability of Success		Apportioned System Reliability
		Both Systems	At Least One System	By Phase - Overall Model
A (2 hr)	Launch and injection of two Planetary Vehicles into acceptable interplanetary transfer trajectories.	0.90*	0.949	0.95 LV; 0.9737; 0.9737
B (185 days)	Separation, acquisition and cruise inclination trajectory correction maneuvers if required to achieve specified interplanetary transfer trajectory.	0.519	0.885	0.7594; 0.7594
C (15 days)	Placement of Planetary Vehicle into an acceptable Mars orbit, including performance of orbit correction maneuvers if required.	0.462	0.863	0.9430; 0.9430
D (3 hr)	Performance of Spacecraft/Capsule separation maneuver at preselected time and location.	0.458	0.861	0.9953; 0.9953
E (30 days)	Obtain data from at least one Spacecraft Science payload for a specified time of one month.	0.406	0.836 (approx. 80*)	0.9421; 0.9421 PV1 PV2

*Used as constraints in apportionment.

17.0 PLANETARY QUARANTINE

17.1 Approach to Planetary Quarantine. The Planetary Quarantine Mission Constraint states that the probability that Mars is contaminated prior to the calendar year 2021 as a result of any single launch shall be less than 10^{-4}.

To satisfy this imposing constraint two steps must be achieved:

a. Identification of every conceivable source of contamination to Mars.
b. Conception and implementation of a satisfactory solution to each case identified in a.

Table 17-1 presents the results of current studies aimed at identifying possible sources of contamination, and potential solutions to the problems associated with each source. These potential solutions have been grouped as follows:

a. 1st-Order Solution. Implementation of this category of solution would have a major adverse influence on the entire program from the standpoints of cost, schedule and reliability.

b. 2nd-Order Solution. Implementation of this category of solution involves significant tradeoffs in one or more areas.

c. 3rd-Order Solution. This category of solutions can be relatively easily implemented, the tradeoffs involved being not too significant.

If any given problem can be solved by a 2nd- or 3rd-order solution, then the use of a 1st-order solution will impose an unwarranted major program penalty. Similarly, choice of a 2nd-order solution will impose an unwarranted penalty if a 3rd-order solution is available. Finally, choice of a 3rd-order solution will impose a penalty if in reality no solution is required. Because of the severe program penalties associated with over solving any of the specific problems, the approach should be to: (a) assign, on the basis of preliminary analysis, a portion of the total 1×10^{-4} probability to each specific problem, as an upper limit, and (b) evaluate each specific problem in sufficient depth so that a conservative probability can be associated with it.

Results of this study will permit choosing the lowest order of solution necessary to assure meeting the planetary quarantine requirement without incurring the severe penalties associated with the choice of an over solution. As indicated in Table 17-1, there is a fairly wide range of mission and hardware solutions for many of the specific problems. Hence, after determining the magnitude of the problem for a given area, suitable tradeoffs can be performed to allow the selection of the optimum solution. Preliminary conclusions are:

a. Because of the large number of ways in which the capsule can become recontaminated, the biobarrier opening or separation should occur as late as possible in the sequence of events.

b. All separation mechanisms, unfold mechanisms and sensor covers should be designed to restrain loose ejecta.

c. The Attitude Control gas system will require at least some degree of decontamination (microbial load reduction), and quite possibly complete sterilization.

d. The OI subsystem and the MC/OA propulsion subsystems will possibly not have to be sterilized.

Each problem listed in Table 17-1 must be considered in a model used to establish an upper-limit goal for each specific problem area. The actual assignment of a portion of the total probability of 1×10^{-4} to each specific problem will be an iterative procedure which will be updated continually as better definition of the problem and the tradeoffs involved with weight, reliability, cost and schedule become available.

TABLE 17-1. CLASSIFICATION OF PLANETARY QUARANTINE PROBLEMS AND SOLUTIONS

Potential Problem		Potential Solution		
Category	Description	1st Order Solution (Major Adverse Influence On Program)	2nd Order Solution (Can Be Implemented, But Involves Significant Tradeoffs)	3rd Order Solution (Relatively Easy To Implement and Not Too Significant Tradeoffs Involved)
A. Spacecraft Impacts Mars	1. Due to failure at midcourse	1. Sterilize entire spacecraft	1. Approach philosophy	
	2. Due to failure at orbit insertion	2. Sterilize entire spacecraft	2. Trajectory selection	
	3. Due to failure at orbit adjust	3. Sterilize entire spacecraft	3. Orbit insertion and adjust philosophy	
	4. Due to orbit decay	4. Sterilize entire spacecraft	4. Orbit selection	
B. Separation Mechanism Ejecta Impacts Mars	5. S-IVB/planetary vehicle separation ejecta		5. Design to constrain loose ejecta	
	6. S-IVB aft shroud unfold operation ejecta		6. Design to constrain loose ejecta	
	7. Spacecraft/forward bio-barrier separation ejecta		7. Design to constrain loose ejecta	
	8. Spacecraft/capsule separation ejecta			8. Sterilize separation mechanism
	9. Capsule emergency separation ejecta		9. Design to constrain loose ejecta	9. Do not execute separation if lander and barrier could impact Mars
	10. Miscellaneous unfold and deployment operation ejecta		10. Design to constrain loose ejecta	
C. Launch Vehicle Impacts Mars	11. S-IC	11. No solution required		
	12. S-II	12. No solution required		
	13. S-IV B			13. Retro fire
D. Particles Impacting Mars	14. From orbit insertion motor	14. Sterilize orbit insertion system	14a. Orbit insertion philosophy 14b. Decontaminate OI system	
	15. From orbit adjust motor	15. Sterilize orbit adjust system	15a. Midcourse adjust philosophy 15b. Orbit adjust philosophy 15c. Decontaminate OA system 15d. Eliminate OA	
	16. From attitude control system		16. Sterilize attitude control system	16. Decontaminate attitude control system
	17. From spacecraft	17a. Sterilize entire spacecraft 17b. Decontaminate external spacecraft surface with ethylene oxide treatment	17. Design all external spacecraft surfaces and parts to minimize loose particles or pieces	
E. Bio-Barrier Impacts Mars	18. Forward bio-barrier impacts Mars	18. Sterilize spacecraft	18a. Separate before OI 18b. Attach to spacecraft 18c. Separate after orbit insertion (i) Select Safe Orbit (ii) Kick Into Good Orbit (iii) Modify $W/C_D A$	
	19. Aft bio-barrier	19. Sterilize spacecraft	19. Do not use emergency capsule separation unless safe orbit is assured	19. Assure non-accidental release
F. Lander Recontaminated (After Launch)	20. Micrometeorites puncturing bio-barrier	20. Sterilize spacecraft	20. Micrometeorite bumper or self-sealing bio-barrier	Locate all nozzles to minimize plume impingement on any portion of the planetary vehicle
	21. By orbit insertion particles direct	21. Sterilize orbit insertion system	21. Keep bio-barrier on until after orbit insertion	
	22. By orbit insertion sweeping dirty spacecraft	22. Sterilize orbit insertion system and decontaminate spacecraft surface	22. Keep bio-barrier on until after orbit insertion	
	23. By orbit adjust particles direct	23. Sterilize orbit adjust system	23a. Keep bio-barrier on until after orbit adjust 23b. Decontaminate orbit adjust system	
	24. By orbit adjust particles sweeping dirty spacecraft	24. Sterilize orbit adjust system and decontaminate spacecraft surface	24. Keep bio-barrier on until after orbit adjust	
	25. By attitude control particles direct	25. Sterilize attitude control system	25a. Keep bio-barrier on until after orbit adjust 25b. Decontaminate attitude control system	
	26. By attitude control particles sweeping dirty spacecraft	26. Sterilize attitude control system and decontaminate spacecraft surface	26a. Decontaminate attitude control system and surface. Decontaminate spacecraft in affected areas 26b. Keep bio-barrier on until after lander separation 26c. Use momentum wheels instead of attitude control gas during period associated with lander separation	
	27. By lander (after separation) going through orbit insertion, orbit adjust attitude control, or spacecraft particles still in orbit	27. Sterilize orbit insertion, orbit adjust and attitude control systems	27. Keep bio-barrier on until sometime after lander separation	
	28. By separation mechanism ejecta and/or miscellaneous unfold and deployment mechanism ejecta		28a. Design all separation and unfold mechanism to constrain loose ejecta 28b. Maintain a bio-barrier over lander as late as possible in mission sequence	

The rest of this section describes the analytical and experimental efforts needed to determine the magnitude of the problem in certain major categories, and some possible hardware and mission approaches.

17.2 Launch Vehicle. The probability of impacting Mars with either the non-sterile S-IC stage or the non-sterile S-II stage is so small that it can be neglected. However, the probability of impacting Mars with the non-sterile S-IVB is sufficiently high, for the planned Mars insertion trajectory, to require a retro-fire by the S-IVB stage. An alternate way to reduce the problem associated with the S-IVB stage is to employ sufficient bias in the initial aim point to reduce the reliability requirements of the retro-rocket.

17.3 Separation Mechanisms. All biologically contaminated particles or material ejected from a Planetary Vehicle are a potential source of biological contamination of Mars. Since it is not presently planned to sterilize the complete Planetary Vehicle, including the adapter, the number of non-sterile ejecta must be minimized. Therefore, all separation devices, deployment mechanisms, and protective cover devices must be designed to minimize the number of free particles and material generated during the operation of these devices and mechanisms. (See VC235FD102 and VC235FD104.)

17.4 Spacecraft. To assure that the non-sterile Spacecraft does not impact Mars, the heliocentric trajectory must be sufficiently biased away from the selected aim point to assure, in the event of failure of subsequent corrections, that injection guidance errors do not result in Mars contamination. This bias may or may not lie along the Mars center-final aim-point line. In other words, it is desirable that the extension of the line connecting the new aim point for a maneuver with the pre-maneuver indicated RT plane arrival point, should not pass too close to Mars.

As a result of the first midcourse maneuver, orbit determination and execution errors will remain, but will be much smaller than the errors attributable to injection guidance. Therefore, a considerable portion of the initial bias can safely be removed by choosing an aim point much closer to the final desired aim point. Similarly, for the second and third midcourse corrections, additional bias can be removed since residual errors after each correction will become progressively smaller. The correction where all bias can be removed will depend upon the convergence accuracy of the midcourse correction sequence which depends on many factors. Conceivably, in some cases all bias could be removed before the final correction.

If perfect navigation and guidance were available, an orbit as low as 600 km x 8000 km could be selected to satisfy the requirement that the spacecraft does not decay out of orbit before the year 2021. However, to allow for navigation and guidance errors a minimum orbit of 1000 km x 10,000 km has been selected.

17.5 Propellants. Table 17-2 summarizes the main properties of the ejecta from the Orbit Injection (OI), the Midcourse/Orbit-Adjust (MC/OA), and the Attitude Control subsystems. Because of the large quantity of ejecta, each of these subsystems presents potential planetary quarantine problems of major concern. The following three sections discuss these systems

TABLE 17-2. ATTITUDE CONTROL AND PROPULSION SYSTEM EJECTA CHARACTERISTICS

System	Ejected Weight (lb)	Ejecta Utilization	Ejecta Composition	Temperature (Chamber/ Exhaust) (°F)	Dwell Time	Exhaust Velocity
1. Orbit Injection Propulsion			Combustion gas (Mol Wt = 28.2 gm/mol)			
Solid	8400	90-sec burning time resulting in Mars orbit	Al_2O_3 particles Insulation and exit cone liner char particles TVC, Freon 114B2	5840/3830	0.01-0.10 sec	9700 ft/sec (2.95 km/sec)
2. Midcourse/Orbit Adjust Propulsion		Event — Propellant Used				
Monopropellant	1900	MC No. 1 645 lb. MC No. 2 105 MC No. 3 105 OA No. 1 50 OA No. 2 50 955 Remainder utilized if required by mission.	Decomposition products (Mol Wt = 14.1 gm/mol) 0.05% catalyst particles	1900/400	msec	7750 ft/sec (2.36 km/sec)
3. Attitude Control System	78	Approximately uniform over mission duration	Gaseous N_2	95	---	2190 ft/sec (0.666 km/sec)

from the standpoint of direct contamination of Mars. Capsule recontamination by contaminated ejecta from these systems is separately covered in Section 17.6.

17.5.1 Orbit Insertion (OI). From the standpoint of adverse effects on reliability, schedule, and cost for the entire program, a requirement to sterilize the OI system would be second only to a requirement to sterilize the complete spacecraft. Consequently, a sizable analytical and experimental effort is justified if it shows that the OI subsystem need not be sterilized.

Figure 17-1 shows a probability tree for direct contamination of Mars by OI ejecta. Each of the individual items indicated will have to be assessed in order to evaluate the potential OI contamination probability. Comments on major blocks in Figure 17-1 are presented below.

ARE VIABLE ORGANISMS INITIALLY PRESENT IN OI SYSTEM?

DO VIABLE ORGANISMS SURVIVE SIX-MONTH TRANSIT PHASE?

Although some early quantative data exist on the microbial population of solid and liquid propellants, samples of the specific propellant selected should be assayed to provide the needed quantitative data. This would include evaluating the survibability/die-off of the natural microbial population in both freshly-prepared samples and samples which have been stored for various time periods. Since the predicted temperature of the propellant during the six-month transit phase is between 40 and 80 °F, the most appropriate test would be to evaluate the effects on samples maintained in this temperature range.

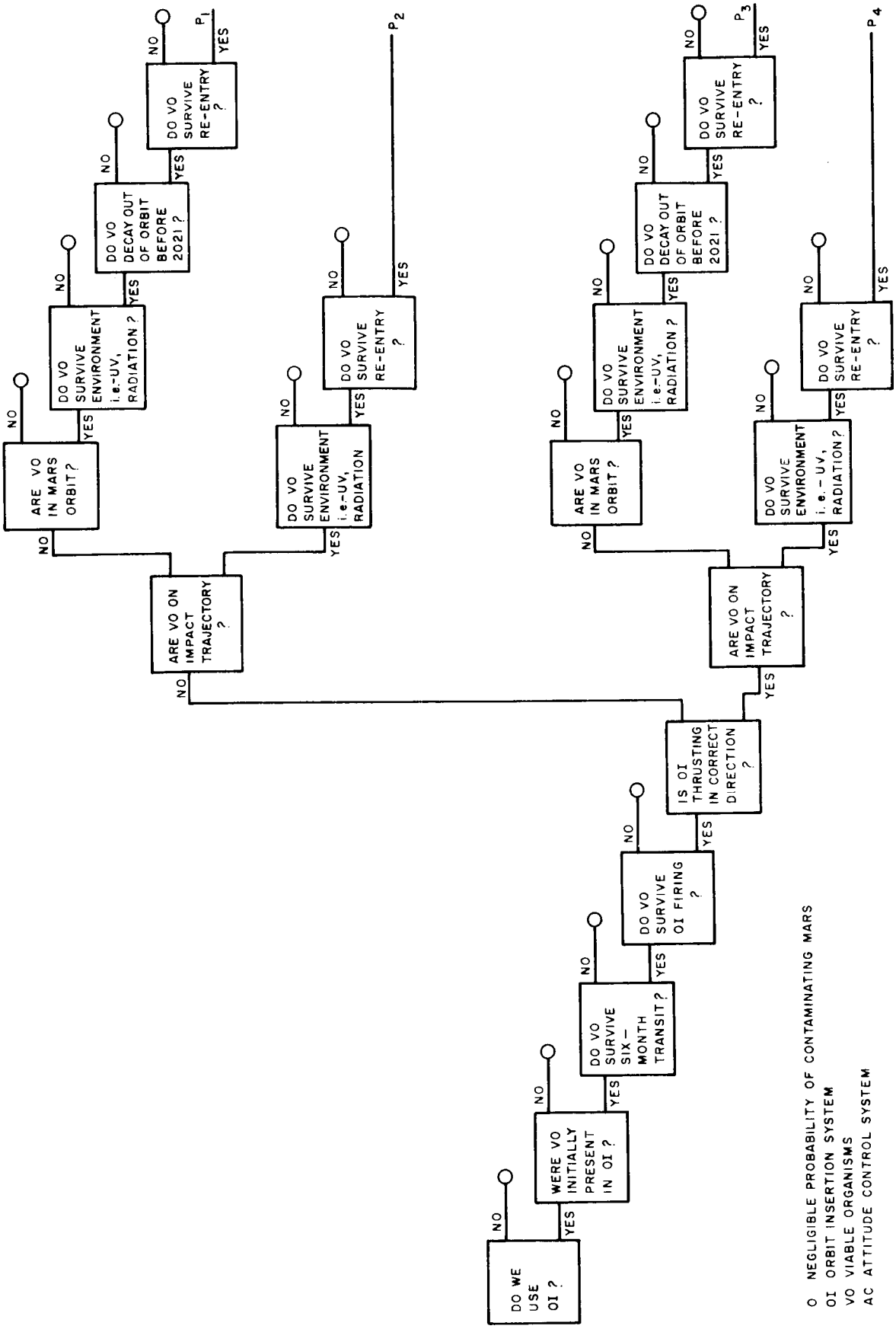
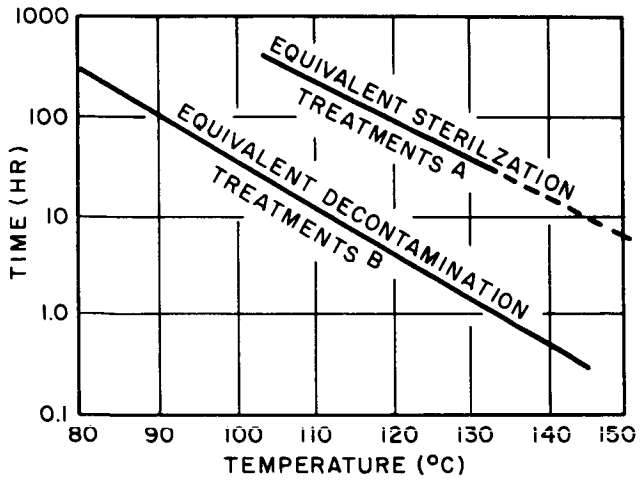


Figure 17-1. Probability Tree, Orbit Insertion Subsystem Particles Contaminating Mars

Because of the difficulty normally encountered in assessing effects on the variable levels and types of microorganisms indigenous to such materials, the employment of known test organisms in such studies is not uncommon. It is envisioned that such organisms could be incorporated into duplicate lots of propellant specimens; it is believed that data obtained with the test organisms would be corroborative of those obtained with the natural micro-flora. The precautions normally required in the use and interpretation of results from experiments employing known test organisms would have to be observed.

DO VIABLE ORGANISMS SURVIVE ORBIT-INSERTION FIRING?

Figure 17-2 presents the NASA Biosciences Office currently-recommended time-temperature treatments for sterilization and decontamination. Figure 17-3, an extrapolation of the curve from Figure 17-2, indicates that temperatures of 300 to 400 °C could sterilize in times of only millisecond durations. Since this is strictly an extrapolation, its validity would have to be proved. Evidence which tends to corroborate this, taken from Decker et al (1954)[1], is presented in Table 17-3 for spores of Bacillus Subtilis var. Niger suspended in a flowing stream of air. The results indicate that "virtual sterilization" — in the author's words, 99.9999 percent reduction — may be achieved at the cited conditions with air-flow rates of from 10 to 75 cfm, and that an even greater reduction can be obtained if the air is maintained at 625 °F for three seconds.



A. BASED ON TDT DATA 0.1 GM SAMPLES OF GARDEN SOIL ASSAYED IN THIOGLYCOLLATE BROTH

B BASED ON TDT DATA DRY SPORES OF BACILLUS SUBTILIS RIGER ASSAYED IN TRYPTICASE SOY BROTH

Figure 17-2. Equivalent Dry Heat Decontamination and Sterilization Treatments for Unmanned Planetary Lander

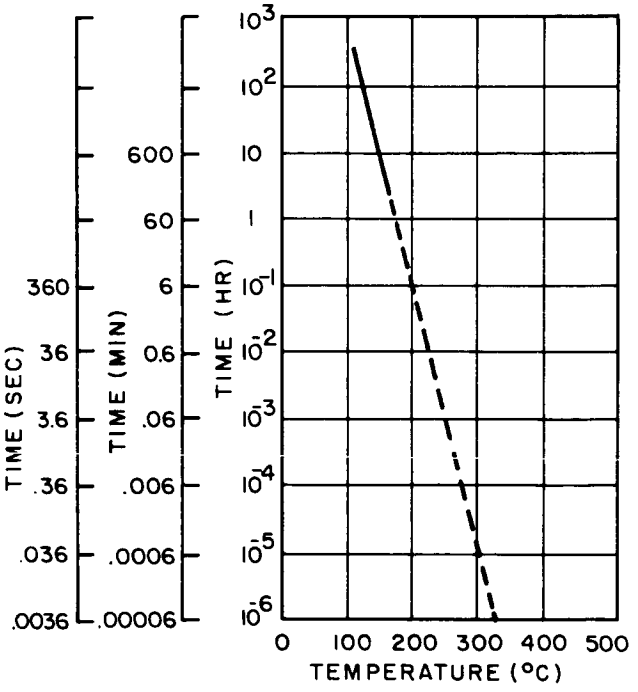


Figure 17-3. Extrapolated Dry Heat Sterilization Treatments

[1] Decker, H.M., Citek, F.J., Harstad, J.B., Gross, W.H. and Piper, F.J.; Time-Temperature Studies of Spore Penetrations through an Electric Air Sterilizer; Applied Microbiology, Vol. 2, No. 1, pp. 33-36; 1954.

TABLE 17-3. STERILIZATION TEMPERATURE VERSUS RETENTION TIME

Temperature		Retention Time (sec)
(°F)	(°C)	
425	218	16
475	246	6-7
525	273	3
575	279	1.8

Other data by Bourdillon et al (1948)[2] reveal that complete sterilization was achievable between 210 and 240 °C with exposure times of from 6 to 8 seconds, for an internally heated furnace, and with times of from 0.4 to 0.6 second for an externally heated furnace. These authors concluded that 250 °C might be adequate to sterilize moving air in a well-designed furnace, but that it was desirable to aim at a possible air-exit temperature of 300 °C (572 °F) if complete freedom from spore-bearing organisms is essential.

Superheated steam, sometimes referred to as analogous to dry heat, used to sterilize empty cans in an aseptic canning process (Pflug, et al 1959)[3] is as high as 525-550 °F, the temperatures in the cans being in the range of 420 to 425°F. The exposure time employed, between 40 seconds and one minute, is adequate for sterilization. Temperatures of from 410 to 415°F for exposure times of from 1 to 1.5 minutes are employed to sterilize the can covers.

The above indicates that a large kill factor could possibly be associated with the OI firing as a result of the high chamber temperature. For example, in solid systems of the type being considered, the chamber and exhaust temperatures are typically 6000 °F and 3000 °F, respectively, the organisms being exposed to these temperatures for durations ranging from 0.01 to 0.1 second.

The feasibility of possible experiments to determine the validity of this hypothesis, and whether organisms experience such temperatures and exposure times in a rocket firing, is being evaluated. A possible experiment would consist of the firing of a small motor, inoculated with known test organisms, in a biologically-clean test chamber, the residue (exhaust products) being collected and bio-assayed. The most meaningful results would include definition of the number and size distribution of the viable organisms, if any, in the rocket exhaust.

ARE VIABLE ORGANISMS ON IMPACT TRAJECTORY?

Assuming that there are viable organisms in the OI exhaust, it then becomes necessary to determine the velocity and size distribution of these organisms in order to assess whether they can get to Mars. A major factor in this determination is the direction of the OI system at the time of firing. Any failure in the Attitude Control subsystem, resulting in a wrong

---

[2] Bourdillon, R.B., Lidwell, O.M., and Lovelock, J.E.; Air Disinfection by Heat; Studies in Air Hygiene; Medical Research Annual Report #262; pp. 190-207; London, 1948.

[3] Pflug, I.J., Hall, C.W., and Trout, G.M.; Aseptic Canning of Dairy Products; Dairy Engineering; 1959.

orientation of the OI system, will have to be considered in the analysis. One way to minimize misalignment is to require attitude verification before orbit insertion.

For the no-failure case, a consideration directly bearing on this problem is the method of orbit insertion. As shown in Figure 17-4, orbit insertion can occur at either of two points on the approach hyperbola. The second point (2) has been tentatively selected. One of the major reasons for this choice is that it will minimize the possible contamination problem from the orbit-insertion particles since, in theory, the larger particulate exhaust from the OI nozzle will be confined within a cone centered along the engine axis.

Dispersion into the upper Martian atmosphere of organic material in the OI propellant can occur if the OI exhaust acts as a carrier for this material, which can exist as large molecular clusters or as a resident on macroscopic-sized particles. These clusters of organic material, if carried into the regions above the Martian atmosphere by the rocket-exhaust plume, could, depending upon the distribution in direction and space, enter the relatively thin Martian atmosphere intact and contaminate the surface. If the contaminant concentrations and their distribution in size and direction of motion are known, an entry analysis of the contaminations can be performed to determine what fraction of the original material would find its way to the surface of the planet. In order to analyze the motions of small particles and molecular clusters, it is necessary to understand the flow in the rocket exhaust plume which will act as the carrier for the material of interest. Expansion of the rocket plume into the vacuum in the upper Martian atmosphere will establish a quite complex rarified flow, since it will be collision-dominated near the nozzle exit plane, but collision-free very far from the nozzle.

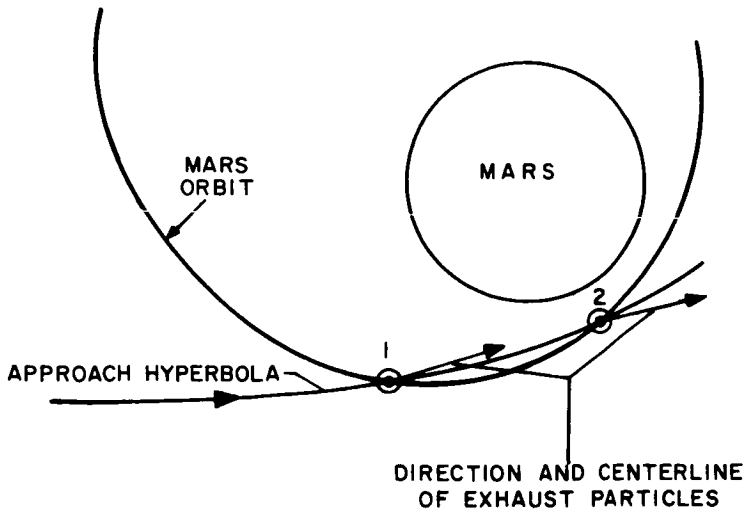


Figure 17-4. Orbit Insertion Alternatives

In the absence of physical boundaries, there is a flow which undergoes a transition from collision-dominated isentropic expansion in the vicinity of the nozzle exit plane, to collision-free or free molecular flow far downstream from the nozzle. This sequence has been established experimentally in several laboratories; measurements show that the Mach number along the centerline of the jet increases according to a collision-dominated isentropic expansion until collisions are too frequent to support the expansion. The Mach number increase then levels off, the expansion being said to freeze. This is in direct contradiction to the prediction by the continuum, isentropic theory of a continual rise.

An aid in modeling this complex two-dimensional free jet flow is the existing work on

the problem of one-dimensional spherical source flow.[4] This source-flow model will probably be a very good representation of events along the jet centerline, but will become progressively worse off-axis as the source Reynolds number decreases. To date, the solution has been obtained for a spherical source flow with near vacuum conditions very far from the source. This problem includes the most important feature of vacuum expansion: the transition to free molecular flow in the absence of boundaries. It is, however, expected that over a wide range of source Reynolds numbers the solution to this problem will represent conditions along the rocket plume centerline. It is planned to extend this analysis to the conditions which exist off-axis, since they will be critical for the determination of the material particle trajectories in the carrier exhaust plume.

Conditions in the carrier exhaust plume having been established, the dispersal of any contaminate material that may be present in the nozzle exit plane must now be investigated. To perform this analysis, the contaminate material can be divided into two classes: those that travel with macroscopic-sized particles and those that are part of large molecular clusters and behave rather as molecules of very large molecular weight. The analysis on the flow of a trace species of large molecular weight in a rocket exhaust plume[4] can be applied to the latter class. This analysis will give the distribution, concentration and direction of motion of these large molecules in the exhaust plume. For the macroscopic particles, an approximate solution is the integration of the equations of motion of typical small particles in the ambient carrier-gas environment.

With this plume analysis available, the dispersal dynamics can now be considered. This can again be treated in two classes: (1) for the large molecular aggregates consider a process of molecular diffusion in the presence of a gravitational field — a process encountered in the dispersal of Stronium 90 in the earth's atmosphere, which has been considered in some detail; and (2) for the larger macroscopic particles, the capability developed by the General Electric Company over the past three years in the analysis of re-entry of small particulate matter into planetary atmospheres can be applied. This capability has been developed in connection with the safety effort of the Nuclear Rocket Program under contract with the AEC, an effort which resulted in a highly accurate computer program for predicting the re-entry and burn-up of small particles, taking into account the various rarified flow regimes encountered during entry, and the continuously varying W/C_DA of a particle which is disintegrating because of re-entry burn-up.

In summary, the above described plume and dispersal analysis would provide the following information:

a. The distribution in size, direction of motion, speed, concentration and temperature within the plume itself of both particulate material and large molecular aggregates.

---

[4] Personnal communication: Hamel, B.B., GE Space Science Laboratory, and Willis, D.R., University of California, Berkeley.

b. The number flux of large molecular aggregates that would reach the planet surface, and the number of macroscopic particles that would impact the planet, as well as their temperatures.

DO VIABLE ORGANISMS SURVIVE ENVIRONMENT?

DO VIABLE ORGANISMS SURVIVE RE-ENTRY?

The major environmental factors near Mars which are potentially capable of reducing the number of viable microorganisms are: ultraviolet (UV) radiation, ionizing radiation, temperature and high vacuum.

It is fairly generally agreed that UV is very effective in destroying viable organisms exposed directly to the flux. However, the main problem is that since UV penetration is very shallow, viable organisms can be easily shielded, even by other organisms. Estimates exist on the UV flux at the top of the Mars atmosphere, Packer et al (1963)[5]. Very little is known regarding the biological effects of the ionizing radiation near Mars. This area should be studied to determine the weighting, if any, to be assigned to this environmental factor.

Another factor which should be investigated is the effect of temperature-shocking on organisms. A sudden fall in temperature may result in death of organisms. Any freezing-thawing cycles (e.g., for particles in orbits which experience an eclipse) could also have a possible effect on the viability of microorganisms. With regard to the effects of high vacuum, up to 10^{-9} torr, for periods as long as 35 days, at 25 °C, there is no known significant loss of viability of microbial spores[6].

Although the possible synergistic effects of all of the above environmental factors have not been investigated, some work has been done with two or three factors at a time. Since the results indicate increased reduction in viability with more factors considered, the possible combined effect on viability of organisms should be investigated.

Little or no reduction in viability of microorganisms, certainly no measurable effects can be expected from any of the above factors with relatively short time exposures. A possible exception is the effect of UV on individual small clusters of viable organisms. However, the effects of previously mentioned agents or factors might be very significant for viable organisms experiencing long exposures, as in a slowly decaying orbit about Mars.

17.5.2 Midcourse Orbit-Adjust (MC/OA). While evaluation of the potential problem of the direct contamination of Mars by MC/OA exhaust products will involve many of the same

---

[5] Packer, E., Scher, S. and Sagan, C.; Biological Contamination of Mars. II Cold and Aridity as Constraints on the Survival of Terrestrial Microorganisms in Simulated Martian Environments. Icarus 2, pp 293-316, 1963.

[6] Morelli, F.A., Fehlner, F.P. and Stembridge, C.H.: Effect of Ultra-High Vacuum on Bacillus subtilis var. niger; Nature, 196, No. 4850, pp 106-107; 1962.

considerations discussed under the OI case, Section 17.5.1, there are several additional mission tradeoffs which will have to be taken into account in the evaluation.

The early midcourse corrections are not likely to present a significant problem, for three reasons. First, the number of particles which will receive the exact velocity increment needed to place them on a Mars impact trajectory will be small. Second, long exposure to solar pressure will result in significant perturbations to the trajectories of the particles. Third, long exposure to the space environment, particularly UV, will result in some reduction in the number of viable organisms reaching the vicinity of Mars. However, since the last midcourse correction will occur close to Mars, the problem from the exhaust products will be aggravated; hence, a tradeoff involving the actual time at which this last midcourse correction is made is required. An additional factor tending to reduce the possible problem from any midcourse maneuver is that these firings are essentially normal to the flight path and in the direction away from Mars.

Another mission tradeoff involves the selection of the orbit periapsis, higher values of periapsis tending to alleviate the problem. However, this tradeoff affects many other areas. For example, increasing the selected orbit from 1000 km x 10,000 to 2000 km x 10,000 km will require:

a. An $\sim$ 140 m/sec higher ΔV for OI

b. An $\sim$ 76 m/sec higher ΔV for capsule de-orbit

c. An increase in the Spacecraft-Capsule range at capsule entry from $\sim$ 1800 km to $\sim$ 3600 km.

Other mission approaches available for alleviating this problem, and requiring tradeoff studies, are:

a. Restriction of orbit adjustments to those which result in a lower energy orbit and in which the OI particles are placed in a higher energy (safer) orbit.

b. Restriction of line-of-apsides adjustments to those which cause the OI particles to be sent away from Mars rather than towards it.

c. Elimination of all orbit adjustments.

17.5.3 Attitude Control (AC) Gas. The potential problem of direct contamination of Mars by AC exhaust particles can be analyzed in a manner similar to that for the OI and MC/OA systems. This problem is expected to be very severe for several reasons:

a. Absence of combustion eliminates the reduction of viable organisms by high temperatures.

b. The exhaust from the AC nozzles is randomly oriented with respect to the velocity vector of the spacecraft.

c. The spacecraft will be operating in a near-Mars orbit for a long period of time.

The only mission approach available for minimizing this problem is the use of a higher orbit. Some of the tradeoffs involved with a higher orbit were previously mentioned. Possible solutions to the hardware aspects of this problem are discussed in Section 17.7.

17.6 Capsule Recontamination. The capsule is subject to recontamination at any time that the integrity of the bio-barrier is violated, either accidentally or by micrometeorites. However, the considerations involved with these methods of recontamination are primarily the concern of the Capsule Contractor. The Spacecraft Contractor is mainly concerned with the problems which can arise after the barrier is intentionally opened, and with the mission tradeoffs associated with the time of opening of the bio-barrier. Detailed analysis, similar to that discussed for the OI system in Section 17.5.1, should be performed to determine the magnitude of the different potential recontamination problems for vaiours bio-barrier concepts and mission tradeoffs. Several hardware and mission tradeoff approaches are discussed below.

At separation, the forward portion of the canister is accelerated away from the capsule by mechanical means, while the aft end remains between the Spacecraft and the capsule. Because of the positive gas pressure (assuming that the capsule is pressurized), any microbes shaken loose from the separation mechanisms or the forward portion of the canister would be forced away from the exposed capsule surface. The major disadvantage of this canister separation procedure, whether performed before or after Planetary Vehicle orbit insertion, is that it causes the exposed capsule to pass through the cloud of spacecraft control gases ejected during the attitude maneuver. Once the Planetary Vehicle is placed in its Martian orbit, the capsule will be exposed to the Attitude Control gas and the exhaust from the orbit-adjust propulsion system, which would have been operated during preceding orbits. No matter how the gas is dispersed, there is a finite probability that the Planetary Vehicle will intercept some microbes. Releasing of the capsule as early as possible will minimize the number of viable organisms intercepted.

An obvious alternative would be the use of two continguous sterilization canisters: one, a rigid outer barrier which aids meteoroid attenuation and separates before orbit insertion and the other, a thin film which can be opened at the time of capsule release or separated with the capsule and ejected later. If the thin-film barrier remains with the Spacecraft, it must be retracted and stowed so that the spacecraft mission is not affected by it. If it is released with the capsule, means must be devised to assure that it does not reach Mars. This could conceivably be achieved as follows:

a. Separate the thin-film barrier and then cause it to be rolled or folded up to increase its W/C_DA to a larger value than that of the spacecraft, thus putting it in a safe orbit.

b. Assure that the film barrier is a self-consumable type, either by an exothermic reaction, or by a sublimating coating.

The first alternative, the thin-film barrier remaining with the Spacecraft, seems to be the more feasible one.

Still another possibility is to keep the canister with the capsule until after capsule-spacecraft separation. The canister would then be separated. To prevent the contaminated canister from eventually decaying in orbit and impacting Mars, two possibilities exist:

a. The spacecraft orbit could be selected so that the canister (having a smaller W/C_DA than the spacecraft) will not decay out of orbit before 50 years, which would require an orbit approximately 2000 km x 10,000 km in altitude.

b. The canister could be provided with a sufficient ΔV (approximately 110 mps) to put it into a safe orbit, which would require a means of orienting and stabilizing the barrier while imparting the ΔV.

Entry will create incinerating heat at the forebody of a sphere-cone configuration; which quickly decrease toward the afterbody or aft cover. The sterilizing effect is a time-temperature function. The time is very short, approximately 45 seconds, for the estimated Mars atmosphere. Present information indicates that the aft temperatures and time of exposure will be relatively ineffective as a sterilizing treatment.

Any viable organisms on the heat shield will be incinerated; any on the aft cover may survive to contaminate Mars. If any viable organisms should be on the capsule after entry velocity is achieved, they may separate from the capsule as the Mars atmosphere is reached. These microbes or microbe colonies may have a W/C_DA which would allow Mars entry without sterilization by entry heating.

17.7 Possible Hardware Approaches to Certain Major Problem Areas

17.7.1 Spacecraft Surface Decontamination. Biological contamination of Mars and recontamination of the capsule by particles from the spacecraft surface must be considered in both the design and handling procedures of the Planetary Vehicle. After normal clean-room handling, loose particles may remain with the Spacecraft. In addition, particles which were attached prior to launch may be dislodged during flight by various agents, including:

a. Shock, vibration, and acceleration loading on the spacecraft during rocket firing, attitude-correction and separation events.

b. The sweeping effect on the spacecraft surface of the impingement of high-velocity exhaust gases from the propulsion and attitude-control nozzles.

c. Outgassing of materials.

d. Meteorite impact.

At present the degree of precaution which must be taken to prevent biological contamination of Mars by these agents is uncertain. The basic requirement that the Spacecraft contain no loose particles greater than four mils in diameter may be adequate. However, if analysis

shows that further precautions are required, several decontamination (load-reduction) measures, short of total heat sterilization, may be utilized. These include:

a. Biological load-reduction controls during manufacturing, assembly and handling.

b. Local surface decontamination by ethylene oxide of areas which are swept by exhaust gases, and of areas which receive the highest shock and vibration loads.

c. A complete surface treatment with ethylene oxide. The use of ethylene oxide imposes a serious compatibility requirement on the materials, which must be considered during design. Therefore, a local surface treatment with minimum ethylene-oxide exposure would be highly preferred over a complete spacecraft purge.

d. An ethylene-oxide purge of the fairing prior to launch.

e. Exposure of the Spacecraft to a decontamination heat cycle (i.e., a heat cycle less severe than the accepted sterilization cycle, but in the range of the upper limit of operating or storage time-temperature product to which components are normally designed. Possible enhancement of this step occurs with higher relative humidity[7]).

17.7.2 Attitude Control/Propulsion Subsystems. As previously mentioned, ejecta from the exhaust of the Propulsion and Attitude Control subsystems are a potential source of Mars contamination, the extent of which must be evaluated. These ejecta consist of unconsumed fuel, exhaust gas, insulation or liner and TVC fluid. Each subsystem must be analyzed individually to determine the degree of decontamination required.

It is presently believed that analysis, and possibly a test program, will show that total heat sterilization of the solid-propellant orbit-injection subsystem will not be necessary. The most difficult problems encountered in total heat sterilization are those which result from subjecting the propellant grain, propellant-to-insulation bonds, and insulation-to-case bonds to the severe thermal stresses induced by the differences in thermal expansion coefficients between the propellant and the chamber, and from the degradation of propellant and propellant bonds during steady-state heating conditions.

It is quite possible that the exhaust gases of a solid rocket motor, resulting from combustion of the propellant at a flame temperature of 6000 °F, will be self-sterilizing. Since this is not an experimentally verified fact, an experimental program should be included if analysis indicates this to be a critical area. If it can be proven that the exhaust gas from propellant combustion is self-sterilizing, and if analysis shows that further decontamination of the system is required (for the other OI ejecta such as TVC, exit-cone liner), the approach can be to heat-sterilize the motor chamber with the insulation installed prior to heat-sterilizing the nozzle, TVC, and ignition subsystems. After propellant casting, the interior surface of the motor can be surface-decontaminated with ethylene oxide to assure that microorganisms are not ejected during ignition.

---

[7] McDade, J.J. and Hall, L.B.; Survival of Gram-Negative Bacteria in the Environment. I. Effect of Relative Humidity on Surface Exposed Organisms; Amer. Jour. Hygiene 80:192-204; 1964.

The problems to be encountered in sterilizing or decontaminating the monopropellant Orbit Adjust subsystem and the cold-gas Attitude Control subsystem are quite similar; the major difference is the use of a liquid in the first case and of a gas in the second. The level of biological control which will be placed on these systems has not been determined. However, if analysis shows that total heat sterilization is required for one or both of these systems, several system constraints may be identified:

a. All parts and components must be designed to withstand ethylene-oxide decontamination and the accepted time-thermal sterilization cycle.

b. The subsystem must be designed in accordance with a modular concept so that it can be heat sterilized as a unit prior to installation in the Spacecraft; alternatively, a sterile method of connecting feed lines must be developed.

c. If the system is heat sterilized with the propellant or gas loaded, the pressure caused by the high-temperature exposure could contribute to the material degradation of the tanks. If the system is heat sterilized empty, a sterile loading procedure must be developed.

d. All possible leak sources, such as valves and nozzles between the inside and outside of the subsystem, must be sealed off until the Spacecraft is beyond the Earth's atmosphere.

Several methods of decontamination of these subsystems less severe than complete heat sterilization may prove adequate to meet the overall planetary quarantine requirements. These methods include:

a. Purge the subsystem with ethylene oxide and then load with sterile or highly-filtered propellant or gas.

b. Mix ethylene oxide with the specific propellant or gas (the feasibility of this approach has not been demonstrated and would require investigation).

c. Install absolute filters in the system (the obvious effects on reliability of the system make this approach unattractive).

Biological control of the Attitude Control subsystem is further discussed in VC234FD104, and of the Propulsion subsystems in VC238TF (Volume C).

CII VC220FD101

TRAJECTORY AND GUIDANCE ANALYSIS

SECTION

1	GENERAL
2	APPLICABLE DOCUMENTS
3	HELIOCENTRIC TRAJECTORY
4	SATELLITE ORBIT
5	MIDCOURSE GUIDANCE
6	ORBIT INSERTION
7	ORBIT TRIM
8	CAPSULE DEORBIT

TRAJECTORY AND GUIDANCE ANALYSIS

1.0 GENERAL. The design trajectories chosen for the 1971 Mars VOYAGER mission and the criteria for their selection, and several trajectory-dependent parameters required for design of the VOYAGER Spacecraft are presented in this section. The parameters include communication ranges, distance from sun, occultation times, and lighting conditions.

The selection of the heliocentric trajectories, satellite orbit, and capsule de-orbit trajectory can not be accomplished independently because of the inter-action between the characteristics of each. Since neither the full requirements of the scientific experiments on the satellite orbit or the capsule design and experiments on the capsule de-orbit trajectory are known, it would not be possible to optimize the selection of the trajectories or orbit at this time. In addition, the inter-actions between their characteristics are such that an optimization can be made only after an extensive parametric analysis. However, the trajectories and orbit selected fulfill all known constraints and offer a good compromise between design and scientific requirements.

The heliocentric trajectory selection, midcourse guidance, satellite orbit selection, satellite orbit insertion guidance, orbit trim maneuvers and capsule de-orbit maneuvers will be discussed independently with the characteristics of each noted as necessary in the discussion of another. Briefly, the trajectories and orbit selected for design study are as follows:

A. Heliocentric Trajectory

Launch Period - April 28 to June 28, 1971

Arrival Date - First Planetary Vehicle, November 1 to November 17, 1971
Second Planetary Vehicle, November 11 to November 27, 1971

Asymptotic approach velocity (first planetary vehicle) - 3.5 km/sec

B. Satellite Orbit

Size - 1,000 by 10,000 kilometer altitude

Inclination - 60 degrees to Mars equator

Line of apsides - Such that the capsule impact is 20 degrees from the terminator for a capsule de-orbit on the first day of the orbiting phase

C. Capsule De-orbit Trajectory

De-orbit point - 230 degrees true anomaly

Entry angle - 16 degrees

De-orbit velocity increment - 217 meters/sec

Thrust angle (measured from orbit velocity direction) - 124 degrees

2.0 APPLICABLE DOCUMENTS

VC211SR101	Mission Objectives and Design Criteria
VC220SR101	Design Characteristics and Restraints
V-MA-004-002-14-03	Voyager 1971 Mission Guidelines

3.0 HELIOCENTRIC TRAJECTORY

3.1 Constraints. The various constraints placed upon the selection of the helicocentric trajectory are as follows:

a. Only type I trajectories are applicable.

b. The departure injection energy, C3, must be less than 25 km^2/sec^2.

c. The absolute magnitude of the declination of the departure asymptote must be greater than 5 degrees.

d. The launch azimuths shall be greater than 60 degrees East of North and less than 115 degrees East of North.

e. The launch period shall be at least 45 days with a daily firing window of at least two hours.

f. The launch site shall be complex 39 of the Kennedy Space Center.

g. The coast times in Earth orbit shall be between 2 and 90 minutes.

h. The absolute magnitude of the inclination to the ecliptic must be greater than 0.1 degree.

i. Two Planetary Vehicles shall be launched on a single booster in 1971.

j. The two Planetary Vehicles must arrive at Mars at least ten days apart.

k. The approach velocity to Mars must be less than 4.5 Km/sec.

These constraints are indicated by the shaded areas of the trajectory map of Figure 3-1. The limitation of -39 degrees for the declination of the departure asymptote results from the requirement of a launch azimuth greater than 60 degrees and at least a two-hour daily firing window.

3.2 Guidelines. The "VOYAGER 1971 Mission Guidelines", dated May 1, 1965, defines the following guidelines for use in selecting heliocentric transfer trajectories.

a. The approach velocity should be nearly constant over the entire launch window.

b. The flight times and communication distances should be kept as short as possible.

c. The arrival dates and geometry should be held as constant as possible over the launch window.

d. The wave of darkening is of interest and arrival dates should be adjusted to view this phenomena, if possible.

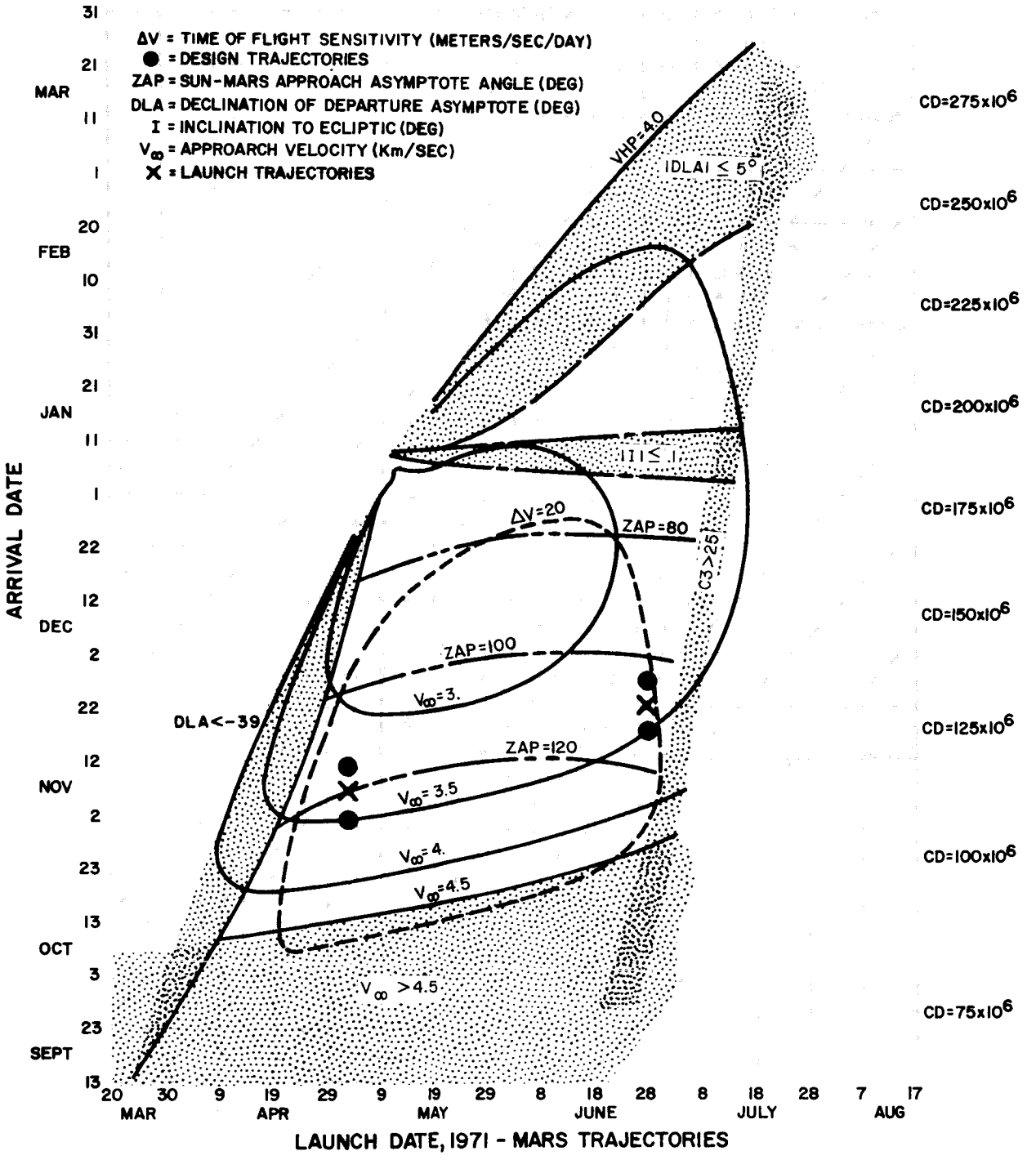


Figure 3-1. VOYAGER Mission Trajectory Map

3.3 Time-of-Arrival Adjustment. A 10-day separation in Planetary Vehicle arrival dates at Mars can be achieved by the following procedure. The Saturn-IVB stage containing the two planetary vehicles is injected into a heliocentric transfer trajectory which would result in the vehicles arriving at Mars midway between the two desired arrival dates. At some time from two to five days after injection, a maneuver is performed on each vehicle to correct for injection guidance errors and to change the time of arrival. One vehicle is changed so as to arrive five days earlier, and the other is changed so as to arrive five days later.

The magnitude of the velocity increment required to change the time of flight by a specified amount is shown in Figure 3-2. This figure shows contours of constant time of flight sensitivity superimposed on the standard time of flight versus launch date map for Mars 1971 Type I trajectories. Time of flight sensitivity is defined here as the magnitude of the velocity impulse (in meters/second) required to change the time of flight by one day. Contours are shown for 10, 20, 30, 40, and 50 meters/sec/day. The absolute minimum sensitivity is 6.4 meters/sec/day and occurs for the trajectory with a May 9 launch date and 186 days flight time.

Of the total ΔV capability of 200 meters/sec which is to be provided for each vehicle, it is expected that 100 meters/sec will be allocated for the first correction. It is desirable to keep the first correction as small as practicable so as to reduce dispersion due to maneuver execution errors. In order to allow a five-day change in time of flight, the transfer trajectory should be within the 20-meter/sec/day contour. This contour is also shown on Figure 3-1.

3.4 Trajectory Selection. In the selection of the design trajectories, the following were considered:

a. Launch - launch period, launch energy, declination of departure asymptote.

b. Spacecraft Design - trip time, communication distance, sun distance and occultations during the orbiting phase.

c. Propulsion - velocity increment for changing the trip time five days, Mars approach velocity, and apsidal rotation.

d. Scientific Experiments - effect of approach conditions on viewing and lighting.

e. Operational - constant arrival date.

f. Guidance - propagation of maneuver errors.

It is noted that the longest launch period for a constant arrival date within the 20 meter/sec/day time of flight change boundary, occurs for arrivals the first week of November. Also, as will be shown in Section 4.9, the amount of apsidal rotation, hence, orbit insertion velocity increment, is lower for the earlier arrival dates; i.e., higher ZAP angle. Generally, the Mars approach speed decreases as the arrival date is delayed from October and November until the middle of December. However, an approach velocity of 3.5 km/sec will allow injection into the desired satellite orbit under all conditions of arrival weight.

Trip time, sun distance, and communication distances are lowest for early arrival dates. Although not shown in this report, it was determined that without apsidal rotations,

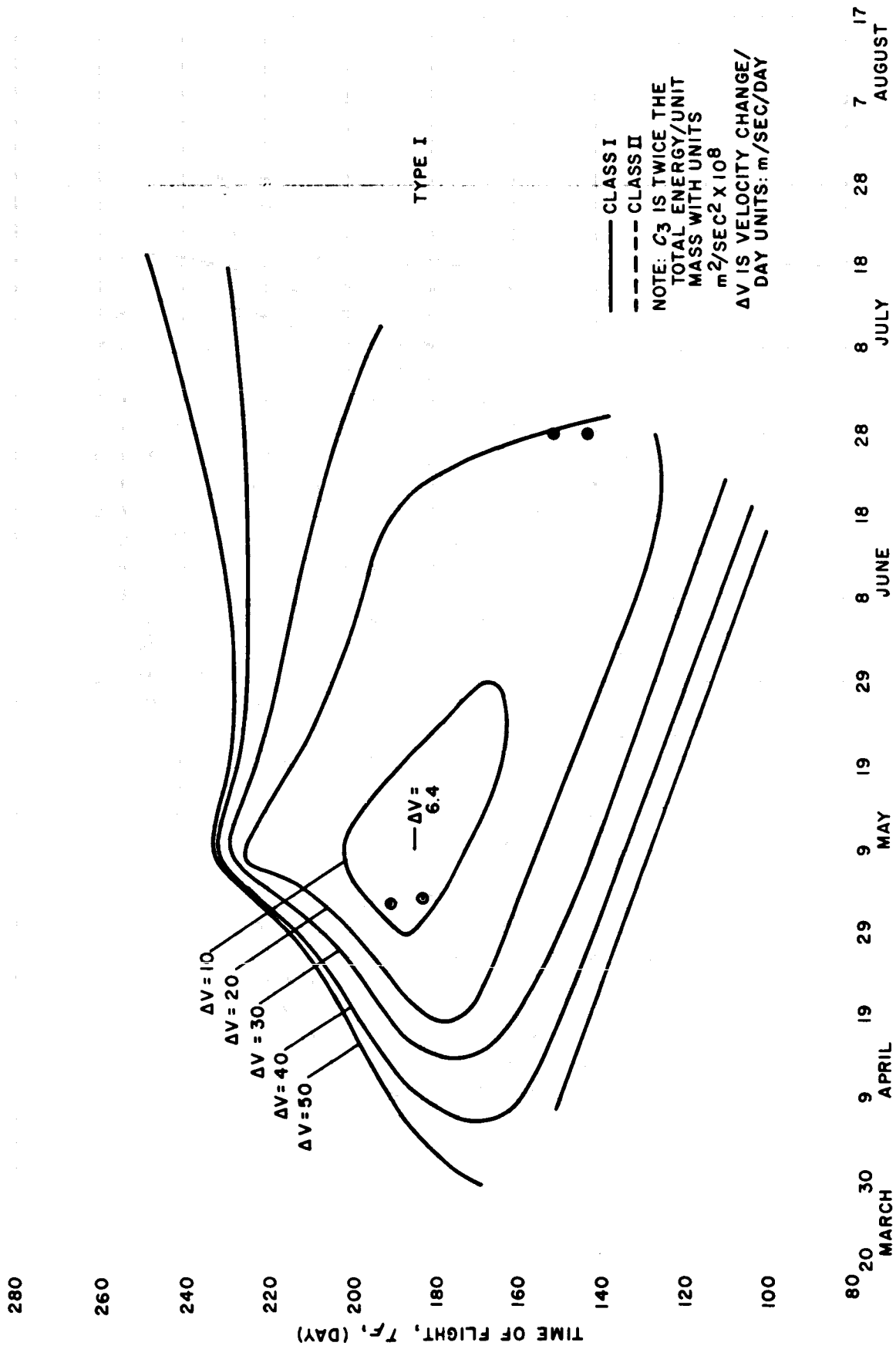


Figure 3-2. Time of Flight Adjustment

occultations and scientific viewing generally are best for trajectories for which the ZAP angle is 100 degrees or more (early November arrival). The propagation of maneuver errors as defined by the dispersion ellipse characteristics in EDP 281, "Trajectory Selection Considerations for VOYAGER Missions to Mars during the 1971-1977 Time Period," is minimum for arrival dates around November 1, 1971. This arrival date is unfortunately not well suited for observing the "wave of darkening". On November 1, 1971, the southern wave has already passed its peak in most regions of interest and the northern wave does not start until well towards the end of the expected useful life of the orbiter. To observe either wave adequately, the arrival date would have to be moved one way or the other by at least three months, which is obviously impractical for the 1971 opportunity. Wave of darkening considerations, therefore, have little influence on the choice of arrival data for 1971.

An arrival date around the first of November adequately fulfills all constraints and selection criteria. From Figure 3-1, it is noted that the locus of trajectories having a constant approach velocity of 3.5 km/sec also defines a region of approximately constant arrival date in the first half of Noevmber and a constant ZAP angle of the preferred higher magnitude. Therefore, this 3.5 km/sec boundary is selected as the trajectory rule for the first Planteary Vehicle. The velocity requirement (100 meters/sec) for time of flight changes, limits the launch period to between April 28 and June 28, 1971. The declination of the departure asymptote for these trajectories is greater than -35 degrees and the DLA related constraints are adequately satisfied.

By selecting a launch period from May 3, 1971 to June 17, 1971, which just meets the 45-day requirement, the velocity requirement for time of flight adjustment can be reduced from 100 meters/sec to 75 meters/sec. Improvements in many other trajectory parameters are also obtained: for instance, the minimum DLA is -32 degrees, (allowing an increase in the daily firing window to over five hours), maximum C_3 is reduced from 21 km^2/sec^2 to 15 km^2/sec^2, and the variation in ZAP angle over the arrival period is reduced from 20 to 15 degrees. The sensitivity of miss distance to midcourse maneuver errors is also slightly less for this reduced launch period.

For design pruposes, design trajectories were chosen as follows (these trajectories are noted on Figure 3-1 by heavy dots):

Launch	Arrival
May 3, 1971	November 1, 1971
May 3, 1971	November 11, 1971
June 28, 1971	November 17, 1971
June 28, 1971	November 27, 1971

The clock angle, earth cone angle, (defined in Figure 3-3) and canopus cone angle as a function of time are given in Figure 3-4 and the communication and Sun distances are shown in Figure 3-5. The clock and cone angles are also shown in Figure 3-6 as a polar plot for ease in determining antenna location and pointing.

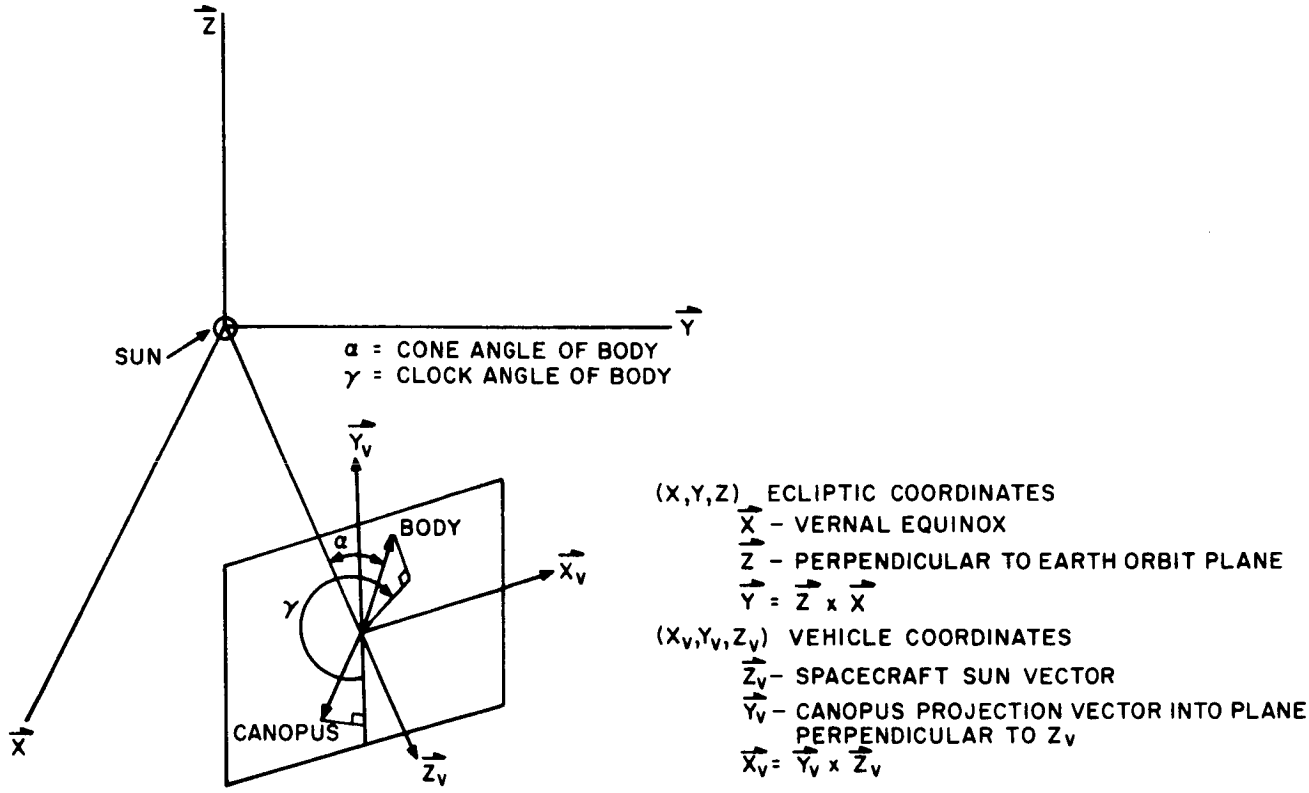


Figure 3-3. Vehicle Coordinate System

3.5 Ground Station Radar Track Profile for Near-Earth Hyperbolic Ascent Trajectories. Radar track profiles from five ground stations were developed utilizing three near-earth hyperbolic ascent trajectories for a launch day of May 3, 1971. These profiles are defined in terms of range and elevation angle above the local horizontal plane from each of the stations. The track period of interest was from the injection point to approximately 22 hours after injection.

The geocentric declination and right ascension of the hyperbolic departure asymptote are -31 and 343.5 degrees, respectively. An injection energy, (C_3) of 10.177 km^2/sec^2 and a parking orbit altitude of 100 nautical miles are used to define the hyperbolic shape parameters. The true anomaly of the injection point is 3.7 degrees.

Two of the three ascent trajectories were generated using the identical launch azimuth of 60 degrees East of North. The launch window period between these two launches is approximately six hours. The third ascent trajectory was chosen with a launch azimuth of 74 degrees East of North to place the launch time approximately in the middle of the six-hour launch window period defined by the 60-degree launch azimuth trajectories. The five radar stations which were utilized for the analysis are: (1) Ascension Island, (2) Madrid, Spain, (3) Johannesburg, South Africa, (4) Woomera, Australia, and (5) Goldstone, U.S.A.

The launch window parameter information was obtained from a launch window analysis computer program utilizing Saturn V booster data. Output from this program was used as the input to the radar track program which computed the range, azimuth and elevation angle of the

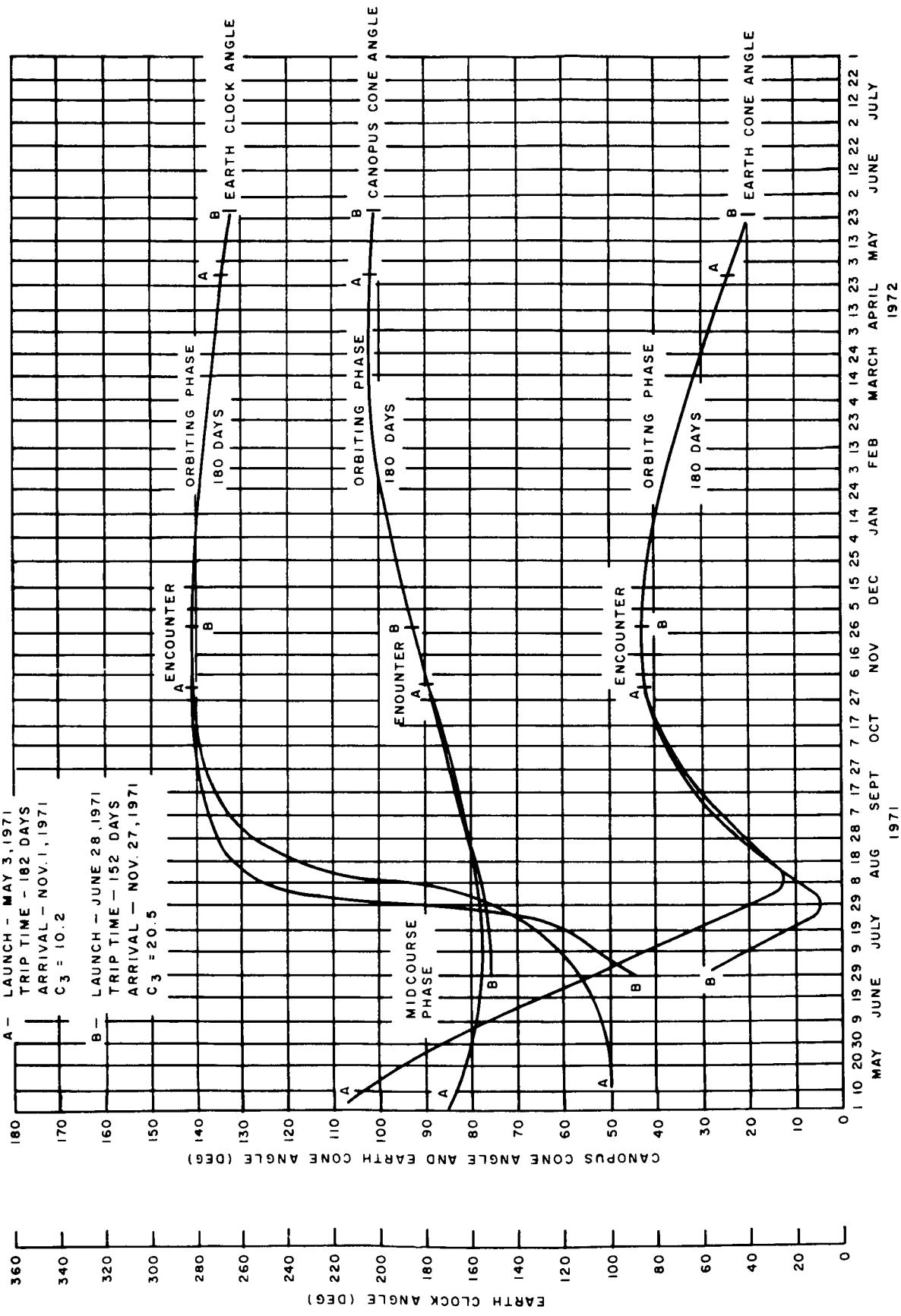


Figure 3-4. Trajectory Geometry, Angles

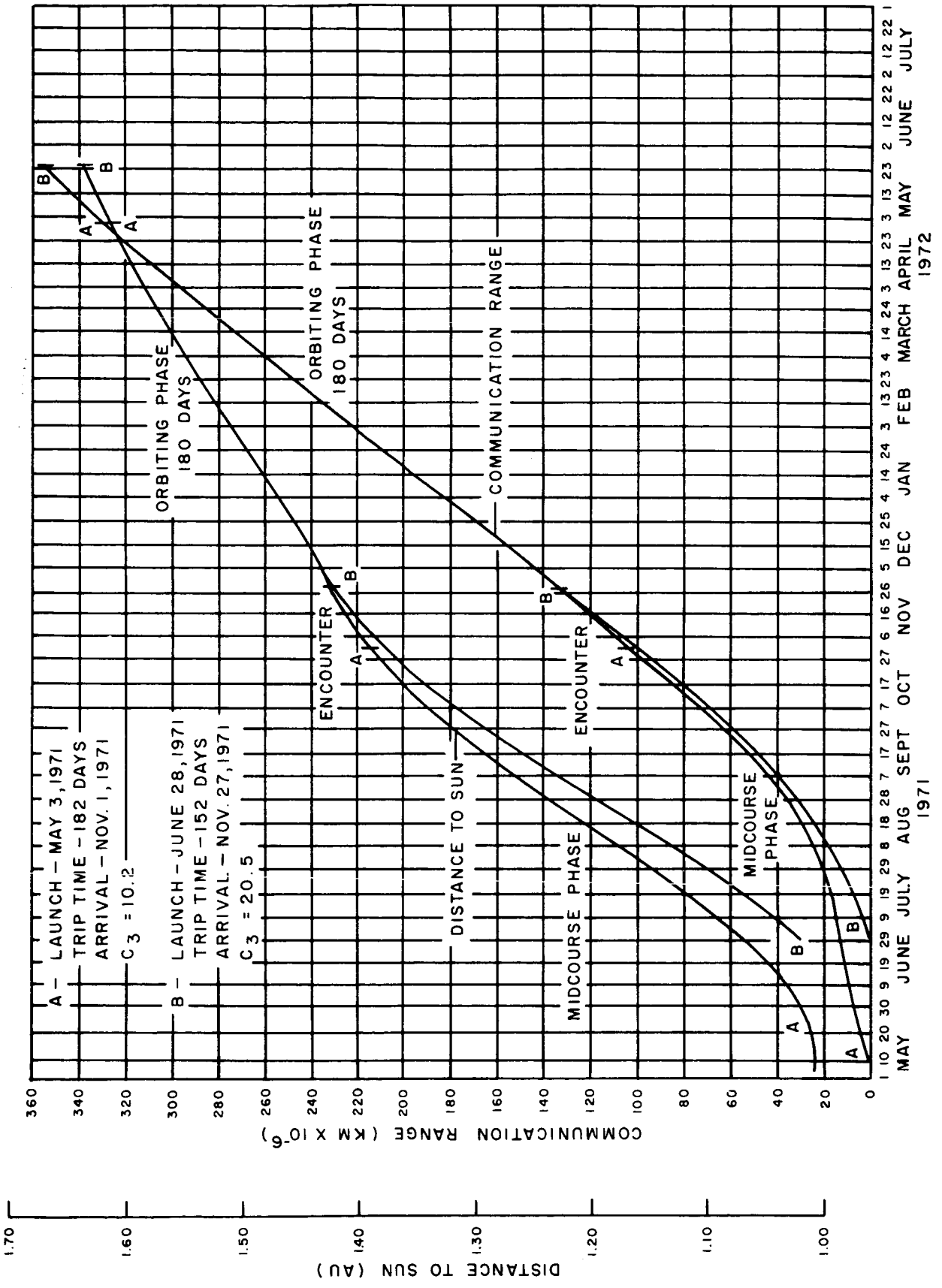


Figure 3-5. Trajectory Geometry, Distances

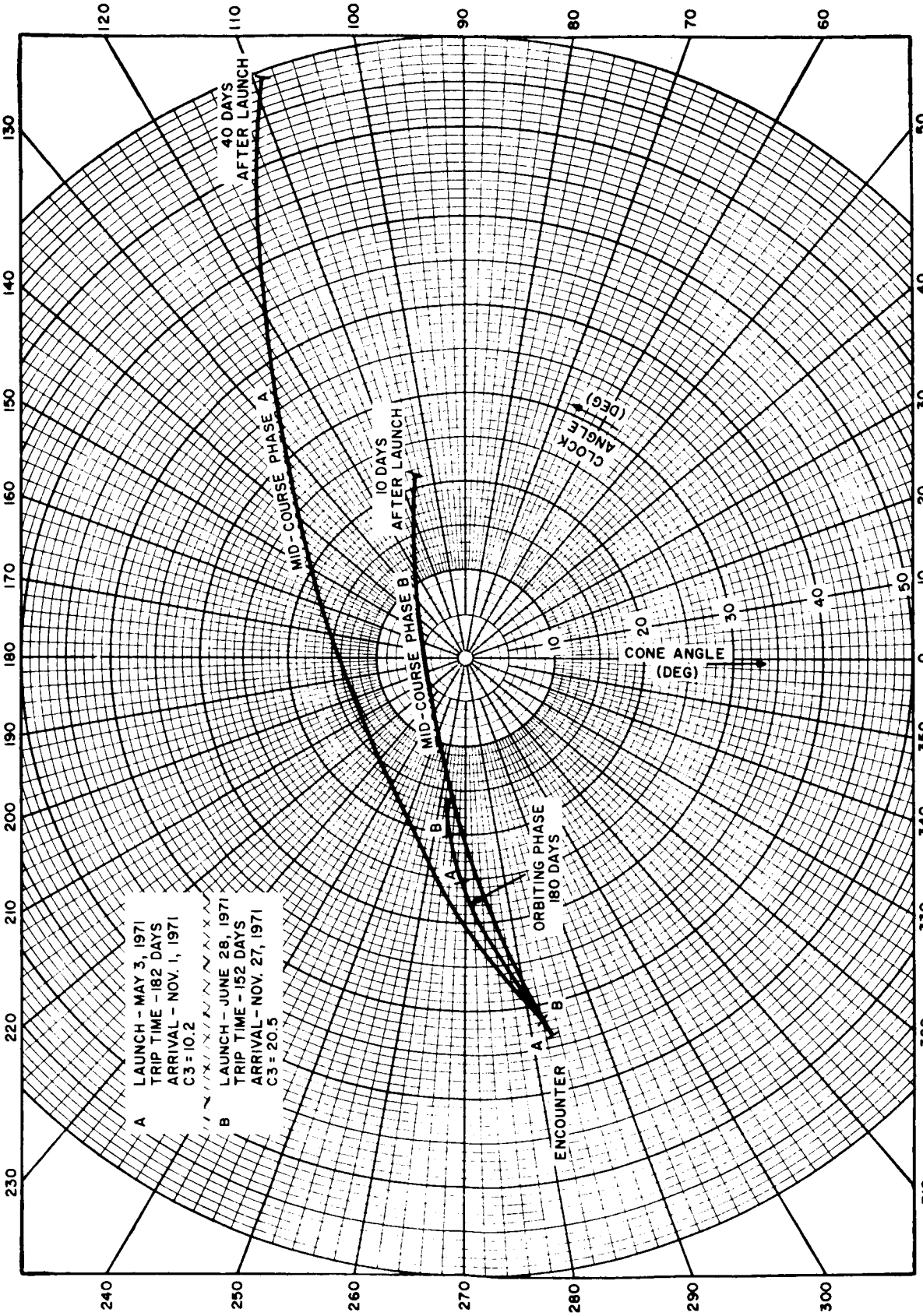


Figure 3-6. Earth Cone and Clock Angles

line-of-sight (LOS) vector between radar stations located on a spherical earth to the space vehicle position. The elevation angle is defined as the angle between the LOS vector and the local horizontal plane at a tracking station. A zero elevation angle corresponds to the LOS vector in the local horizontal plane.

The range and elevation angles versus flight time from the injection point are shown in Figures 3-7 through 3-12 (range is plotted for Woomera and Johannesburg only). The elevation angles for the LOS that fall below zero are not shown; consequently, dead bands on the elevation angle plots correspond to those time periods when the radar site cannot track the vehicle. The range plots for Woomera and Johannesburg are shown only for those time periods when the station can see the vehicle.

4.0 SATELLITE ORBIT

4.1 Constraints. The "VOYAGER 1971 Preliminary Mission Description", dated October 15, 1965 and subsequent direction from JPL defines the following constraints on the selection of the Satellite Orbit:

a. The probability of contaminating Mars as a result of any single launch for 50 years after arrival must be less than 10^{-4}.

b. The insertion velocity shall be less than 2.2 km/sec.

c. The orbit insertion maneuvers at Mars must take place in view of Goldstone.

d. No orbit shall be selected which will cause loss of the spacecraft roll reference for a period of time which may impair Flight Spacecraft control in the normal mode operations.

e. The capsule deorbit velocity increment must be less than 550 m/sec.

f. Capsule separation to occur 3 to 10 days after arrival at Mars.

g. Capsule separation and deorbit maneuvers must take place in view of Goldstone.

h. The capsule entry angle shall be between 20 degrees and vacuum graze.

i. The time from deorbit thrust to capsule entry must be greater than 50 minutes, but less than 12 hours.

j. The angle of attack at entry must be less than 60 degrees.

k. The landing site must be between 15 and 30 degrees of the terminator, preferably the evening terminator.

l. The maximum atmospheric descent time shall be less than 900 seconds.

4.2 Guidelines. The following guidelines are useful in selecting the satellite Orbit:

a. A fixed amount of retro-propellant should be used for both Planetary Vehicles throughout the launch window.

b. Sun occultation should be avoided for as long as possible after arrival.

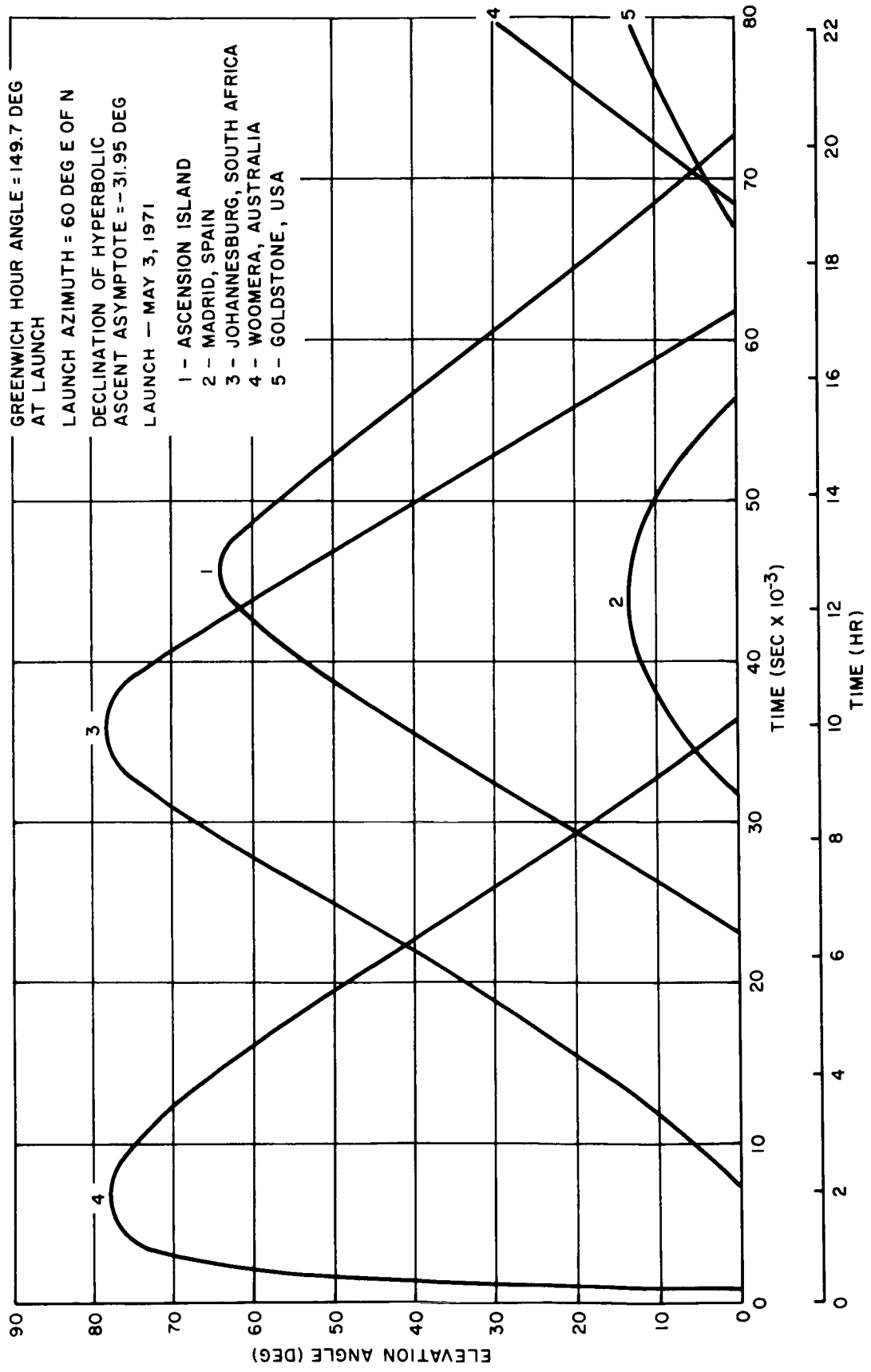


Figure 3-7. Earth Tracking Elevation Angle, Start of Window

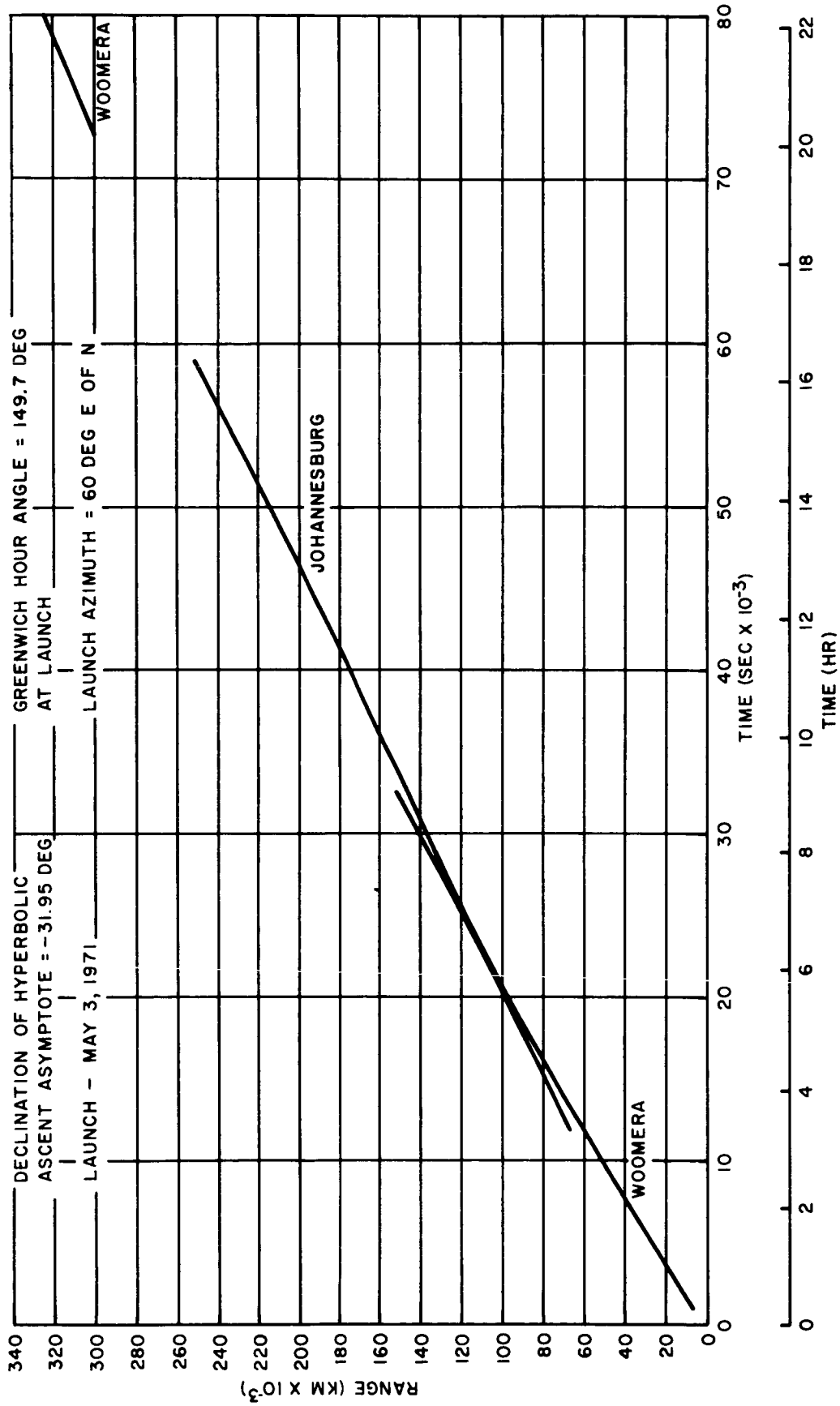


Figure 3-8. Earth Tracking Range, Start of Window

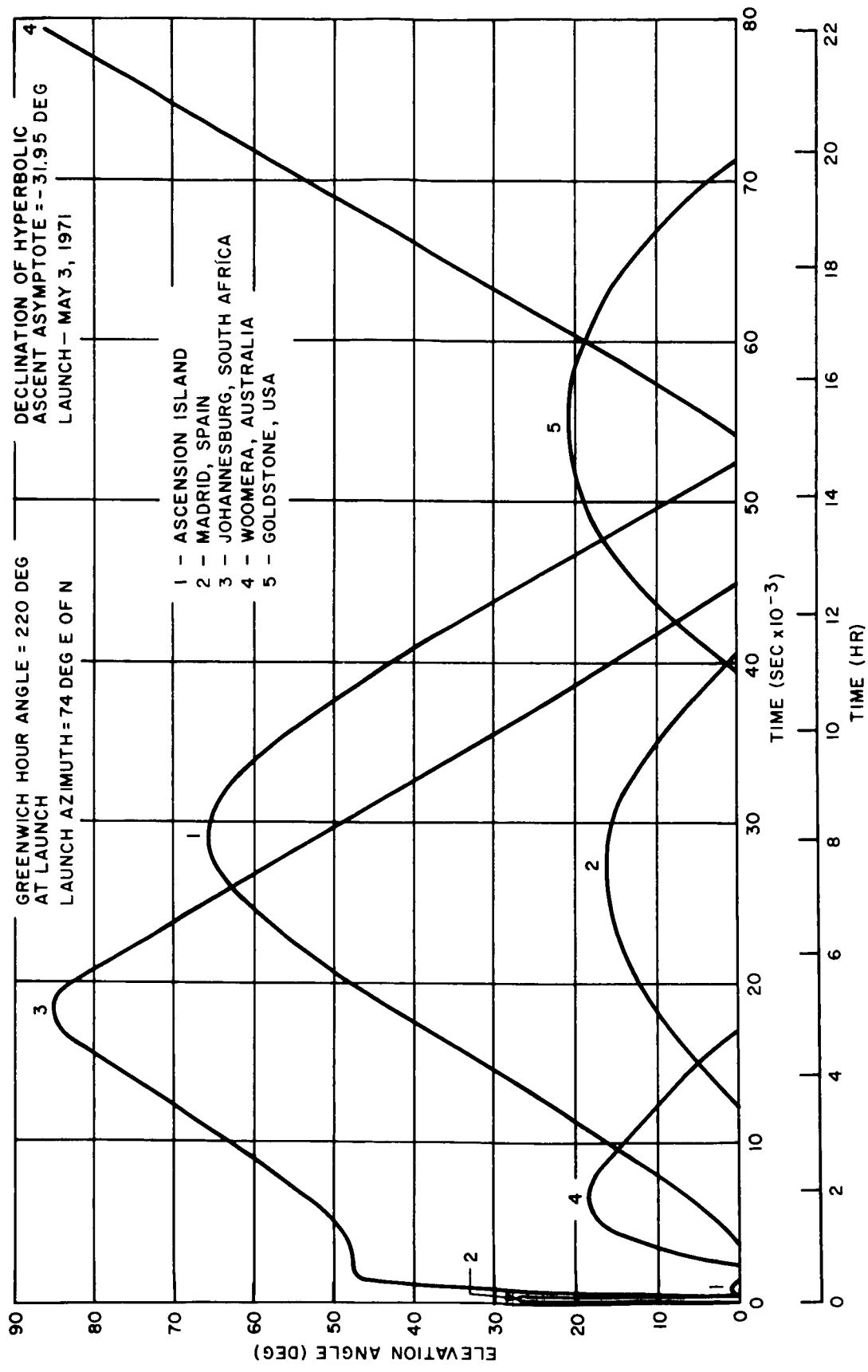


Figure 3-9. Earth Tracking Elevation Angle, Middle of Window

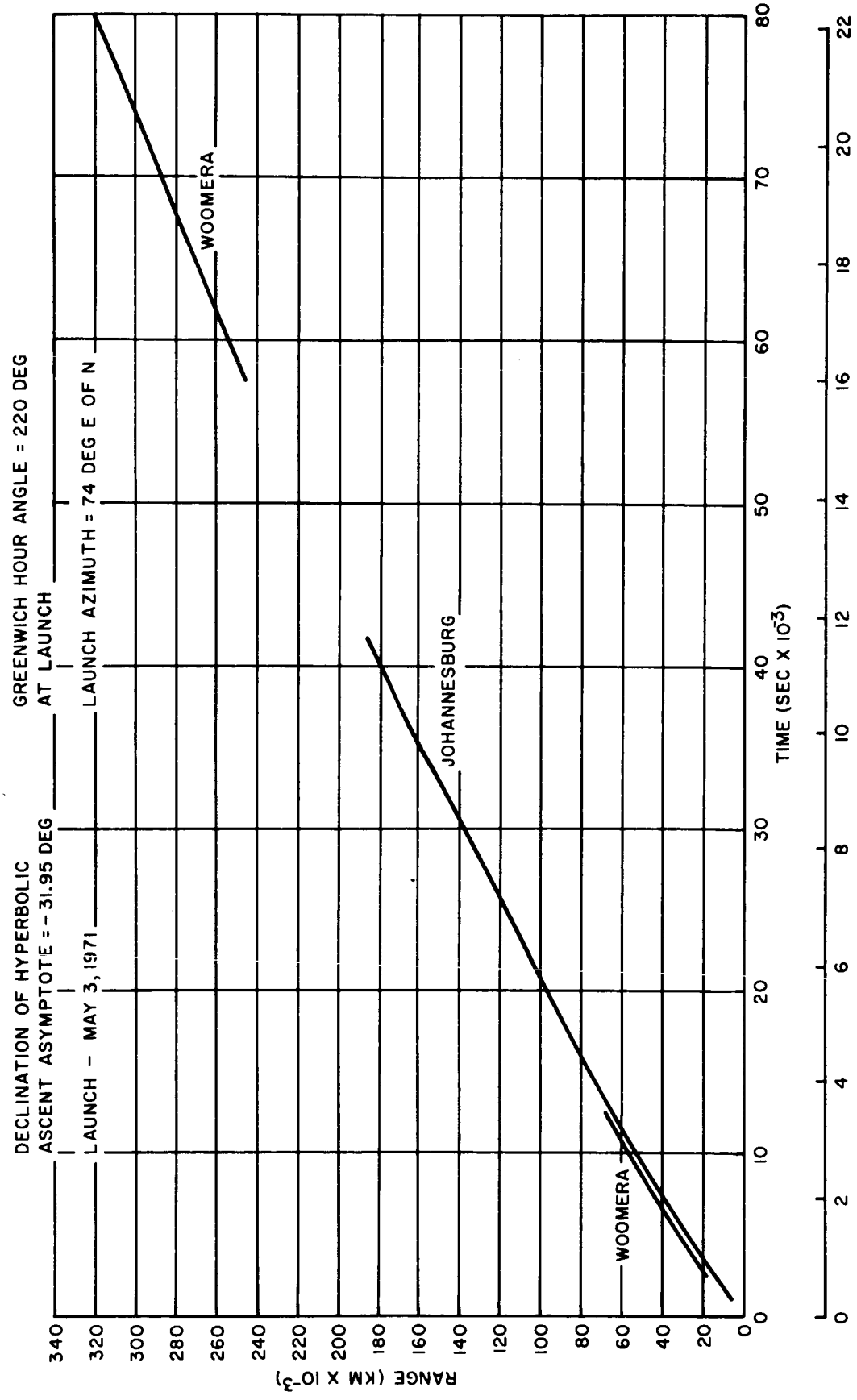


Figure 3-10. Earth Tracking Range, Middle of Window

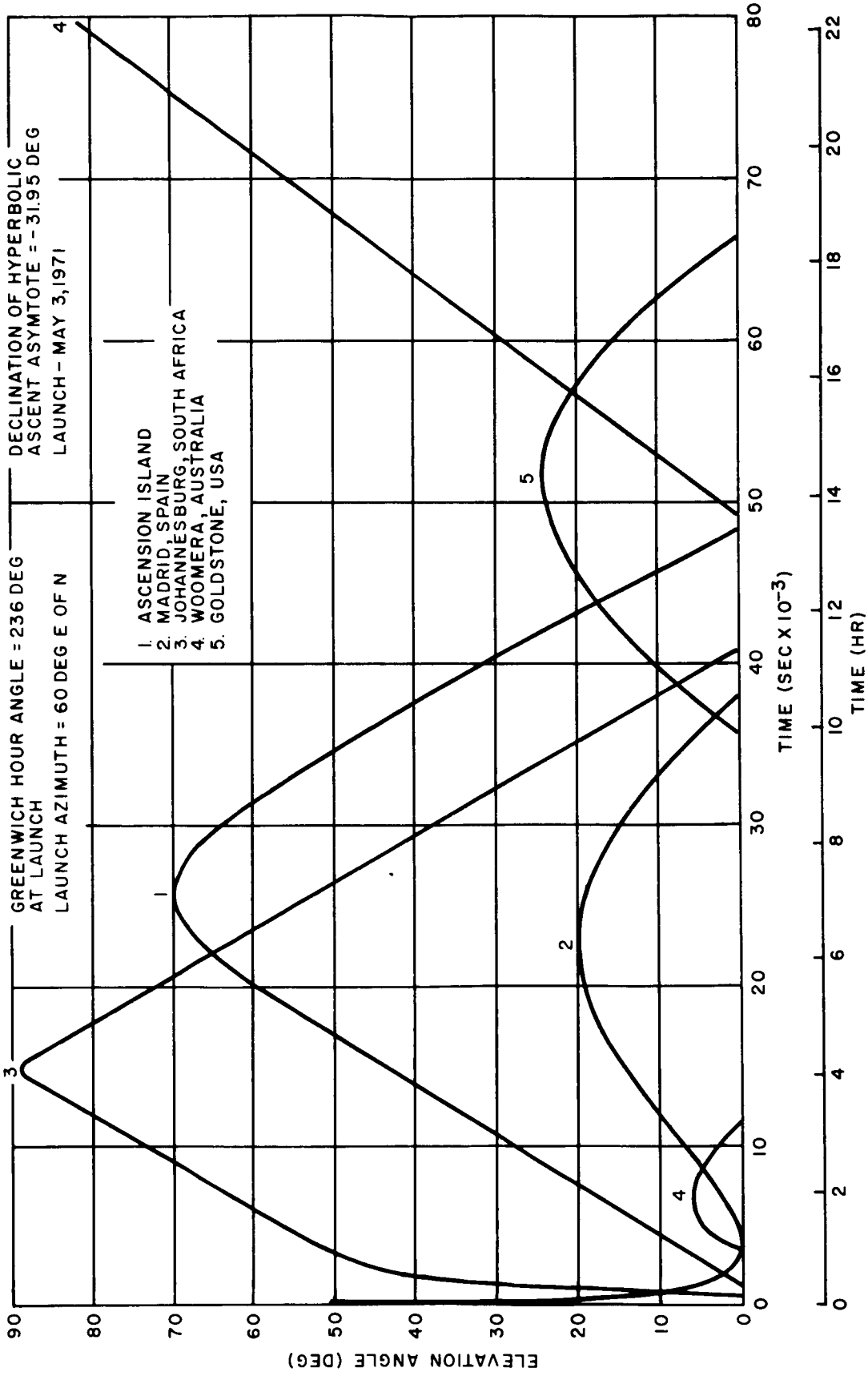


Figure 3-11. Earth Tracking Elevation Angle, End of Window

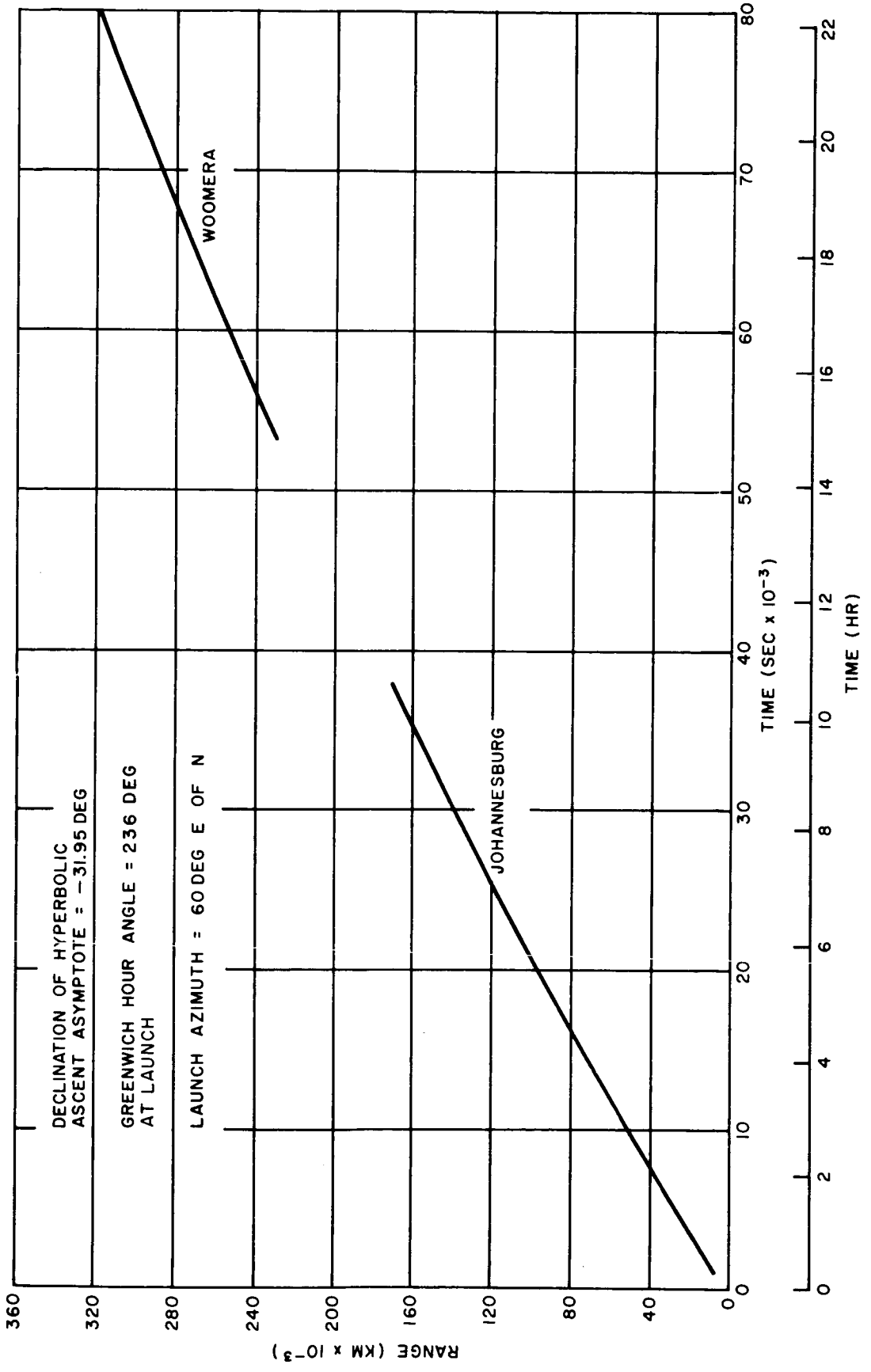


Figure 3-12. Earth Tracking Range, End of Window

c. The following combination of conditions should not hold for more than one to two hours per orbit:

Clock angles of the bright limb of Mars ± 35 degrees
Cone angles of the bright limb of Mars 90 ± 60 degrees

d. The areocentric orbit plane should not be perpdedicular to the Earth-Mars line.

e. The orbit rate should not be zero with respect to the Earth-Mars line.

f. Scientific Guidelines (see Note)

1. Topographic TV Experiment

(a) The area of interest on the planet is between 10 degrees north and 40 degrees south latitude.

(b) The local vertical cone angle must be between 100 and 140 degrees.

(c) The altitude should be as low as possible without causing image motion compensation problems.

2. Color TV Experiment

(a) The area of interest on the planet is between 10 degrees north and 40 degrees south latitude.

(b) The local vertical cone angle should be as close to 180 degrees as possible.

(c) The altitude should be as low as possible without causing image motion compensation problems.

3. Mars Scanner Experiment

(a) The orbital altitude and velocity should be kept constant.

(b) The local vertical cone angle should be greater than 80 degrees.

4. Ultraviolet Spectrometer

(a) The altitude should be kept as low as possible.

(b) The inclination to the ecliptic should be 30 degrees.

5. Dual Frequency Occultation Receiver. Atfer the first few days of arrival, the Earth should be occultated during every orbit for less than a month and then not again.

NOTE

The experiments listed are considered to be typical for a Mars orbiter mission. The selection of a typical set of experiments was made in order to determine the effect of various scientific instrument requirements on the trajectory selection and does not mean that these particular experiments are being proposed for the mission. In the case of the TV and Scanner Experiments, it is desirable to have the ground traces to repeat once every one to three months. The swath widths should be evenly spaced and the period should not exceed the orbital period of Mars.

g. The capsule angle of attack at entry should be as small as possible.

h. The capsule-orbiter range should be as small as possible.

i. The capsule deorbit velocity should be as small as possible.

j. The capsule entry velocity should be as low as possible.

4.3 Capsule Deorbit Maneuver. Several factors, essential to a successful capsule mission, influences not only the choice of the capsule deorbit velocity increment, but also the choice of the deorbit point in the spacecraft orbit and even, to some degree, the spacecraft orbit itself. The factors are shown in Table 4-1. Improvements in any one of these factors usually are accompanied by worsening of others. It has been found, however, that a good compromise solution is achieved when the descent orbit can be made, through rotation of its line of apsides, to intersect the spacecraft orbit at any desired deorbit point as shown in Figure 4-1. That is, the descent path should have the same semimajor axis and eccentricity regardless of the deorbit point.

Selection of a given descent orbit as represented by this compromise solution and an entry path angle fixes the entry velocity and entry location. The effect of deviations from this descent orbit resulting in higher or lower entry velocities and path angles are shown in Figures 4-2, 4-3 and 4-4. Higher velocities and path angles, for example, mean higher ΔV, longer descent time, higher communication range and more positive angles of attack, while entry and landing position angles increase. All of these effects are most pronounced for deorbit near apoapsis.

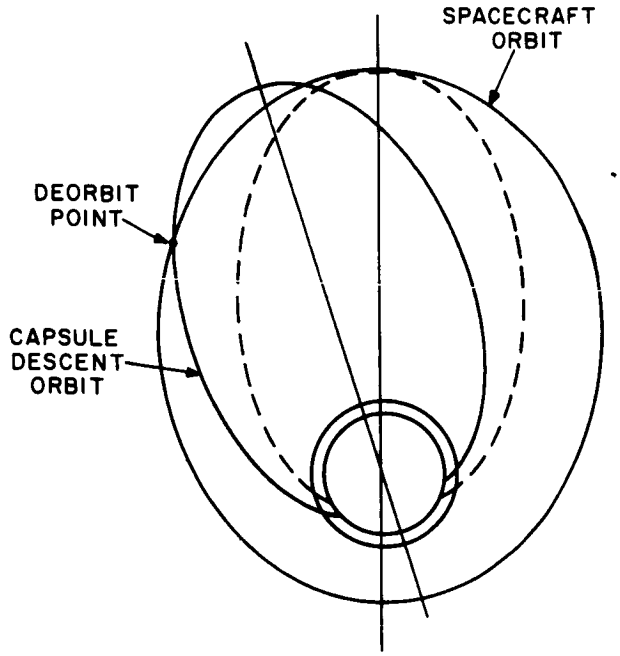


Figure 4-1. Capsule Deorbit Geometry

TABLE 4-1. CAPSULE DEORBIT CONSIDERATIONS

Factor	Influence	Constraints
Magnitude of deorbit velocity increment	Capsule weight, Angular errors	$\Delta V = 550$ m/sec
Direction of deorbit velocity increment	Dispersion, Angle of attack at entry	Minimize dispersion and variation angle of attack at entry
Time elapsed from deorbit to entry	Capsule power requirements, View period from Goldstone, Angular dispersions	12 hr > Time > 50 min
Communication distance from capsule to spacecraft during entry	Communication power, antenna gain	Range < 4000 km
Elevation of spacecraft above capsule horizon during entry	Clear communication line of sight	Elev. > 15 degrees
Entry and impact points relative to spacecraft periapsis point	Location of area for television coverage, Dispersion	Dispersion required, 500 km 3σ desired, 300 km 3σ desired, Control of entry point
Entry angle of attack	Effective M/CDA Stability requirements Exospheric attitude control	< 60 deg definitely without attitude control. < 40 deg desired.
Entry path angle	Loads, Heating, Parachute deployment, Altitude	Vacuum graze to 20 deg
Entry Velocity	Loads, Heating, Parachute deployment, Altitude	< 4.6 km/sec

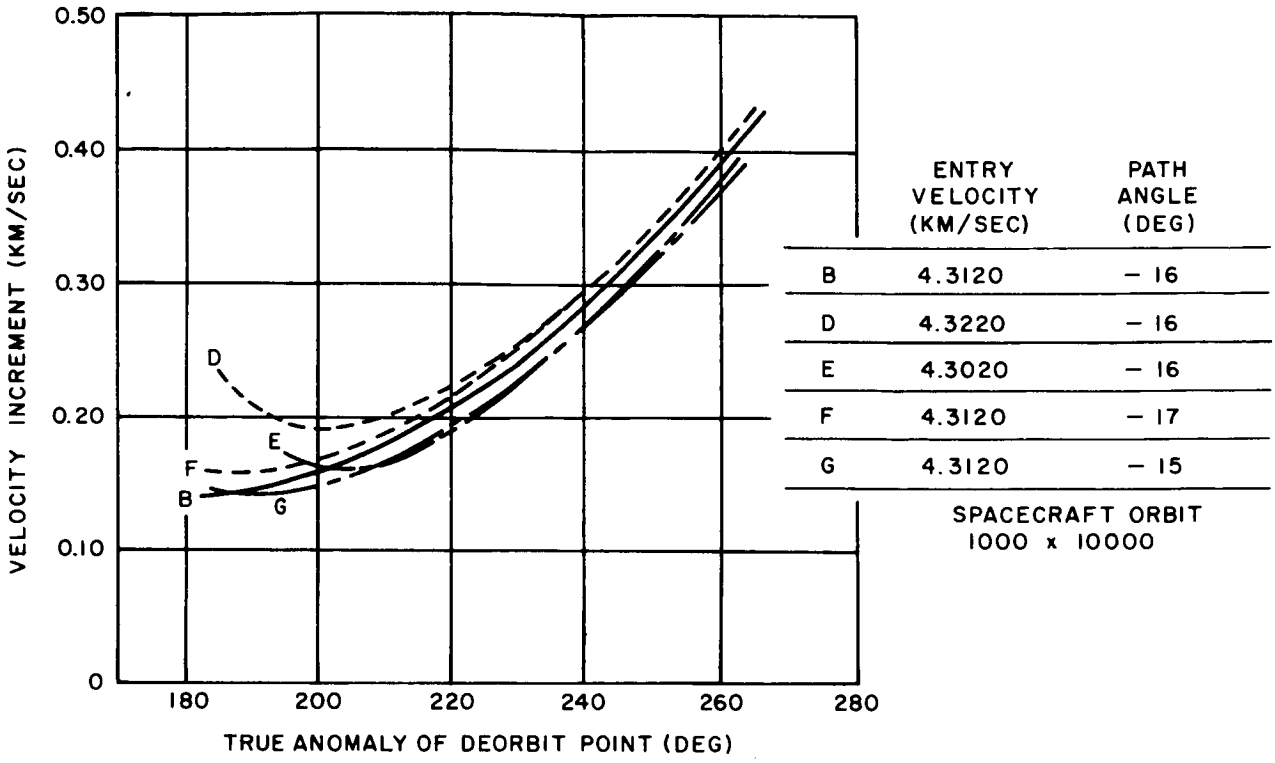


Figure 4-2. Capsule Deorbit, Velocity Increment

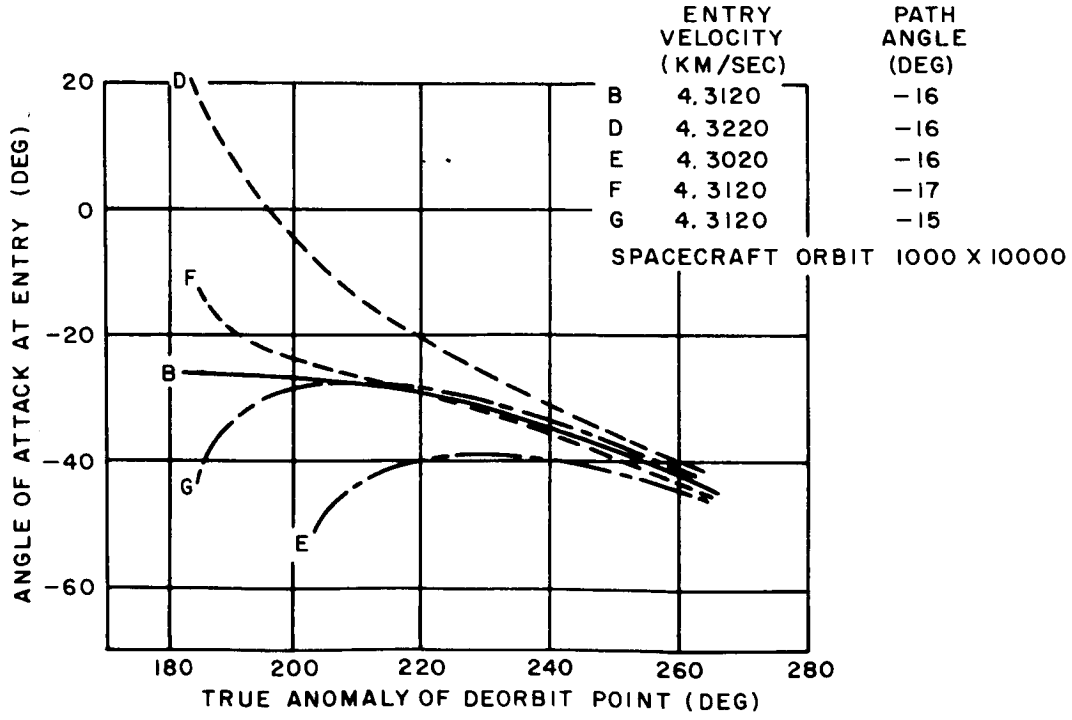


Figure 4-3. Capsule Deorbit, Entry Angle of Attack

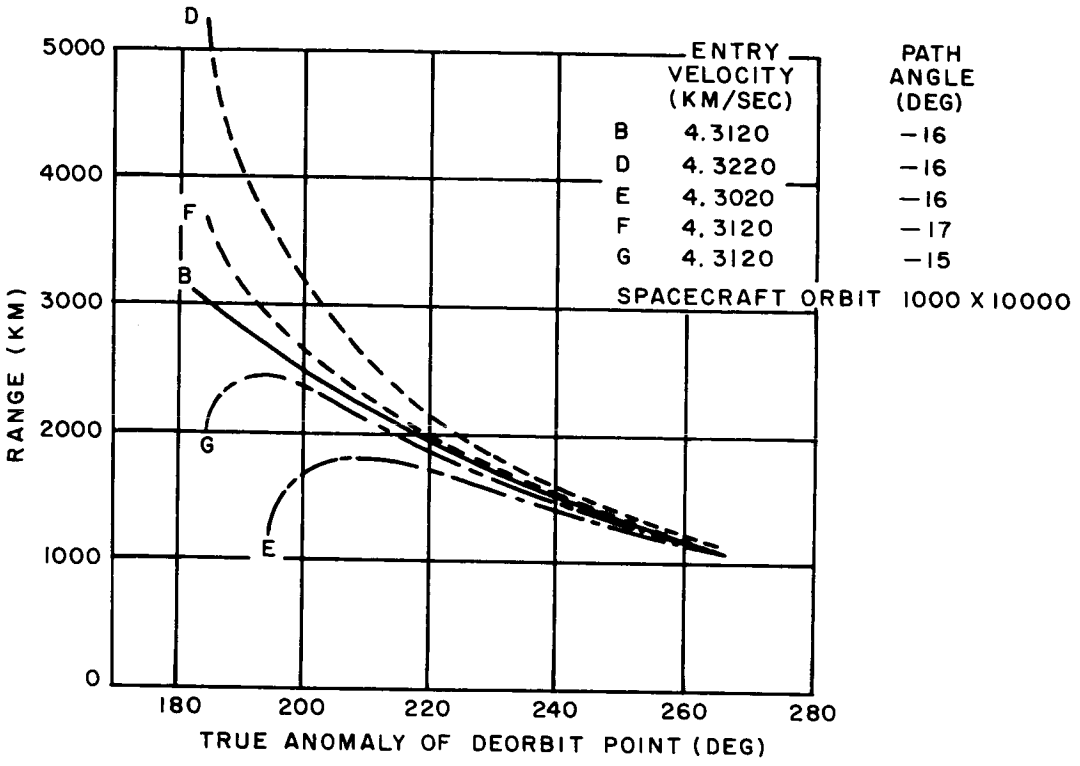


Figure 4-4. Capsule Deorbit, Capsule-Orbiter Range

An analysis constrained to a single set of entry conditions will suffice to evaluate the deorbit opportunities from all points in any given orbit. Applied to a series of orbits, this method enables a rapid screening of deorbit possibilities, and reduces the points of interest to a relatively narrow band in a selected range of spacecraft orbits. Small adjustments in ΔV and entry path angle can be examined about these few points and error sensitivities determined about the most optimum conditions to refine the deorbit point selection.

Table 4-2 indicates the effects of the orbiter true anomaly at the separation point for several orbit altitudes. A good compromise point appears to be a true anomaly of 230 degrees since for higher true anomalies, the velocity increment and angle of attack increase while for

TABLE 4-2. EFFECT OF SEPARATION POINT ON ENTRY PARAMETERS

Orbit		Velocity Increment (km/sec)				Range at Entry (km)				Angle of Attack at Entry (deg)				Time to Entry (min)			
Peri-apsis	Apo-apsis	True Anomaly at Separation				True Anomaly at Separation				True Anomaly at Separation				True Anomaly at Separation			
		220	230	240	250	220	230	240	250	220	230	240	250	220	230	240	250
1000	6000	0.243	0.275	0.314	0.360	1701	1532	1381	1251	34	36	38	41	64.8	55.1	46.6	39.4
2000	6000	0.375	0.413	0.459	0.512	3006	2807	2626	2466	50	31	32	33	73.5	64.8	57.2	50.5
1000	10000	0.201	0.254	0.276	0.325	1926	1690	1491	1325	29	31	35	38	85.4	69.0	55.9	45.5
2000	10000	0.319	0.363	0.416	0.479	3468	3150	2872	2634	25	27	29	31	98.1	81.5	68.5	57.8
1000	15000	0.171	0.206	0.249	0.301	2079	1787	1550	1361	27	30	34	38	106.0	82.2	63.9	50.3
2000	15000	0.275	0.323	0.381	0.458	3800	3374	3017	2725	23	26	28	31	122.0	97.8	78.7	64.1

lower true anomalies the range and time to entry increase. Any of these true anomalies would be acceptable, since none of the parameters violates the constraints.

4.4 Orbit Altitude Selection. The contamination constraint affects the minimum orbital altitude for the areocentric orbit. Using the "Realistic Atmosphere" model in EPD 281, the associated lifetime curves and a ballistic parameter of $M/C_DA = 0.22$ slug/ft^2, the minimum orbit altitude curve shown in Figure 4-5 was derived. The assumed ballistic coefficient is lower than that anticipated for a vehicle of the VOYAGER class giving an additional safety factor in the orbit selection. Next allocating a probability of contamination due to orbiter decay of 2×10^{-5}, a 30% variation in periapsis altitude as specified in the Preliminary Mission Description, and a 1% variation in the injection velocity in the worst case direction, the guidance boundary in Figure 4-5 was derived. In Figure 4-5, only orbits to the right of the curve are allowable. The curves of constant approach velocity shown in Figure 4-5 indicate the minimum orbit altitude obtainable within the 2.2 km/sec specified velocity increment. Capsule deorbit trajectory analyses (Section 4.3) indicate that investigating deorbit trajectories

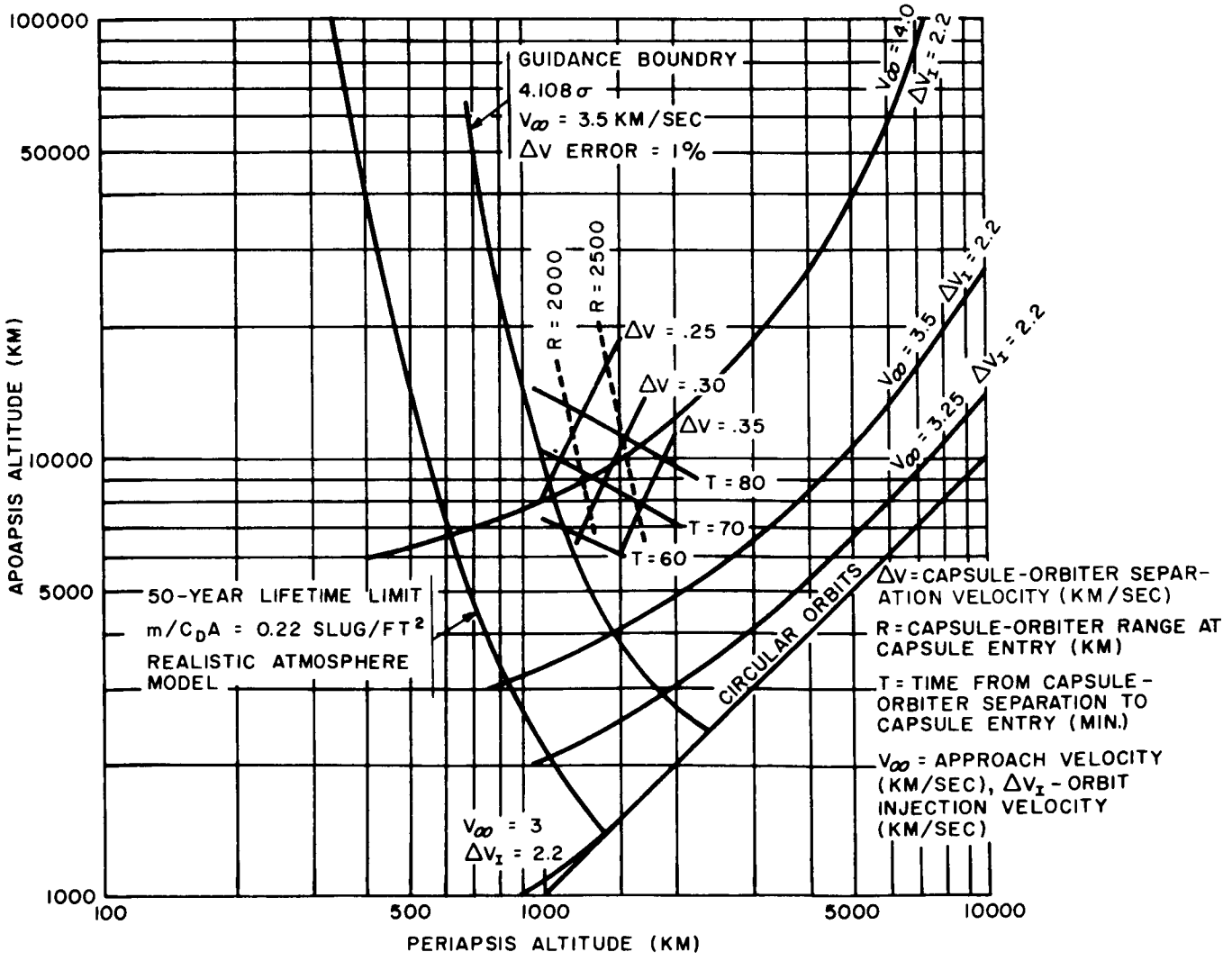


Figure 4-5. Allowable Orbit Altitudes

with entry angles of 16 degrees and separation true anomalies of 230 degrees represents a good compromise with respect to velocity increment, angle of attack, and range. For these conditions lines of constant orbiter-capsule range at entry, separation velocity increment and time from separation to entry are also shown in Figure 4-5.

Examination of Figure 4-5 indicates that a wide range or orbiter altitudes satisfy the constraints as listed. From the scientific measurement viewpoint, a low altitude is desirbale in order to achieve maximum obtainable resolution. The lower altitudes, however, may cause image motion problems. In addition, highly elliptical orbits are undesirable due to the wide variations in sensor focal length requirements. From an engineering viewpoint, the lower altitude orbits result in more frequent occultations and shorter communication time per orbit.

A reasonable orbit altitude which provides a compromise between the competing capsule parameters, planetary contamination constraint, and occultations is an orbit with a periapsis altitude of 1000 kilometers and an apoapsis altitude of 10,000 kilometers. Raising the periapsis to higher values increases the orbiter-capsule range at entry. Decreasing the apoapsis causes an increase in the Sun, Earth and Canopus occultations.

4.5 Capsule Deorbit Trajectory Parameters. The following parameters describe the capsule deorbit trajectory from a 1000 by 10,000 kilometer (altitude) orbit. This trajectory is used for design purposes.

a. Orbiter true anomaly at separation, 230 degrees
b. Deorbit velocity, 217 m/sec
c. Angle between orbiter velocity and separation velocity, 124 degrees
d. Entry velocity, 4.30 km/sec
e. Entry angle, 16 degrees
f. Angle of attach at entry, 39.9 degrees
g. Central angle travel from separation to entry, 100 degrees

The Orbiter-Capsule range and range rate are shown in Figures 4-6 and 4-7, for the standard orbits. The angle between the capsule thrusting direction and the line of sight from the orbiter to the capsule is shown in Figure 4-8. For the four design trajectories, the spacecraft attitude will go off the sun line by 24.7 to 40 degrees. With only this amount of deviation from the sun line, the power output from the solar array will not be less than 76.5% of that when the spacecraft is stabilized to the sun. Thus, with the line of sight to the capsule as shown by Figure 4-8, the spacecraft can be maintained in the capsule separation attitude until after capsule impact; this is desirable in order to provide a high reliability of receiving the capsule data.

4.6 Occultations. The occultations for the 1000 x 10,000 km (altitude) orbit and various launch and arrival dates and orbit inclinations are shown in Table 4-3. The line of apsides of all the trajectories have been rotated such that the capsule will impact 20 degrees from the evening terminator, if deorbit occurs on the day of arrival and the standard capsule descent trajectory is used. The orbit insertion maneuver is visible from the Earth for all the trajectories listed in the table. The orbiter is also visible during the entire capsule descent,

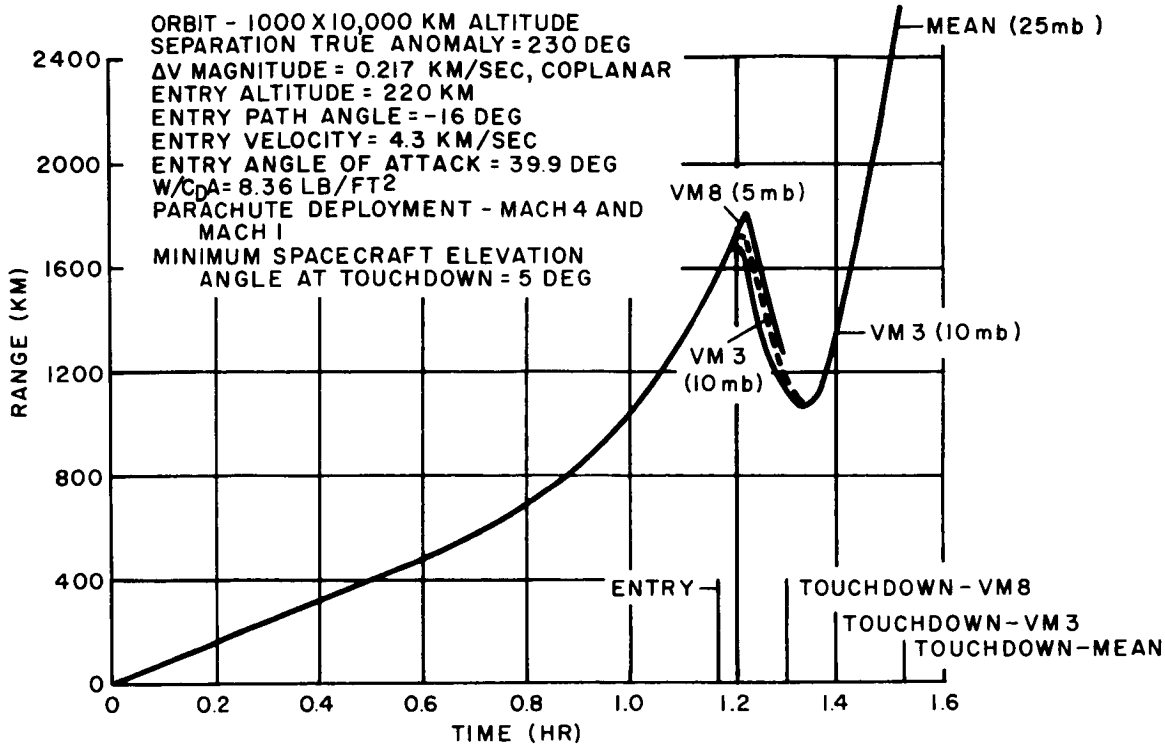


Figure 4-6. Capsule-Orbiter Range

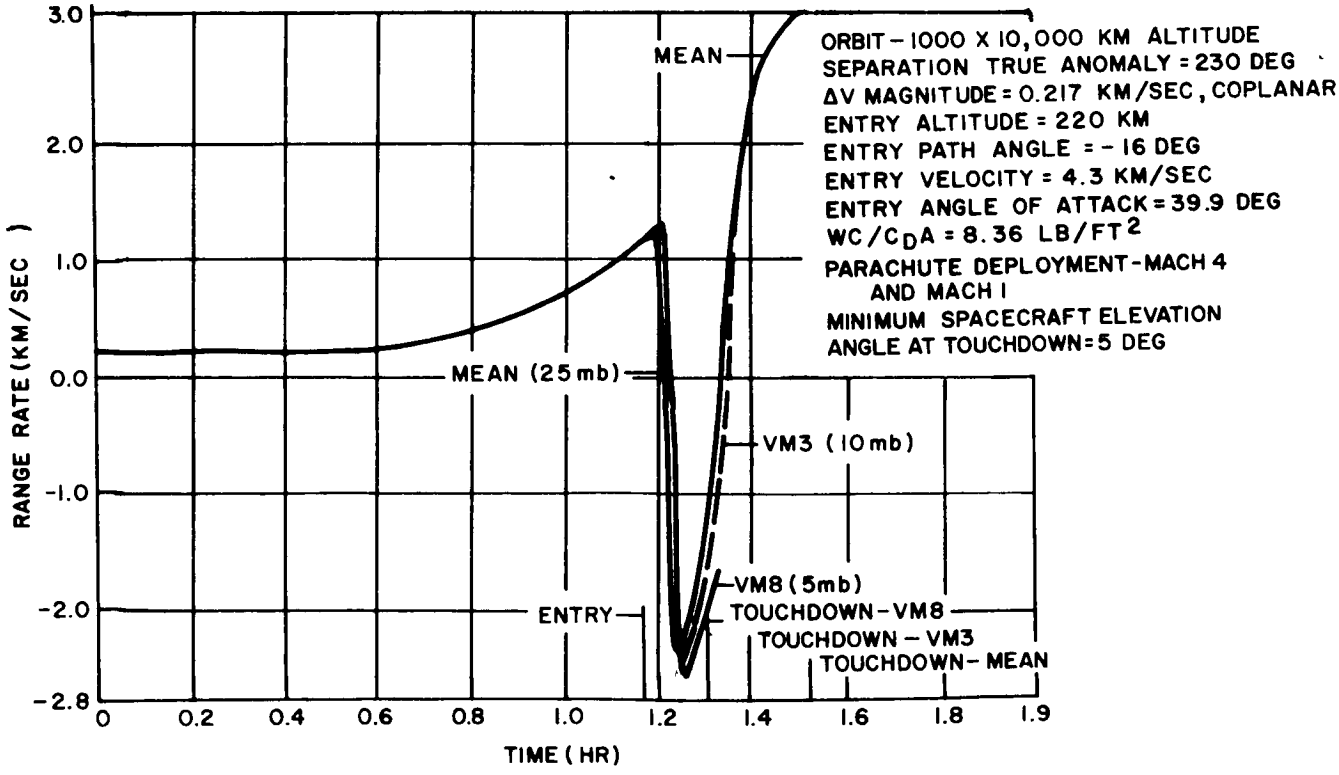


Figure 4-7. Orbiter-Capsule Range Rate

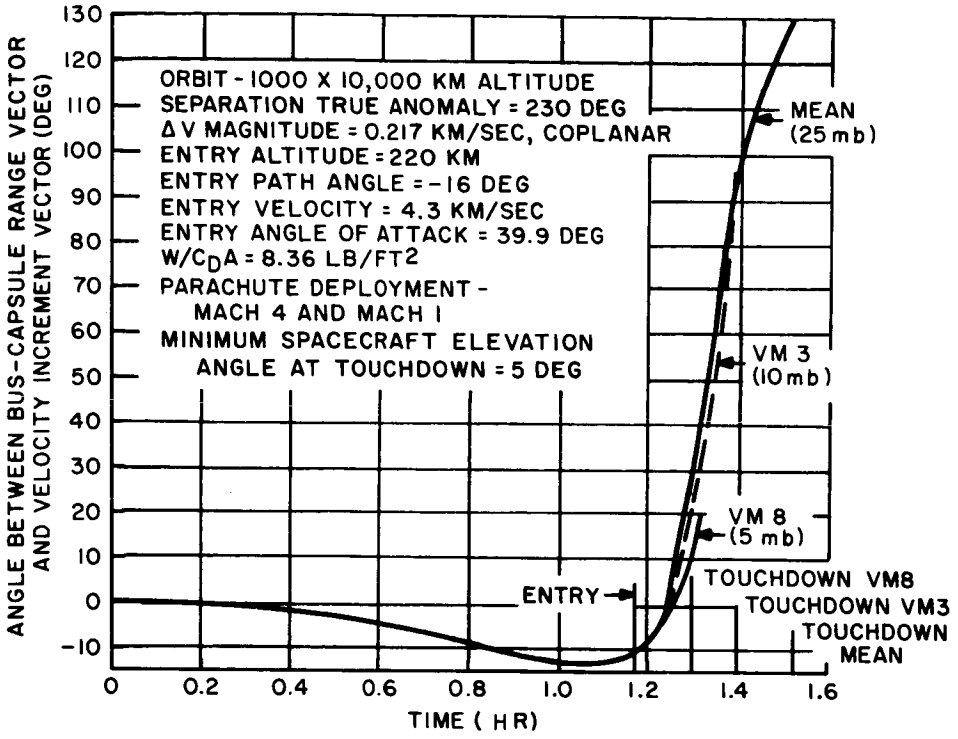


Figure 4-8. Capsule-Orbiter, Line-of-Sight Angle

TABLE 4-3. OCCULTATION TIMES

Launch Date	Arrival Date	Peri-apsis Altitude (km)	Apo-apsis Altitude (km)	Incli-nation (deg)	Rotation (deg)	Earth Occultation Time ~ Minutes Days after Encounter							Sun Occultation Time ~ Minutes Days after Encounter							Star Occultation Time ~ Minutes Days after Encounter						
						0	30	60	90	120	150	180	0	30	60	90	120	150	180	0	30	60	90	120	150	180
May 3	November 1	1000	10000	60	11.5	36.7	26.5	0	0	85.0	0	0	0	0	0	83.4	0	0	0	0	0	0	0	0	10.0	26.7
May 3	November 11	1000	10000	60	19.0	35.5	19.8	0	0	92.3	0	0	0	0	0	93.4	0	0	0	0	0	0	0	0.7	21.7	28.0
June 28	November 17	1000	10000	60	26.0	38.0	26.0	0	0	83.4	0	0	0	0	0	73.3	48.2	0	0	0	0	0	0	0	0	21.7
June 28	November 27	1000	10000	60	34.1	35.3	17.8	0	0	90.9	0	0	0	0	0	87.2	0	0	0	0	0	0	0	0	13.8	24.7
May 3	November 1	1000	10000	40	21.7	35.8	35.3	40.5	42.0	16.7	0	0	41.8	48.8	57.9	10.8	0	0	0	0	0	0	7.5	16.7	11.5	25.7
May 3	November 11	1000	10000	40	28.9	36.3	35.2	40.0	40.8	0	0	0	40.2	50.0	55.7	0	0	0	0	0	0	0	7.0	16.5	20.8	24.0
June 28	November 17	1000	10000	40	34.0	36.8	36.5	39.7	45.2	32.2	0	0	40.8	41.7	59.5	49.7	0	0	0	0	0	0	0	0	13.3	17.8
June 28	November 27	1000	10000	40	42.0	37.3	36.2	39.8	45.7	25.5	0	0	38.3	43.3	54.2	43.3	0	0	0	0	0	0	0	0	7.8	9.3
June 8	December 19	1000	10000	60	53.5	29.9	0	0	57.3	56.3	0	0	0	0	31.5	82.2	0	0	0	0	0	0	0	12.3	21.2	27.2
June 8	November 29	1000	10000	60	31.5	34.8	16.4	0	0	93.0	0	0	0	0	0	91.5	0	0	0	0	0	0	0	0	12.8	24.7
June 8	November 8	1000	10000	60	14.6	38.3	31.4	0	0	57.2	60.2	0	0	0	0	40.8	71.7	0	0	0	0	0	0	0	0	17.2

entry and impact period. The arrival time must be adjusted to ensure that Goldstone is in view during the capsule separation and deorbit maneuvers.

Comparing the last three trajectories in the table indicates that the early arrival dates delay Canopus occultations until a later time in the mission and are, therefore, more desirable from this view point. The first eight trajectories shown in Table 4-3 have relatively early arrival dates and span the launch period. Comparing these indicates that a 60-degree inclination is more favorable (when considering occultation effects) than a 40-degree inclined orbit.

4.8 TV Viewing Parameters. The topographical TV experiment requires low altitude and local vertical cone angles between 100 and 140 degrees. The cone angle is defined in Figure 3-3 as the Sun-orbiter-body angle. In this case the body is the center of Mars. Table 4-4 indicates the altitudes and latitudes of coverage for several early arrival trajectories. The table indicates that the altitudes are optimum near the evening terminator at the start of the mission and at the morning terminator after 180 days in orbit. The 40-degree inclination covers the more desirable latitudes, 10 °N to 40 °S, for topographical TV.

The color TV experiment requires high cone angles near 180 degrees along with low altitudes for best results. Table 4-5 indicates the best color TV conditions exist in the middle of the mission for the 60-degree inclined orbits and near the end of the mission for the 40-degree inclined orbits. The 60-degree inclination orbit gives color TV coverage of scientifically more interesting latitudes.

TABLE 4-4. CONDITIONS FOR TOPOGRAPHIC TV AT DAY ZERO CONE ANGLE 100 ° - 140 °

Days In Orbit	Launch Date	Arrival Date	Inclination (Deg)	Morning Terminator Region					Evening Terminator Region				
				Altitude		Latitude			Altitude		Latitude		
				Min	Max	In	Out	Max	Min	Max	In	Out	Max
0	May 3, 1971	November 1, 1971	60	4250	9200	7	-39	-39	1000	1850	-60	-28	-60
0	May 3, 1971	November 11, 1971	60	3750	9100	- 2	-50	-50	1000	2000	-59	-20	-59
0	June 28, 1971	November 17, 1971	60	4000	9150	7	-42	-42	1000	1900	-60	-28	-60
0	June 28, 1971	November 27, 1971	60	3350	9000	- 2	-53	-53	1000	2150	-60	-20	-60
0	May 3, 1971	November 1, 1971	40	5650	9550	- 3	-29	-29	1000	1550	-33	-10	-33
0	May 3, 1971	November 11, 1971	40	5600	9500	- 9	-32	-32	1000	1550	-30	- 4	-30
0	June 28, 1971	November 17, 1971	40	5600	9050	1	-25	-25	1000	1550	-36	-14	-36
0	June 28, 1971	November 27, 1971	40	5500	9500	- 4	-29	-29	1000	1550	-33	-10	-33
60	May 3, 1971	November 1, 1971	60	1550	3600	-50	-55	-60	1050	1950	- 6	34	34
60	May 3, 1971	November 11, 1971	60	1700	3850	-54	-53	-60	1050	1900	3	40	40
60	June 28, 1971	November 17, 1971	60	1500	3500	-51	-53	-60	1050	1950	- 6	35	35
60	June 28, 1971	November 27, 1971	60	1600	3600	-55	-51	-60	1050	1950	3	41	41
60	May 3, 1971	November 1, 1971	40	4300	8050	-39	-34	-40	1050	1150	11	33	33
60	May 3, 1971	November 11, 1971	40	4400	8150	-40	-31	-40	1030	1200	16	35	35
60	June 28, 1971	November 17, 1971	40	4200	7850	-38	-36	-40	1050	1150	8	31	31
60	June 28, 1971	November 27, 1971	40	4250	7950	-39	-34	-40	1050	1150	12	34	34
120	May 3, 1971	November 1, 1971	60	1050	1850	-57	-29	-57	1800	3800	35	59	59
120	May 3, 1971	November 11, 1971	60	1100	2000	-54	-21	-54	1600	3550	38	60	60
120	June 28, 1971	November 17, 1971	60	1075	1850	-56	-27	-56	1850	3850	37	60	60
120	June 28, 1971	November 27, 1971	60	1050	1095	-53	-22	-53	1700	3150	40	60	60
120	May 3, 1971	November 1, 1971	40	2000	6100	-17	23	23	1050	1300	36	30	40
120	May 3, 1971	November 11, 1971	40	1950	6050	-12	27	27	1200	1300	37	26	40
120	June 28, 1971	November 17, 1971	40	2650	6450	-23	9	-23	1140	1150	36	34	40
120	June 28, 1971	November 27, 1971	40	2650	6450	-19	13	-19	1150	1150	40	28	40
180	May 3, 1971	November 1, 1971	60	1000	2250	-11	-	60	2250	7750	-	37	60
180	May 3, 1971	November 11, 1971	60	1000	2250	- 2	-	60	2250	7900	-	29	60
180	June 28, 1971	November 17, 1971	60	1000	2200	-14	-	60	2200	7650	-	38	60
180	June 28, 1971	November 27, 1971	60	1000	2250	- 6	-	60	2250	7700	-	30	60
180	May 3, 1971	November 1, 1971	40	1700	3850	-20	8	-20	1050	1850	39	32	40
180	May 3, 1971	November 11, 1971	40	1900	4100	33	39	40	1020	1750	4	23	23
180	June 28, 1971	November 17, 1971	40	1800	4250	26	40	40	1000	1700	16	-13	16
180	June 28, 1971	November 27, 1971	40	2000	4400	28	40	40	1000	1600	12	-16	-16

TABLE 4-5. CONDITIONS FOR COLOR TV EXPERIMENT 1971 EXAMPLE MARS ORBITS

Launch Date	Arrival Date	Inclination (Deg)	Day 0			Day 60			Day 120			Day 180		
			Cone ∠	Alt	Lat	Cone ∠	Alt	Lat	Cone ∠	Alt	Lat	Cone ∠	Alt	Lat
May 3, 1971	November 1, 1971	60	146	2900	-53	155	1100	-33	164	1100	3	131	2300	50
May 3, 1971	November 11, 1971	60	143	2700	-58	159	1100	-27	158	1100	9	131	2300	56
June 28, 1971	November 17, 1971	60	145	2900	-55	152	1100	-32	167	1100	7	135	2200	48
June 28, 1971	November 27, 1971	60	142	2700	-58	156	1100	-26	162	1100	11	134	2200	56
May 3, 1971	November 1, 1971	40	163	3000	-39	175	2200	-14	142	1600	30	157	1100	28
May 3, 1971	November 11, 1971	40	163	2900	-39	173	2200	-10	142	1600	33	162	1100	25
June 28, 1971	November 17, 1971	40	163	2900	-39	175	2000	-17	150	1700	25	155	1200	35
June 28, 1971	November 27, 1971	40	161	2900	-39	176	2100	-13	149	1700	29	159	1200	32

4.8 Orbit Inclination Selection. The choice between a 40- and a 60-degree inclination is a compromise between the scientific and engineering parameters. The 40-degree inclination is more favorable for the topographical TV experiment while a 60-degree inclined orbit probably gives better overall color TV coverage when considering lighting, altitude and latitude. The 60-degree inclination, however, eliminates solar occultations in the early parts of the mission and requires less apsidal rotation. Since the scientific experiments are not drastically compromised, a 60-degree inclination orbit is chosen for design purposes.

The selection of the orbit inclination completes the definition of the design orbit. The apsidal rotations, approach velocities, maneuver orbit insertion velocity increment, and location of the line of apsides for the design trajectories and orbit are shown in Table 4-6.

TABLE 4-6. APSIDAL ROTATION PARAMETERS FOR DESIGN TRAJECTORIES

Distance From Terminator if Impact Occurs on Day 1				Case 1*			Case 2*	
Launch Date	Arrival Date	I	V_∞	φr	ΔV_{min}	θT	φr	ΔV_{min}
May 3	Nov. 1	60	3.502	11.5	1.81	27.6	17.5	1.94
May 3	Nov. 11	60	3.195	19.0	1.665	28.1	24.5	1.885
June 28	Nov. 17	60	3.507	26.0	1.895	28.2	32.0	1.84
June 28	Nov. 27	60	3.2865	34.1	1.825	27.7	40.4	1.70
June 8	Dec. 19	60		53.5				
June 8	Nov. 29	60		31.5				
June 8	Nov. 8	60		14.6				

I - Satellite Orbit Inclination
V_∞ - Approach velocity
φr - Apsidal rotation
ΔV - Injection velocity
θT - Angle to terminator of impact point 10 days after arrival

*Case 1 - Capsule impact 20 degrees from the terminator for separation on same day as the orbit injection.

*Case 2 - Capsule impact 15 degrees from the terminator for separation on same day as the orbit injection.

5.0 MIDCOURSE GUIDANCE.

5.1 Guidance Policy. This section presents the results of an investigation to determine required midcourse maneuver execution accuracies which, with a representative guidance policy, will satisfy the following guidance performance requirements for the VOYAGER 1971 Mission:

a. 100 km (3σ) semi-major axis for the aim point dispersion ellipse in the $\overline{R}$, $\overline{T}$ plane at Mars (maximum value).

b. One min (3σ) time of arrival uncertainty (maximum value).

c. Contamination probability of less than 10^{-4} for a single launch; 10^{-4} is assumed for each midcourse maneuver on the basis of an allowable contamination probability due to a maneuver and the probability of correcting the maneuver error.

A precise pre-mission analysis of the multiple maneuver problem requires a complex technique such as Monte Carlo simulation; however, an approximate approach along the lines presented in the JPL document EPD-250* has been utilized in this investigation.

The midcourse requirements investigated for the selected trajectories include:

a. Number of maneuvers and their timing — the velocity correction for a 10-day time of arrival separation is assumed to occur at the first midcourse maneuver.

b. Velocity correction execution accuracies including proportional and non-proportional errors.

c. Biasing of the aim point to satisfy the non-contamination constraint.

In addition, an investigation was made to determine trajectory correction accuracies satisfying a set of guidance conditions initially stipulated in the document "VOYAGER 1971 Preliminary Mission Description", October 15, 1965, p. 35.

5.2 Mathematical Modeling. The velocity correction, $\bar{v}$, for a midcourse maneuver is assumed to be the sum of a constant and a random correction. Assuming an error model developed by C. R. Gates**, the covariance matrix, L_e, for the resultant random execution errors is given by the equation:

$$L_e = (\sigma_s^2 - \sigma_p^2) \quad E(\bar{v}\,\bar{v}^T) \quad + \quad (\sigma_p^2 \bar{V}^2 + \sigma_c^2)\, I$$

where

σ_s = standard deviation of proportional shut-off error

σ_p = standard deviation of per axis pointing error

σ_c = standard deviation of non-proportional errors; the shut-off resolution error σ_r and autopilot error σ_a are assumed to have the value σ_c

$E(\bar{v}\bar{v}^T)$ = second moment of velocity correction

$\bar{V}^2$ = mean square velocity magnitude

This velocity error covariance matrix is then linearly propagated to the target $\bar{T}$, $\bar{R}$, $\bar{S}$ coordinates using the transition matrix, F, to obtain the covariance matrix, Λ , for the target dispersion errors,

$$\Lambda = F\, L_e\, F^T$$

*"Mariner Mars 1969 Orbiter Technical Feasibility Study", 16 November 1964

**C.R. Gates, "A Simplified Model of Midcourse Maneuver Execution Errors", JPL TR-32-504

The transition matrix sensitivity coefficients for the first midcourse correction are obtained from the JPL compilation of Earth-Mars Trajectories (JPL TM 33-100 Vol. 1, Part A). For the subsequent midcourse corrections, the sensitivity coefficients are assumed to be directly proportional to the propagation time with no coordinate rotation.

To determine the required biasing to satisfy the non-contamination constraint, the following assumptions are made concerning the probability distribution of the target dispersion errors:

a. Since the first velocity correction is predominately a constant correction for time of arrival separation, the resultant dispersion errors are approximately gaussian. A biasing locus in the $\overline{R}$, $\overline{T}$ plane satisfying the probability constraint is then obtained by integrating this assumed gaussian distribution over the effective capture area.

b. Since the second velocity correction is highly random, the resultant dispersion errors (products of gaussian errors) are decidedly non-gaussian. A biasing locus in the $\overline{R}$, $\overline{T}$ plane is obtained assuming a 3.9σ dispersion ellipse (see EPD-250).

5.3 Maneuver Requirements. Using the analysis described in Section 5.2, an investigation of midcourse maneuver requirements satisfying the performance requirements listed in Section 5.1, was performed for the following selected trajectories:

Designation	A	D
Launch Date	5/3/71	6/28/71
Arrival Date	11/1/71	11/27/71
Flight Time (days)	182	152
Time of Arrival Separation Velocity (m/sec)	44.3 (-5 days)	96.6 (+ 5 days)

The assumed values for the error sources are:

a. Velocity correction for injection errors is assumed spherically distributed with $V_{rms} = 10$ m/sec.

b. The following 1σ execution errors are considered:

Pointing	σ_p	= 0.87 deg and 0.57 deg
Shutoff	σ_s	= 0.2%
Resolution	σ_r	= 0.009 m/sec
Autopilot	σ_a	= 0.009 m/sec

c. The following orbit determination uncertainties are assumed when determing the velocity correction for the last maneuver:

SG1 = 500 km (3σ)
SG2 = 500 km (3σ)
SG3 = 3 min (3σ)

Table 5-1 presents the maneuver sequence and resulting dispersion errors for a pointing error of 1.7 and 2.6 (3σ) degrees and for the two trajectories A and D. No biasing from the first aim point is assumed at injection. Actually a bias will be required to satisfy the non-contamination constraint. The removal of this bias at the first maneuver will require a velocity correction of the order of 10 m/sec and will be nearly perpendicular to the velocity correction for time of arrival separation; hence, its effect on these results will be very small. A minimum bias distance was used in determining the first aim point. The effective capture radii were assumed to be 6570 km for trajectory D and 6300 km for trajectory A. Radial biasing was used in determining the second aim point (the resulting bias distance is nearly minimal).

Comparison of the results in Table 5-1 indicates that trajectory D is a worst case trajectory with respect to the propagation of maneuver errors. This is due to:

a. The larger velocity correction required for the five-day time of flight adjustment.
b. The larger sensitivity coefficients for propagation of velocity errors to the $\bar{R}$, $\bar{T}$ target plane.

For trajectory D and a 2.6-degree pointing error, the dispersion values of 82.8 (3σ) km and 24.9 (3σ) seconds, SG1 and SG3, respectively, satisfy the guidance requirements of 100 km and 60 seconds.

TABLE 5-1. MANEUVER SEQUENCES AND GUIDANCE ERRORS

Trajectory	Pointing Accuracy (3σ) (deg)	Maneuver Time	Velocity Correction Mean m/sec	Velocity Correction RMS m/sec	Aiming Point Impact Parameter (km)	Aiming Point θ (deg)	Bias (km)	SG1 (1σ) (km)	SG2 (1σ) (km)	THA (deg)	SG3 (1σ) (sec)
D	2.6	Injection + 5 days	96.6	97.0	39,200	94.3	34,400	23,300	9770	16.9	9340
		Encounter - 30 days	13.3	20.3	9260	41.6	1470	710	585	12.6	196
		Encounter - 10 days	1.7	2.2	7790	41.6	0	27.6	16.3	-50.1	8.3
D	1.7	Injection + 5 days	96.6	97.0	28,500	89.5	23,900	15,400	6440	16.9	6120
		Encounter - 30 days	9.2	13.7	7790	41.6	0	319	256	13.7	89
		Encounter - 10 days	0	0.6	7790	41.6	0	9.3	9.1	-76.2	2.8
A	2.6	Injection + 5 days	44.3	45.4	15,800	71.0	10,370	6410	2830	7.7	5630
		Encounter - 30 days	3.9	9.0	7580	40.5	540	336	311	+ 1.6	54
		Encounter - 10 days	0.6	0.9	7040	40.5	0	13.2	10.5	-51.2	3.9

The most significant error source is the pointing error in that the values for the final dispersions after the third correction are almost entirely dependent on pointing error. In fact, with a 2.6-degree (3σ) pointing accuracy, the resolution and autopilot errors can be doubled and the shutoff error increased by a factor of three without exceeding the 100 km guidance requirement. Table 5-1 also indicates that a 1.7-degree (3σ) pointing accuracy is required to eliminate the need for biasing at the second maneuver for trajectory D.

An investigation was also made to determine required trajectory correction accuracies to achieve a maximum 3σ semi-major axis for the dispersion ellipse in the $\overline{R}$, $\overline{T}$ plane at Mars of 100 km under the following assumed conditions:

a. Launch date 5/24/71
   Arrival date 11/18/71

b. A 3σ injection error (a 1σ miss is assumed to be correctable with a velocity increment of 10 m/sec)

c. First maneuver at 5 days after injection; second maneuver at 30 days prior to encounter.

d. No orbit determination error

e. No arrival date separation or biasing

Assuming the following 1σ execution errors:

Shutoff	σ_s	=	0.2%
Resolution	σ_r	=	0.005 m/sec
Autopilot	σ_a	=	0.005 m/sec

the required pointing accuracy is

Pointing Accuracy (3σ)	Injection Error Spherically Distributed
1.43 deg	V_{RMS} = 10 m/sec (random)
0.82 deg	V = 30 m/sec (constant)

6.0 ORBIT INSERTION.

6.1 Orbit Insertion Guidance Analysis. Analysis of desirable capsule descent trajectories indicates that the periapsis of the satellite orbit should be close to the evening terminator to ensure capsule impact within a region 15 to 30 degrees from the terminator. This requires a positive (in the direction of motion) apsidal rotation at injection of varying amounts depending on arrival velocity and arrival date. For the four trajectories considered, ranging from a May 3, 1971 launch and arrival dates of November 1 and November 11, 1971 to a June 28, 1971 launch date and arrival dates of November 17, 1971 and November 23, 1971, the required apsidal rotation (for a 60-degree inclination) varies from 11.5 to 34.1 degrees. The approach velocity varies from 3.195 km/sec to 3.507 km/sec.

For a given approach velocity, apsidal rotation and orbit shape, there is an optimum impact parameter and transfer point which results in a minimum orbit insertion velocity increment which is given in Figure 6-1. For the above cases this minimum varies from 1.665 km/sec to 1.895 km/sec. Since a solid retro engine is to be used, it is desirable to plan the orbit injection maneuver so that a fixed impulse will suffice for all cases. This can be done by

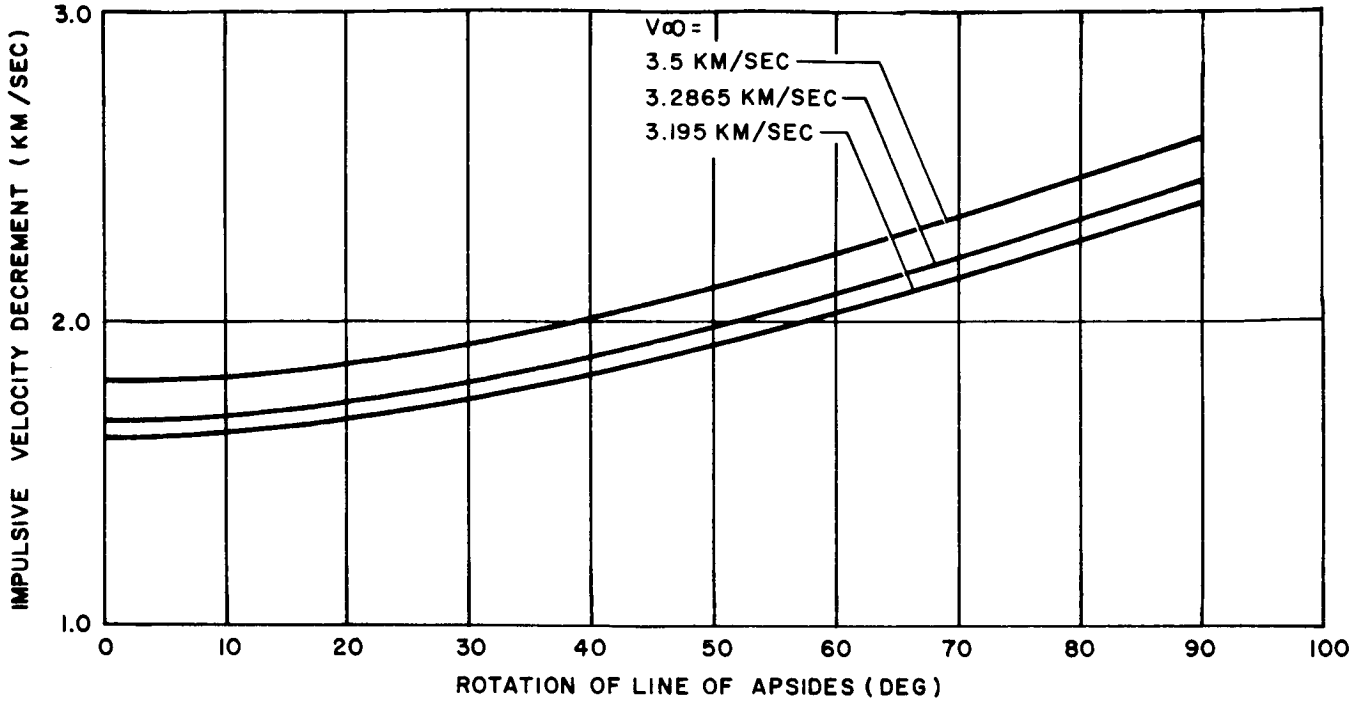
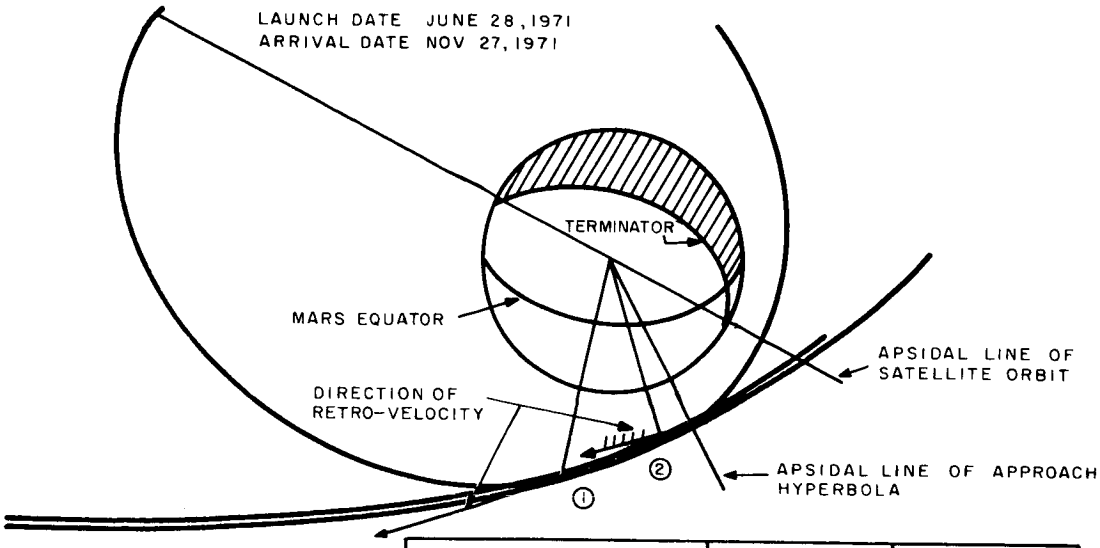


Figure 6-1. Minimum Insertion Velocity with Apsidal Rotation

using an impact parameter and transfer point which are different from the optimum so as to increase the required ΔV by an amount sufficient to bring the impulse for all cases, required ΔV and injected weight, to the same value. For such non-optimum transfers, there are always two combinations of impact parameter and transfer point which yield the same orbit using a given ΔV; Figure 6-2 shows these two injection conditions for a typical case. Table 6-1 lists the approach velocity, impact parameter, apsidal rotation, true anomaly of transfer point and angle of the ΔV direction with respect to the local horizonal, resulting in a fixed ΔV of 1.90 km/sec for the four selected trajectories. Two injection conditions are listed for each case. The higher impact parameter trajectory is designated condition (1) and the lower impact parameter condition (2). The higher impact parameter is preferable from a guidance viewpoint; however, since transfer occurs earlier, the sensitivity of the orbit to injection errors is larger and there is a higher probability of exhaust products impacting Mars. The preferred injection condition, therefore, is the one associated with a lower impact parameter and injection close to the periapsis of the approach hyperbola.

In the event of a premature capsule separation (prior to orbit insertion), the orbit insertion ΔV obtained, assuming all the retro fuel is burned, is increased by about 1 km/sec. For most injection conditions, if the nominal time and direction of retro thrust are used, the resulting orbit would impact the planet. By changing the time and direction of retro thrust, a 1000 by 10,000 km orbit can still be obtained; however, the apsidal line will be rotated by about 70 degrees. If the impact parameter of the approach hyperbola is reduced by 500 km, a 1,000 by 10,000 KM altitude orbit can be obtained with about 55 degrees apsidal rotation.



V ∞ = 3.286 KM/SEC

ΔV INJECTION = 1.90 KM/SEC

1000 X 10000 ORBIT

APSIDAL ROTATION = -34.1 DEG.

	CONDITION ①	CONDITION ②
HYPERBOLIC PERIAPSIS ALTITUDE (KM)	1574 KM	1365 KM
HYPERBOLIC TRUE ANOMALY AT INJECTION (DEG)	-36.1	-4.7
DIRECTION OF RETRO THRUST (MEASURED CCW FROM DIRECTION OF TRAVEL) (DEG)	184.3	160.6

Figure 6-2. Orbit Insertion Geometry

TABLE 6-1. ORBIT INSERTION PARAMETERS

	Condition	i (deg)	V_{hp}	$\Delta\varphi$	ΔV	h_p	h_i	ν_h	V_h	V_e	ν_e	γ_h	γ_e	β
May 3-Nov. 1	1	60	3.50	11.5	1.9	1009.5	1300.4	-24.40	5.527	3.670	-35.93	-16.97	11.89	189.81
May 3-Nov. 1	2	60	3.50	11.5	1.9	953.0	1000.3	10.12	5.639	3.836	-1.21	7.00	-0.41	164.92
May 3-Nov. 1	1	40	3.50	21.7	1.9	1216.1	1517.5	-24.19	5.453	3.558	-46.64	-16.95	-15.26	183.16
May 3-Nov. 1	2	40	3.50	21.7	1.9	1137.0	1140.2	-2.59	5.585	3.756	-24.76	-1.80	-8.26	167.15
May 3-Nov. 11	1	60	3.195	19.0	1.9	985.4	1985.6	-43.11	5.125	3.351	-62.05	-29.25	-19.85	196.74
May 3-Nov. 11	2	60	3.195	19.0	1.9	841.0	1000.1	18.94	5.455	3.836	0.55	12.67	0.18	154.12
June 28-Nov. 17	1	60	3.507	26.0	1.9	1310.4	1459.3	-17.00	5.477	3.587	-44.07	-11.94	-14.46	175.23
June 28-Nov. 17	2	60	3.507	26.0	1.9	1298.4	1405.9	-14.51	5.495	3.614	-41.54	-10.19	-13.67	173.36
June 28-Nov. 27	1	60	3.2865	34.1	1.9	1573.7	1365.4	-36.14	5.078	3.187	-72.20	-25.22	-22.64	184.34
June 28-Nov. 27	2	60	3.2865	34.1	1.9	2337.9	1376.3	-4.67	5.367	3.630	-40.06	3.21	-13.20	160.64

i - inclination
V_{hp} - approach velocity
$\Delta\varphi$ - apsidal rotation
ΔV - injection velocity impulse
h_p - periapsis altitude of approach hyperbola
h_i - injection altitude
ν_h - true anomaly of injection point on hyperbola
V_h - velocity before injection
V_e - velocity after injection
ν_e - true anomaly of injection point on ellipse
γ_h - path angle of hyperbola at injection
γ_e - path angle of ellipse at injection
β - firing angle

6.2 Orbit Insertion Error Analysis. A previous study of the orbit insertion problem (Task A, VOYAGER Study, CII-VB220AA102-5) provided the following conclusions:

a. For small dispersions in the error sources, the results obtained using impulsive thrusting are in good agreement with the results obtained using non-impulsive thrusting (non-zero burn time).

b. The approach velocity (v_∞) can be determined very accurately so that the effect of this error source can be neglected.

c. The error in the knowledge of the gravitational constant of Mars can also be neglected since the present uncertainty in this quantity should be greatly reduced by 1971.

d. The following error sources have been shown to be the major contributors to deviations from the desired nominal orbit:

1. DSIF Timing Error - This error source corresponds to a translation along the nominal approach trajectory (time of flight error).

2. DSIF Impact Parameter Error - This error source corresponds to an in-plane translation of the trajectory which is normal to the nominal approach asymptote. This error results in an off-nominal approach trajectory which affects time and location of periapsis passage (hyperbolic trajectory) and produces correlated position and velocity errors at the nominal time of orbit injection.

3. Velocity Increment Error - This is an error which results from off-nominal operation of the solid fuel rocket used for orbit injection and small variations in vehicle weight.

4. Thrust Orientation Error - The attitude control system is the major contributor to this error.

e. The four error sources listed in d, above, can be considered to be independent of each other.

Studies of the orbit injection propulsion system, which utilizes a solid fuel rocket, indicate that the three sigma error in velocity increment can be held to within 1% of the nominal velocity increment. The three sigma values for the error in thrust direction is two degrees or less when all factors which contribute to this error source are considered. These two error sources are associated with the injection process.

The specified errors as given in the "Preliminary Mission Description" result in the following navigation and guidance errors:

a. The timing error has a three-sigma value of 67.2 seconds.
b. The impact parameter error has a three-sigma value of 316 kilometers.

All statistical values given above assume a Gaussian distribution with zero bias.

Since previous studies have demonstrated that results obtained by considering the error sources to be independent are in good agreement with results obtained using Monte Carlo techniques, the dispersions in the orbital elements given in Table 6-2 are obtained by calculating the square root of the sum of the squares of the three-sigma dispersions obtained for each of the four contributing error sources defined above.

TABLE 6-2. ORBIT PARAMETER DEVIATION

Injection Conditions	DISPERSION IN ORBITAL ELEMENTS			
	Periapsis Altitude (3 σ) (Km)	Apoapsis Altitude (3 σ) (Km)	Apsidal Rotation (3 σ) (Deg)	Period (3 σ) (hr)
Nov. 1, 1971				
Condition (1)*	316	1910	4.83	1.30
Condition (2)*	260	1340	4.31	0.89
Nov. 27, 1971				
Condition (1)*	326	1210	4.33	0.88
Condition (2)*	244	1290	3.72	0.84

*Refer to Figure 6-2.

The breakdown of the total errors for Condition (2) of the November 1, 1971 arrival date is given in Table 6-3. Periapsis altitude, the element which most affects orbit decay, is not appreciably affected by any of the error sources except for errors in the impact parameter. However, relatively large changes in apoapsis altitude can result from each of the error sources considered and these result in corresponding changes in the period.

TABLE 6-3. ORBIT INSERTION ERROR SENSITIVITIES

Error Source	Periapsis Altitude (km)	Apoapsis Altitude (km)	Apsidal Rotation (Deg)	Period (Hr)
Thrust direction, -2 deg	-3	+799	+2.60	+0.50
Thrust direction, +2 deg	0	-644	-2.80	-0.40
Time of flight, -67.2 sec	-54	-625	+3.25	-0.40
Time of flight, +67.2 sec	+48	+851	-2.85	+0.54
Thrust magnitude, +1%	0	-481	+0.35	-0.30
Thrust magnitude, -1%	0	+512	-0.33	+0.30
Impact parameter, +316 km	+254	+427	+0.02	+0.41
Impact parameter, -316 km	-248	-198	-0.06	-0.27
RSS error	260	1340	4.31	0.89

On the basis of these results, even the worst case combination of errors will not prevent capture of the spacecraft by Mars. The injection conditions corresponding to Condition (2) for both injection dates result in smaller dispersions in the orbital elements as compared with the corresponding Condition 1 results. Also, for both of these Condition (2) injection conditions, the velocity increment of 1.9 km/sec can be added to the initial velocity vector in any direction without causing the spacecraft to pass below an altitude of 220 km at the point of closest approach to Mars on the resulting trajectory. In contrast, for both of the Condition (1) injection conditions, impact will occur if the same velocity increment is added to the initial velocity vector in certain directions. Condition (1) results. Therefore, Condition (2) injection should be used for orbit injection. The maximum three-sigma dispersions in periapsis altitude and apoapsis altitude are 260 km and 1340 km, respectively, with a corresponding dispersion in period of 0.89 hour. Based on present estimates of the Martian atmosphere, atmospheric capture of the spacecraft will not occur during the fifty-year period following orbit insertion for the worst case orbit. The corresponding three-sigma dispersion in the in-plane orbit rotation is 4.31 degrees.

The nominal inclination of the orbital plane is 60 degrees. The inclination is influenced by errors in impact parameter which are normal to the nominal plane of the approach trajectory, and by errors in thrust direction which are also normal to the nominal plane of the approach trajectory. Using the same values for the three-sigma dispersions of these error sources as were used for the in-plane errors, the three-sigma dispersion for orbit inclination is approximately 2 degrees for condition (2) of the November 1, 1971 arrival date.

7.0 ORBIT TRIM. Four orbit parameters are considered as subject to adjustment after injection into the areocentric orbit. They are: periapsis altitude, apoapsis altitude, inclination, and argument of periapsis, in order of priority. No adjustment of the line of nodes is considered. A solution for the optimum maneuver to accomplish the forementioned adjustments (minimum ΔV) has not been found, but even if it were available, it would not necessarily be suitable because of limited ΔV available for orbit adjustment. For this reason, the requirements for adjustment of each parameter are first presented independently of the other corrections, and secondly the possibility of combining a high and low priority correction in a single maneuver is examined.

Figures 7-1 and 7-2 present the velocity increment required to correct periapsis and apoapsis errors as a function of those errors. A typical maneuver to correct the orbit shape (with the correct priorities) would be a ΔV applied at apoapsis (Figure 7-1) to correct the periapsis error and a ΔV applied at the corrected periapsis (Figure 7-2).

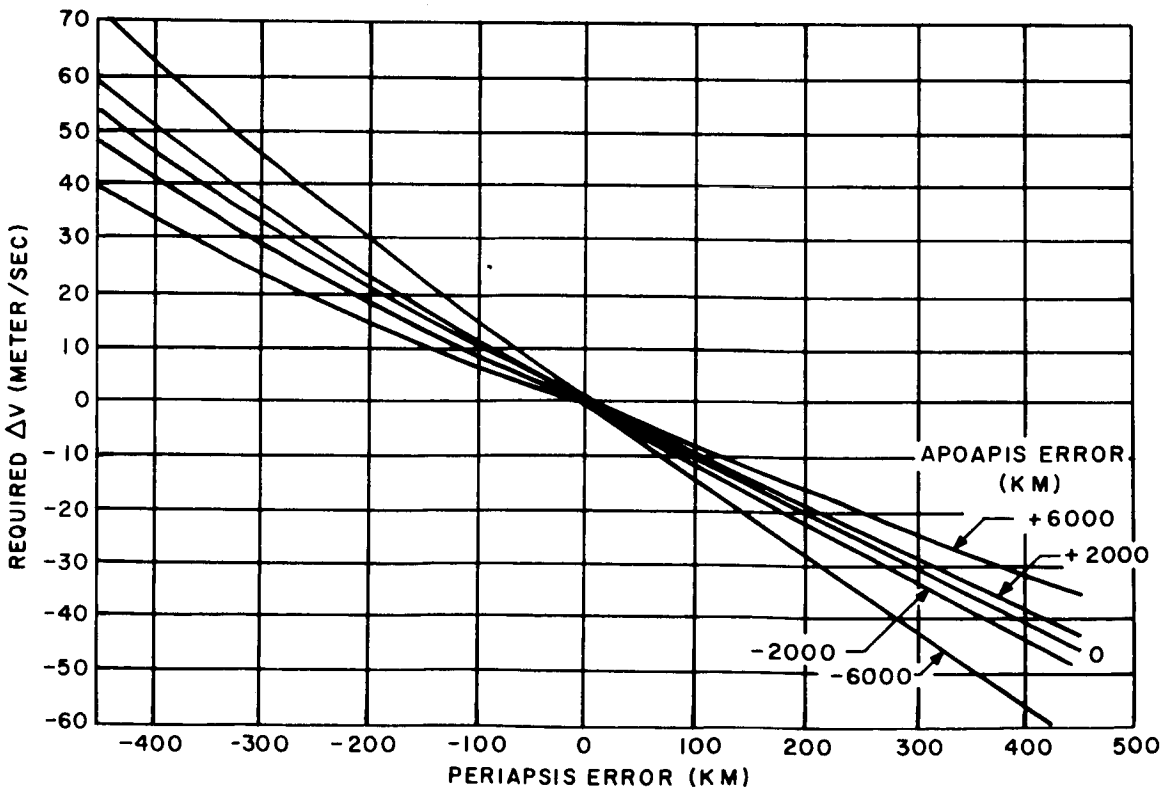


Figure 7-1. Periapsis Error Correction

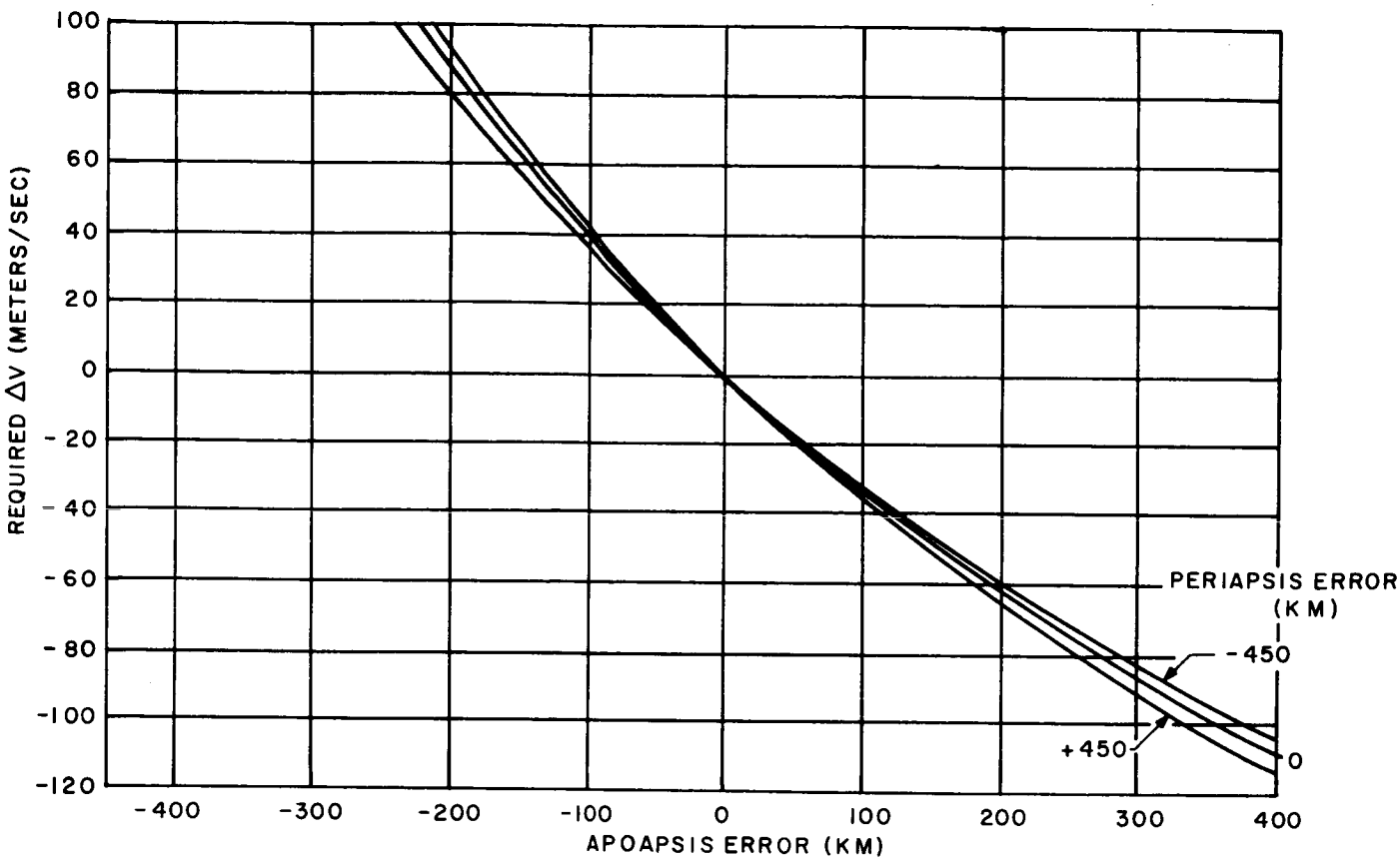


Figure 7-2. Apoapsis Error Correction

Figure 7-3 shows the velocity increment required for a plane (inclination) change or apsidal rotation. The plane change is conducted at the node, and is a function of true anomaly at that point. The ΔV required is, therefore, a function of the argument of periapsis, with the maneuver being conducted at whichever node is closer to the apoapsis. Assuming that orbit trim maneuvers can be executed with the same accuracy as the midcourse corrections, the residual errors in the orbit parameters due to execution errors are negligible compared with the orbit determination errors, so that the accuracy of the orbit after trim is dependent primarily on orbit determination accuracy.

Two methods of accomplishing the apsidal rotation are given. The single impulse maneuver is conducted at the intersection of the old and new orbits. This method has the advantage of requiring a single maneuver, but is relatively costly in terms of velocity change. The optimum method requires two symmetrical impulses applied at the semi-latus-rectums of the old and new orbits, with a large transfer orbit between them.

Figure 7-4 considers a series of combined maneuvers using the total ΔV budget (100 m/sec) for the case when the line of apsides coincides with the line of nodes. This is an idealization, but illustrates the savings obtainable by combining the periapsis correction with a plane change or apsidal rotation. Combining apoapsis corrections with other changes is less advantageous for this situation.

Figures 7-1 through 7-4 show that the assumed errors of ±300 km periapsis altitude, ±5 degrees inclination, and ±10 degrees apsidal rotation cannot all be corrected with a ΔV

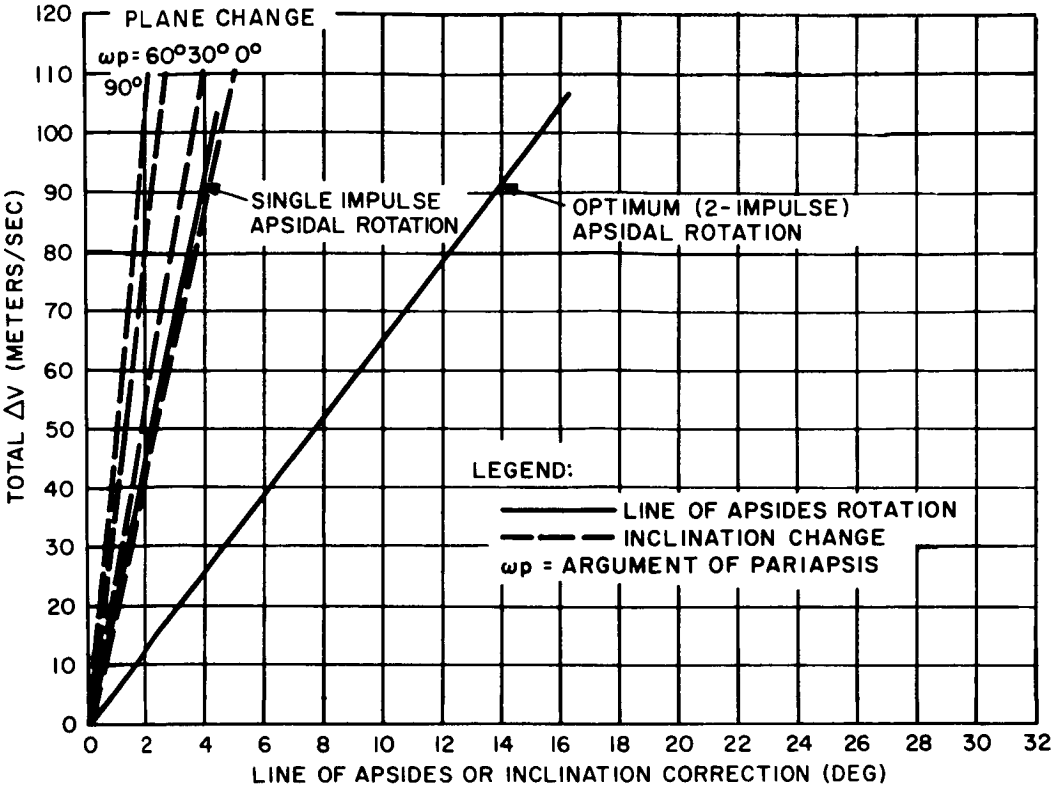


Figure 7-3. Inclination and Line of Apsides Error Correction

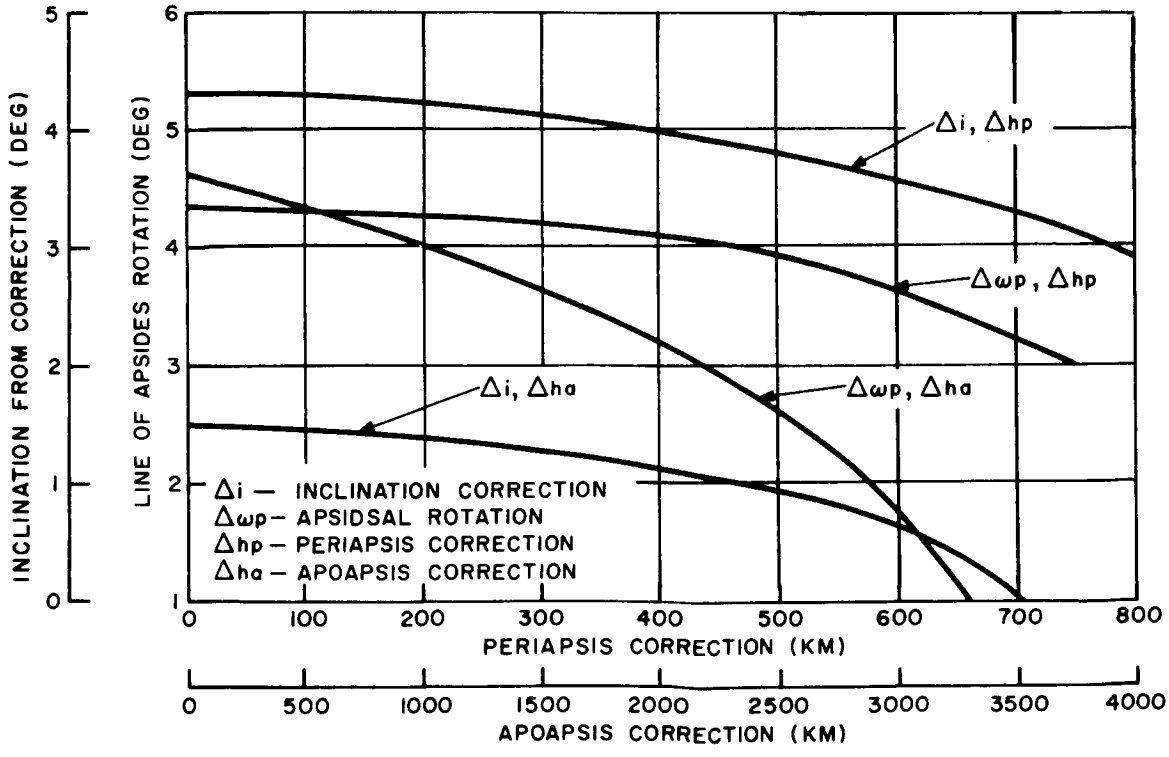


Figure 7-4. Orbit Error Corrections for 100 Meters/Second

capability of 100 m/sec. Figure 7-4 shows (for the idealization considered) that along with a 300-km periapsis correction an apsidal rotation or plane change of slightly more than 4 degrees can be accomplished, but not both. Removal of the idealized restriction and optimization of the trim maneuver requires refinement of injection errors and further analysis.

8.0 CAPSULE DEORBIT

8.1 Orbiter-Lander Separation. Prior to the actual deorbit maneuver, it is necessary to separate the capsule from the orbiter. A small separation velocity is applied to the capsule before the capsule is spun-up. This separation maneuver is made in such a manner that the orientation of the capsule is held fixed to the direction required for the deorbit maneuver. By necessity, the separation velocity is applied in this direction. This separation maneuver is performed to allow the capsule to move far enough away from the orbiter so that after retro propulsion subsequent motion of the capsule and/or large particles from the deorbit rocket will not result in collision with the orbiter.

The maximum coast time from separation to deorbit maneuver is specified as 20 minutes. Using the following nominal deorbit conditions, the separation dynamics betwen orbiter and capsule as a function of time from separation, were analyzed:

True anomaly = 230 deg
Firing angle = 124 deg

The firing angle is measured from the velocity direction, see Figure 8-1. Note that the capsule can be ejected in either of two directions along the firing direction. The results of the analysis are shown in Figure 8-2. The angle, α_{LOS}, is the angle between the line-of-sight from the orbiter to the capsule and the deorbit firing direction. The range, R_{LOS}, is the line-of-sight distance from the orbiter to the capsule.

From the data of Figure 8-2 it is possible to determine the probability of collision between deorbit rocket particles. The probability density representing the dispersion due to pointing inaccuracies during firing is:

$$p(d, \sigma) = \frac{1}{2\pi\sigma^2} \quad e^{-1/2 \frac{d^2}{\sigma^2}}$$

where

σ is the standard deviation of dispersion
d is the minimum distance between capsule or capsule rocket pieces and the orbiter

The probability of impacting an area A centered at a distance d from the center of the dispersion is approximately:

$$p(\sigma) \approx \frac{A}{2\pi\sigma^2} \quad e^{-1/2 \frac{d^2}{\sigma^2}}$$

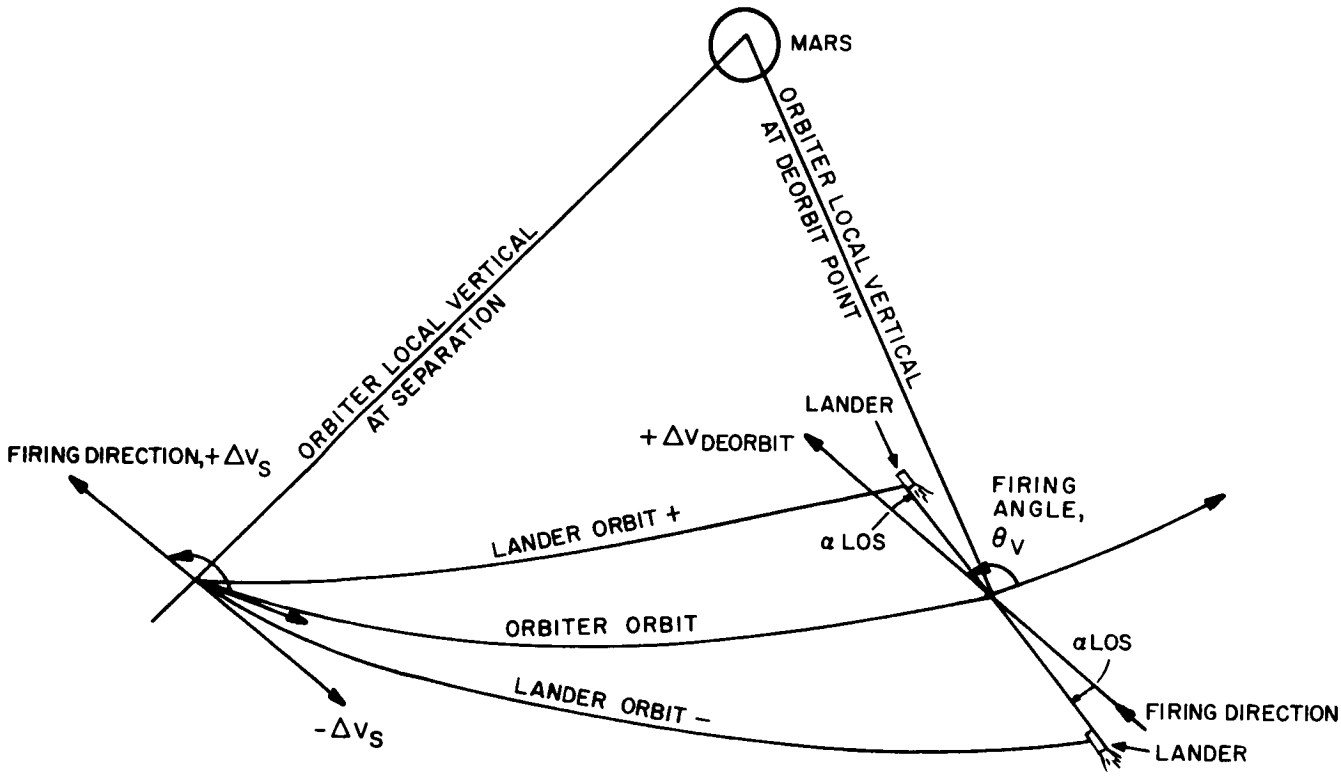


Figure 8-1. Capsule Separation Geometry

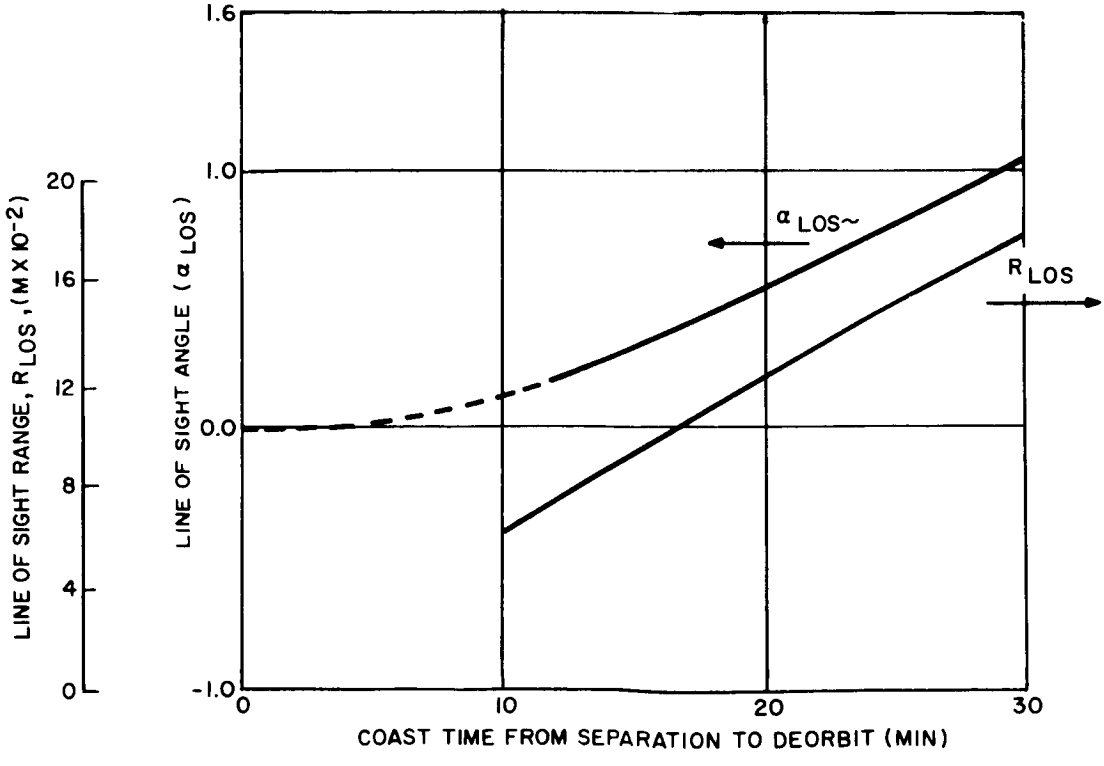


Figure 8-2. Capsule-Orbiter Separation

Assuming a one-m/sec separation velocity between the capsule and the orbiter and a 20-minute separation time before firing of the capsule engine, the maximum probability (assuming a dispersion $\sigma = d/\sqrt{2}$) of large engine particles striking the orbiter (assumed three-meter radius) is 0.022. For release of the capsule in the opposite direction, the maximum probability of the capsule striking the orbiter is 0.057.

The probability of collision can be reduced by increasing the separation velocity or the time between separation and engine firing. For instance, if the time is increased to 30 minutes, the minimum distance between the center of the orbiter and the capsule or engine particles is increased to approximately three times (36.2 meters) that for a separation time of 20 minutes. This decreases the probability of collision between capsule and orbiter or capsule engine pieces and orbiter by a factor of nine.

8.2 Satellite Orbit Deviation. The flexibility of the capsule deorbit system to accommodate changes in spacecraft orbit is illustrated in Figures 8-3, 8-4, and 8-5. Figure 8-3 shows that for the nominal 1000 x 10000-km orbit the fixed deorbit velocity increment selected for a nominal deorbit at 230 degrees true anomaly can be used at earlier or later deorbit points to provide a shifting of the entry point by nearly 10 degrees central angle. Figures 8-4 and 8-5 show that this same Δ V can be used to deorbit successfully from a larger orbit (1300 x 13000 km) or smaller orbit (700 x 8000 km) with a similar range of entry points; a considerable overlap of entry points for this range of orbits is also possible. Therefore, expected deviations in the orbit size and location of the line of apsides of the spacecraft orbit can, within generous limits, be accommodated by adjustment of the deorbit point and Δ V direction without change in the ΔV magnitude so as to achieve impact at the desired location.

Figure 8-3 also shows that the same entry point can be met with a ΔV which is 50 m/sec lower than the nominal. This permits orientation of the ΔV vector to achieve nearly 140 m/sec velocity increment normal to the plane of the orbit. This would result in a successful deorbit to the same entry point with approximately 4 degrees central angle cross range at the entry point.

In Figures 8-3 through 8-5, the range of entry path angles is approximately vacuum graze to 20 degrees.

8.3 Capsule Deorbit Error Sensitivities. Error sensitivity from deorbit to entry is shown in Table 8-1 for typical errors in both orbit determination and deorbit execution for a 230-degree deorbit true anomaly. The orbit determination errors include periapsis altitude orbital period, gravitational parameter and direction of the line of apsides in the orbital plane. The deorbit execution errors are velocity increment error, velocity increment direction error, and error in time since periapsis passage at which the velocity increment is added. Table 8-2 shows error sensitivities during the atmospheric entry portion of the capsule flight. The total RSS landing dispersion due to these error sensitivities that are based on direct coupling between down-range dispersion and entry path angle errors but otherwise random, normally distributed errors is shown in Table 8-3 to be 242 km and is well within the goal of 300 km. The assumptions of random error, normal distributions and non-coupling of orbit determination errors are subject to correction based on the orbit determination method. Also, the assumed error magnitudes may be inconsistent with orbit

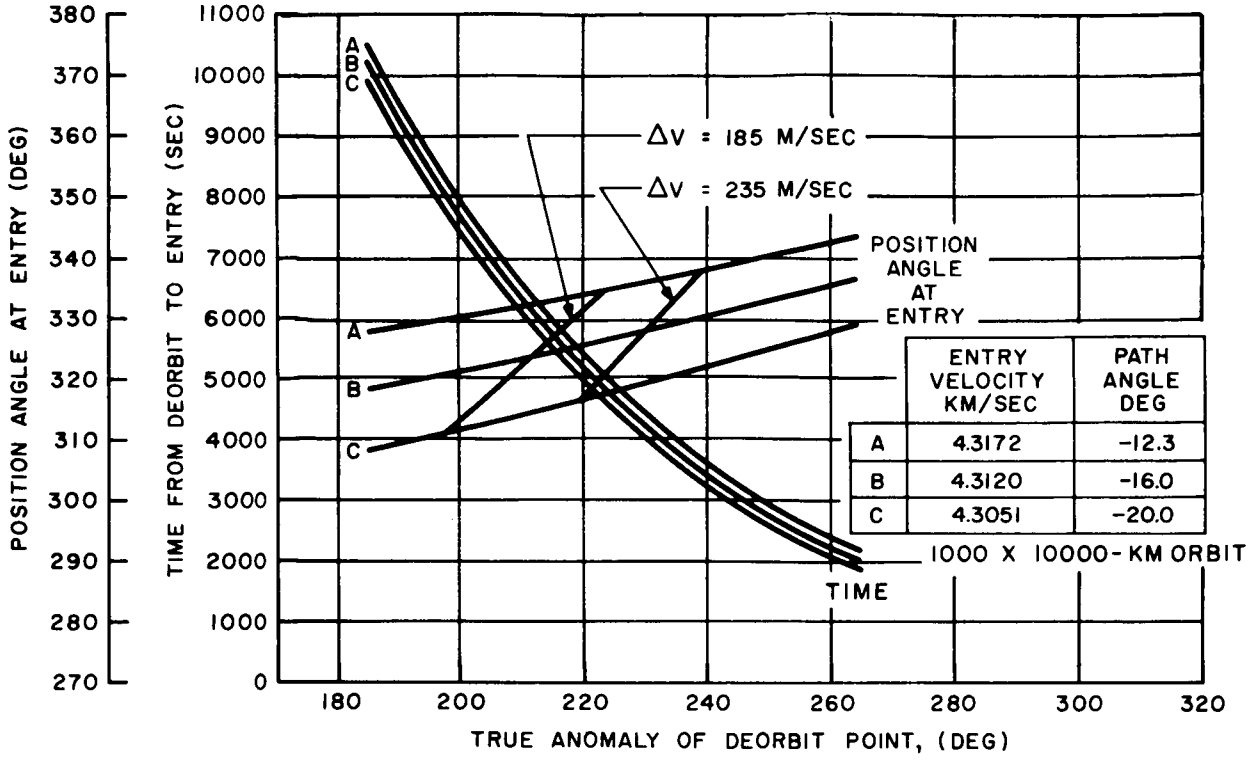


Figure 8-3. Capsule ΔV Range, Nominal Orbit

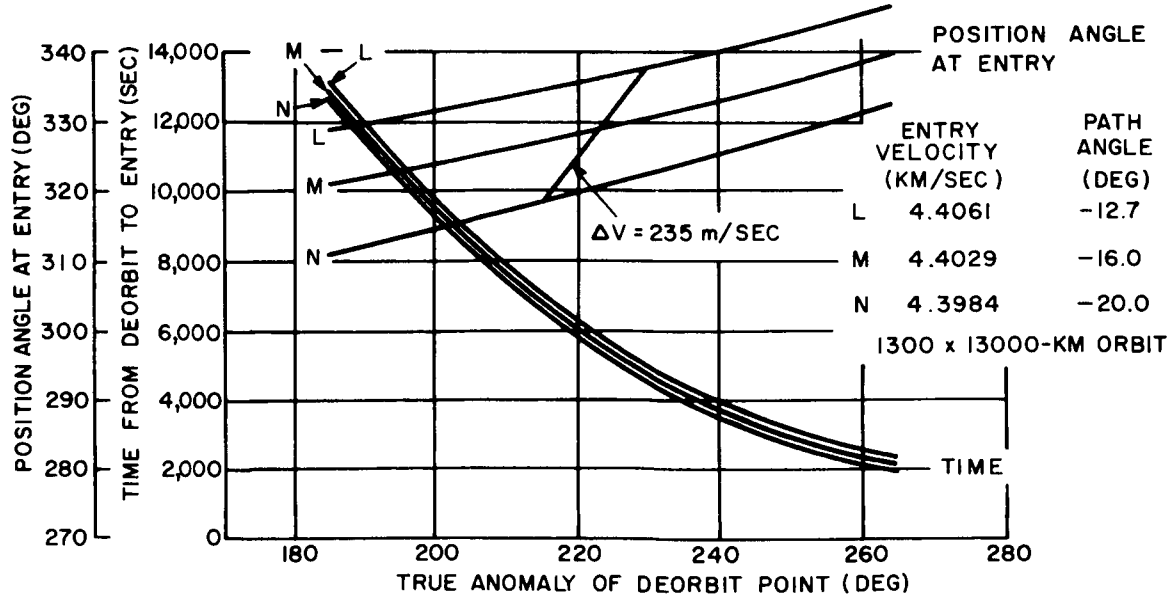


Figure 8-4. Capsule Deorbit, 1300 by 13000-Kilometer Orbit

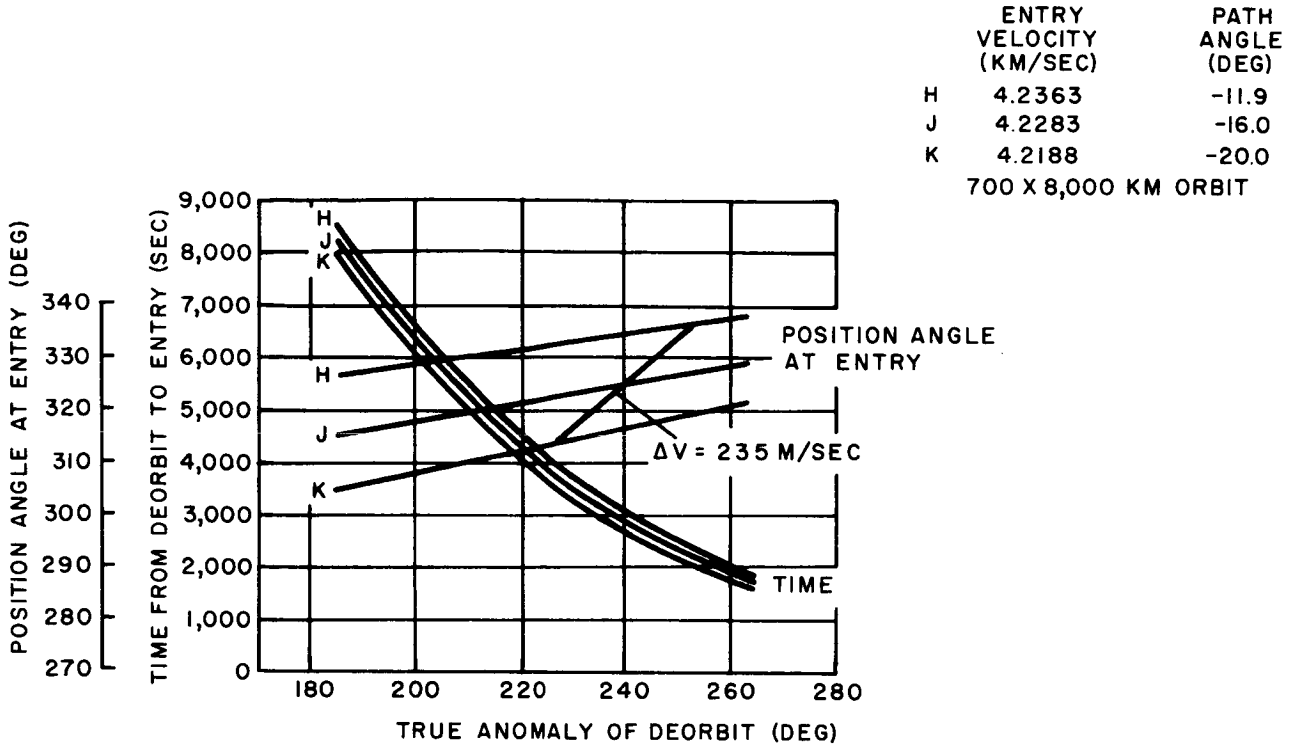


Figure 8-5. Capsule Deorbit, 7500 by 8000-Kilometer Orbit

TABLE 8-1. CAPSULE DEORBIT MANEUVER ERROR SENSITIVITIES

Error Source	Error Magnitude	TRAJECTORY PARAMETER VARIATIONS				
		Entry Velocity (M/sec)	Entry Path Angle (deg)	Entry Position Angle (deg)	Deorbit to Entry Time (sec)	Capsule Spacecraft Range (km)
Periapsis Radius	5 km	0.152	0.11	0.30	3.6	4.4
Orbital Period	0.2%	0.228	.24	0.60	36.0	12.5
Gravitational Parameter	0.3%	7.09	0.0	0.007	1.7	1.2
Line of Apsides	0.2%	0.328	0.05	0.28	0.60	2.2
Velocity Increment	3%	0.914	0.71	1.56	36.0	16.0
Pointing	2%	3.28	0.50	0.80	6.0	22.0
Time (Periapsis to deorbit)	0.1%	0.38	0.10	0.26	7.0	5.0
RSS		7.89	0.92	1.92	51.9	30.8

NOMINAL CONDITIONS

Entry Velocity, 4.3 km/sec
Entry Path Angle, 16 degrees
Entry Position Angle, 327 degrees
Deorbit to Entry Time, 4167 sec
Capsule-Spacecraft Range, 1724 km

determination practice. However, at the assumed levels, the deorbit execution errors which are within current demonstrated state-of-the-art, are the principal influence on dispersion so it seems safe to expect that the RSS values shown are realistic. The errors shown are in-plane errors. Cross range errors can also result from ΔV alignment errors or orbit determination errors, but they should be small compared with the in-plane errors.

TABLE 8-2. CAPSULE DEORBIT ENTRY ERROR SENSITIVITIES

Error Source	Error Magnitude	Parameter Variation: Position Angle, Entry (deg)	Parameter Variation: Main Chute Deployment Height (m)
Entry Velocity	±8.5 m/sec	0.4	7
Entry Path Angle	±1 deg	2.25	387
Atmosphere	VM8, VM3	0.93	7920
Parachute Deployment Velocity	±30.5 m/sec	Neg.	887

Nominal Vehicles

Diameter, 12 ft

Weight, 1200 lb at entry (M/C_DA = 0.261 slug/ft^2)

Drogue chute, 24-ft diameter, deployed at 716 m/sec

Main chute, 50.5-ft diameter, deployed at 183 m/sec

Nominal Entry Conditions

Entry Velocity, 4.30 km/sec

Entry path angle, 16 degrees

TABLE 8-3. CAPSULE IMPACT DISPERSION

Entry Position Angle Entry Due to Deorbit (deg)	1.916 deg
Entry Position Angle Error During Entry Due to Path Angle Error of 0.915 deg	2.06 deg
Sum	3.976 deg
Entry Path Angle Position Angle Error Due to Entry Velocity Error of 7.9 m/sec (deg)	0.037 deg
Entry Position Angle Error Due to Atmosphere Variations (deg)	0.93 deg
Entry Position Angle Error Due to Parachute Deployment Velocity Error of 30.5 m/sec	Neg.
RSS Error	4.083 deg 242.3 km

CII VC220FD103

COMPONENT DESIGN PARAMETERS

SECTION

1 SCOPE
2 APPLICABLE DOCUMENTS
3 DESIGN PARAMETERS

COMPONENT DESIGN PARAMETERS

1.0 SCOPE. This document defines the weight, the electrical power requirements, and the temperature environment of all spacecraft components. In its final form, it shall serve as the control document for these parameters.

2.0 APPLICABLE DOCUMENTS.

VC211SR101	Mission Objectives and Design Criteria	VC220SR101	Design Characteristics and Restraints

3.0 DESIGN PARAMETERS. Table 3-1 lists the weight, power parameters, and thermal parameters of all applicable spacecraft components. The operating and nonoperating temperature limits present the minimum and maximum subassembly temperature in degrees Fahrenheit that the component can reliably withstand without failure.

Table 3-2 lists the average power parameters for the subsystems as a function of the flight sequence. It is identical to the energy balance sheet discussed in VC236FD101. Under each event in the flight sequence, the average power is listed for those components and subsystems which are drawing power during that phase.

TABLE 3-1. COMPONENT DESIGN PARAMETERS

Description	Weight (lb.)	Reference Number	Power Input (Watts)		Power Dissipated (Watts)		Power Source	Allowable Temp(°F)	
			Avg.	Peak	Avg.	Peak		Min	Max
POWER SUBSYSTEM, BAY NO. 1									
Battery No. 1	43.0	01001	(1)		13.0	100.0	Charge Reg.	40.0	80.0
Main Buck Regulator	11.5	01002	(1)		36.0	39.6	DC	14.0	167.0
Charge Regulator	1.5	01003	(1)		12.0	19.0	Array	14.0	167.0
3 Phase Inverter	3.5	01004	(1)			7.0	Reg DC	14.0	167.0
2.4KC Inverter	4.5	01005	(1)		30.0	33.0	Reg DC	14.0	167.0
1 Phase Inverter	1.5	01006	(1)			2.5	Reg DC	14.0	167.0
Bay No. 1 Wire Harness	4.6	01007						-200.0	250.0
Chassis	3.1	01008							
Mics. Hardware	1.0	01009							
Batt Temp Sensors	0.1	01010						0.0	100.0
Bay Temp Sensors	0.1	01011						-300.0	300.0
Shutter Angle Sensors	0.4	01012						-300.0	300.0
Weight Subtotal	74.8								
POWER SUBSYSTEM, BAY NO. 2									
Battery No. 2	43.0	02001	(1)		13.0	100.0	Charge Reg.	40.0	80.0
Main Buck Regulator	11.5	02002	(1)		36.0	39.6	DC	14.0	167.0
Charge Regulator	1.5	02003	(1)		12.0	19.0	Array	14.0	167.0
3 Phase Inverter	4.5	02004	(1)		30.0	33.0	Reg DC	14.0	167.0
2.4KC Inverter	4.5	02005	(1)				Reg DC	14.0	167.0
1 Phase Inverter	1.5	02006	(1)			2.5	Reg DC	14.0	167.0
Bay No. 2 Wire Harness	4.6	02007						-200.0	250.0
Chassis	3.1	02008							
Misc. Hardware	1.0	02009							
Batt Temp Sensors	0.1	02010						0.0	100.0
Bay Temp Sensors	0.1	02011						-300.0	300.0
Shutter Angle Sensor	0.4	02012						-300.0	300.0
Weight Subtotal	74.8								
SCIENCE ELECTRONICS, BAY NO. 3									
Electronics	45.0	03001	(1)		(1)			14.0	167.0
Chassis	3.1	03002							
Misc. Hardware	1.0	03003							
Bay Temp Sensor	0.1	03004						-300.0	300.0
Shutter Angle Sensor	0.4	03005						-300.0	300.0
Weight Subtotal	49.6								

TABLE 3-1. COMPONENT DESIGN PARAMETERS (Continued)

Description	Weight (lb.)	Reference Number	Power Input (Watts)		Power Dissipated (Watts)		Power Source	Allowable Temp(°F)	
			Avg.	Peak	Avg.	Peak		Min	Max
SPARE BAY NO. 4									
Chassis	3.1	04001							
Misc Hardware	1.0	04002							
Bay Temp Sensor	0.1	04003						-300.0	300.0
Weight Subtotal	4.2								
SCIENCE ELECTRONICS, BAY NO. 5									
Electronics	45.0	05001	(1)		(1)			14.0	167.0
Chassis	3.1	05002							
Misc. Hardware	1.0	05003							
Bay Temp Sensors	0.1	05004						-300.0	300.0
Shutter Angle Sensor	0.4	05005						-300.0	300.0
Weight Subtotal	49.6								
SCIENCE DAE, BAY NO. 6									
Electronics	55.0	06001	(1)		(1)			14.0	167.0
Chassis	3.1	06002							
Misc. Hardware	1.0	06003							
Bay Temp Sensor	0.1	06004						-300.0	300.0
Shutter Angle Sensor	0.4	06005						-300.0	300.0
Weight Subtotal	59.6								
DATA STORAGE, BAY NO. 7									
Tape Recorder	18.0	07001	5.5	5.5	5.5	5.5	2400~	0.0	158.0
Tape Recorder	18.0	07002	5.5	5.5	5.5	5.5	2400~	0.0	158.0
Tape Recorder	18.0	07003	5.5	5.5	5.5	5.5	2400~	0.0	158.0
Control Logic	0.4	07004	0.2	0.2	0.2	0.2	2400~	0.0	176.0
Control Logic	0.4	07005	0.2	0.2	0.2	0.2	2400~	0.0	176.0
Control Logic	0.4	07006	0.2	0.2	0.2	0.2	2400~	0.0	176.0
Playback Sequencer	0.6	07007	0.2	0.2	0.2	0.2	2400~	0.0	176.0
Power Supply	2.0	07008	17.9	17.9	0.6	0.6	2400~	0.0	176.0
Bay No. 7 Wire Harness	4.6	07009						-200.0	250.0
Chassis	3.1	07010						0.0	200.0
Misc. Hardware	1.0	07011						-200.0	300.0
Bay Temp Sensor	0.1	07012						-300.0	300.0
Shutter Angle Sensor	0.4	07013						-300.0	300.0
Weight Subtotal	67.0								

TABLE 3-1. COMPONENT DESIGN PARAMETERS (Continued)

Description	Weight (lb.)	Reference Number	Power Input (Watts)		Power Dissipated (Watts)		Power Source	Allowable Temp(°F)	
			Avg.	Peak	Avg.	Peak		Min	Max
DATA STORAGE, BAY NO. 8									
Tape Recorder	18.0	08001	5.5	5.5	5.5	5.5	2400~	0.0	158.0
Tape Recorder	18.0	08002	5.5	5.5	5.5	5.5	2400~	0.0	158.0
Tape Recorder	18.0	08003	5.5	5.5	5.5	5.5	2400~	0.0	158.0
Control Logic	0.4	08004	0.2	0.2	0.2	0.2	2400~	0.0	176.0
Control Logic	0.4	08005	0.2	0.2	0.2	0.2	2400~	0.0	176.0
Control Logic	0.4	08006	0.2	0.2	0.2	0.2	2400~	0.0	176.0
Playback Sequencer	0.6	08007	0.2	0.2	0.2	0.2	2400~	0.0	176.0
Power Supply	2.0	08008	17.9	17.9	0.6	0.6	2400~	0.0	176.0
Bay No. 8 Wire Harness	4.6	08009						-200.0	250.0
Chassis	3.1	08010							
Misc. Hardware	1.0	08011							
Bay Temp Sensors	0.1	08012						-300.0	300.0
Shutter Angle Sensor	0.4	08013						-300.0	300.0
Weight Subtotal	67.0								
TELEMETRY SUBSYSTEM, BAY NO. 9									
Commutator	7.0	09001						0.0	176.0
Signal Conditioning	0.7	09002						0.0	176.0
Command Storage	0.4	09003						0.0	176.0
Command Storage	0.4	09004						0.0	176.0
Power Supply	1.4	09005	4.1	4.1	0.8	0.8	2400~	0.0	176.0
Power Supply	1.4	09006	4.1	4.1	0.8	0.8	2400~	0.0	176.0
ADC	0.4	09007					(2)	0.0	176.0
ADC	0.4	09008					(2)	0.0	176.0
Frequency Divider	0.1	09009					(2)	0.0	176.0
Rate Control (2)	0.1	09010					(2)	0.0	176.0
By-Pass Logic (2)	0.1	09011					(2)	0.0	176.0
Phaser	0.1	09012					(2)	0.0	176.0
PNG (4)	0.2	09013					(2)	0.0	176.0
Format Programer	0.4	09014					(2)	0.0	176.0
Format Programer	0.4	09015					(2)	0.0	176.0
Decoding Matrix (2)	0.2	09016					(2)	0.0	176.0

TABLE 3-1. COMPONENT DESIGN PARAMETERS (Continued)

Description	Weight (lb.)	Reference Number	Power Input (Watts)		Power Dissipated (Watts)		Power Source	Allowable Temp(° F)	
			Avg.	Peak	Avg.	Peak		Min	Max
Subcom. Drive	0.5	09017					(2)	0.0	176.0
Subcom. Drive	0.5	09018					(2)	0.0	176.0
Digital Accumulator	0.6	09019					(2)	0.0	176.0
Digital Accumulator	0.6	09020					(2)	0.0	176.0
Transfer Register 2	0.1	09021					(2)	0.0	176.0
Data Selector (2)	0.1	09022					(2)	0.0	176.0
Modulator	0.5	09023					(2)	0.0	176.0
Bay No. 9 Wire Harness	1.1	09024						-200.0	250.0
Chassis	3.1	09025							
Misc. Hardware	1.0	09026							
Bay Temp Sensors	0.1	09027						-300.0	300.0
Shutter Angle Sensor	0.4	09028	8.2					-300.0	300.0
Weight Subtotal	22.3								
COMMAND SUBSYSTEM, BAY NO. 10									
Comm Det & Prog Control	4.2	10001	2.0	2.0	2.0	2.0	(2)	0.0	185.0
Comm Det & Prog Control	4.2	10002	2.0	2.0	2.0	2.0	(2)	0.0	185.0
Comm Det & Prog Control	4.2	10003	2.0	2.0	2.0	2.0	(2)	0.0	185.0
Command Decoder	5.6	10004	4.5	4.5	4.5	4.5	(2)	0.0	185.0
Command Decoder	5.6	10005	4.5	4.5	4.5	4.5	(2)	0.0	185.0
Decoder Acess Switch	3.0	10006	0.2	0.2	0.2	0.2	(2)	0.0	185.0
Power Supply	3.1	10007	20.2	20.2	5.0	5.0	2400~	0.0	185.0
Bay No. 10 Wire Harness	3.0	10008						-200.0	250.0
Chassis	3.1	10009							
Misc. Hardware	1.0	10010							
Bay Temp Sensors	0.1	10011						-300.0	300.0
Shutter Angle Sensor	0.4	10012						-300.0	300.0
Weight Subtotal	37.5								
RADIO SUBSYSTEM, BAY NO. 11									
Transponder No. 2	13.3	11001	15.5	15.5	15.5	15.5	2400~	- 10.0	180.0
Transponder No. 3	13.3	11002	15.5	15.5	15.5	15.5	2400~	- 10.0	180.0
Bay No. 11 Wire Harness	1.4	11003						-200.0	250.0
Chassis	3.1	11004							
Misc. Hardware	1.0	11005							
Bay Temp Sensors	0.1	11006						-300.0	300.0
Shutter Angle Sensor	0.4	11007						-300.0	300.0
Weight Subtotal	32.6								

TABLE 3-1. COMPONENT DESIGN PARAMETERS (Continued)

Description	Weight (lb.)	Reference Number	Power Input (Watts)		Power Dissipated (Watts)		Power Source	Allowable Temp(°F)	
			Avg.	Peak	Avg.	Peak		Min	Max
RADIO SUBSYSTEM, BAY NO. 12									
Power Amplifier No. 2	7.5	12001	147.0	147.0	97.0	97.0	DC	- 35.0	245.0
Power Amplifier No. 3	7.5	12002	147.0	147.0	97.0	97.0	DC	- 35.0	245.0
Power Amplifier No. 1	3.0	12003	36.0	50.0	46.0	46.0	DC	- 10.0	180.0
Transponder No. 1	13.3	12004	15.5	15.5	15.5	15.5	2400~	- 10.0	180.0
Diplexer Switch Assembly	13.4	12005	0.0	15.0	0.0	15.0	DC	- 10.0	180.0
Bay No. 12 Wire Harness	3.7	12006						-200.0	250.0
Chassis	3.1	12007							
Misc. Hardware	1.0	12008							
Bay Temp Sensors	0.1	12009						-300.0	300.0
Weight Subtotal	52.6								
RADIO SUBSYSTEM, BAY No. 13									
Relay Radio	25.0	13001	12.0	12.0	12.0	12.0	2400~	- 10.0	180.0
Bay No. 13 Wire Harness	1.4	13002						-200.0	250.0
Chassis	3.1	13003							
Misc. Hardware	1.0	13004							
Bay Temp Sensors	0.1	13005						-300.0	300.0
Shutter Angle Sensor	0.4	13006						-300.0	300.0
Weight Subtotal	31.0								
COMPUTER AND SEQUENCER SUBSYSTEM, BAY NO. 14									
Computer and Sequencer	35.0	14001	50.0	50.0	50.0	50.0	2400~	0.0	120.0
Solar Aspect Sensor	5.0	14002						0.0	220.0
Earth Null Sensor	2.0	14003						0.0	150.0
Bay No. 14 Wire Harness	2.1	14004						-200.0	250.0
Chassis	3.1	14005							
Misc. Hardware	1.0	14006							
Bay Temp Sensors	0.1	14007						-300.0	300.0
Shutter Angle Sensor	0.4	14008						-300.0	300.0
Weight Subtotal	48.7								

TABLE 3-1. COMPONENT DESIGN PARAMETERS (Continued)

Description	Weight (lb.)	Reference Number	Power Input (Watts)		Power Dissipated (Watts)		Power Source	Allowable Temp(° F)	
			Avg.	Peak	Avg.	Peak		Min	Max
GUIDANCE AND CONTROL SUBSYSTEM, BAY NO. 15									
AC Electronics	8.6	15001	9.6	9.6	9.6	9.6	2400~	0.0	160.0
Auto Pilot Electronics	6.0	15002	12.0	12.0	3.5	3.5	2400~	0.0	160.0
Accel and Gyro Electronics	14.5	15003	29.0	29.0	29.0	29.0	(3)	0.0	160.0
Accel and Gyro Electronics	14.5	15004	29.0	29.0	29.0	29.0	(3)	0.0	160.0
Bay No. 15 Wire Harness	5.7	15005						-200.0	250.0
Chassis	3.1	15006							
Misc. Hardware	1.0	15007							
Gyro Temp Sensors	0.1	15008						0.0	200.0
Accel Temp Sensors	0.1	15009						0.0	200.0
Bay Temp Sensors	0.1	15010						-300.0	300.0
Shutter Angle Sensor	0.4	15011						-300.0	300.0
Weight Subtotal	54.1								
POWER SUBSYSTEM, BAY NO. 16									
Battery No. 3	35.0	16001	(1)		13.0	100.0	Charge Reg	40.0	80.0
Charge Regulator	1.5	16002	(1)		12.0	19.0	Array	14.0	167.0
Pyro Controller	7.5	16003	2.0		2.0		2400~	15.0	185.0
Synchronizer and Clock	6.0	16004	8.5	8.5	8.5	8.5	Reg DC	14.0	167.0
Power Logic and Switch	5.5	16005		10.0		10.0	Reg DC	14.0	167.0
Bay No. 16 Wire Harness	4.1	16006						-200.0	250.0
Chassis	3.1	16007							
Misc. Hardware	1.0	16008							
Bay Temp Sensors	0.1	16009						-300.0	300.0
Shutter Angle Sensor	0.4	16010						-300.0	300.0
Weight Subtotal	64.2								

TABLE 3-1. COMPONENT DESIGN PARAMETERS (Continued)

Description	Weight (lb.)	Reference Number	Power Input (Watts)		Power Dissipated (Watts)		Power Source	Allowable Temp(° F)	
			Avg.	Peak	Avg.	Peak		Min	Max
PRIMARY STRUCTURE									
Capsule Sep. Frame	9.3	17001							
Tapered Longeron	35.0	17002							
Kick Frame	38.9	17003							
Equip Channel	26.4	17004							
Support Angle	1.0	17005							
Support Angle	0.4	17006							
Outer Cap	6.9	17007							
Tapered Strut	94.0	17008							
Shear Panels	89.1	17009							
Ftgs Structure	31.4	17010							
Hardware	38.0	17011							
Separation Fittings	21.0	17012							
Weight Subtotal	391.4								
METEOROID PROTECTION									
Meteoroid Shield	70.1	18001							
Weight Subtotal	70.1								
SCAN PLATFORM									
Prime Sensors	120.5	19001	(1)		(1)		(1)		
Structure-Boom-Actuator	25.0	19002							
Thermal Control	4.5	19003							
Weight Subtotal	150.0								
SOLAR ARRAY									
Solar Panel 1	14.6	20001						-250.0	250.0
Solar Panel 2	14.6	20002						-250.0	250.0
Solar Panel 3	14.6	20003						-250.0	250.0
Solar Panel 4	14.6	20004						-250.0	250.0
Solar Panel 5	14.6	20005						-250.0	250.0
Solar Panel 6	14.6	20006						-250.0	250.0
Solar Panel 7	14.6	20007						-250.0	250.0
Solar Panel 8	14.6	20008						-250.0	250.0
Solar Panel 9	14.6	20009						-250.0	250.0
Solar Panel 10	14.6	20010						-250.0	250.0
									250.0

TABLE 3-1. COMPONENT DESIGN PARAMETERS (Continued)

Description	Weight (lb.)	Reference Number	Power Input (Watts)		Power Dissipated (Watts)		Power Source	Allowable Temp(° F)	
			Avg.	Peak	Avg.	Peak		Min	Max
Solar Panel 11	14.6	20011						-250.0	250.0
Solar Panel 13	14.6	20012						-250.0	250.0
Solar Panel 14	14.6	20013						-250.0	250.0
Solar Panel 15	14.6	20014						-250.0	250.0
Solar Panel 16	14.6	20015						-250.0	250.0
Spar and Caps	67.2	20016							
Zener Regulators	8.0	20017						-250.0	250.0
Panel Temp Sensors	0.2	20018						-250.0	250.0
Wiring	25.0	20019						-250.0	250.0
Weight Subtotal	319.4								
ATTITUDE CONTROL GAS SYSTEM									
Nitrogen Tank and Gas	46.4	21001						- 50.0	160.0
Nitrogen Tank and Gas	46.4	21002						- 50.0	160.0
Nitrogen Tank and Gas	46.4	21003						- 50.0	160.0
Nitrogen Tank and Gas	46.4	21004						- 50.0	160.0
Hardware and Tube Fittings	13.0	21005						- 50.0	160.0
Heaters	0.5	21006		5.0		5.0	DC		
Fill Valves (2)	0.5	21007							
Temperature Sensors (2)	0.5	21008						- 50.0	160.0
Press Xducers (4)	2.0	21009						- 50.0	160.0
Filters (2)	0.5	21010						- 50.0	160.0
Press Regulators (2)	4.0	21011						- 50.0	160.0
Solenoid Valves (48)	24.0	21012		5.0		8 0	DC	- 50.0	160.0
Nozzles (24)	2.4	21013						- 50.0	160.0
Mount Str. and Misc.	14.0	21014							
Weight Subtotal	247.0								

VC220FD103

TABLE 3-1. COMPONENT DESIGN PARAMETERS (Continued)

Description	Weight (lb.)	Reference Number	Power Input (Watts)		Power Dissipated (Watts)		Power Source	Allowable Temp(° F)	
			Avg.	Peak	Avg.	Peak		Min	Max
A/C INDEPENDENTLY MOUNTED SENSORS									
Sun Gate Sensor	0.2	22001						30.0	130.0
Cruise Sun Sensor	1.2	22002						30.0	130.0
Secondary Acquisition Sensor	1.2	22003						30.0	140.0
Canopus Tracker	6.3	22004	1.8	1.8	1.8	1.8	2400 ~	- 30.0	100.0
Canopus Tracker	6.3	22005	1.8	1.8	1.8	1.8	2400 ~	- 30.0	100.0
Support Structure and Hardware	1.2	22006							
Temperature Sensors	0.2	22007						-300.0	300.0
Weight Subtotal	16.6								
SCIENCE (BODY MOUNTED SENSORS)									
Misc. Science	105.0	23001	(1)		(1)				
Temperature Sensors	0.4	23002						-300.0	300.0
Weight Subtotal	105.4								
ANTENNA ASSEMBLIES									
Relay Antenna	2.0	24001						-300.0	200.0
Associated Structure	2.0	24002						-300.0	200.0
Hi Gain Antenna, Structure and Actuation	80.0	24003						-300.0	200.0
Low Gain Antennas (2)	1.6	24004						-300.0	200.0
Medium Gain Antenna	4.4	24005						-300.0	200.0
Supt. Structure	2.0	24006							
Temperature Sensors	0.1	24007						-300.0	300.0
Weight Subtotal	92.1								
THERMAL CONTROL									
Shutter Assembly and Face Sheet 1	8.1	25001						-200.0	200.0
Shutter Assembly and Face Sheet 2	8.1	25002						-200.0	200.0
Shutter Assembly and Face Sheet 3	8.1	25003						-200.0	200.0

TABLE 3-1. COMPONENT DESIGN PARAMETERS (Continued)

Description	Weight (lb.)	Reference Number	Power Input (Watts)		Power Dissipated (Watts)		Power Source	Allowable Temp (°F)	
			Avg.	Peak	Avg.	Peak		Min	Max
Insul and Face Sheet 4	4.1	25004						-300.0	+300.0
Shutter Assembly and Face Sheet 5	8.1	25005						-200.0	200.0
Shutter Assembly and Face Sheet 6	8.1	25006						-200.0	200.0
Shutter Assembly and Face Sheet 7	7.0	25007						-200.0	200.0
Shutter Assembly and Face Sheet 8	7.0	25008						-200.0	200.0
Shutter Assembly and Face Sheet 9	7.0	25009						-200.0	200.0
Shutter Assembly and Face Sheet 10	7.2	25010						-200.0	200.0
Shutter Assembly and Face Sheet 11	8.1	25011						-200.0	200.0
Insul. and Face Sheet 12	11.6	25012						-300.0	300.0
Shutter Assembly and Face Sheet 13	7.2	25013						-200.0	200.0
Shutter Assembly and Face Sheet 14	8.1	25014						-200.0	200.0
Shutter Assembly and Face Sheet 15	7.2	25015						-200.0	200.0
Shutter Assembly and Face Sheet 16	8.1	25016						-200.0	200.0
Insul A/C	2.5	25017						-200.0	200.0
Paint	4.0	25018						-300.0	300.0
Insulation Orbiter	15.2	25019						-200.0	200.0
Weight Subtotal	144.8								
PYROTECHNIC									
Pin Pullers	2.2	26001						- 70.0	167.0
Squibs	2.2	26002					Pyro	- 65.0	167.0
Weight Subtotal	4.4								

TABLE 3-1. COMPONENT DESIGN PARAMETERS (Continued)

Description	Weight (lb.)	Reference Number	Power Input (Watts)		Power Dissipated (Watts)		Power Source	Allowable Temp(°F)	
			Avg.	Peak	Avg.	Peak		Min	Max
HARNESS									
Main Harness	35.0	27001						-200.0	250.0
Relay Cable	1.0	27002						- 76.0	752.0
High-Gain Cable	4.0	27003						- 76.0	752.0
Low-Gain Cable	5.0	27004						- 76.0	752.0
Medium-Gain Cable	2.0	27005						- 76.0	752.0
Umbilical	4.5	27006						- 10.0	167.0
Weight Subtotal	51.5								
PROPULSION HARDWARE									
RETRO			(4)						
Retro Engine	9513.0	28001	872.0	872.0	872.0	72.0	DC	0.0	110.0
Tapered Strut	60.8	28002							
Kick Ring	12.5	28003							
Tubular Strut	16.4	28004							
Kick Ring	3.8	28005							
Weight Subtotal	9606.5								
MIDCOURSE PROPULSION									
Engine 4-Mono	32.4	29001						1800.0	1900.0
Jet Vane Assembly (4)	9.6	29002	0.0	69.0	0.0	69.0	AUTO PILOT	35.0	250.0
Quad Sol Valves (4)	20.0	29003		135.0		135.0	DC	35.0	150.0
Cav Vent Assembly (4)	2.0	29004						35.0	125.0
B-D-Relief Valves (2)	2.8	29005						35.0	125.0
Valve 2 Position	0.5	29006					Pyro	35.0	125.0
Filter 3	1.2	29007						35.0	125.0
Valve, Ex. Oper	8.0	29008					Pyro	- 65.0	167.0
Valve, Ex. Oper	6.0	29009					Pyro	- 65.0	167.0
Valve, Fill, Vent	3.2	29010						- 65.0	167.0
Switch, Pressure	0.4	29011						0.0	167.0
Regulator (2)	4.6	29012						0.0	125.0
Transducers Press (7)	3.5	29013	3.2				DC	0.0	167.0
Lines, Trays, and Brackets	12.0	29014							

TABLE 3-1. COMPONENT DESIGN PARAMETERS (Continued)

Description	Weight (lb.)	Reference Number	Power Input (Watts)		Power Dissipated (Watts)		Power Source	Allowable Temp(° F)	
			Avg.	Peak	Avg.	Peak		Min	Max
Supt Struct	38.0	29015							
Propellant Tnks (4)	93.0	29016						35.0	100.0
Bladders (4)	12.0	29017						35.0	100.0
Gas	9.5	29018						0.0	125.0
Gas Tank (2)	102.0	29019						0.0	125.0
Prop Tank Supt	13.8	29020						0.0	125.0
Tank Supt Tubes	4.3	29021							
MTG Frames	20.0	29022							
Weight Subtotal	398.8								
PROPELLANT-LIQUID	1788	3001						35.0	100.0
CAPSULE	2600.0	31001							
BIO-BARRIER (LOWER PORTION)	250.0	32001							
BIO-BARRIER (UPPER PORTION)	150.0	33001							
SPACECRAFT TO BOOSTER ADAPTER									
Adapter Ftgs and Hardware	50.0	34001							
Piston System	25.6	34002							
Gas System	37.7	34003							
Weight Subtotal	113.3								

(1) See Table 3-2 for power input for various mission phases.

(2) Power input from subsystem T/R.

(3) Heaters 12 watts, unregulated battery; gyros 9 watts, 400 cps, 3 φ; electronics 8 watts, 2400 cps.

(4) Power consumption during 90 second engine burn only.

TABLE 3-2. AVERAGE POWER PARAMETERS

Mission Phase	Launch to Acquisition (Typical)	Cruise	Midcourse Maneuver (Typical)	Orbit with Capsule Spacecraft Day				Orbit without Capsule Spacecraft Day			
				Mars Orbit Insertion (Typical)	Full Science (2 hr 14 min)	Other Times	Eclipse (41.8 min)	Capsule Separation (Typical)	Full Science, (2 hr 14 min)	Other Times	Eclipse (66 min)
2400-cps Inverter Loads:											
Radio	30	30	30	30	30	30	30	30	30	30	30
Telemetry	8	8	8	8	8	8	8	8	8	8	8
Command	20	20	20	20	20	20	20	20	20	20	20
Data Storage	36	3	9	9	25	9	9	9	25	9	9
Guidance and Control	20	12	32	40	21	21	21	21	21	21	21
Articulation	3	3	3	3	3	3	3	3	3	3	3
Pyrotechnic	2	2	2	2	2	2	2	2	2	2	2
Computer and Sequencer	50	50	50	50	50	50	50	50	50	50	50
Science		29	29	29	96	11	11	11	125	40	40
Clock and Synchronizer	9	9	9	9	9	9	9	9	9	9	9
Environmental Control							9				9
Inverter Load Subtotal	178	166	192	200	264	163	172	163	293	192	201
Harness Loss	1.8	1.7	1.9	2.0	2.7	1.6	1.7	1.6	3.0	1.9	2.0
Total Inverter Output	179.8	167.7	193.9	202.0	266.7	164.6	173.7	164.6	296.0	193.9	203.0
2400-cps Inverter Efficiency	0.87	0.87	0.88	0.88	0.90	0.86	0.86	0.86	0.90	0.88	0.88
2400-cps Inverter Thermal Loss	26.5	25.8	27.3	27.7	31.3	25.6	26.1	25.6	32.9	27.3	27.8
Total 2400-cps Inverter Input	206.3	193.5	221.2	229.7	298.0	190.2	200.8	190.2	328.9	221.2	230.8
400-cps, 3 φ Inverter Loads:											
Guidance and Control (PF = 0.35)	9		9	18	9	9	9	9	9	9	9
Inverter Load Subtotal	9		9	18	9	9	9	9	9	9	9
Harness Loss	0.1		0.1	0.2	0.1	0.1	0.1	0.1	0.1	0.1	0.1
Total Inverter Output	9.1		9.1	18.2	9.1	9.1	9.1	9.1	9.1	9.1	9.1
400-cps, 3φ Inverter Efficiency	0.56		0.56	0.56	0.56	0.56	0.56	0.56	0.56	0.56	0.56
400-cps, 3φ Inverter Thermal Loss	7.0		7.0	14.0	7.0	7.0	7.0	7.0	7.0	7.0	7.0
Total 400-cps, 3 φ Inverter Input	16.1		16.1	32.2	16.1	16.1	16.1	16.1	16.1	16.1	16.1
400-cps, 1 φ Inverter Loads:											
Science					10	5	5		10	5	5
Inverter Load Subtotal					10	5	5		10	5	5
Harness Loss					0.1	0.1	0.1		0.1	0.1	0.1
Total Inverter Output					10.1	5.1	5.1		10.1	5.1	5.1
400-cps, 1φ Inverter Efficiency					0.80	0.73	0.73		0.80	0.73	0.73
400-cps, 1φ Inverter Thermal Loss					2.5	1.9	1.9		2.5	1.9	1.9
Total 400-cps, 1 φ Inverter Input					12.6	7.0	7.0		12.6	7.0	7.0
400-cps Inverter Input Subtotal	16.1		16.1	32.2	28.7	23.1	23.1	16.1	28.7	23.1	23.1
Diode Thermal Loss	0.1		0.1	0.2	0.2	0.2	0.2	0.1	0.2	0.2	0.2
Main Regulator Output	222.5	193.5	237.4	262.1	326.9	213.5	224.1	206.4	356.8	244.5	254.1
Main Regulator Efficiency	0.87	0.86	0.88	0.88	0.90	0.87	0.87	0.87	0.90	0.88	0.88
Main Regulator Thermal Loss	32.2	30.6	33.0	34.4	38.0	31.7	32.3	31.3	39.6	33.4	33.9
Main Regulator Input	254.7	224.1	270.4	296.5	364.9	245.2	256.4	237.7	396.4	277.9	288.0
Unregulated D-C Loads:											
Capsule		200			200	200		200			
Radio	50	147	147	147	147	147	147	147	147	147	147
Gyro Heaters	6		6	12	6	6	6	6	6	6	6
Unregulated D-C Load Subtotal	56	347	153	159	353	353	153	353	153	153	153
Harness Loss	0.6	3.5	1.5	1.6	3.6	3.6	1.5	3.6	1.5	1.5	1.5
Total Unregulated D-C Load	56.6	350.5	154.5	160.6	356.6	356.6	154.5	356.6	154.5	154.5	154.5
Unregulated Bus Power	311.3	574.6	424.9	457.1	721.5	601.8	410.9	594.3	550.9	432.4	442.5
Direct Battery Loads:											
Fault Sensors	2	2	2	2	2	2	2	2	2	2	2
Thrust Vector Control Engine (Pk)				(875)							
Direct Battery Load Subtotal	2	2	2	2	2	2	2	2	2	2	2
Harness Loss											
Total Direct Battery Load	2	2	2	2	2	2	2	2	2	2	2
Battery Bus Power	313.3	2	426.9	459.1	2	2	412.9	196.3	2	2	444.5
Thermal Loss	3.2		4.3	4.6			4.2	2.0			4.5
Battery Power Output	316.5	2	431.2	463.7	2	2	417.1	198.3	2	2	449.0
Battery Energy Output (W-hr)	532		696	1593			290.7	347			493.9
Battery Thermal Loss	86		118	126	1.4	12.4	114	54	8.6	18.1	122
Battery Energy Input (W-hr)					33	522			199	760	
Battery Power Input					14.9	128.3			89.1	186.8	
Charger Output		2			16.9	130.3			91.1	188.8	
Battery Charger Efficiency					50.3/53	50.3/53			50.3/53	50.3/53	
Battery Charger Thermal Loss		1			1.0	7.3			4.8	9.9	
Charger Input		3			17.9	137.6			95.9	198.7	
Array Bus Power		577.6			739.4	739.4			646.8	631.1	
Harness Loss		5.8			7.5	7.5			6.5	6.4	
Array Power Requirement		583.4			746.9	746.9			653.3	637.5	
Array Power Available		817			802	802		400	721	721	

CII VC220FD105

LAUNCH VEHICLE INTERFACE

SECTION

1 SCOPE
2 FUNCTIONAL INTERFACE
3 PHYSICAL INTERFACE
4 ELECTRICAL SIGNAL AND POWER INTERFACE
5 RF INTERFACE
6 ENVIRONMENTAL CONTROL INTERFACE

LAUNCH VEHICLE INTERFACE

1.0 SCOPE. This document specifies the requirements placed on the Planetary Vehicles by the Launch Vehicle System and the requirements placed on the Launch Vehicle System by the Planetary Vehicles. Each Planetary Vehicle includes a Flight Capsule, and a Flight Spacecraft. These requirements are based upon JPL data and, where necessary, assumptions which are explained in the appropriate sections. It is assumed for this study that the Launch Vehicle System includes the Launch Vehicle, the nose fairing and structural shroud, encapsulation diaphragms, umbilical lines, VOYAGER launch complex facilities, and all other supporting equipment for prelaunch and launch activities. The nose fairing is defined as that portion of the enclosure which protects the forward Planetary Vehicle. The structural shroud is defined as that portion of the enclosure which provides support for the forward Planetary Vehicle and protection for the aft Planetary Vehicle.

All Planetary Vehicle interfaces with the Launch Vehicle are the responsibility of the Spacecraft System. The Spacecraft System and the Launch Vehicle System have functional, physical, electrical signal and power, RF, and environmental control interfaces. Each of the interfaces is shown in Figure 1-1 and described below.

2.0 FUNCTIONAL INTERFACE. Two identical Planetary Vehicles will be launched together on the specified trajectory. The Spacecraft System will be able to maintain launch readiness in fueled and mated condition for the duration of the launch opportunity. The Launch Vehicle System will be capable of maintaining readiness for a daily firing window of 2 hours for a 20 day period and have a probability of 0.99 for accomplishing the launch. The Launch Vehicle will have parking-orbit capability and a guaranteed gross injection weight capability of 63,000 lb on a Mars trajectory with a C_3 of 25 km^2/sec^2 based upon a launch azimuth of 115 degrees. The Saturn-IVB stage will be capable of providing the final burn after an interval of 2 to 90 minutes in nominal parking orbit.

During ascent through the Earth's atmosphere the Planetary Vehicles are enclosed in the launch vehicle nose fairing and structural shroud. The aerodynamic nose fairing is jettisoned at approximately 350,000 feet altitude.

Each Planetary Vehicle will be separated from the Launch Vehicle by firing the squib-actuating valves of the separation system which in turn release high-pressure gas to each of the 16 separation thrusters.

At the time of separation of the forward Planetary Vehicle, it is given a relative velocity of 3.4 ft/sec by the separation system. The maximum angular rate at separation must be less than 3 deg/sec. The Launch Vehicle will contribute less than 1 deg/sec and the maximum angular tip-off rate attributable to the spacecraft separation system must be less than 2 deg/sec.

It is assumed that after separation of the forward Planetary Vehicle, the structural shroud can be ruptured and folded back, as shown in Figure 1-1 and remain attached to the Launch Vehicle to satisfy the planetary quarantine constraint. The forward Planetary Vehicle

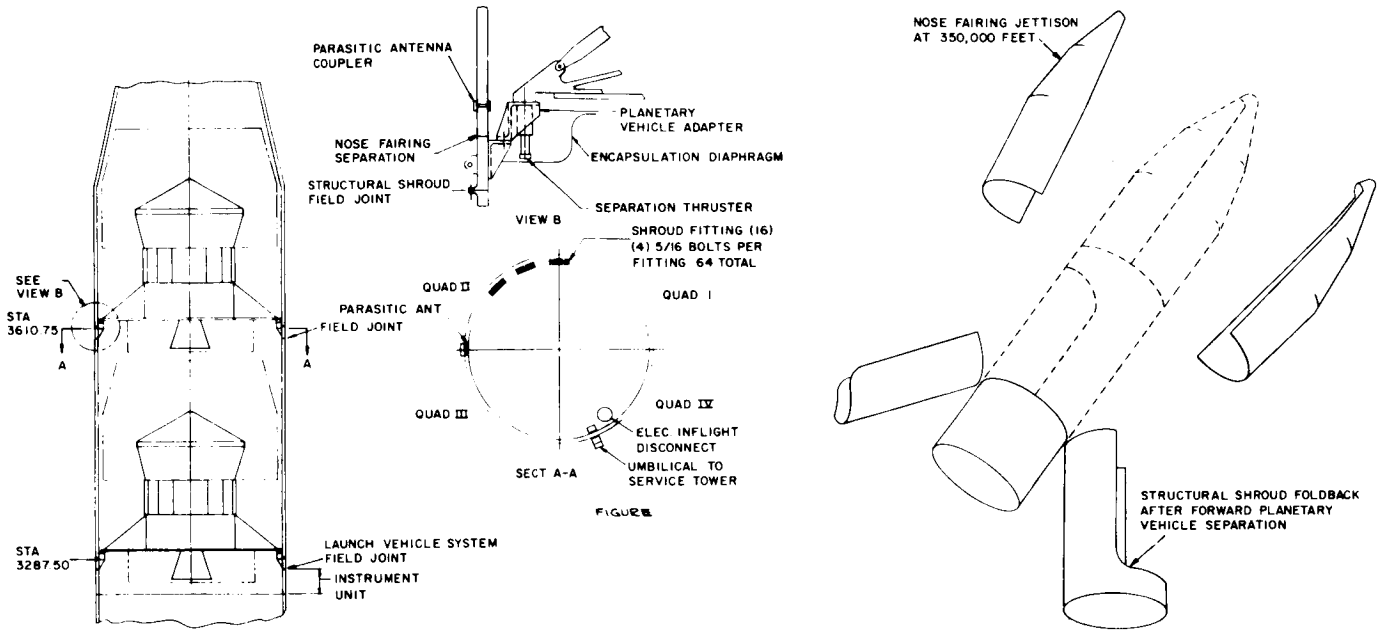


Figure 1-1. Launch Vehicle/Planetary Vehicle Interface

adapter is attached to the shroud, and likewise remains with the Launch Vehicle. Subsequent to the assumed 5 minute fold-back operation, the aft Planetary Vehicle is given a relative velocity of 2.5 ft/sec by its separation system. The resultant nominal separation velocity, between the two Planetary vehicles, of 1.9 ft/sec $\left[3.4-2.5\left(\frac{30660}{51160}\right)\right]$ insures the necessary dispersion at the time of the first mid-course maneuver 2 to 5 days after injection. The maximum angular separation rates for the aft Planetary Vehicle are the same as for the forward Planetary Vehicle.

The 1σ miss plus time of flight dispersions of each Planetary Vehicle shall be correctable with a velocity increment of 10 m/sec or less, 2 days after injection.

3.0 PHYSICAL INTERFACE. The identical mechanical interfaces between the Planetary Vehicles and the Launch Vehicle System are the field joints, stations 3610.75 and 3287.5, formed by the bottom surfaces of the Planetary Vehicle adapters and the shroud fittings as shown in Figure 1-1. These mechanical interfaces are the only structural supports for the Planetary Vehicles. Approximately at these station planes are the encapsulation diaphragms and the launch vehicle inflight electrical disconnects. The Planetary Vehicle adapters are attached to the shroud fittings by means of 64, 5/16-inch-diameter shear and tension bolts, located on a 251.8-inch diameter, inserted from the underside of the interface.

Before mating, the aft Planetary Vehicle is encapsulated in the structural shroud with both ends sealed by a diaphragm. This total assembly is supported and handled by lugs which are adjacent to the lower structural shroud fittings. The forward Planetary Vehicle is likewise encapsulated in the nose fairing with an end diaphragm and is handled and supported by handling lugs adjacent to the upper structural shroud fittings below which is the mating field joint to the structural shroud.

In addition to the structural interface, the Launch Vehicle System provides two umbilical connections in the structural shroud which are adjacent to each of the Planetary Vehicle adapters. The design of the electrical connectors in the encapsulation diaphrams is the responsibility of the Planetary Vehicle contractor. The Launch Vehicle System provides access ports to the mating connectors in the Launch Vehicle structural shroud and instrument unit.

4.0 ELECTRICAL SIGNAL AND POWER INTERFACE. The electrical interface between the Planetary Vehicles and the Launch Vehicle System is illustrated in Figure 4-1 and includes ground power, launch monitor control, spacecraft, capsule and environmental telemetry, and firing circuits for the various separation events. Prior to liftoff, the Planetary Vehicles are switched from launch complex to internal power.

All electrical exchanges are accomplished by means of launch complex umbilicals to each Planetary Vehicle and wires from the Planetary Vehicles down to the Launch Vehicle. The umbilical connections are located in the structural shroud adjacent to each Planetary Vehicle adapter. The leads between the Planetary Vehicles and the Launch Vehicle consist of the firing circuits and the inflight disconnect telemetry circuits.

4.1 Launch Complex Umbilicals. The launch complex umbilical harnesses shall provide wiring for ground power and the monitor and control signal exchanges between each Planetary Vehicle and the launch complex. Each harness contains an estimated 108 leads to each Planetary Vehicle as shown in Table 4-1.

TABLE 4-1. NUMBER OF WIRES PER PLANETARY VEHICLE UMBILICAL

Subsystem	No. Wires	Subsystem	No. Wires
Power	12	G&C	6
Radio	5 coax	Propulsion	8
Telemetry	1 coax	Science	12 (assumed)
C&S	30	Capsule	24 (assumed)
Pyrotechnic	10		

The Planetary Vehicles shall be capable of withstanding a failure (open or short) of the launch complex umbilicals. Complete discussion of the launch complex umbilicals can be found in CII VC280FD100 of Volume B.

4.2 Launch Vehicle Inflight Disconnect. Planetary Vehicle environmental measurements such as vibration, acoustic, pressure, and temperature will be made and transmitted over the Launch Vehicle telemetry system. In addition, spacecraft telemetry signals will be provided for transmission over the Launch Vehicle telemeter. The disconnect leads from each Planetary Vehicle are routed to the Launch Vehicle as shown in Figure 4-1.

Prior to each Planetary Vehicle separation, the inflight disconnects at the Planetary Vehicle adapter are pulled by a mechanism which is released by a squib-actuated pin-puller.

4.3 Launch Vehicle Direct Wiring. Since squib-firing circuits are not routed through inflight separation connectors certain direct wiring is required from the Launch Vehicle. The squib-actuated pin-pullers which release the pull mechanism of the inflight disconnects and the actuating valves of the Planetary Vehicle separation systems are activated by the Launch

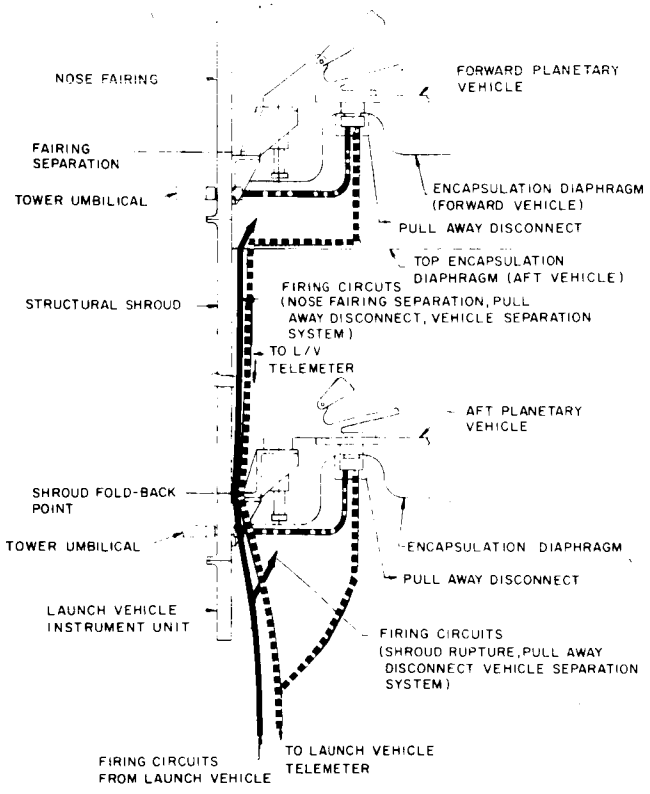


Figure 4-1. Launch Vehicle/Planetary Vehicle Electrical Interface

Vehicle in the proper timing sequence. It is also assumed that the Launch Vehicle will supply the power since the Planetary Vehicle pyrotechnics subsystem is not armed until separation so that an inadvertent or spurious command prior to that time cannot cause a premature squib firing.

Each of the pin-pullers and each of the actuating valves for each Planetary Vehicle has two electro-explosive devices. Each device has 2 bridges which require 5 amps for 10 milliseconds. Thus a total of 16 wires are required for each Planetary Vehicle. Each Planetary Vehicle provides the ignitor wiring, safe-arm devices, and connectors on the Planetary Vehicle adapters.

5.0 RF INTERFACE. The output RF signals from each Planetary Vehicle are picked up by means of a parasitic antenna coupler. One coupler is mounted on the shroud adjacent to the aft Planetary Vehicle adapter and one is mounted on the shroud adjacent to the forward Planetary Vehicle adapter. Each signal is carried to an antenna on the exterior surface of the structural shroud. The antennas are located so that both flight spacecraft are in communication with the Cape 71 DSIF station during the launch phase.

6.0 ENVIRONMENTAL CONTROL INTERFACE. Thermal, humidity, and contamination control (gas flow) environments are provided by the Launch Vehicle System to the encapsulated Planetary Vehicles from time of explosive safe/sterile assembly through nose fairing separation. It is assumed that the encapsulating diaphragms are supplied with the nose fairing and structural shroud. The diaphragms are located in the adapters, approximately in the structural mating planes and remain with the adapters.

The Launch Vehicle System will supply bacteriologically filtered gas through each umbilical, at $60 \pm 10°$ F, $30 \pm 10\%$ humidity, to maintain a positive pressure in the shroud to preclude inward leaks. The gas selection will be dictated by engineering and biological considerations. The flow rate is such that there is an air change approximately every 5-10 minutes. A return exhaust line is also provided by the Launch Vehicle System for each Planetary Vehicle.

Each vent hole to the exhaust lines is required to have a bacteriological filter to prevent contamination after hose disconnect as well as to provide a means of pressure equalization during atmospheric ascent. A second bacteriological filter is required at the vehicle end of the exhaust line to prevent laminar flow back into the nose fairing and shroud filters.

The Planetary Vehicles will be delivered to the launch complex for mating enclosed in their encapsulated nose fairing or shroud and attached to their handling and mating AHSE. The encapsulated Planetary Vehicles will be lifted and mated by the Launch Vehicle contractor. From the time the Planetary Vehicles leave the explosive-safe sterile assembly facility in fueled and ready condition, they will remain encapsulated for launch pad operations.

CII VC220FD106

FLIGHT CAPSULE INTERFACE

SECTION

1	SCOPE
2	APPLICABLE DOCUMENTS
3	FLIGHT SPACECRAFT/FLIGHT CAPSULE RELATIONSHIPS
4	MECHANICAL INTERFACE
5	THERMAL INTERFACE
6	ELECTRICAL INTERFACE
7	CAPSULE RELAY RECEIVER INTERFACE
8	PYROTECHNIC INTERFACE

FLIGHT CAPSULE INTERFACE

1.0 SCOPE. This document covers the interface design and functional relationships between the Flight Spacecraft and Flight Capsule. It will serve to specify those design features which are considered necessary for the successful accomplishment of the VOYAGER Mission. The assumptions which have been made about the Flight Capsule and its mission are outlined, as well as those interface solutions which would be desirable to the Flight Spacecraft. Furthermore, this document will serve as the first Flight Spacecraft input to the Spacecraft-Capsule Interface Control Document.

2.0 APPLICABLE DOCUMENTS

VC220SR101 - Design Characteristics and Constraints
VD220FD101 - Trajectories and Guidance

3.0 FLIGHT SPACECRAFT/FLIGHT CAPSULE RELATIONSHIPS. For purposes of describing a meaningful interface, certain assumptions have been made and, where it was found necessary, investigations of critical aspects of the Flight Capsule were carried out.

Entry trajectories are based on a 60-degree half angle sphere-cone Capsule configuration with a 12-foot base diameter into the VOYAGER-Mars (VM) atmospheres No. 3, 7, and 8. Capsule entry stability characteristics were studied assuming use of a passive spin stabilization system. From these studies, reasonable limits could be placed on angle-of-attack at entry.

Capsule descent times were based upon deployment of a parachute at Mach 1. The Sterilization Canister is assumed to be of rigid construction, made in two parts, mating circumferentially at the Capsule base diameter. In flight, only the forward portion is separated. It is further assumed that this separation takes place prior to Mars orbit insertion; however, it is recognized that further tradeoff studies will have to be made in this area. This is further discussed in Section 2 of VC220SR101.

3.1 Capsule Flight Profile. During Interplanetary Cruise, Capsule status, such as internal temperatures, pressures, battery charge state, etc., will be monitored via hardwire across the interface using the Flight Spacecraft commutator for sampling.

Approximately 7 hours before separation, the Flight Capsule is commanded to initiate a system checkout sequence. Required power is supplied by the Flight Spacecraft and regulated and distributed by the Flight Capsule power controller. As a part of the checkout sequence, quantitative and discrete commands will be verified and initiate times updated, as required. The checkout data consists of the output of the Capsule telemetry encoder which is accepted by the spacecraft telemetry subsystem and multiplexed with the Spacecraft engineering data for transmission to the Deep Space Instrumentation Facility (DSIF). The Flight Capsule continues in the checkout mode until separation.

During the Flight Spacecraft separation attitude maneuver, approximately 1 hour before separation, the Flight Capsule will be transferred to internal power. The separation

sequence begins by enabling the Flight Capsule Separation Sequencer. All Capsule events leading up to and including physical separation are timed and controlled by the Separation Sequencer.

While the Flight Spacecraft is performing the separation attitude maneuver, the Capsule shares equally the 7 7/24 bps transmission data rate with Flight Spacecraft engineering data. The Spacecraft will supply the Capsule commutator with clock pulses, allowing synchronization with its decoder and providing for a simple interface.

The Flight Capsule Separation Sequencer will count down to the last event before separation and will hold a specified period for final go-ahead from the Spacecraft Control and Sequencer (C&S). If this signal is not received, the Sequencer will recycle and shut down the Flight Capsule system. If the command is received, the Capsule sequencer will continue its countdown to the command to separate.

Before firing the de-orbit rocket, the Flight Capsule will be given a separation rate of approximately 0.85 mps and allowed to drift a distance of about 1000 meters to minimize plume impingement on the Spacecraft. Angular rates transferred to the Spacecraft pitch and yaw axes must not exceed 0.85 deg/sec to ensure attitude recovery within the dynamic range of the Spacecraft gyros.

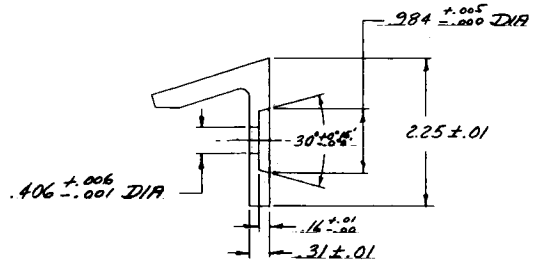
Events subsequent to separation can be timed by the action of a separation switch or Inflight Disconnect (IFD) circuit opening. The Spacecraft will continue to hold the separation attitude until Capsule impact, which, for a 1 x 10,000 km orbit and chosen de-orbit conditions, will last about 75 minutes.

The Flight Capsule can begin relaying separation events and engineering data shortly after separation at 100 bps. This data mode will continue until just prior to entry, when the data rate will be changed to 200,000 bps. The signal for this command will come from a timer initiated at separation by the Separation Sequencer. The Flight Capsule will be telemetering diagnostic and engineering data, atmospheric information, and descent TV all the way to impact.

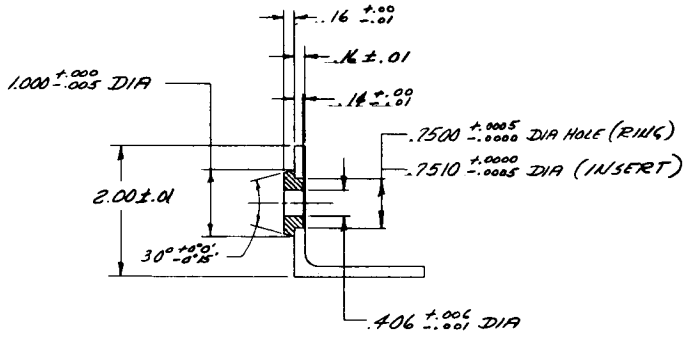
4.0 MECHANICAL INTERFACE

4.1 General Arrangement. Each Flight Capsule is mounted to the forward portion of its Flight Spacecraft and is wholly contained within the envelope described in the Preliminary Mission Description. The only attachment will be at the interface plane. The Spacecraft-to-Capsule field joint lies at Planetary Vehicle station 101.25.

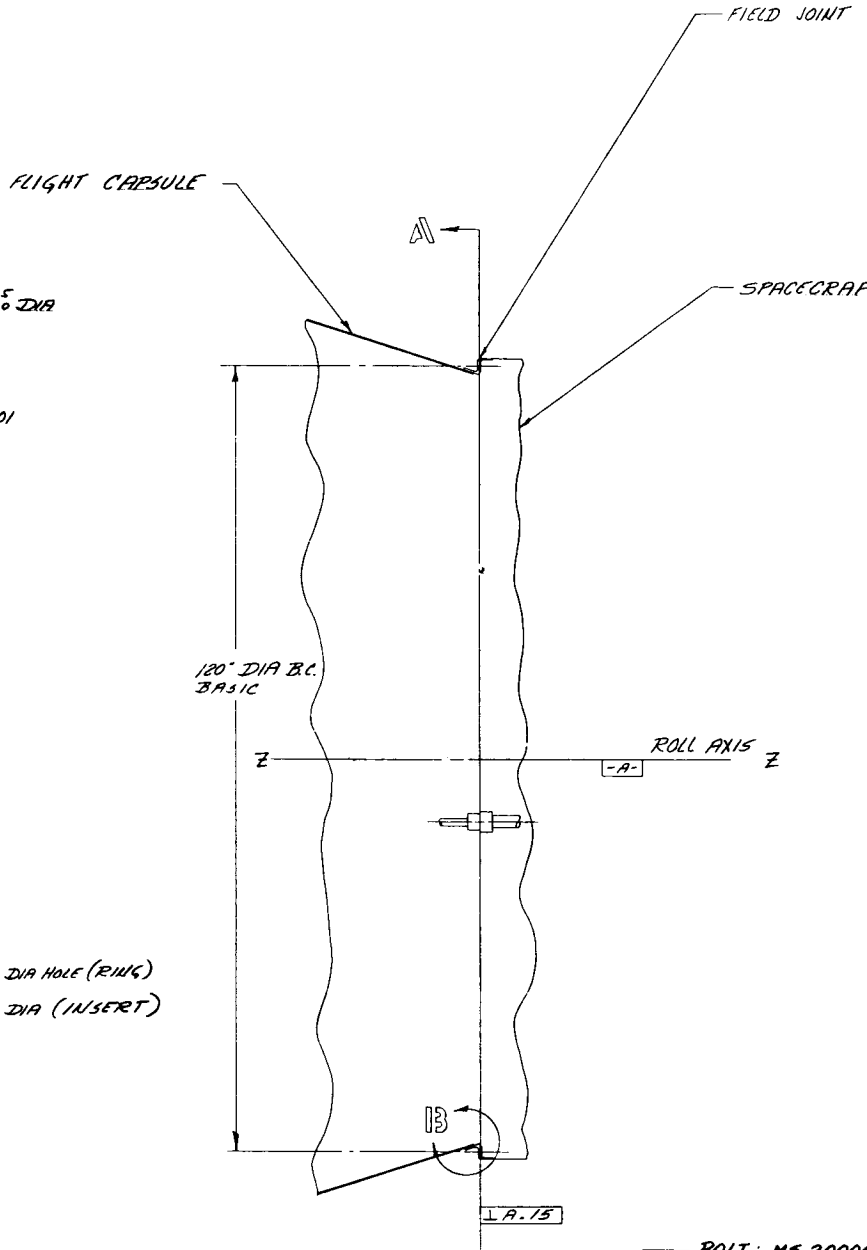
The Flight Capsule/Flight Spacecraft interface is a field joint as shown in Figure 4-1. This interface comprises two circular mating rings, one terminating the Flight Capsule adapter and the other terminating the Flight Spacecraft adapter structure. The mechanical interface is structurally joined by 16 nut/bolt/tapered insert attachments symmetrically located around the interface rings on a nominal 120-inch-diameter bolt circle. One bolt hole is offset circumferentially to key the rotational position of the Flight Capsule to the position of the Flight Spacecraft. Tapered inserts are assumed to transfer the compressive and shear loads across

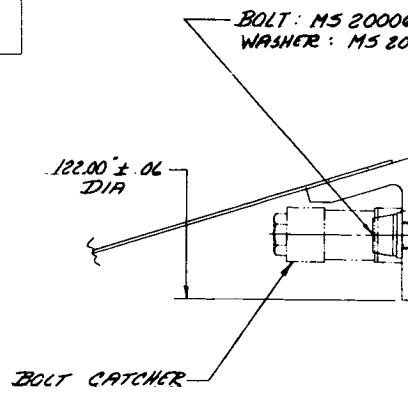


DETAIL - C
FLIGHT CAPSULE RING
TAPERED HOLE INTERFACE
TYP 16 PLACES
SCALE: 1/1



DETAIL - D
SPACECRAFT RING
ALIGNING INSERT INTERFACE
TYP 16 PLACES
SCALE: 1/1





the interface. The taper is used to compensate for hole pattern or mounting ring misalignment. Ample bolt hole clearance around the bolts can be provided to ease attachment/detachment procedures.

The field joint can also serve as the emergency separation joint through use of gas-operated separation nuts as shown in Figure 4-1. Gas supplied from a common storage tank operates simultaneously on each piston and collar which separates a segmented nut. Rotational rates are held to a minimum. A further discussion on the emergency separation design can be found in VC235FD102.

4.2 Mating Tolerances. Tolerances assumed for mating parts are shown in Figure 4-1.

4-3. Design Loads Criteria. The primary load conditions for the Flight Spacecraft/Flight Capsule interface are ground handling, boost, Mars orbit injection, and Flight Capsule separation. The maximum design loads for this interface occur during the boost condition. These loads are the result of various combinations of Flight Capsule inertial reactions to booster rigid body accelerations and vibratory accelerations. The interface structure is designed to withstand the maximum Flight Capsule inertial reactions occurring during boost with a 1.25 factor of safety.

The vibratory load factors were converted to equivalent rigid body load factors to obtain maximum total Flight Capsule load factors. These load factors and resulting interface ultimate loads for a 3000-pound Flight Capsule are shown in Table 4-1, where (-) indicates tension in the bolt.

4.4 Accessibility. The interface is designed such that visible and physical access is available to install and torque the mating bolts. Access is also provided to allow stray voltage tests of the Flight Spacecraft/Flight Capsule electrical connector and the capability for connection/disconnection while the vehicles are mechanically mated.

4.5 Flight Capsule Mass Properties. Flight Spacecraft design has been based upon the Capsule mass properties as shown in Table 4-2.

5.0 THERMAL INTERFACE. The configuration and orientation of the Sterilization Canister structure, which mates to the Flight Spacecraft, is such that it exerts a minimum thermal influence on the Spacecraft. Total Spacecraft-to-Sterilization-Canister heat flow at the interface is assumed not to exceed 50 watts with a Spacecraft structure temperature at 90°F.

TABLE 4-1. FLIGHT CAPSULE LOAD FACTORS

	Load Factor	Max Ultimate Loads
Longitudinal	+ 10.91 - 7.67	+ 41,000 lb - 28,000 lb
Lateral	1.65	6,200 lb
Total Bending	$\ddot{\theta}_y$ = .004 rad/sec^2	756,000 in. lb (max bending arm 122 inches)
Torsion	$\ddot{\theta}_z$ = 44.34 rad/sec^2	540,800 in.-lb

TABLE 4-2. CAPSULE MASS PROPERTIES

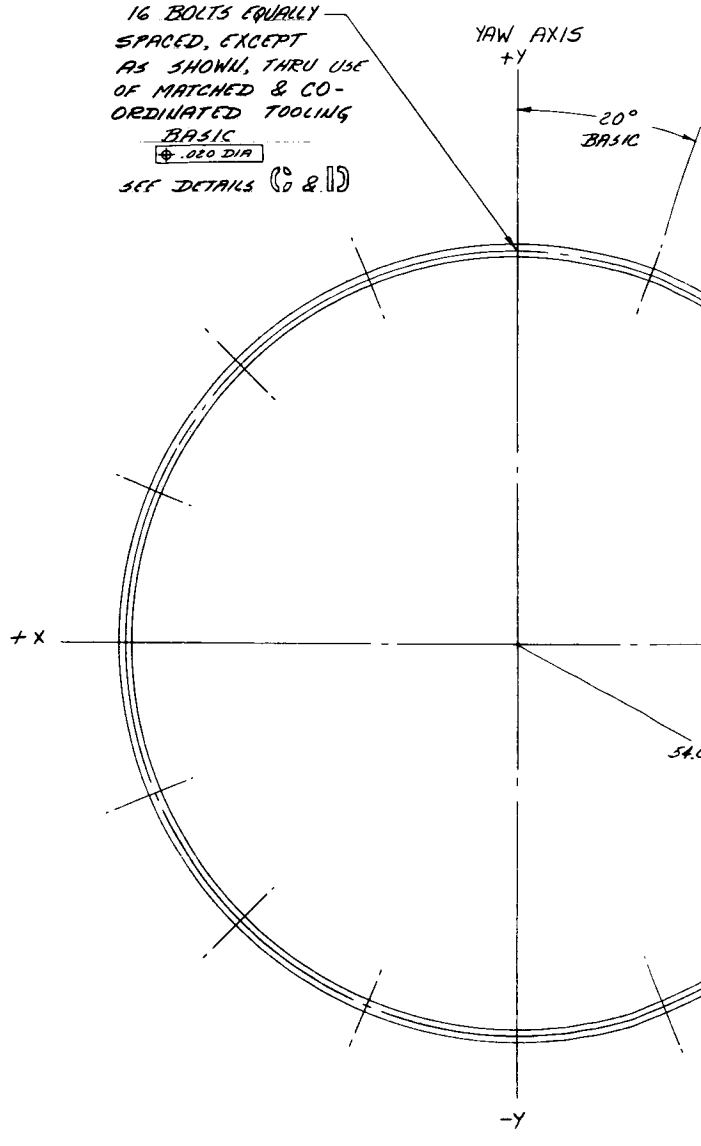
Opportunity	Total Weight (lb)	cg Location* (in.)	I_x	I_y	I_z	
1971-1973	3,000	122	1500	1500	1500	Slug Ft^2 (max)
1975-1577	10,000	122	8000	8000	8000	

*cg is maximum forward position measured from interface joint.

16 BOLTS EQUALLY SPACED, EXCEPT AS SHOWN, THRU USE OF MATCHED & CO-ORDINATED TOOLING

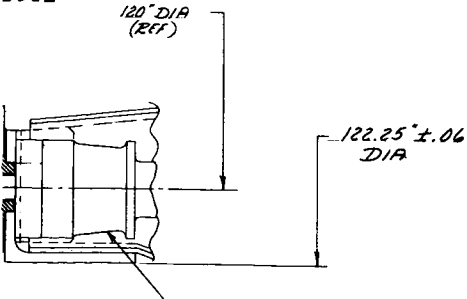
BASIC ⌖ .020 DIA

SEE DETAILS C & D



SECT. A-A

02C6



ETAIL - B

D BOLT
TALLATION
LE: 1/1

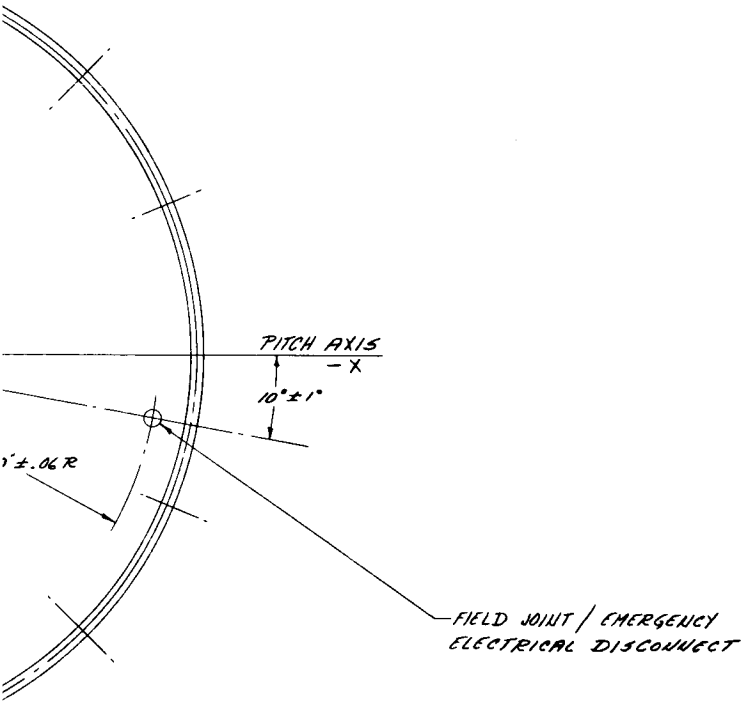


Figure 4-1. VOYAGER Flight Capsule/ Spacecraft Interface

Total heat flow from Sterilization Canister to Spacecraft is assumed not to exceed 30 watts for a Spacecraft structure temperature of 50°F. This flow includes both conduction across the mechanical joint and radiation between canister and the spacecraft inside the 120-inch interface structure, but not radiation exchange outside this point. This requirement does not apply during short-term periods of maneuvering or attitude correction; the time period for this condition shall be less than 3.3 hours in any 24-hour period.

Provisions will be made for periodic monitoring of Capsule temperature sensors during all phases of the mission.

The Sterilization Canister configuration and orientation will be such that the Flight Spacecraft will receive no direct infrared illumination from Canister surfaces having temperatures $\geq$ 180°F. The infrared emissivity of all Sterilization Canister surfaces which are visible to the Flight Spacecraft shall not exceed 0.1

During Spacecraft cruise attitude, solar energy incident upon the Sterilization Canister is negligible; however, significant Solar energy incidence can be expected for the short periods of maneuvering ($\leq$3.3 hours max/day).

Table 5-1 lists Flight Capsule Thermal conditions.

TABLE 5-1. FLIGHT CAPSULE THERMAL CONDITIONS

Mission Phase	Requirements
Pre-Launch	Aerodynamic shroud temperature maintained ±80°F.
Launch and Parking Orbit	Maximum time before removal of aerodynamic shroud after launch is 110 minutes (P/V No 2). No heater power required unless parking orbit > 3.3 hr.
Interplanetary Cruise and Orbit	200 watts DC power will be supplied to Flight Capsule Heater power may be interrupted up to 3.3 hr/day.

6.0 ELECTRICAL INTERFACE

6.1 Power Transfer. Flight Spacecraft supplies to the Flight Capsule an average of 200 watts (34-62 v dc) of power for Flight Capsule environmental control, Capsule system monitoring and checkout, battery heaters and battery charging. The Flight Spacecraft protects against Flight Capsule faults with resetable circuit breakers.

Transfer to Flight Capsule internal power occurs upon receipt of a pre-separation discrete command from the Spacecraft. Pre-separation sequencing of the Flight Capsule is made utilizing the Capsule power. Battery status will be monitored by the Flight Spacecraft telemetry via hardwire lines between the Capsule and Spacecraft. Inverter output voltage and frequency will be sampled, encoded, and sent through the Capsule-Spacecraft data link.

6.2 Grounding, Shielding, and Cabling. The Flight Capsule electrical system will utilize a single-point grounding philosophy. All signal and power circuits will be referenced to a single vehicle ground point. The Flight Capsule VGP will be part of the Capsule structure and will be tied to the Flight Spacecraft SGN by at least one No. 16 gage wire through the electrical interface.

All shielded wires crossing the Spacecraft-Capsule electrical interface will have the shields grounded to the Flight Spacecraft structure ground within the Spacecraft and at the Flight Capsule structure within the Capsule. The shields will not be carried through the interface. Shields will not be used as the return path for power or signal currents.

6.3 Electromagnetic Interference (EMI). The Flight Capsule and Flight Spacecraft equipment will not generate stray voltages or fields that would adversely affect the operation of their particular or mutual equipments.

6.4 Field Joint Electrical Connector. An electrical connector will be provided between the Flight Capsule and the Flight Spacecraft to provide circuit continuity for power, command, monitor, and checkout functions between the Flight Capsule and Flight Spacecraft during the Interplanetary Cruise phase and between Capsule, Spacecraft, and Operational Support Equipment (OSE) during prelaunch checkout. By utilizing a pin puller-actuated, pull-away type of electrical connector, it serves in concert with the emergency separation event.

6.5 Flight Capsule-Flight Spacecraft Signal Interface

6.5.1 Capsule-Spacecraft Hardwire Telemetry

6.5.1.1 Capsule Versus Bus Commutation. Transmittal of Capsule diagnostic information can be accomplished either by commutating the data in the Flight Capsule and transmitting digitally or by allowing the individual sensor leads to cross the interface and process the signal within the Flight Spacecraft.

The advantages of commutating the cruise diagnostic measurements from the Capsule prior to crossing the interface are: (1) Only one pair of wires is required to carry the commutated signal across the Capsule/Spacecraft interface. Control signals (three at most) would be required to start/stop and clock the commutator. (2) The commutator can be used after separation to sample the same sensors for transmission via the relay link to the bus. (3) Minimum in-flight disconnect weight results.

The advantages of having the individual sensor outputs available at the interface are: (1) The Flight Capsule telemetry equipment will not be used until pre-separation checkout; hence, increased reliability will result; (2) the interface is simplified in that all data processing is done on the Flight Spacecraft; (3) a failure in the Flight Capsule cruise instrumentation will not affect the engineering instrumentation used from pre-separation checkout to impact.

The strongest influence on the choice of data transmittal is the fact that with individual sensor outputs the Flight Capsule equipment can be dormant until pre-separation checkout. In this way the Flight Capsule Data Handling System is not called upon to continually be activated when a Capsule status check is required. By providing individual sensor outputs, flexibility is maintained in obtaining diagnostic data at any required frequency.

The Flight Capsule commutator must function after separation and is, of course, a vital link in the telemetry system. A failure in the commutator is catastrophic to the mission, whereas, a failure of one or possibly several interface sensor wires leads only to a

somewhat degraded mission. The tradeoff is not complete, since it requires an investigation of redundancy of the Flight Capsule commutator; however, for the purposes of the present study, individual sensor outputs will be assumed.

6.5.1.2 Capsule Diagnostic Measurements. It is assumed that a total of 30 unique diagnostic measurements will be made aboard the Flight Capsule during cruise.

6.5.1.3 Capsule Check-Out Telemetry. The Flight Capsule will undergo a complete system checkout approximately seven hours prior to separation by energizing as many of the components as possible except for those of a one-shot nature and possibly the transmitter. All sensor outputs will be sampled by the Flight Capsule Data Handling System, encoded, ordered, and sent through the interface connector. The rate at which data is transmitted across the interface will be controlled by the bit synchronization signal provided by the Spacecraft. The rate for checkout will be 116 2/3 bits per second for about 86% of the time. The data will be generated as long as the 116 2/3 pulses per second synchronization signal is present. During the Capsule separation maneuver, the synchronization signal will be 7 7/24 pulses per second for 50% of the time so that the Capsule status may be monitored. Pre-separation Flight Capsule status data will be added serially to Bus engineering data during the separation attitude maneuver and transmitted to the DSIF.

6.5.2 Hardwire Commands

6.5.2.1 Capsule Command List. The discrete commands anticipated to be required by Flight Capsule are:

a. End Launch Mode
b. Arm Bio-barrier Pyro (destination: Spacecraft Pyro Subsystem)
c. Release Bio-barrier (destination: Spacecraft Pyro Subsystem)
d. Switch to Internal Power
e. Initiate Capsule Checkout
f. Initiate Capsule Separation Sequencer
g. Enable Separation Sequence
h. Unassigned
i. Unassigned

The Flight Spacecraft can also provide six quantitative commands to the Flight Capsule.

6.5.2.2 Command Signal Description. Quantitative commands will be sent to the Capsule on three different lines. An "Alert and End of Word Line" is tied to each of the user elements. A "Sync" line is provided in common to all users as is the line which carries the information. The 32 pulses per second "Sync" line will be used to read the information bits into the various decoders.

Discrete commands will be accomplished by providing a separate switch closing for each discrete command required.

7.0 CAPSULE RELAY RECEIVER INTERFACE

The Capsule Relay Receiver carried aboard the Flight Spacecraft has the following interfaces with the spacecraft bus.

7.1 Command Interface. Discrete commands from the Flight Spacecraft C&S to the Capsule relay receiver equipment will be provided as shown in Table 7-1.

TABLE 7-1. DISCRETE COMMANDS FROM FLIGHT SPACECRAFT C&S TO CAPSULE RELAY RECEIVER

Function	Destination
Low-Rate Tape Recorder	Relay Recorder
On or Off	
Read Out	
High-Rate Tape Recorder	Relay Recorder
On or Off	
Read Out	
Relay Receiver	Relay Receiver
On or Off (via Power Subsystem)	

Bit synchronization will be supplied to the relay tape recorders.

7.2 Telemetry Interface. Operating status of the Capsule relay receiver will be made by monitoring the receiver AGC. Sampling rate will be a 77-second interval during pre-separation checkout.

Data will be received from the Flight Capsule at two rates, 100 bits per second from separation until 240 km altitude. From 240 km until impact, the rate will be in the range of 200,000 bps. The low- and high-rate data will be received, demodulated, detected, and stored in the Capsule relay recorders on the spacecraft. The recorded data is played back through the Flight Spacecraft Telemetry Subsystem in phase with the bit sync signal.

7.3 Thermal Control Interface. The Capsule relay receiver equipment is located in bay No. 13 and will be thermally controlled by means of thermal louvers. Average minimum bay temperature is estimated at 50° F, and an average maximum bay temperature is 90° F, based upon an assumed equipment dissipation of 10 watts.

7.4 Power Interface. 2.4 kc, single-phase, square-wave power will be supplied to the Capsule Relay Receiver Subsystem at 50 V RMS ±2%. Fault protection is to be provided by Capsule Relay Receiver Subsystem. Flight Spacecraft C&S will provide a signal to the Power Subsystem to furnish power to the Relay Receiver Subsystem.

The design of all Capsule Relay receiver electronic equipment shall be compatible with the electrical transients and the electromagnetic environment estimated in the VOYAGER Environmental Prediction Document.

7.5 Physical Interface. The Capsule Relay Receiver Subsystem is mounted in Flight Spacecraft equipment bay No. 13. Equipment should be mounted in a standard level III electronic bay assembly and adhere to specifications described in VC235FD106.

Total Relay Subsystem weight has been assumed to be 25 pounds and total power required is 12 watts.

7.6 Relay Antenna. The relay antenna is assumed to be a 400-mc turnstile with ground plane located on the +X axis of the Spacecraft. The Flight Spacecraft will maintain separation attitude until Capsule impact to permit antenna coverage of the Capsule during this time. A further discussion can be found in VC233FD101.

8.0 PYROTECHNIC INTERFACE

In order to ensure the proper connection of the electroexplosive devices (EED) used in the Flight Capsule, a continuity loop through each EED capable of being monitored through the Spacecraft/Capsule interface connector must exist. In addition, the position of any safe-arm device must also be monitored through the interface connector. All pyrotechnic devices and their associated firing circuitry must conform to the Mission Specification Document which includes strict adherence to the requirements of AFETRM 127-1, Range Safety Manual.

CII VC220FD107

MOS/DSN INTERFACE REQUIREMENTS

SECTION

1	SCOPE
2	APPLICABLE DOCUMENTS
3	DESCRIPTION
4	PLANETARY VEHICLE
5	LAUNCH OPERATION
6	FLIGHT OPERATIONS

MOS/DSN INTERFACE REQUIREMENTS

1.0 SCOPE. This document specifies the restraints placed upon the Planetary Vehicle by the Mission Operations System (MOS) and the requirements placed on the MOS by the Planetary Vehicle.

2.0 APPLICABLE DOCUMENTS

EPD-283 - The Deep Space Network, 15 Sept 1965

General Specification for Performance and Design Requirements for the VOYAGER 1971 Spacecraft System, dtd 17 Sept 1965

VOYAGER 1971 Preliminary Mission Description, 15 Oct 1965

CII VC 220SR101 - Design Characteristics and Restraints

CII VC 211SR101 - Mission Objectives and Design Criteria

3.0 DESCRIPTION. The direct interface of the Planetary Vehicle with the MOS is the telecommunications link between the radio subsystem on the Planetary Vehicle and the stations of the Deep Space Network (DSN). The Planetary Vehicle and MOS interface also includes the operational interface with the Space Flight Operations Facility (SFOF). In establishing the restraints and requirements stated below, the configuration and capability of the DSN have been assumed to be as described in EPD-283 the Deep Space Network and the General Specification for Performance and Design Requirements for the VOYAGER Spacecraft System. The MOS support is assumed to be as defined in the VOYAGER 1971 Preliminary Mission Description. The restraints and requirements have been grouped into three categories: Planetary Vehicle, launch operations and space flight operations.

4.0 PLANETARY VEHICLE. These requirements and restraints are based upon the Planetary Vehicle characteristics required for the Planetary Vehicle to achieve its mission.

a. The Planetary Vehicle shall maintain 2-way communication for tracking, telemetry, and command in all mission phases.

b. Planetary Vehicle and Deep Space Information Facility (DSIF) antenna polarization shall be right-hand circular.

c. Planetary Vehicle shall minimize loss in communications with the DSIF during all maneuvers and shall remain in communication with the DSIF at all other times except during ascent or when occulted from Earth by Mars.

d. Suitable calibration data of all transponders flown shall be made available to the DSIF stations.

e. The maximum error rate for communication of telemetry data shall be 5×10^{-3} errors per bit.

f. The bit error probability for the command link at threshold shall be less than $P_e^b = 10^{-5}$.

g. Information required for 2-way communications lock and command shall be transmitted in all telemetry modes.

h. During a normal command lock sequence, the spacecraft receiver static phase error shall be zeroed.

i. No real-time external commands shall be necessary for routine spacecraft flight operations.

j. Calculations shall be made on the ground for the following functions and shall be transmitted to the Spacecraft for execution at the appropriate time.

   1. In-flight maneuver quantitative values

   2. Mars orbit trim quantitative values

   3. Enabling signal for capsule separation from the Spacecraft

   4. The Spacecraft shall verify the reception and correctness of all external commands.

k. Telemetry, ranging and science data shall be source identified for all mission phases.

l. The capsule telemetry shall be a functional interface of MOS via the Spacecraft.

5.0 LAUNCH OPERATIONS. These requirements and restraints are based upon the configuration of the Planetary Vehicles enclosed in the nose fairing. During launch preparations at the launch pad, spacecraft telecommunication signals are picked up by an antenna directed toward DSIF Cape 71 Station and passed through the Launch Vehicle and its umbilical. In addition signals are carried through the nose fairing parasitic antennas. At the Explosive Safe Facility (ESF) the input and output signals of both Planetary Vehicles are relayed by antennas directed toward the DSIF Cape 71 Station. Adequate launch preparation is based upon the following requirements:

a. The MOS shall be capable of supporting the launch of one Space Vehicle, i.e., two Planetary Vehicles on one Launch Vehicle.

b. DSIF Station Cape 71 shall be capable of performing communication tests with the Planetary Vehicles in the ESF and at the launch pad during the seven weeks immediately preceding launch.

c. DSIF Station Cape 71 shall be capable of performing communications tests with the Proof Test Model (PTM) Planetary Vehicle during its cycle of launch preparation verification at Kennedy Space Center (KSC).

d. Ascent mode telemetry capability will be provided through the Launch Vehicle for specified environmental measurements.

e. The final telecommunication checkout and frequency determination shall be provided by DSIF 71 Cape Station.

f. The Eastern Test Range (ETR) shall provide range safety and other launch range services.

6.0 FLIGHT OPERATIONS. These requirements and restraints are based upon the operational considerations of tracking, telemetry, and command.

a. The MOS shall provide 24 hour/day coverage from launch through the end of the mission.

b. The MOS shall be capable of tracking and controlling two Planetary Vehicles during the interplanetary phase of the mission.

c. All prime DSIF Stations shall be able to command for Planetary Vehicle maneuvers during the interplanetary phase.

d. Planetary Vehicle checkout data and simulation tape exercises shall be employed in DSIF compatible form for operational capability tests, including final system rehearsals just prior to launch.

e. No spacecraft event requiring DSN monitoring before acquisition by the DSIF shall be planned.

f. The SFOF shall support 24 hour/day mission coverage from one week before launch through the end of the mission.

g. Mission Dependent Equipment (MDE) shall be provided for each DSIF Station to convert the received spacecraft data into the format required for local processing and for transmission to the SFOF.

h. The Goldstone DSIF Station shall be capable of supporting design verification tests with an RF model of the Spacecraft during the design phase of the program.

i. The Goldstone DSIF Station and the SFOF shall be capable of supporting proof and operational tests with the PTM.

j. The encounters of each Spacecraft with Mars shall take place over the Goldstone Station. Encounters shall occur not less than 10 days apart. The Goldstone Station shall be capable of commanding the first Spacecraft during its encounter, while simultaneously tracking and monitoring the second.

k. The MOS shall be capable of simultaneous tracking and controlling of two Spacecraft during the post-encounter phase of the mission.

l. All orbital trim maneuvers of the Planetary Vehicle or Spacecraft shall be accomplished through Goldstone.

m. Orbit trim maneuvers shall ensure that the probability of impact on Mars before 2021 shall be less than 2×10^{-5}.

CII VC220FD108

EXPERIMENT INTERFACE

SECTION

1 SCOPE
2 APPLICABLE DOCUMENTS
3 FUNCTIONAL DESCRIPTION OF INTERFACE

EXPERIMENT INTERFACE

1.0 SCOPE. This document describes the interface between the spacecraft science payload and the Spacecraft Bus which has been assumed for purposes of spacecraft design for Task B. These assumptions are consistent with information contained in the JPL documentation provided but are necessarily more detailed in order to permit adequate definition of the Flight Spacecraft configuration and functional requirements.

2.0 APPLICABLE DOCUMENTS

VC211SR101, Mission Objectives and Design Criteria
VC220SR101, Design Characteristics and Restraints

3.0 FUNCTIONAL DESCRIPTION OF INTERFACE

3.1 Orientation and Location. Articulation of the span platform support structure will be accomplished by the Science Subsystem. The scan platform is deployed from the outer edge of the solar array. This location permits the planet pointing instruments to view Mars by day or night without intrusion of any part of the Planetary Vehicle into the field of view. However, the gimbal mechanism is designed to provide only the travel required to accommodate viewing of the daylight side of Mars plus 10 degrees beyond each terminator, as specified for the Task A study. Mechanical modifications to the preferred design would be required to permit night viewing of Mars. The transmission of power, data, and synchronizing information between the scan platform and the Spacecraft Bus is accomplished via a hard-wire cable which is designed to accommodate the movement of the scan platform.

Special attachments or locations can be provided as required for individual body-mounted instruments. The electronic equipment part of the Science subsystem will be contained in three of the equipment bays.

3.2 Weight and Volume. The spacecraft Bus is prepared to carry a Science subsystem of the weight and volume described in Table 3-1.

3.3 Control and Sequencing. Provision can be made for the Computer and Sequencer to provide sequencing signals to the Data Automatic Equipment if desired. Detailed sequencing of the individual scientific instruments is assumed to be carried on normally by the Data Automatic Equipment. It has been assumed that for automatic operation over the anticipated lifetime of the vehicle, the in-orbit sequencing will be based upon the true anomaly obtained from gimbal E, the gimbal about which the scan platform rotates in the orbit plane. The terminology is borrowed from the Task A report in which gimbals C and D erected a vertical to the orbit plane and gimbal E permitted rotation about this vertical. A

TABLE 3-1. SCIENCE SUBSYSTEM WEIGHT AND VOLUME

	Weight (lb)	Volume (ft^3)
Platform and platform mounted equipment	150	7
Bay mounted equipment	150	3
Equipment mounted elsewhere	100	2

typical orbit sequence for platform-mounted instruments based upon a gimbal E signal is shown in Table 3-2. In this sequence gimbal E angles are assumed to be zero at high noon.

The following list illustrates the kind of control signals which are likely to cross the Science-Spacecraft Bus interface.

Signals provided by the Science subsystem.

a. Gimbal E position signals consisting of pulses indicating positive or negative incremental angular movement.

b. End of travel signals, positive and negative, for gimbal E.

c. Planet angle signal indicating half angle or angle subtended by Mars. This information and gimbal E information are combined to produce a limb crossing signal.

d. Tape recorder control signals.

e. Power signal to control 400-cps Science inverter.

Signals provided by the Spacecraft Bus.

a. Scientific instrument sequencing signals as required.
b. End of tape signals.
c. Real-time and nonreal-time data gates, and timing pulses.
d. Limb crossing signal.

3.4 Power

3.4.1 Type. 50 volts rms ±2% at 2400 cps ±0.10% square wave, single phase and 28 volts rms ±2% at 400 cps ±0.01% square wave, single phase power will be required by the Science subsystem.

3.4.2 Quantity. Quantitative estimates of the maximum power required are as follows:

		2400 cps	400 cps
a.	During cruise	30 watts	0
b.	In orbit during day-side passage	115 watts	10 watts
c.	During remainder of orbit	40 watts	0

TABLE 3-2. TYPICAL ORBIT SEQUENCE FOR PLATFORM-MOUNTED INSTRUMENTS

Experiment	Start Recording	Stop Recording
Black and White TV	280°	25 minute timer or 320°
	40°	Tape full or 80°
Color TV	350°	Tape Full
	260°	285°
IR Scanner	330°	30°
IR Spectrometer	330°	30°
UV Spectrometer	Limb crossing	5 minute timer
	70°	100°

3.4.3 Frequency Stability. The Science subsystem should be able to continue to operate despite degradation of the stability of the power supply frequency from ±0.01% to ±1%, in the event of a sync signal failure in a power invertor, and from ±1% to -4 to -6% in the event of a subsequent back-up oscillator failure.

3.4.4 Load Fault Protection. The Science subsystem will provide the means for load fault protection (e.g., fuses).

3.4.5 Power Control. The Science subsystem will provide the means for switching power to specific loads within the Science subsystem. It will also provide a signal for switching input power to the 400-cps inverter.

3.5 Data Handling. The Spacecraft Bus will accept data from the Science subsystem in two general modes; cruise and orbit. In cruise mode all data will be clocked out by the Telemetry subsystem, the rate depending upon the mode in which the Bus Telemetry is operating. In orbit mode, all data will be directed by the Data Automatic Equipment to the tape recorders in the Data Storage subsystem.

The Spacecraft Bus will accept all cruise science data, place it in the real-time format and then either have it transmitted or recorded for playback later, depending upon the mode in which the Spacecraft Bus Telemetry is operating. During orbit the Data Storage subsystem will record all planetary data given to it by the Science subsystem and then read it at the telemetry transmitting rate. The read-out periods will have to be carefully sequenced, or phased, with the periods of data recording in order to make best use of the available transmission time. It has been assumed, in selecting the characteristics of the Data Storage subsystem, that no more than 10^8 digital data bits will be generated by any one instrument during one orbit and the total amount of data generated during one orbit might typically be about 2.2×10^8 bits.

3.6 Environment

3.6.1 Electromagnetic Interference

3.6.1.1 Insulation and Grounding. The construction of all scientific instruments and their associated electronics will be such that all circuitry will be insulated from chassis and vehicle structure. Conductors will be provided within the Science subsystem leading from circuits requiring reference to ground. These conductors will be brought to a common ground point within the Spacecraft Bus. Lumped capacitance within individual components greater than 50 pf must not exist between circuits and chassis and/or vehicle structure.

3.6.1.2 Short Circuit Protection. In the event of an accidental short-circuit within the Science subsystem, it is assumed that damage to any component within either the Flight Spacecraft or Operational Support Equipment is to be prevented with load fault protection of each instrument in power lines, and resistors in series with signal lines.

3.6.2 Thermal

3.6.2.1 Electronic Bays. Except during periods in which the Spacecraft is not oriented to the celestial references, the temperature of the scientific experiment equipment located in the electronics bays will be maintained between 40 and 90° F. During short periods of time such as orbit insertion engine firing and earth ascent, the temperature may reach 110° F. These temperatures are for a maximum power dissipation of 37 watts per electronic bay.

3.6.2.2 Body-Mounted Experiments. The locations and techniques used in mounting the body-mounted instruments will be arranged to suit the individual requirements of the experiment, but the temperature of the mounting surfaces may be expected to be within the range 50 to 90° F for instruments mounted inside the Spacecraft Bus.

3.6.3 Magnetic. The Spacecraft Bus will contribute less than one gamma of magnetic field intensity at the magnetometer sensor under all normal operating conditions and less than ten gamma after exposure to a magnetic field of 25 oersteds. The field at the magnetometer sensor will not vary by more than 0.1 gamma during normal operation of the Spacecraft Bus.

3.7 Pointing Accuracy. For VOYAGER 1971, ±1 degree has been assigned as a suitable goal for the maximum uncertainty with which the platform-mounted instruments are pointed toward Mars. The amount of uncertainty in the location of fields of view upon the Martian surface to which this ±1 degree leads is shown in Table 3-3.

TABLE 3-3. UNCERTAINTY IN LOCATION OF FIELDS OF VIEW

Altitude (km)	Linear Range (km)	Central Angle (deg)
1000	15	0.3
2000	35	0.6
3000	50	0.9
4000	70	1.1
5000	85	1.4
10000	170	2.9

CII VC220FD109

TELEMETRY DATA CRITERIA

SECTION

1	SCOPE
2	APPLICABLE DOCUMENTS
3	TELEMETRY DATA CRITERIA
4	DATA COMPRESSION
5	TELEMETRY CHANNEL ASSIGNMENT

TELEMETRY DATA CRITERIA

1.0 SCOPE. This section defines the rationale for telemetry measurement selection and organization. It also contains a first-cut telemetry list, presented in terms of deck format (Figure 5-1, "Telemetry Deck Format") and of subsystem listing (Table 5-2, "Telemetry Channel Assignment").

2.0 APPLICABLE DOCUMENTS

VC220SR101	Design Characteristics and Restraints
VC233FD101	Telecommunication Subsystem

3.0 TELEMETRY DATA CRITERIA. The VOYAGER Spacecraft shall be capable of transmitting telemetry data to the Deep Space Instrumentation Facility (DSIF) during all mission phases from launch to encounter and during its orbital lifetime (except during earth occultation).

3.1 Data Groups

3.1.1 Spacecraft Engineering Data. All measurements of spacecraft parameters, plus some engineering measurements of the on-board relay-radio and science subsystem, are included in this category. These measurements may be subdivided into three types, in order of priority:

a. Spacecraft Operational - data that are necessary for normal operation of the Spacecraft, and hence are continuously transmitted in all data modes. A good example is the two-words-per-minor-frame required to establish frame sync. Since the only normal operations of the spacecraft which are dependent upon ground command are spacecraft maneuvers, most "operational data" are those related to performance of maneuvers, such as the output from solar-aspect sensors for attitude verification, and that from the Canopus tracker.

b. Spacecraft Integrity - data that monitor the normal operations of the Spacecraft so that malfunctions may be corrected by ground command. Data in this category include parameters that may indicate malfunctions requiring the discontinuation of a maneuver in process, such as low battery-charge state. Other corrective command actions include backing up of C&S commands in the event of a false-dismiss in the C&S; switching to redundant components, where a command to perform this is not provided by the spacecraft; or reprogramming of the C&S to permit the mission to continue in a non-nominal and possibly degraded mode in order to offset the effect of some component malfunction.

c. Post-maneuver and Post-flight Analysis - data that relate to parameters for which no timely ground command action is possible, but whose performance must be known for the analysis of maneuvers and/or normal operations. This analysis will provide a basis for improving spacecraft performance on subsequent launch opportunities. Data of this kind include those related to autopilot and propulsion-system performance.

3.1.2 Capsule Data

a. Capsule Diagnostic - data needed for analysis of capsule system and subsystem performance.

b. Capsule Checkout - data needed for establishing the operational readiness of the capsule for separation from the Spacecraft.

c. Capsule Science - science data accumulated by the capsule instrumentation.

3.1.3 Scanned Science Data. Data in the form of serial digital bit trains containing image information, obtained from instrumentation on the planet-scan package.

3.1.4 Nonscanned Science Data. Data obtained from cruise and orbit body-mounted instrumentation, such as the fields and particles data.

3.2 Channel Selection. In the interest of maximum transmission efficiency, information channels are, in general, transmitted only during those mission phases for which they are applicable. To accomplish this, the telemetry data-handling subsystem has been arranged to operate in the following data-transmission modes (also see Table 5-1):

1A	Maneuver	3B	Orbit (Earth-occultation)
1B	Maneuver (Capsule-separation)	4	Cruise (Recorder-readout)
2	Cruise	5	Capsule Checkout.
3A	Orbit		

The information transmitted during each of these modes comprises only that which is necessary to support a particular mission phase or to prepare for subsequent phases, some exceptions being allowed in the interest of hardware optimization and reliability enhancement. The manner of handling this information is shown in Figure 3-1, "Telemetry System Information Flow," and Figure 3-2, "Telemetry Mode Sampling and Transmission Rates."

3.3 Data Acceptance. Data are accepted for transmission in an appropriate telemetry mode if they meet at least one of the following requirements:

a. They contain status information required by the ground complex in order to generate corrective-action commands.

b. They contain support or calibration information necessary for establishing the significance or validity of measurements.

c. They contain scientific information whose accumulation is a Mission objective.

d. They contain information required for post-flight analysis in order to effect design improvement and/or advance the state-of-the-art. Such data shall be stored during critical operations, such as maneuvers, when the transmission rate is low, in order to maintain an adequate sampling rate of critical parameters.

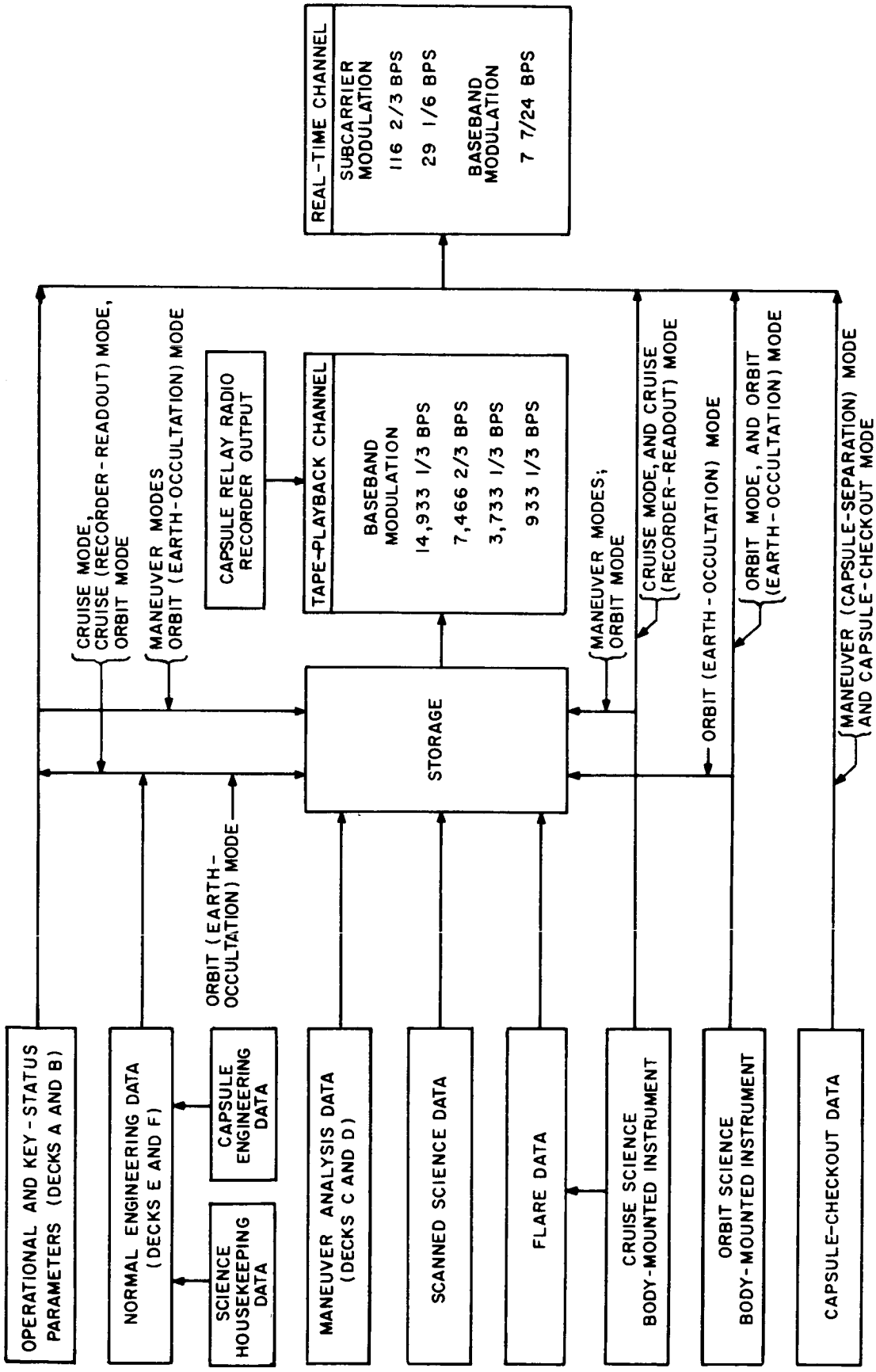


Figure 3-1. Telemetry System Information Flow

Modes / Real-Time Channel Rates / Sampled Data	1A Maneuver		1B Maneuver (Capsule-Separation)		2 Cruise	3A Orbit	3B Orbit (Earth Occultation)	4 Cruise (Recorder-Readout)	5 Capsule Checkout
	XMIT: 7-7/24 BPS	Store: 116 BPS	XMIT: 7-7/24 BPS	Store: 116 BPS	XMIT: 116 BPS	XMIT: 116 BPS	Store: 116 BPS	XMIT: 116 BPS	XMIT: 116 BPS
Operational and Key-Status Information									
12 Words - Fast Sampling	15.4 sec/sample	3.85 sec/sample	30.8 sec/sample	1.9 sec/sample	3.85 sec/sample	3.85 sec/sample	3.85 sec/sample	3.85 sec/sample	7.7 sec/sample
36 Words - Medium Sampling	154 sec/sample	38.5 sec/sample	308 sec/sample	19 sec/sample	38.5 sec/sample	38.5 sec/sample	38.5 sec/sample	38.5 sec/sample	77 sec/sample
80 Words - Slow Sampling (Decks A and B)	3080 sec/sample	770 sec/sample	6160 sec/sample	385 sec/sample	770 sec/sample	770 sec/sample	770 sec/sample	770 sec/sample	1540 sec/sample
Maneuver Analysis Data									
15 Words - Fast Sampling	3.85 sec/sample		1.9 sec/sample						
10 Words - Medium Sampling (Decks C and D)	38.5 sec/sample		19 sec/sample						
Normal Engineering Data									
6 Words - Fast Sampling					3.85 sec/sample	3.85 sec/sample	3.85 sec/sample	3.85 sec/sample	
52 Words - Medium Sampling					38.5 sec/sample	38.5 sec/sample	38.5 sec/sample	38.5 sec/sample	
150 Words - Slow Sampling					770 sec/sample	770 sec/sample	770 sec/sample	770 sec/sample	
30 Capsule Words - Slow Sampling					770 sec/sample	770 sec/sample	770 sec/sample	770 sec/sample	
4 Science Words - Fast Sampling (Decks E and F)					3.85 sec/sample	3.85 sec/sample	3.85 sec/sample	3.85 sec/sample	
Recorder Playback						Planet-Scan Playback at 15 KBPS or Less	(Inhibited)	Flare or Maneuver Data Playback at 3733-1/3 BPS	Planet-Scan Playback at 15 KBPS or Less
Capsule Data 16 or 112 Words			16 words at 30.8 sec per 7-Bit word						112 words at 7.7 sec per 7-Bit word
Science Data 32 Words	Store 32 words @ 3.85 sec per 7-Bit word				3.85 sec per 7-Bit word			32 words at 3.85 sec per 7-Bit word	
Science-Equipment Data 32 words						32 words at 3.85 sec per 7-Bit word	32 words at 3.85 sec per 7-Bit word		
Minor-Frame Size	16-word	64-word	32-word	32-word	64-word	64-word	64-word	64-word	128-word

Figure 3-2. Telemetry Mode Sampling and Transmission Rates

3.4 Priority Ordering. The seven telemetry modes have been arranged to accomplish the following priority ordering:

a. Operational and key-status information is transmitted during all modes for maximum DSIF exposure.

b. Normal engineering data are transmitted in all except the Maneuver Modes and the Capsule-checkout Mode. These data relate to the normal operational parameters, and provide routine vehicle, capsule and science-equipment monitoring for diagnostic purposes and for post-maneuver and post-flight analysis.

c. Maneuver analysis data are recorded during Maneuver Mode and Capsule-separation Mode for playback upon return to the Cruise Mode. These data permit post-maneuver and post-flight analysis of the operation of subsystems utilized during maneuvers.

d. Science data, including flight capsule relay data, required to accomplish all mission objectives are transmitted whenever the Spacecraft is Sun/Canopus oriented, and the high-gain antenna is pointed toward the earth, except when maneuver analysis data are being played back.

4.0 DATA COMPRESSION

4.1 General. During the Phase IA/Task-B study, an investigation was made of the use of data compression. It was realized at the outset that the application of data-compression techniques to the scientific data stream is beyond the present task scope of the Flight Spacecraft study contractors, and is indeed pointless without detailed interaction with the principal investigators of the VOYAGER experiments. Therefore, data compression was considered only with regard to operational and housekeeping data on the Spacecraft and its experiments. Since this involves only 50% of the Cruise-mode data-transmission rate and less than 1% of the data-rate capability for Cruise or Orbit Modes, the need for data compression during these modes is clearly not worth the added equipment complexity involved. Only during a Maneuver Mode, when the data-transmission rate drops to 7-7/24 bps but the data activity is high, might any real advantage be gained from data compression. Therefore, only this possibility was considered in any detail.

4.2 Possible Usefulness. Depending on spacecraft distance from earth at the time of a maneuver, the round-trip communication time could be as long as 16 minutes. Evaluation of telemetry data and the making of a ground-command decision will require additional minutes. Hence, ground command action during short periods, such as propulsion-system firing, is not feasible. However, in each case the total maneuver sequence is long enough to permit useful ground command action based upon received telemetry. For example, if during a midcourse trajectory-correction maneuver a serious fault were observed in the operation of the Attitude Control subsystem, a ground command to abort the maneuver could be transmitted to the spacecraft; the maneuver could be attempted again later in the mission after the fault had been corrected or a redundant system had been switched in.

If a data compression scheme could permit more frequent sampling of critical maneuver operations, several advantages would accrue. Frequent sampling of G&C parameters affecting maneuver turns, such as gyro-torquer current or gyro output, would not only serve as a back-up of the solar aspect sensor attitude-verification method, but would also indicate where in the maneuver procedure any malfunction occurred. This would permit more intelligent ground override of the Computer and Sequencer to save the maneuver. It would be especially valuable for the orbit-insertion maneuver, which is the only spacecraft maneuver which can not be deferred. More frequent sampling of vital parameters might also reveal trends leading to failure which could be prevented by proper command action. More data, especially from G&C and Propulsion, would be useful in post-maneuver and post-flight analysis, leading to design refinements for future flights. Finally, frequent sampling might reveal the cause of a catastrophic failure which occurred too quickly to be seen at a slower sampling rate.

4.3 Concepts Considered. Several data-compression concepts to increase sampling frequency during a maneuver mode were considered:

a. Programmable format (changeable by ground command).

b. Asynchronous schemes, such as the following:

   1. Zero-order, floating-aperture techniques.

   2. Run-length encoding.

   3. Delta encoding.

c. Alarm Schemes.

Of these three concepts the last seemed the most promising and was explored farthest. One version consists of a fixed-subframe-length, fixed-word technique not requiring either buffer storage or arithmetic processing from implementation. In this concept, important spacecraft maneuver parameters (for example, gyro-torquing-current magnitude) would be sampled at short intervals; any out-of-limit reading would be transmitted as a six-bit address, plus another bit to show whether the particular reading was out of limits on the high side or on the low side. Several blank words, say five, would be left in the maneuver format for insertion of out-of-limit readings. If all these words appeared blank in the received telemetry, it would be known that all sampled channels were behaving properly. If all five blank words were filled with repetitions of the same few out-of-limit conditions, it would be known that only these few readings indicated malfunctioning. If the five blank words were filled with different out-of-limit readings, it would be known that at least five spacecraft conditions were out of limit, from which it might be concluded that ground intervention to abort the maneuver was required.

However, the inclusion of such a data-compression scheme would involve the addition of considerable functional and hardware complexity, for at least the following reasons:

a. Many of the readings that need to be monitored do not lend themselves readily to simple out-of-limit statements. An instance of this is the gyro-torquing-current magnitude, mentioned in the preceding paragraph, which goes from zero to a nominal value and then back to zero. Proper measurement of this variable requires rather complex logic, in order not to report as out-of-limit a condition which is normal.

b. It is very difficult to clear enough high-speed-deck words of operational data, such as frame-sync words, to provide the blank words required.

4.4 Conclusion. No special provision for data compression was incorporated in the telemetry subsystem for two reasons: first, after a telemetry list had been compiled it was apparent that even without any special provisions for data compression, all vital telemetry information could be transmitted with sampling intervals small enough to permit ground decision of whether or not to allow a particular maneuver to continue; second, it was found that the tradeoff of functional and hardware complexity, and therefore of long-life reliability, versus useful performance enhancement was unfavorable.

5.0 TELEMETRY CHANNEL ASSIGNMENT

5.1 Assignment Priority. The selection of engineering (including capsule) measurements, was made in accordance with the following order of priority:

a. Measurement of those system parameters where an abnormal indication might require aborting of a maneuver to save the mission.

b. Measurement of those system parameters where an abnormal indication might require corrective action to avoid degraded mission performance.

c. Measurements to obtain data required for verifying the achievement of mission objectives.

d. Measurements to obtain data required for diagnosing the cause of any malfunctions and incipient failures in order to enhance the mission performance of later flights.

5.2 Channel Assignment. Channel locations and resulting sampling rates were selected to comply as closely as possible with the following requirements:

a. Nonessential data transmitted during each mission phase must be minimized.

b. The number of voltage references required on each deck must be minimized.

c. Measurements which are closely related to each other and which collectively should be made at nearly the same instant for an analysis must be grouped as closely together as possible in time when making channel selections. An example of this is the -15 volts, +15 volts and AGC signals measured at each of three receivers in the Radio Subsystem.

d. Deck sizes must be consistent for the sake of design simplicity.

e. Deck sizes must be kept low in order to minimize the effect of deck loss.

f. Two or more measurements which could be used for the same analysis must be located in separate decks, as a precaution against deck loss.

5.3 Spare Channels. Provision has been made for 15% spare channels on the high and medium decks. This can easily be extended to the low decks during the design phase. Should there be no additional measurement requirements, these spare channels could be used to provide redundancy and/or more frequent measurement of critical parameters.

5.4 Deck Format. Figure 5-1, "Telemetry Deck Format" is a functional diagram of the commutator distribution, with channel assignments. High decks A and B, with their associated medium and low decks, are used for both real-time transmission and storage during all modes; high decks C and D serve for storage only, and only during the two Maneuver Modes; high decks E and F serve for real-time transmission during only the Cruise, Orbit, and Cruise Recorder Readout Modes and for storage during only the Orbit (Earth-occultation) Mode.

5.5 Data Modes. The modes, and the kinds of data handled during each mode, are defined in Table 5-1, "Telemetry Mode Assignment."

5.6 Channel Assignment. Table 5-2, "Telemetry Channel Assignment," presents, by subsystems, the telemetry measurments and their respective channel assignments. The table also contains the kind of variable being measured and its range and the kind of voltage reference used, plus its range (if analog) in each case.

TABLE 5-1. TELEMETRY MODE ASSIGNMENT

Mode		Real Time or Stored	Kind of Data Handled
No.	Name		
1A	Maneuver	RT ST	Critical Maneuver data Maneuver and motor-burn data Cruise science data
1B	Maneuver (Capsule	RT ST	Capsule Checkout data Critical Maneuver data Maneuver and motor-burn data
2	Cruise	RT	Cruise/Orbit engineering data Cruise science data Capsule diagnostic data
3A	Orbit	RT	Cruise/Orbit engineering data Orbit science Capsule diagnostic data (prior to separation) Planet-scan science data (Playback of recorders)
3B	Orbit (earth Occultation	ST	Cruise/Orbit engineering data Orbit science data Planet-scan science data
4	Cruise (Recorder Readout)	RT	Cruise/Orbit engineering data Cruise science data Manuever or solar flare recorded data
5	Capsule Checkout	RT	Spacecraft operational data Capsule checkout data

TRANSMISSION MODES				
NO.	MISSION PHASE	REAL TIME OR STORED	HD MD LD	INTERVAL SECONDS

HIGH DECKS

A1	TLM	MAIN FRAME SYNC
A2	TLM	MAIN FRAME SYNC

MEDIUM DECKS

M101	TLM	MED DECK SYNC
M102	RAD	CAPSULE

LOW DECKS

L101	C/S	TTG REGISTER 1
L102	C/S	TTG REGISTER 2
L103	C/S	TTG REGISTER 3
L104	C/S	TTG REGISTER 4
L105	C/S	WORD AND ADDRESS 1

1A	MANEUVER	REAL TIME	15.4 154 3080
1A	MANEUVER	STORED	3.85 38.5 770
1B	MANEUVER (CAPSULE-SEPARATION)	REAL TIME	30.8 308 6160
1B	MANEUVER (CAPSULE-SEPARATION)	STORED	1.92 19.2 385
2	CRUISE	REAL TIME	3.85 38.5 770
3A	ORBIT	REAL TIME	3.85 38.5 770
3B	ORBIT (EARTH-OCCULT)	STORED	3.85 38.5 770
4	CRUISE (RECORDER READOUT)	REAL TIME	3.85 38.5 770
5	CAPSULE X-OUT	REAL TIME	7.7 77 1540

A4	CMD	COMMAND ERROR AND ACCEPT/ C/S INHIBIT
A5	C/S	COMPUTER AND SEQUENCER SEQ TIME 1
A6	C/S	COMPUTER AND SEQUENCER SEQ TIME 2
A7	C/S	COMPUTER AND SEQUENCER SEQ TIME 3
A8		M100
M104	G/C	PITCH CRUISE SUN SENSOR
M105	G/C	YAW CRUISE SUN SENSOR
M106	TLM	LOW DECK POSITION A
M107	G/C	PITCH GYRO RATE/POS (-3/+3 DPS)
M108		SPARE
M109		L100
M110		L200
L109	PRO	MCOA JET VANE POSITION LOGIC
L110	PWR	CHARGE REGULATOR 1 STATE
L111	PWR	CHARGE REGULATOR 2 STATE
L112	PWR	CHARGE REGULATOR 3 STATE
L113	VEH	PYRO CONTROLLER 1
L114	VEH	PYRO CONTROLLER 2
L115	VEH	PYRO CONTROLLER 3
L116	VEH	PYRO CONTROLLER 4
L117	VEH	HIGH GAIN ANT A ACTUATOR TEMP
L118	VEH	HIGH GAIN ANT B ACTUATOR TEMP
L119	VEH	HIGH GAIN ANT FLEX CABLE TEMP
L120	PWR	BACKUP OSC IN USE
L201	G/C	COLD GAS TANK 1 PRESSURE
L202	RAD	POWER AMP 1 OUTPUT
L203		SPARE
L204	PRO	RPS TVC PRESS
L205	PWR	REGULATOR 1 OUTPUT VOLTAGE
L206	G/C	COLD GAS TANK 2 PRESSURE
L207	G/C	REGULATOR 1 PRESSURE
L208	G/C	REGULATOR 2 PRESSURE
L209	VEH	PYRO 1 VOLTAGE
L210	VEH	PYRO 2 VOLTAGE
L211	G/C	COLD GAS TANK 3 PRESSURE
L212	RAD	POWER AMP 2 OUTPUT
L213		SPARE
L214	RAD	POWER 3 WATT TRANSMITTER
L215	PWR	2.4 KC INVERTER 2 VOLTAGE
L216	G/C	COLD GAS TANK 4 PRESSURE
L217	PWR	400 CPS 3PH INVERTER 1 VOLT
L218	PWR	400 CPS 3PH INVERTER 2 VOLT
L219	PWR	400 CPS 1PH INVERTER VOLT
L220	PWR	2.4 KC INVERTER 1 VOLTAGE

B1	C/S	ATTITUDE VERIFICATION 1
B2	C/S	ATTITUDE VERIFICATION 2
B3	C/S	ATTITUDE VERIFICATION 3
B4	G/C	CANOPUS INTENSITY
B5	G/C	GYRO TORQUER CURRENT SUM
B6		M200
B7		M300
B8		M400
M201	PWR	BATTERY 1 CURRENT
M202	PWR	BATTERY 2 CURRENT
M203	PWR	BATTERY 3 CURRENT
M204	RAD	AGC RECEIVER 1 COARSE
M205	RAD	AGC RECEIVER 2 COARSE
M206	G/C	YAW GYRO RATE/POS (-3/+3 DPS)
M207	PRO	MCOA PROPELLANT TANK PRESS
M208	PWR	ARRAY VOLTAGE
M209	PWR	BATTERY AMP-HR DISCHARGE
M210		SPARE
M301	RAD	STATIC PHASE ERROR 1
M302	RAD	STATIC PHASE ERROR 2
M303	G/C	ROLL GYRO RATE/POS (-3/+3 DPS)
M304	TLM	LOW DECK POSITION B
M305	VEH	HIGH GAIN ANT A GIMBAL POS 1
M306	G/C	ATTITUDE CONTROL LOGIC STATUS 1
M307	VEH	HIGH GAIN ANTENNA B GIMBAL POS 1
M308		SPARE
M309		L300
M310		L400
L301	VEH	BAY 1 TEMP SENSOR 1
L302	VEH	BAY 2 TEMP SENSOR 1
L303	VEH	BAY 3 TEMP SENSOR 1
L304	VEH	BAY 4 TEMP SENSOR 1
L305	VEH	BAY 5 TEMP SENSOR 1
L306	VEH	BAY 6 TEMP SENSOR 1
L307	VEH	BAY 7 TEMP SENSOR 1
L308	VEH	BAY 8 TEMP SENSOR 1
L309	VEH	BAY 9 TEMP SENSOR 1
L310	VEH	BAY 10 TEMP SENSOR 1
L311	VEH	BAY 11 TEMP SENSOR 1
L312	VEH	BAY 12 TEMP SENSOR 1
L313	VEH	BAY 13 TEMP SENSOR 1
L314	VEH	BAY 14 TEMP SENSOR 1
L315	VEH	BAY 15 TEMP SENSOR 1
L316	VEH	BAY 16 TEMP SENSOR 1
L317	G/C	PRIMARY GYRO SYSTEM BLOCK TEMP
L318	G/C	ALTERNATE GYRO SYSTEM BLOCK TEMP
L319		SPARE
L320	TLM	TEMP SENSOR REF CURRENT B
L401	G/C	COLD GAS TANK 1 TEMP
L402	PRO	MCOA PROPELLANT TANK 1 TEMP
L403	G/C	SOL VALVE TEMP 1
L404	PRO	MCOA HE TANK 1 TEMP
L405	PWR	SOLAR ARRAY TEMP 1
L406	G/C	COLD GAS TANK 2 TEMP
L407	PRO	MCOA PROPELLANT TANK 2 TEMP
L408	G/C	SOL VALVE TEMP 2
L409	G/C	PITCH ACQUISITION SUN SENSOR TEMP
L410	G/C	YAW ACQUISITION SUN SENSOR TEMP
L411	G/C	COLD GAS TANK 3 TEMP
L412	PRO	MCOA PROPELLANT TANK 3 TEMP
L413	G/C	SOL VALVE TEMP 3
L414	PRO	MCOA HE TANK 2 TEMP
L415	PWR	SOLAR ARRAY TEMP 2
L416	G/C	COLD GAS TANK 4 TEMP
L417	PRO	MCOA PROPELLANT TANK 4 TANK
L418	G/C	SOL VALVE TEMP 4
L419	G/C	ACCELEROMETER TEMP

M401	TLM	MED DECK SYNC B	L501	PRO	RPS AND MCOA SQUIB VALVE EVENT COUNTER
M402	G/C	ATTITUDE CONTROL LOGIC STATUS 2	L502	PWR	SOLAR ARRAY TEMP 3
M403	G/C	THRESHOLD DETECTOR COUNTER PITCH POS	L503	CMD	DET A LOCK AND SYNC
M404	G/C	THRESHOLD DETECTOR COUNTER YAW POS	L504	CMD	DET B LOCK AND SYNC
M405	G/C	THRESHOLD DETECTOR COUNTER ROLL POS	L505	CMD	DET C LOCK AND SYNC
M406	G/C	THRESHOLD DETECTOR COUNTER PITCH NEG	L506	VEH	HIGH GAIN ANT LATCH AND A/B LIM LOGIC
M407	G/C	THRESHOLD DETECTOR COUNTER YAW NEG	L507	VEH	HIGH GAIN ANT LATCH AND A/B LIM LOGIC
M408	G/C	THRESHOLD DETECTOR COUNTER ROLL NEG	L508	G/C	CONOPUS TRACKER TEMP 2
M409	D/S	MTR ID	L509	C/S	COMPUTER AND SEQUENCER STATUS 1
M410		L500	L510	C/S	COMPUTER AND SEQUENCER STATUS 2
			L511	C/S	COMPUTER AND SEQUENCER STATUS 3
			L512	C/S	COMPUTER AND SEQUENCER STATUS 4
			L513	D/S	MTR 5 TAPE MOTION
			L514	D/S	MTR 6 TAPE MOTION
			L515	PWR	SOLAR ARRAY TEMP 4
			L516	PWR	400 CPS INVERTER CURRENT
			L517	VEH	MAGNETOMETER AND MED GAIN ANT LOGIC
			L518	PRO	RPS SAFE/ARM LOGIC
			L519	PWR	SOLAR ARRAY TEMP 5
			L520	PWR	SOLAR ARRAY TEMP 6

				C1	G/C	AUTOPILOT OUTPUT PITCH
				C2	G/C	AUTOPILOT OUTPUT YAW
				C3	G/C	AUTOPILOT OUTPUT ROLL
				C4	PRO	RPS CHAMBER PRESS
			3.85	C5	PRO	MCOA ENGINE CHAMBER PRESS 1
IA	MANEUVER	STORED	38.5	C6	PRO	MCOA ENGINE CHAMBER PRESS 2
			770	C7	PRO	MCOA ENGINE CHAMBER PRESS 3
				C8	PRO	MCOA ENGINE CHAMBER PRESS 4
	MANEUVER		1.92	D1	G/C	PITCH ACQ SUN SENSOR
IB	(CAPSULE-	STORED	19.2	D2	G/C	YAW ACQ SUN SENSOR
	SEPARATION)		385	D3	G/C	ACCELEROMETER
				D4	G/C	PITCH GYRO RATE/POS (-3/+3 DPS)
				D5	G/C	YAW GYRO RATE/POS (-3/+3 DPS)
				D6	G/C	ROLL GYRO RATE/POS (-3/+3 DPS)
				D7		SPARE
				D8		M500

M501	TLM	MED DECK SYNC D
M502	PRO	MCOA PROPELLANT MANIFOLD PRESS
M503	PRO	MCOA HE TANK PRESS
M504	G/C	ALT PITCH GYRO
M505	G/C	ALT YAW GYRO
M506	G/C	ALT ROLL GYRO
M507		SPARE
M508		SPARE
M509		SPARE
M510		SPARE

(3)

E1	SCI	ENG SCIENCE BODY MOUNTED SENSORS	M601		SPARE	L601	RAD	COLLECTOR 1 TEMP
E2	SCI	ENG SCIENCE BODY MOUNTED SENSORS	M602	RAD	COLLECTOR VOLTAGE PWR AMP 1	L602	RAD	COLLECTOR 2 TEMP
E3		SPARE	M603	RAD	COLLECTOR VOLTAGE PWR AMP 2	L603	RAD	BASE PLATE TEMP 3W TRANSMITTER
E4		SPARE	M604	RAD	-25 VOLTS EXCITER 1	L604	RAD	VCO TEMP RECEIVER 1
E5		SPARE	M605	RAD	-25 VOLTS EXCITER 2	L605	RAD	VCO TEMP RECEIVER 2
E6		M600	M606	RAD	-25 VOLTS EXCITER 3	L606	RAD	VCO TEMP RECEIVER 3
E7		M700	M607	RAD	-25 VOLTS 3 WATT TRANSMITTER	L607	RAD	L.O. DRIVE 1
E8		M800	M608		L60	L608	RAD	L.O. DRIVE 2
			M609		L70	L609	RAD	L.O. DRIVE 3
			M610		L80	L610	VEH	HIGH GAIN ANT DEPLOY AXIS POS
						L611	CAP	CAPSULE
						L612	CAP	CAPSULE
						L613	CAP	CAPSULE
						L614	CAP	CAPSULE
						L615	CAP	CAPSULE
						L616	CAP	CAPSULE
						L617	CAP	CAPSULE
						L618	CAP	CAPSULE
						L619	CAP	CAPSULE
						L620	CAP	CAPSULE

L701		SPARE
L702		SPARE
L703	SCI	INSTRUMENT PKG GIMBAL C ACT TEMP

			3.85
2	CRUISE	REAL TIME	38.5
			770
			3.85
3A	ORBIT	REAL TIME	38.5
			770
	ORBIT		3.85
3B	(EARTH-	STORED	38.5
	OCCULT)		770
	CRUISE		3.85
4	(RECORDER-	REAL TIME	38.5
	READOUT)		770

F1	SCI	ENG SCIENCE BODY MOUNTED SENSORS
F2	SCI	ENG SCIENCE BODY MOUNTED SENSORS
F3		SPARE
F4		SPARE
F5		SPARE
F6		M900
F7		M1000
F8		M1100

M701	TLM	MED DECK SYNC E
M702	PWR	ARRAY CURRENT
M703	PWR	BATTERY 1 VOLTAGE COARSE
M704	PWR	BATTERY 2 VOLTAGE COARSE
M705	PWR	BATTERY 3 VOLTAGE COARSE
M706	PWR	REGULATOR 1 OUTPUT CURRENT
M707	G/C	CANOPUS SENSOR
M708	TLM	LOW DECK POSITION E
M709	RAD	AGC RECEIVER 3 COARSE
M710		SPARE

301	D/S	MTR 1 TAPE MOTION
M802	D/S	MTR 2 TAPE MOTION
M803	D/S	MTR 3 TAPE MOTION
M804	D/S	MTR 4 TAPE MOTION
M805		SPARE
M806		SPARE
M807		SPARE
M808		SPARE
M809		SPARE
M810		SPARE

M901	RAD	-15V RECEIVER 1
M902	RAD	-15V RECEIVER 2
M903	RAD	-15V RECEIVER 3
M904	RAD	-15V EXCITER 1
M905	RAD	-15V EXCITER 2
M906	RAD	-15V EXCITER 3
M907	RAD	HELIX VOLTAGE PWR AMP 1
M908	RAD	STATIC PHASE ERROR 3
M909	VEH	HIGH GAIN ANT A GIMBAL POS 2
M910	TLM	LOW DECK POSITION F

M1001	TLM	MED DECK SYNC F
M1002	PWR	BATTERY RAW BUSS VOLTAGE
M1003	PWR	REGULATOR 2 OUTPUT VOLTAGE
M1004	PWR	REGULATOR 2 OUTPUT CURRENT
M1005	G/C	PITCH GYRO PKG TEMP
M1006	G/C	YAW GYRO PKG TEMP
M1007	G/C	ROLL GYRO PKG TEMP
M1008	G/C	ACCELEROMETER PKG TEMP
M1009		L90
M1010		L10

L701	SCI	INSTRUMENT PKG GIMBAL E ACT TEMP
L705	SCI	INSTRUMENT PKG GIMBAL E ACT TEMP
L706		SPARE
L707	VEH	SCAN PKG FLEX CABLE TEMP
L708	D/S	MTR 1 PRESSURE
L709	D/S	MTR 2 PRESSURE
L710	D/S	MTR 3 PRESSURE
L711	SCI	TEMP SCAN PKG 1
L712	SCI	TEMP INST PKG 1
L713	SCI	TEMP SCAN PKG 2
L714	SCI	TEMP INST PKG 2
L715	SCI	TEMP SCAN PKG 3
L716	SCI	TEMP INST PKG 3
L717	SCI	TEMP INST PKG 4
L718	SCI	TEMP INST PKG 5
L719	SCI	TEMP INST PKG 6
L720	TLM	TEMP SENSOR REF CURRENT E

L801	SCI	INSTRUMENT PKG GIMBAL C POSITION
L802	SCI	INSTRUMENT PKG GIMBAL C POSITION
L803	SCI	INSTRUMENT PKG GIMBAL D POSITION
L804	SCI	INSTRUMENT PKG GIMBAL D POSITION
L805	SCI	INSTRUMENT PKG GIMBAL E POSITION
L806	SCI	INSTRUMENT PKG GIMBAL E POSITION
L807	D/S	MTR 4 PRESSURE
L808	D/S	MTR 5 PRESSURE
L809	D/S	MTR 6 PRESSURE
L810		SPARE
L811	CAP	CAPSULE
L812	CAP	CAPSULE
L813	CAP	CAPSULE
L814	CAP	CAPSULE
L815	CAP	CAPSULE
L816	CAP	CAPSULE
L817	CAP	CAPSULE
L818	CAP	CAPSULE
L819	CAP	CAPSULE
L820	CAP	CAPSULE

L901	VEH	SHUTTER 1 POSITION
L902	VEH	SHUTTER 3 POSITION
L903	VEH	SHUTTER 5 POSITION
L904	VEH	SHUTTER 7 POSITION
L905	VEH	SHUTTER 9 POSITION
L906	VEH	SHUTTER 11 POSITION
L907	VEH	SHUTTER 13 POSITION
L908	VEH	SHUTTER 15 POSITION
L909	RAD	COLLECTOR CURRENT PWR AMP 1
L910	RAD	CATHODE CURRENT PWR AMP 2
L911	C/S	+3 VOLTS
L912	C/S	+6 VOLTS
L913	C/S	+15 VOLTS
L914	RAD	EXCITER 1 POWER OUT
L915	RAD	EXCITER 2 POWER OUT
L916	RAD	EXCITER 3 POWER OUT
L917	PWR	BATTERY 1 VOLTAGE FINE
L918	PWR	BATTERY 2 VOLTAGE FINE
L919	PWR	BATTERY 3 VOLTAGE FINE
L920		SPARE

L1001	VEH	SHUTTER 2 POSITION
L1002		SPARE
L1003	VEH	SHUTTER 6 POSITION
L1004	VEH	SHUTTER 8 POSITION
L1005	VEH	SHUTTER 10 POSITION
L1006		SPARE
L1007	VEH	SHUTTER 14 POSITION
L1008	VEH	SHUTTER 16 POSITION
L1009	PWR	ARRAY/BATTERY BUSS CURRENT
L1010	RAD	HELIX CURRENT 1
L1011	RAD	+15 VOLTS RECEIVER 1
L1012	RAD	+15 VOLTS RECEIVER 2
L1013	RAD	+15 VOLTS RECEIVER 3
L1014		SPARE
L1015	VEH	HIGH GAIN ANT A MOTOR PRESS
L1016	VEH	HIGH GAIN ANT B MOTOR PRESS

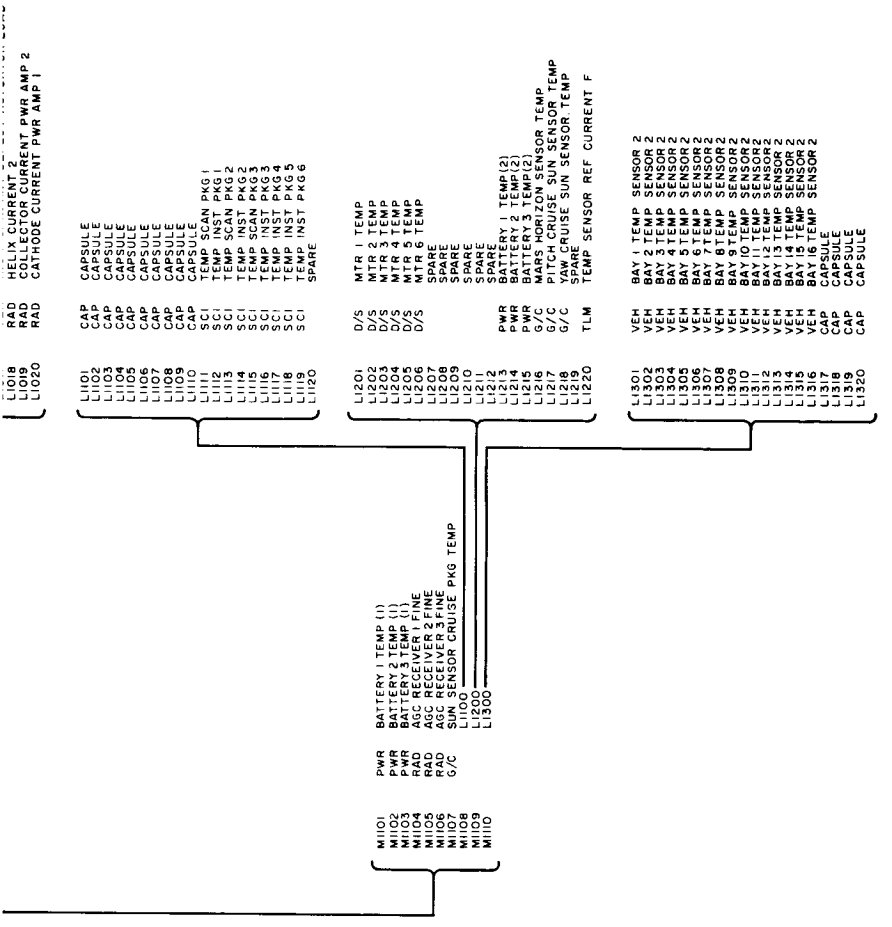


Figure 5-1. Telemetry Deck Format

TABLE 5-2. CHANNEL ASSIGNMENTS

Deck Location	Sub-System	Variable Measured	Ref Volt	Range of Variable	Unit of Variable
1. GUIDANCE AND CONTROL					
B4	G/C	CANOPUS INTENSITY	3.2	10XCANOPUS	
B5	G/C	GYRO TORQUER CURRENT SUM	3.2		
C1	G/C	AUTOPILOT OUTPUT PITCH	3.2	-30/+30	VDC
C2	G/C	AUTOPILOT OUTPUT YAW	3.2	-30/+30	VDC
C3	G/C	AUTOPILOT OUTPUT ROLL	3.2	-30/+30	VDC
D1	G/C	PITCH ACQ SUN SENSOR	1.6	-10/+10	DEG
D2	G/C	YAW ACQ SUN SENSOR	1.6	-10/+10	DEG
D3	G/C	ACCELEROMETER	3.2	0/50	F/S
D4	G/C	PITCH GYRO RATE/POS (-3/+3 DPS)	1.6	-6/+6	DEG
D5	G/C	YAW GYRO RATE/POS (-3/+3 DPS)	1.6	-6/+6	DEG
D6	G/C	ROLL GYRO RATE/POS (-3/+3 DPS)	1.6	-6/+6	DEG
M104	G/C	PITCH CRUISE SUN SENSOR	1.6	-2/+2	DEG
M105	G/C	YAW CRUISE SUN SENSOR	1.6	-2/+2	DEG
M107	G/C	PITCH GYRO RATE/POS (-3/+3 DPS)	1.6	-6/+6	DEG
M206	G/C	YAW GYRO RATE/POS (-3/+3 DPS)	1.6	-6/+6	DEG
M303	G/C	ROLL GYRO RATE/POS (-3/+3 DPS)	1.6	-6/+6	DEG
M306	G/C	ATTITUDE CONTROL LOGIC STATUS 1	DIG	7 BITS	
M402	G/C	ATTITUDE CONTROL LOGIC STATUS 2	DIG	7 BITS	
M403	G/C	THRESHOLD DETECTOR COUNTER PITCH POS	DIG	COUNTS	
M404	G/C	THRESHOLD DETECTOR COUNTER YAW POS	DIG	COUNTS	
M405	G/C	THRESHOLD DETECTOR COUNTER ROLL POS	DIG	COUNTS	
M406	G/C	THRESHOLD DETECTOR COUNTER PITCH NEG	DIG	COUNTS	
M407	G/C	THRESHOLD DETECTOR COUNTER YAW NEG	DIG	COUNTS	
M408	G/C	THRESHOLD DETECTOR COUNTER ROLL NEG	DIG	COUNTS	
M504	G/C	ALT PITCH GYRO	1.6	-04/+04	DEG
M505	G/C	ALT YAW GYRO	1.6	-04/+04	DEG
M506	G/C	ALT ROLL GYRO	1.6	-04/+04	DEG
M707	G/C	CANOPUS SENSOR	1.6	-1/+1	DEG
M1005	G/C	PITCH GYRO PKG TEMP	3.2	30/200	DEG
M1006	G/C	YAW GYRO PKG TEMP	3.2	30/200	DEG
M1007	G/C	ROLL GYRO PKG TEMP	3.2	30/200	DEG
M1008	G/C	ACCELEROMETER PKG TEMP	3.2		DEG
M1107	G/C	SUN SENSOR CRUISE PKG TEMP	100MV	-200/+200	DEG
L201	G/C	COLD GAS TANK 1 PRESSURE	3.2	0/3250	PSI
L206	G/C	COLD GAS TANK 2 PRESSURE	3.2	0/3250	PSI
L207	G/C	REGULATOR 1 PRESSURE	3.2	0/100	PSI
L208	G/C	REGULATOR 2 PRESSURE	3.2	0/100	PSI
L211	G/C	COLD GAS TANK 3 PRESSURE	3.2	0/3250	PSI
L216	G/C	COLD GAS TANK 4 PRESSURE	3.2	0/3250	PSI
L317	G/C	PRIMARY GYRO SYSTEM BLOCK TEMP	100MV	30/200	DEG
L318	G/C	ALTERNATE GYRO SYSTEM BLOCK TEMP	100MV	30/200	DEG
L401	G/C	COLD GAS TANK 1 TEMP	100MV	0/200	DEG
L403	G/C	SOL VALVE TEMP 1	100MV	-100/+200	DEG
L406	G/C	COLD GAS TANK 2 TEMP	100MV	0/200	DEG
L408	G/C	SOL VALVE TEMP 2	100MV	-100/+200	DEG
L409	G/C	PITCH ACQUISITION SUN SENSOR TEMP	100MV	-200/+200	DEG
L410	G/C	YAW ACQUISITION SUN SENSOR TEMP	100MV	-200/+200	DEG
L411	G/C	COLD GAS TANK 3 TEMP	100MV	0/200	DEG
L413	G/C	SOL VALVE TEMP 3	100MV	-100/+200	DEG
L416	G/C	COLD GAS TANK 4 TEMP	100MV	0/200	DEG
L418	G/C	SOL VALVE TEMP 4	100MV	-100/+200	DEG
L419	G/C	ACCELEROMETER TEMP	100MV	0/200	DEG
L420	G/C	CANOPUS TRACKER TEMP 1	100MV	-200/+200	DEG
L508	G/C	CONOPUS TRACKER TEMP 2	DIG		
L1216	G/C	MARS HORIZON SENSOR TEMP	100MV	0/200	DEG
L1217	G/C	PITCH CRUISE SUN SENSOR TEMP	100MV	-200/+200	DEG
L1218	G/C	YAW CRUISE SUN SENSOR TEMP	100MV	-200/+200	DEG
2. COMMAND					
A4	CMD	COMMAND ERROR AND ACCEPT/. C/S INHIBIT	DIG		
L503	CMD	DET A LOCK + SYNC	DIG		
L504	CMD	DET B LOCK + SYNC	DIG		
L505	CMD	DET C LOCK + SYNC	DIG		

TABLE 5-2. CHANNEL ASSIGNMENTS (Continued)

Deck Location	Sub-System	Variable Measured	Ref Volt	Range of Variable	Unit of Variable
3. COMPUTER AND SEQUENCER					
A5	C/S	COMPUTER AND SEQUENCER SEQ TIME 1	DIG		
A6	C/S	COMPUTER AND SEQUENCER SEQ TIME 2	DIG		
A7	C/S	COMPUTER AND SEQUENCER SEQ TIME 3	DIG		
B1	C/S	ATTITUDE VERIFICATION 1	DIG		
B2	C/S	ATTITUDE VERIFICATION 2	DIG		
B3	C/S	ATTITUDE VERIFICATION 3	DIG		
L102	C/S	TTG REGISTER 2	DIG		
L101	C/S	TTG REGISTER 1	DIG		
L103	C/S	TTG REGISTER 3	DIG		
L104	C/S	TTG REGISTER 4	DIG		
L105	C/S	WORD AND ADDRESS 1	DIG		
L106	C/S	WORD AND ADDRESS 2	DIG		
L107	C/S	WORD AND ADDRESS 3	DIG		
L108	C/S	WORD AND ADDRESS 4	DIG		
L509	C/S	COMPUTER AND SEQUENCER STATUS 1	DIG		
L510	C/S	COMPUTER AND SEQUENCER STATUS 2	DIG		
L511	C/S	COMPUTER AND SEQUENCER STATUS 3	D16		
L512	C/S	COMPUTER AND SEQUENCER STATUS 4	DIG		
L911	C/S	+3 VOLTS	3.2		
L912	C/S	+6 VOLTS	3.2		
L913	C/S	+15 VOLTS	3.2		
4. DATA HANDLING AND STORAGE					
M409	D/S	MTR ID	DIG		
M801	D/S	MTR 1 TAPE MOTION	3.2		IPS
M802	D/S	MTR 2 TAPE MOTION	3.2		IPS
M803	D/S	MTR 3 TAPE MOTION	3.2		IPS
M804	D/S	MTR 4 TAPE MOTION	3.2		IPS
L513	D/S	MTR 5 TAPE MOTION	3.2		IPS
L514	D/S	MTR 6 TAPE MOTION	3.2		IPS
L708	D/S	MTR 1 PRESSURE	3.2		PSI
L709	D/S	MTR 2 PRESSURE	3.2		PSI
L710	D/S	MTR 3 PRESSURE	3.2		PSI
L807	D/S	MTR 4 PRESSURE	3.2		PSI
L808	D/S	MTR 5 PRESSURE	3.2		PSI
L809	D/S	MTR 6 PRESSURE	3.2		PSI
L1201	D/S	MTR 1 TEMP	100MV		DEG
L1202	D/S	MTR 2 TEMP	100MV		DEG
L1203	D/S	MTR 3 TEMP	100MV		DEG
L1204	D/S	MTR 4 TEMP	100MV		DEG
L1205	D/S	MTR 5 TEMP	100MV		DEG
L1206	D/S	MTR 6 TEMP	100MV		DEG
5. TELEMETRY					
A1	TLM	MAIN FRAME SYNC	DIG	1111111	SYN
A2	TLM	MAIN FRAME SYNC	DIG	1111111	SYN
A3	TLM	MODE IDENT	DIG		
M101	TLM	MED DECK SYNC A	DIG		
M106	TLM	LOW DECK POSITION A	DIG		
M304	TLM	LOW DECK POSITION B	DIG		
M401	TLM	MED DECK SYNC B	DIG		
M501	TLM	MED DECK SYNC D	DIG		
M701	TLM	MED DECK SYNC E	DIG		
M708	TLM	LOW DECK POSITION E	DIG		
M910	TLM	LOW DECK POSITION F	DIG		
M1001	TLM	MED DECK SYNC F	DIG		
L320	TLM	TEMP SENSOR REF CURRENT B	100MV		
L720	TLM	TEMP SENSOR REF CURRENT E	100MV		
L1220	TLM	TEMP SENSOR REF CURRENT F	100MV		

TABLE 5-2. CHANNEL ASSIGNMENTS (Continued)

Deck Location	Sub-System	Variable Measured	Ref Volt	Range of Variable	Unit of Variable
6. RADIO					
M102	RAD	CAPSULE RELAY RCVR 1 AGC	1.6		
M103	RAD	CAPSULE RELAY RCVR 2 AGC	1.6		
M204	RAD	AGC RECEIVER 1 COARSE	3.2	-90/-150	DBM
M205	RAD	AGC RECEIVER 2 COARSE	3.2	-90/-150	DBM
M301	RAD	STATIC PHASE ERROR 1	1.6	-600/+600	CPS
M302	RAD	STATIC PHASE ERROR 2	1.6	-600/+600	CPS
M602	RAD	COLLECTOR VOLTAGE PWR AMP 1	1.6		VDC
M603	RAD	COLLECTOR VOLTAGE PWR AMP 2	1.6		VDC
M604	RAD	-25 VOLTS EXCITER 1	1.6	-20/-30	VDC
M605	RAD	-25 VOLTS EXCITER 2	1.6	-20/-30	VDC
M606	RAD	-25 VOLTS EXCITER 3	1.6	-20/-30	VDC
M607	RAD	-25 VOLTS 3 WATT TRANSMITTER	1.6	-20/-30	VDC
M709	RAD	AGC RECEIVER 3 COARSE	3.2	-90/-150	DBM
M901	RAD	-15V RECEIVER 1	1.6	-12/-18	VDC
M902	RAD	-15V RECEIVER 2	1.6	-12/-18	VDC
M903	RAD	-15V RECEIVER 3	1.6	-12/-18	VDC
M904	RAD	-15V EXCITER 1	1.6	-12/-18	VDC
M905	RAD	-15V EXCITER 2	1.6	-12/-18	VDC
M906	RAD	-15V EXCITER 3	1.6	-12/-18	VDC
M907	RAD	HELIX VOLTAGE PWR AMP 1	1.6		VDC
M908	RAD	STATIC PHASE ERROR 3	1.6	-600/+600	CPS
M1104	RAD	AGC RECEIVER 1 FINE	100MV	-118/+142	DBM
M1105	RAD	AGC RECEIVER 2 FINE	100MV	-118/+142	DBM
M1106	RAD	AGC RECEIVER 3 FINE	100MV	-118/+142	DB4
L202	RAD	POWER AMP 1 OUTPUT	3.2	0/50	WAT
L212	RAD	POWER AMP 2 OUTPUT	3.2	0/50	WAT
L214	RAD	POWER 3 WATT TRANSMITTER	3.2	0/5	WAT
L601	RAD	COLLECTOR 1 TEMP	100MV		DEG
L602	RAD	COLLECTOR 2 TEMP	100MV		DEG
L603	RAD	BASE PLATE TEMP 3W TRANSMITTER	100MV	0/200	DEG
L604	RAD	VCO TEMP RECEIVER 1	100MV	25/150	DEG
L605	RAD	VCO TEMP RECEIVER 2	100MV	25/150	DEG
L606	RAD	VCO TEMP RECEIVER 3	100MV	25/150	DEG
L607	RAD	L.O. DRIVE 1	100MV	0/3	MW
L608	RAD	L.O. DRIVE 2	100MV	0/3	MW
L609	RAD	L.O. DRIVE 3	100MV	0/3	MW
L909	RAD	COLLECTOR CURRENT PWR AMP 1	3.2		MA
L910	RAD	CATHODE CURRENT PWR AMP 2	3.2		MA
L914	RAD	EXCITER 1 POWER OUT	3.2	0/.6	WAT
L915	RAD	EXCITER 2 POWER OUT	3.2	0/.6	WAT
L916	RAD	EXCITER 3 POWER OUT	3.2	0/.6	WAT
L1010	RAD	HELIX CURRENT 1	3.2		MA
L1011	RAD	+15 VOLTS RECEIVER 1	3.2	12/18	VDC
L1012	RAD	+15 VOLTS RECEIVER 2	3.2	12/18	VDC
L1013	RAD	+15 VOLTS RECEIVER 3	3.2	12/18	VDC
L1018	RAD	HELIX CURRENT 2	3.2		MA
L1019	RAD	COLLECTOR CURRENT PWR AMP 2	3.2		MA
L1020	RAD	CATHODE CURRENT PWR AMP 1	3.2		MA
7. PROPULSION					
C4	PRO	RPS CHAMBER PRESS	3.2	0/600	PSI
C5	PRO	MCOA ENGINE CHAMBER PRESS 1	3.2	0/250	PSI
C6	PRO	MCOA ENGINE CHAMBER PRESS 2	3.2	0/250	PSI
C7	PRO	MCOA ENGINE CHAMBER PRESS 3	3.2	0/250	PSI
C8	PRO	MCOA ENGINE CHAMBER PRESS 4	3.2	0/250	PSI
M207	PRO	MCOA PROPELLANT TANK PRESS	3.2	0/350	PSI
M502	PRO	MCOA PROPELLANT MANIFOLD PRESS	3.2	0/350	PSI
M503	PRO	MCOA HE TANK PRESS	3.2	0/4000	PSI
L109	PRO	MCOA JET VANE POSITION LOGIC	DIG		
L204	PRO	RPS TVC PRESS	3.2	0/4000	PSI
L402	PRO	MCOA PROPELLANT TANK 1 TEMP	100MV	0/130	DEG
L404	PRO	MCOA HE TANK 1 TEMP	100MV	50/150	DEG
L407	PRO	MCOA PROPELLANT TANK 2 TEMP	100MV	0/130	DEG
L412	PRO	MCOA PROPELLANT TANK 3 TEMP	100MV	0/130	DEG
L414	PRO	MCOA HE TANK 2 TEMP	100MV	50/150	DEG
L417	PRO	MCOA PROPELLANT TANK 4 TEMP	100MV	0/130	DEG
L501	PRO	RPS + MCOA SQUIB VALVE EVENT COUNTER	DIG		
L518	PRO	RPS SAFE/ARM LOGIC	DIG		

TABLE 5-2. CHANNEL ASSIGNMENTS (Continued)

Deck Location	Sub-System	Variable Measured	Ref Volt	Range of Variable	Unit of Variable
8. POWER					
M201	PWR	BATTERY 1 CURRENT	3•2	-7/+25	AMP
M202	PWR	BATTERY 2 CURRENT	3•2	-7/+25	AMP
M203	PWR	BATTERY 3 CURRENT	3•2	-7/+25	AMP
M208	PWR	ARRAY VOLTAGE	3•2	30/70	VDC
M209	PWR	BATTERY AMP-HR DISCHARGE	3•2	0/2	AHR
M702	PWR	ARRAY CURRENT	3•2	0/25	AMP
M703	PWR	BATTERY 1 VOLTAGE COARSE	3•2	30/50	VDC
M704	PWR	BATTERY 2 VOLTAGE COARSE	3•2	30/50	VDC
M705	PWR	BATTERY 3 VOLTAGE COARSE	3•2	30/50	VDC
M706	PWR	REGULATOR 1 OUTPUT CURRENT	3•2	0/15	AMP
M1002	PWR	BATTERY RAW BUSS VOLTAGE	3•2	30/55	VDC
M1003	PWR	REGULATOR 2 OUTPUT VOLTAGE	3•2	28/32	VDC
M1004	PWR	REGULATOR 2 OUTPUT CURRENT	3•2	0/15	AMP
M1101	PWR	BATTERY 1 TEMP (1)	100MV	0/130	DEG
M1102	PWR	BATTERY 2 TEMP (1)	100MV	0/130	DEG
M1103	PWR	BATTERY 3 TEMP (1)	100MV	0/130	DEG
L110	PWR	CHARGE REGULATOR 1 STATE	DIG		
L111	PWR	CHARGE REGULATOR 2 STATE	DIG		
L112	PWR	CHARGE REGULATOR 3 STATE	DIG		
L120	PWR	BACKUP OSC IN USE	DIG		
L205	PWR	REGULATOR 1 OUTPUT VOLTAGE	3•2	28/32	VDC
L215	PWR	2•4KC INVERTER 2 VOLTAGE	3•2	45/55	VAC
L217	PWR	400 CPS 3PH INVERTER 1 VOLT	3•2	22/30	VAC
L218	PWR	400 CPS 3PH INVERTER 2 VOLT	3•2	22/30	VAC
L219	PWR	400 CPS 1PH INVERTER VOLT	3•2	25/33	VAC
L220	PWR	2•4KC INVERTER 1 VOLTAGE	3•2	45/55	VAC
L405	PWR	SOLAR ARRAY TEMP 1	100MV	-100/+250	DEG
L415	PWR	SOLAR ARRAY TEMP 2	100MV	-100/+250	DEG
L502	PWR	SOLAR ARRAY TEMP 3	100MV	-100/+250	DEG
L515	PWR	SOLAR ARRAY TEMP 4	100MV	-100/+250	DEG
L516	PWR	400 CPS INVERTER CURRENT	3•2	0/1•5	AMP
L519	PWR	SOLAR ARRAY TEMP 5	100MV	-350/+100	DEG
L520	PWR	SOLAR ARRAY TEMP 6	100MV	-350/+100	DEG
L917	PWR	BATTERY 1 VOLTAGE FINE	3•2	45/50	VDC
L918	PWR	BATTERY 2 VOLTAGE FINE	3•2	45/50	VDC
L919	PWR	BATTERY 3 VOLTAGE FINE	3•2	45/50	VDC
L1009	PWR	ARRAY/BATTERY BUSS CURRENT	3•2	0/13	AMP
L1213	PWR	BATTERY 1 TEMP (2)	100MV	0/130	DEG
L1214	PWR	BATTERY 2 TEMP (2)	100MV	0/130	DEG
L1215	PWR	BATTERY 3 TEMP (2)	100MV	0/130	DEG
9. VEHICLE					
M305	VEH	HIGH GAIN ANT A GIMBAL POS 1	DIG	-50/+120	DEG
M307	VEH	HIGH GAIN ANT B GIMBAL POS 1	DIG	-10/+22	DEG
M909	VEH	HIGH GAIN ANT A GIMBAL POS 2	DIG	-50/+120	DEG
L113	VEH	PYRO CONTROLLER 1	DIG		
L114	VEH	PYRO CONTROLLER 2	DIG		
L115	VEH	PYRO CONTROLLER 3	DIG		
L116	VEH	PYRO CONTROLLER 4	DIG		
L117	VEH	HIGH GAIN ANT A ACTUATOR TEMP	100MV	-200/200	DEG
L118	VEH	HIGH GAIN ANT B ACTUATOR TEMP	100MV	-200/+200	DEG
L119	VEH	HIGH GAIN ANT FLEX CABLE TEMP	100MV	-100/+200	DEG
L209	VEH	PYRO 1 VOLTAGE	3•2	3/15	VDC
L210	VEH	PYRO 2 VOLTAGE	3•2	3/15	VDC
L301	VEH	BAY 1 TEMP SENSOR 1	100MV	0/250	DEG
L302	VEH	BAY 2 TEMP SENSOR 1	100MV	0/250	DEG
L303	VEH	BAY 3 TEMP SENSOR 1	100MV	0/250	DEG
L304	VEH	BAY 4 TEMP SENSOR 1	100MV	0/250	DEG
L305	VEH	BAY 5 TEMP SENSOR 1	100MV	0/250	DEG
L306	VEH	BAY 6 TEMP SENSOR 1	100MV	0/250	DEG
L307	VEH	BAY 7 TEMP SENSOR 1	100MV	0/250	DEG
L308	VEH	BAY 8 TEMP SENSOR 1	100MV	0/250	DEG
L309	VEH	BAY 9 TEMP SENSOR 1	100MV	0/250	DEG
L310	VEH	BAY 10 TEMP SENSOR 1	100MV	0/250	DEG
L311	VEH	BAY 11 TEMP SENSOR 1	100MV	0/250	DEG
L312	VEH	BAY 12 TEMP SENSOR 1	100MV	0/250	DEG
L313	VEH	BAY 13 TEMP SENSOR 1	100MV	0/250	DEG
L314	VEH	BAY 14 TEMP SENSOR 1	100MV	0/250	DEG
L315	VEH	BAY 15 TEMP SENSOR 1	100MV	0/250	DEG

TABLE 5-2. CHANNEL ASSIGNMENTS (Continued)

Deck Location	Sub-System	Variable Measured	Ref Volt	Range of Variable	Unit of Variable
L316	VEH	BAY 16 TEMP SENSOR 1	100MV	0/250	DEG
L506	VEH	HIGH GAIN ANT LATCH + A/B LIM LOGIC	DIG		
L507	VEH	HIGH GAIN ANT LATCH + A/B LIM LOGIC	DIG		
L517	VEH	MAGNETOMETER AND MED GAIN ANT LOGIC	DIG		
L610	VEH	HIGH GAIN ANT DEPLOY AXIS POS	3.2	0/132	DEG
L707	VEH	SCAN PKG FLEX CABLE TEMP	100MV	-100/+200	DEG
L901	VEH	SHUTTER 1 POSITION	3.2	0/90	DEG
L902	VEH	SHUTTER 3 POSITION	3.2	0/90	DEG
L903	VEH	SHUTTER 5 POSITION	3.2	0/90	DEG
L904	VEH	SHUTTER 7 POSITION	3.2	0/90	DEG
L905	VEH	SHUTTER 9 POSITION	3.2	0/90	DEG
L906	VEH	SHUTTER 11 POSITION	3.2	0/90	DEG
L907	VEH	SHUTTER 13 POSITION	3.2	0/90	DEG
L908	VEH	SHUTTER 15 POSITION	3.2	0/90	DEG
L1001	VEH	SHUTTER 2 POSITION	3.2	0/90	DEG
L1003	VEH	SHUTTER 6 POSITION	3.2	0/90	DEG
L1004	VEH	SHUTTER 8 POSITION	3.2	0/90	DEG
L1005	VEH	SHUTTER 10 POSITION	3.2	0/90	DEG
L1007	VEH	SHUTTER 14 POSITION	3.2	0/90	DEG
L1008	VEH	SHUTTER 16 POSITION	3.2	0/90	DEG
L1015	VEH	HIGH GAIN ANT A MOTOR PRESS	3.2	0/3000	LBS
L1016	VEH	HIGH GAIN ANT B MOTOR PRESS	3.2	0/3000	LBS
L1017	VEH	HIGH GAIN ANT DEPLOY ACTUATOR LOAD	3.2	0/3000	LBS
L1301	VEH	BAY 1 TEMP SENSOR 2	100MV	0/250	DEG
L1302	VEH	BAY 2 TEMP SENSOR 2	100MV	0/250	DEG
L1303	VEH	BAY 3 TEMP SENSOR 2	100MV	0/250	DEG
L1304	VEH	BAY 4 TEMP SENSOR 2	100MV	0/250	DEG
L1305	VEH	BAY 5 TEMP SENSOR 2	100MV	0/250	DEG
L1306	VEH	BAY 6 TEMP SENSOR 2	100MV	0/250	DEG
L1307	VEH	BAY 7 TEMP SENSOR 2	100MV	0/250	DEG
L1308	VEH	BAY 8 TEMP SENSOR 2	100MV	0/250	DEG
L1309	VEH	BAY 9 TEMP SENSOR 2	100MV	0/250	DEG
L1310	VEH	BAY 10 TEMP SENSOR 2	100MV	0/250	DEG
L1311	VEH	BAY 11 TEMP SENSOR 2	100MV	0/250	DEG
L1312	VEH	BAY 12 TEMP SENSOR 2	100MV	0/250	DEG
L1313	VEH	BAY 13 TEMP SENSOR 2	100MV	0/250	DEG
L1314	VEH	BAY 14 TEMP SENSOR 2	100MV	0/250	DEG
L1315	VEH	BAY 15 TEMP SENSOR 2	100MV	0/250	DEG
L1316	VEH	BAY 16 TEMP SENSOR 2	100MV	0/250	DEG

10. SCIENCE

E1	SCI	ENG SCIENCE BODY MOUNTED SENSORS	3.2		
E2	SCI	ENG SCIENCE BODY MOUNTED SENSORS	3.2		
F1	SCI	ENG SCIENCE BODY MOUNTED SENSORS	DIG		
F2	SCI	ENG SCIENCE BODY MOUNTED SENSORS	DIG		
L703	SCI	INSTRUMENT PKG GIMBAL C ACT TEMP	100MV	-200/+200	DEG
L704	SCI	INSTRUMENT PKG GIMBAL D ACT TEMP	100MV	-200/+200	DEG
L705	SCI	INSTRUMENT PKG GIMBAL E ACT TEMP	100MV	-200/+200	DEG
L711	SCI	TEMP SCAN PKG 1	100MV	-100/+200	DEG
L712	SCI	TEMP INST PKG 1	100MV	-100/+200	DEG
L713	SCI	TEMP SCAN PKG 2	100MV	-100/+200	DEG
L714	SCI	TEMP INST PKG 2	100MV	-100/+200	DEG
L715	SCI	TEMP SCAN PKG 3	100MV	-100/+200	DEG
L716	SCI	TEMP INST PKG 3	100MV	-100/+200	DEG
L717	SCI	TEMP INST PKG 4	100MV	-100/+200	DEG
L718	SCI	TEMP INST PKG 5	100MV	-100/+200	DEG
L719	SCI	TEMP INST PKG 6	100MV	-100/+200	DEG
L801	SCI	INSTRUMENT PKG GIMBAL C POSITION	DIG		
L802	SCI	INSTRUMENT PKG GIMBAL C POSITION	DIG		
L803	SCI	INSTRUMENT PKG GIMBAL D POSITION	DIG		
L804	SCI	INSTRUMENT PKG GIMBAL D POSITION	DIG		
L805	SCI	INSTRUMENT PKG GIMBAL E POSITION	DIG		
L806	SCI	INSTRUMENT PKG GIMBAL E POSITION	DIG		
L1111	SCI	TEMP SCAN PKG 1	100MV	-100/+200	DEG
L1112	SCI	TEMP INST PKG 1	100MV	-100/+200	DEG
L1113	SCI	TEMP SCAN PKG 2	100MV	-100/+200	DEG
L1114	SCI	TEMP INST PKG 2	100MV	-100/+200	DEG
L1115	SCI	TEMP SCAN PKG 3	100MV	-100/+200	DEG
L1116	SCI	TEMP INST PKG 3	100MV	-100/+200	DEG
L1117	SCI	TEMP INST PKG 4	100MV	-100/+200	DEG
L1118	SCI	TEMP INST PKG 5	100MV	-100/+200	DEG
L1119	SCI	TEMP INST PKG 6	100MV	-100/+200	DEG

TABLE 5-2. CHANNEL ASSIGNMENTS (Continued)

Deck Location	Sub-System	Variable Measured	Ref Volt
11. CAPSULE			
L611	CAP	CAPSULE	100MV
L612	CAP	CAPSULE	100MV
L613	CAP	CAPSULE	100MV
L614	CAP	CAPSULE	100MV
L615	CAP	CAPSULE	100MV
L616	CAP	CAPSULE	100MV
L617	CAP	CAPSULE	100MV
L618	CAP	CAPSULE	100MV
L619	CAP	CAPSULE	100MV
L620	CAP	CAPSULE	100MV
L811	CAP	CAPSULE	100MV
L812	CAP	CAPSULE	100MV
L813	CAP	CAPSULE	100MV
L814	CAP	CAPSULE	100MV
L815	CAP	CAPSULE	100MV
L816	CAP	CAPSULE	100MV
L817	CAP	CAPSULE	100MV
L818	CAP	CAPSULE	100MV
L819	CAP	CAPSULE	100MV
L820	CAP	CAPSULE	100MV
L1101	CAP	CAPSULE	100MV
L1102	CAP	CAPSULE	100MV
L1103	CAP	CAPSULE	100MV
L1104	CAP	CAPSULE	100MV
L1105	CAP	CAPSULE	100MV
L1106	CAP	CAPSULE	100MV
L1107	CAP	CAPSULE	100MV
L1108	CAP	CAPSULE	100MV
L1109	CAP	CAPSULE	100MV
L1110	CAP	CAPSULE	100MV
L1317	CAP	CAPSULE	100MV
L1318	CAP	CAPSULE	100MV
L1319	CAP	CAPSULE	100MV
L1320	CAP	CAPSULE	100MV

CII VC220FD111

ACCURACY ANALYSES

SECTION

1	SCOPE
2	APPLICABLE DOCUMENTS
3	ANALYTICAL APPROACH
4	HIGH-GAIN ANTENNA POINTING ACCURACY
5	PLANETARY SCAN PLATFORM POINTING ACCURACY
6	MANEUVER POINTING ACCURACY

ACCURACY ANALYSES

1.0 SCOPE. This document presents pointing error analyses for the high-gain antenna, the planetary science package, and for spacecraft maneuvers. All major identifiable error contributions have been included. The results indicate that the proposed system meets the accuracy requirements of the VOYAGER mission.

2.0 APPLICABLE DOCUMENTS.

VC220SR101	Design Characteristics and Restraints
VC220FD101	Trajectories and Guidance
VC220FD113	Layout and Configuration

3.0 ANALYTICAL APPROACH. Error analyses for High-Gain Antenna (HGA) pointing, Planetary Scan Platform (PSP) pointing, and maneuvering are contained in the following sections. To permit consideration of the problem geometry, successive multiplications of coordinate transformation matrices were made to include the effect of each system error and the nominal rotations required for the reorientation or maneuver. A similar matrix product was formed from the nominal rotations and the final orthogonal pointing errors. Since both resultant matrices define the actual attitude after reorientation, equating their like parts yields expressions for orthogonal errors in terms of the system errors and their respective weighting functions. Error contributors are assumed to be independent, although orthogonal components of the final error may or may not be independent. In the maneuvering error analysis, two final pointing errors are presented: one assuming independent orthogonal errors, and the other dependent errors. In reality, final errors will fall somewhere between these two values.

The HGA error analysis has been conducted to produce results approaching the worst case. Known errors, such as control system deadband, gimbal servo quantization, and curve fit accuracy have been added algebraically to the 3σ root-mean-squared value of the gaussian-distributed errors. Polarities of the known errors have been selected to maximize the resultant errors. The final result yields an error within the tolerable value.

Error analyses of PSP pointing accuracy and maneuvering accuracy have been conducted by computing the standard deviation of each error source. The standard deviation of the resultant error in each of the two orthogonal axes defining the pointing error was computed by calculating the square root of the sum of the variances. Since most of the resultant error is contributed by uniformly distributed control system deadbands, results should not be treated as normal distributions. This implies that the resultant error standard deviations are incorrect. However, the results should be on the conservative side, and, since all requirements are met without undue design penalty, further refinement was not warranted.

4.0 HIGH-GAIN ANTENNA POINTING ACCURACY. The HGA is attached to the Spacecraft by a gimbal mechanism providing two degrees of freedom. With gimbal angles at zero positions, the antenna boresight axis is oriented parallel to the -Z body axis. The first

rotation with respect to the Sun-Canopus coordinate system is about the Spacecraft Y-axis through an angle referred to as "B." The second rotation is about the transformed X-axis through an angle referred to as "A."

Error sources contributing to the resultant pointing error are deviations of the body axes from the stellar references, gimbal position errors, and errors in definition of the boresight axis. The latter errors have been mathematically lumped with gimbal errors for computational convenience. Since the second gimbal rotation (A) is small, this is acceptable. The two orthogonal error equations are

$$\Delta y = \delta x \text{ Sin A Sin B} + \delta y \text{ Cos A} + \delta z \text{ Sin A Cos B} + \Delta B \text{ Cos A}$$

$$\Delta x = \delta x \text{ Cos B} - \delta z \text{ Sin B} - \Delta A$$

Error sources, identification, magnitude, and variances for the HGA pointing accuracy are listed in Table 4-1. Magnitudes indicated represent three times the standard deviation for gaussian distributed errors, the design value of the maximum error excursion for uniformly distributed errors, and curve fit errors. All error sources are presumed to be independent. Standard deviations of the two orthogonal errors are

$$\sigma \Delta_y = [\delta x^2 \text{ Sin}^2 A \text{ Sin}^2 B + \delta y^2 \text{ Cos}^2 A + \delta z^2 \text{ Sin}^2 A \text{ Cos}^2 B + \Delta B^2 \text{ Cos}^2 A]^{1/2}$$

$$\sigma \Delta_x = [\delta x^2 \text{ Cos}^2 B + \delta z^2 \text{ Sin}^2 B + \Delta A^2]^{1/2}$$

where

$$(\text{Delta})^2 = \Sigma \text{ Delta Variances}$$

All of these errors are assumed to be gaussian distributed, except for control system deadband, gimbal servo quantization, and curve fit accuracy. Summing the gaussian distributed variances yields

$\Sigma \delta x$ Variances = 0.00141

$\Sigma \delta y$ Variances = 0.00304

$\Sigma \delta z$ Variances = 0.00141

$\Sigma \Delta A$ Variances = 0.00139

$\Sigma \Delta B$ Variances = 0.00139

During the orbit phase, the gimbal angles are approximately

A = 10 degrees

B = 40 degrees

For this case, the standard deviations of the two orthogonal errors are

$\sigma \Delta_y$ = 0.07 degree

$\sigma \Delta_x$ = 0.05 degree

TABLE 4-1. HGA ERROR ANALYSIS

Error Source	Identification	3σ or Max Value Magnitude (deg)	Variance
Control System Deadband	δx, δy, δz	0.458	0.06992
Canopus Sensor Repeatability	δy	0.141	0.00222
Sun Sensor Repeatability	δx, δz	0.071	0.00055
Control Electronics Drift	δx, δy, δz	0.046	0.00024
Sensor Mounting Alignment	δx, δy, δz	0.050	0.00028
Threshold Detector Variations	δx, δy, δz	0.023	0.00006
Gimbal Alignment	δx, δy, δz	0.050	0.00028
Gimbal Servo Quantization	ΔA, ΔB	0.125	0.00521
Curve Fit Accuracy	ΔA, ΔB	0.250	0.03125
Antenna To Gimbal	ΔA, ΔB	0.050	0.00028
Antenna Beam to Antenna	ΔA, ΔB	0.100	0.00111

And the nongaussian errors are

$$\delta x = \delta y = \delta z = +0.458$$

$$\Delta A = -0.375$$

$$\Delta B = +0.375$$

Then

$$\Delta y = 0.83 \text{ degree}$$

$$\Delta x = 1.02 \text{ degrees}$$

The pointing error (ΔP) should always be

$$\Delta P < [(\Delta y + 3\sigma \Delta_y)^2 + (\Delta X + 3\sigma \Delta_x)^2]^{1/2}$$

$$< 1.60 \text{ degrees}$$

Therefore, if the antenna is sized to deliver the desired bit rate with a 1.75 degree pointing error, there should be an adequate safety margin.

As a comparison, it is of interest to compute what is here erroneously labeled as the standard deviation of the final pointing error. The sums of all the appropriate variances yield

$\Sigma \delta x$ Variances = 0.07133

$\Sigma \delta y$ Variances = 0.07300

$\Sigma \delta z$ Variances = 0.07133

$\Sigma \Delta A$ Variances = 0.03785

$\Sigma \Delta B$ Variances = 0.03785

For the orbiting situation gimbal angles, the orthogonal errors are

$$\sigma \Delta_y = 0.331 \text{ degree}$$

$$\sigma \Delta_x = 0.330 \text{ degree}$$

which yield for this manner of computation a worst-case pointing error standard deviation of 0.468 degree, or a 3 σ value of 1.4 degrees.

5.0 PLANETARY SCAN PLATFORM POINTING ACCURACY. The Planetary Scan Platform (PSP) is attached to the spacecraft by a gimbal mechanism with three degrees of freedom. Two gimbals are employed to establish an axis perpendicular to the Satellite orbital plane while the third points the PSP optical axis along the local vertical vector. When nulled, the gimbals point the perpendicular axis along the Y-Axis of the Sun-Canopus coordinate system and the optical axis along the X-axis. The first rotation is through an angle C about the + Z axis, and the second an angle D about the transformed + X axis. The final rotation takes place through an angle E about the axis perpendicular to the orbital plane. A horizon sensor is used to determine a local vertical reference for the closed loop system providing this rotation.

Similar to the High-Gain Antenna situation, sources contributing to the resultant PSP pointing error are deviations of the body axes from stellar references, gimbal position errors, and errors in the definition of the instrument optical axis. The out-of-plane component becomes

$$-\Delta z = \delta x\,(\sin E \cos C + \sin C \cos E \sin D)$$

$$+ \delta y\,(\sin E \sin C - \cos C \cos E \sin D)$$

$$+ \delta z\,(\cos E \cos D + \Delta C \cos E \cos D + \Delta D \sin E)$$

In the orbital plane, however, the closed loop control system is not affected by the usual body axis errors but does have its own sources of error designated as $\delta y'$. Therefore, the in-plane pointing error component becomes

$$\Delta y = \delta y' + \Delta E$$

Table 5-1 identifies, in a manner similar to Table 4-1, the error sources contributing to the PSP pointing error. If the body axis errors are the same in each axis, the resultant out-of-plane error is equal to the magnitude of the contribution to a single axis. The same argument applies in the case of gimbal errors if the worst case of D = 0 degrees is assumed so that

$$\delta \Delta_z = (\delta^2 + \Delta^2)^{1/2}$$

The table of errors, however, shows that the stellar sensor for the body Y-axis contributes a larger error than the other sensors. This can be treated by adding a term, which is a function of the error increment, to the variance. In other terms

$$\sigma \Delta_z = [\,\delta^2 + \Delta^2 + K_n\,(n + Z)\,\delta n^2\,]^{1/2}$$

Where $K = (\sin E \sin C - \cos C \cos E \sin D)^2$

TABLE 5-1. PLANETARY SCIENCE PACKAGE ERROR ANALYSIS

Error Source	Identification	Magnitude (deg)	Variance
Control System Deadband	δx, δy, δz	0.458*	0.00992
Canopus Sensor Repeatability	δy,	0.141	0.00222
Sun Sensor	δx, δz	0.071	0.00055
Control Electronics Drift	δx, δy, δz	0.046	0.00024
Sensor Mounting Alignment	δx, δy, δz	0.050	0.00028
Horizon Sensor Alignment	δy,	0.050	0.00028
Horizon Sensor Resolution	δy,	0.100	0.00111
Servo Hang-off	δy,	0.100	0.00111
Planet Ellipticity	δy,	0.120	0.00160
False Horizon	δy	0.200	0.00444
Orbit Inclination	δx, δy, δz	0.100	0.00111
Threshold Magnitude	δy	-0.250*	0.02080
Gimbal Alignment	ΔC, ΔD, ΔE	0.050	0.00028
Actuation Variations	ΔC, ΔD, ΔE	0.050	0.00028
Curve Fit Accuracy	ΔC, ΔD	0.250*	0.03125
Gimbal Servo Quantization	ΔC, ΔD	0.125*	0.00521
*non-Gaussian errors			

and n = factor used to denote the magnitude of the increment as a function of an error source, δ n.

During the orbital phase

$$C \cong -5 \text{ degrees}$$

$$D \cong -15 \text{ degrees}$$

so that $K \cong (-0.087 \sin E + 0.258 \cos E)^2$

which reaches a maximum value of $(0.272)^2 = 0.074$

The combination of in-plane errors is much simpler, the in-plane component being obtained from

$$\delta \Delta_y = (\delta y'^2 + \Delta E^2)^{1/2}$$

From the error table, the variances of the Gaussian errors may be obtained and summed.

$\Sigma\delta$ Variance = 0.00230 $\quad$ $\Sigma\delta$ y' Variance = 0.00854

$\Sigma\Delta$ Variance = 0.00056 $\quad$ $\Sigma\Delta$ E Variance = 0.00056

There are also the non-Gaussian errors

δ = 0.458

Δ = ±0.375

δ y' = -0.0250

By adding the non-Gaussian errors arithmetically to the 3σ values of the Gaussian errors,

$3\sigma\ \Delta_z = 0.995$

$3\sigma\ \Delta_y = 0.535$

Assuming the in-plane and out-of-plane errors to be orthogonal and independent, the total pointing error will be less than 0.89 degree, with a probability of 99%.

6.0 MANEUVER POINTING ACCURACY. In performing midcourse correction, orbit insertion, and orbit adjust maneuvers, a pair of turns about two body axes is required to properly orient the propulsive thrust vector. This thrust vector is nominally coincident with the spacecraft + Z axis and will be reoriented as required through a pitch-yaw or yaw-pitch turn combination. Flexibility in choosing the order of these two turns is required to minimize the resultant pointing error for each maneuver. (One sequence of turns for a given maneuver will have a lower sum of turn magnitudes and, consequently, will yield a lower error than the other). A combination of pitch and yaw turns are chosen because a solar aspect sensor is used for turn verification.

Contributing error sources are deviations of the body axes from the celestial references, control system deadband in the inertial-sensing mode, uncertainties in actual magnitudes of executed turns, the autopilot error (which includes thrust axis misalignments and center-of-gravity location uncertainty), and gyro drift. Gyro deadbands contribute to the final pointing errors only through misalignment of the axes about which the required maneuver turns are made. These deadbands do not contribute directly to the final errors, since each turn is referenced to the appropriate gyro null and not to the actual vehicle attitude (within the deadband) about the turn axis.

A yaw (through angle Y) - pitch (through angle P) turn sequence was arbitrarily chosen for the analysis. From the matrix equation described in Section 3.0, the two orthogonal error equations are

$$\epsilon x = Gx - \delta z - \Delta Z \sin Y + \Delta P + \Delta X (\cos Y - 1) + \delta x \cos Y + Ax$$

$$\epsilon y = Gy + \Delta X \sin Y \sin P + \delta x \sin Y \sin P + \delta z \cos Y \sin P + \Delta Z \cos Y \sin P + \Delta Y (\cos P - 1) + \Delta' Y \cos P + \delta y \cos P + \Delta y$$

Since the body axis deviations from the celestial references are essentially equal for all three axes, the above expressions are simplified by replacing δx, δy, and δz with δ. Similarly, the gyro deadbands, gyro drifts, and autopilot errors are simplified to Δ, G and A, respectively. Converting the orthogonal errors to their standard deviations,

$$\sigma_{\epsilon x} = \left[G^2 + \delta^2 + \Delta P^2 + 2\Delta^2 (1 - \cos Y) + A^2 \right]^{1/2}$$

$$\sigma_{\epsilon y} = \left[G^2 + \delta^2 + \Delta' Y^2 \cos^2 P + 2\Delta^2 (1 - \cos P) + A^2 \right]^{1/2}$$

All contributing errors are identified in the summations of Tables 6-1, 6-2, and 6-3.

6.1 Error Summations. To illustrate the effects of turn magnitude on the resultant pointing error, two representative maneuvers have been analyzed. The first is a yaw 45 degrees-pitch 45 degrees sequence; the second is a yaw 165 degrees - pitch 10 degrees sequence. It can be seen from Table 6-4 that the resultant pointing error is greater for the maneuver which requires turn magnitudes whose sum is the greater. This effect is generally true; thus, errors are minimized by choosing the turn pair with the smallest sum.

TABLE 6-1. MANEUVER ERROR ANALYSIS Standard Deviation of Final Pitch Error, $\sigma_{\epsilon x}$ (Yaw 45 degrees - Pitch 45 degrees Sequence)

Error Source	Symbol	Magnitude	Variance
Control System Deadband[1] (Optical Sensing Mode)	δ	0.458	0.06992
Sensor Repeatability[2]	δ	0.141	0.00222
Control Electronics Drift	δ	0.046	0.00024
Sensor Mounting Alignment	δ	0.050	0.00028
Threshold Detector Variations	δ	0.023	0.00006
Control System Deadband[1] (Gyro Sensing Mode)	Δ	0.458	0.04102*
C&S Timer Resolution[3]	ΔP	0.089	0.00090
Turn Rate Uncertainty[4]	ΔP	0.178	0.00348
Gyro Drift[5]	G	0.154	0.00260
Autopilot	A	0.300	0.01000
			0.13072

σ_{ϵ_x} = (0.13072) 1/2 power = 0.362 degree

Notes

1 Magnitudes are for uniform distribution. Equivalent 3σ value is $\sqrt{3}$ times the magnitude shown.

2 Includes variations in linearity and null position with time and temperature. (Canopus value chosen as worst case.)

3 ± 0.5 sec

4 ± 0.4% of 3.14 mrad/sec

5 ± 0.25 deg/hr

* Variance multiplied by the appropriate functions of y as indicated in the expressions for σ_{ϵ_x}.

TABLE 6-2. MANEUVER ERROR ANALYSIS Standard Deviation of Final Pitch Error, $\sigma_{\epsilon x}$ (Yaw 165 degree - Pitch 10 degree Sequence)

Error Source	Symbol	Magnitude (deg)	Variance
Control System Deadband (Optical Sensing Mode)	δ	0.458	0.06992
Sensor Repeatability	δ	0.141	0.00222
Control Electronics Drift	δ	0.046	0.00024
Sensor Mounting Alignment	δ	0.050	0.00028
Threshold Detector Variations	δ	0.023	0.00006
Control System Deadband (Gyro Sensing Mode)	Δ	0.458	0.27524*
C&S Times resolution	ΔP	0.089	0.00090
Turn Rate Uncertainty	ΔP	0.036	0.00014
Gyro Drift	G	0.186	0.00372
Autopilot	A	0.300	0.01000
			0.36272

$\sigma_{\epsilon x}$ = (0.36272) 1/2 power
= 0.602°

* Variance multiplied by the appropriate functions of y as indicated in the expressions for $\sigma_{\epsilon x}$.

TABLE 6-3. MANEUVER ERROR ANALYSIS Standard Deviation of Final Yaw Error, $\sigma_{\epsilon y}$ (Yaw 165 degree - Pitch 10 degree Sequence)

Error Source	Symbol	Magnitude (deg)	Variance
Control System Deadband (Optical Sensing Mode)	δ	0.458	0.06992
Sensor Repeatability	δ	0.141	0.00222
Control Electronics Drift	δ	0.046	0.00024
Sensor Mounting Alignment	δ	0.050	0.00028
Threshold Detector Variations	δ	0.023	0.00006
Control System Deadband (Gyro Sensing Mode)	Δ	0.458	0.00210*
C&S Timer Resolution	Δ_y	0.089	0.00087*
Turn Rate Uncertainty	Δ_y	0.226	0.04973
Gyro Drift	G	0.186	0.00372
Autopilot	A	0.300	0.01000
			0.13914

$\sigma_{\epsilon y}$ = (0.13914) 1/2 power
= 0.373 degree

* Variances multiplied by the appropriate functions of Y & P as indicated in the expressions for $\sigma_{\epsilon y}$.

TABLE 6-4. LIMITS OF MANEUVER POINTING ERRORS

Pointing Error Limits	Y = 45°, P = 45°		Y = 165°, P = 10°	
	1σ	3σ	1σ	3σ
Upper	0.509°	1.527°	0.708°	2.124°
Lower *	0.360°	1.080°	0.488°	1.626°

* For two-dimensional errors, probabilities equivalent to 1σ and 3σ are 39% and 99%, respectively.

Gyro drifts are considered to be essentially undirectional, and the drift errors are entered in the summations as a single value based on the total time for each maneuver during which the spacecraft is "on gyros." While it is recognized that this is a simplification, the inaccuracy introduced is considered negligible.

The error magnitudes listed in Tables 6-1, 6-2, and 6-3 are three times the standard deviation for the gaussian-distributed errors. Errors having uniform distributions (control system deadbands in the optical and gyro

sensing modes) have been converted to the equivalent 3σ values. Therefore, since all errors are gaussian-distributed (or equivalent), the square root of the sum of the variances (modified by the appropriate functions of the turn angles) which contribute to each orthogonal error yields the standard deviation of that error.

For the yaw 45 degree - pitch 45 degree maneuver, the error summations for $\sigma_{\epsilon x}$ is presented in Table 6-1. The summation for $\sigma_{\epsilon y}$ is identical to that for $\sigma_{\epsilon x}$ except that the pitch turn magnitude error, ΔP (including the timer resolution and turn rate uncertainty errors), is replaced by the modified yaw turn magnitude error, $\Delta Y \cos P$. The resulting standard deviation of the final yaw error is

$$\sigma_{\epsilon y} = 0.358 \text{ degree}$$

Thus, for the yaw 45 degree - pitch 45 degree maneuver the standard deviations of the orthogonal errors are

$$\sigma_{\epsilon x} = 0.362 \text{ degree}$$

$$\sigma_{\epsilon y} = 0.358 \text{ degree}$$

It is clear from the expressions for $\sigma_{\epsilon x}$ and $\sigma_{\epsilon y}$ that these errors are neither completely independent nor completely correlated. This fact is significant, since the choice of techniques used to convert these two one-dimensional errors into a single two-dimensional pointing error depends upon the degree of correlation. Since, as stated in Section 4.0, a technique more rigorous than RSS summations is required to yield truly meaningful values for the pointing error (such as Monte Carlo), it appears sufficient in this analysis to define the range within which the values of the pointing errors will fall. To establish the upper limit for this range, the orthogonal errors are assumed to be completely correlated and, for the lower limit, completely independent.

Thus, the limits on the pointing error range are as follows:

	Probability	
	1σ	3σ
Upper Limit, deg (Errors correlated)	0.509	1.527
Lower Limit, deg * (Errors independent)	0.360	1.080

* For two-dimensional errors, probabilities equivalent to 1σ and 3σ are 39% and 99%, respectively.

For the yaw 165 degree - pitch 10 degree maneuver, the error summations for $\sigma_{\epsilon x}$ and $\sigma_{\epsilon y}$ are presented in Tables 6-2 and 6-3. Thus, for the yaw 165 degree - pitch 10 degree maneuver, the standard deviations of the orthogonal errors are

$$\sigma_{\epsilon x} = 0.602 \text{ degrees}$$

$$\sigma_{\epsilon y} = 0.373 \text{ degrees}$$

Using the previously described technique for conversion to a two-dimensional distribution, the limits on the pointing error range are as follows:

	Probability	
	1σ	3σ
Upper Limit, deg (Errors correlated)	0.708	2.124
Lower Limit, deg (Errors independent)	0.488	1.626

6.2 Conclusion. For comparison, the resulting pointing error limits for the two maneuvers analyzed are presented in Table 6-4.

The error limits shown are directly applicable to midcourse correction and orbit trim maneuvers. For the orbit injection maneuver, the errors are slightly greater for the same turn sequences, since the spacecraft is "on gyros" for nearly two hours from the start of the first turn until ignition of the retroengine. This prolonged gyro hold increases the upper limits of the pointing error by about 0.03 degrees (1σ) and 0.1 degree (3σ). These upper limits are considered to be essentially the worst-case errors.

In determining the capsule pointing error at the time of separation, the error limits are essentially as shown in Table 6-4, since the autopilot error can be replaced by the capsule alignment error, the two being nearly equal. The accuracy with which the proposed system can control the propulsive impulse, or ΔV, in a maneuver is discussed in the autopilot description.

Since the analysis of the VOYAGER trajectory and orbital requirements has indicated a maximum allowable pointing error of 2.60 degrees (3σ), the maneuver accuracy of the proposed system is satisfactory. In conclusion, it is well to restate that in the design phase, Monte Carlo techniques should be used to determine the probability distribution of the final pointing errors.

CII VC220FD112

FLIGHT SEQUENCE

SECTION

1	SCOPE
2	APPLICABLE DOCUMENTS
3	MISSION SUMMARY
4	NOMENCLATURE AND USE OF TABLES
5	SEQUENCE OF EVENTS AND POWER PROFILE
6	COMMAND LIST

FLIGHT SEQUENCE

1.0 SCOPE. This document describes in detail the sequence of operations performed by the two VOYAGER spacecraft from the period immediately preceding launch until completion of the mission.

2.0 APPLICABLE DOCUMENTS. The following list of documents is directly applicable to the Flight Sequence:

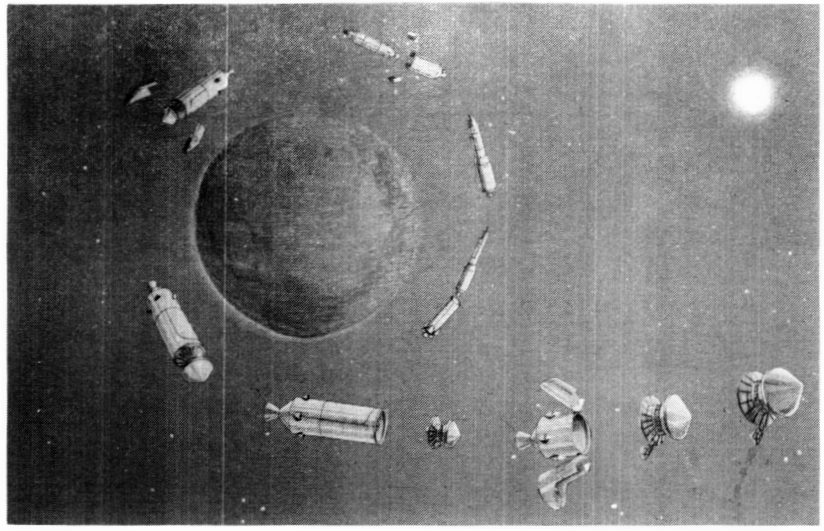
VC220SR101 Design Characteristics and Restraints
VC220FD101 Trajectories and Guidance

3.0 MISSION SUMMARY. The mission phases which comprise a nominal mission profile are as defined on pages 13, 14, 15, and 16 of the "VOYAGER 1971 Preliminary Mission Description" dated October 15, 1965. This defined phase format is utilized throughout the Flight Sequence listing, and a summary of the highlights of these phases follows.

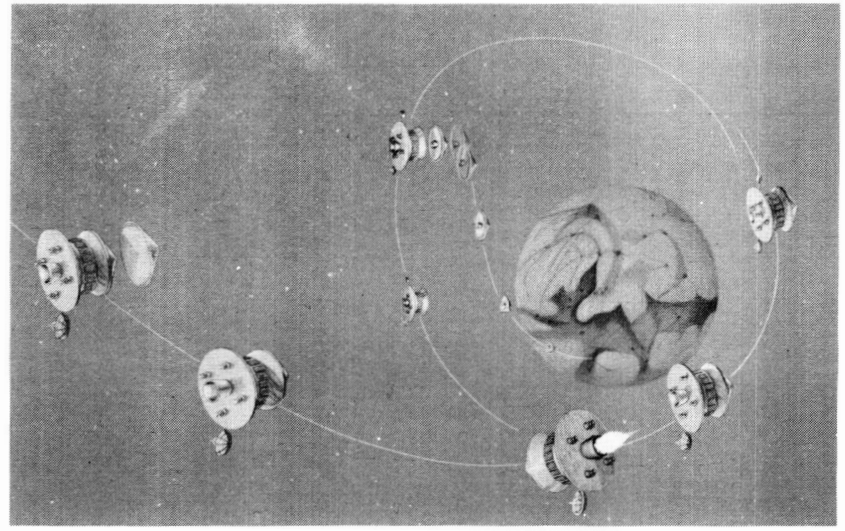
The Planetary Vehicles are initialized for launch prior to lift-off, and the Forward Planetary Vehicle (P/V1) separates from the Launch Vehicle soon after injection on the transfer trajectory. The Aft Planetary Vehicle (P/V2) separates from the Saturn-IVB stage 10 minutes after the separation of P/V1, and a nominal ΔV of 2 feet per second is provided between the Forward and Aft Planetary Vehicles to eliminate the possibility of collision. (See Figure 3-1.)

The Flight Spacecraft has the capability of performing three interplanetary trajectory corrections. The first and second midcourse maneuvers for P/V1 are planned for three and thirty days from launch with those of P/V2 being performed one day later. The third trajectory correction is performed seven days before encounter with a ten day encounter time difference existing for P/V1 and P/V2. A pitch and yaw or yaw and pitch turn sequence is used for orienting the spacecraft prior to adding the ΔV velocity increment during trajectory corrections, and solar aspect sensor data is obtained during the turns and is used for attitude verification following completion of the orientation procedure. Two turns are used for orienting the Planetary Vehicles during maneuvers, since attitude verification from solar aspect sensor data is more readily obtainable; total maneuver time is less than when three turns are used (requiring less time on gyros and batteries); and it is easier to retrace the turns as a backup to the automatic C&S celestial reference reacquisition technique. Two turns have the disadvantages of making antenna pattern pointing more difficult and possibly requiring larger individual turns. Ample time is allotted to inhibit engine burn by ground command if attitude verification is not achieved. The high-gain antenna is not reoriented during maneuvers, and data reception on Earth following a maneuver and switch to Cruise Radio Mode verifies proper reacquisition of celestial references. Stored maneuver data is not played back until adequate time has elapsed for Sun and Canpous reacquisition verification.

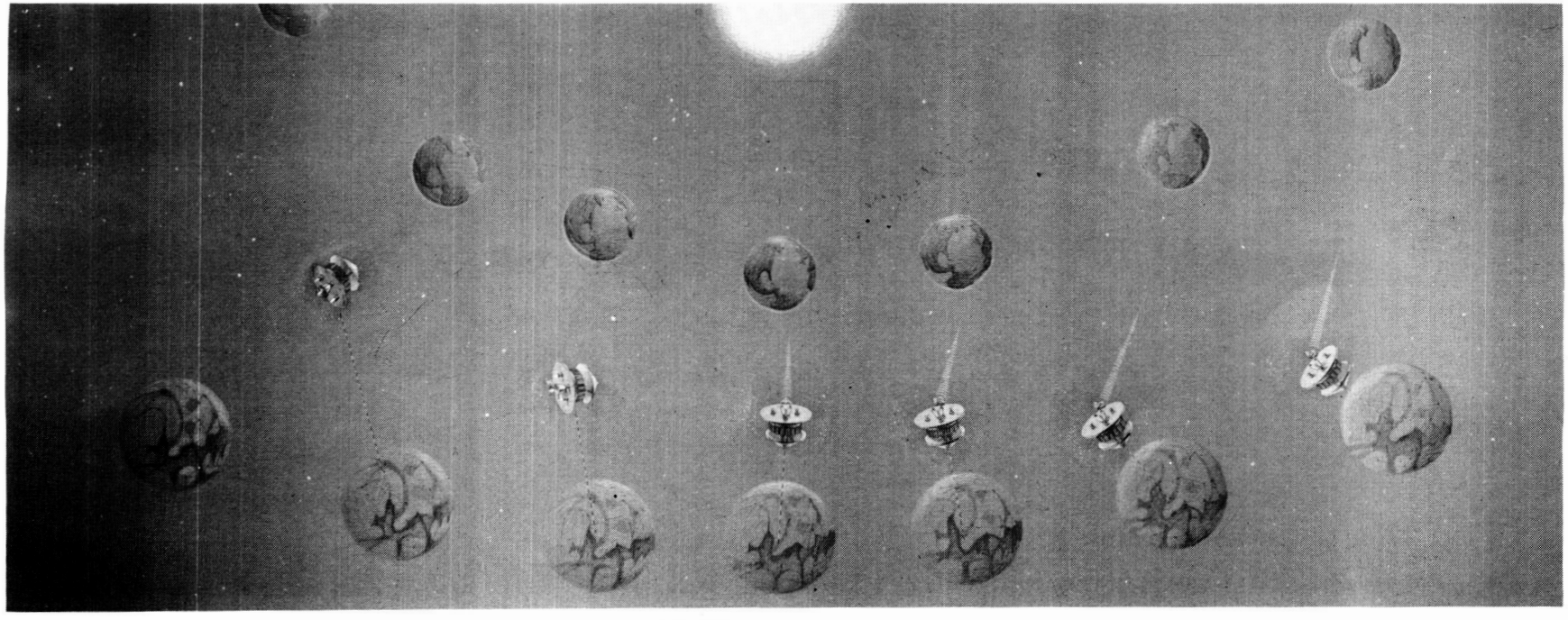
The Flight Capsule canister is jettisoned one day prior to orbit insertion, and the canister is separated while the Planetary Vehicle is Sun-Canopus oriented.



LAUNCH AND INJECTION PHASE



MARS ORBIT INSERTION AND CAPSULE SEPARATION PHASES



INTERPLANETARY CRUISE AND TRAJECTORY CORRECTION PHASES

VC220FD112

Figure 3-1. Flight Sequence of Events

During orbit insertion, redundant gyro packages are operated to provide momentary switching capability. Approximately 100 minutes are allowed to correct abnormalities (if necessary) between desired attitude attainment and orbit injection engine firing. Attitude verification is again obtained by solar aspect sensor data, and the high-gain antenna is not reoriented during the maneuver.

Orbit geometry is determined during the first two orbits with Orbit and PSP Science power off. Although a 1,000-km x 10,000-km 60-degree inclined orbit is recommended, a 40-degree inclination is portrayed in the Flight Sequence and is used as a design guide for the Flight Spacecraft (since the 60-degree inclination leads to a simpler sequence). Science power is limited in the 40-degree inclination prior to Flight Capsule separation, and a modified data gathering sequence is specified during this period of time.

The Flight Spacecraft has the capability of performing two Mars orbit trim maneuvers both prior to and after Flight Capsule separation. These maneuvers (if necessary) are nominally performed two, four, eight, and ten days after encounter. The orbit trim maneuvers are basically identical to the interplanetary trajectory correction maneuvers.

Flight Capsule separation occurs four to six days after orbit insertion (depending upon the number of required orbit trim maneuvers and the desired impact area - orbit plane geometry). Flight Capsule checkout begins one orbit prior to separation, and a yaw - pitch turn sequence is utilized to properly orient the relay antenna for Flight Capsule data reception. Separation does not occur until a ground command enable signal is received, and the Flight Spacecraft maintains its separation attitude until after impact. Following reacquisition of celestial references, stored Flight Capsule data is transmitted to Earth. All science data gathering is inhibited from the beginning of Flight Capsule checkout until completion of stored data transmission.

Late in the mission (55 days after encounter for the 40-degree inclination), a 180-degree roll reorientation is performed to avoid Flight Capsule bio-barrier interference with the PSP Science field-of-view.

4.0 NOMENCLATURE AND USE OF TABLES. The Flight Sequence is presented with the following column heading format:

Days
Hours
Minutes
Seconds

Refers to time from launch. The times shown are based on a nominal May 3, 1971 launch date and November 1, 1971 and November 11, 1971 nominal arrival dates.

Mission Phase: As defined by the nominal profile.
Events: Occurrences within a mission phase.
Source: Command source to initiate an event.
Backup: Command backup source, if required.
Destination Subsystem: Primary and backup command destination.

Destination: Bay location of effected components, etc.
Raw DC: DC bus sum power load with event occurrence.
2.4 Kc: 2400 cps sum power load with event occurrence.
400 cps: 400 cps sum power load with event occurrence.

The radio modes, data modes, science categories, and abbreviations shown in Table 4-1 are used in the Command and Flight Sequence Lists.

TABLE 4-1. MODES AND ABBREVIATIONS USED IN COMMAND AND FLIGHT SEQUENCE LISTS

Launch Radio Mode: 3-watt amplifier, primary low-gain and parasitic antenna	RADIO: Radio Subsystem
Maneuver Radio Mode: 50-watt amplifier, secondary low-gain antenna	R RAD: Relay Radio Subsystem
Cruise Radio Mode: 50-watt amplifier, high-gain antenna	DAE: Data Automation Equipment
Data Mode 1A: Maneuver Mode	TVC: Thrust Vector Control
Data Mode 1B: Flight Capsule Separation Maneuver Mode	S/C: Flight Spacecraft
Data Mode 2: Cruise Mode	P/V2: Aft Planetary Vehicle
Data Mode 3A: Normal Orbit Mode	M/C or MC: Midcourse maneuver
Data Mode 3B: Earth Occultation Mode	MTR: Magnetic Tape Recorder
Data Mode 4: Cruise Recorder Readout Mode	PSP: Planet Scan Platform
Data Mode 5: Capsule Checkout Mode	TCA: Thrust Chamber Assembly
Cruise Science: Science used throughout interplanetary cruise	S1: Separation Switch No. 1
Orbit Science: Science used in orbit but not PSP-mounted	SO: Sun Occultation
PSP Science: Science mounted on PSP	CO: Canopus Occultation
G&C: Guidance and Control Subsystem	ANT: High-gain antenna
AC: Attitude Control	LG: Low gain
IGP: Integrating Gyro Package	CD: Command Decoder
D/S or DS: Data Storage Subsystem	LV: Launch Vehicle
SCI: Science Subsystem	P/V1: Forward Planetary Vehicle
C&S or CS: Computer and Sequencer	LCE: Launch Complex Equipment
AP: Autopilot	OTM or OA: Orbit trim maneuver
POWER: Power Subsystem	PSC: Playback sequencer control
PYRO: Pyrotechnics Subsystem	CAPS: Flight Capsule
T/M: Telemetry Subsystem	S2: Separation Switch No. 2
	EO: Earth Occultation
	TTG: Time-to-Go Register
	HG: High gain

5.0 SEQUENCE OF EVENTS AND POWER PROFILE. Table 5-1 is a detailed listing of the primary events for a nominal 1971 VOYAGER mission. An upper-bound power profile is also presented.

TABLE 5-1. FLIGHT SEQUENCE OF EVENTS AND POWER PROFILE

Day	Hr	Mn	Sc	Ph	Event	Source	Bk/Up	Dest s/s	Dest	Raw d c	2.4 kc	400 cps
1 Prelaunch Mission Phase												
-02	00	00	00	01	INSERT STORED COMMANDS	LCE		C+S				
-00	00	09	00	01	INITIALIZE PLANETARY VEHICLES FOR LAUNCH							
-00	00	09	00	01	ATTITUDE CONT. INITIAL.	LCE		G+C				
-00	00	09	00	01	SCIENCE TO LAUNCH MODE	LCE		SCI				
-00	00	09	00	01	RECORDERS TO LAUNCH MD.	LCE		DS				
-00	00	09	00	01	RADIO TO LAUNCH MODE	LCE		RADIO				
-00	00	09	00	01	SWITCH TO DATA MODE 2	LCE		T/M				
-00	00	09	00	01	CAPSULE TO LAUNCH MODE	LCE		CAPS				
-00	00	09	00	01	SWITCH TO INT. POWER	LCE		POWER				
-00	00	03	00	01	INITIALIZE C+S	LCE		C+S				
2 Launch + Injection Mission Phase												
-00	00	01	00	02	UMBILICAL(S) RELEASE	LCE		LV				
000	00	00	00	02	LIFT-OFF					056W	169W	009W
000	00	00	0	02	APPROXIMATE + WORST CASE TIMES ARE SHOWN THROUGHOUT PHASES							
000	00	02	34	02	S-IC ENGINE CUT-OFF	LV		LV				
000	00	02	34	02	S-IC STAGE JETTISON	LV		LV				
000	00	02	44	02	S-II STAGE BURN	LV		LV				
000	00	03	28	02	JETTISON FWD. NOSE FRG.	LV		LV				
000	00	03	28	02	NOSE FAIRING JETTISONED AT 350.000 FEET ALTITUDE							
000	00	04	00	02	CRUISE SCIENCE ON IF NEAR EARTH DATA DESIRED							
000	00	08	59	02	S-II STAGE ENG. CUT-OFF	LV		LV				
000	00	08	59	02	S-II STAGE SEPARATION	LV		LV				
000	00	09	04	02	S-IVB STAGE INIT. BURN	LV		LV				
000	00	09	49	02	S-IVB STAGE CUT-OFF	LV		LV				
000	00	09	49	02	PARKING ORBIT INJECTION	LV		LV				
000	00	34	49	02	S-IVB STAGE SEC. BURN	LV		LV				
000	00	34	49	02	P/V TRANS. TRAJ. INJ.	LV		LV				
000	00	34	49	02	ASSUMES 25 MIN. PARKING ORBIT-VARIABLE TIME CORRECTED BY M/C							
000	00	44	25	02	INFLIGHT DISC. SEP.	LV		ADAPT.				
000	00	44	30	02	P/V1 SEPARATION	LV		ADAPT.				
000	00	44	30	02	SEPARATION VELOCITY INCREMENT 3FT./SEC.							
000	00	44	30	02	ARM PYROTECHNICS (P/V1)	S1	S2	PYRO				
000	00	44	30	02	ENABLE C+S (P/V1)	S1	S2	C+S				
3 Acquisition Mission Phase (P/V1)												
000	00	45	30	03	ENABLE PNEUM. DRIVERS	CS000	CD600	G+C	15	080W	169W	009W
000	00	46	30	03	END RECORDER LAUNCH MD.	CS083	CD757	DS	08	080W	136W	009W
000	00	47	30	03	END CAPSULE LAUNCH MD.	CS093	CD788	CAPS				
000	00	48	30	03	INIT. HG ANT. DPLYMT.	CS025	CD648	PYRO	00	160W	136W	009W
000	00	48	30	03	DEP. SEC. LG ANTENNA	CS026	CD649	PYRO				
000	00	48	30	03	DEP. MAGNETOMETER	CS027	CD650	PYRO				
000	00	49	30	03	REMOVE CR. SCI. COVERS	CS028	CD651	PYRO				
000	00	50	30	03	2.4KC SCI. POWER ON	CS039	CD699	POWER				
000	00	51	30	03	CRUISE SCIENCE ON	CS103	CD820	DAE	06	160W	165W	009W
2 Launch + Injection Mission Phase (P/V2)												

5-10

```
000 00 51 30 02 REMOVE P/V2 FAIRING          LV              LV
000 00 54 25 02 INFLIGHT DISC. SEP.          LV              ADAPT.
000 00 54 30 02 P/V2 SEPARATION              LV              ADAPT.
000 00 54 30 02 SEPARATION VELOCITY INCREMENT 1FT./SEC.
000 00 54 30 02 ARM PYROTECHNICS (P/V2)      S1      S2      PYRO
000 00 54 30 02 ENABLE C+S (P/V2)            S1      S2      C+S
```

3 Acquisition Mission Phase (P/V2)

```
000 00 55 30 03 PERFORM 10 ACQ. EVENTS ENUMERATED FOR P/V1
```

3 Acquisition Mission Phase (P/V1 + P/V2 - P/V1 Times Noted)

```
000 00 55 30 03 P/V2 EVENT TIMES DENOTED BY COMMENT WHEN APPROPRIATE
000 00 56 30 03 S-IVB RETROMANEUVER          LV              LV
000 00 56 30 03 ANTENNA DEPLOYMENT COMPLETE                      00   080W 165W 009W
000 01 25 30 03 SUN ACQUISITION COMPLETE                         15   056W 165W 009W
000 01 25 30 03 CAPSULE POWER ON             CS037 CD697  POWER 00   256W 165W 009W
000 01 25 30 03 MAGNETOMETER CALIBRATION ROLL STARTS
000 18 05 30 03 MAGNETOMETER CALIBRATION COMPLETE
000 18 05 30 03 SW. TO CRUISE MODE           CS001 CD606  G+C
000 19 15 30 03 CANOPUS ACQUISITION COMPLETE
000 19 15 30 03 HG ANTENNA CONTROL ON        CS042 CD703  POWER 00   416W 165W 009W
000 19 15 30 03 ANTENNA MOVES TO PREPROGRAMMED POSITION
000 19 25 00 03 SW. TO CRUISE RADIO MD.      CS085        RADIO 12   353W 165W 009W
000 19 25 00 03 DATA RECEPTION ON EARTH WILL VERIFY CANOPUS ACQUISITION
000 19 50 00 03 GYRO SET 1 OFF               CS046 CD707  POWER 15   347W 157W 000W
```

4 Interplanetary Cruise Mission Phase

```
000 19 50 00 04 UPDATE ANTENNA PTG.- AS REQUIRED THROUGHOUT MISSION
000 19 50 00 04 STEP ANTENNA GIMBAL A        CS057 CD722  ANT.
000 19 50 00 04 STEP ANTENNA GIMBAL B        CS061 CD726  ANT.
000 19 50 00 04 INCREMENT CANOPUS FUNCT.     CS018 CD628  G+C
```

175 05 41 26 10 OBTAIN SOLAR FLARE DATA (SAME AS PHASE 4)
175 05 41 26 10 SUN LOOPS TO HIGH GAIN CS015 CD621 G+C

11 Flight Capsule Canister Separation (P/V1)

181 12 00 00 11 P/V2 CANISTER JETTISONED 10 DAYS LATER
181 12 00 00 11 INIT. STER. CAN. PYRO CS035 CD673 PYRO

12 Interplanetary Cruise Mission Phase

13 Mars Orbit Insertion Mission Phase (P/V1)

182 12 30 20 13 P/V2 PERFORMS SAME MANEUVER SEQUENCE 10 DAYS LATER
182 12 31 20 13 GYRO SET 1 ON CS045 CD706 POWER 15 353W 165W 009W
182 12 32 20 13 GYRO SET 2 ON CS047 CD708 POWER 15 359W 173W 018W
182 12 32 20 13 TWO GYRO PACKAGES OPERATE DURING ORBIT INSERTION
182 13 02 20 13 GYRO TEMP. OVERRIDE CS020 CD630 G+C
182 13 55 20 13 SW. TO DATA MODE 1A CS074 CD744 T/M 08 359W 179W 018W
182 13 56 20 13 SW.TO MANEUVER RADIO MD.CS086 RADIO
182 14 01 20 13 AUTOPILOT POWER ON CS040 CD701 POWER 15 359W 191W 018W
182 14 01 50 13 CAPSULE POWER OFF CS038 CD698 POWER 00 159W 191W 018W
182 14 02 20 13 SW. TO FULL INERT. CONT.CS002 CD607 G+C
182 14 03 20 13 START PITCH TURN (+) CS006 CD611 G+C
182 14 11 40 13 STOP PITCH TURN CS008 CD613 G+C
182 14 12 40 13 START YAW TURN (+) CS003 CD608 G+C
182 14 21 00 13 STOP YAW TURN CS005 CD610 G+C
182 14 21 00 13 TURN TIMES DESIGNATED ARE MAXIMUM EXPECTED
182 14 21 00 13 ASSUMES PITCH + YAW OR YAW + PITCH SEQUENCE
182 15 59 00 13 ATTITUDE VERIFICATION COMPLETE (SOLAR ASPECT SENSOR DATA)
182 15 59 30 13 HG ANT. GIMBAL LOCKS ON CS066 CD731 ANT. 00 419W 191W 018W
182 15 59 40 13 TVC POWER ON CS052 CD716 POWER 00 1.3K 191W 018W
182 15 59 40 13 AEROJET THRUST VECTOR CONTROL SYSTEM REQUIRES 875W DC
182 15 59 45 12 CLOSE RETRO INJECTORS CS072 CD741 PROP.
182 15 59 50 13 FIRE TVC PRES. SQUIBS CS029 CD664 PYRO
182 15 59 58 13 ENABLE AUTOPILOT CS023 CD646 G+C
182 16 00 00 13 INITIATE ENGINE BURN CS030 CD665 PYRO
182 16 00 00 13 THRUST VECTOR CONTROL PROVIDED BY AUTOPILOT
182 16 01 29 13 ENGINE BURNOUT (MINUTEMAN SYSTEM)
182 16 01 34 13 AUTOPILOT POWER OFF CS041 CD702 POWER 15 1.3K 179W 018W
182 16 01 35 13 HG ANT.GIMBAL LOCKS OFF CS067 CD732 POWER 00 1.0K 179W 018W
182 16 01 36 13 TVC POWER OFF CS053 CD717 POWER 00 159W 179W 018W
182 16 01 37 13 SW. TO CRUISE MODE CS001 CD606 G+C 15 183W 179W 018W
182 16 01 38 13 ENABLE SUN OCCULT. MODE CS012 CD617 G+C
182 16 11 06 13 PERIAPSIS PASSAGE OCCURS
182 16 11 06 13 EVENTS FOR WORST CASE 40 DEGREE INCLINED ORBIT
182 16 12 21 13 EARTH OCCULTATION ENCOUNTERED (40 DEGREE INCLINED ORBIT)
182 16 12 21 13 DATA MODES, ETC. NOT SWITCHED SINCE P/V IS OFF CELESTIAL REF.
182 16 32 46 13 SUN OCCULTATION ENCOUNTERED (40 DEGREE INCLINED ORBIT)
182 16 32 46 13 SW. TO YAW + PITCH INERTIAL CONTROL 15 159W 179W 018W
182 16 32 46 13 THERMAL CONTROL ON 00 159W 188W 018W
182 16 32 46 13 THERMAL CONTROL FOR ANTENNA GIMBAL + LINES TO PROPELLANT TANKS
182 16 48 09 13 EARTH OCCULTATION COMPLETE
182 17 14 34 13 SUN OCCULTATION COMPLETE
182 17 14 34 13 COMMENCE SUN ACQUISITION 15 183W 188W 018W
182 17 14 34 13 THERMAL CONTROL OFF 00 183W 179W 018W
182 17 23 25 13 SUN ACQUISITION COMPLETE 15 159W 179W 018W
182 17 23 25 13 CAPSULE POWER ON CS037 CD697 POWER 00 359W 179W 018W
182 18 33 25 13 CANOPUS ACQUIRED
182 18 33 25 13 GYRO SET 2 OFF CS048 CD709 POWER 15 353W 171W 009W

TABLE 5-1. FLIGHT SEQUENCE OF EVENTS AND POWER PROFILE (Continued)

Day	Hr	Mn	Sc	Ph	Event	Source	Bk/Up	Dest s/s	Dest	Raw d c	2.4 kc	400 cps
5 First Interplanetary Trajectory Correction (P/V1) (Continued)												
003	02	10	20	05	STOP PITCH TURN	CS008	CD613	G+C				
003	02	11	20	05	START YAW TURN (+)	CS003	CD608	G+C				
003	02	19	40	05	STOP YAW TURN	CS005	CD610	G+C				
003	02	19	40	05	TURN TIMES DESIGNATED ARE BASED ON SUM TOTAL OF 180 DEGREES MAX							
003	02	19	40	05	ASSUMES PITCH + YAW OR YAW + PITCH SEQUENCE							
003	02	44	39	05	ATTITUDE VERIFICATION COMPLETE (SOLAR ASPECT SENSOR DATA)							
003	02	44	40	05	IF ATTITUDE NOT VERIFIED, INHIBIT BURN SEQ. BY GROUND COMMAND							
003	02	44	40	05	HG ANT. GIMBAL LOCKS ON	CS066	CD731	ANT.	00	413W	183W	009W
003	02	44	45	05	MONOPROPELLANT ENGINES + MAXIMUM EXPECTED BURN TIME							
003	02	44	46	05	START ENGINE BURN	CS069	CD734	PROP	00	548W	183W	009W
003	02	44	46	05	ENGINE THRUST VECTOR CONTROL PROVIDED BY AUTOPILOT							
003	02	50	47	05	STOP ENGINE BURN	CS070		PROP	00	413W	183W	009W
003	02	50	50	05	STOP ENGINE BURN (BKUP)	CS071		PROP				
003	02	50	50	05	PROPELLANT IS NOT DEPRESSURIZED + ISOLATED UNTIL AFTER M/C2							
003	02	51	00	05	HG ANT.GIMBAL LOCKS OFF	CS067	CD732	ANT.	00	153W	183W	009W
003	02	51	30	05	AUTOPILOT POWER OFF	CS041	CD702	POWER	15	153W	171W	009W
003	02	52	00	05	SW. TO CRUISE MODE	CS001	CD606	G+C	15	177W	171W	009W
003	03	32	00	05	SUN ACQUISITION COMPLETE							
003	03	32	00	05	CAPSULE POWER ON	CS037	CD697	POWER	00	353W	171W	009W
003	04	42	00	05	CANOPUS ACQUIRED							
003	04	42	00	05	SW. TO CRUISE RADIO MD.	CS085		RADIO				

```
003 05 07 01 05 GYRO SET I OFF                    CS046 CD707  POWER 15   347W 163W 000W
003 05 07 01 05 SW. TO DATA MODE 4                CS079 CD749  T/M
003 05 13 01 05 SW. TO DATA MODE 2                CS076 CD746  T/M        347W 157W 000W
```

6 Interplanetary Cruise Mission Phase

```
003 05 13 01 06 UPDATE ANTENNA POINTING + CANOPUS CONE ANGLE (SAME AS PHASE 4)
003 05 13 01 06 OBTAIN SOLAR FLARE DATA (SAME AS PHASE 4)
```

7 Second Interplanetary Trajectory Correction (P/V1)

```
029 12 00 00 07 P/V2 PERFORMS SAME MANEUVER SEQUENCE 1 DAY LATER
029 12 00 00 07 REPEAT FIRST INTERPL. TRAJECTORY CORRECTION SEQUENCE EXCEPT
029 12 00 00 07 DO NOT OPEN + CLOSE QUAD. SOL VALVES TO EXPELL AIR
029 12 00 00 07 DO NOT PRESSURIZE + ENABLE PROPELLANT FLOW
030 05 41 26 07 DISABLE M/C PROP.FLOW 1 CD658          PYRO
030 05 41 26 07 DEPRESS. M/C PROP. 1    CD661          PYRO
```

8 Interplanetary Cruise Mission Phase

```
030 05 41 26 08 UPDATE ANTENNA POINTING + CANOPUS CONE ANGLE (SAME AS PHASE 4)
030 05 41 26 08 OBTAIN SOLAR FLARE DATA (SAME AS PHASE 4)
060 00 00 00 08 SUN LOOPS TO MED. GAIN  CS014 CD620  G+C
```

9 Third Interplanetary Trajectory Correction (P/V1)

```
174 12 00 00 09 P/V2 PERFORMS SAME MANEUVER SEQUENCE 10 DAYS LATER
174 12 00 00 09 REPEAT FIRST INTERPL. TRAJECTORY CORRECTION SEQUENCE EXCEPT
174 12 00 00 09 DO NOT OPEN + CLOSE QUAD. SOL. VALVES TO EXPELL AIR
175 00 40 00 09 PRES. MC/OA PROP. 2      CD653          PYRO
175 00 40 00 09 ENABLE MC/OA PROP. FL.2  CD656          PYRO
```

10 Interplanetary Cruise Mission Phase

```
175 05 41 26 10 UPDATE ANTENNA POINTING + CANOPUS CONE ANGLE (SAME AS PHASE 4)
```

```
000 19 50 00 04 OBTAIN SOLAR FLARE DATA - AS REQUIRED THROUGHOUT MISSION
000 19 50 00 04 TURN ON TAPE RECORDER    DAE              DS    08   347W 163W 000W
001 00 27 46 04 TURN OFF TAPE RECORDER   DAE              DS
001 00 27 46 04 ASSUMES 10,000,000 BITS OF SOLAR FLARE DATA STORED (600BPS)
001 00 27 46 04 SW. TO DATA MODE 4       DS               T/M
001 01 12 26 04 SW. TO DATA MODE 2       DS               T/M   08   347W 157W 000W
```

5 First Interplanetary Trajectory Correction (P/V1)

```
002 12 00 00 05 P/V2 PERFORMS SAME MANEUVER SEQUENCE 1 DAY LATER
002 12 00 00 05 LOAD MIDCOURSE MANEUVER 1 QUANTITATIVE COMMANDS
002 12 10 00 05 PITCH TURN START TIME    CD914            C+S
002 12 10 00 05 PITCH STOP - YAW START   CD915            C+S
002 12 10 00 05 YAW STOP                 CD916            C+S
002 12 10 00 05 M/C ENGINE START TIME    CD917            C+S
002 12 10 00 05 M/C ENGINE STOP TIME     CD919            C+S
002 14 00 00 05 PITCH TURN POLARITY (+)  CD798            C+S
002 14 00 00 05 YAW TURN POLARITY (+)    CD800            C+S
003 00 30 00 05 GYRO SET 1 ON            CS045 CD706      POWER 15   353W 165W 009W
003 00 31 00 05 OPEN QUAD. SOL. VALVES   CS069 CD734      PROP  00   488W 165W 009W
003 00 32 00 05 CLOSE QUAD. SOL. VALVES  CS070 CS071      PROP  00   353W 165W 009W
003 00 32 00 05 AIR IS EXPELLED PRIOR TO PROPELLANT PRESSURIZATION
003 00 40 00 05 PRESSURIZE PROPELLANT 1  CD652            PYRO
003 00 40 00 05 ENABLE PROPELL. FLOW 1   CD655            PYRO
003 01 30 00 05 GYRO TEMP. OVERRIDE      CS020 CD630      G+C
003 01 54 00 05 SW. TO DATA MODE 1A       CS074 CD744      T/M   08   353W 171W 009W
003 01 55 00 05 SW.TO MANEUVER RADIO MD.  CS086            RADIO
003 02 00 00 05 AUTO PILOT POWER ON      CS040 CD701      POWER 15   353W 183W 009W
003 02 00 30 05 CAPSULE POWER OFF        CS038 CD698      POWER 00   153W 183W 009W
003 02 01 00 05 SW.TO FULL INERT. CONT.  CS002 CD607      G+C
003 02 02 00 05 START PITCH TURN (+)     CS006 CD611      G+C
```

TABLE 5-1. FLIGHT SEQUENCE OF EVENTS AND POWER PROFILE (Continued)

Day	Hr	Mn	Sc	Ph	Event	Source	Bk/Up	Dest s/s	Dest	Raw d c	2.4 kc	400 cps
14 Planetary Vehicle Orbital Operations Mission Phase												
182	18	33	26	14	SW. TO CRUISE RADIO MD.	CS085		RADIO				
182	18	33	27	14	DEPLOY PLANET SCAN PLTM	CS031	CD666	PYRO				
182	18	33	30	14	400 CPS SCI. POWER ON	CS049	CD710	POWER				
182	18	34	00	14	PSP CONTROL ON	CS104	CD820	DAE	00	353W	171W	014W
182	18	34	00	14	PSP MOVES TO PREPROGRAMMED POSITION FOR GIMBALS C + D							
182	18	34	30	14	ENABLE EO DATA MODE SW.	CS102	CD815	C+S	00	353W	172W	014W
182	18	35	00	14	REMOVE SCIENCE COVERS	CS032	CD667	PYRO				
182	18	36	00	14	PSP GIMBAL E CONTROL ON	CS115	CD820					
182	18	36	00	14	TERMINATOR CROSSING + PLANET LIMB SIGNALS DEDUCED FROM (CONT.)							
182	18	36	00	14	GIMBAL E PICKOFF AND C+S KNOWLEDGE OF PLANET HALF ANGLE							
182	18	58	26	14	SW. TO DATA MODE 4	CS079	CD749	T/M				
182	19	07	54	14	SW. TO DATA MODE 2	CS076	CD746	T/M	08	353W	166W	014W
182	19	41	06	14	APOAPSIS PASSAGE OCCURS							
182	19	43	00	14	MORNING TERM. PASSAGE	CS117		SCI				
182	22	56	06	14	PLANET LIMB CROSSING	CS116		SCI				
182	23	11	06	14	PERIAPSIS PASSAGE OCCURS							
182	23	12	21	14	EARTH OCCULTATION OCCURS (40 DEGREE INCLINED ORBIT)							
182	23	12	21	14	SW. TO DATA MODE 3B	CS078	CD748	T/M	08	353W	172W	014W
182	23	12	36	14	EVENING TERM. PASSAGE	CS118		SCI				
182	23	32	46	14	SUN OCCULTATION OCCURS (40 DEGREE INCLINED ORBIT)							
182	23	32	46	14	CAPSULE POWER OFF				00	153W	172W	014W
182	23	32	46	14	THERMAL CONTROL ON				00	153W	181W	014W
182	23	32	46	14	SWITCH TO YAW + PITCH INERTIAL CONTROL							
182	23	48	09	14	EARTH OCCULTATION COMPLETE							
182	23	48	09	14	SW. TO DATA MODE 4	CS079	CD749	T/M				
182	23	49	16	14	SW. TO DATA MODE 2	CS076	CD746	T/M	08	153W	175W	014W
183	00	14	34	14	SUN OCCULTATION COMPLETE							
183	00	14	34	14	SWITCH TO CELESTIAL REFERANCES							
183	00	14	34	14	CAPSULE POWER ON				00	353W	175W	014W
183	00	14	34	14	THERMAL CONTROL OFF					353W	166W	014W
183	02	41	06	14	APOAPSIS PASSAGE OCCURS							
183	02	43	00	14	MORNING TERM. PASSAGE	CS117		SCI				
183	05	56	06	14	PLANET LIMB CROSSING	CS116		SCI				
183	06	11	06	14	PERIAPSIS PASSAGE OCCURS (COMPLETION OF TWO ORBITS)							
183	06	11	06	14	TURN OFF CRUISE SCIENCE	CS103	CD820	DAE	06	353W	137W	014W
183	06	11	07	14	TURN ON ORBIT SCIENCE	CS105	CD820	DAE	06	353W	148W	014W
183	06	12	21	14	EARTH OCCULTATION OCCURS (40 DEGREE INCLINED ORBIT)							
183	06	12	21	14	SW. TO DATA MODE 3B	CS078	CD748	T/M	08	353W	154W	014W
183	06	12	36	14	EVENING TERM. PASSAGE	CS118		SCI				
183	06	32	46	14	SUN OCCULTATION OCCURS (40 DEGREE INCLINED ORBIT)							
183	06	32	46	14	SWITCH TO PITCH + YAW INERTIAL CONTROL							
183	06	32	46	14	CAPSULE POWER OFF				00	153W	154W	014W
183	06	32	46	14	THERMAL CONTROL ON				00	153W	163W	014W
183	06	48	09	14	EARTH OCCULTATION COMPLETE (EARTH OCCULTATION SENSOR)							

183	07	14	34	14	SUN OCCULTATION COMPLETE						
183	07	14	34	14	SWITCH TO CELESTIAL REFERENCES						
183	07	14	34	14	CAPSULE POWER ON						
183	07	14	34	14	THERMAL CONTROL OFF				00	353W	163W 014W
183	09	41	06	14	APOAPSIS PASSAGE OCCURS				00	353W	154W 014W
183	09	43	00	14	MORNING TERM. PASSAGE	CS117		SCI			
183	11	11	00	14	PSP SCIENCE POWER ON	CS106	CD820	DAE	06	353W	255W 019W
183	11	41	00	14	COLOR TV ON	CS110	CD820	DAE			
183	11	41	01	14	IR SCANNER ON	CS107	CD820	DAE			
183	11	41	02	14	IR SPECTROMETER ON	CS109	CD820	DAE			
183	12	01	00	14	COLOR TV OFF	CS110	CD820	DAE			
183	12	20	00	14	IR SCANNER OFF	CS107	CD820	DAE			
183	12	25	00	14	IR SPECTROMETER OFF	CS109	CD820	DAE			
183	12	45	00	14	BLACK + WHITE TV ON	CS108	CD820	DAE			
183	12	56	06	14	PLANET LIMB CROSSING	CS116		SCI			
183	13	00	00	14	IR SCANNER ON	CS107	CD820	DAE			
183	13	10	00	14	UV SPECTROMETER ON	CS111	CD820	DAE			
183	13	11	06	14	PERIAPSIS PASSAGE OCCURS						
183	13	12	10	14	BLACK + WHITE TV OFF	CS108	CD820	DAE			
183	13	12	21	14	EARTH OCCULTATION OCCURS (40 DEGREE INCLINED ORBIT)						
183	13	12	21	14	SW. TO DATA MODE 3B	CS078	CD748	T/M			
183	13	12	36	14	EVENING TERM. PASSAGE	CS118		SCI			
183	13	20	00	14	UV SPECTROMETER OFF	CS111	CD820	DAE			
183	13	24	00	14	IR SCANNER OFF	CS107	CD820	DAE			
183	13	25	00	14	PSP SCIENCE POWER OFF	CS106	CD820	DAE	06	353W	154W 014W
183	13	25	00	14	PRECEDING IS TIME APPROXIMATION OF PSP SCIENCE SEQ. (CONT.)						
183	13	25	00	14	USING PSP GIMBAL E PICKOFF + ENCOUNTER ORBIT GEOMETRY						
183	13	26	00	14	PSP REPOSITIONED						
183	13	32	46	14	SUN OCCULTATION OCCURS (40 DEGREE INCLINED ORBIT)						
183	13	32	46	14	SWITCH TO PITCH + YAW INERTIAL CONTROL						
183	13	32	46	14	CAPSULE POWER OFF						
183	13	32	46	14	THERMAL CONTROL ON				00	153W	154W 014W
183	13	48	09	14	EARTH OCCULTATION COMPLETE (EARTH OCCULTATION SENSOR)				00	153W	163W 014W
183	13	48	09	14	SW. TO DATA MODE 3A	CS077	CD747	T/M			
183	14	14	34	14	SUN OCCULTATION COMPLETE						
183	14	14	34	14	SWITCH TO CELESTIAL REFERENCES						

17 Flight Spacecraft - Flight Capsule Separation Mission Phase

188	10	48	54	17	P/V2 PERFORMS SAME MANEUVER SEQUENCE 10 DAYS LATER								
188	10	48	54	17	MAY BE PERFORMED EARLIER IF ORBIT TRIM MANEUVER(S) NOT REQ•								
188	10	48	54	17	SW• TO DATA MODE 5	CS080	CD750	T/M					
188	10	48	55	17	START CAPSULE CHECKOUT	CS094	CD789	CAPS					
188	10	48	55	17	UPDATE + VERIFY STORED QUANTITATIVE COMMANDS IN CAPSULE								
188	10	48	56	17	INH•PSP GIMBAL E MOTION	CS119	CD820	DAE	06	353W	154W	009W	
188	10	48	56	17	PRECEDING INHIBITS PSP SCIENCE ON								
188	10	48	57	17	ORBIT SCIENCE OFF	CS105	CD820	DAE	06	353W	143W	009W	
188	11	11	06	17	PERIAPSIS PASSAGE OCCURS								
188	11	11	06	17	INH• SO CAPS• POWER OFF	CS054	CD718	POWER					
188	11	12	21	17	EARTH OCCULTATION OCCURS (40 DEGREE INCLINED ORBIT)								
188	11	12	21	17	SW• TO DATA MODE 3B	CS078	CD748	T/M	08	353W	137W	009W	
188	11	32	46	17	SUN OCCULTATION OCCURS (40 DEGREE INCLINED ORBIT)								
188	11	32	46	17	SWITCH TO PITCH + YAW INERTIAL CONTROL								
188	11	32	46	17	THERMAL CONTROL ON				00	353W	146W	009W	
188	12	07	34	17	EARTH OCCULTATION COMPLETE (EARTH OCCULTATION SENSOR)								
188	12	07	34	17	SW• TO DATA MODE 5	CS080	CD750	T/M	08	353W	152W	009W	
188	12	14	34	17	SUN OCCULTATION COMPLETE								
188	12	14	34	17	SWITCH TO CELESTIAL REFERENCES								
188	12	14	34	17	THERMAL CONTROL OFF				00	353W	143W	009W	
188	15	38	00	17	SW• TO DATA MODE 1B	CS075	CD745	T/M					
188	15	39	00	17	INH•EO DATA MODE SWITCH	CS101	CD814	C+S	00	353W	142W	009W	
188	15	40	00	17	SW•TO MANEUVER RADIO MD	CS086		RADIO					
188	15	41	13	17	SW• TO FULL INERT• CONT•	CS002	CD607	G+C					
188	15	41	14	17	START YAW TURN (+)	CS003	CD608	G+C					
188	15	49	34	17	STOP YAW TURN	CS005	CD610	G+C					
188	15	50	34	17	START PITCH TURN (+)	CS006	CD611	G+C					
188	15	58	54	17	STOP PITCH TURN	CS008	CD613	G+C					
188	15	58	54	17	PRECEDING ASSUMES A YAW - PITCH TURN SEQUENCE								
188	15	58	54	17	TURN TIMES ARE MAXIMUM POSSIBLE EXPECTED								
188	15	58	55	17	RELAY RADIO ON	CS043	CD704	POWER	13	353W	154W	009W	
188	15	58	56	17	SW• TO INTERNAL POWER	CS095	CD790	CAPS	00	153W	154W	009W	
188	16	38	54	17	ATTITUDE VERIFIED - CAPSULE CHECKOUT COMPLETE								
188	16	39	54	17	ENABLE CAPSULE SEP•	CD792		CAPS					
188	16	40	54	17	INIT•CAPS•SEP•SEQUENCE	CS096	CD791	CAPS					
188	16	45	54	17	LOW RATE RECORDER ON	CS088	CD782	R•RAD•					
188	16	48	50	17	S/C - CAPSULE IN-FLIGHT DISCONNECT CONNECTOR SEPARATED								
188	16	48	54	17	CAPSULE SEPARATION								
188	16	49	00	17	INIT• COLD GAS JET SQ•	CS033	CD668	PYRO					
188	17	08	54	17	CAPSULE DEORBIT MOTOR FIRES								
188	18	00	00	17	HIGH RATE RECORDER ON	CS089	CD783	R•RAD•					
188	18	00	01	17	LOW RATE RECORDER OFF	CS088	CD782	R•RAD•					
188	18	11	06	17	PERIAPSIS PASSAGE OCCURS								

TABLE 5-1. FLIGHT SEQUENCE OF EVENTS AND POWER PROFILE (Continued)

Day	Hr	Mn	Sc	Ph	Event	Source	Bk/Up	Dest s/s	Dest	Raw d c	2.4 kc	400 cps
15 First Planetary Vehicle Mars Orbit Trim Maneuver (P/V1) (Continued)												
184	14	56	20	15	ORBIT SCIENCE OFF	CS105	CD820	DAE	06	353W	143W	014W
184	14	57	20	15	INH. PSP GIM. E MOTION	CS119	CD820	DAE	06	353W	143W	009W
184	14	57	20	15	PRECEDING INHIBITS PSP SCIENCE ON							
184	14	58	20	15	SW. TO DATA MODE 1A	CS074	CD744	T/M				
184	16	20	00	15	INH.EO DATA MODE SWITCH	CS101	CD814	C+S	00	353W	142W	009W
184	16	21	20	15	SW.TO MANEUVER RADIO MD.	CS086		RADIO				
184	16	26	20	15	AUTOPILOT POWER ON	CS040	CD701	POWER	15	353W	154W	009W
184	16	26	50	15	CAPSULE POWER OFF	CS038	CD698	POWER	00	153W	154W	009W
184	16	27	20	15	SW. TO FULL INERT. CONT.	CS002	CD607	G+C				
184	16	28	20	15	START PITCH TURN (+)	CS006	CD611	G+C				
184	16	36	40	15	STOP PITCH TURN	CS008	CD613	G+C				
184	16	37	40	15	START YAW TURN (+)	CS003	CD608	G+C				
184	16	46	00	15	STOP YAW TURN	CS005	CD610	G+C				
184	16	46	00	15	TURN TIMES DESIGNATED ARE BASED ON SUM TOTAL OF 180 DEGREES MAX							
184	16	46	00	15	ASSUMES PITCH + YAW OR YAW + PITCH SEQUENCE							

```
184 17 10 55 15 ATTITUDE VERIFICATION COMPLETE (SOLAR [illegible]  ANT.  00   413W 154W 009W
184 17 11 00 15 HG ANT. GIMBAL LOCKS ON CS066 CD731   ANT.  00   413W 154W 009W
184 17 11 00 15 IF ATTITUDE NOT VERIFIED. INHIBIT BURN SEQ. BY GROUND COMMAND
184 17 11 00 15 MONOPROPELLANT ENGINES + MAXIMUM EXPECTED ENGINE BURN TIME
184 17 11 05 15 PERIAPSIS PASSAGE OCCURS
184 17 11 06 15 START ENGINE BURN          CS069 CD734   PROP  00   548W 154W 009W
184 17 12 21 15 EARTH OCCULT. OCCURS
184 17 17 06 15 STOP ENGINE BURN           CS070         PROP  00   413W 154W 009W
184 17 17 09 15 STOP ENGINE BURN (BKUP)    CS071         PROP
184 17 17 09 15 PROPELLANT IS NOT DEPRESSURIZED + ISOLATED UNTIL AFTER OTM 4
184 17 17 09 15 HG ANT.GIMBAL LOCKS OFF    CS067 CD732   ANT.  00   153W 154W 009W
184 17 18 08 15 AUTOPILOT POWER OFF        CS041 CD702   POWER 15   153W 142W 009W
184 17 18 38 15 SW. TO CRUISE MODE         CS001 CD606   G+C   15   177W 142W 009W
184 17 18 40 15 SUN OCCULTATION OCCURS                             15   153W 142W 009W
184 17 32 46 15 SWITCH TO PITCH + YAW INERTIAL CONTROL             00   153W 151W 009W
184 17 32 46 15 THERMAL CONTROL ON
184 17 58 04 15 EARTH OCCULTATION COMPLETE                         15   177W 151W 009W
184 18 14 34 15 SUN OCCULTATION COMPLETE                           00   177W 142W 009W
184 18 14 34 15 THERMAL CONTROL OFF                                15   153W 142W 009W
184 18 40 28 15 SUN ACQUISITION COMPLETE
184 18 40 28 15 CAPSULE POWER ON           CS037 CD697   POWER 00   353W 142W 009W
184 19 48 58 15 CANOPUS ACQUIRED
184 19 48 58 15 SW. TO CRUISE RADIO MD.    CS085         RADIO
184 20 13 58 15 SW. TO DATA MODE 3A        CS077 CD747   T/M
184 20 14 58 15 ORBIT SCIENCE ON           CS105 CD820   DAE   06   353W 153W 009W
184 20 15 58 15 PSP GIMBAL E CONTROL ON    CS115 CD820   SCI   06   353W 153W 014W
184 20 16 58 15 EN.EO DATA MODE SWITCH     CS102 CD815   C+S   00   353W 154W 014W
184 20 16 58 15 REPEAT ORBIT GEOMETRY DETERMINATION AS WELL AS PSP SCIENCE(CONT
184 20 16 58 15 DATA GATHERING AS FOLLOWING ORBIT INJECTION
```

16 Second Planetary Vehicle Mars Orbit Trim Maneuver (P/V1)

```
186 07 25 20 16 PERFORMED ONLY IF NECESSARY - ENGINE BURN ASSUMED AT APOAPSIS
186 07 25 20 16 REPEAT FIRST PLANETARY VEHICLE MARS ORBIT TRIM SEQUENCE
186 07 25 20 16 OCCULTATIONS WILL OCCUR AT DIFFERENT TIMES DURING SEQUENCE
186 07 25 20 16 REPEAT ORBIT GEOMETRY DETERMINATION AS WELL AS PSP SCIENCE(CONT
186 07 25 20 16 DATA GATHERING AS FOLLOWING ORBIT INJECTION
```

183	14	14	34	14	CAPSULE POWER ON		00	353W 163W 014W
183	14	14	34	14	THERMAL CONTROL OFF		00	353W 154W 014W
183	14	14	34	14	CONTINUE REPEATING PREVIOUS ORBITAL SEQUENCE			

15 First Planetary Vehicle Mars Orbit Trim Maneuver (P/V1)

184	02	55	20	15	PERFORMED ONLY IF NECESSARY - ENG. BURN ASSUMED AT PERIAPSIS		
184	02	55	20	15	P/V2 PERFORMS SAME MANEUVER SEQUENCE 10 DAYS LATER IF NECESSARY		
184	02	55	20	15	SCIENCE DATA GATHERING CONTINUES UNTIL INHIBITED BY PSP MOTION		
184	02	55	20	15	LOAD ORBIT TRIM MANEUVER 1 QUANTITATIVE COMMANDS		
184	03	00	00	15	PITCH TURN START TIME	CD914	C+S
184	03	00	00	15	PITCH STOP - YAW START	CD915	C+S
184	03	00	00	15	YAW STOP	CD916	C+S
184	03	00	00	15	OTM ENG. START TIME	CD917	C+S
184	03	00	00	15	OTM ENG. STOP TIME	CD919	C+S
184	05	00	00	15	PITCH TURN POLARITY (+)	CD798	C+S
184	05	00	00	15	YAW TURN POLARITY (+)	CD800	C+S

TABLE 5-1. FLIGHT SEQUENCE OF EVENTS AND POWER PROFILE (Continued)

Day	Hr	Mn	Sc	Ph	Event	Source	Bk/Up	Dest s/s	Dest d	Raw c	2.4 kc	400 cps
17 Flight Spacecraft - Flight Capsule Separation Mission Phase (Continued)												
188	18	12	21	17	EARTH OCCULTATION OCCURS (40 DEGREE INCLINED ORBIT)							
188	18	29	54	17	CAPSULE IMPACT							
188	18	32	46	17	SUN OCCULTATION OCCURS (40 DEGREE INCLINED ORBIT)							
188	18	32	46	17	THERMAL CONTROL ON				00	153W	163W	009W
188	18	48	09	17	EARTH OCCULTATION COMPLETE							
188	19	00	00	17	HIGH RATE RECORDER OFF	CS089	CD783	R•RAD•				
188	19	01	00	17	RELAY RADIO OFF	CS044	CD705	POWER	13	153W	151W	009W
188	19	14	34	17	SUN OCCULTATION COMPLETE							
188	19	14	34	17	THERMAL CONTROL OFF				00	153W	142W	009W
188	19	14	34	17	SW• TO CRUISE MODE	CS001	CD606	G+C	15	177W	142W	009W
188	19	54	34	17	SUN ACQUISITION COMPLETE				00	153W	142W	009W
188	21	04	34	17	CANOPUS ACQUIRED							
188	21	04	34	17	SW• TO CRUISE RADIO MD•	CS085		RADIO				
188	21	29	34	17	SW• TO DATA MODE 3A	CS077	CD747	T/M				
188	21	54	34	17	ENABLE RELAY REC• RDT•	CS090	CD784	R•RAD•				
189	01	10	00	17	CAPSULE ENTRY RECORDED DATA PLAYBACK COMPLETE							
189	01	10	00	17	EN• EO DATA MODE SWITCH	CS102	CD815	C+S		153W	143W	009W
189	01	11	00	17	PSP GIMBAL E CONTROL ON	CS115	CD820	DAE		153W	143W	014W
189	01	11	06	17	PERIAPSIS PASSAGE OCCURS							
189	01	12	00	17	CRUISE SCIENCE ON	CS103	CD820	DAE		153W	172W	014W
189	01	12	21	17	EARTH OCCULTATION OCCURS (EARTH OCCULTATION SENSOR)							
189	01	12	21	17	SW• TO DATA MODE 3B	CS078	CD748	T/M				
189	01	12	36	17	EVENING TERM• PASSAGE	CS118		SCI				
189	01	13	00	17	ORBIT SCIENCE ON	CS105	CD820	DAE		153W	183W	014W
18 Flight Spacecraft Orbital Operations Mission Phase												
189	01	32	46	18	SUN OCCULTATION OCCURS (40 DEGREE INCLINED ORBIT)							
189	01	32	46	18	SWITCH TO PITCH + YAW INERTIAL CONTROL							
189	01	32	46	18	THERMAL CONTROL ON				00	153W	192W	014W
189	01	48	09	18	EARTH OCCULTATION COMPLETE (EARTH OCCULTATION SENSOR)							
189	01	48	09	18	SW• TO DATA MODE 3A	CS077	CD747	T/M				
189	02	14	34	18	SUN OCCULTATION COMPLETE							
189	02	14	34	18	SWITCH TO CELESTIAL REFERENCES							
189	02	14	34	18	THERMAL CONTROL OFF				00	153W	183W	014W
189	03	50	00	18	PSP SCIENCE POWER ON	CS106	CD820	DAE	06	153W	284W	019W
189	04	25	00	18	IR SCANNER ON	CS107	CD820	DAE				
189	04	34	00	18	UV SPECTROMETER ON	CS111	CD820	DAE				
189	04	41	06	18	APOAPSIS PASSAGE OCCURS							
189	04	43	00	18	MORNING TERM• PASSAGE	CS117		SCI				
189	04	53	00	18	UV SPECTROMETER OFF	CS111	CD820	DAE				
189	05	00	00	18	BLACK + WHITE TV ON	CS108	CD820	DAE				

```
189 05 25 00 18 BLACK + WHITE TV OFF      CS108 CD820  DAE
189 06 25 00 18 IR SCANNER ON             CS107 CD820  DAE
189 06 30 00 18 IR SPECTROMETER ON        CS109 CD820  DAE
189 06 41 00 18 COLOR TV ON               CS110 CD820  DAE
189 07 01 00 18 COLOR TV OFF              CS110 CD820  DAE
189 07 20 00 18 IR SCANNER OFF            CS107 CD820  DAE
189 07 25 00 18 IR SPECTROMETER OFF       CS109 CD820  DAE
189 07 45 00 18 BLACK + WHITE TV ON       CS108 CD820  DAE
189 07 56 06 18 PLANET LIMB CROSSING      CS116        SCI
189 08 00 00 18 IR SCANNER ON             CS107 CD820  DAE
189 08 10 00 18 UV SPECTROMETER ON        CS111 CD820  DAE
189 08 11 06 18 PERIAPSIS PASSAGE OCCURS
189 08 12 10 18 BLACK + WHITE TV OFF      CS108 CD820  DAE
189 08 12 21 18 EARTH OCCULTATION OCCURS (EARTH OCCULTATION SENSOR)
189 08 12 21 18 SW. TO DATA MODE 38       CS078 CD748  T/M
189 08 12 36 18 EVENING TERM. PASSAGE     CS118        SCI
189 08 20 00 18 UV SPECTROMETER OFF       CS111 CD820  DAE
189 08 24 00 14 IR SCANNER OFF            CS107 CD820  DAE
189 08 25 00 18 PSP SCIENCE OFF           CS106 CD820  DAE   06   153W 183W 014W
189 08 26 00 18 PSP REPOSITIONED
189 08 26 00 18 CONTINUE REPEATING PREVIOUS ORBITAL SEQUENCE
```

(25)

19 First Flight Spacecraft Mars Orbit Trim Maneuver (P/V1)

```
190 04 55 20 19 PERFORMED ONLY IF NECESSARY - ENGINE BURN ASS. AT PERIAPSIS
190 04 55 20 19 P/V2 PERFORMS SAME MANEUVER SEQUENCE 10 DAYS LATER IF NECESSARY
190 04 55 20 19 REPEAT FIRST PLANETARY VEHICLE MARS ORBIT TRIM MANEUVER
190 04 55 20 19 EARTH + SUN OCCULTATIONS OCCUR AT DIFFERENT TIMES DURING OTM
190 04 55 20 19 REPEAT ORBIT GEOMETRY DETERMINATION AS WELL AS PSP SCIENCE(CONT
190 04 55 20 19 DATA GATHERING AS FOLLOWING CAPSULE SEPARATION
```

20 Second Flight Spacecraft Mars Orbit Trim Maneuver (P/V1)

```
192 09 25 20 20 PERFORMED ONLY IF NECESSARY - ENGINE BURN ASSUMED AT APOAPSIS
```

[redacted]

```
192 09 25 20 20 P/V2 PERFORMS SAME MANEUVER SEQUENCE 10 DAYS LATER IF NECESSARY
192 09 25 20 20 REPEAT FIRST PLANETARY VEHICLE MARS ORBIT TRIM MANEUVER
192 09 25 20 20 EARTH + SUN OCCULTATIONS OCCUR AT DIFFERENT TIMES DURING MAN.
192 09 25 20 20 REPEAT ORBIT GEOMETRY DETERMINATION AS WELL AS PSP SCIENCE(CONT
192 09 25 20 20 DATA GATHERING AS FOLLOWING CAPSULE SEPARATION
193 03 25 00 20 DISABLE OTM PROP.FLOW 2 CD658          PYRO
193 03 25 00 20 DEPRESS. OTM PROP.2     CD661          PYRO
```

21 Flight Spacecraft Orbital Operations Mission Phase (P/V1)

```
193 03 25 00 21 CONTINUE SCIENCE DATA GATHERING
193 03 25 00 21 UPDATE ANTENNA POINTING + CANOPUS CONE ANGLE (SAME AS PHASE 4)
```

22 Flight Spacecraft 180 Degree Roll Reorientation Sequence

```
237 00 00 00 22 ASSUMES THAT REORIENTATION TAKES PLACE WITHOUT OCCULT. INTERF.
237 00 01 00 22 CANOPUS TRACKER 2 ON    CS051 CD714  POWER
237 00 30 00 22 SW. TO DATA MODE 1A     CS074 CD744  T/M
237 00 30 01 22 SW.TO MANEUVER RADIO MD CS086        RADIO
237 00 30 02 22 REORIENT HIGH GAIN ANTENNA (PROGRAMMED CONTROL)
237 00 35 00 22 INH.PSP GIMBAL E MOTION CS119 CD820  DAE
```

TABLE 5-1. FLIGHT SEQUENCE OF EVENTS AND POWER PROFILE (Continued)

Day	Hr	Mn	Sc	Ph	Event	Source	Bk/Up	Dest s/s	Dest d	Raw c	2.4 kc	400 cps
22 Flight Spacecraft 180 Degree Roll Reorientation Sequence (Continued)												
237	00	35	00	22	PRECEDING INHIBITS PSP SCIENCE ON							
237	00	39	00	22	UPDATE PSP GIMBAL C	CS113	CD820	DAE				
237	00	39	00	22	UPDATE PSP GIMBAL D	CS114	CD820	DAE				
237	00	39	55	22	SW. TO ROLL INERT. MODE	CS013	CD618	G+C				
237	00	40	00	22	START 180 DEGREE ROLL	CS009	CD614	G+C				
237	00	56	40	22	STOP 180 DEGREE ROLL	CS011	CD616	G+C				
237	00	56	40	22	SW. TO CAN. 2 SIG. INP.	CS120	CD605	G+C				
237	00	56	41	22	SW. TO CRUISE RADIO MD.	CS085		RADIO				
237	01	22	40	21	TURN OFF CANOPUS TKR.1	CS050	CD713	POWER				
237	01	22	41	22	SW. TO DATA MODE 3A	CS077	CD747	T/M				
237	01	30	00	22	PSP GIMBAL E CONTROL ON	CS115	CD820	DAE				
237	01	30	00	22	CONTINUE SCIENCE DATA GATHERING							
23 Canopus Star Occultation												
272	00	00	00	23	SW. TO ROLL INERT. CONT.	CS013	CD618	G+C				
272	00	30	00	23	CANOPUS OCCULTATION							
272	00	37	30	23	CANOPUS PRESENT							
272	01	07	30	23	SW. TO CRUISE MODE	CS001	CD606	G+C				
272	01	07	30	23	PRECEDING SEQUENCE BECOMES INTEGRATED WITH NORMAL ORBIT SEQ.							

VC220FD112

6.0 COMMAND LIST.

Discrete Commands: Commands which provide momentary switch closure to Planetary Vehicle subsystems.

Quantitative Commands: Commands which provide a stream of digital information to the subsystem user.

The commands originating from the following sources are numbered as follows:

Computer and Sequencer (Discrete): CS000 to CS549.
Command Decoder (Discrete): CD600 to CD899.
Computer and Sequencer (Quantitative): CS900 to CS905.
Command Decoder (Quantitative): CD906 to CD999.

The Command List consists of all commands required for the Forward Planetary Vehicle. A duplicate set of commands is required for P/V2.

6.1 Guidance and Control Subsystem.

6.1.1 Attitude Control.

Command Source		Command
Primary	Backup	
CS000	CD600	Enable Pneumatic Drivers
CD601	———	Disable Pneumatic Drivers
CD602	———	Switch to I.G.P. No. 1 Signal Input
CD603	———	Switch to I.G.P. No. 2 Signal Input
CD604	———	Switch to Canopus No. 1 Signal Input
CS120	CD605	Switch to Canopus No. 2 Signal Input
CS001	CD606	Switch to Cruise Mode
CS002	CD607	Switch to Full Inertial Control
CS003	CD608	Start Yaw Turn (+)
CS004	CD609	Start Yaw Turn (-)
CS005	CD610	Stop Yaw Turn
CS006	CD611	Start Pitch Turn (+)
CS007	CD612	Start Pitch Turn (-)

Command Source		Command
Primary	Backup	
CS008	CD613	Stop Pitch Turn
CS009	CD614	Start Roll Turn (+)
CS010	CD615	Start Roll Turn (-)
CS011	CD616	Stop Roll Turn
CS012	CD617	Enable Sun Occultation Mode
CS013	CD618	Switch to Roll Inertial Mode
CD619	———	Roll Override
CS014	CD620	Sun Loops to Medium Gain
CS015	CD621	Sun Loops to High Gain
CD622	———	Spare
CS016	CD623	Select Canopus No. 1 for Incrementing
CS017	CD624	Select Canopus No. 2 for Incrementing
CD625	———	Enable Canopus High-Gate Function
CD626	———	Enable Canopus Low-Gate Function
CD627	———	Enable Cone Angle Function
CS018	CD628	Increment Canopus Function (+)
CS019	CD629	Increment Canopus Function (-)
CS020	CD630	Gyro Temperature Override
CS046	CD707	Gyro Set No. 1 Off
CS048	CD709	Gyro Set No. 2 Off
CS021	CD631	Spare
CS022	CD632	Spare
CD633	———	Spare
↓	↓	↓
CD645	———	Spare

6.1.2 Autopilot.

Command Source		Command
Primary	Backup	
CS023	CD646	Enable Autopilot (and Enable Retroengine Injectors Open)
CS024	CD647	Spare

6.2 Pyrotechnic Subsystem

Command Source		Command
Primary	Backup	
CS025	CD648	Initiate High-Gain Antenna Deployment
CS026	CD649	Deploy Secondary Low-Gain Antenna
CS027	CD650	Deploy Magnetometer
CS028	CD651	Remove Cruise Science Covers
CD652	———	Pressurize MC/OA Propellant 1
CD653	———	Pressurize MC/OA Propellant 2
CD654	———	Pressurize MC/OA Propellant 3
CD655	———	Enable MC/OA Propellant Flow 1
CD656	———	Enable MC/OA Propellant Flow 2
CD657	———	Enable MC/OA Propellant Flow 3
CD658	———	Disable MC/OA Propellant Flow 1
CD659	———	Disable MC/OA Propellant Flow 2
CD660	———	Disable MC/OA Propellant Flow 3
CD661	———	Depressurize MC/OA Propellant 1
CD662	———	Depressurize MC/OA Propellant 2
CD663	———	Depressurize MC/OA Propellant 3
CS029	CD664	Initiate TVC Pressurization Squibs
CS030	CD665	Initiate Retroengine Burn
CS031	CD666	Initiate PSP Deployment
CS032	CD667	Remove Orbit and PSP Science Instrument Covers
CS033	CD668	Initiate Cold Gas Jet Squibs

Command Source		Command
Primary	Backup	
CD669	———	Initiate 2 Position Valve (Propulsion S/S)
CD670	———	Isolate TCA No. 1 and 3 (Propulsion S/S)
CD671	———	Isolate TCA No. 2 and 4 (Propulsion S/S)
CS034	CD672	Spare
CS035	CD673	Initiate Sterilization Canister Pyro
CD674	———	Separate Emergency Spacecraft-Capsule Connector
CD675	———	Initiate Emergency Capsule Separation Pyro
CS036	CD676	Spare
CD677	———	Spare
CD678	———	Spare

6.3 Power Subsystem.

Command Source		Command
Primary	Backup	
CD679	———	Charge Regulator No. 1 Off
CD680	———	Setting A - Charge Regulator No. 1
CD681	———	Setting B - Charge Regulator No. 1
CD682	———	Setting C - Charge Regulator No. 1
CD683	———	Charge Regulator No. 2 Off
CD684	———	Setting A - Charge Regulator No. 2
CD685	———	Setting B - Charge Regulator No. 2
CD686	———	Setting C - Charge Regulator No. 2
CD687	———	Charge Regulator No. 3 Off
CD688	———	Setting A - Charge Regulator No. 3
CD689	———	Setting B - Charge Regulator No. 3
CD690	———	Setting C - Charge Regulator No. 3
CD691	———	Main Regulator No. 1 On/Off
CD692	———	Main Regulator No. 2 On/Off

Command Source		Command
Primary	Backup	
CD693	———	2.4-Kc Inverter No. 1 On/Off
CD694	———	2.4-Kc Inverter No. 2 On/Off
CD695	———	Switch to 400 cps 1Ø Inverter No. 1
CD696	———	Switch to 400 cps 1Ø Inverter No. 2
CS037	CD697	Capsule Power On
CS038	CD698	Capsule Power Off
CS039	CD699	2.4-Kc Science Power On
CD700	———	2.4-Kc Science Power Off
CS040	CD701	Autopilot Power On
CS041	CD702	Autopilot Power Off
CS042	CD703	Articulation Power On/Off
CS043	CD704	Relay Radio Power On
CS044	CD705	Relay Radio Power Off
CS045	CD706	Gyro Set No. 1 On
CS046	CD707	Gyro Set No. 1 Off
CS047	CD708	Gyro Set No. 2 On
CS048	CD709	Gyro Set No. 2 Off
CS049	CD710	Power to Science On (400 cps)
CD711	———	Power to Science Off (400 cps)
CD712	———	Power to Canopus Tracker No. 1 On
CS050	CD713	Power to Canopus Tracker No. 1 Off
CS051	CD714	Power to Canopus Tracker No. 2 On
CD715	———	Power to Canopus Tracker No. 2 Off
CS052	CD716	Thrust Vector Control Power On
CS053	CD717	Thrust Vector Control Power Off
CS054	CD718	Inhibit Solar Occultation Capsule Power Off
CD719	———	Enable Solar Occultation Capsule Power Off
CS055	CD720	Spare
CS056	CD721	Spare

6.4 High-Gain Antenna Articulation/Actuation Subsystem.

Command Source		Command
Primary	Backup	
CS057	CD722	Rotate 1/4° A axis (+)
CS058	CD723	Rotate 1/4° A axis (-)
CS059	CD724	Slew (+) A axis
CS060	CD725	Slew (-) A axis
CS061	CD726	Rotate 1/4° B axis (+)
CS062	CD727	Rotate 1/4° B axis (-)
CS063	CD728	Slew (+) B axis
CS064	CD729	Slew (-) B axis
CS065	CD730	Stop Slew
CS066	CD731	HG Ant Gimbal Locks On
CS067	CD732	HG Ant Gimbal Locks Off
CS068	CD733	Spare

6.5 Propulsion Subsystem

Command Source		Command
Primary	Backup	
CS069	CD734	Open Quad. Sol. Valves (4)
CS070	CS071	Close Quad. Sol. Valves (4)
CD735	———	Open Quad. Sol. Valves 1 and 3
CD736	———	Open Quad. Sol. Valves 2 and 4
CD737	———	Close Quad. Sol. Valves 1 and 3
CD738	———	Close Quad. Sol. Valves 2 and 4
CD739	———	Arm Retroengine (Safe and Arm)
CD740	———	Inhibit Retroengine Burn (S&A)
CS072	CD741	Close Retroengine Injectors
CS073	CD742	Spare
CD743	———	Spare

6.6 Telemetry Subsystem.

Command Source		Command
Primary	Backup	
CS074	CD744	Switch to Data Mode 1A
CS075	CD745	Switch to Data Mode 1B
CS076	CD746	Switch to Data Mode 2
CS077	CD747	Switch to Data Mode 3A
CS078	CD748	Switch to Data Mode 3B
CS079	CD749	Switch to Data Mode 4
CS080	CD750	Switch to Data Mode 5
CS081	CD751	Toggle High Data Rate
CD752	———	Toggle Low Data Rate
CD753	———	Phaser Bypass
CD754	———	Toggle Real Time Channel Activity
CD755	———	Toggle Stored Data Channel Activity
CS082	CD756	Spare

6.7 Data Storage Subsystem.

Command Source		Command
Primary	Backup	
CS083	CD757	End Recorder Launch Mode
CD758	———	PSC Function Switch Toggle
CD759	———	Advance MTR Input Switch
CD760	———	Advance MTR Address
CD761	———	Reset Playback Control
CD762	———	Playback Start
CD763	———	Spare

6.8 Radio Subsystem

Command Source		Command
Primary	Backup	
CS084	———	Switch to Launch Radio Mode
CS085	———	Switch to Cruise Radio Mode
CS086	———	Switch to Maneuver Radio Mode
CD764	———	Exciter No. 1 On/Off
CD765	———	Exciter No. 2 On/Off
CD766	———	Exciter No. 3 On/Off
CD767	———	Power Amplifier No. 1 On/Off
CD768	———	Power Amplifier No. 2 On/Off
CD769	———	Power Amplifier No. 3 On/Off
CD770	———	Receiver No. 1 On/Off
CD771	———	Receiver No. 2 On/Off
CD772	———	Receiver No. 3 On/Off
CD773	———	Antenna Transfer Switch No. 1 Norm/ Reverse
CD774	———	Antenna Transfer Switch No. 2 Norm/ Reverse
CD775	———	Backup Antenna Switch No. 3 Norm/ Backup
CD776	———	Ranging On/Off
CS087	CD777	Spare
CD778	———	Spare
↓	↓	↓
CD781	———	Spare

6.9 Relay Radio Subsystem

Command Source		Command
Primary	Backup	
CS088	CD782	Low-Rate Recorder On/Off
CS089	CD783	High-Rate Recorder On/Off

Command Source		Command
Primary	Backup	
CS090	CD784	Enable Relay Recorder Readout
CD785	———	Disable Relay Recorder Readout
CS091	CD786	Spare
CS092	CD787	Spare

6.10 Flight Capsule.

Command Source		Command
Primary	Backup	
CS093	CD788	End Capsule Launch Mode
CS094	CD789	Start Capsule Checkout
CS095	CD790	Switch to Internal Power
CS096	CD791	Initiate Capsule Separation Sequence
CD792	———	Enable Capsule Separation
CD793	———	Disable Capsule Separation
CS097	CD794	Spare
↓	↓	↓
CS100	CD797	Spare
CS900	———	Spare
↓	↓	↓
CS902	———	Spare
CD923	———	Spare
↓	↓	↓
CD925	———	Spare

6.11 Computer and Sequencer Subsystem.

Command Source		Command
Primary	Backup	
CD906	———	Gimbal Angle A Slope
CD907	———	Gimbal Angle B Slope

Command Source		Command
Primary	Backup	
CD908	———	Gimbal Angle C Slope
CD909	———	Gimbal Angle D Slope
CD910	———	Modify or Scan Word in Memory Sequence
CD911	———	TTG 1 Update
CD912	———	TTG 2 Update
CD913	———	TTG 3 Update
CD914	———	TTG 4 Update
CD915	———	TTG 5 Update
CD916	———	TTG 6 Update
CD917	———	TTG 7 Update
CD918	———	TTG 8 Update
CD919	———	ΔV Register Update
CD920	———	PSP Turn On Threshold
CD921	———	PSP Turn Off Threshold
CD798	———	Pitch Turn (+)
CD799	———	Pitch Turn (-)
CD800	———	Yaw Turn (+)
CD801	———	Yaw Turn (-)
CD802	———	Roll Turn (+)
CD803	———	Roll Turn (-)
CD804	———	Update Master Sequence
CD805	———	Start Special Sequence 1
CD806	———	Start Special Sequence 2
CD807	———	Start Special Sequence 3
CD808	———	Start Special Sequence 4
CD809	———	Start Master Sequence
CD810	———	Set Time Base to 1 Second
CD811	———	Set Time Base to 1 Minute
CD812	———	Set Time Base to 1 hour

Command Source		Command
Primary	Backup	
CD813	———	Spare
CS101	CD814	Inhibit Earth Occultation Data Mode Switch
CS102	CD815	Enable Earth Occultation Data Mode Switch
CD816	———	Spare
↓	↓	↓
CD819	———	Spare

6.12 Science and Data Automation Subsystem

Command Source		Command
Primary	Backup	
CS103	CD820	Cruise Science On/Off
CS104	CD820	PSP Control On/Off
CS105	CD820	Orbit Science On/Off
CS106	CD820	PSP Science On/Off
CS107	CD820	Infrared Scanner On/Off
CS108	CD820	Black and White TV On/Off
CS109	CD820	IR Spectrometer On/Off
CS110	CD820	Color TV On/Off
CS111	CD820	UV Spectrometer On/Off
CS112	CD820	Bistatic Radar On/Off
CS113	CD820	Update PSP Gimbal C
CS114	CD820	Update PSP Gimbal D
CS115	CD820	PSP Gimbal E Control On
CS116	———	Planet Limb Crossing
CS117	———	Morning Terminator Crossing
CS118	———	Evening Terminator Crossing
CS119	CD820	Inhibit PSP Gimbal E Motion
CD821	———	Spare
CD822	———	Spare

Command Source		Command
Primary	Backup	
CD922	———	Spare
CS903	———	Spare
↓	↓	↓
CS905	———	Spare

CII VC220FD113

LAYOUT AND CONFIGURATION

SECTION

1	SCOPE
2	APPLICABLE DOCUMENTS
3	SPACECRAFT DESCRIPTION
4	PACKAGING OF ELECTRONIC BAYS
5	SPACECRAFT COORDINATE SYSTEM
6	MASS PROPERTIES
7	ALIGNMENT ACCURACY

LAYOUT AND CONFIGURATION

1.0 SCOPE. This document describes the layout and configuration of the 1971 spacecraft. A detailed description of the vehicle is given, and structural references and alignments are discussed. In addition, the packaging of the electronic bays is illustrated.

2.0 APPLICABLE DOCUMENTS

The following documents directly apply to the layout and configuration of the 1971 spacecraft:

VC220SR101 - Design Characteristics and Restraints

VC238FD101 - Propulsion System Selection

3.0 SPACECRAFT DESCRIPTION

3.1 Configuration Elements. This section describes briefly the major configuration elements and their mounting locations on the VOYAGER Flight Spacecraft. Figure 3-1 is a detailed layout and configuration drawing showing the location of major subsystem elements and the overall geometry. The following discussion refers to this drawing when locations and views are mentioned. For more detail concerning geometry and dimensions, see the VOYAGER Spacecraft Basic Gemoetry drawing in VC220SR101. The rationale for the preferred configuration is also discussed in Section 4.0 of this document.

The 1971 VOYAGER Flight Capsule has been defined as a 12-foot diameter, 60-degree sphere cone. It is mounted forward of the Flight Spacecraft on its adapter which interfaces with the Flight Spacecraft at the 120-inch diameter field joint at station 101.25. The capsule weighs 3000 pounds including sterilization canister, and is shown with a center of gravity at station 169.25. The Flight Spacecraft meets the performance requirements of the given geometric envelope and weight allocation of 17500 pounds, and houses the equipment which obtains and transmits to earth the scientific data required from the VOYAGER Mission.

The Flight Spacecraft is composed basically of the following subsystems:

a. Telecommunications - Consists of the Radio, Command, Telemetry, and Data Storage subsystems.

b. Guidance and Control - Consists of Attitude Control, Cold Gas Jets and Autopilot.

c. Power - Consists of an electrical generation and distribution subsystem.

d. Computer and Sequencer - Consists of the necessary command processing and storage devices, and sensors needed to provide attitude verification and orbit sequencing.

e. Propulsion - Consists of a Midcourse Correction and Orbit Adjust (MC/OA) Subsystem and a Retro-propulsion (RPS) Subsystem.

f. Engineering Mechanics - Consists of the vehicle structure, Thermal Control, electronic packaging and harnessing, separation and deployment subsystems, and High Gain Antenna articulation subsystem.

3.1.1 Telecommunications Subsystem. The Major elements of the Telecommunications Subsystem are the antennas and the associated electronics. These items are briefly discussed in the following paragraphs.

3.1.1.1 Antennas

a. High Gain Antenna - A 90-inch diameter wire-mesh antenna made of aluminum wire with a magnesium supporting frame structure. It is stowed as shown in Figure 3-1 and is deployed to its operating position. An IR sensor is mounted to, and boresighted with this antenna to provide earth occultation signals to the Computer and Sequencer.

b. Medium Gain Antenna - A Mariner C type elliptical parabolic dish antenna approximately 21 x 46 inches in size. It is mounted below blank panel 14 to provide an unobstructed field of view.

c. Primary Low Gain Antenna - Used to provide communication capability during launch and for command throughout the mission. It is oriented with the beam center 25 degrees off the Z axis and is located in the vicinity of the -X axis at the outer edge of the solar array.

d. Secondary Low Gain Antenna - Used to provide communications capability during maneuvers and is located and deployed in the vicinity of the +X axis at the outer edge of the solar array.

e. VHF Relay Antenna - Used to relay data from the Flight Capsule during its entry and impact. It is located on the +X axis.

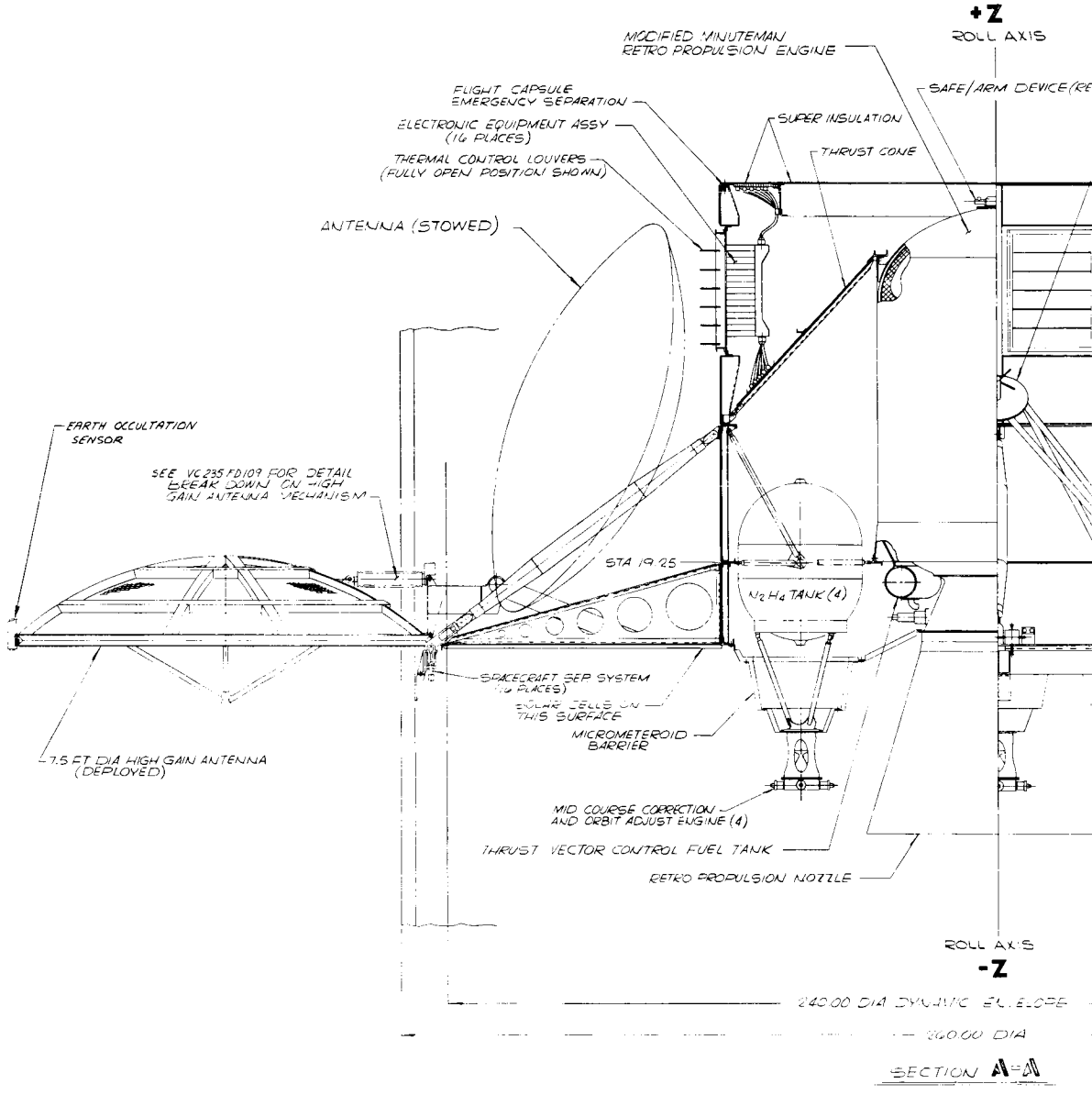
3.1.1.2 Associated Electronics. The Telecommunications Subsystem electronic components are located in Bays 7, 8, 9, 10, 11, 12 and 13. The high gain antenna coaxial cable runs along a spacecraft support tube and enters the spacecraft lower bus structure at approximately station 50.0.

3.1.2 Guidance and Control. The Guidance and Control Subsystem consists of position sensors (sun sensors and Canopus star sensors), a gyro package, associated electronics, and a cold gas mass expulsion system with nozzles, associated plumbing, and valving.

3.1.2.1 Position Sensors. The position sensors are located in various positions on the spacecraft such as to satisfy their field of view requirements. These sensors are aligned with relatively close tolerances to the reference planes, and the individual sensors and their locations are enumerated as follows:

a. The sun gate sensor and cruise sun sensors are housed in a unit located on the aft micrometeoroid shield under Bay 15.

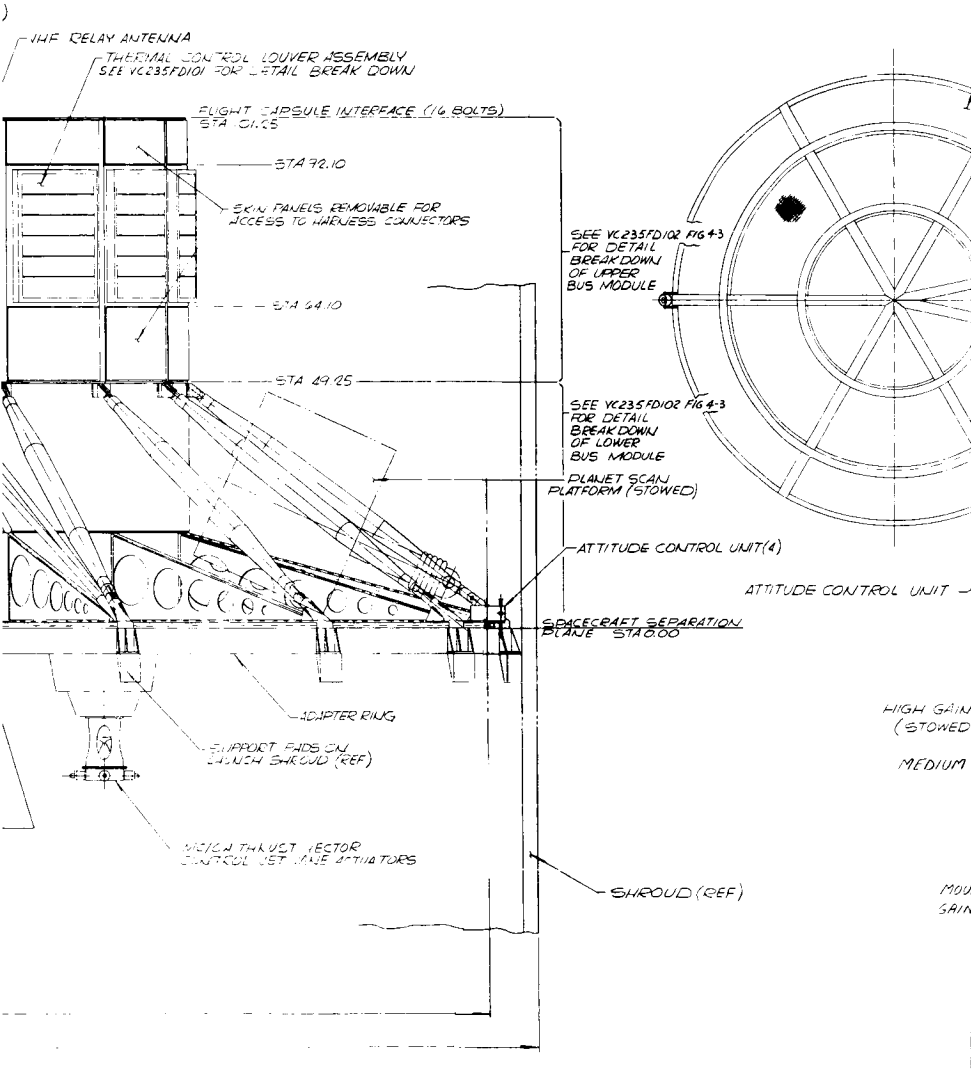
b. The secondary acquisition sun sensors and solar aspect sensors are in four units. These units are located near the outer edge of the solar array on the X and Y axes; the sensors are mounted to provide 4π steradians unobstructed field of view.

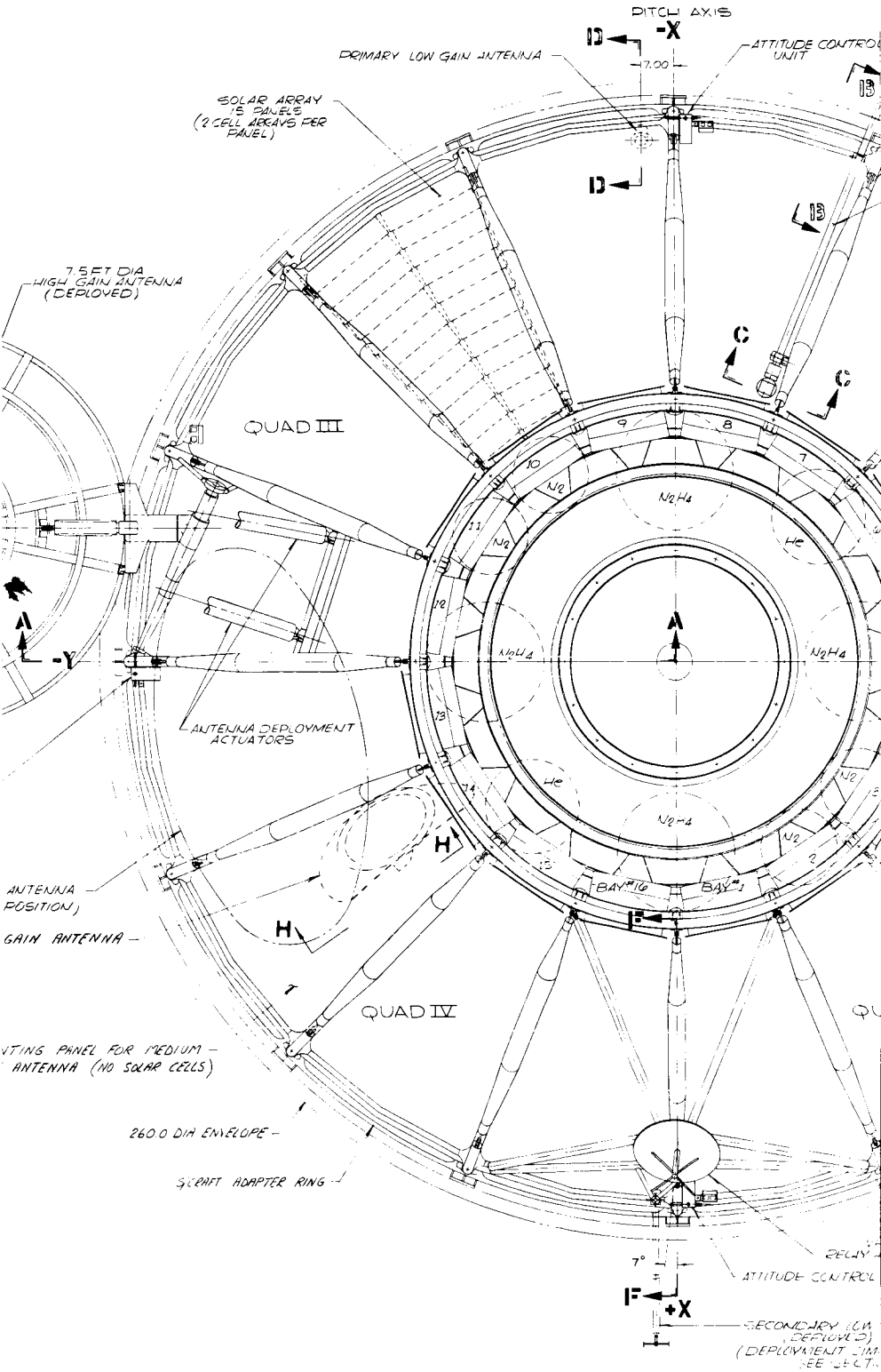

+Z
ROLL AXIS
MODIFIED MINUTEMAN
RETRO PROPULSION ENGINE
SAFE/ARM DEVICE(RE
FLIGHT CAPSULE
EMERGENCY SEPARATION
ELECTRONIC EQUIPMENT ASSY
(16 PLACES)
SUPER INSULATION
THRUST CONE
THERMAL CONTROL LOUVERS
(FULLY OPEN POSITION SHOWN)
ANTENNA (STOWED)
EARTH OCCULTATION
SENSOR
SEE VC235FD109 FOR DETAIL
BREAK DOWN ON HIGH
GAIN ANTENNA MECHANISM
STA 19.25
N2H4 TANK (4)
SPACECRAFT SEP SYSTEM
(6 PLACES)
SOLAR CELLS ON
THIS SURFACE
MICROMETEROID
BARRIER
7.5 FT DIA HIGH GAIN ANTENNA
(DEPLOYED)
MID COURSE CORRECTION
AND ORBIT ADJUST ENGINE (4)
THRUST VECTOR CONTROL FUEL TANK
RETRO PROPULSION NOZZLE
ROLL AXIS
-Z
240.00 DIA DYNAMIC ENVELOPE
260.00 DIA

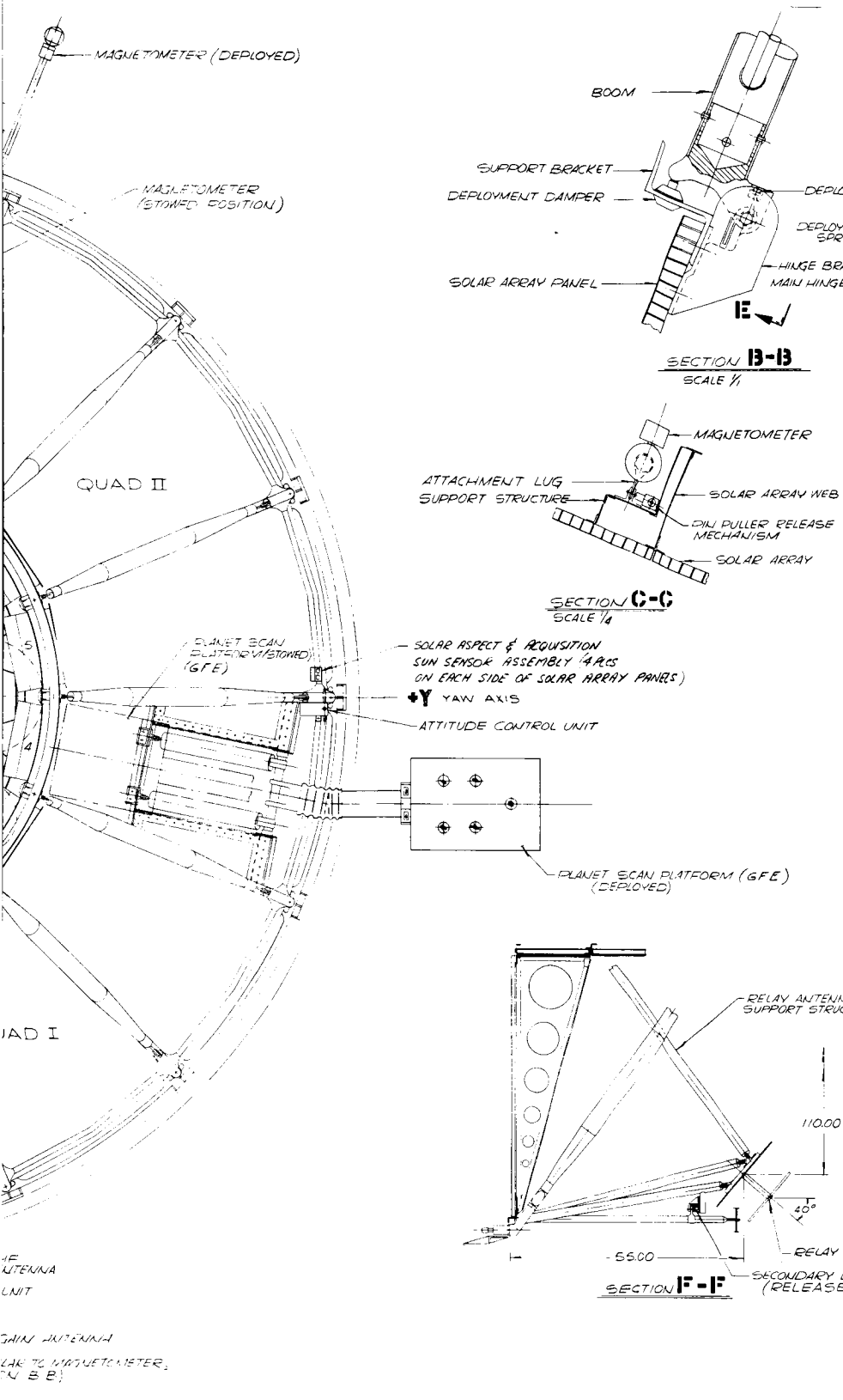
SECTION A-A

BAY NO	SUBSYSTEM	BAY NO	SUBSYSTEM
1	POWER S/S	11	RADIO S/S
2	POWER S/S	12	RADIO S/S
3	SCIENCE ELECTRONICS	13	RELAY RADIO
4	SPARE	14	GUIDANCE & CONTROL S/S
5	SCIENCE ELECTRONICS	15	GUIDANCE & CONTROL
6	SCIENCE DAE	16	POWER S/S
7	DATA STORAGE		
8	DATA STORAGE		
9	TELEMETRY S/S		
10	COMMAND S/S		

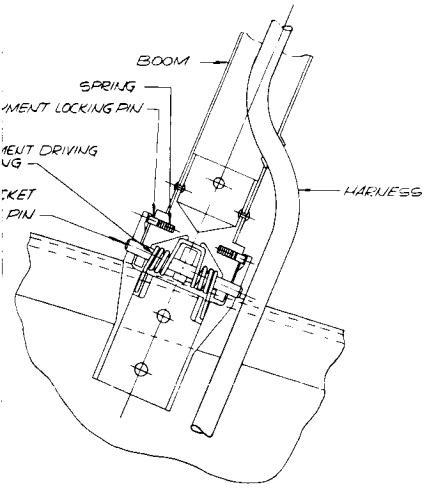
TABLE SHOWING BAY ALLOCATIONS OF ELECTRONIC EQUIPMENT



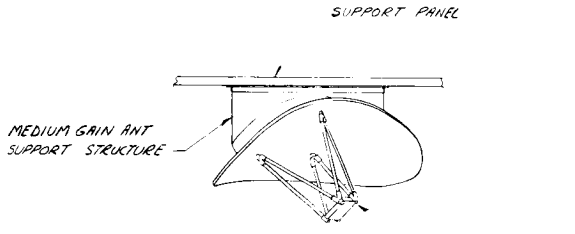

PITCH AXIS
-X
PRIMARY LOW GAIN ANTENNA
ATTITUDE CONTROL UNIT
SOLAR ARRAY 15 PANELS (2 CELL ARRAYS PER PANEL)
7.5 FT DIA HIGH GAIN ANTENNA (DEPLOYED)
QUAD III
QUAD IV
ANTENNA DEPLOYMENT ACTUATORS
-Y
+X
BAY 16
BAY 1
N_2H_4
He
N_2
ATTITUDE CONTROL
SECONDARY (LOW
(DEPLOYED)
260.0 DIA ENVELOPE
S/CRAFT ADAPTER RING


MAGNETOMETER (DEPLOYED)
MAGNETOMETER (STOWED POSITION)
QUAD II
QUAD I
PLANET SCAN PLATFORM (STOWED) (GFE)
SOLAR ASPECT & ACQUISITION SUN SENSOR ASSEMBLY (4 REQ'S ON EACH SIDE OF SOLAR ARRAY PANELS)
+Y YAW AXIS
ATTITUDE CONTROL UNIT
PLANET SCAN PLATFORM (GFE) (DEPLOYED)
BOOM
SUPPORT BRACKET
DEPLOYMENT DAMPER
SOLAR ARRAY PANEL
SECTION B-B
SCALE 1/1
MAGNETOMETER
ATTACHMENT LUG
SUPPORT STRUCTURE
SOLAR ARRAY WEB
DIN PULLER RELEASE MECHANISM
SOLAR ARRAY
SECTION C-C
SCALE 1/4
110.00
40°
55.00
SECTION F-F

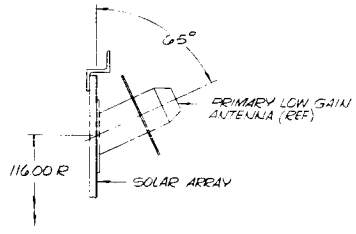
3(f)



VIEW E-E
SCALE 1/1



SECTION H-H

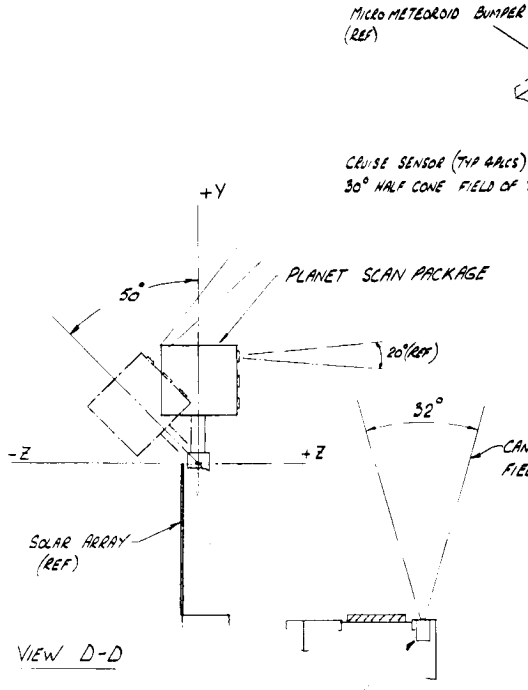


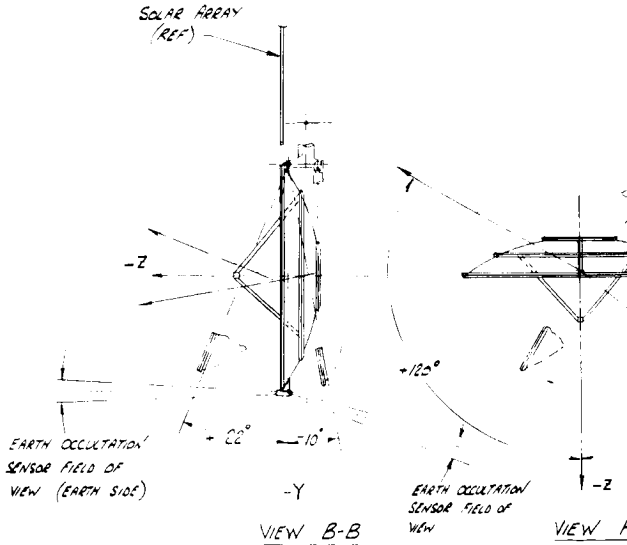
SECTION D-D
SCALE 1/4

TURE

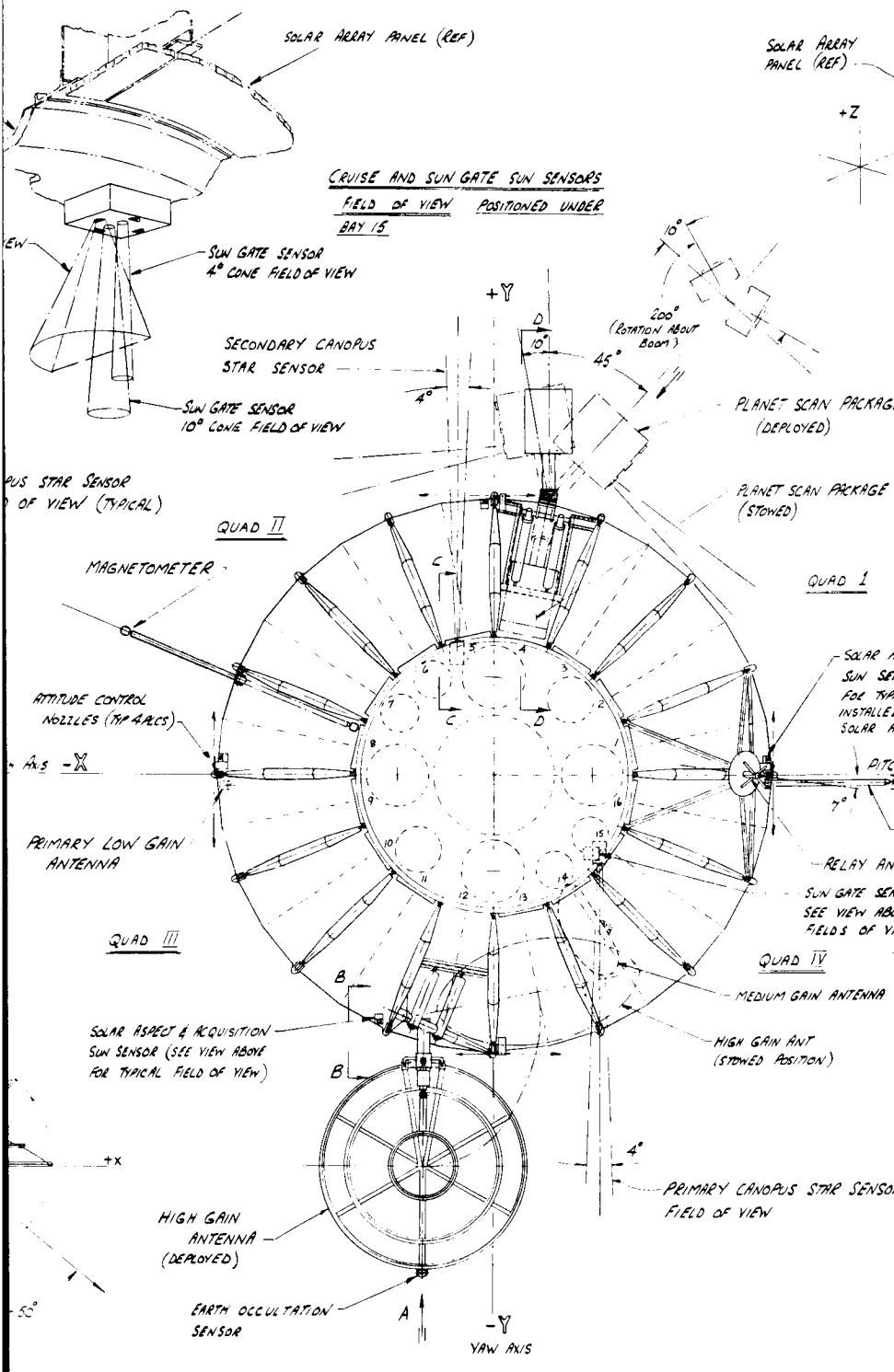
NTENNA (REF)
W GAIN ANTENNA (REF)
MECHANISM SAME AS SECTION C-C)

Figure 3-1. Overall Spacecraft Layout and Configuration

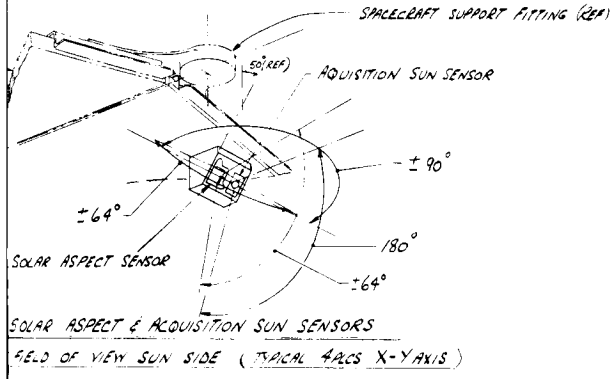




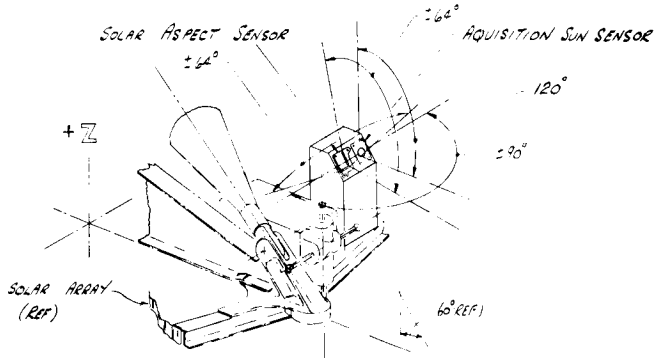
HIGH GAIN ANTENNA MOTIO


SOLAR ARRAY PANEL (REF)
SOLAR ARRAY PANEL (REF)
+Z
CRUISE AND SUN GATE SUN SENSORS FIELD OF VIEW POSITIONED UNDER BAY 15
SUN GATE SENSOR 4° CONE FIELD OF VIEW
SUN GATE SENSOR 10° CONE FIELD OF VIEW
+Y
D
10°
200° (ROTATION ABOUT BOOM)
45°
SECONDARY CANOPUS STAR SENSOR
4°
PLANET SCAN PACKAG (DEPLOYED)
PLANET SCAN PACKAGE (STOWED)
QUAD II
QUAD I
MAGNETOMETER
ATTITUDE CONTROL NOZZLES (TYP 4 PLCS)
AXIS -X
PRIMARY LOW GAIN ANTENNA
QUAD III
QUAD IV
MEDIUM GAIN ANTENNA
HIGH GAIN ANT (STOWED POSITION)
SOLAR ASPECT & ACQUISITION SUN SENSOR (SEE VIEW ABOVE FOR TYPICAL FIELD OF VIEW)
+X
4°
PRIMARY CANOPUS STAR SENSO FIELD OF VIEW
HIGH GAIN ANTENNA (DEPLOYED)
53°
EARTH OCCULTATION SENSOR
A
-Y
YAW AXIS
RELAY AN
7°

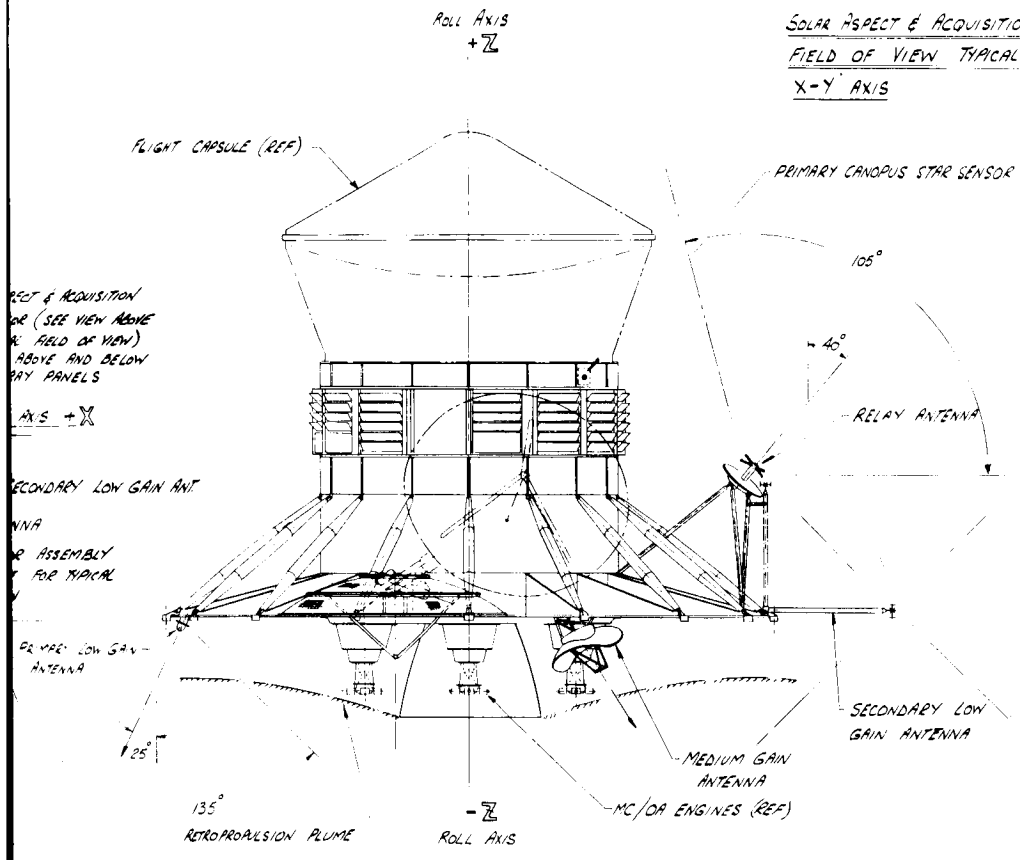
4 (2)



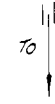
SOLAR ASPECT & ACQUISITION SUN SENSORS
FIELD OF VIEW SUN SIDE (TYPICAL 4 ACS X-Y AXIS)



SOLAR ASPECT & ACQUISITION SUN SENSOR
FIELD OF VIEW TYPICAL 4 PLACES ON
X-Y AXIS



SIDE VIEW OF SPACECRAFT
LOOKING ALONG Y AXIS



4 (B)

Figure 3-2. Spacecraft Fields of View

c. The two Canopus star sensors are mounted with their optical axes parallel to the Y-axis and pointing in opposite directions. They are located at station 97.5 on the upper bus module structure with the lens and sensor outside the shell and associated electronics contained within the controlled environment area.

3.1.2.2 Integrating Gyro Package. The gyro package is located in Bay 15 and is mounted on an aligned, machined surface.

3.1.2.3 Attitude Control Pneumatics System. Two cold gas tanks (16-inch diameter spheres) containing pressurized gaseous nitrogen are oppositely mounted in Quadrants II and IV at a radial distance of 50.6 inches from the vehicle centerline. Pneumatic lines are run from the tanks to the nozzle-valve assemblies, and the entire system is provided with wire heating elements and super-insulation as required for thermal control of the nitrogen.

The 24 nozzles (eight each for pitch, yaw, and roll control, respectively) are located on the outer edge of the solar arrays at the ±X and ±Y axis locations. They are oriented with opposing nozzles per control axis at each specific mounting location (yaw and roll control nozzles at the ±X axis locations, pitch and roll nozzles located along the ±Y axis).

3.1.3 Power. The electrical power generation system is a photovoltaic system utilizing silicon cells mounted on 15 panels which are essentially trapezoidal in shape. The panels are rigidly mounted on 16 support ribs extending radially from the spacecraft structure. The panel surface is located at approximately spacecraft station 0.75.

3.1.4 Computer and Sequencer. The computer and Sequencer Subsystem consists of the required command processing and storage devices and timers which initiate various spacecraft functions. The required electronic equipment is located in Bay No. 14.

3.1.5 Propulsion Subsystem. The Propulsion Subsystem consists of the Retro-Propulsion System and the Midcourse Correction and Orbit Adjust System. The Retro-Propulsion System consists of a modified Minuteman solid fuel engine mounted with its thrust axis along the spacecraft Z axis; thrust vector control is provided by injection of liquid fuel contained in a torus tank surrounding the nozzle throat.

The Midcourse Correction and Orbit Adjust System provides small vernier corrections to the transit trajectory as well as Mars orbit adjustments. This system consists of four monopropellant thrust chambers located on the X and Y axes at stations 29.60 and 42.75 radius with their thrust vectors parallel to the spacecraft Z axis. Thrust vector control is by nozzle vanes.

The engines mount directly to the underside of each of the four cylindrical fuel tanks. Two pressurized helium spheres of 20-inch diameter are used for propellant transfer and are mounted between the fuel tanks. The complete system with associated valves, regulators, plumbing, etc. is mounted on its own modular structure.

3.1.6 Engineering Mechanics. The Engineering Mechanics Subsystem provides basic support and protection for all other spacecraft subsystems. It, in turn, includes the Thermal Control, Separation and Deployment, and Vehicle Structure subsystems.

3.1.6.1 Thermal Control. Thermal control of the spacecraft bus is provided by louvers on the equipment modules and a super-insulation blanket which surrounds the entire bus surface with the exception of the thermal louvers on the equipment bays.

3.1.6.2 Separations and Deployments. Table 3-1 summarizes the pertinent details of the Pyrotechnic Subsystem as well as other deployment devices. The controller for the pyrotechnic devices is located in Bay 16.

TABLE 3-1. SEPARATION AND DEPLOYMENT SUMMARY

Component	Type of Mechanism	No. of Series Items	Type of Initiator	Actuator
Booster-Spacecraft Adapter	Separation	1	Squib	Pneumatically Actuated Thruster-Release
High Gain Antenna	Unlocking and Deployment	1	Squib	Pin-puller and motor
Secondary Low Gain Antenna	Unlocking and Deployment	1	Squib	Pin-puller and Spring-damper
Magnetometer	Unlocking and Deployment	1	Squib	Pin-puller and Spring-damper
Planet Scan Platform	Unlocking and Deployment	1	Squib	4 Pin-pullers and linear actuator
Capsule Sterile Canister Capsule ejection	Capsule Manufacturer Responsibility			
Emergency Separation	Separation	1	-	One separation nut per bolt pneumatically actuated

3.1.6.3 Spacecraft Structure. The spacecraft configuration with the basic arrangement of equipment is shown in Figure 3-1. The spacecraft bus structure provides for the overall mounting of equipment as well as serving as the load carrying media between the capsule and the launch vehicle shroud. The bus structural arrangement has been designed as two separate module sections; (1) an upper bus module, station 49.25 to 101.25, and (2) a lower bus module extending from station 0.00 to 49.25. The modules are joined at the production break at station 49.25 which consists of thirty-two tension bolts designed to carry axial and shear loads across the joint.

The upper bus module primarily contains the equipment bays, divided into sixteen modular packages. In addition, the module serves as the primary mounting support for the forward thrust cone adapter to the modified Minuteman engine. The structure is designed as a sixteen-sided polygon in the equipment support bays consisting of longerons and shear carrying skin sections. The longerons serve to transmit axial loads through the section and also provide mounting support for the equipment modules. The equipment modules are designed integrally with the structure to carry primary shear loads through thermal radiating cover plates which provide for heat dissipation and thermal control of the components. Thirty-two structural load carrying doors are provided adjacent to the equipment bays for ready access to the main system harness and connectors.

The lower bus module serves as the mounting structure for the fixed solar array, medium and high gain antennas, relay antenna, and the planet scan platform. The module also shrouds and houses the midcourse propulsion system, and the gas jet system together with associated equipment.

The lower module structure is designed into two separate submodule sections for ease of assembly and installation of equipment. The lower portion contains the solar array and antenna supports and provides integral mounting structure for the Attitude Control system. This arrangement permits modular removal of the attitude control subsystem without disassembly of interconnecting plumbing joints and fittings. The upper portion of the module (MC/OA submodule) provides mounting and modular installation of the midcourse propulsion

system which may be bench assembled as a separate unit. The submodular sections are joined at the production joint at station 19.25.

The lower bus module structure is constructed as a cylindrical sheet-stringer stiffened arrangement. Primary shear is transferred through beaded shear panels and then, in turn, through the solar array honeycomb panels to the bus adapter section. Sixteen tubular support members provide axial load continuity for the lower bus module between the production break at station 49.25 and the adapter interface connection at station 0.00.

4.0 PACKAGING OF ELECTRONIC BAYS. The electronic equipment is packaged in sixteen bays of the equipment module. This equipment is assembled into a unifying structure to provide load and thermal paths which can be integrated with the vehicle structure. When bolted into the vehicle, the electronic assembly provides rigid support for the electronic equipment and externally mounted items as well as protection against environmental factors.

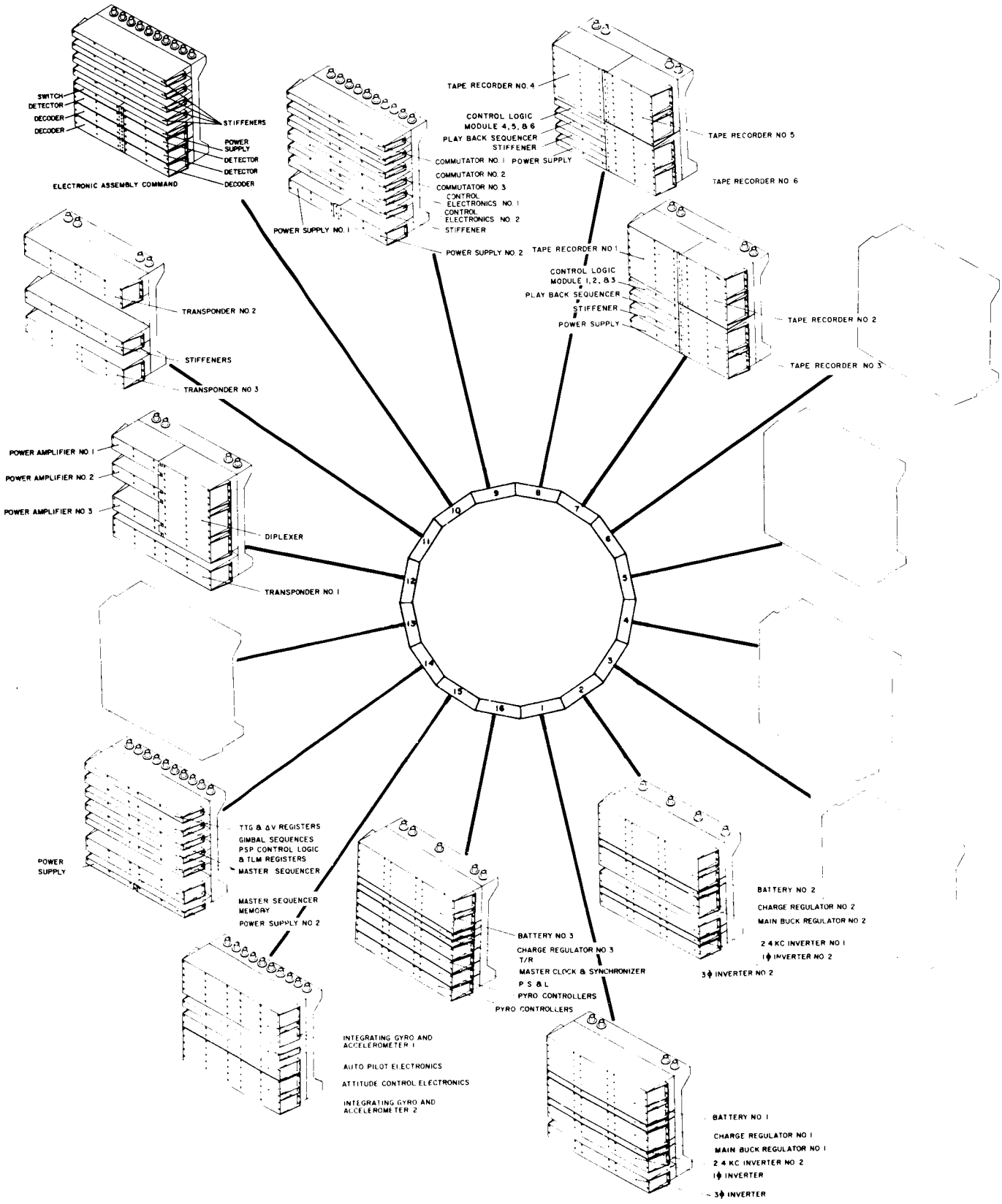
The assemblies are of standardized size and shape. To be consistent with system requirements, functional subsystems are arranged in one or more bays to enhance spacecraft reliability by increasing ease of fabrication, testing, and configuration management. Sharing of a bay by two or more functional subsystems is avoided where possible.

The equipment allocations for the various bays are shown in Figure 4-1. The location of the bays with respect to the vehicle axes is shown in Figure 3-1. Each electronic bay assembly has approximately 15% spare subassembly volume to accommodate growth during development. Relocation of the equipment can accumulate the available spare volume to provide an empty bay if required. This can be accomplished without combining separate subsystems into one bay.

The allocation of the equipment in the bays was done in a manner to provide center-of-gravity location and thermal balance as well as the additional following criteria:

a. Radio Subsystem located next to antennas.
b. Science package next to planet scan platform.
c. Proximity of Data Encoder and Storage to Science DAE and Radio subsystem.

5.0 SPACECRAFT COORDINATE SYSTEM. (Refer to Figure 5-1, the Planetary Vehicle and Booster Coordinate System for the following discussion.) The coordinate system consists of three mutually perpendicular reference axes; the pitch (X), yaw (Y), and roll (Z) axes which form a conventional Cartesian coordinate system. The roll axis is defined normal to the primary reference plane (A) (defined below) with +Z FWD, bisecting reference plane (B) (defined below) as it passes through the center of the equipment module structure. The yaw axis is defined coincident to the secondary reference plane (B) and parallel to the primary reference plane (A), bisecting bays 12 and 13 in the -Y and bays 4 and 5 in the +Y direction. The pitch axis is defined as being normal to the yaw (Y) axis forming a conventional right-hand system. The +X direction bisects Bays 1 and 16. Positive pitch, yaw, and roll angles and moments are defined as clockwise when looking from the origin along the positive reference axis. This is a conventional right-hand coordinate system in all respects.


SWITCH DETECTOR
DECODER
DECODER
STIFFENERS
POWER SUPPLY
DETECTOR
DETECTOR
DECODER
ELECTRONIC ASSEMBLY COMMAND
COMMUTATOR NO. 1
COMMUTATOR NO. 2
COMMUTATOR NO. 3
CONTROL ELECTRONICS NO. 1
CONTROL ELECTRONICS NO. 2
STIFFENER
POWER SUPPLY NO. 1
POWER SUPPLY NO. 2
TAPE RECORDER NO. 4
CONTROL LOGIC MODULE 4, 5, & 6
PLAY BACK SEQUENCER STIFFENER
POWER SUPPLY
TAPE RECORDER NO. 5
TAPE RECORDER NO. 6
TRANSPONDER NO. 2
STIFFENERS
TRANSPONDER NO. 3
TAPE RECORDER NO. 1
CONTROL LOGIC MODULE 1, 2, & 3
PLAY BACK SEQUENCER STIFFENER
POWER SUPPLY
TAPE RECORDER NO. 2
TAPE RECORDER NO. 3
POWER AMPLIFIER NO. 1
POWER AMPLIFIER NO. 2
POWER AMPLIFIER NO. 3
DIPLEXER
TRANSPONDER NO. 1
1
2
3
4
5
6
7
8
9
10
11
12
13
14
15
16
POWER SUPPLY
TTG & ΔV REGISTERS
GIMBAL SEQUENCES
PSP CONTROL LOGIC & TLM REGISTERS
MASTER SEQUENCER
MASTER SEQUENCER MEMORY
POWER SUPPLY NO. 2
BATTERY NO. 3
CHARGE REGULATOR NO. 3
T/R
MASTER CLOCK & SYNCHRONIZER
P S & L
PYRO CONTROLLERS
PYRO CONTROLLERS
BATTERY NO. 2
CHARGE REGULATOR NO. 2
MAIN BUCK REGULATOR NO. 2
2.4 KC INVERTER NO. 1
1φ INVERTER NO. 2
3φ INVERTER NO. 2
INTEGRATING GYRO AND ACCELEROMETER 1
AUTO PILOT ELECTRONICS
ATTITUDE CONTROL ELECTRONICS
INTEGRATING GYRO AND ACCELEROMETER 2
BATTERY NO. 1
CHARGE REGULATOR NO. 1
MAIN BUCK REGULATOR NO. 1
2.4 KC INVERTER NO. 2
1φ INVERTER
3φ INVERTER

3

8

Bay No.	Assembly Function	W
1	1/3 POWER SUBSYSTEM - Battery No. 1; Charge Regulator No. 1; Main Buck Regulator No. 1; 2.4 Kc Inverter No. 2, 3 Φ No. 1	
2	1/3 POWER SUBSYSTEM - Battery No. 2, Charge Regulator No. 2; Main Buck Regulator No. 2; 2.4 Kc Inverter No. 1; 3 Φ Inverter No. 2	
3	SCIENCE ELECTRONICS	
4	SPARE	
5	SCIENCE ELECTRONICS	
6	SCIENCE DAE	
7	1/2 DATA STORAGE SUBSYSTEM 3 ea. Tape Recorders, 3 ea. CLM, 1 ea. PBS	
8	1/2 DATA STORAGE SUBSYSTEM 3 ea. Tape Recorders, 3 ea. CLM, 1 ea. PBS; 1 ea. Power Supply	
9	RADIO SUBSYSTEM	
10	COMMAND SUBSYSTEM Command Detectors, Command Decoders, Command Access Switch, Power Supply	
11	1/2 RADIO SUBSYSTEM Transponders No. 2 and 3	
12	1/2 RADIO SUBSYSTEM 2 ea. TWT's, 1 ea. Solid State Exciter, 1 ea. Diplexer Assembly, 1 ea. Transponder	
13	RELAY RADIO SUBSYSTEM	
14	COMPUTER AND SEQUENCER SUBSYSTEM	
15	GUIDANCE AND CONTROL SUBSYSTEM Integrating Gyro & Accelerometer Package, A/C Electric, Auto Pilot Electr.	
16	1/3 POWER SUBSYSTEM - BATTERY No. 3, Charge Regulator, PS&L, Pyro Controller, Synchronizer, Charge Control	
	Total	

*Weight estimate based on PIR 5200-JHC-008
Weight does not include harness trays, cablin
**Power estimates based on PIR 5200-JHC-008
represents worst case.

Figure 4-1. Equipment Allocation for Sixteen-Sided Configuration

eight* (Est) (lb)	Power** (Est)* (Watts)	No. of System Connections	Volumetric Efficiency %
74	78.5	8-10	60
74	17.3	8-10	60
45	33		
45	33		
55	30	8	
55.5	18	4	92
60.5	12.2	4	92
18	8.2	15-16	28
30	20.2	12	48
26.6	15	4	45
43.3	110	4	79
25	10	4	44
35	30	13	52
28.4	65.8	13	50
68.5	27.3	10	79
683.8	508.3	112	60 Aug.

re later inputs from Subsystem Engineers.
; and other hardware.
PIR 4428-07 Rev. C and VB236FD101 and

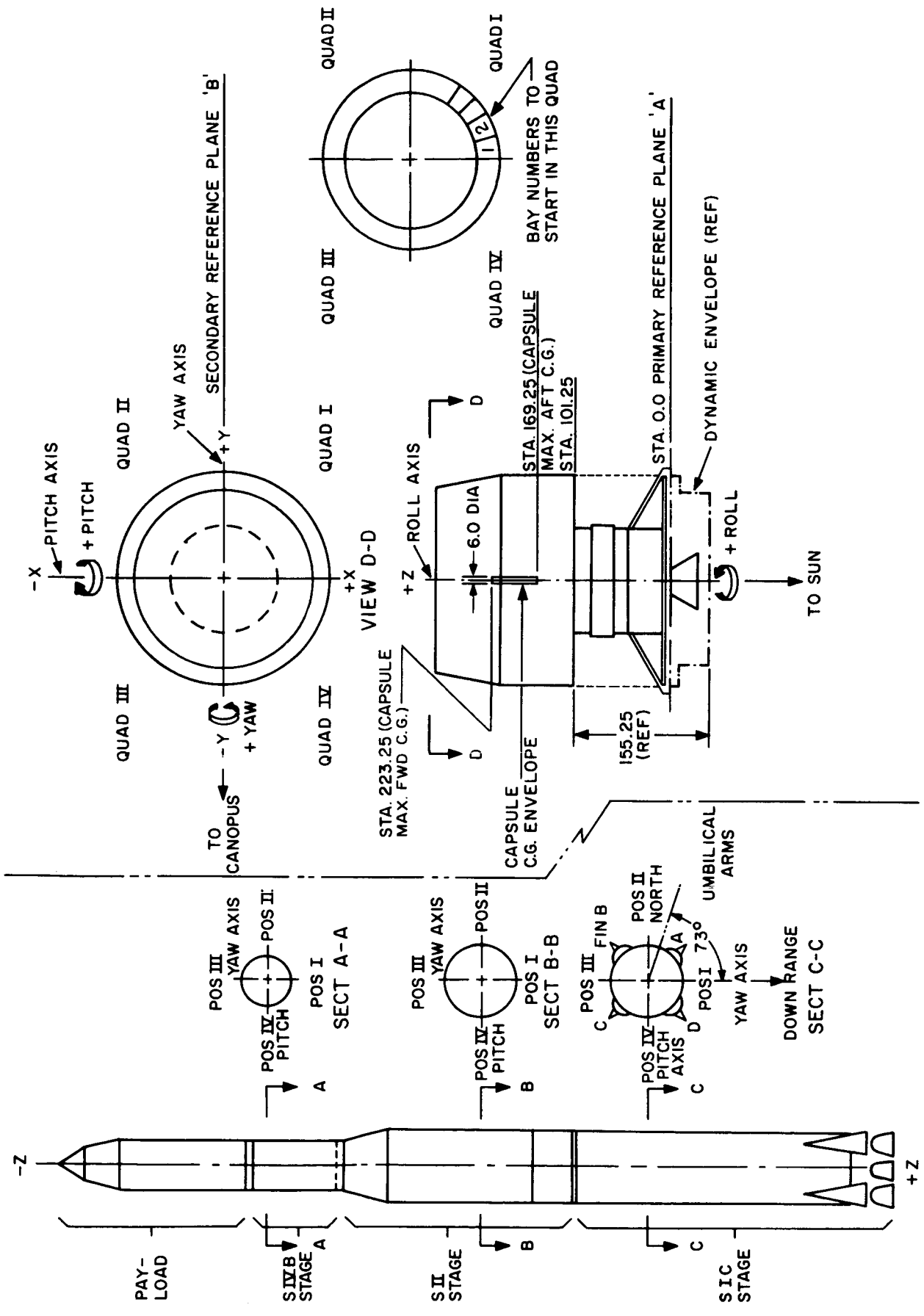


Figure 5-1. Planetary Vehicle and Booster Coordinate System

The primary reference plane (A) is defined as the planetary vehicle adapter separation plane. The secondary reference plane (B) is the imaginary plane generated by the yaw (Y) axis (fixed by the nominal intersection of the bays 4 and 5, and bays 12 and 13) and a perpendicular from the yaw (Y) axis to the primary reference plane (A). The allowable alignment tolerances between the primary (A) and secondary (B) reference planes are defined in Section 7.0 of this document, and a general location of the reference plans are shown in Figure 3-1.

VOYAGER Station 0.00 is defined as the Flight Spacecraft Separation Plane, and is the primary reference plane (A). Positive station numbers run up the Spacecraft in the +Z direction.

6.0 MASS PROPERTIES. Table 6-1 presents weight, center of gravity, moments and products of inertia information at specific times in the mission. This information is presented with the center-of-gravity of the capsule assumed on the spacecraft roll axis for two conditions, the aft and forward positions of the capsule allowable envelope. A third condition with a three-inch offset of the capsule center-of-gravity in the forward position of the envelope is also given.

TABLE 6-1. MASS PROPERTIES

Flight Sequence Description	Case No.	Weight (lb)	$\bar{Z}$	$\bar{X}$	$\bar{Y}$	Ioz	Iox	Ioy	Wzx	Wzy	Wxy
Aft CG on 3000-lb Capsule											
Launch - (on pad) 1-Planetary Vehicle	1	17289	67.12	0.41	0.23	8187	14747	14497	- 22.5	- 15.9	30.7
Transit Antenna Deployed	2	17176	67.49	0.23	0.05	8179	14720	14314	12.6	61.2	80.3
After Midcourse Correction	3	15780	71.03	0.25	0.06	7577	13831	13425	9.6	60.5	80.3
After Retro Burn (Orbiting)	4	7322	91.41	0.54	0.12	6997	11542	11136	- 7.7	56.5	80.2
PSP Deployed	5	7322	90.91	1.17	1.66	7626	12203	11348	-120.0	-217.4	300.8
After Capsule Separation	6	4572	42.47	1.83	2.61	3970	3634	2781	- 30.6	- 90.0	299.1
After Orbit Adjust	7	4266	43.52	1.96	2.79	3841	3554	2701	- 32.5	- 92.8	298.7
Forward CG on 3000-lb Capsule											
Launch - (on pad) 1-Planetary Vehicle	1	17289	76.50	0.41	0.23	8187	23362	23109	- 36.8	- 23.8	30.7
Transit Antenna Deployed	2	17176	76.93	0.23	0.05	8179	23307	22901	4.6	59.3	80.3
After Midcourse Correction	3	15780	81.31	0.25	0.06	7577	22141	21735	0.9	58.5	80.3
After Retro Burn (Orbiting)	4	7322	113.52	0.54	0.12	6997	18013	17607	- 26.4	52.2	80.2
PSP Deployed	5	7322	113.02	1.17	1.66	7626	18709	17855	-160.9	-275.6	300.8
After Capsule Separation	6	4572	42.47	1.83	2.61	3970	3634	2781	- 30.6	- 90.0	299.1
After Orbit Adjust	7	4266	43.52	1.96	2.79	3841	3554	2701	- 32.5	- 92.8	298.7
Forward CG on 3000-lb Capsule with 3-inch Offset											
Launch - (on pad) 1-Planetary Vehicle	1	17289	76.50	0.41	0.75	8191	23366	23109	- 36.8	258.9	29.9
Transit Antenna Deployed	2	17176	76.93	0.23	0.58	8184	23312	22901	4.6	341.2	79.9
After Midcourse Correction	3	15780	81.31	0.25	0.63	7581	22146	21735	0.9	331.8	79.8
After Retro Burn (Orbiting)	4	7322	113.52	0.54	1.35	7000	18016	17607	- 26.4	262.9	79.2
PSP Deployed	5	7322	113.02	1.17	2.90	7623	18706	17855	-160.9	- 63.9	298.5
After Capsule Separation	6	4572	42.47	1.83	2.61	3970	3634	2781	- 30.6	- 90.0	299.1
After Orbit Adjust	7	4266	43.52	1.96	2.79	3841	3554	2701	- 32.5	- 92.8	298.7
			Center of Gravity in Inches from Ref.			Inertia about the Center of Gravity (Slug ft^2)			Product of Inertia about the Center of Gravity (Slug ft^2)		

TABLE 7-1. MECHANICAL ALIGNMENTS AND ALIGNMENT TOLERANCES

Function Accuracy Requirement (3σ)	Alignment	Alignment Reference	Alignment Tolerance (3σ)	Comments
Center-of-gravity	Dry Spacecraft Bus CG	Spacecraft Axes	±0.05 inch	These tolerances are a conservative estimate of measuring uncertainty
	Midcourse Prop. System	Spacecraft Axes	±0.10 inch	These tolerances represent the allowable location uncertainties from desired nominal locations following addition or assembly and the preceding center-of-gravity measurements
	Retro Prop. System	Spacecraft Axes	±0.10 inch	
	Planet Scan Platform	Spacecraft Axes	±0.10 inch	
	High Gain Antenna	Spacecraft Axes	±0.10 inch	
	Overall Planetary Vehicle Longitudinal Axis	Perpendicular to Launch Vehicle Longitudinal Axis	±0.15 inch	This tolerance is desirable, but not totally expedient
	Flight Spacecraft Field Joint Plane	Landing Vehicle Longitudinal Axis	±10.0 minutes	Flatness and concentricity alignment tolerances of 0.010 and 0.050 inch respectively are specified to control localized stresses at tie down
	Spacecraft Separation Plane	Parallel to Primary Ref. Plane A	±10.0 minutes	
	Secondary Reference Plane B	Perpendicular to Primary Ref. Plane A	±1.0 minute	The secondary reference plane (B) is determined by the Y axis (fixed by optical means) and the perpendicular from the Y axis to the primary reference plane (A)
Celestial References	Acquisition Sun Sensors			
	Mounting Surfaces	Sun Sensor Assembly		
	(Parallelism)	Mounting and Indexing	±10.0 minutes	
	(Indexing)	Surfaces	±10.0 minutes	
	Cruise Sun Sensors			
	Mounting Surfaces	Sun Sensor Assembly		
	(Parallelism)	Mounting and	±2.0 minutes	
	(Indexing)	Indexing Surfaces	±6.0 minutes	
	Sun Sensor Assembly	Primary (A)		
	Mounting Surfaces	or Secondary (B)	±2.0 minutes	
	(Parallelism)	Reference Planes	±6.0 minutes	
	(Indexing)			
	Acquisition Sun Sensors			Individual mounting surfaces on the basic solar array structure are aligned such as to negate the array structure alignment tolerances
	Mounting Surfaces	Primary (A) or		
	(Parallelism)	Secondary (B)	±10.0 minutes	
	(Indexing)	Reference Planes	±10.0 minutes	

	Sun Gate Sensor Mounting Surfaces (Parallelism) (Indexing)	Sun Sensor Assembly Mounting and Indexing Surfaces	±2.0 minutes ±6.0 minutes	
	Canopus Star Sensor Mounting Surface (Parallelism) (Indexing)	Primary (A) or Secondary (B) Reference Planes	±2.0 minutes ±6.0 minutes	
Attitude Control	Gyro Package Block (Parallelism and Indexing)	Primary (A) or Secondary (B) Reference Planes	±10.0 minutes	Gyro input axes are aligned with respect to the block and mutually perpendicular to each other within ±8 minutes
	Attitude Control Nozzle Mounting Surface (Parallelism) (Indexing)	Primary (A) or Secondary (B) Reference Planes	±1.5 degrees ±1.5 degrees	
High Gain Antenna	Antenna Beam Center Antenna Mounting Surface Antenna Gimbal Axes	Antenna Mounting Surface Antenna Gimbal Axes Primary (A) or Secondary (B) Reference Planes	±6.0 minutes ±3.0 minutes ±3.0 minutes	The solar array structure alignment tolerance is negated at the antenna mounting interface
Monopropellant Engines	Midcourse Engine (4) Thrust Vectors	Thrust Chamber Centerlines	±0.10 inch (radially) ±15.0 minutes (half cone)	Typical maximum midcourse engine thrust vector-thrust chamber centerline misalignments
	Thrust Chamber Centerlines	Nominal location	±0.05 inch (radially)	
	Thrust Chamber Centerlines	Secondary Reference Plane B	±1.0 degree (indexing)	
	Thrust Chamber Centerlines	Primary Reference Plane A (Perpendicular)	±30.0 minutes (half cone)	
Solid Propellant Engine	Retro Engine Thrust Vector	Thrust Chamber Centerline	±0.03 inch (radially) 12.0 minutes (half cone)	Typical maximum thrust vector-chamber centerline misalignments
	Thrust Chamber Centerline	Nominal CG location (Roll Axis) and Perpendicular to Primary Reference Plane A	±0.0625 inch (radially) 30.0 minutes (half cone)	
Accelerometer	Accelerometer Package (Parallelism and Indexing)	Primary (A) and Secondary B Reference Planes	±10.0 minutes	
Medium Gain Antenna	Antenna Beam Center	Antenna Mounting Surface	±8.0 minutes	The solar array structure alignment tolerance is negated at the antenna mounting surface
	Antenna Mounting Surface (Parallelism and Indexing)	Primary (A) and Secondary (B) Reference Planes	±8.0 minutes	
Capsule Mounting	Capsule Mounting Plane (Perpendicular to capsule roll axis)	Parallel to Primary Reference Plane A	±30.0 minutes (half cone)	
	Spacecraft center-of-gravity	Separation maneuver ΔV impulse thrust vector	±1.0 degree (half cone)	
Scientific Experiments	Instrument (Experiment) Mounting Surfaces	Planet Scan Platform Gimbal Axes	±3.0 minutes	Scientific alignment requirements will be defined upon further definition of the instrumentation
	PSP Gimbal Axes	Primary (A) and Secondary (B) Reference Planes	±3.0 minutes	
	Mars Planet Sensor Optical Axis	Planet Scan Platform Gimbal Axes	±3.0 minutes	
	Magnetometer Base (Parallelism and Indexing)	Magnetometer Mounting Surface on Boom	±3.0 minutes	It is desirable that one axis of the magnetometer be parallel to the Spacecraft Z axis to within ±1.0 degree
	Magnetometer Mounting Surface on Boom	Primary (A) or Secondary (B) Reference Planes	±58.0 minutes	

Table 6-2 presents the uncertainty in the spacecraft center-of-gravity determination. The uncertainty is provided as an arithmetic sum of error contributions and as a root sum square total. Uncertainties in distance from the Z axis are totaled separately as coordinate-independent contributions. The antenna and scan package movements are considered variables and summed by coordinate and are presented as coordinate-dependent contributions. Coordinate-dependent and coordinate-independent contributions are combined to show total center-of-gravity uncertainty.

TABLE 6-2. UNCERTAINTY SUMMATIONS

Sources of CG Error / Coordinate Independent	Weight or Weight Tolerance Per Phase					Radius or Radius Tolerance (In.)	After Booster Separation (Spacecraft = 17000 lb)		Before Cannister Separation (Spacecraft = 15300 lb)		Before Orbit Insertion (Spacecraft 15100 lb)		After Orbit Insertion (Spacecraft 6700 lb)		After Capsule Release (Spacecraft = 3900 lb)	
	Phase 1	2	3	4	5		Phase 1		Phase 2		Phase 3		Phase 4		Phase 5	
CG Measurement Errors							ρ (in)	$\rho^2 \times 10^{-4}$ (in.^{2})	ρ (in.)	$\rho^2 \times 10^{-4}$ (in.^{2})	ρ (in.)	$\rho^2 \times 10^{-4}$ (in.^{2})	ρ (in.)	$\rho^2 \times 10^{-4}$ (in.^{2})	ρ (in.)	$\rho^2 \times 10^{-4}$ (in.^{2})
Dry Spacecraft Minus (lbs) Solid Motor (lbs)	2900	2900	2900	2900	2900	± 0.05	0.0085	0.72	0.0095	0.90	0.0096	0.92	0.0216	4.66	0.0371	13.75
Capsule (lbs)	3000	3000	2800	2800		± 0.05	0.0088	0.77	0.0098	0.9C	0.0099	0.98	0.0224	5.01		
Solid Motor (lbs)	9500	9500	9500	1300	1300	± 0.03	0.0168	2.82	0.0186	3.46	0.0189	3.57	0.0425	18.10	0.075	56.3
Assembly Location Errors																
Capsule (lbs)	3000	3000	2800	2800		±0.10	0.0176	3.10	0.0196	3.84	0.0185	3.42	0.0418	17.50		
Planet Scanner (lbs)	150	150	150	150	150	±0.10	0.0009	0.01	0.001	0.01	0.001	0.01	0.0022	0.48	0.004	0.16
Solid Motor (lbs)	9500	9500	9500	1300	1300	±0.10	0.0557	31.0	0.062	38.50	0.0628	39.40	0.0194	3.76	0.033	11.22
MCS Propellant Errors																
Unequal Filling (%)	±2.13	±2.13	±2.13	±2.13	±2.13	42	0.0052	0.27	0.006	0.36	0.006	0.36	0.013	1.69	0.023	5.3
Unequal Usage (%)	0.38	0.38	0.38	0.38	0.38	42	0.0009	0.01	0.001	0.01	0.001	0.01	0.0024	5.76	0.004	0.16
	Subtotals						0.1144	38.71	0.1275	4804	0.1277	48.67	0.1653	56.96	0.176	87.89
Coordinate-Dependent																
Antenna Rotation	50 Pounds All Phases															
-X Contribution							0.0496	24.6	0.055	30.2	0.056	31.4	0.126	159.0	0.217	470.0
+Y Contribution							0.0066	0.4	0.007	0.5	0.007	0.5	0.017	2.9	0.029	8.4
+X Contribution							0.0377	13.7	0.043	18.5	0.042	17.66	0.096	92.0	0.165	272.0
Planet Scanner Movement	150 Pounds All Phases															
-X Contribution												-X	0.084	70.5	0.144	207
+X Contribution												+X	0.560	3140	0.962	9800
-Y Contribution												-Y	0.236	557	0.406	1650
Coordinate Sums Extreme Uncertainty																
-X							0.164		0.183		0.184		0.375		0.535	
+X							0.152		0.171		0.170		0.821		1.303	
+Y							0.121		0.135		0.135		0.182		0.205	
-Y							0.114		0.127		0.128		0.401		0.582	
Total RSS Uncertainty																
-X							0.079		0.088		0.090		0.169		0.288	
+X							0.072		0.082		0.085		0.573		1.01	
+Y							0.063		0.070		0.070		0.074		0.127	
-Y							0.062		0.069		0.070		0.248		0.425	

7.0 ALIGNMENT ACCURACY. Table 7-1 defines the mechanical alignments and alignment tolerances deemed necessary for successfully meeting the various mission phase accuracy requirements. All alignment tolerances specified in Table 7-1 are three sigma (normal distribution) unless otherwise specified. In most cases, the effects of structural and thermal deformations have not been included; in the mission phases where these and other factors are of significance, adequate safety margins are included as a conservative measure.

ACKNOWLEDGEMENTS

The following documents of this Final Report were prepared by the Motorola, Inc., Military Electronics Division, and by Texas Instruments, Apparatus Division:

Motorola

VC233FD102	Radio Subsystem
VC233FD103	Command Subsystem
VC263FD104	Radio Subsystem OSE
VC263FD103	Command Subsystem OSE

Texas Instruments

VC233FD105	Data Storage Subsystem
VC233FD106	Telemetry Subsystem
VC263FD105	Data Storage Subsystem OSE
VC263FD106	Telemetry Subsystem OSE

Both Motorola and Texas Instruments contributions are incorporated in:

VC280FD105	MDE Functional Description

CII VC233FD101

TELECOMMUNICATION SUBSYSTEM

SECTION	
1	SCOPE
2	APPLICABLE DOCUMENTS
3	FUNCTIONAL DESCRIPTION
4	INTERFACE DEFINITIONS
5	PERFORMANCE PARAMETERS
6	PHYSICAL CHARACTERISTICS
APPENDIX A	PERFORMANCE CURVES

TELECOMMUNICATIONS SUBSYSTEM

1.0 SCOPE. This document describes the 1971 Voyager Flight Spacecraft Telecommunication system. The requirements placed on the subsystems, the operation during a typical mission, and the performance parameters are given. Complete graphs of the telemetry, tracking and command performance are included.

2.0 APPLICABLE DOCUMENTS. The following documents contain information which applies to the Telecommunication System:

JPL Documents

EPD-283	Planned Capabilities of the DSN for Voyager
MC4-310A	Functional Specification, Mariner C Flight Equipment, Telecommunication System
-	"Contractor Performance Measures of the Telecommunication System," letter from A. Gluckson, 17 May 1965

GE Documents

VC211SR101	Mission Objectives and Design Criteria
VC220SR101	Design Characteristics and Restraints
VC220FD112	Flight Sequence
VC220FD113	Layout and Configuration
VB233AA101	Telecommunication Trade-Off Studies

3.0 FUNCTIONAL DESCRIPTION. The 1971 Voyager Telecommunication System represents a logical extension of the techniques and equipment designs developed and demonstrated by JPL on the Ranger and Mariner programs. The increased size of the Voyager spacecraft has permitted significant increase in storage capacity and in reliability through equipment redundancy. The increased size of Voyager, coupled with the increased capability of the DSIF, permits a large increase in transmission capability. Extensive use of integrated circuits for digital functions has reduced the weight of many elements of the Voyager Telecommunication System, compared with their counterparts in the Mariner System.

The Telecommunication System described in this document is the result of many tradeoff studies and the use of engineering judgment based on past experiences. A ground rule was to keep the system conceptually simple and based on proven techniques wherever possible. A 50-watt power amplifier was selected as a reasonable step forward in the area of power amplifiers. A 7.5-foot diameter parabolic antenna was selected as the best compromise from weight, simplicity, and reliability considerations. A strong program on optimum redundancy was undertaken to maximize reliability versus weight.

In the following pages, a telecommunication system is described which is the result of the considerations indicated above, as well as many others which are documented in the tradeoff studies.

3.1 Communication Requirements. The Spacecraft Telecommunication System must perform the following general functions:

a. Telemeter spacecraft and capsule engineering data throughout the mission. Telemeter data from interplanetary science instruments throughout the mission, and data from planet scan instruments during the orbital phase. Provide a relay antenna, and transmit capsule engineering and science data that was stored during capsule de-orbit and entry phases up through capsule impact.

b. Receive commands from the stations of the DSIF, and decode and provide switch enclosures or quantitative data to the spacecraft and capsule subsystems.

c. Provide for range rate, range and angular tracking of the spacecraft by the DSIF stations.

The above general requirements are expanded by mission phase to delineate the requirements imposed on the system by the mission operations in the following section.

3.1.1 Launch Phase. Two phases of the launch phase are considered: pre-launch and launch through injection.

a. Pre-launch. In the 45 to 60 days before launch, all operational modes must be checked out. The telecommunications subsystems will be checked by use of the umbilical and by radio link.

b. Launch Through Injection. From launch to separation of each spacecraft from the booster, radio communications must be accomplished through parasitic antennas on the shroud. The DSIF stations No. 71 at KSC and No. 72 at Ascension may view the spacecraft during ascent to parking orbit. Depending on the length of the parking orbit (< 90 minutes) communications with the other stations of the DSN may be possible for brief periods. Communications are required for the transmission of engineering data from the spacecraft and capsule. Command for back-up to on-board commands, and range rate and range tracking are also required. Telemetry data will also be relayed via the launch vehicle. The transmitted telemetry spectrum will be compatible with DSN automatic acquisition.

3.1.2 Acquisition Phase. Depending on the duration of the parking orbit, the spacecraft may be in view of Johannesburg, Woomera or possibly the Goldstone station during injection and acquisition of celestial attitude references. During the acquisition period, and subsequently during cruise in the heliocentric transfer trajectory, the spacecraft will come into view of all the DSIF stations.

During acquisition, the spacecraft may initially tumble at rates up to 3 degrees per second. After the tumbling rates are damped and the spacecraft becomes stabilized to the Sun, the spacecraft will roll to calibrate science instruments and then to acquire Canopus. In order to provide communications prior to Canopus lock, the antenna must provide coverage at cone angles up to at least 100 degrees for all roll positions. The high gain antenna will be used to verify Canopus acquisition.

Telemetry, command and tracking requirements are the same as during launch, except that spacecraft interplanetary science data must be transmitted. The required transmission capability is 2.5×10^6 bits per day. The goal is 5×10^6 bits per day (an average of 58 bps).

3.1.3 Interplanetary Cruise (Before First Maneuver). The spacecraft will be fully stabilized. Coverage by the DSIF stations will be continuous. The spacecraft interplanetary science instruments will store up to 10^6 bits of data during a solar flare. The telemetry subsystem will transmit this data at a high rate. The command subsystem must accept quantitative commands that specify the turns and velocity magnitude that the spacecraft must accomplish for trajectory corrections.

3.1.4 Interplanetary Trajectory Correction. The first trajectory correction occurs 2 to 10 days after launch. It is assumed that the spacecraft may assume any attitude during the maneuver. During the turns to and from the stabilized motor burn attitude, continuous communication is not required. After achieving the motor burn attitude, telemetry is required to verify that the correct attitude has been achieved. Command is required so that the burn may be inhibited if the proper attitude was not reached. Storage of science and engineering data is required while the spacecraft is not in the normal cruise attitude. Tracking is not required. Later trajectory corrections have the same requirements.

3.1.5 Interplanetary Cruise. After a maneuver, the stored data will be dumped at a high rate. All other requirements are the same as the first cruise phase.

3.1.6 Mars Orbit Insertion. The requirements are the same as for earlier maneuvers.

3.1.7 Orbital Operations.

After two orbits, high rate planet scan data is stored. Data is collected at rates up to 50,000 bps. The required storage capacity is 5×10^7 bits; the goal is 5×10^8 bits. After a recorder is full or the DAE indicates no more data to be stored, transmission of the stored data may begin. In addition to the planet scan science data, spacecraft engineering data and science instrument housekeeping data shall be transmitted in real time. The maximum transmission rate shall not exceed 15,000 bps. After the second spacecraft achieves orbit, the rate from the two spacecraft together shall be less than 15,000 bps. After six months, the data transmission capability shall exceed 5×10^7 bits per day, with a goal of 10^8 bits per day. During capsule checkout prior to capsule separation, data shall be transmitted at a rate of 100 bps. Commands shall be received for orienting the spacecraft to the capsule separation attitude. Provision shall be made for handling up to six quantitative commands for the capsule as well as updating capability for up to ten Computer and Sequencer commands for the capsule. During the capsule separation maneuver, communication requirements are the same as for earlier maneuvers. While the spacecraft remains in the separation attitude, the capsule relay data will be received via a 400 mc antenna provided. The relay antenna shall provide coverage such that the antenna gain in db will exceed the factor G, given by:

$$G\ (\text{db}) = -5 + 20 \log_{10} (\text{range to capsule in thousands of km})$$

After capsule impact and resumption of cruise attitude by the spacecraft, the data stored in the relay subsystem recorder shall be transmitted to the DSIF stations.

3.1.8 Mars Orbit Trim. During orbit trim maneuvers, communication requirements are the same as in earlier maneuvers.

3.2 System Description. The Voyager Telecommunication System is composed of four subsystems. These subsystems are: (1) radio, (2) telemetry, (3) data storage and (4) command. A simplified block diagram of the Telecommunication System is given in Figure 3-1.

3.2.1 Radio Subsystem. The radio subsystem, Figure 3-2, is capable of transmitting at either three or fifty watts, at S-band. The three-watt power amplifier is employed during launch and acquisition; the fifty-watt power amplifiers are used throughout the remainder of the mission. The power amplifiers are driven by the exciter section of the transponders, in which the telemetry data and ranging signal phase modulate the carrier. The receiver section of each transponder demodulates the command or ranging signals transmitted by the DSIF stations, and provides the coherent carrier reference for the exciters for range rate tracking. The command subcarrier signal is processed in the command subsystem; the turn-around ranging signal is filtered and limited in the transponder.

Four S-band antennas are located as shown in Figure 3-3. During launch, the fixed primary low gain antenna is rf-coupled to the launch vehicle shroud antenna. After separation the primary low gain antenna provides essentially hemispherical coverage, with the center of the beam near the sun pointing (-Z) axis. Acceptable gain is achieved at cone angles up to 110 degrees in the direction of earth in the early cruise phases (approximately the -X direction).

The 7.5-foot high-gain parabolic reflector antenna may also be used in the early cruise phases after the spacecraft is fully stabilized. It is stowed behind the solar panels during launch, and is deployed after injection. It is steered by commands from the Computer and Sequencer subsystem so that it can point to Earth throughout the cruise and orbit phases of the mission.

During maneuvers it is not planned to swing the high gain antenna around, but the capability could be provided so that the high gain antenna could be used as a back-up means of verifying the maneuver attitude, or to provide the best possibility of obtaining tracking data during motor burn, if this should be required. The secondary low gain antenna is deployed on the +X axis. It provides a toroidal pattern, with the axis of the toroid along the X axis. Its coverage is broader than the primary low gain antenna, and it is therefore the preferred antenna for use during maneuvers.

The fourth S-band antenna is the fixed medium gain antenna of the Mariner C-type which produces a beam of elliptical cross section. This antenna is provided as a back-up to the high gain antenna, and for the 1971 mission will support a data rate of 933-1/3 bps for four months after encounter.

A 400 mc antenna is provided for the relay subsystem. This antenna is mounted on the + X side of the vehicle as shown in Figure 3-3, and is supported far enough away from the body

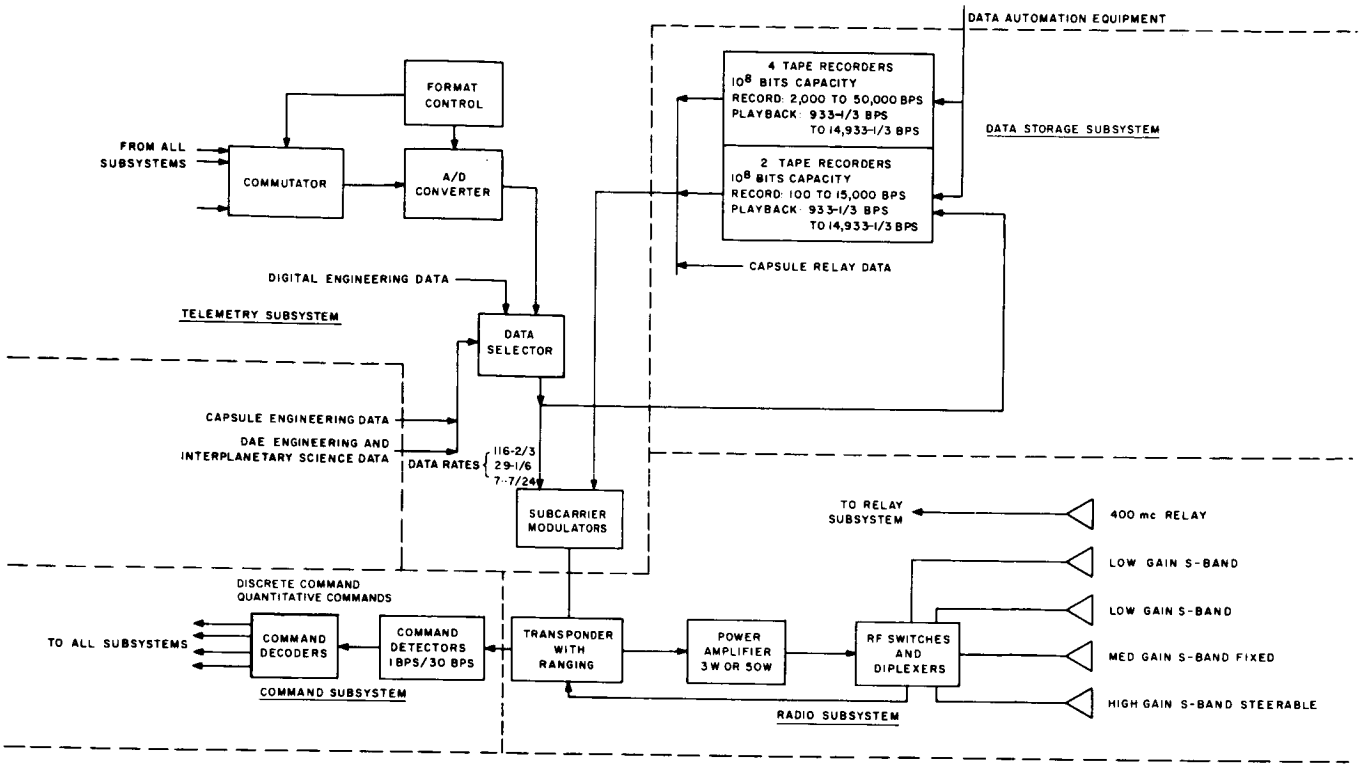


Figure 3-1. Telecommunication System

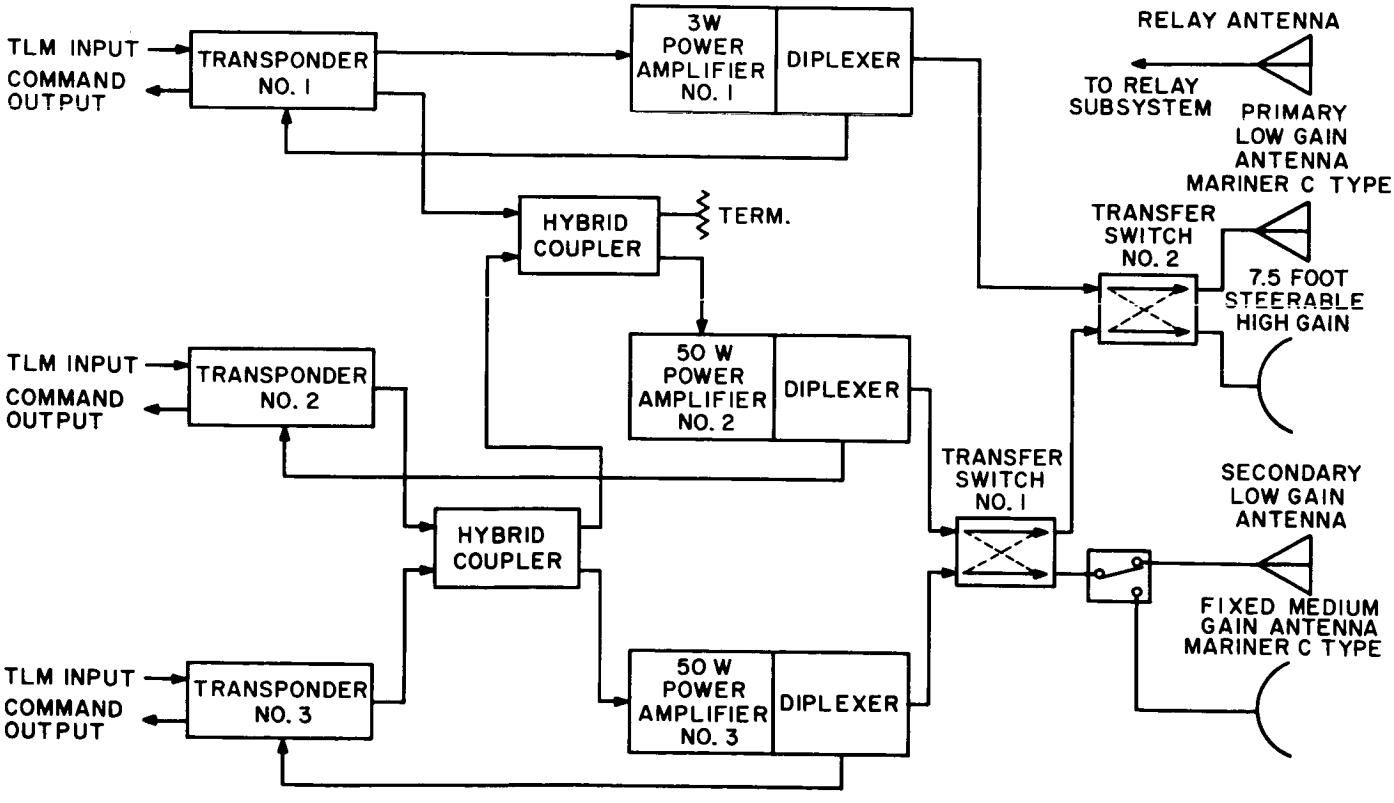


Figure 3-2. Radio Subsystem

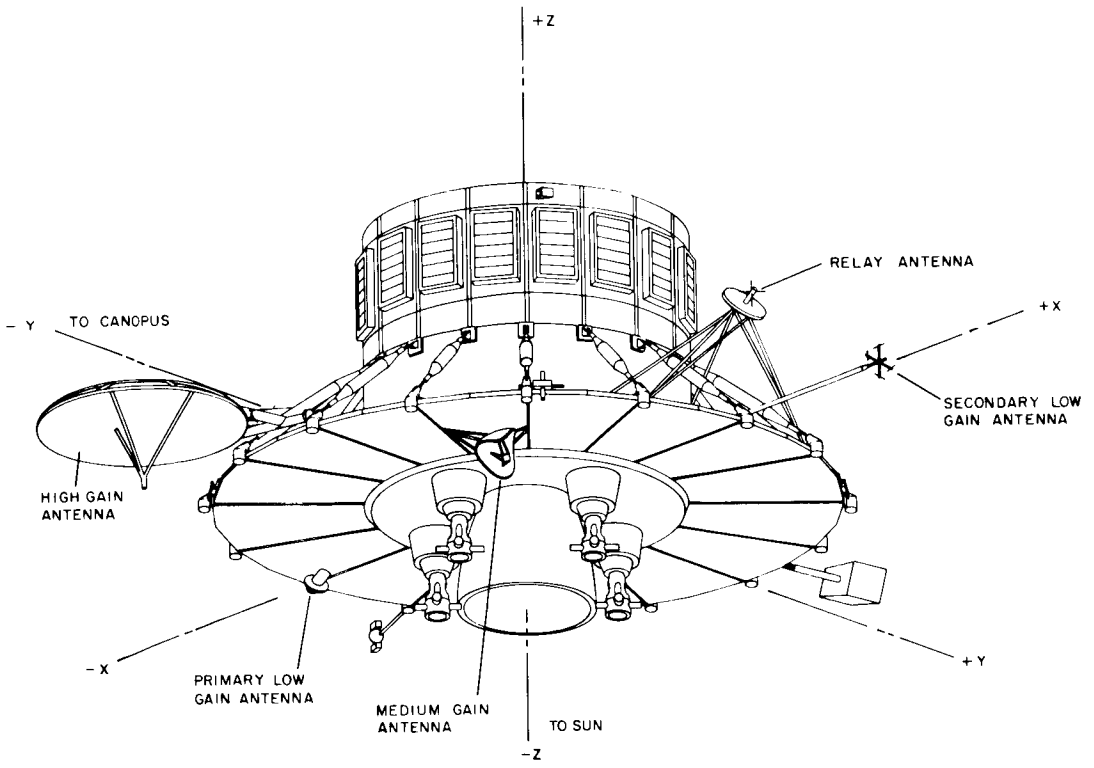


Figure 3-3. Antenna Locations

so that it may view the capsule during descent through capsule impact, while the spacecraft maintains the attitude from which the capsule was separated.

3.2.2 Telemetry Subsystem. The Telemetry subsystem has five basic modes of operation (as given in Table 3-1) in which engineering, capsule, and science data are collected and processed for storage or transmission. During normal cruise and orbital operations, all non-stored data is transmitted at 116 2/3 bps on a 268.8 kc subcarrier, while all recorded data is simultaneously transmitted at 3,733 1/3, 7,466 2/3, or 14,933 1/3 bps. During maneuvers and emergencies, engineering data is transmitted at 7 7/24 bps. Stored science and engineering data is transmitted at 933 1/3 bps and 29 1/6 bps respectively during the orbit science back-up mode in case of loss of the high-gain antenna system.

A functional block diagram of the telemetry subsystem is given in Figure 3-4. Analog engineering data is multiplexed and conditioned, if required, by the commutator. The multiplexed analog data is encoded into seven bit words by the ADC. The encoded analog data is time-multiplexed with digital engineering data and presented to the data selector. The data selector time-multiplexes the engineering data with the digital capsule and/or real time DAE data.

The two format programmers and their associated PNG's provide functional redundancy, and provide as well a means for effectively running two commutators at the same time. This feature is useful during maneuvers in which one format must be stored and a different one transmitted.

TABLE 3-1. DATA TRANSMISSION MODES

Mode	Title	Description
1A	Maneuver	Transmitted - Maneuver engineering data, including attitude verification channels, transmitted at 7 7/24 bps. Stored - Collection rate of 116 2/3 bps. 58 1/3 bps maneuver, motor burn, and capsule engineering data 58 1/3 bps cruise science data.
1B	Capsule Separation	Transmitted - Maneuver engineering and capsule data transmitted at 7 7/24 bps. 3 31/48 bps maneuver engineering data 3 31/48 bps capsule status data Stored: Maneuver engineering data only, collected at 116 2/3 bps.
2	Cruise	Transmitted - Cruise/Orbit engineering and cruise science data transmitted at 116 2/3 bps. 58 1/3 bps cruise/orbit engineering 58 1/3 bps cruise science
3A	Orbit	Transmitted - Stored data from planet scan, and fields and particles instruments is transmitted at 14,933 1/3; 7,466 2/3; or 3,733 1/3 bps. Engineering data (58 1/3 bps) and DAE orbit data (58 1/3 bps) transmitted at 116 2/3 bps. Backup rates of 933 1/3 bps together with 29 1/6 bps are also available. Stored - Planet scan, and fields and particle data stored on recorders.
3B	Earth Occultation	As above but all data stored. Science playback is inhibited.
4	Cruise Recorder Readout	Transmitted - Stored data, either maneuver or flare data, transmitted at 3733 1/3 bps. Cruise/Orbit engineering and cruise science data transmitted at 116 2/3 bps as in Mode 2.
5	Capsule Checkout	Transmitted - Stored data from planet scan and fields and particles instruments is transmitted at 14,933 1/3 or 7,466 2/3 bps. Engineering data (14 7/12 bps) and Capsule checkout data (102 1/12 bps) transmitted at 116 2/3 bps. Science data stored as in normal orbit operations.

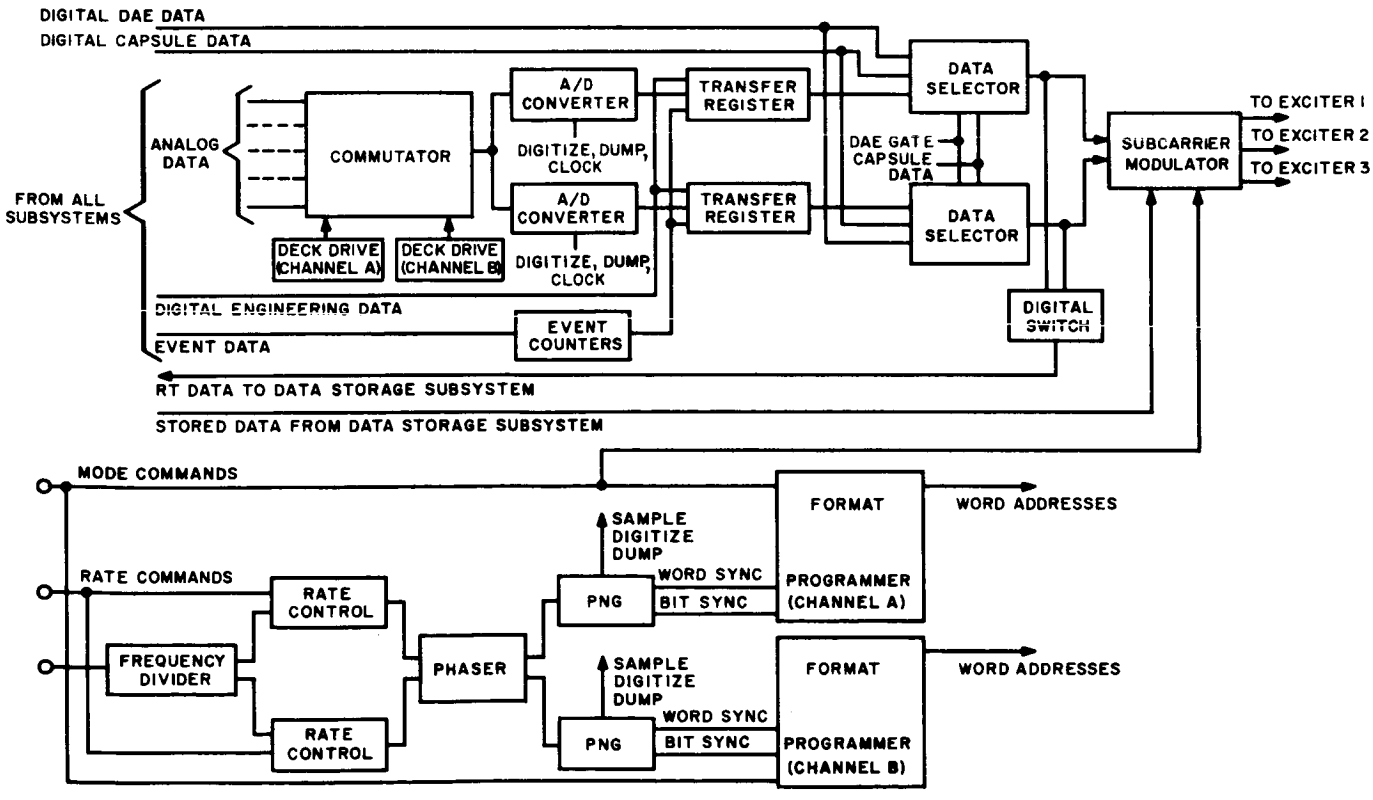


Figure 3-4. Telemetry Subsystem

The format programmer has the basic function of selecting the data source, and determining the number of words to be clocked out of the data source.

The subcarrier modulator receives two inputs: (1) the time-multiplexed real time data stream consisting of engineering, capsule and/or real time DAE data, and (2) the stored data input consisting of recorded planet scan data, recorded fields and particle data or recorded maneuver data. Each input is combined with synchronization information (PN) and placed on a subcarrier ($2\,f_S$). In addition, the real time data stream modulates a 268.8 kc subcarrier. The two channels are linearly summed, as in the case of orbit operations, or only the real time data channel is transmitted, as in the case of normal cruise operations.

3.2.3 Data Storage Subsystem. The data storage subsystem as shown in Figure 3-5 provides for the storage of digital data from the science and telemetry subsystems. The data storage subsystem is composed of six magnetic tape recorders and their associated control and power supply electronics. It performs the following primary functions:

a. Storage of spacecraft maneuver engineering data, cruise science data, and capsule diagnostic data during trajectory corrections.

b. Storage of science data in orbit from fields and particle instruments, IR scanner, IR/UV spectrometers, and two video instruments.

c. Storage of high rate science data during solar flares.

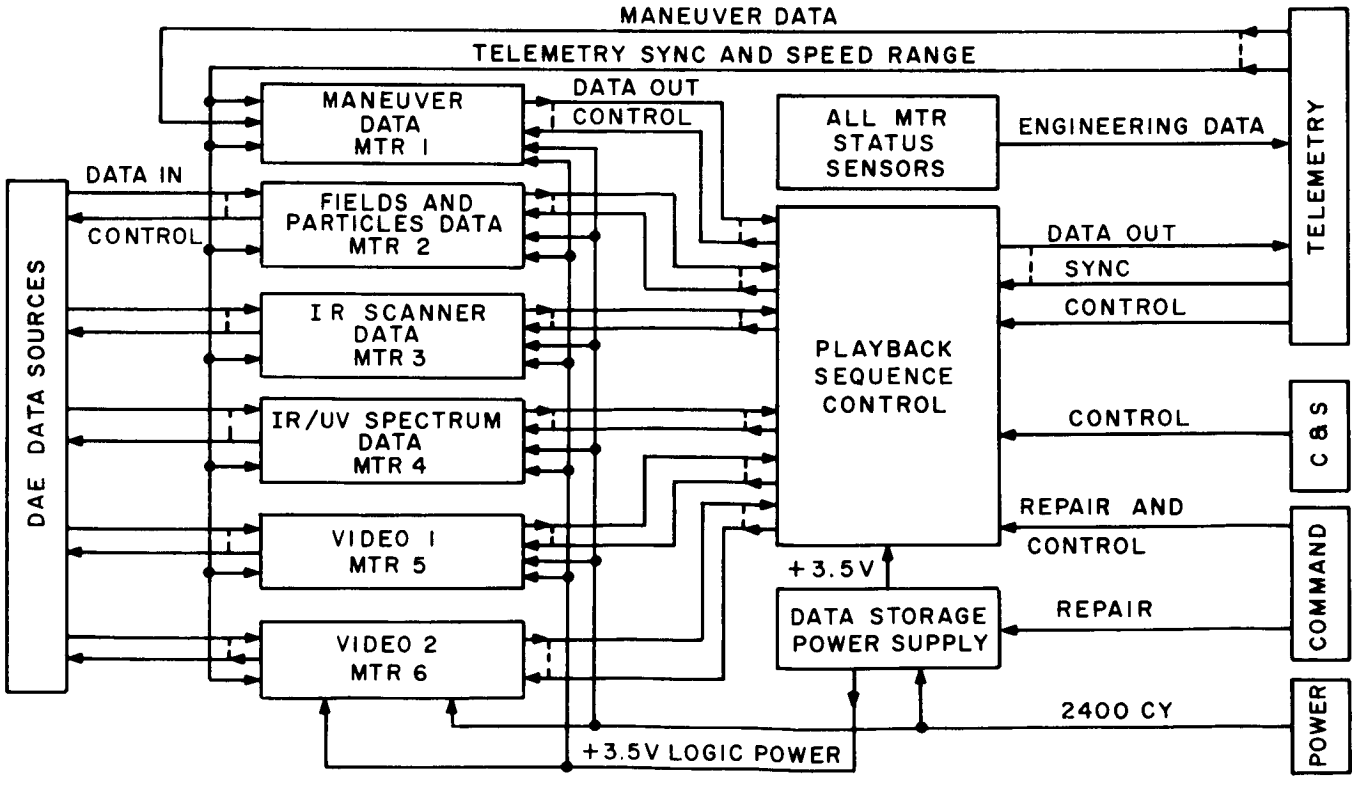


Figure 3-5. Data Storage Subsystem

The recorders are all physically identical peripheral drive, parallel-recording types, with identical tape pack sizes. The units differ only in having one or two motors, depending on the record/playback speed ratio. Each recorder is primarily associated with one data input, and recording may proceed independently on any or all units. Playback is sequential, one recorder at a time. Functional redundancy is achieved by allowing units to exchange input functions in case of recorder failure.

3.2.4 Command Subsystem. The command subsystem, Figure 3-6, performs the functions of detecting and passing execute pulses or digital information streams to various spacecraft users as addressed from the ground via the radio subsystem. It is basically a modification and extension of the Mariner B and C command systems. Command data may be relayed to the spacecraft through any one of the three channels shown on the block diagram. There are two command bit rates that may be used:

a. A 15 bps rate, which can be attained through any of the three receiving channels for high rate programming of C and S, and/or DAE functions.

b. A 1/2 bps rate, available through receiving channels A and C.

The command subcarrier is demodulated in the Detector, and the command data signal is matched-filtered. The Manchester coded data bits are checked for errors in the Program Control Unit, which recognizes the word synchronization pattern and generates the required timing signals for discrete and quantitative commands. The Decoder Access Unit selects the decoder configuration to be used by decoding the first two bits of each command. The outputs of the two decoders are in series, and normally both decoders operate to produce a command. In the event of failure of one decoder, it may be bypassed by the Decoder Access Unit. The Command Decoders provide dc isolated switch closures for each discrete command output. The quantitative command data bits are transferred to the addressed subsystem through isolated switches also. The Command Subsystem has the capability for up to 246 discrete and/or quantitative commands, which exceeds the requirements defined in the "Flight Sequence", VC220FD112, by 23% thus allowing for growth.

3.3 Operation. In the following section, the operations of the telecommunication subsystems are described. Table 3-2 summarizes the operations by mission phase.

3.3.1 Launch Operations. During the portions of the launch phase in which the two spacecraft are mated to the booster, the communication systems on the booster will relay the spacecraft telemetry data signal and will provide the primary means of obtaining tracking data. No command capability will be provided, although normally no commands are required. Radio links with the two spacecraft provide the following capabilities:

a. Back-up direct telemetry data
b. Emergency command capability
c. Acquisition by the DSIF stations of the spacecraft signal prior to separation

The radio links during launch are through parasitic antennas on the shroud which are rf-coupled to the primary low gain antenna on each spacecraft. Because of the limitations of rf

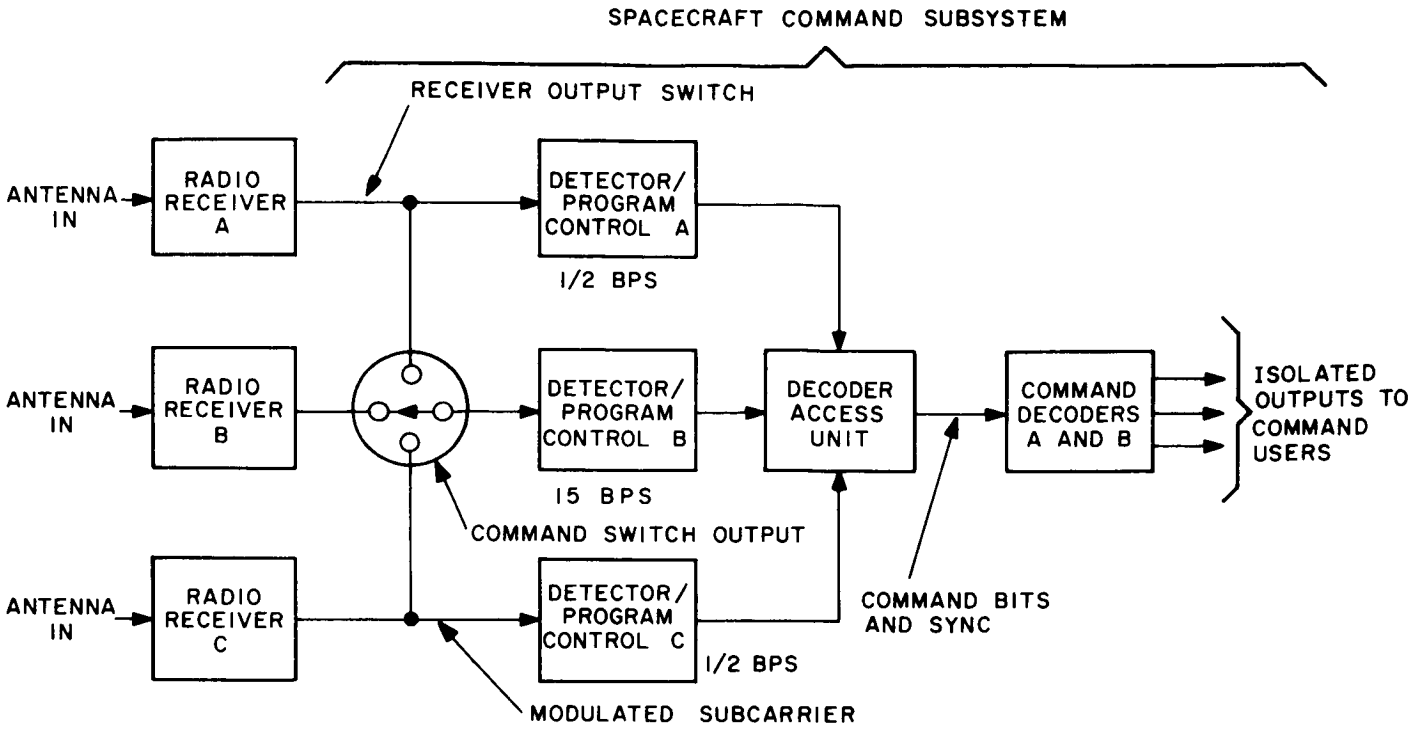


Figure 3-6. Command Flow Diagram

power and dc voltage which must be observed in order to prevent breakdown as the vehicle passes through the altitudes of critical pressure, a three watt solid state transmitter is employed. This transmitter is diplexed with a receiver to the antenna.

The data collection and transmission requirements during launch are for spacecraft and capsule engineering data. There is no data storage requirement. Spacecraft and capsule engineering data, and interplanetary science data is transmitted throughout the mission (except during maneuvers) at a rate of 116 2/3 bps on a 268.8 kc subcarrier. The same data rate and subcarrier were chosen for use in launch. Not only does this provide a capability which satisfies the launch telemetry requirements without adding an additional data rate, sampling format or subcarrier modulator, but it provides a free spectral band of greater than 400 kc about the carrier, so that a DSIF automatic acquisition sweep of ± 150 kc can be readily accommodated without the possibility of false lock on a sideband.

3.3.2 Acquisition. After injection and separation from the booster, the telemetry, tracking and command requirements are the same as during launch, except that the cruise science instruments are energized. These instruments are continuously operating, and the average rate at which data is generated corresponds to 29 and 58 bps for the specified requirement and goal respectively. Adding 58 bps to the expected spacecraft engineering and capsule data rate requirements leads to a rate consistent with the 116 2/3 bps rate selected.

The vehicle may initially tumble at rates as high as 3 degrees per second until the attitude control system damps out the motions. After acquiring the Sun and stabilizing in pitch and

TABLE 3-2. OPERATIONS BY MISSION PHASE

Phase	Time	DSIF Station	Tracking	Command	Data Collection	Data Transmission
Pre-Launch	45-60 days	DSIF 71,	Checkout of ranging	Checkout of all operational modes	Checkout of telemetry S/S and Data Storage S/S	Transmission at all rates and modes

					at all rates	
Launch & Injection	45 min	DSIF 71, Ascension	Doppler tracking	Command capability at 1/2 bps or 15 bps through primary low gain via parasitic antenna on shroud	TLM S/S in Mode 2 (Cruise Mode). Spacecraft, engineering, capsule, and science data is collected for transmission.	Transmission at 116 2/3 bps, 3-watts, through primary low gain antenna to shroud antenna. Telemetry data also relayed to the launch vehicle.
Acquisition	19 hr	Johannesburg, Woomera Goldstone	Doppler tracking	Command through either low gain antenna by transmitter frequency selection	Same as above. Engineering data includes roll rate and roll position information.	Transmission at 116 2/3 bps, 3 watts, through primary low gain antenna. At completion of acquisition, transmission at 50 W through high-gain antenna (used for Canopus verification).
Initial Interplanetary Cruise		Johannesburg, Woomera, Madrid, Canberra, Goldstone	Doppler tracking and ranging as required	Command capability at 1/2 bps or 15 bps. The Command S/S accepts quantitative command specifying turns and velocity magnitude for trajectory correction. The high gain antenna may be used in addition to the low gain antennas.	Same as above. If solar flare occurs, science data in format is deleted. Solar flare data is stored on fields and particle data recorder. 10^8 bit capacity provided. TLM S/S automatically goes to Mode 4 upon receipt of signal indicating flare ended. Normal cruise engineering, capsule, and science data is collected as in normal cruise operation.	Transmission at 116 2/3 bps, 50 watts, through high-gain antenna during normal cruise. If solar flare occurs, at completion of flare simultaneous transmission of real time data at 116 2/3 bps, and stored data at 3733 1/3 bps, 50 watts, through high-gain antenna.
First Inter-Planetary Trajectory Correction Turn, Thrust, Turn	2 to 10 days after launch Duration 3.5 hr	Goldstone	Tracking not required	Command capability at 1/2 bps or 15 bps when spacecraft has assumed motor burn attitude	TLM S/S in Mode 1A. Manuever engineering data is collected for transmission. Attitude verification data in for-	Transmission at 7 7/24 bps, 50 watts, through secondary low-gain antenna.

					mat. Maneuver engineering, motor burn, science, and capsule data is collected for storage. 10^8 bit capacity provided.	
Reacquisition Completed		Goldstone			TLM S/S is commanded by the C&S to Mode 4. Real time data is collected as in normal cruise. Stored maneuver data is played back. At completion of playback TLM S/S goes to Mode 2.	Simultaneous transmission of real time data at 116 2/3 bps and stored maneuver data at 3733 1/3 bps, 50 watts through high-gain antenna.
Additional Interplanetary Cruise Phases	← Same as Initial Interplanetary Cruise →					
Additional Interplanetary Trajectory Correction Phases	← Same as First Interplanetary Trajectory Correction →					
Orbit Insertion Turn, Thrust, Turn	6 months after launch 2 hr 30 min	Goldstone		Command capability at 1 bps when spacecraft has assumed motor burn attitude	TLM S/S in Mode 1A. Maneuver engineering data is collected for transmission. Attitude verification data in format. Maneuver engineering, motor burn, science and capsule data is collected for storage.	Transmission at 7 7/24 bps, 50 watts, through secondary low-gain antenna.
First and Second Orbit Earth Occultation	36 min	NA	NA	NA	TLM S/S remains in Mode 1A stor-	NA

					ing maneuver data	
Sun Occultation	42 min				Same as above	Transmission at 7 7/24 bps, 50 watts, through secondary low-gain antenna.
Reacquisition					TLM S/S is commanded by C&S to Mode 4. Stored maneuver data is played back. At completion of playback TLM S/S goes to Mode 2.	Simultaneous transmission of real time data at 117 2/3 bps and stored data at 3733 1/3 bps, 50 watts through high-gain antenna. At completion of stored data readout, transmission is at 116 2/3 bps, 50 watts, through high-gain antenna.
Orbital Operations (Pre-capsule separation)		All stations	Doppler tracking and ranging as required	Command capability at 1/2 bps and 15 bps. Science sequencing commands and C&S command may be updated	TLM S/S in Mode 3A. Spacecraft engineering and science engineering data is collected for real time transmission. Capsule diagnostic data is contained in format. Science data (scan and non-scan) is collected and stored. Playback of recorded data begins when recorder is full or DAE indicates no more data for storage. 4×10^8 bit capacity available for scan science, 1×10^8 bit capacity available for fields and particle data.	Simultaneous transmission of real time data at 116 2/3 bps and stored data at 14933 1/3 or 7466 2/3 or 3733 1/3 bps at 50 watts through high-gain antenna
Orbit Trim	Same as Orbit Injection					
Capsule Checkout	3 hr 30 min			Command capability at 1/2 bps or 15 bps. Commands are accepted for orienting the capsule	TLM S/S in Mode 5. Spacecraft engineering and capsule checkout data (102 bps) is collected for real	Same as in Orbital Operations

				separation attitude. Capsule quantitative commands and updated C&S commands for the capsule are accepted.	time transmission. Science data is processed as in normal orbit operations.	
Capsule Separation		Goldstone	Tracking not required			
Turn to Separation	1 hr, 30 min			Command capability at 1 bps after spacecraft has assumed separation attitude	TLM S/S in Mode 1B. Spacecraft maneuver and capsule engineering data is collected for real time transmission. Science data collected and stored as required. Spacecraft maneuver engineering data is stored in manuever recorder.	Transmission at 7/7/24 bps, 50 watts through secondary low-gain antenna.
Separation to Reacquisition	5 hrs				Same as above Capsule relay data is stored by Relay S/S.	Same as above
Orbital Operation Post Separation		All stations	Doppler tracking and ranging as required	Same as Orbital Operations (Pre-Capsule Separation)	Same as Orbital Operations (Pre-Capsule Separation). Capsule relay data is handled same as recorded science data.	Same as Orbital Operations (Pre-Capsule Separation)
Earth Occultations					TLM S/S in Mode 3B. Same as Mode 3A, with real time data stored and science playback inhibited.	NA
Sun Occultations	◄ Same as Orbital Operation ►					

yaw, the spacecraft rolls to calibrate the science instruments. In order to provide nearly continuous coverage the primary low gain antenna is provided. The pattern has a broad lobe so that for any orientation of the vehicle tumbling motion with respect to the ground station, communications will be possible for a period of time long enough to achieve synchronization and transmit a command or obtain telemetry data. At the short range at which injection takes place, very low vehicle antenna gains can be accepted. Relatively narrow lobes are useful. For example, with a lobe of 90 degrees, the time in the lobe is at least 30 seconds. For the 116 2/3 bps telemetry system, the mean time for acquisition of bit and word sync is 18.9 seconds*, and a frame period is 3.8 seconds. For command**, mean time for sync acquisition is less than 1/4 second, while the time to transmit a discrete command is only 1 second. Thus, it is conceivable that, if necessary, a command could be successfully accomplished even under these extreme conditions.

As described in Section 3.4.3, two low-gain antennas are used. The primary low-gain antenna was chosen for telemetry during launch and injection. Either the primary or secondary low-gain antenna may be used for command by selecting the transmitter frequency. If range rate tracking is desired, the primary low-gain antenna must be used.

3.3.3 Interplanetary Cruise. After acquisition of celestial references, normal cruise operations are required. The telemetry transmission is switched to the steerable high-gain antenna to verify Canopus acquisition. During cruise, the science instruments collect data at the normal rate (a capability for 58 bps is provided) except during solar flares, when the collection rate is assumed to be as high as 15,000 bps. The capability to store 10^8 bits at this rate for subsequent transmission is provided. The stored data is transmitted simultaneously with the real time science, engineering, and capsule data by employing frequency division multiplexing. Also during the cruise phase, the spacecraft will perform trajectory correction maneuvers. In order to orient the motor in the proper direction, the vehicle may assume any attitude. Further, the magnitude of the velocity change to be accomplished cannot be determined before launch. Therefore, the command system must provide for transmitting the turn and velocity magnitude data to the Spacecraft. This data, in the form of quantitative commands, is addressed to the user subsystems by the command decoder.

3.3.4 Interplanetary Trajectory Corrections. As the vehicle turns to the attitude at which the motor will be fired, it is deemed impractical to maintain the high-gain antenna oriented to Earth. Therefore, if communications are required during the turn, a low-gain antenna system must be used. During early maneuvers it would be feasible to maintain the normal cruise data transmission rate of 116 2/3 bps for the science, capsule and engineering data. However, during late maneuvers, only a much lower rate can be accommodated; with an antenna gain of zero db, a rate of 116 2/3 bps can only be supported to a range of 55×10^6 km. The direction of the turns may cause a null in the antenna pattern to be directed to the Earth, so that communications during the turn cannot be guaranteed. However, after the spacecraft stabilizes at the proper attitude for motor burn, it is possible to use a low-gain antenna and assure that nulls are avoided. Because the secondary low-gain antenna provides such wide

*VC233FD106 Voyager Telemetry Subsystem, Section 5.0
**VC233FD103 Voyager Command Subsystem, Section 5.0

coverage, the normal procedure is considered to include only two turns. If the desired attitude would result in a null in the antenna pattern being directed to Earth, the procedure would have to be altered to include a roll so that the null could be avoided.

As discussed in the Task A study, it would also be possible to use the high-gain antenna for telemetry after reaching the maneuver attitude, by providing at least 180 degrees pointing arc in a plane including the vehicle roll axis from the -Z to +Z directions. In this case it would be necessary to choose a particular roll attitude to obtain coverage. Use of the high-gain antenna has the advantage of confirming that the spacecraft has achieved the proper maneuver attitude. However, it requires programming the antenna reorientation and carrying it out, as well as switching telemetry transmission modes if telemetry during the turn is required. For these reasons, the present design does not employ the high-gain antenna during maneuvers in the primary operating mode; it uses instead the secondary low-gain antenna. With the 50-watt power amplifiers and a 5-cps ground receiver carrier loop bandwidth, a data rate of 7 7/24 bps can be supported to a range of 240×10^6 km. This rate provides capsule data and considerable spacecraft engineering data, including attitude sensor data to confirm that the proper maneuver turns have been made. Because the data rate is so much less than the normal engineering data rates and because continuous coverage cannot be guaranteed, the normal engineering data, cruise science data, and capsule data is stored during the maneuver, for transmission after the Spacecraft returns to the normal cruise attitude.

Command capability is required to back up on-board commands and to inhibit motor burn if there is a malfunction. Either of the two low-gain antenna-receiver combinations may be used for command by selecting the appropriate frequency of the ground transmitter.

3.3.5 Mars Orbit Insertion. The telecommunications requirements are the same as during interplanetary trajectory connections. Communications during the turns and telemetry reception during motor burn are not required.

3.3.6 Mars Orbital Operations. During the first two orbits, on-board sensors are used to establish the time reference to initiate the orbit sequence of operations of the scientific instruments. Depending on the exact orbit, Earth and Sun occultations may occur soon after achieving orbit. Reacquisition of Canopus after the orbit insertion maneuver is not accomplished during the occultations. Therefore the maneuver telemetry mode is used, in which 7 7/24 bps engineering data is transmitted through the secondary low-gain antenna, while 116 2/3 bps engineering, capsule and science data are stored for transmission after reacquisition. After transmission of the stored data, using the high-gain antenna, the normal cruise mode of operation is resumed.

Subsequent to the second orbit, normal orbit operations begin, and the planet scan science data is stored as it is collected. A capability of 4×10^8 bits is provided. Transmission may begin as soon as a recorder is full or the DAE indicates playback should start. Data from the interplanetary science instruments is also recorded. The recorders are read out in sequence, each recorder being available for new data as soon as it is emptied. The recorders may be read out at rates of 14933 1/3, 7466 2/3 and 3733 1/3 bps, consistent with the constraint that the data rate not exceed 15,000 bps. When the second Spacecraft achieves orbit and begins transmitting science data, the maximum data rate from the two Spacecraft

together may not exceed 15,000 bps. The rate of 3733 1/3 bps may be maintained to a range of 390 x 10^6 km, which exceeds the maximum end of mission range for a late 1973 encounter (arrival January 26, 1974).

Concurrently with the high rate science data from the recorders, spacecraft science and capsule engineering data are transmitted at 116 2/3 bps on a 268.8 kc subcarrier. Commands may be received to backup on-board commands. Range and range rate tracking may be used for orbit determination.

Before capsule separation, orbit trim maneuvers may be required. The command system is required to receive turn and velocity data as for interplanetary trajectory correction maneuvers. During the maneuver, telemetry data transmission is reduced to 7 7/24 bps, and engineering and capsule data are recorded for transmission after the maneuver is complete. Command capability is required after achieving the maneuver attitude.

Also, prior to capsule separation, capsule check-out operations require the transmission of 100 bps data. Normal science data storage and playback may be accomplished simultaneously. However, the Spacecraft engineering data transmission rate is reduced so that the capsule checkout data may be accommodated with the 116 2/3 bps data rate.

During capsule separation, operations are required as in a maneuver. After separation, capsule data are received and stored by the relay system, which is not part of the Spacecraft telecommunications system, although a 400 mc relay antenna is provided. Following capsule impact, normal orbital operations are resumed, and the telecommunications requirements are the same as before. The stored relay data may be read out.

3.4 Alternatives. In the following sections are discussed some of the principal alternatives considered in the system design, and the rationale for the approach selected. Included are: (1) data rate selection, (2) time versus frequency multiplexing, (3) antenna system considerations, and (4) error control coding.

3.4.1 Data Rate Selection. In this section, the selection of the data rates for the transmission of data is discussed. The rates selected for the transmission of stored data are 14,933 1/3 bps, 7466 2/3 bps, 3733 1/3 bps and 933 1/3 bps. Real time engineering, capsule and interplanetary science data are transmitted at 116 2/3 bps, and 29 1/6 bps. During maneuvers, engineering data is transmitted at 7 7/24 bps.

For the selected radio subsystem parameters of 50-watt transmitter power and a 7.5-foot antenna, the maximum usable data rate of 15,000 bps (14,933 1/3 bps is provided) may be readily achieved at nominal encounter times for 1971 and 1973 opportunities, and maintained well into the orbit phases. When the second spacecraft successfully reaches orbit and begins transmitting high rate data, the maximum usable rate from each spacecraft is 7500 bps (7466 2/3 bps is provided). After several months in orbit, the system data rate capability under worst case conditions drops below 7500 bps. Therefore, the data rate of 3733 1/3 bps is also provided for the primary data transmission system. This rate can be maintained through the entire mission, even when worst case negative tolerances hold.

The specified minimum science data return capability of 5×10^7 bits per day corresponds to an average continuous transmission rate of 580 bps; the design goal is twice as high. The system capability exceeds the requirement by more than six to one. Two backup configurations for the radio subsystem can be used: the first uses the 3-watt amplifier with the high gain antenna; the second uses either of the two 50-watt amplifiers with the medium-gain Mariner C type antenna. A lower science data rate of 933 1/3 bps is provided to lengthen the coverage period of these backup systems. An even lower data rate such as 466 2/3 bps would lengthen the coverage of the 3-watt transmitter backup by 60 days, but would not extend the coverage of the medium-gain antenna system significantly. It would also increase the speed range required of the tape recorders beyond the range that may be accomplished with a single motor. Therefore, a data rate of 933 1/3 bps was chosen.

The data return capability is less than the data storage capability. For example, at the highest transmission rate of 14,933 1/3 bps, the total quantity of data that can be returned in the period of one orbit is 3.8×10^8 bits for the selected 1,000 x 10,000 km orbit, which has a period of about 7 hours. Also, the estimated science data collection rate yields about 2.5×10^8 bits per orbit. On the other hand, the data storage capacity assigned to the collection of planet scan science is 4×10^8 bits, excluding the 10^8 bit capacity assigned to the collection of fields and particle science data. Therefore, the storage subsystem has an excess capacity which can be used to accommodate longer orbit periods or partial loss of capacity due to failures, and to provide operational flexibility to prolong the period between collecting data if desired.

A higher rate than 116 2/3 bps for the transmission of real time data could have been provided without requiring a significant change in the system. This rate was selected to be no higher than necessary to satisfy user requirements to avoid increasing the ground data handling requirement. During the six-month interplanetary cruise phase except during maneuvers), the interplanetary science data is allocated 58 1/3 bps, the capsule approximately one bps, and spacecraft subsystems, 57 1/3 bps. During capsule checkout prior to separation, the 102 1/2 bps capsule data utilizes the majority of this transmission capability; the remaining 14 7/12 bps capacity is used for real time engineering data (during normal orbit operations, interplanetary science data is stored for transmission at the high rates). After capsule separation, the spacecraft and DAE engineering data share the capacity.

Under normal conditions, when the full link transmission capability is available, the real time data transmission reduces the power available for the high rate data by less than 0.9 db. If the backup transmission systems are used, however, so that the high rate must be reduced to 933 1/3 bps, the 116 2/3 bps data would cause a 2.1 db loss. For this reason, the real time data transmission rate is reduced to 29 1/6 bps, so that the loss is held below 0.9 db.

During maneuvers and emergencies, the low-gain antennas are used. A coherent transmission system is chosen to satisfy the low data rate requirements. A rate of 7 7/24 bps can be supported by a zero db gain antenna to a range of 254×10^6 km under worst case conditions. This range exceeds that required for the capsule separation maneuver of 120×10^6 km for an early 1971 encounter by a factor of 2, giving an additional margin above worst case tolerances of 6 db (for a late 1973 encounter, the surplus margin is 3 db).

3.4.2 Time Versus Frequency Multiplexing. Frequency multiplexing was chosen over time multiplexing based on tradeoffs in the following three areas: (1) implementation, (2) DAE interface, and (3) transmission efficiency. The additional transmission losses are offset by savings in hardware and the simplification of the DAE interface. A summary of the considerations in the three areas is given below:

3.4.2.1 Implementation. It was assumed that real time data must be transmitted during periods of stored data playback.

a. Frequency multiplexing of two subcarriers (stored data and real-time data) requires an additional modulator and an analog summer. Both suppressed and non-suppressed subcarriers were considered. From an implementation standpoint, the suppressed subcarrier modulator is preferred since it requires about one-fifth the hardware. The implementation of the summer is similar to the Mariner C summer.

b. Two time multiplexing schemes were considered: (1) sampling real time data continuously and (2) sampling real time data only during "no data present" periods while playing back stored data.

   1. Continuous sampling of real-time data requires a storage element to store the data until a "no-data present" period occurs on the tape, at which time the stored real time data is read out (Task A approach). Assuming 10^6 bit blocks of recorded data as a maximum, and a transmission rate of 15,000 bps, approximately 67 seconds are required to read out the data. For a real time collection rate of 117 bps, a 7800-bit memory and its associated control circuitry are required.

   2. Sampling and transmitting only during a "no data present" period, though requiring a minimum of hardware, results in a varying and long sampling interval. The "no-data-present" period will occur at different intervals, depending on the science instrument and/or the start-stop time of the recorder in the record mode. Assuming again a 10^6 bit block of data as a maximum, the minimum sampling interval would be 67 seconds.

3.4.2.2 DAE Interface. For the DAE interface, it was found that:

a. Frequency multiplexing in no way constrains the DAE/data storage interface. Data can be presented to the recorders in any block size and to all at the same time.

b. For the time multiplexing schemes considered, a constraint of 10^6 bits maximum block size is imposed on the DAE in order to make the schemes practical. In addition, formatting of the data into blocks with associated labeling is required by the DAE.

3.4.2.3 Transmission Efficiency. To compare the transmission efficiency of the two general techniques the following assumptions are made:

a. The time multiplexing technique is ideal in that real time data is interlaced with stored data, with no gaps in the resultant data stream.

b. The frequency multiplexing technique is implemented as described in this report. A single set of modulation indices have been selected such that both channels threshold simultaneously in the 3733/117 bps and 933/29 bps modes. Additional losses in efficiency have been accepted in the 14933/117 bps and 7467/117 bps modes, in order to eliminate the elements required for additional modulation index switching.

c. For both techniques, 25% of the total transmitted power is allotted to the RF carrier.

d. E/N_0 for the composite time multiplexed data is 5.9 db; for frequency multiplexed data it is 5.9 db for stored data and 8.0 db for real time data.

Since total transmitted power is proportional to the SNR referenced to a one-cps bandwidth in the thresholding channel divided by the modulation loss associated with that channel, the following defines the ratio of total power required:

$$\frac{P_{TM}}{P_{FM}} = \frac{\left[1/L_m \left(R_s + R_{RT}\right) {}^{E}/_{N_o}\right]_{TM}}{\left[1/L_{ms} \left(R_s \; {}^{E}/_{N_o}{}_s\right)\right]_{FM}}$$

where:

L_m = modulation loss in time multiplexed channel (0.75)

L_{ms} = modulation loss in stored data channel for frequency multiplexing (0.615)

R_s = bit rate of stored data

R_{RT} = bit rate of real time data

E/N_0 = ratio of signal energy per bit to noise density for time multiplexed data (5.9)

$(E/N_0)_s$ = ratio of signal energy per bit to noise density for stored data channel (5.9)

The resulting efficiency comparison is shown in Table 3-3.

TABLE 3-3. TRANSMISSION EFFICIENCY LOSS WITH FREQUENCY MULTIPLEXING

FM		TM	FM Efficiency	FM Loss (db)
R_s (bps)	R_{RT} (bps)	$(R_s + R_{RT})$ (bps)		
14933	117	15050	0.826	-0.82
7467	117	7584	0.833	-0.79
3733	117	3850	0.845	-0.73
933	29	962	0.845	-0.73

3.4.3 Antenna System Considerations. The S-band antennas are the high-gain steerable antenna, the fixed medium-gain antenna, and the primary and secondary low-gain antennas. A 400 mc relay antenna is also provided. In this section, the changes made to the Task A designs and the alternatives considered during the Task B study are discussed.

3.4.3.1 High Gain Antenna. The steerable high-gain antenna is the same as recommended in the Task A study, and is a 7.5-foot parabolic reflector antenna, providing a beamwidth of 4 degrees and a peak gain of 32.5 db. In the course of the study both smaller and larger steerable antennas were considered. The nominal power gain product of the 7.5-foot antenna/

50-watt power amplifier combination is about 90,000; because of pointing losses, the worst case power gain product is 62,500. This combination will support a data rate of 4900 bps at a range of 328 x 10^6 km, which is the end of mission range for the early 1971 encounter considered. For a late 1973 encounter, a rate of 3950 bps may be supported at the end of mission range of 375 x 10^6 km. Thus, even for a late 1973 encounter, the data rate goal of 1160 bps may be achieved with a much lower power gain product of about 19,000, which is a factor of 3.23 less than the worst case product of the proposed system. Either the transmitted power could be reduced to below 20 watts, or the antenna diameter could be decreased to about 4 feet. However, the higher data rate capability of the proposed system affords the opportunity of obtaining a large amount of additional scientific data at the short ranges near encounter, as shown in Table 3-4. For example, with the proposed system a data rate of 15,000 bps can be maintained for a period of 2-1/2 months for an early 1971 encounter, compared with two weeks for the minimum capability system considered, with a power gain product of 19,000. Of course, if both spacecraft successfully achieve orbit, this increased capability cannot be taken advantage of, because of the data rate restriction for both spacecraft of 15,000 bps. However, with the proposed system a data rate capability of 7500 bps can be maintained for almost 4-1/2 months, compared with less than 2 months for the minimum system. For a late 1973 encounter, 7500 bps can be maintained for over 2 months, compared with less than 10 days for the minimum system.

TABLE 3-4. COMPARISON OF DATA RATE CAPABILITY OF PROPOSED SYSTEM WITH THE MINIMUM SYSTEM

Data Rate	15,000 bps		7,500 bps	
	Early 1971	Late 1973	Early 1971	Late 1973
Proposed System 50 watts, 7 1/2 foot PG = 62,500	75 days	20 days	135 days	72 days
Minimum System 50 watts, 4 feet PG = 19,000	14 days		54 days	6 days

An antenna as large as ten feet was also considered. The peak gain would be 2.75 db greater than the 7.5-foot antenna, but the pointing loss would be greater by 1.4 db for the same 1.5 degree pointing error. Therefore, the net increase in worst case gain is only 1.35 db. The added weight (at least 50 pounds) and the increased difficulty in stowing and deploying ruled out such a large antenna.

The 7.5-foot antenna is a reasonable design for Voyager. Preliminary studies of the system pointing error show that the three σ error will be less than 1.5 degrees, corresponding to a gain loss of 1.6 db. An analysis of the effect of thermal gradients for worst case attitudes with respect to the Sun indicates that the distortion will be much less than 1/16 wavelength, and will cause negligible gain degradation. A structural design analysis has been made to ensure that the required strength to withstand vibration and acceleration loads can be obtained within the allocated weight. Thus, the 7.5-foot antenna is selected because of the large increase in data return capability it affords, and because its design can be carried out with high confidence of success.

3.4.3.2 Medium-Gain Antenna. As a backup to the steerable high-gain antenna, a fixed medium-gain antenna of the same type as the Mariner C high-gain antenna is selected. During the Task B study, a computer program was prepared to enable alternate antenna configurations and aiming points to be readily evaluated. The program computes the worst-case antenna gain, taking into account pointing error, as a function of time in orbit. Figure 3-7 shows

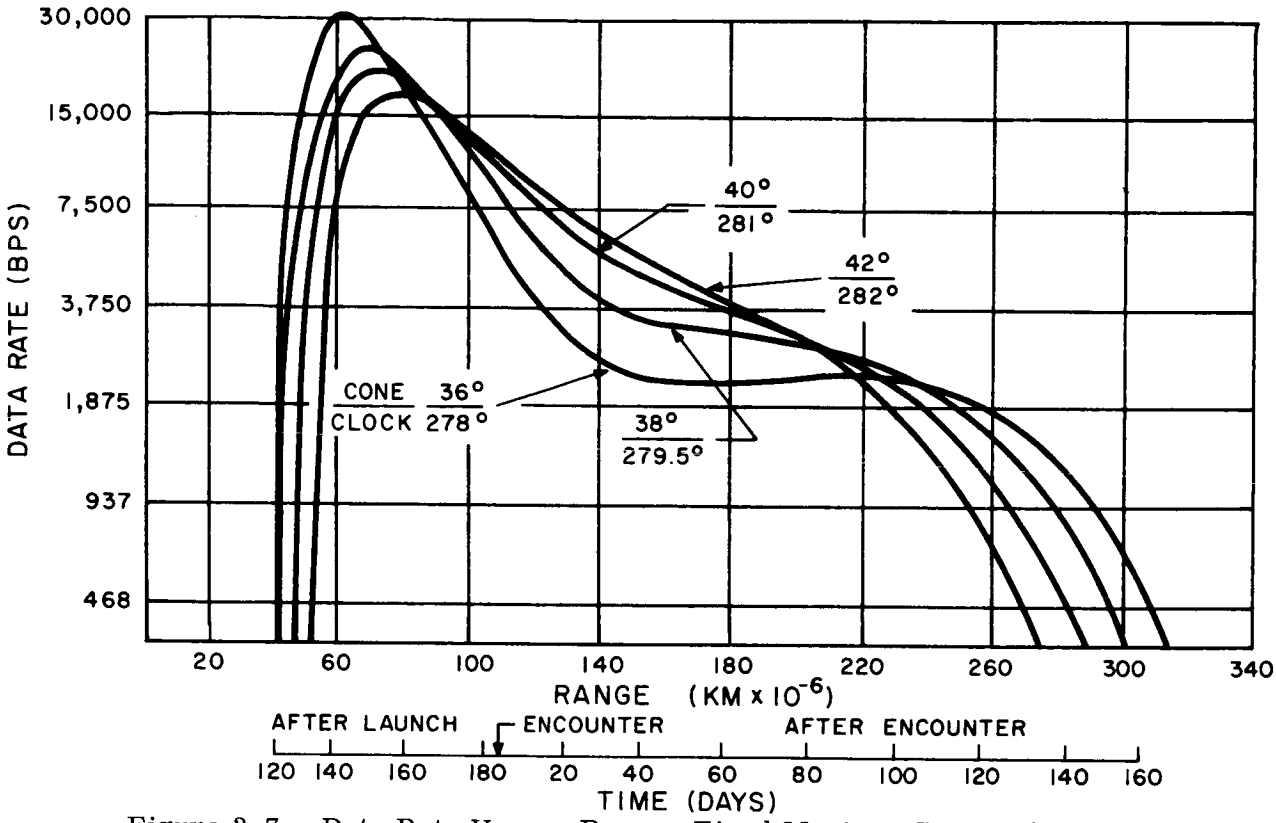


Figure 3-7. Data Rate Versus Range, Fixed Mariner C Type Antenna

the results for the Mariner C antenna for a typical 1971 trajectory with an early arrival date (November 1, 1973). The system data rate capability is plotted as a function of range, and time referenced to encounter, for different aiming points of the antenna. The aiming points are designated as the cone and clock angles to which the peak of the beam is pointed. Encounter occurs at cone and clock angles of 42° and 282° respectively. As time passes, the cone angle to the Earth increases to a maximum of about 43 degrees, and then decreases. The communication range increases after encounter until after the end of the nominal mission. If the peak of the antenna beam is aimed at the Earth at encounter, the period of communication coverage is the shortest.

The period of coverage may be increased by aiming the antenna at lower cone angles so that the peak of the beam points to the Earth at some time after encounter, compensating for the increased communication range. However, this increased coverage is accomplished at the expense of obtaining a high data rate for a longer period of time shortly after encounter. For example, comparing the curves for the extreme cases considered which correspond to aiming points of 42°/282° and 36°/278°, the former will support the lowest data rate for the return of planet scan data of 933 1/3 bps until 120 days after encounter, while the latter will support it until 150 days after encounter. However, with the beam aimed at 42°/282°, 7500 bps may be supported to 20 days after encounter, while with it pointed at 36°/278°, 7500 bps can not be achieved at all after encounter. Thus the total data return is much greater when the beam is aimed at the cone and clock angles to the Earth at encounter, even though the total coverage time is shorter. Assuming that the increased data return is more valuable than the longer coverage, aiming the antenna at the Earth at encounter is more desirable, and is therefore selected. Similar plots were made for other possible fixed antenna configurations.

For the 1971 trajectory resulting in an early encounter, higher-gain antennas than the Mariner C antenna would be desirable, based on the criterion of maximizing the data return. For example, a 3 x 5-foot antenna with a peak gain of 25 db, compared with the gain of 23.5 db for the Mariner C antenna, will support 7500 bps for 40 days after encounter and 933 1/3 bps for about 120 days. More detailed studies should be made considering other arrival times and antenna configurations as well as the data return optimization criteria. For the present design the already developed and proven Mariner C design provides a powerful backup capability.

3.4.3.3 Low-Gain Antennas. To meet the communications requirements during all mission phases at least two low-gain antennas are required. Type and location of these antennas are influenced by factors such as size and shape of the planetary vehicle and its varying attitude with respect to Earth, ease of stowage and deployment, redundancy and backup considerations, and interference by other deployed elements (high-gain antenna and planet scan package).

A test program was conducted with the objective to evaluate, by actual measurement, the relevant performance characteristics of several candidate low-gain antennas in the presence of the interfering vehicle. Measurements were performed on a scale model basis, using a scale factor of 1:5 at a test frequency of 5 x 2.2 = 11.0 Gc. This scale factor results in a vehicle model of reasonable size and in model antennas which can be built with practical tolerances. Figure 3-8 shows the configuration used. It shows the model of the vehicle with the two low-gain antennas mounted and with mockups of the deployed high-gain antenna and planet scan package. It should be noted that the vehicle model shape had to be selected before the preferred configuration was finalized. The model envelope is representative of a vehicle with a large capsule, except for the transition between the cylindrical spacecraft body and the capsule. This transition should be gradual by a cone tapering down to the diameter of the spacecraft body. Measurements were also made with a small capsule model (12-foot diameter).

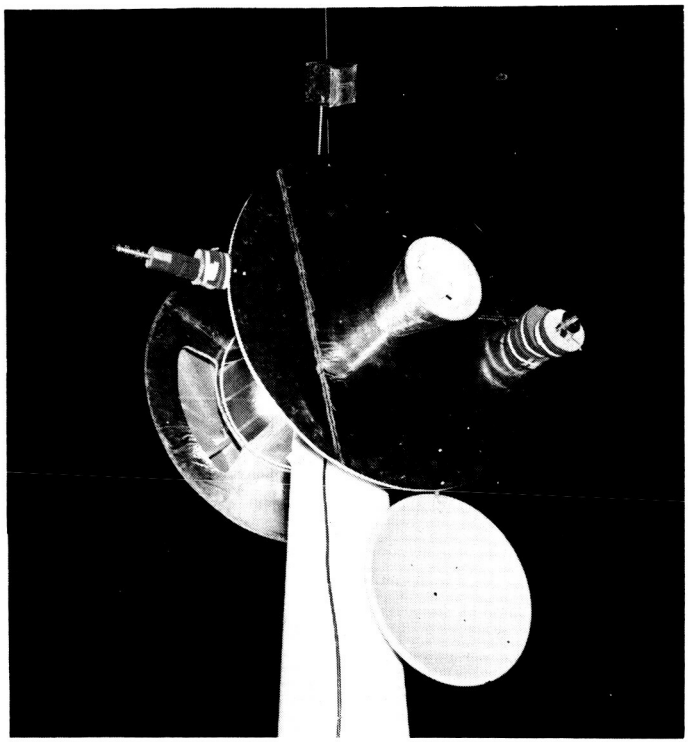
Three antennas, shown in Figure 3-8, were investigated:

a. A crossed slot, Mariner C-type antenna with a hemispherical pattern

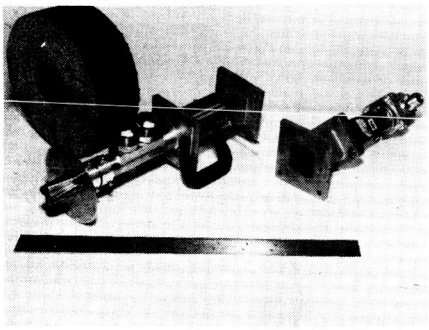
b. A parallel plate antenna with a toroidal pattern

c. A turnstile antenna over a conical ground plane with a flat-nosed hemispherical pattern.

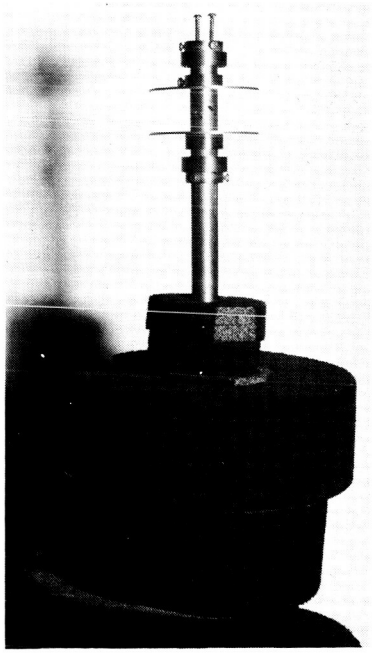
All three antennas were initially adjusted for a desirable "free space" pattern and for optimum on-axis circular polarization. The impedance match at the test frequency was accomplished by external stub tuning. These preliminary pattern measurements were made on a short outdoor range (15 feet long, 18 feet above ground); the circularity measurements were made on a short (4-foot), absorber-lined indoor range. Pattern and circularity measurements were then made with the antennas mounted on the vehicle model. These measurements were made on an indoor, anechoic chamber range (120 feet long x 40 feet wide x 24 feet high). The entire room (which is also used for radar cross section measurements) is lined with broadband, high-frequency absorber material. All test equipment, except for the source antenna, is located outside the chamber. Due to the near-isotropic character of these low-gain antennas,



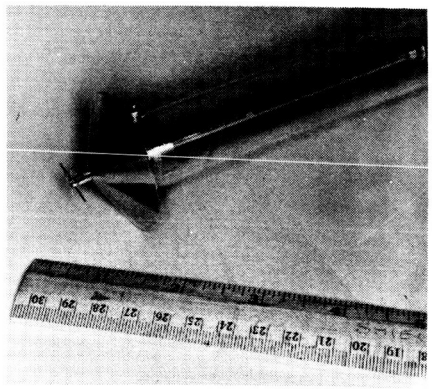
SCALE MODEL WITH TEST ANTENNAS MOUNTED ON INDOOR RANGE



MARINER C TYPE
CROSSED SLOT ANTENNA



PARALLEL PLATE ANTENNA



TURNSTILE ANTENNA OVER
CONICAL GROUND PLANE

Figure 3-8. Antenna Tests on Low Gain Antennas

range reflections are a problem and considerable effort was expended to determine the nature and magnitude of the reflections and to reduce them to an acceptable level by selecting the proper range geometry and by the use of additional RF absorber material.

The measuring program included tests under the following conditions:

a. Various boom lengths for the crossed slot antenna
b. Various boom lengths for the parallel plate antenna
c. Various look angles for the parallel plate antenna
d. Various orientations of the high-gain antenna and planet scan package

Patterns were measured in planes where shadowing by the vehicle body or reflections from the vehicle body were judged to be critical for the configuration under test. For the configuration shown in Figure 3-8, patterns were measured in a sufficient number of roll planes to prepare signal level contour plots for the entire 4 π solid angle.

The significant results and conclusions can be summarized as follows:

a. For maximum reliability it is desirable to have at least one low-gain antenna mounted in a fixed position. A modified Mariner C-type antenna selected as the primary low-gain antenna meets this requirement best. When mounted in the preferred configuration as shown, this antenna will provide coverage at high cone angles for the near-Earth phase. By tilting it away from the -Z axis, blockage by, and reflections from, the rocket motor are minimized. If the nozzle is RF-transparent, tilting the antenna would not be required. A longer fixed support would be desirable to make full use of the broad pattern that can be obtained from this type antenna. The present envelope restrictions however, prohibit this. With an optimized design the following minimum gain levels should be obtained in the X-Z plane:

Angle Off Thrust Axis (-Z Axis)	Gain
110° (near Earth)	-5 db
90° (near Earth)	0 db
0° (-Z axis)	+2 db
40° (encounter)	0 db

b. The secondary low-gain antenna should be as omnidirectional as possible since (it is used during maneuvers) and should complement the primary low-gain antenna, while providing maximum possible gain in the direction of the -Z axis. The size of the planetary vehicle (spacecraft and capsule) dictates the use of a boom-deployed antenna, to reduce the shadow region. The measurements on the model vehicle with a large capsule, using a 5-foot (full size) long support boom, show that the coverage at the -6 db gain level is reduced to 67% of the entire 4 π solid angle, from 87%

obtainable without shadowing. An optimized design should result in the following nominal gain levels in the X-Z plane:

Angle Off Thrust Axis (-Z Axis)	Gain
-90° (near Earth)	-∞ db (pattern null)
0° (-Z axis)	0 db
+40° (encounter)	-1.5 db

c. Measurements on the toroidal pattern antenna with smaller boom lengths show unacceptable ripple in the plane of the toroid due to reflections off the vehicle body in addition to an increased shadow region.

d. A broad hemispherical pattern, similar to the pattern of the primary antenna, was also considered for the secondary low-gain antenna. This pattern would have maximum gain in the direction of the +X axis and would eliminate the null of the toroidal pattern. This would be at the expense of gain in the hemisphere centered about the -Z axis and at the expense of omnidirectional coverage. It is concluded that the toroidal pattern is the best choice for the case of a vehicle with a small capsule (1971). Further detailed studies are required to optimize for specific, large-capsule configurations.

e. Altering the position of the high-gain antenna and the planet scan package did not show any significant effects on the radiation characteristics in the X-Z plane. More complete investigations are required to confirm this observation.

f. The desired flat-nosed hemispherical pattern was not readily obtained on the turnstile antenna. No measurements with this antenna mounted on the spacecraft model were performed.

g. The test program improved the skill in development and design of antennas of this type and demonstrated the adequacy of the test facilities for acceptance and qualification testing.

3.4.3.4 Relay Antenna. The 400 mc relay antenna selected is a turnstile above a ground plane. Figure 3-9 shows the required gain of this antenna as well as the idealized gain obtained plotted as a function of the angle between the line of sight to the capsule from the spacecraft and the spacecraft +Z axis. This angle is based on the spacecraft maintaining the attitude it had at capsule separation until capsule impact. The required gain was calculated using the formula:

$$G = -5 + 10 \log_{10} R$$

where:

G = the required antenna gain in db
R = the range from the spacecraft to capsule in thousands of kilometers

During descent from orbit, the capsule is generally in the +Z direction as viewed from the spacecraft; the range increases to a maximum of about 1800 km at capsule entry. The

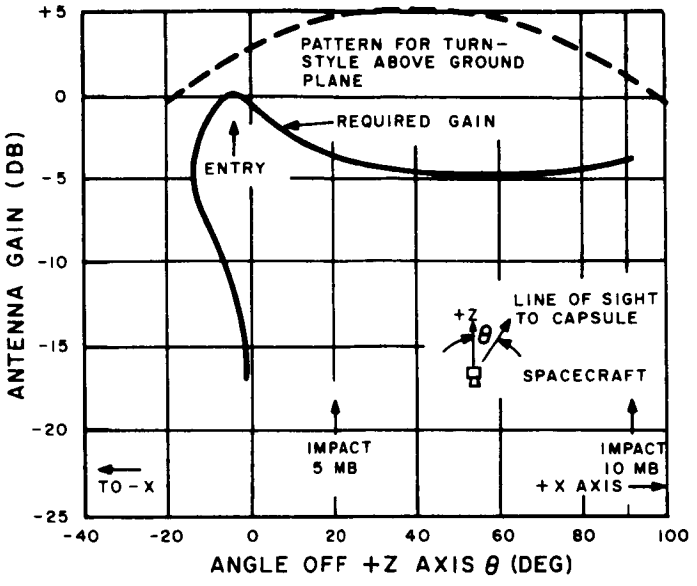


Figure 3-9. Relay Antenna Coverage

angular excursion of the line of sight from separation to entry is less than 15 degrees. As the capsule enters, the communication range decreases and the angle increases between the +Z axis and the line of sight. For the atmosphere corresponding to a 5 millibar (mb) surface pressure, the line of sight has moved 20 degrees toward the +X axis at impact; for a 10 mb atmosphere, the line of sight has moved to near the +X axis at impact.

The beamwidth of the selected antenna is broad enough so that the antenna may be fixed to the spacecraft body for this trajectory. The peak of the antenna beam is pointed 40 degrees off the +Z axis in the X-Z plane. The principal obstruction to the antenna view is the capsule biological barrier. For the 1971 capsule, it was assumed that the barrier is less than 12 feet in diameter, and the angle from the beam center to the edge of the barrier is greater than 60 degrees. The antenna gain at this point will be more than 5 db below the peak gain of 5 db. The effect of reflections off the barrier must be studied in depth, but it is expected that the pattern degradation will be acceptable. The nominal gain margin of the selected antenna above the minimum requirement is about 4 db at capsule impact for the 10 mb atmosphere, and is 8.5 db for the 5 mb atmosphere.

For the case shown, a single fixed antenna will satisfy the requirements. More detailed studies must be made for a variety of spacecraft orbits and entry trajectories, and to determine the effect of the vehicle and biological barrier on the antenna pattern.

3.4.4 Error Control Coding. Error control coding was again reviewed for use in the telemetry link. A more powerful code than was considered in the Task A study was examined, and the results of the studies are reported here. The code is a "regular bi-simplex" (63, 7) code which provides at threshold a theoretical performance improvement (compared to no coding) of 2.3 db on the basis of equivalent bit error probability, and 3.4 db on the basis of equivalent word error probability.

The principal reason it was not recommended was that it is not a proven deep-space technique, and therefore a development program with attendant uncertainties in cost, schedule and realizable performance must be undertaken. Because it appears to offer a significant improvement in performance for a small reliability penalty, it is recommended that the development of the system be carried out so that it may be considered for future VOYAGER spacecraft. For this reason, the work which has been carried out to date in estimating the

performance capability of the code and in defining an approach to implementing an encoder and decoder, including a synchronization scheme, is described in the following sections.

3.4.4.1 Selection of the Code. From the class of all binary group codes one code, the (63,7), has been selected as the most promising for application to the Voyager telemetry link. Initially, attention was focused on this code because: (1) its seven-bit word length is the same as that of the data; (2) its performance closely approximates that of the (64,7) bi-orthogonal code (and also that of the (127,7) regular simplex code, which is generally thought to be the optimum seven-bit code); and (3) the integer ratio (9) of total digits to information digits simplifies the necessary timing circuits. Investigation of the performance of the (63,7) code and the complexity of the decoder (correlator) required at the receiver confirmed that it provides a very good balance between power of performance and complexity of implementation. This investigation is presented in the following three sections.

3.4.4.2 Performance of the (63,7) Code. For direct transmission without any error correction coding the probability of error of a seven bit word is:

$$p_7 = 1 - (1 - p_1)^7 = 7\,p_1 - \binom{7}{2} p_1^2 + \binom{7}{3} p_1^3 - \cdots \qquad (1)$$

where p_1 is the probability of error of a single bit. For optimum signals optimally detected, in white gaussian noise, p_1 is given as a function of the ratio of the signal energy per bit to the noise spectral density by:[1]

$$p_1 = R\left(\sqrt{2E/N_o}\right) \qquad (2)$$

where

$$R(x) = \frac{1}{\sqrt{2\pi}} \int_x^\infty e^{-t^2/2}\,dt$$

In order to give a good estimate of the performance of the (63,7) code, it is necessary first to investigate some closely related codes.

There is general agreement (although no proof) that, for a fixed number of information bits per word, the optimum code for the white gaussian noise channel is a regular simplex code. The signals of such a code can be constructed from those of an orthogonal code by shifting the origin of the signal vectors of an orthogonal code to the point which is the sum of the signal vectors. Hence the performance of a regular simplex code is readily obtained given that of an orthogonal code. There is a cyclic group code having 2^m-1 total digits, m information

---

1 Eq. (2) is derived in many places, including:
"On Coded Phase Coherent Communications", A. J. Viterbi, IRE Transactions on Space Electronics and Telemetry, SET - 7, No. 1, March 1961.

bits, and a Hamming distance of 2^{m-1}, for every positive integer m, which is a regular simplex code. For m = 7, such a code has 127 digits and a Hamming distance of 64, and can correct 31 or fewer errors per word.

Signals which form a regular bi-simplex code can be obtained from the signals for a regular simplex code by including the (negative) complements of all the signals. There is a group code version of a regular bi-simplex code also. It has $2^{m-1}-1$ total digits, m information bits, and a Hamming distance of $2^{m-2}-1$. For m = 7, this is the (63,7) code, which has Hamming distance 31 and can correct 15 or fewer errors per word.

Assuming correlation detection, which is optimum, the theoretical probability or word error for the white gaussian noise channel is plotted in Figure 3-10 for the (127,7) regular simplex code, the (64,7) biorthogonal code, and no coding.[1]

From the binary code version of a biorthogonal (64,7) code it is possible to construct a regular bi-simplex (63,7) code by deleting one digit. By this process, the distances between some of the code words will be reduced, but none will be increased. From these observations a lower bound on the probability of error for the regular bi-simplex (63,7) code can be obtained; however, it is of little value since it falls to the left of the curve for the (127,7) regular simplex code. Now an upper bound on the probability of error for the regular bi-simplex (63,7) code is provided by shifting the curve for the probability of error for the bi-orthogonal (64,7) code to the right by 10 log 32/31 = 0.138 db, because if all the distances of the (63,7) code were increased by the factor 32/31 the resulting distances will equal or exceed those of a (64,7) code whose minimum distance is 32/31 times that of the original (63,7) code.

This bound on performance of the regular bi-simplex (63,7) code is also plotted in Figure 3-10. Because the number of distances affected by the code alterations is very nearly one-half the total number of distances, an excellent estimate of the performance of the (63,7) code will result by a curve just halfway between the bound and the curve for the (64,7) code. Such an estimate along with the curve for no coding is shown in Figure 3-11.

For a regular bi-simplex code a good estimate of bit error probability is obtained by taking one half the word error probability, because, given a word error, all words other than the transmitted word and its complement are nearly equally likely to result; i.e., the resulting word is selected nearly at random and so any digit has nearly equal probability of being a "1" or a "0". Figure 3-12 shows this estimate of the probability of bit error for the regular bi-simplex (63,7) code along with the probability, p_1 of error without coding.

Since the performance of the regular bi-simplex (63,7) code so closely approximates that of the regular simplex (127,7) code as well as that of the biorthogonal (64,7) code, it suffices to limit consideration of seven-bit codes to only one of these codes. Because of the integer ratio of total digits to information bits of the (63,7) code, it requires less complex timing

1. Ibid.

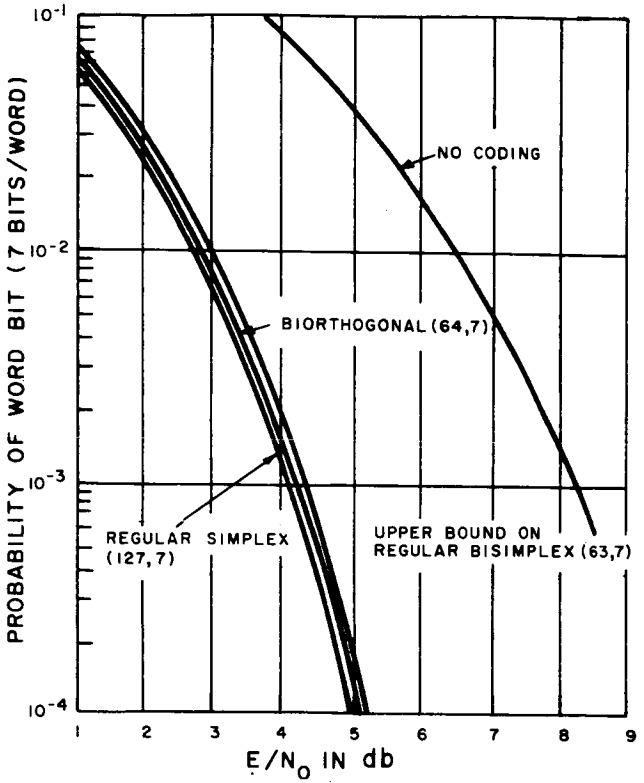


Figure 3-10. Word Error Probability for Codes Bounding (63, 7) Code

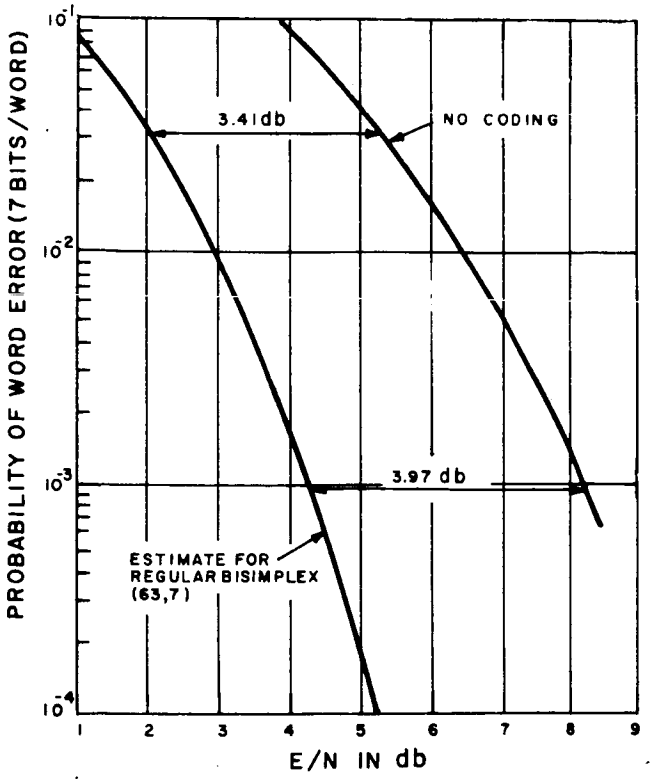


Figure 3-11. Word Error Probability for (63, 7) Code

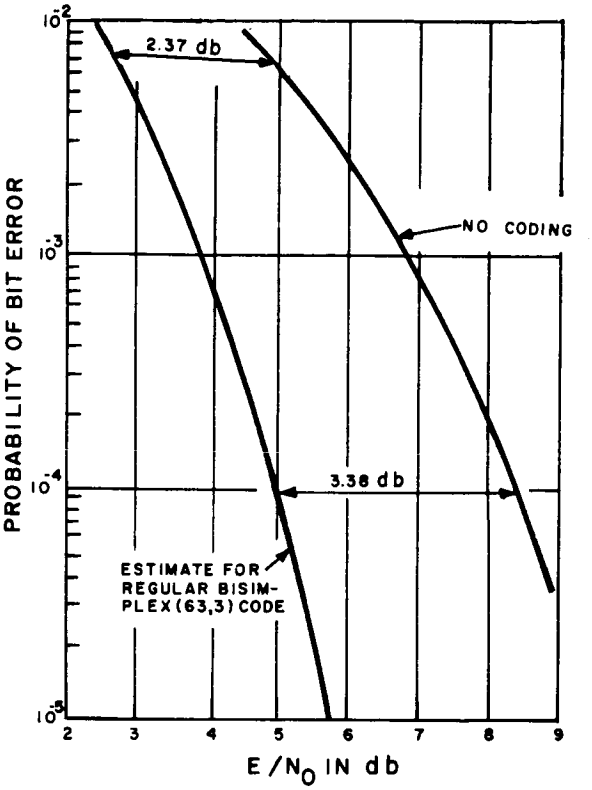


Figure 3-12. Equivalent Bit Error Probability for (63, 7) Code

circuitry for encoding and decoding than do the others. As the encoder must be aboard the spacecraft, the (63, 7) code is to be preferred over the others.

The improvement obtained by using a code is most conveniently expressed as the db increase in E/N_0 required to achieve some specified error rate without coding over that using the code. From Figures 3-11 and 3-12 it is evident that the improvement depends upon whether word error rate or bit error rate is specified as well as the error rate or E/N_0. Table 3-5 lists some representative data obtained from the figures. The last line of the table indicates the limiting value of improvement as E/N_0 approaches infinity.*

*For a derivation, see: "Word Error Rate for Group Codes Detected by Correlation and Other Means", C. M. Hackett, Jr., IRE Transaction on Information Theory, Vol. IT 9, No. 1, pp. 24-33, Jan. 1963.

TABLE 3-5. IMPROVEMENT FOR (63,7) CODE

E/N_o No Coding (db)	Probability of Word Error	Probability of Bit Error	Improvement Based on Word Error (db)	Improvement Based on Bit Error (db)
5.22	3.45×10^{-2}	5.00×10^{-3}	3.41	2.37
6.47	1.00×10^{-2}	1.46×10^{-3}	3.63	2.82
7.33	3.45×10^{-3}	5.00×10^{-4}	3.79	3.11
8.17	1.00×10^{-3}	1.46×10^{-4}	3.97	3.38
8.79	3.45×10^{-4}	5.00×10^{-5}	4.08	3.56
∞	0	0	5.37	5.37

It is generally true that a good error correcting block code shows more improvement on a word-error basis than on a bit-error basis, and that the improvement increases with E/N_o. Thus it is important to specify as accurately as possible the conditions under which the code will be applied so that its performance can properly be assessed.

For the VOYAGER telemetry link, the highest acceptable bit error rate is specified to be 5×10^{-3}. From the above analysis, it is estimated that the theoretical improvement afforded by the (63,7) regular bisimplex code under this criterion is 2.37 db. If the data comes naturally in 7-bit blocks, the appropriate criterion is word error rate, and for a word error rate of 3.45×10^{-2} (corresponding to a bit error rate of 5×10^{-3}), the improvement is 3.41 db. As indicated above, both measures of improvement increase with E/N_o, both having an asymptotic limit of 5.37 db.

If the data occurs in blocks of length other than 7 (or a multiple of 7), and a 7-bit error correcting code is used, the proper measure of improvement lies between that for bit error rate and that for word error rate. For any specified format, it is possible to calculate an estimate of improvement, using no more approximations than were used above.

3.4.4.3 Encoder-Decoder. The functional design and operation of the encoder-decoder will be broadly described in this section. Many variations in detail are possible, and may in fact be desirable, but their discussion will be sacrificed so that attention can be concentrated on the basic features of the encoder, decoder, and the requisite synchronization. A simplified diagram of the encoder-decoder is shown in Figures 3-13 and 3-14 respectively.

3.4.4.3.1 Encoder. The input data is assumed to be a stream of binary digits. The encoder takes the input data 7 bits at time and generates 63-digit (cyclic) code words. A 63-digit pseudo-random binary pattern is generated and added mod-two synchronously with the code word. The resulting digits are Manchester-coded and then used to phase modulate the carrier. The pattern enhances the difference between any code word and every sequence which results from the end of one code word and the start of the next, so that word synchronization is better achieved. Manchester coding removes the spectrum of the data from the neighborhood of the carrier so that it can be easily tracked as doppler and oscillator instability cause variations.

3.4.4.3.2 Decoder. To obtain data from the incoming waveform the decoder must:

a. Recover half-digit synchronization
b. Determine word synchronization
c. Determine the most likely transmitted code words
d. Convert these code words into data bits

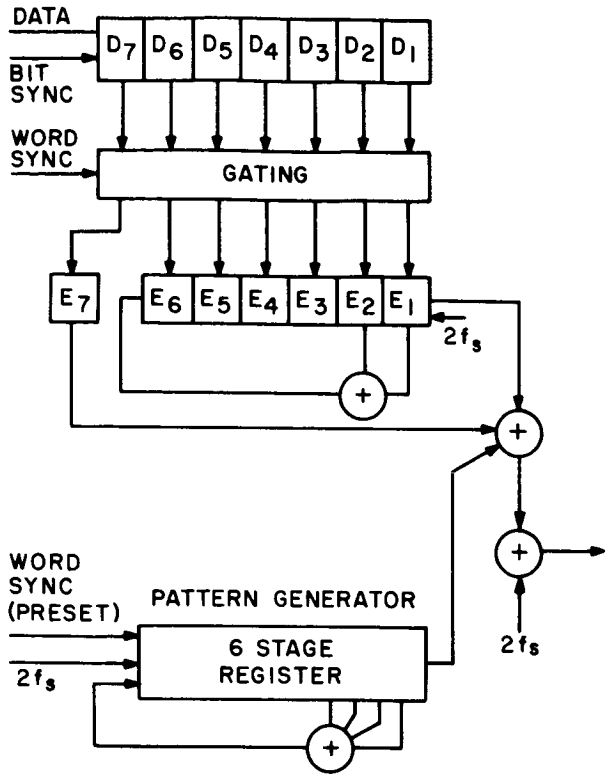


Figure 3-13. Error Control Encoder

Word synchronization is established by correlating the incoming waveform with locally-generated signals at each possible word phase, and determining by the highest output level which word phase is most likely. This technique depends on the correlation being high when synchronization is correct, and low when synchronization is incorrect. *

As shown in Figure 3-14 the incoming waveform following translation to baseband consists of the Mod 2 sum of a PN pattern (P), code words drawn from a regular bi-simplex code (C), and a subcarrier (2 f_s). The pattern and code digits are of equal duration, while the subcarrier rate is one cycle per digit. The combined signal

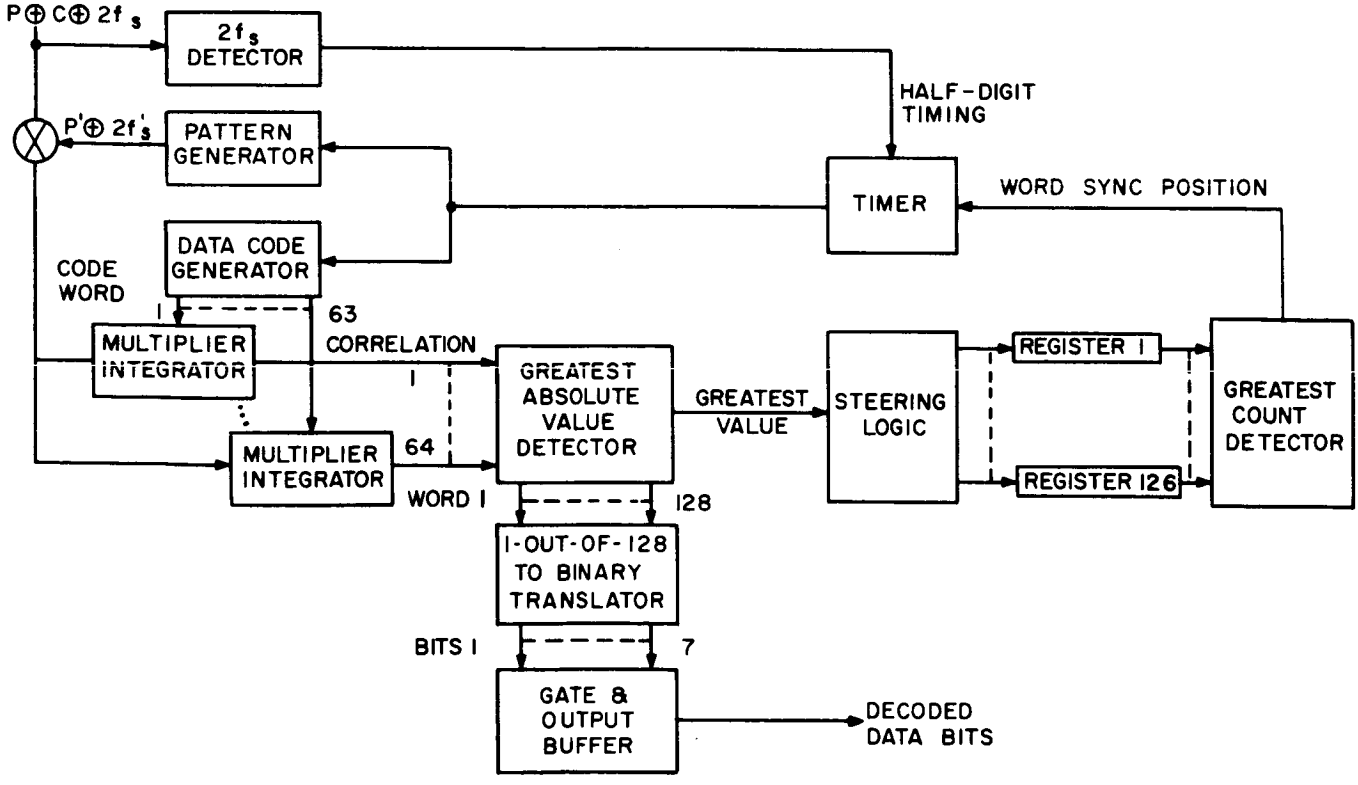


Figure 3-14. Error Control Decoder

* S. W. Golomb et al., "Digital Communications With Space Applications," pp. 142-159, Prentice-Hall, 1964.

enters the $2f_S$ detector* where the subcarrier is recovered, although with a 180 degree ambiguity in phase. The $2f_S$ detector provides half-digit timing to the timer, which drives the pattern generator and data code generator. The timer also causes the generators to slip bits during the sync acquisition interval, and presets the generators when proper bit and word timing have been found. The pattern generator produces a $P' + 2f_S'$ sequence which is multiplied by the incoming waveform. The pattern P' is identical to the received pattern P, but P' is in general phase-shifted with respect to P when sync acquisition begins.

The composite waveform is then fed to a bank of 64 integrators. One of these corresponds to the all-zero code word, while the other 63 are driven from the data code generator with the remaining words in the code vocabulary. After integration by an integrate-and-dump filter in each channel, the correlations (which are bipolar) are fed to the greatest absolute value detector. This detector selects the channel having the level of greatest magnitude, and feeds this level through an A/D converter to one of 126 registers. If the initial phase chosen by the timer is called (arbitrarily) sync position 1, then the greatest absolute value resulting from this sync position is entered in register 1.

The timer then causes the pattern and code generators to slip a half-digit to sync position 2, and the greatest absolute value resulting from correlation over this word interval is entered in register 2. The procedure is repeated until all of the 126 possible sync positions have been used.

At this point a decision could be made as to the most likely sync position by determining which register holds the greatest value. The probability of error is reduced, however, by further averaging. The procedure described above is repeated two or more times and at each subsequent sync position the greatest absolute value is added to the value held in the register corresponding to that sync position. After a predetermined number of cycles, the register holding the greatest sum is located by the greatest value detector, and word sync position is determined from the position of this register in the register bank. The timer slips the phase of the pattern and word code generators to this position, and data is decoded. To guard against subsequent loss of synchronization, one of the registers continues to operate as data is decoded. If the value summed over a given number of words fails to exceed a threshold, resynchronization is initiated.

The code word correlations upon which the word decisions are based can be implemented in either an analog or digital fashion; in the preceding discussion, analog was assumed.

4.0 INTERFACE DEFINITIONS. The detailed boundary definitions and interface characteristics between the telecommunication subsystem and other spacecraft systems are specified in the individual subsystem functional descriptions.

5.0 PERFORMANCE PARAMETERS. This section summarizes the parameters and performance characteristics of the telecommunications system.

---

*J. C. Springett, "Telemetry and Command Techniques For Planetary Spacecraft," Technical Report No. 32-495, pp. 28-29, JPL, Jan. 15, 1965.

5.1 System Parameters. Tables 5-1 and 5-2, together with Figures 5-1 and 5-2, give the values of the significant parameters that determine the performance of the telemetry and command links. The parameters have been grouped into four categories (Transmission Mode, Channel, Reception Mode, and Polarization Loss) such that their combinations provide all inputs to the design control tables for the selected links. Sample design control tables for telemetry and command links have been included in Appendix A to indicate changes made in the normal format to describe the characteristics of the recommended system.

In addition to the parameters contained in Tables 5-1 and 5-2 are the following characteristics of the telemetry, command, and ranging channels (see VC233FD103 for characteristics related to command word structure).

5.1.1 Telemetry

a. Type of Encoding.

1. 7.3-bps channel: single-channel, square-wave, phase-shift keying with PN sync, 9 PN bits per data bit (NRZ).

   Waveform = data $\oplus$ PN $\oplus$ $2f_s$.

2. 117-bps channel: single-channel, square-wave, phase-shift keying with PN sync, 9 PN bits per data bit (MNRZ) on 270-kc square-wave subcarrier (f_o).

   Waveform = data $\oplus$ PN $\oplus$ $2f_s \oplus f_o$.

3. 14933/117; 7467/117; 3733/117; 933/29: two-channel, square-wave, phase-shift keying with PN sync, 9 PN bits per data bit (NRZ lower channel, MNRZ upper channel); upper channel (117 or 29 bps) on 270-kc square-wave subcarrier (f_o).

   Waveform = $K_1\ data_1 \oplus PN_1 \oplus 2f_{s1} + K_2\ data_2 \oplus PN_2 \oplus 2f_{s2} \oplus f_o$

b. Channel Requirements.

1. Engineering measurements: 394.
2. Event counters: 4.

c. Word length: 7 bits.

d. Transmission rates.

1. 7.3 bps.
2. 117 bps.
3. 933/29 bps.
4. 3733/117 bps.
5. 7467/117 bps.
6. 14933/117 bps.

e. Threshold telemetry data signal-to-noise ratio in a 1-cps noise bandwidth that results in the minimum acceptable telemetry bit error probability ($5x10^{-3}$).

1. 7.3 bps : 15.12 db/cps
2. 29 bps : 22.64 db/cps
3. 117 bps : 28.67 db/cps
4. 933 bps : 35.6 db/cps
5. 3733 bps : 41.6 db/cps
6. 7467 bps : 44.6 db/cps
7. 14933 bps : 47.6 db/cps

f. Mean bit acquisition time as a function of threshold SNR.

1. 7.3 bps : 181 sec
2. 29.2 bps : 75.8 sec
3. 117 bps : 18.9 sec
4. 933 bps : 2.36 sec
5. 3733 bps : 0.590 sec
6. 7467 bps : 0.296 sec
7. 14933 bps : 0.148 sec

5.1.2 Command

a. Number of Commands

1. Discrete : 183
2. Quantitative: 23

} 246 available

b. Modulation Type: Digital PSK with PN sync

c. Transmission Rate

1. Sub-bit rate: 1 or 30 SBPS
2. Command bit rate: 1/2 or 15 BPS

d. Threshold command data SNR in a 1-cps noise bandwidth that results in the minimum acceptable bit error rate (2×10^{-6}).

1. 13.2 db for 1 SBPS
2. 25.2 db for 30 SBPS

e. Mean bit sync acquisition time at the threshold SNR.

1. 4.25 minutes per code try at 1 SBPS
2. 15.5 seconds per code try at 30 SBPS

5.1.3 Ranging

a. Type: DSIF Mark I.

b. Maximum unambiguous range.

1. Short code : 10,000 km
2. Lunar code : 800,000 km
3. Planetary code: 40×10^6 km

c. Code Components.

Component	Bit Length		
	Short	Lunar	Planetary
Clock	2	2	2
X	11	11	7
A	31	31	11
B	63	7	23
C	127	15	31
D	-	-	47
E	-	-	103

TABLE 5-2. COMMAND PARAMETERS

COMMAND TRANSMISSION PARAMETERS

Parameter \ MODE	DSIF 71	DSIF 72	Acquisition	85 Ft 100kw	85 Ft 400kw	210 Ft 100kw
Power Transmitted (watts)	5	10^4	10^4	10^5	$4x10^5$	10^5

31	Modulation Loss (Sync A)	-2.4 + 0.6 - 0.7	----	----	-2.1 + 0.5 - 0.6	-2.1 + 0.5 - 0.6	-2.1 + 0.5 - 0.6	-2.1 + 0.5 - 0.6
33	Sync APC Noise BW (Sync A)	-6.0 ± 0.4	----	----	10.5 ± 0.4	9 ± 0.4	7.5 ± 0.4	4.5 ± 0.4
34	Threshold SNR in $2B_{Lo}$ (Sync A)	18.6 ± 0	----	----	26.9 ± 0	26.1 ± 0	25.4 ± 0	23.9 ± 0
37	Modulation Loss (Subcarrier)	----	-1.3 + 0.4 - 0.6	-1.3 + 0.4 - 1.6	-14 + 1.3 - 1.6	-14 + 1.3 - 1.6	-14 + 1.3 - 1.6	-14 + 1.3 - 1.6
39	Subcarrier APC Noise BW	----	0 + 0 - 0.5	0 + 0 - 0.5	0 + 0 - 0.5	0 + 0 - 0.5	0 + 0 - 0.5	0 + 0 - 0.5
40	Threshold SNR in $2B_{Lo}$ (Subcarrier)	----	26.2 ± 0	26.2 ± 0	26.2 ± 0	26.2 ± 0	26.2 ± 0	23.2 ± 0
43	Modulation Loss (Data B)	----	-1.3 + 0.4 - 0.6	-1.3 + 0.4 - 0.6	-14 + 1.3 - 1.6	-14 + 1.3 - 1.6	-14 + 1.3 - 1.6	-14 + 1.3 - 1.6
45	Bit Rate (Data B)	----	20.7 ± 0	20.7 ± 0	20.7 ± 0	20.7 ± 0	20.7 ± 0	14.7 ± 0
46	Required ST/N/B (Data B)	----	8.0 ± 0.5	8.0 ± 0.5	8.0 ± 0.5	8.0 ± 0.5	8.0 ± 0.5	8.0 ± 0.5
49	Modulation Loss (Sync B)	----	-1.3 + 0.4 - 0.6	-1.3 + 0.4 - 0.6	-14 + 1.3 - 1.6	-14 + 1.3 -1.6	-14 + 1.3 - 1.6	-14 + 1.3 - 1.6
51	Sync APC Noise BW (Sync B)	----	0 ± 0.4	0 ± 0.4	0 ± 0.4	0 ± 0.4	0 ± 0.4	-3 ± 0.4
52	Threshold SNR in $2B_{Lo}$ (Sync B)	----	21.6 ± 0	21.6 ± 0	21.6 ± 0	21.6 ± 0	21.6 ± 0	20.1 ± 0

Telemetry Reception Parameters

	Mode / Parameter	DSIF 71	DSIF 72	Acquisition	85 Ft.	210 Ft.
	Antenna	4-ft dish	30-ft dish	2-ft dish	85-ft dish	85-ft dish
	Antenna Pointing Error (deg)	5 + 0 - 5	0.5 + 0 - 5	0.22 + 0 - 0.22	0.02 + 0 -0.02	0.02 + 0 - 0.02
	Antenna Axial Ratio (db)	Linear	1 ± .5	< 1.5	0.7 ± 0.3	0.7 ± 0.3
	System Noise Temperature (°k)	3000	290	300	55	35

DCT No. DCT Parameters

DCT No.						
7	(e) Receiving Antenna Gain	26 ± 1	44 ± 1	22 ± 1	53.3 ± 1	61.9 ± 1
8	Receiving Antenna Pointing Loss	$-4.8 \begin{smallmatrix}+4.8\\-0\end{smallmatrix}$	$-0.5 \begin{smallmatrix}+0.5\\-0\end{smallmatrix}$	0 ± 0	$-0.1 \begin{smallmatrix}+0.1\\-0\end{smallmatrix}$	$-0.3 \begin{smallmatrix}+0.3\\-0\end{smallmatrix}$
9	(f) Receiving Circuit Loss	0 ± 0	0 ± 0	0 ± 0	0 ± 0	0 ± 0
12	(e) Receiver Noise Spectral Density (dbm)	$-163.9 \begin{smallmatrix}+0\\-1\end{smallmatrix}$	$-174.0 \begin{smallmatrix}+0\\-1\end{smallmatrix}$	$-173.9 \begin{smallmatrix}+0\\-1\end{smallmatrix}$	$-181.2 \begin{smallmatrix}+0\\-1\end{smallmatrix}$	$-183.2 \begin{smallmatrix}+0\\-1\end{smallmatrix}$

Polarization Loss - Telemetry Links (db)

Spacecraft Antenna \ Ground Antenna	DSIF 71	DSIF 72	Acquisition	85 Ft.	210 Ft.
(g) Parasitic	-3 ± 0	0 ± 0	0 ± 0	0 ± 0	----
Primary Low-Gain	----	$-0.1 \begin{smallmatrix}+0.1\\-0.1\end{smallmatrix}$	$-0.1 \begin{smallmatrix}+0.1\\-0\end{smallmatrix}$	$0 \begin{smallmatrix}+0\\-0.1\end{smallmatrix}$	$0 \begin{smallmatrix}+0\\-0.1\end{smallmatrix}$
Secondary Low-Gain	----	$-0.1 \begin{smallmatrix}+0.1\\-0.1\end{smallmatrix}$	$-0.1 \begin{smallmatrix}+0.1\\-0\end{smallmatrix}$	$0 \begin{smallmatrix}+0\\-0.1\end{smallmatrix}$	$0 \begin{smallmatrix}+0\\-0.1\end{smallmatrix}$
Medium-Gain	----	----	----	$0 \begin{smallmatrix}+0\\-0.1\end{smallmatrix}$	$0 \begin{smallmatrix}+0\\-0.1\end{smallmatrix}$
High-Gain	----	----	$-0.1 \begin{smallmatrix}+0.1\\-0\end{smallmatrix}$	$0 \begin{smallmatrix}+0\\-0.1\end{smallmatrix}$	$0 \begin{smallmatrix}+0\\-0.1\end{smallmatrix}$

NOTES

(a) Ideal circularly polarized isotropic antenna assumed for reference.
(b) See Figure 5-1 for combined gain and pointing loss vs. mission time.
(c) Zero pointing error assumed for reference.
(d) See Figure 5-2 for combined gain and pointing loss vs. mission time.
(e) The nominal value plus worst-case tolerance is equal to the worst-case value given in EPD 283; best-case value is estimated.
(f) Circuit losses are included in antenna gain.
(g) Ideal circularly polarized isotropic antenna assumed for reference.

VC233FD101

TABLE 5-1. TELEMETRY PARAMETERS

Telemetry Transmission Parameters

	Mode / Parameter	3-Watt Parasitic	3-Watt Primary Low-Gain	50-Watt Primary Low-Gain	50-Watt Secondary Low-Gain	50-Watt Medium-Gain	50-Watt High-Gain	3-Watt High-Gain
	Power Transmitted (watts)	3.8 +.9 -0.8	3.8 +.9 -0.8	50 + 13 - 10	50 + 13 - 10	50 + 13 - 10	50 + 13 - 10	3.8 +.9 -0.8
	Antenna	Parasitic on shroud	Crossed Slot	Crossed Slot	Quad-dipoles	Mariner-C 46x21.2-in. elliptical	7.5-ft dish	7.5-ft dish
	Antenna Pointing Error (deg)	(a)	(b)	(b)	(c)	(d)	1.5 + 0 - 1.5	1.5 + 0 - 1.5
	Antenna Axial Ratio (db)	(a)	1 ± 1	1 ± 1	1 ± 1	1 ± 1	1 ± 1	1 ± 1
DCT No.	DCT Parameters							
1	Total Transmitter Power (dbm)	35.8 ± 1	35.8 ± 1	47 ± 1	47 ± 1	47 ± 1	47 ± 1	35.8 ± 1
2	Transmitting Circuit Loss	-22.1 ± 0	-2.1 ± 0.4	-2.3 ± 0.4	-2.5 ± 0.4	-1.6 ± 0.4	-3.0 ± 0.5	-2.7 ± 0.5
3	Transmitting Antenna Gain	0 ± 0 (a)	2.0 ± 0.5	2.0 ± 0.5	0.0 + 1.0 - 0.5	23.5 + 0.3 - 0.5	32.5 + 0.4 - 0.6	32.5 + 0.4 - 0.6
4	Transmitting Antenna Pointing Loss	0 ± 0 (a)	(b)	(b)	0 ± 0 (c)	(d)	-1.5 + 1.5 - 0	-1.5 + 1.5 - 0

Telemetry Signal and Demodulation Parameters

	Channel / Parameter	7 bps	117 bps	117 bps	14933/117	7467/117	3733/117	933/29
	Data Rate-Ch A (bps)	7.3	----	----	14933	7467	3733	933
	Data Rate - Ch B (bps)	----	116.7	116.7	116.7	116.7	116.7	116.7
	Phase Deviation Ch A (rad.)	0.86 ± .086	----	----	1 ± 0.1	1 ± 0.1	1 ± 0.1	1 ± 0.1
	Phase Deviation Ch B (rad.)	----	1.05 ± 0.1	1.05 ± 0.1	0.38 ± 0.038	0.38 ± 0.038	0.38 ± 0.038	0.38 ± 0.038
	Bit Error Probability	5×10^{-3}	5×10^{-3}	5×10^{-3}	5×10^{-3}	5×10^{-3}	5×10^{-3}	5×10^{-3}
	$2B_{Lo}$-Carrier (cps)	5 + 0 - 0.55	0.12 + 0 - 1.3	152 + 0 - 26	48 + 0 - 5	48 + 0 - 5	48 + 0 - 5	48 + 0 - 5
	$2B_{Lo}$-Sync A (cps)	0.25 ± .025	----	----	11.2 ± 0.11	8 ± 0.8	5.6 ± 0.56	2.8 ± 0.28
	$2B_{Lo}$ Subcarrier (cps)	----	1 + 0 - 0.11	1 + 0 - 0.11	1 + 0 - 0.11	1 + 0 - 0.11	1 + 0 - 0.11	1 + 0 - 0.11
	$2B_{Lo}$-Sync B (cps)	----	1 ± 0.1	1 ± 0.1	1 ± 0.1	1 ± 0.1	1 ± 0.1	0.5 ± 0.05
DCT No.	DCT Parameters							
13	Carrier Modulation Loss	-3.7 + 0.8 - 1	-6 + 1.4 - 1.8	-6 + 1.4 - 1.8	-6 + 1.3 - 1.7	-6 + 1.3 - 1.7	-6 + 1.3 - 1.7	-6 + 1.3 - 1.7
15	Carrier APC Noise BW	7.0 + 0 - 0.5	10.8 + 0 - 0.5	21.8 + 0 - 0.5	16.8 + 0 - 0.5	16.8 + 0 - 0.5	16.8 + 0 - 0.5	16.8 + 0 - 0.5
16	Threshold SNR in $2B_{Lo}$ (1-way)	0 ± 0	0 ± 0	15 ± 0	0 ± 0	0 ± 0	0 ±0	0 ± 0
19	Threshold SNR in $2B_{Lo}$ (2 way)	----	2 ± 0	15 ± 0	2 ± 0	2 ± 0	2 ± 0	2 ± 0
22	Threshold SNR in $2B_{Lo}$ (data Demod)	7 ± 0	10 ± 0	10 ± 0	10 ± 0	10 ± 0	10 ± 0	10 ± 0
25	Modulation Loss (Data A)	-2.4 + 0.6 - 0.7	----	----	-2.1 + 0.5 - 0.6	-2.1 + 0.5 - 0.6	-2.1 + 0.5 - 0.6	-2.1 + 0.5 - 0.6
27	Bit Rate (Data A)	8.6 ± 0	----	----	41.7 ± 0	38.7 ± 0	35.7 ± 0	29.7 ± 0
28	Required ST/N/B (Data A)	6.5 + 0.5	----	----	5.9 + 0.5	5.9 + 0.5	5.9 + 0.5	5.9 + 0.5

	Antenna	4-ft dish	30-ft dish	2-ft dish	85-ft dish	85-ft dish	210-ft dish
	Transmission Frequency (mc)	2113	2113	2113	2113	2113	2113
	Antenna Pointing Error (deg)	5^{+0}_{-5}	$0.2^{+0}_{-0.2}$	$0.22^{+0}_{-0.22}$	$0.02^{+0}_{-0.02}$	$0.02^{+0}_{-0.02}$	$0.02^{+0}_{-0.02}$
	Antenna Axial Ratio (db)	linear	1 ± 0.5	< 1.5	1 ± 0.5	1 ± 0.5	1 ± 0.5
DCT No.	DCT Parameters						
1	[a] Total Transmitter Power (dbm)	$37^{+0.5}_{-0}$	$70^{+0.5}_{-0}$	$70^{+0.5}_{-0}$	$80^{+0.5}_{-0}$	$86^{+0.5}_{-0}$	$80^{+0.5}_{-0}$
2	[b] Transmitting Circuit Loss	0 ± 0	0 ± 0	0 ± 0	0 ± 0	0 ± 0	0 ± 0
3	[a] Transmitting Antenna Gain	24 ± 1	43 ± 1	20 ± 1	51.1 ± 1	51.1 ± 1	60.8 ± 1
4	Transmitting Antenna Pointing Loss	$-3.8^{+3.8}_{-0}$	$-0.5^{+0.5}_{-0}$	0 ± 0	$-0.1^{+0.1}_{-0}$	$-0.1^{+0.1}_{-0}$	$-0.2^{+0.2}_{-0}$

COMMAND SIGNAL AND DEMODULATION PARAMETERS

CHANNEL / Parameter	1 SBPS	30 SBPS
Data Rate (bps)	1	30
Phase Deviation -Data and Subcarrier Sync (rad.)	0.53 ± 0.053	$1.15 \pm .115$
Phase Deviation -PN Sync (rad.)	0.27 ± 0.027	0.6 ± 0.06
Bit Error Probability	2×10^{-6}	2×10^{-6}
$2B_{lo}$ - Carrier (cps)	20 ± 1	20 ± 1
$2B_{lo}$ - Subcarrier Sync (cps)	$0.4^{+0.08}_{-0.07}$	$3^{+0.6}_{-0.6}$

DCT No.	DCT Parameters		
13	Carrier Modulation Loss	$-0.9^{+0.3}_{-0.2}$	-4.8 ± 1.0
15	Carrier APC Noise BW	13 ± 0.2	13 ± 0.2

19	Threshold SNR in $2B_{lo}$ (2-way)	3.8 ± 0	3.8 ± 0
22	Threshold SNR in $2B_{lo}$ (Data Demodulator)	$8.5 + 1.0 - 0$	$8.5 + 1.0 - 0$
25	Modulation Loss (Data)	$-9.2 + 0.6 - 0.7$	$-5.0 + 0.3 - 0.2$
27	Bit Rate	0 ± 0	14.8 ± 0
28	Required ST/N/B	13.2 ± 0	10.4 ± 0
31	Modulation Loss (Data Subcarrier)	$-9.2 + 0.6 - 0.7$	$-5.0 + 0.3 - 0.2$
33	Data Subcarrier APC Noise BW	-4 ± 0.8	$4.8 + 0.8 - 1$
34	Threshold SNR in $2B_{lo}$ (Data Subcarrier)	16.4 ± 0	19.6 ± 0

COMMAND RECEIPTION PARAMETERS

	Mode / Parameter	Parasitic	Primary Low-Gain	Secondary Low-Gain	Medium-Gain	High-Gain
	Antenna	Parasitic on shroud	Crossed slot	Quad-Dipoles	Mariner C 46 x 21.2-in. elliptical dish	7.5-ft. dish
	Antenna Pointing Error (deg)	(c)	(d)	0 (e)	(f)	$1.5 + 0 - 1.5$
	Antenna Axial Ratio (db)	(c)	3 ± 3	1.5 ± 1	4 ± 3	4 ± 2
	System Noise Temperature (°K)	1750 +450 -425	1750 +450 -425	1750 +450 -425	1750 +450 -425	1750 +450 -425
DCT No.	DCT Parameters					
7	Receiving Antenna Gain	0 ± 0 (c)	1.3 ± 0.5	$-0.5 + 0.5 - 1$	$20.8 + 1.3 - 1.3$	30.3 ± 1
8	Receiving Antenna Pointing Loss	0 ± 0 (c)	(d)	0 ± 0 (e)	(f)	$-1.3 + 1.3 - 0$
9	Receiving Circuit Loss	-22.5 ± 0.7	-3.2 ± 0.8	-3.3 ± 0.8	-2.5 ± 0.8	-3.9 ± 0.9
12	Receiver Noise Spectral Density (dbm)	-166.2 ± 1.1	-166.2 ± 1.1	-166.2 ± 1.1	-166.2 ± 1.1	-166.2 ± 1.1

POLARIZATION LOSS-COMMAND LINK (db)

Spacecraft Antenna / Ground Antenna	DSIF 71	DSIF 72	Acquisition	85 Ft	210 Ft
Parasitic (g)	-3 ± 0	0 ± 0	0 ± 0	0 ± 0	-
Primary Low-Gain	-	$-0.2 + 0.2 - 0.5$	$-0.3 + 0.3 - 0.4$	$-0.2 + 0.2 - 0.5$	$-0.2 + 0.2 - 0.5$
Secondary Low-Gain	-	$-0.1 + 0.1 - 0.1$	$-0.2 + 0.2 - 0$	$-0.1 + 0.1 - 0.1$	$-0.1 + 0.1 - 0.1$
Medium-Gain	-	-	-	$-0.3 + 0.3 - 0.4$	$-0.3 + 0.3 - 0.4$
High-Gain	-	-	$-0.4 + 0.4 - 0.3$	$-0.3 + 0.3 - 0.4$	$-0.3 + 0.3 - 0.4$

NOTES

(a) The nominal value plus worst-case tolerance is equal to the worst-case value given in EPD-283; best-case value is estimated.
(b) Circuit losses are included in antenna gain.
(c) Ideal circularly polarized isotropic antenna assumed for reference.
(d) See Figure 5-1 for combined gain and pointing loss vs. mission time.
(e) Zero pointing error assumed for reference.
(f) See Figure 5-2 for combined gain and pointing loss vs. mission time.
(g) Ideal circularly polarized isotropic antenna assumed for reference.

VC233FD101

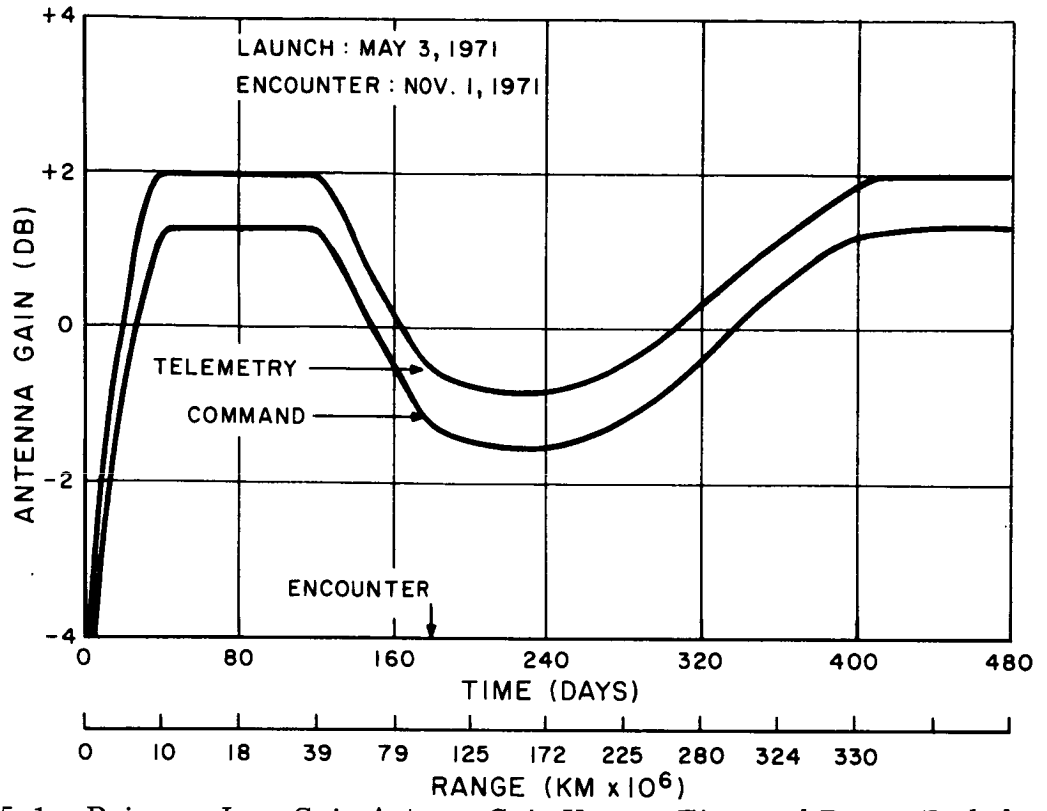


Figure 5-1. Primary Low-Gain Antenna Gain Versus Time and Range (Includes All Pointing Losses)

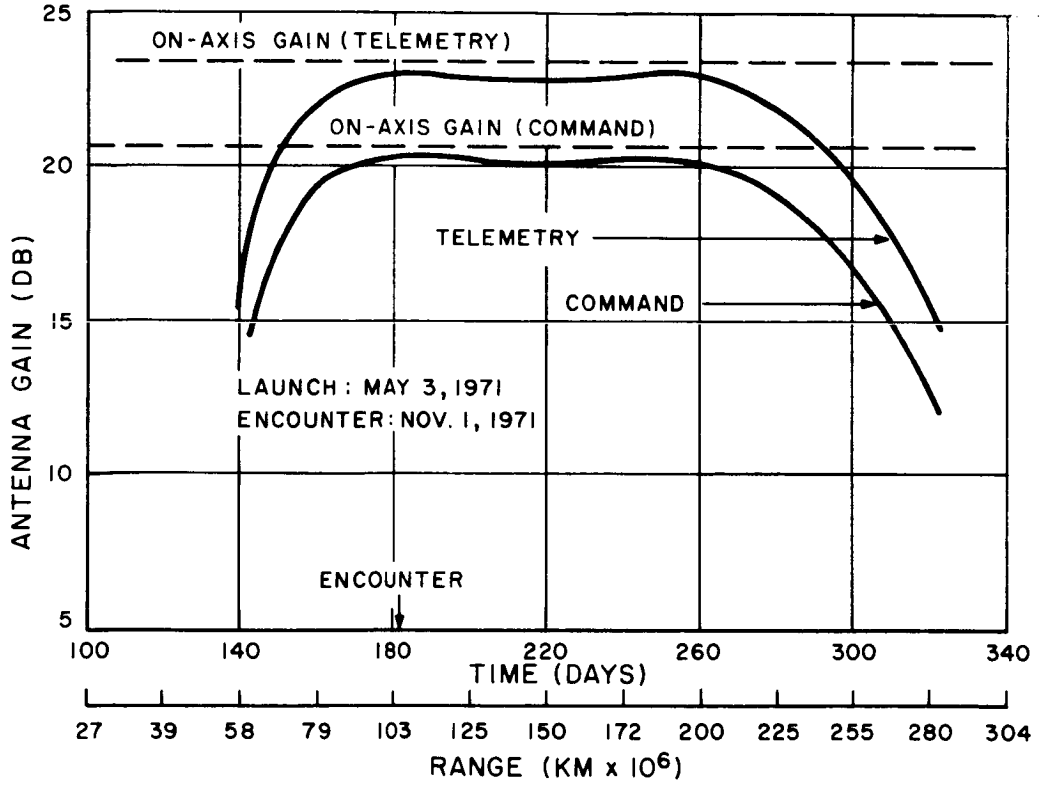


Figure 5-2. Medium-Gain Antenna Gain Versus Time and Range (Includes All Pointing Losses)

d. Threshold signal-to-noise ratio in a 1-cps noise bandwidth that results in minimum acceptable performance for the ranging system: 16 db.

e. Maximum acceptable code acquisition time at threshold.

1. Short code: 380 sec (6.3 minutes)
2. Lunar code: 1625 sec (27.0 minutes)
3. Planetary code: 1545 sec (25.8 minutes)

f. Ranging phase-lock-loop threshold noise bandwidth: $0.8\ ^{+0}_{-0.16}$ cps

g. Transponder turn-around ranging channel noise bandwidth: 2.5 ± 0.25 mc

h. Modulation Index (both transmitters: 1.0 ± 0.1 radians

i. Carrier Modulation Loss: $-5.5\ ^{+1.5}_{-1.3}$ db

j. Ranging Modulation Loss: $-1.5\ ^{+0.6}_{-0.5}$

5.2 Performance Summary. Figures A-1 through A-29, showing the performance of the telecommunication links versus range, are included in Appendix A. Tabular summaries of the results for telemetry and command are given in Tables 5-3 and 5-4. The "greyout" range is given for each link. Listed values of received carrier power and channel performance margins correspond to that range. They include all adverse tolerances and are, therefore, worst-case values.

Four cases are given in Figure A-29 for the ranging channel. For nominal link parameter values, the 210-ft/100-kw ground station and 50-watt/High-Gain spacecraft mode provide ranging to 1.7×10^9 km. This range is reduced to 5.5×10^8 km if the 85-ft/100-kw ground station is used. Assuming worst-case tolerances in both up- and down-links, the range capability of the above systems are reduced to 10^9 km and 3.2×10^8 km, respectively. Command (either 1 or 30 sbps) and telemetry (117 bps) transmitted simultaneously with ranging result in approximately a 2-db loss in performance in the ranging channel.

5.3 Performance Definitions. The following definitions shall apply to the overall telecommunications system performance.

5.3.1 Performance Margin. The performance margin is defined as the ratio of the nominal received signal level (carrier or modulation) to the nominal threshold signal level expressed in db. It shall be considered acceptable when the margin is positive and equal to or greater than the magnitude of the linear sum of the adverse system tolerances. When the performance margin drops below the sum of negative tolerances, the channel shall be defined to be in the "greyout" area. When the performance margin is negative, the channel shall be defined to be in the blackout area.

5.3.2 Nominal Received Signal Level. The nominal received signal level is defined as the received signal level calculated from the nominal system parameters (gains, losses, and power levels). The calculation excludes, as far as possible, all arbitrary margins, pads, or unknown factors.

TABLE 5-3. SUMMARY OF TELEMETRY LINK PERFORMANCE

Transmission Mode	Channel	Reception Mode	Min.* Range (KM)	Carrier Power Received (dbm)	1-Way Track (Carrier) (db)	2-Way Track (Carrier) (db)	Data Demodulator (Carrier) (db)	Data A (db)	Sync A (db)	Subcarrier (db)	Data B (db)	Sync B (db)	Figure No.
3-Watt Parastic	117 BPS	DSIF 71	1.41×10^3	-140.6	12.5	10.5	2.5	-	-	3.0	0	7.2	A-1
	117 BPS	DSIF 72	8.3×10^4	-150.7	12.5	10.5	2.5	-	-	3.0	0	7.2	A-2
	Auto-track 117 BPS	Acquisition	1.46×10^3	-137.1	0	0	5.0	-	-	16.5	13.5	20.7	A-3
	117 BPS	Acquisition	6.9×10^3	-150.6	12.5	10.5	2.5	-	-	3.0	0	7.2	A-4
	117 BPS	85 ft	5.8×10^5	-157.9	12.5	10.5	2.5	-	-	3.0	0	7.2	A-5
3-Watt Primary Low-Gain	Auto-track 117 BPS	Acquisition	1.64×10^4	-137.1	0	0	5.0	-	-	16.5	13.5	20.7	A-6
	117 BPS	Acquisition	7.76×10^4	-150.6	12.5	10.5	2.5	-	-	3.0	0	7.2	A-7
	117 BPS	85 ft	6.69×10^6	-157.9	12.5	10.5	2.5	-	-	3.0	0	7.2	A-8
	117 BPS	210 ft	2.16×10^7	-159.9	12.5	10.5	2.5	-	-	3.0	0	7.2	A-8
50-Watt High-Gain	117 BPS	85 ft	5.68×10^8	-157.9	12.5	10.5	2.5	-	-	3.0	0	7.2	A-9
	117 BPS	210 ft	1.88×10^9	-159.9	12.5	10.5	2.5	-	-	3.0	0	7.2	A-9
50-Watt Primary Low-Gain	117 BPS	85 ft	2.32×10^7	-157.9	12.5	10.5	2.5	-	-	3.0	0	7.2	A-10
	117 BPS	210 ft	6.3×10^7	-159.9	12.5	10.5	2.5	-	-	3.0	0	7.2	A-10
50-Watt Medium-Gain	117 BPS	85 ft	2.5×10^8	-157.9	12.5	10.5	2.5	-	-	3.0	0	7.2	A-11
	117 BPS	210 ft	2.9×10^8	-159.9	12.5	10.5	2.5	-	-	3.0	0	7.2	A-11
3-Watt High-Gain	117 BPS	85 ft	1.62×10^8	-157.9	12.5	10.5	2.5	-	-	3.0	0	7.2	A-12
	117 BPS	210 ft	5.36×10^8	-159.9	12.5	10.5	2.5	-	-	3.0	0	7.2	A-12
50-Watt High-Gain	14983/117	210 ft	1.95×10^8	-140.1	26.3	24.3	16.3	0	10.3	9.0	6.0	13.2	A-13
	7467/117	210 ft	2.75×10^8	-143.1	23.3	21.3	13.3	0	9.6	6.0	3.0	10.2	A-13
	3733/117	210 ft	3.9×10^8	-146.1	20.3	18.3	10.3	0	8.8	3.0		7.2	A-13
50-Watt Medium-Gain	7467/117	210 ft	1.3×10^8	-143.1	23.3	21.3	13.3	0	9.6	6.0	3.0	10.2	A-14
	3733/117	210 ft	1.75×10^8	-146.1	20.3	18.3	10.3	0	8.8	3.0	0	7.2	A-14
	933/29	210 ft	2.5×10^8	-152.1	14.3	12.3	4.3	0	7.3	0	0	5.7	A-14
3-Watt High-Gain	3733/117	210 ft	1.11×10^9	-146.1	20.3	18.3	10.3	0	8.8	3.0	0	7.2	A-15
	933/29	210 ft	2.21×10^8	-152.1	14.3	12.3	4.3	0	7.3	0	0	5.7	A-15
50-Watt Secondary Low-Gain	7 BPS	85 ft	7.24×10^7	-167.2	7.0	5.0	0	0	2.6	-	-	-	A-16
	7 BPS	210 ft	2.4×10^8	-169.2	7.0	5.0	0	0	2.6	-	-	-	A-16

* Range at which performance of weakest channel equals the sum of the negative tolerances in that channel.

TABLE 5-4. SUMMARY OF COMMAND PERFORMANCE

Reception Mode	Transmission Mode	Channel (SBPS)	Minimum Range* (Km)	Figure No.
Parasitic	DSIF 71	1	4.12×10^3	A-17
		30	1.93×10^3	
Parasitic	DSIF 72	1	3.4×10^6	A-18
		30	1.59×10^6	
Parasitic	Acquisition	1	2.54×10^5	A-19
		30	1.19×10^5	
Primary Low-Gain	Acquisition	1	2.34×10^6	A-20
		30	1.1×10^6	
Primary Low-Gain	85 ft/100 kw	1	1.8×10^8	A-21
		30	0.9×10^8	
Primary Low-Gain	85 ft/400 kw	1	5.26×10^8	A-22
		30	1.5×10^8	
Primary Low-Gain	210 ft/100 kw	1	7.95×10^8	A-23
		30	3.72×10^8	
Secondary Low-Gain	85 ft/100 kw	1	2.11×10^8	A-24
		30	1.11×10^8	
Secondary Low-Gain	85 ft/400 kw	1	4.22×10^8	A-25
		30	2.22×10^8	
Secondary Low-Gain	210 ft/100 kw	1	6.38×10^8	A-26
		30	2.98×10^8	
Medium-Gain	85 ft/100 kw	1	3.0×10^8	A-27
		30	2.8×10^8	
High-Gain	85 ft/100 kw	1	5.5×10^9	A-28
		30	2.57×10^9	

*Range at which performance margin of weakest channel equals the sum of the negative tolerances in that channel. Minimum carrier power received and worst-case performance margins at this range are as follows:

	1 SBPS	30 SBPS
Carrier power	-142.4 dbm	-140.5 dbm
2-way track	5.7 db	7.6 db
Data demodulator (Carrier)	0.0 db	1.9 db
Data	0.7 db	0.0 db
Subcarrier	0.7 db	0.0 db

5.3.3 Nominal Threshold Signal Level. The nominal threshold signal level shall be the received signal level required to achieve a specified threshold signal-to-noise ratio in the effective noise bandwidth of the detector or demodulator given the system noise spectral density.

5.3.4 Threshold Signal-to-Noise Ratio. The threshold signal-to-noise power ratio shall be the signal-to-noise ratio required at the detector that will result in the minimum acceptable system performance.

6.0 PHYSICAL CHARACTERISTICS. The detailed physical characteristics are specified in the individual subsystem functional descriptions.

APPENDIX A. PERFORMANCE CURVES

Appendix A contains performance curves (Figures A1 through A-29) for the telecommunication links for both the prime modes and major backup modes of operation. Two sample design control tables (Tables A-1 and A-2) are also included to define parameters and to indicate the method of calculation.

TABLE A-1. SAMPLE DESIGN CONTROL TABLE (TELEMETRY)

Channel 14933/117 BPS, Mode 50W, Hi-Gain/210 ft.

No.	Parameter	Value	Tolerance	
1	Total Transmitter Power	47.0	+1.0	-1.0
2	Transmitting Circuit Loss	-3.0	+0.5	-0.5
3	Transmitting Antenna Gain	32.5	+0.4	-0.6
4	Transmitting Antenna Pointing Loss	-1.5	+1.5	-0.0
5	Space Loss	-259.7	+0.0	-0.0
	.2295 MC, R = 10^8 KM			
6	Polarization Loss	0.0	+0.0	-0.10
7	Receiving Antenna Gain	61.9	+1.0	-1.0
8	Receiving Antenna Pointing Loss	-0.3	+0.3	-0.0
9	Receiving Circuit Loss	0.0	+0.0	-0.0
10	Net Circuit Loss	-170.1	+3.7	-2.2
11	Total Received Power	-123.1	+4.7	-3.2
12	Receiver Noise Spectral Density (N/B)	-183.2	+0.0	-1.0
	T System = 35°K			
13	Carrier Modulation Loss	-6.0	+1.3	-1.7
14	Received Carrier Power	-129.1	+6.0	-4.9
15	Carrier APC Noise BW ($2B_{LO}$ = 48 cps)	16.8	+0.0	-0.5
	CARRIER PERFORMANCE-TRACKING (one-way)			
16	Threshold SNR in $2B_{LO}$	0.0	+0.0	-0.0
17	Threshold Carrier Power	-166.4	+0.0	-1.5
18	Performance Margin	37.3	+7.5	-4.9
	CARRIER PERFORMANCE-TRACKING (two-way)			
19	Threshold SNR in $2B_{LO}$	2.0	+0.0	-0.0
20	Threshold Carrier Power	-164.4	+0.0	-1.5
21	Performance Margin	35.3	+7.5	-4.9
	CARRIER PERFORMANCE-TELEMETRY			
22	Threshold SNR in $2B_{LO}$	10.1	+0.0	-0.0
23	Threshold Carrier Power	-156.4	+0.0	-1.5
24	Performance Margin	27.3	+7.5	-4.9
	DATA CHANNEL A			
25	Modulation Loss	-2.1	+0.5	-0.6
26	Received Data Subcarrier Power	-125.2	+5.2	-3.8
27	Bit Rate (1/T)	41.7	+0.0	-0.0
28	Required ST/N/B	5.9	+0.5	-0.5
29	Threshold Subcarrier Power	-135.6	+0.5	-1.5
30	Performance Margin	10.4	+6.7	-4.3
	SYNC CHANNEL A			
31	Modulation Loss	-2.1	+0.5	-0.6
32	Receiver SYNC Subcarrier Power	-125.2	+5.2	-3.8
33	SYNC APC Noise BW($2B_{LO}$ =11.2 cps)	10.5	+0.4	-0.4
34	Threshold SNR in $2B_{LO}$	26.9	+0.0	-0.0
35	Threshold Subcarrier Power	-145.8	+0.4	-1.4
36	Performance Margin	20.6	+6.6	-4.2
	SUBCARRIER PERFORMANCE			
37	Modulation Loss	-14.0	+1.3	-1.6
38	Received Subcarrier Power	-137.1	+6.0	-4.8
39	Subcarrier APC Noise BW($2B_{LO}$ = 1 cps)	0.0	+0.0	-0.5
40	Threshold SNR in $2B_{LO}$	26.2	+0.0	-0.0
41	Threshold Subcarrier Power	-157.0	+0.0	-1.5
42	Performance Margin	19.9	+7.5	-4.8
	DATA CHANNEL B			
43	Modulation Loss	-14.0	+1.3	-1.6
44	Received Data Subcarrier Power	-137.1	+6.0	-4.8
45	Bit Rate (1/T)	20.7	+0.0	-0.0
46	Required ST/N/B	8.0	+0.5	-0.5
47	Threshold Subcarrier Power	-154.5	+0.5	-1.5
48	Performance Margin	17.4	+7.5	-5.3
	SYNC CHANNEL B			
49	Modulation Loss	-14.0	+1.3	-1.60
50	Receiver SYNC Subcarrier Power	-137.1	+6.0	-4.8
51	SYNC APC Noise BW($2B_{LO}$ = 1 cps)	0.0	+0.4	-0.4
52	Threshold SNR in $2B_{LO}$	21.6	+0.0	-0.0
53	Threshold Subcarrier Power	-161.6	+0.4	-1.4
54	Performance Margin	24.5	+7.4	-5.2

COMMENTS:

TABLE A-2. SAMPLE DESIGN CONTROL TABLE (COMMAND)

Channel 15 BPS, Mode 85 ft; 100 kw/Hi-Gain

No.	Parameter	Value	Tolerance	
1	Total Transmitter Power	80.0	+0.5	-0.0
2	Transmitting Circuit Loss	0.0	+0.0	-0.0
3	Transmitting Antenna Gain	51.1	+1.0	-1.0
4	Transmitting Antenna Pointing Loss	-0.1	+0.1	-0.0
5	Space Loss	-259.0	+0.0	-0.0
	2113 MC, R = 10^8 KM			
6	Polarization	-0.3	+0.3	-0.4
7	Receiving Antenna Gain	30.3	+1.0	-1.0
8	Receiving Antenna Pointing Loss	-1.3	+1.3	-0.0
9	Receiving Circuit Loss	-3.9	+0.9	-0.9
10	Net Circuit Loss	-183.2	+4.6	-3.3
11	Total Received Power	-103.2	+5.1	-3.3
12	Receiver Noise Spectral Density (N/B)	-166.2	+1.1	-1.1
	T System = 1750°K			
13	Carrier Modulation Loss	-0.9	+0.3	-0.2
14	Received Carrier Power	-104.1	+5.4	-3.5
15	Carrier APC Noise BW ($2B_{LO}$ = 20 cps)	13.0	+0.2	-0.2
	CARRIER PERFORMANCE-TRACKING (one-way)			
16	Threshold SNR in $2B_{LO}$	--	--	--
17	Threshold Carrier Power	--	--	--
18	Performance Margin	--	--	--
	CARRIER PERFORMANCE-TRACKING (two-way)			
19	Threshold SNR in $2B_{LO}$	3.8	+0.0	-0.0
20	Threshold Carrier Power	-149.4	+1.3	-1.3
21	Performance Margin	45.3	+6.7	-4.8
	CARRIER PERFORMANCE-COMMAND			
22	Threshold SNR in $2B_{LO}$	8.5	+1.0	-0.0
23	Threshold Carrier Power	-144.7	+2.3	-1.3
24	Performance Margin	40.6	+6.7	-5.8
	DATA CHANNEL			
25	Modulation Loss	-9.2	+0.6	-0.7
26	Received Data Subcarrier Power	-112.4	+5.7	-4.0
27	Bit Rate (1/T)	0.0	+0.0	-0.0
28	Required ST/N/B	13.2	+0.0	-0.0
29	Threshold Subcarrier Power	-153.0	+1.1	-1.1
30	Performance Margin	40.6	+6.8	-5.1
	SUBCARRIER SYNC CHANNEL			
31	Modulation Loss	-9.2	+0.6	-0.7
32	Received SYNC Subcarrier Power	-112.4	+5.7	-4.0
33	SYNC APC Noise BW ($2B_{LO}$ = 0.4 cps)	-4.0	+0.8	-0.8
34	Threshold SNR in $2B_{LO}$	16.4	+0.0	-0.0
35	Threshold Subcarrier Power	-153.8	+1.9	-1.9
36	Performance Margin	41.4	+7.6	-5.9

COMMENTS:

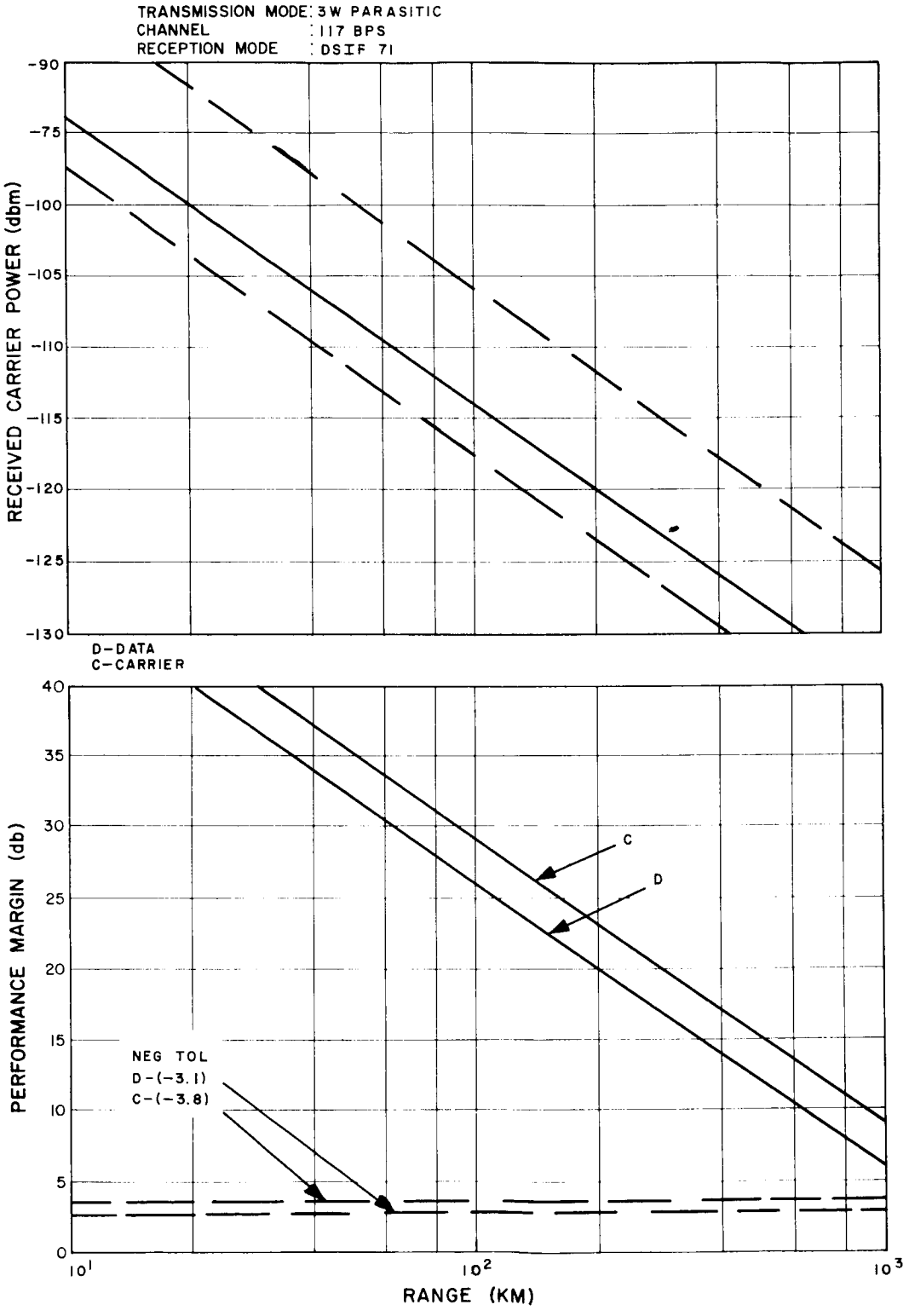


Figure A-1. Link Performance Versus Range (Telemetry)

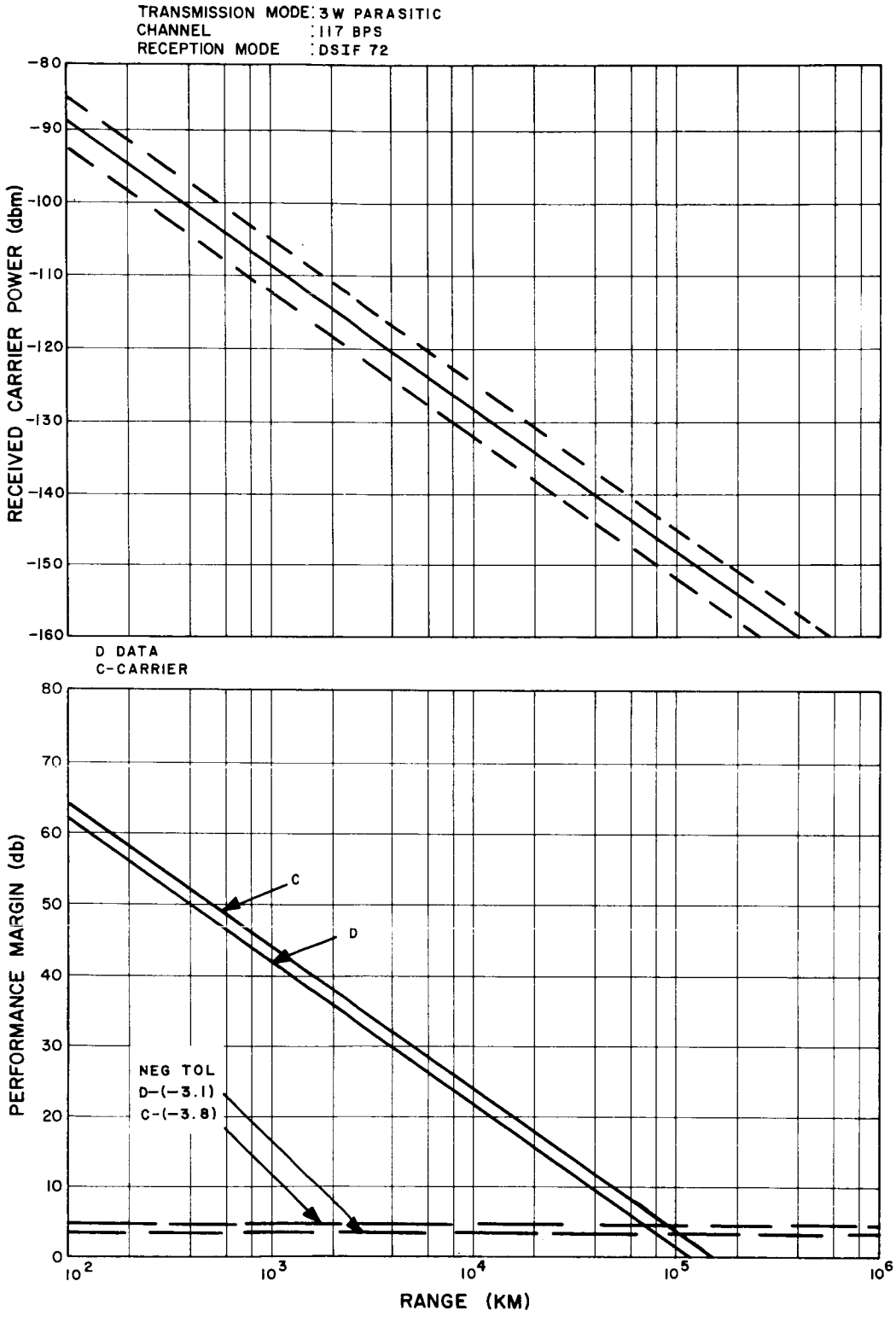


Figure A-2. Link Performance Versus Range (Telemetry)

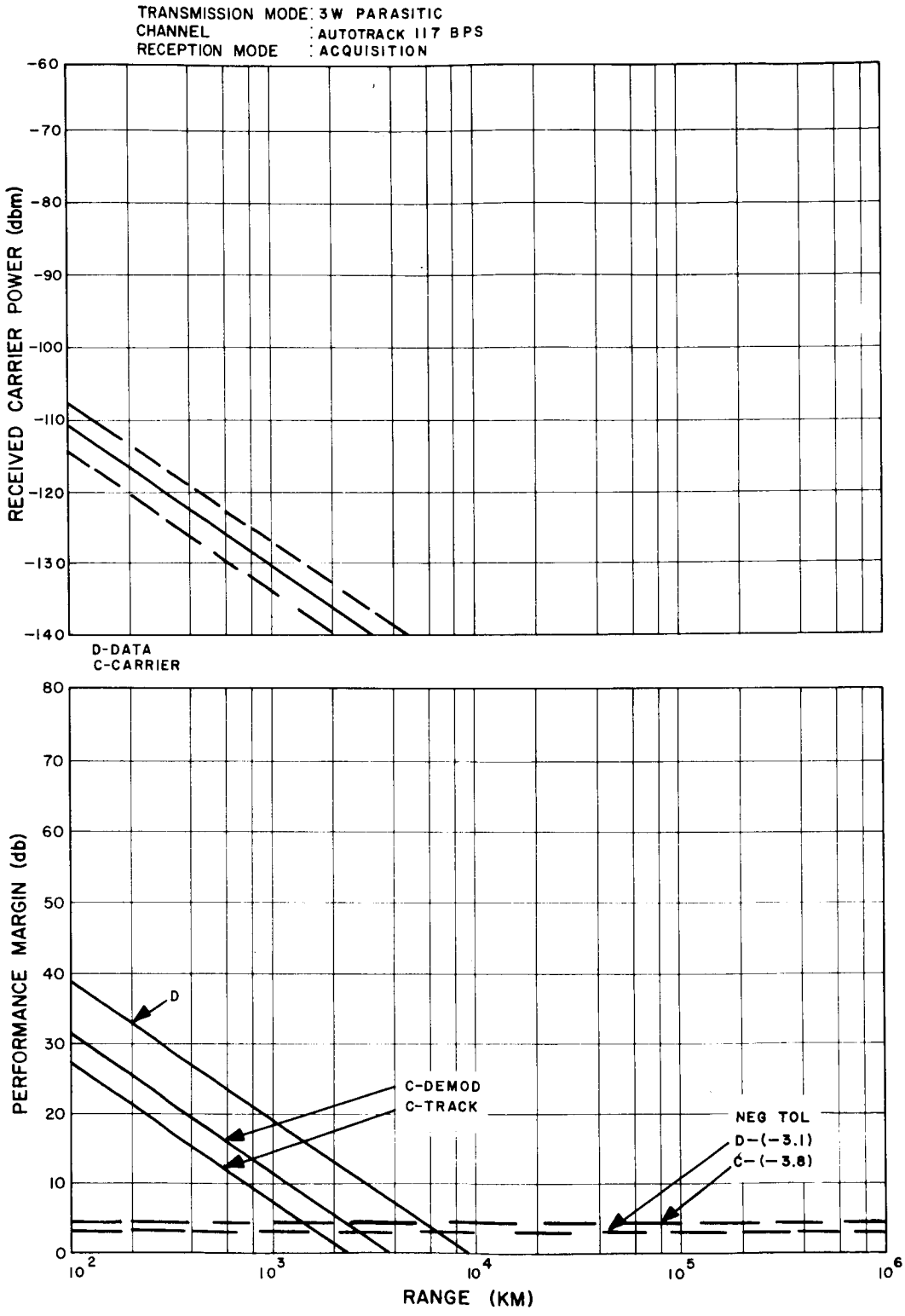


Figure A-3. Link Performance Versus Range (Telemetry)

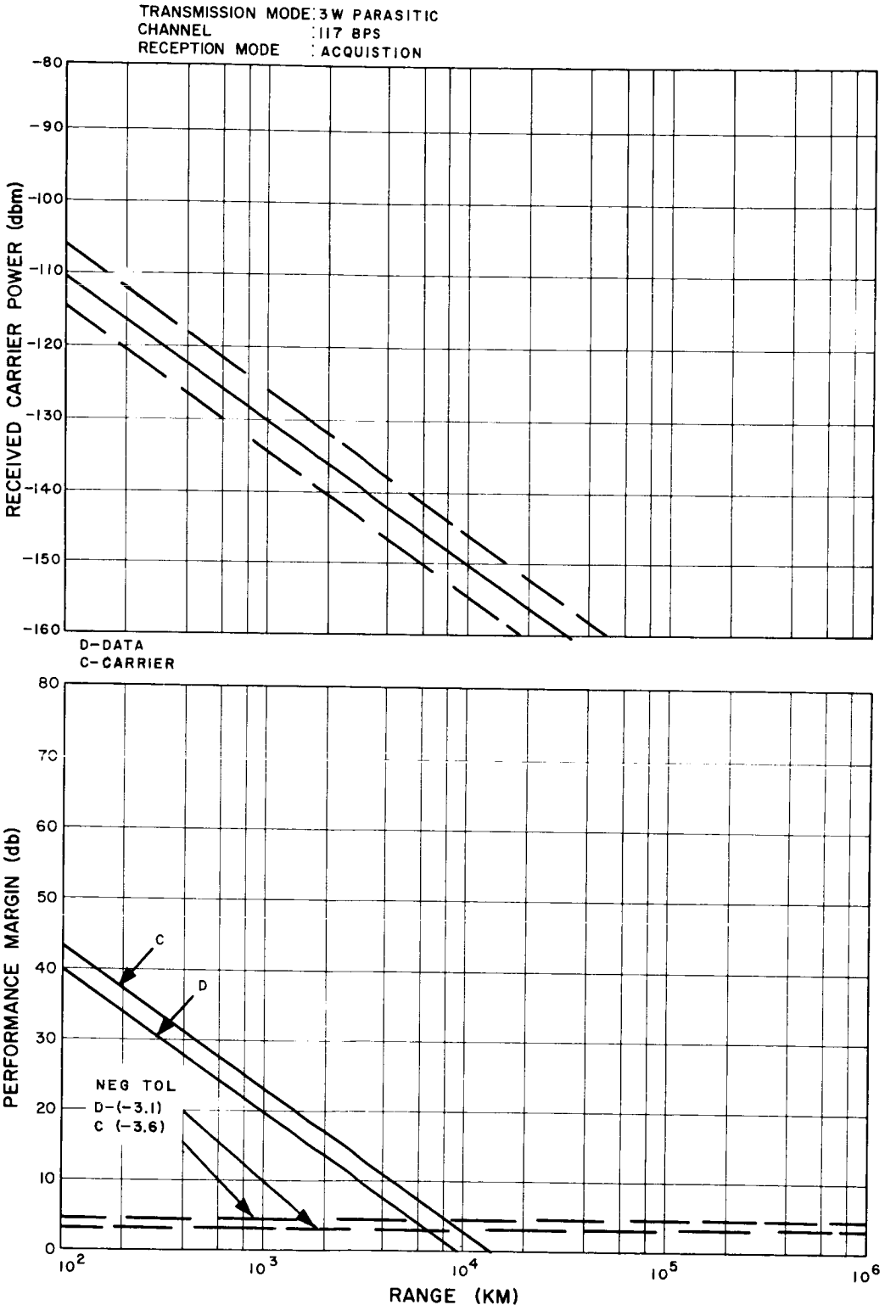


Figure A-4. Link Performance Versus Range (Telemetry)

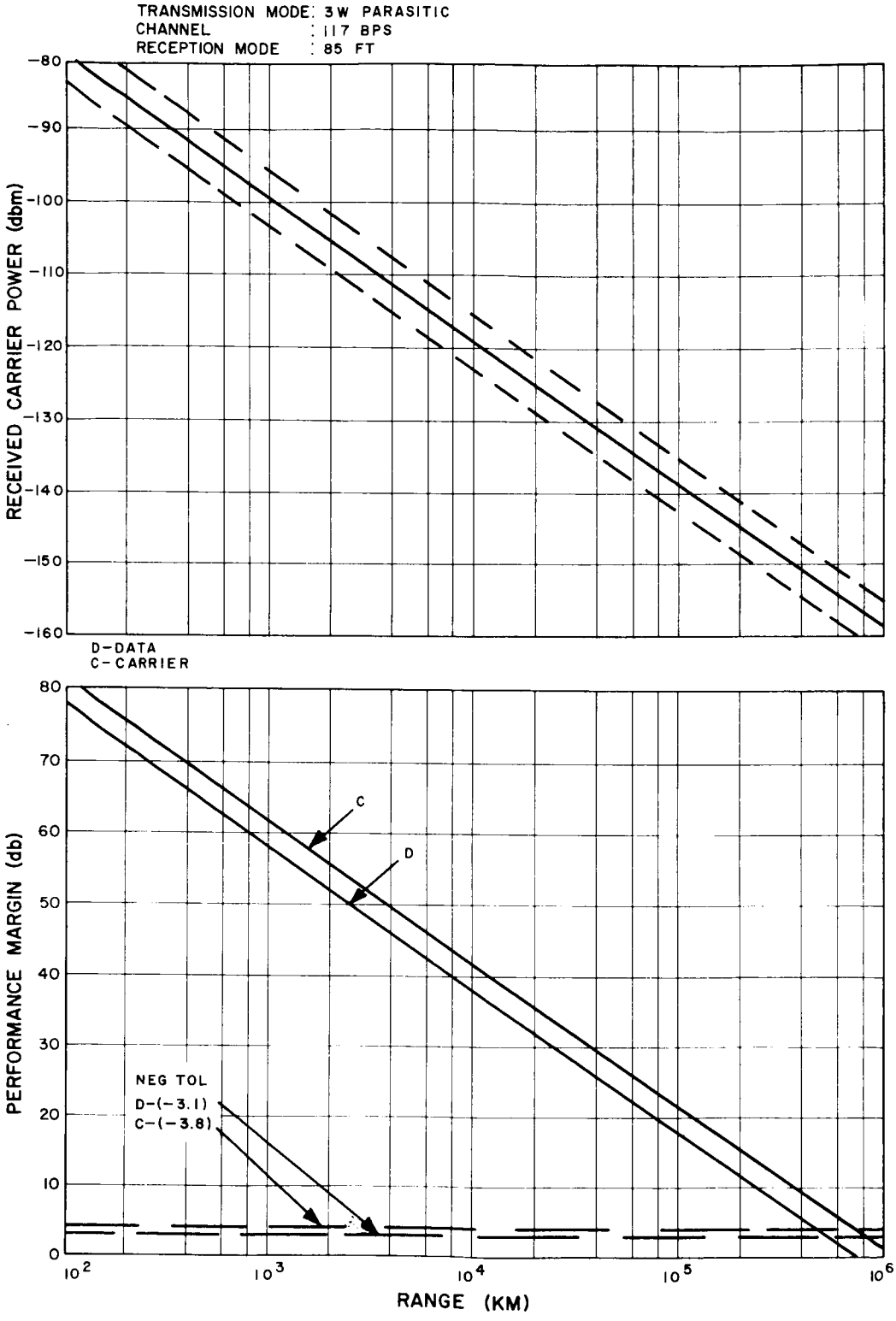


Figure A-5. Link Performance Versus Range (Telemetry)

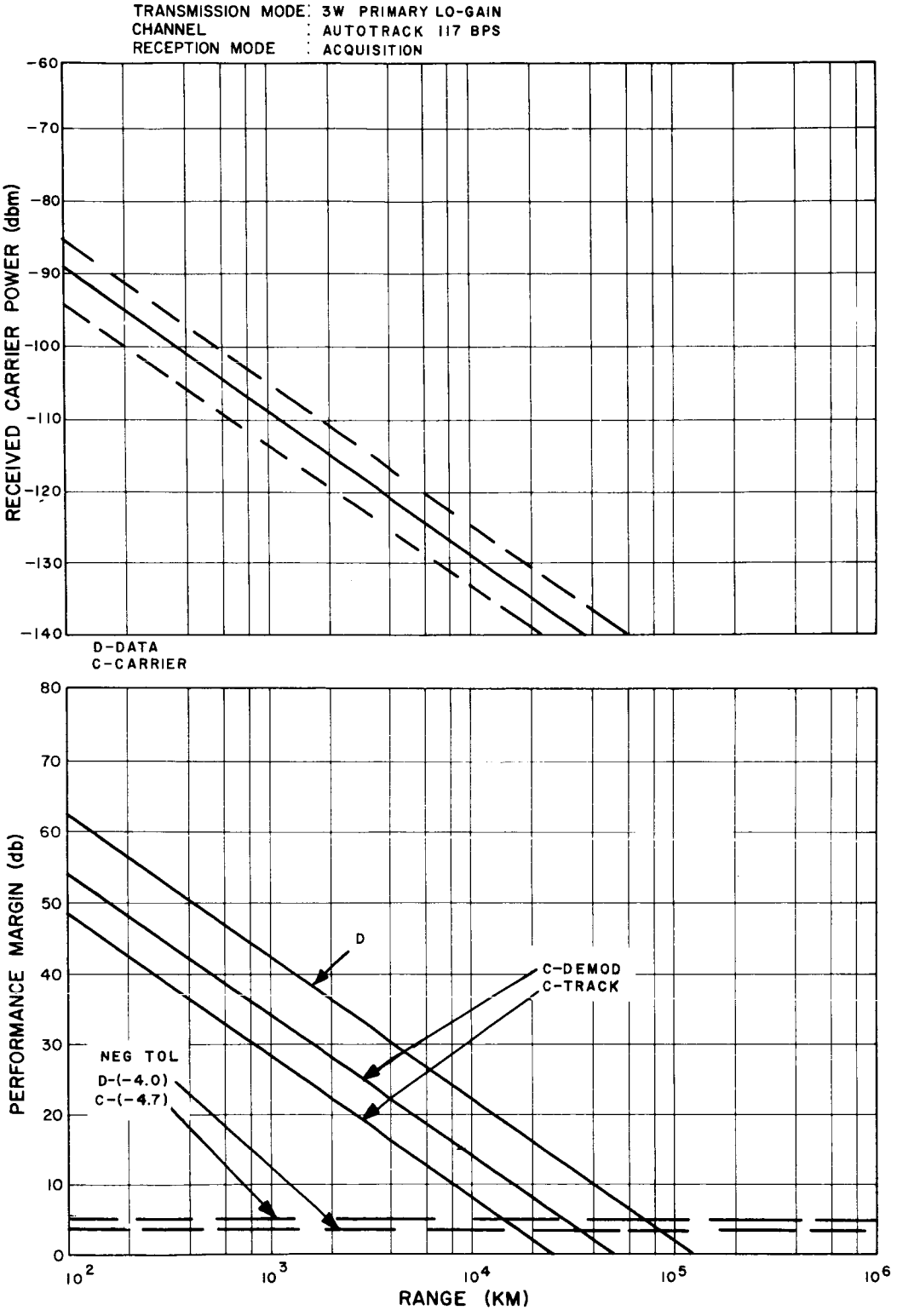


Figure A-6. Link Performance Versus Range (Telemetry)

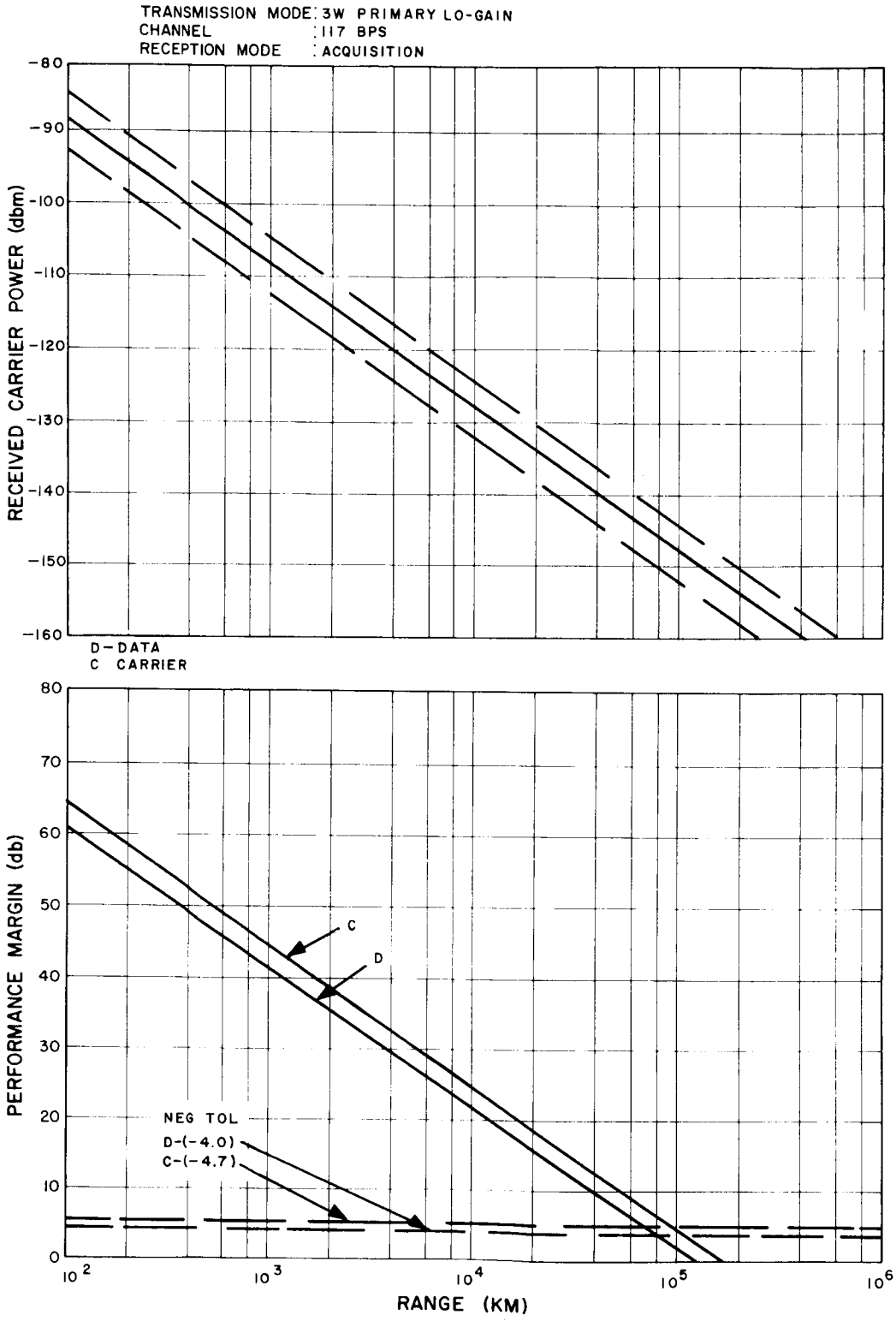


Figure A-7. Link Performance Versus Range (Telemetry)

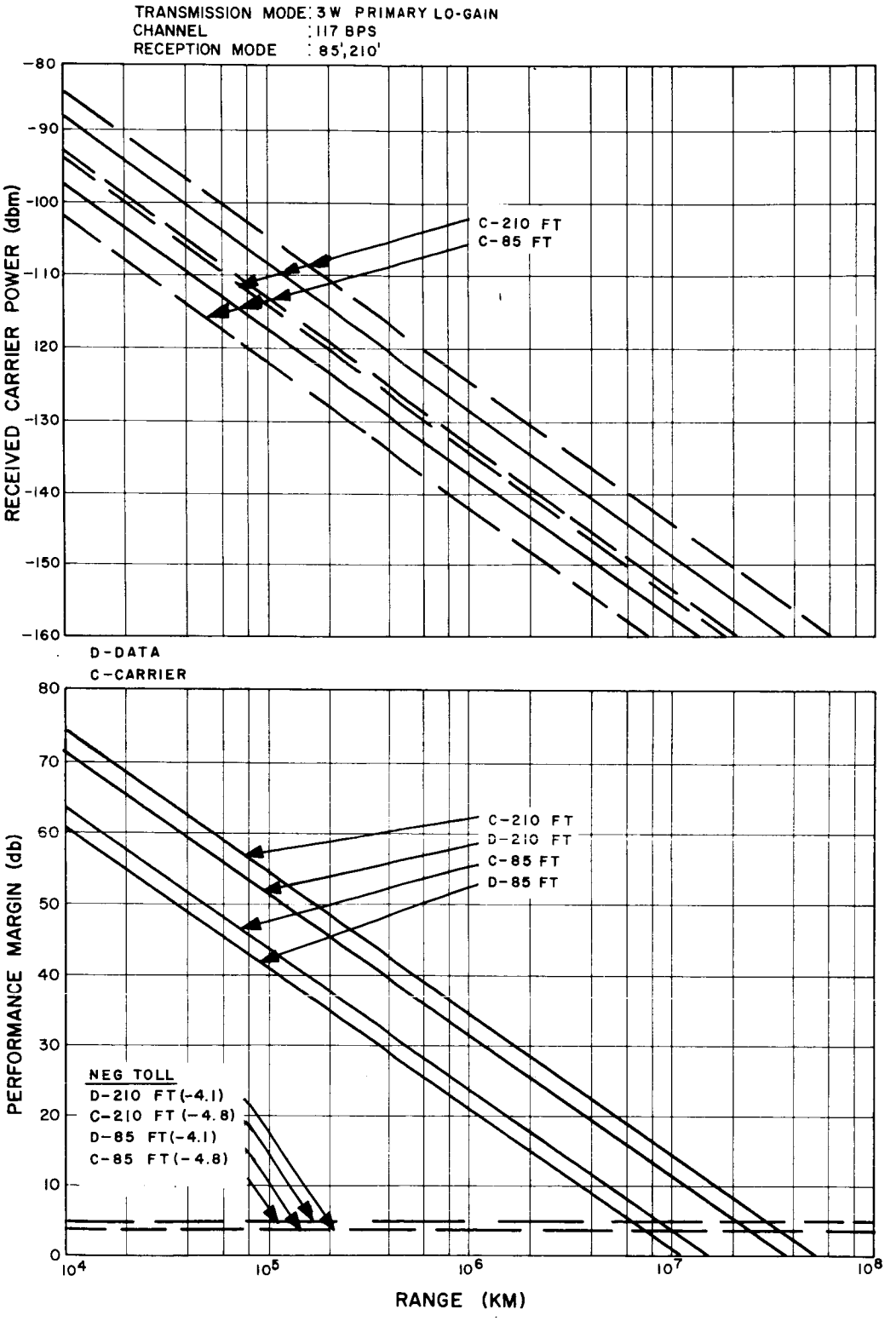


Figure A-8. Link Performance Versus Range (Telemetry)

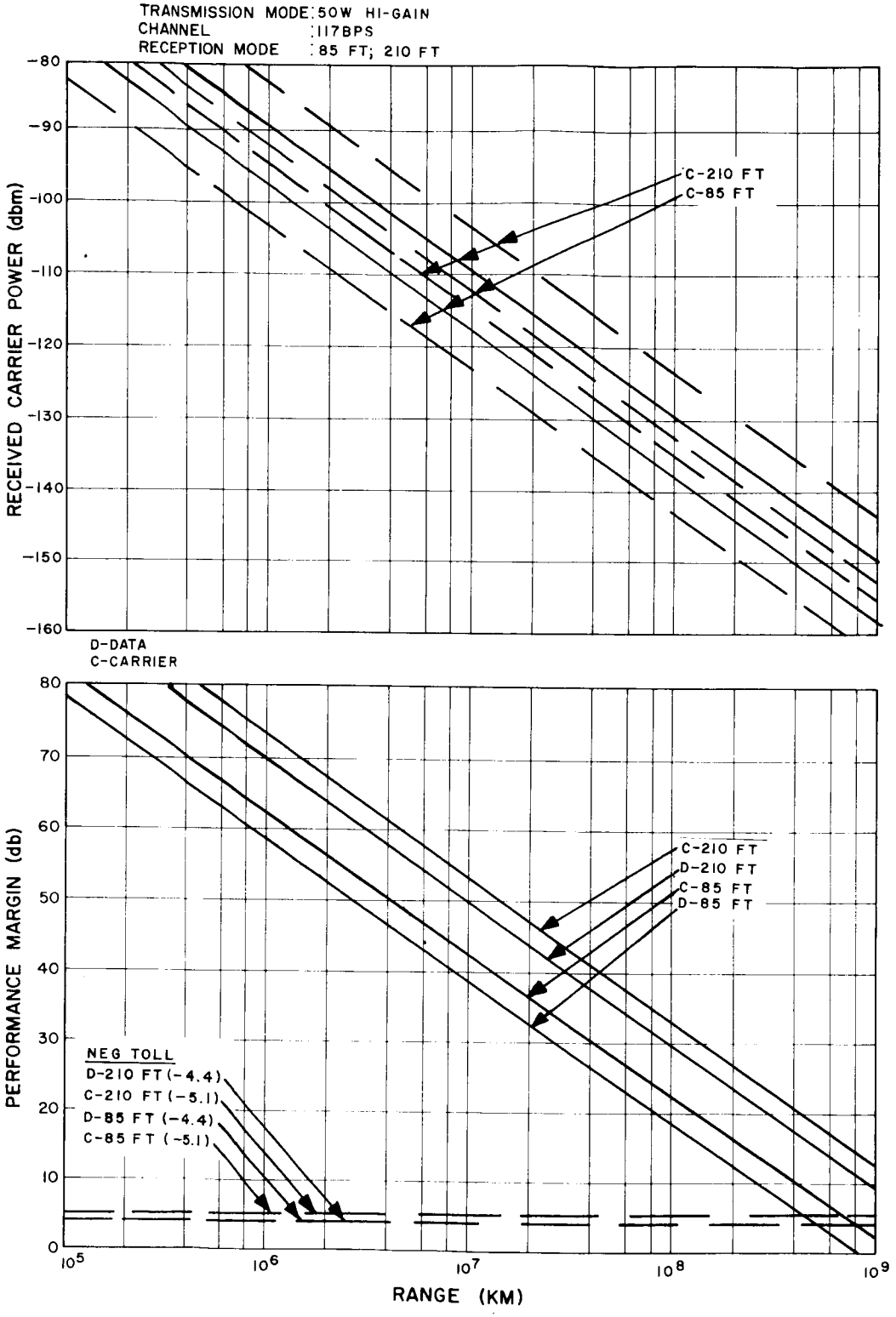


Figure A-9. Link Performance Versus Range (Telemetry)

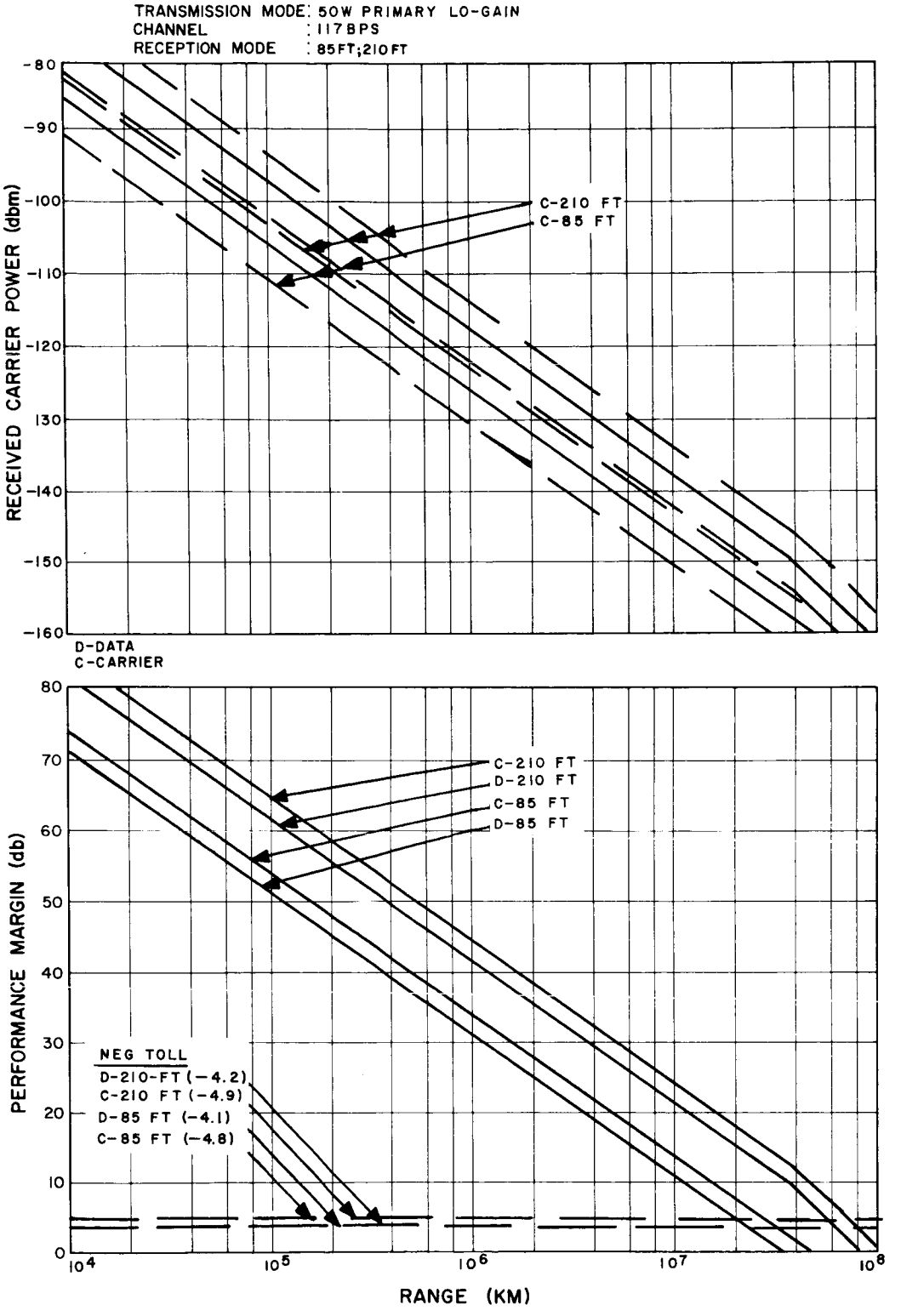


Figure A-10. Link Performance Versus Range (Telemetry)

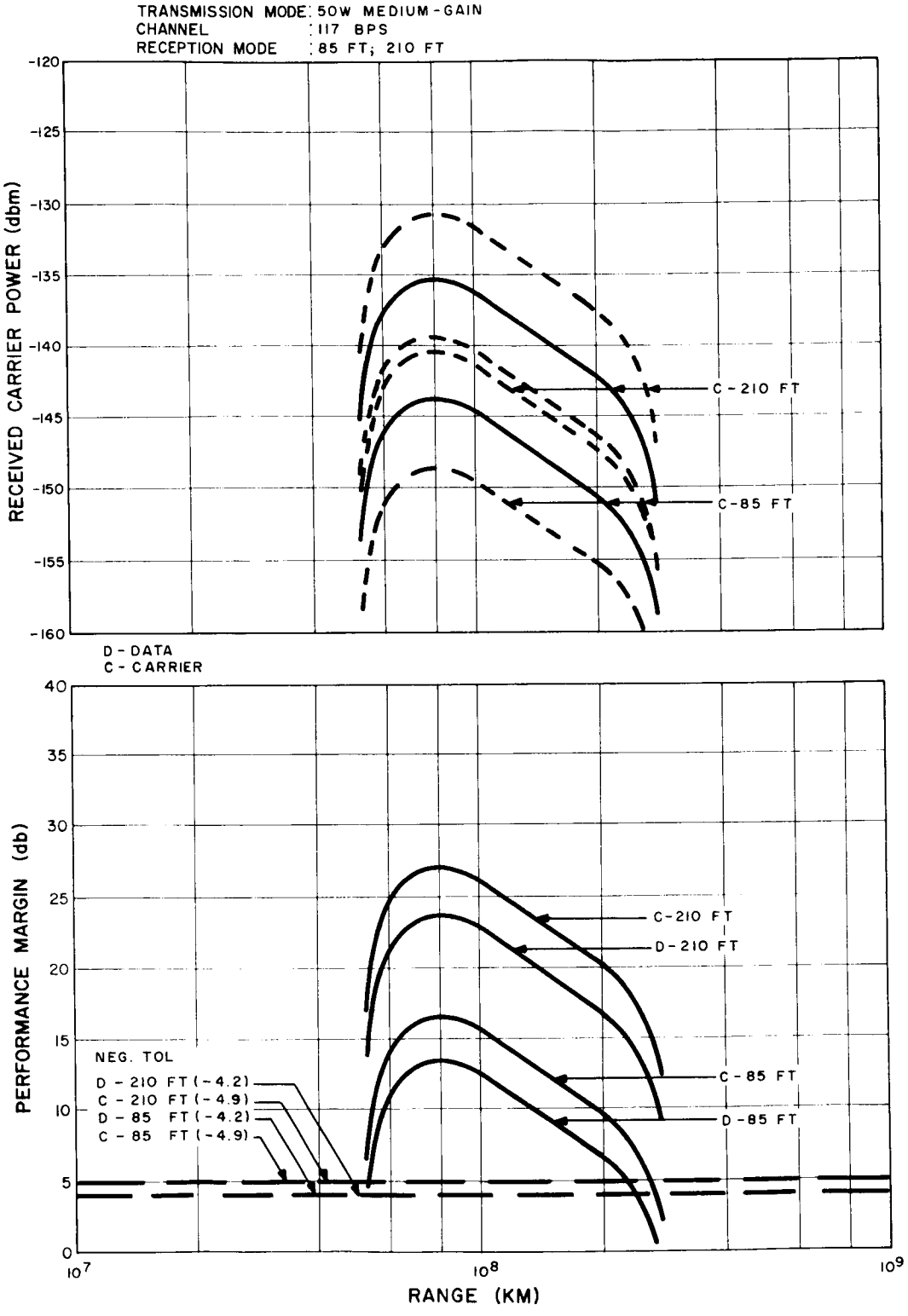


Figure A-11. Link Performance Versus Range (Telemetry)

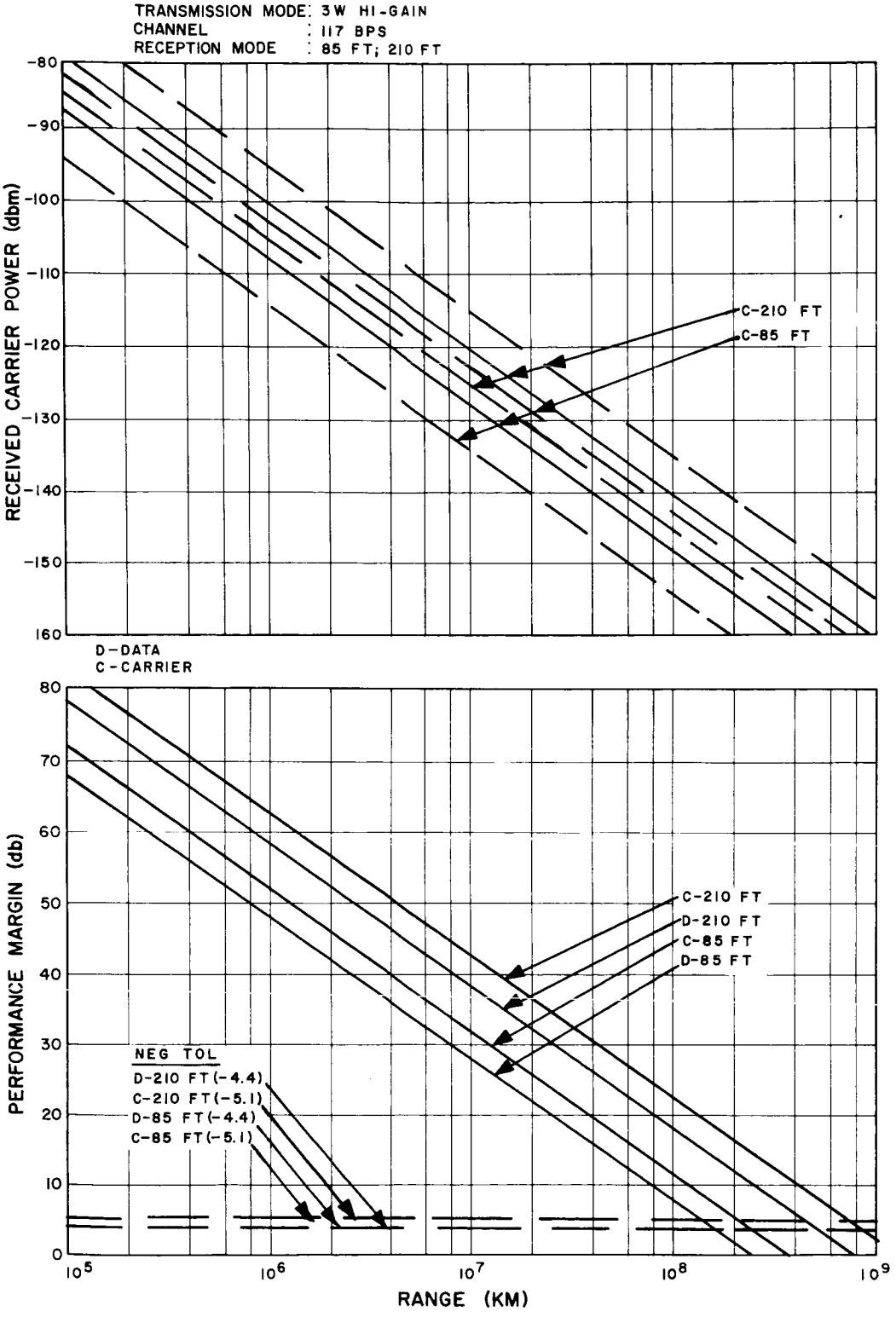


Figure A-12. Link Performance Versus Range (Telemetry)

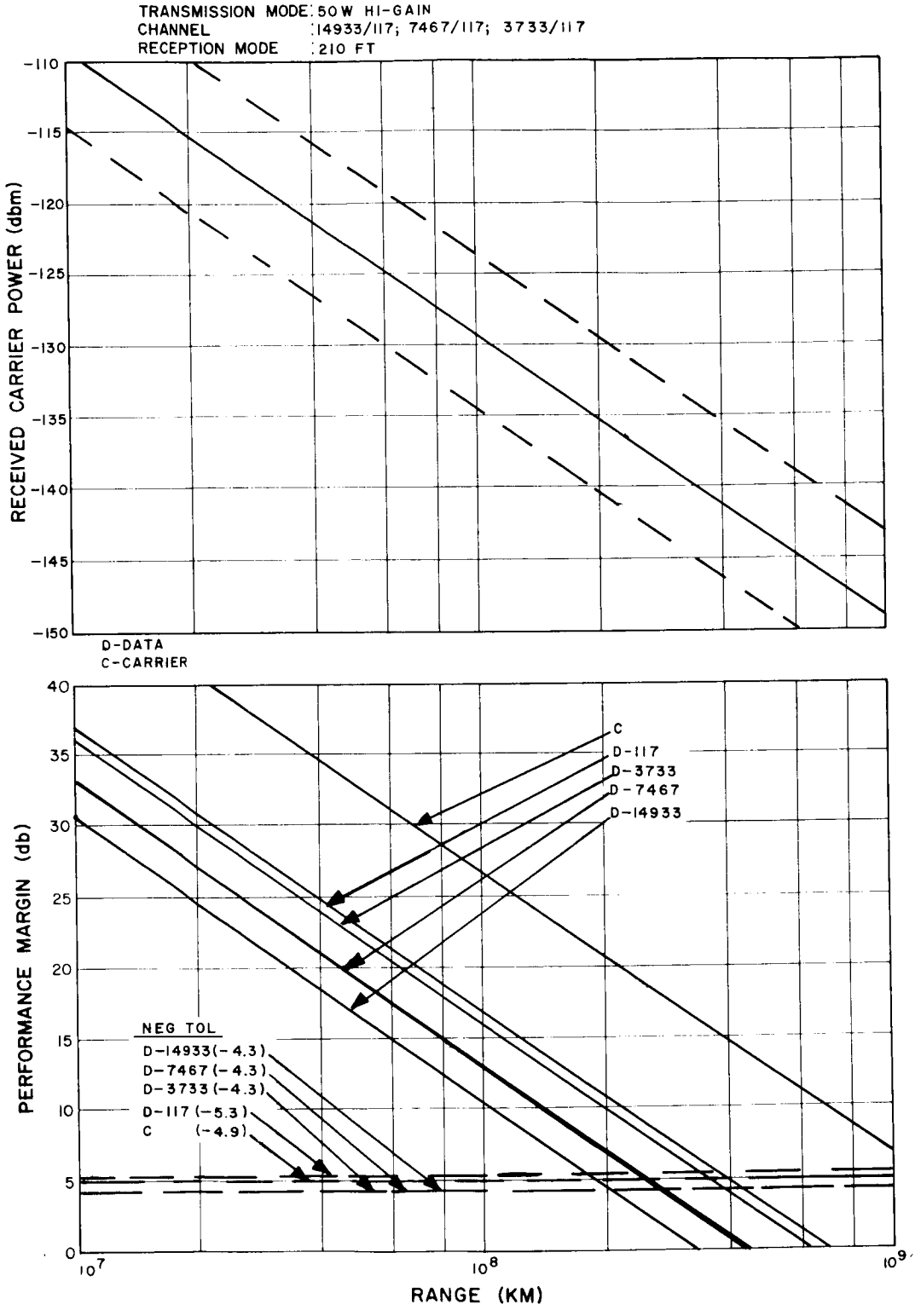


Figure A-13. Link Performance Versus Range (Telemetry)

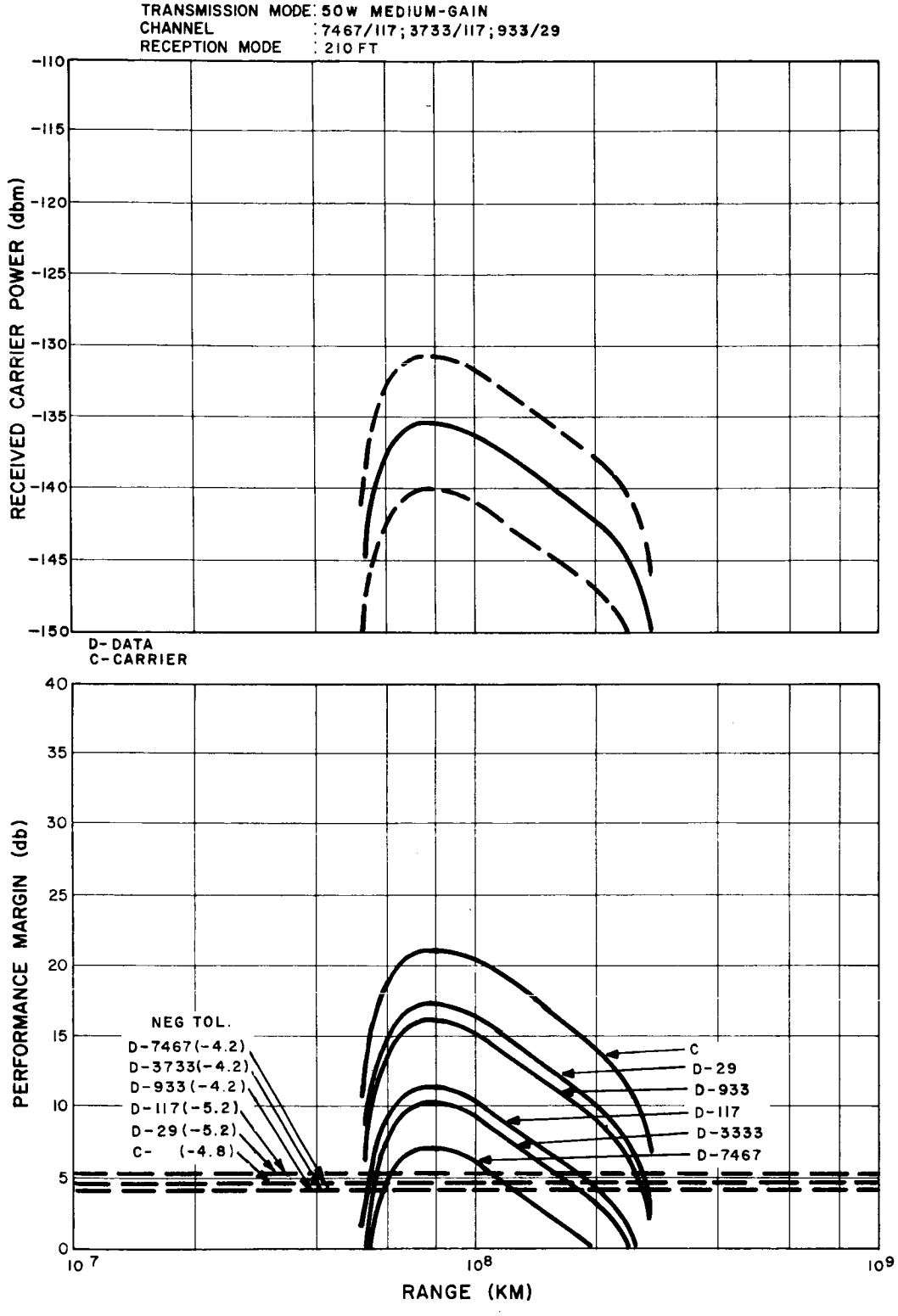


Figure A-14. Link Performance Versus Range (Telemetry)

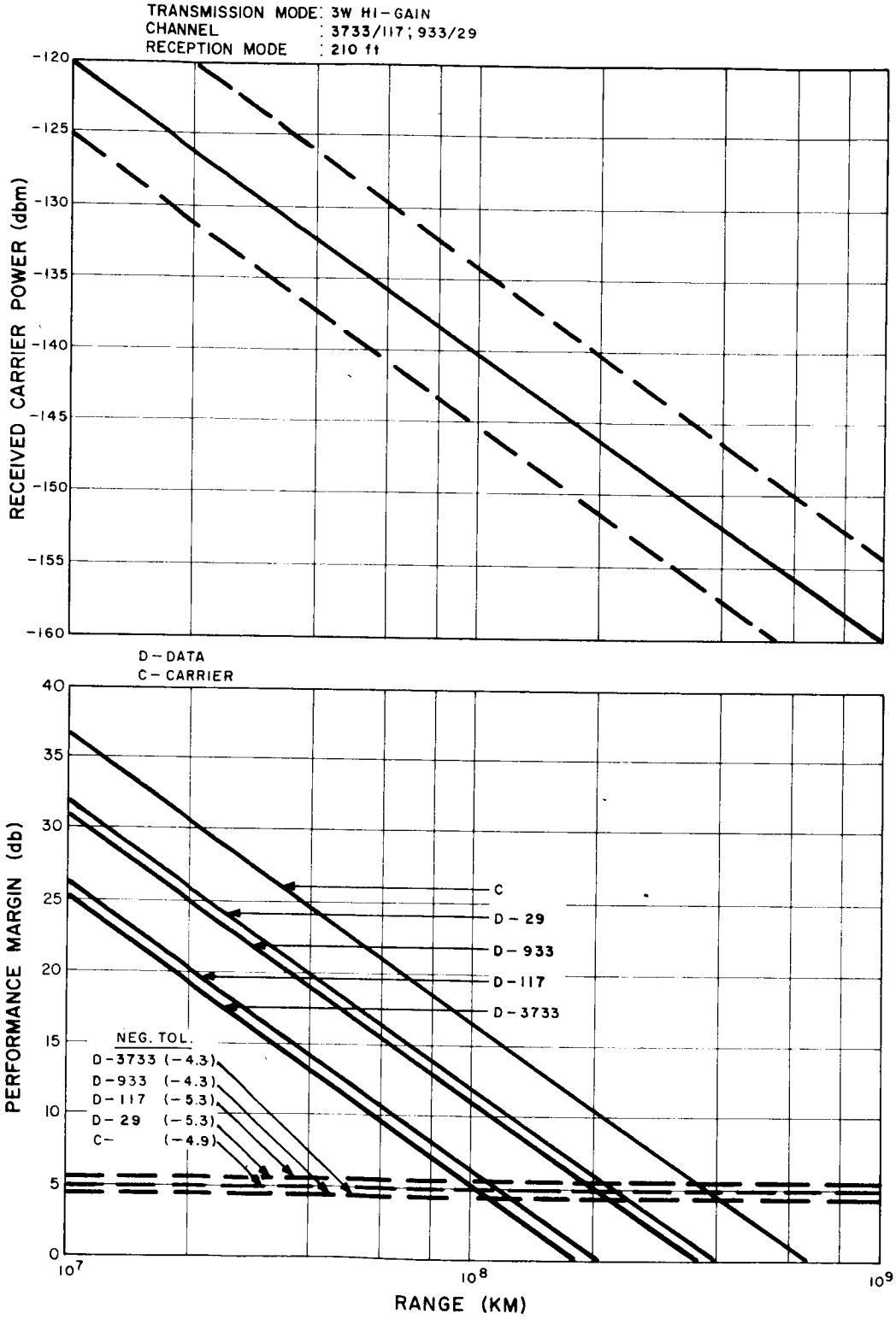


Figure A-15. Link Performance Versus Range (Telemetry)

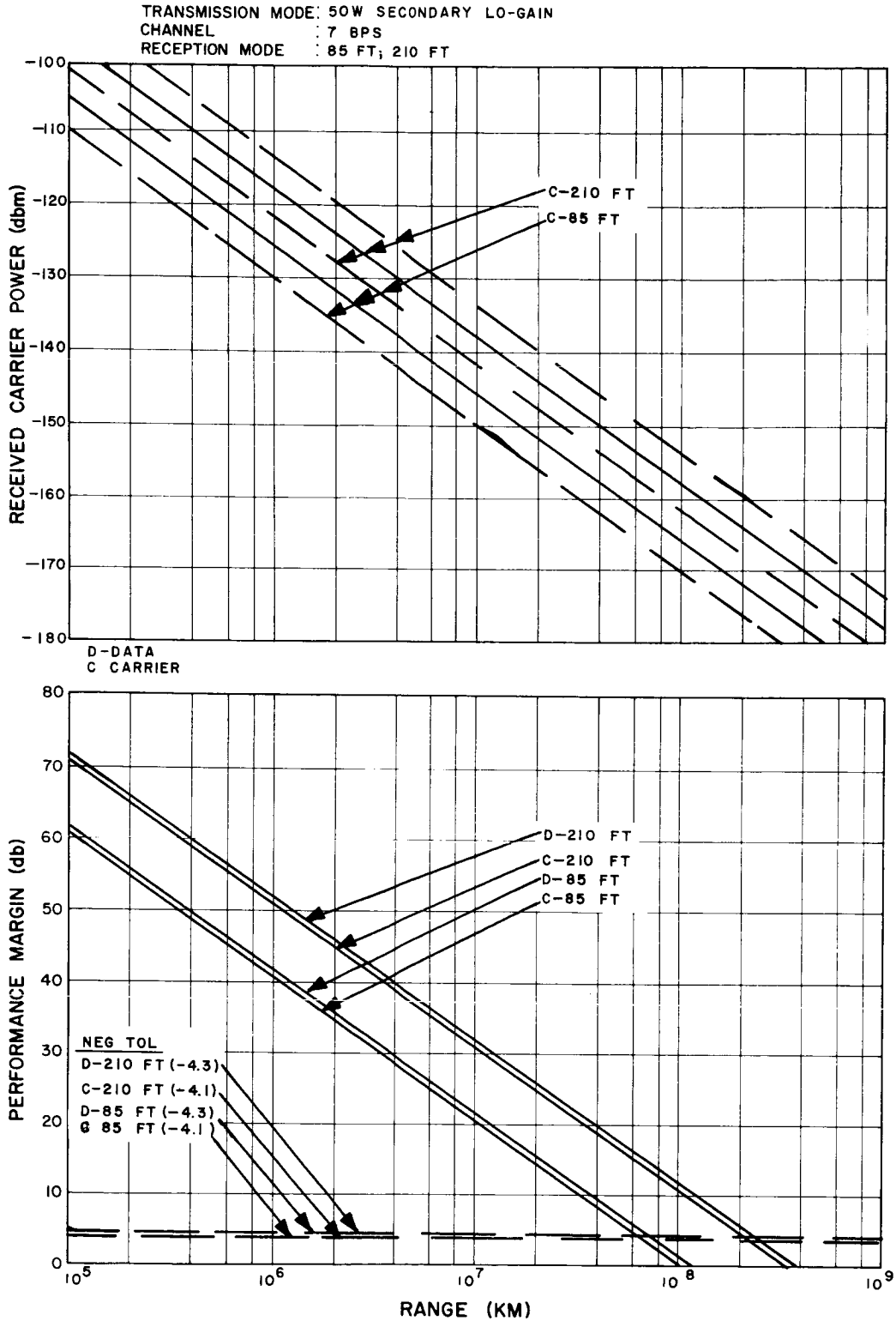


Figure A-16. Link Performance Versus Range (Telemetry)

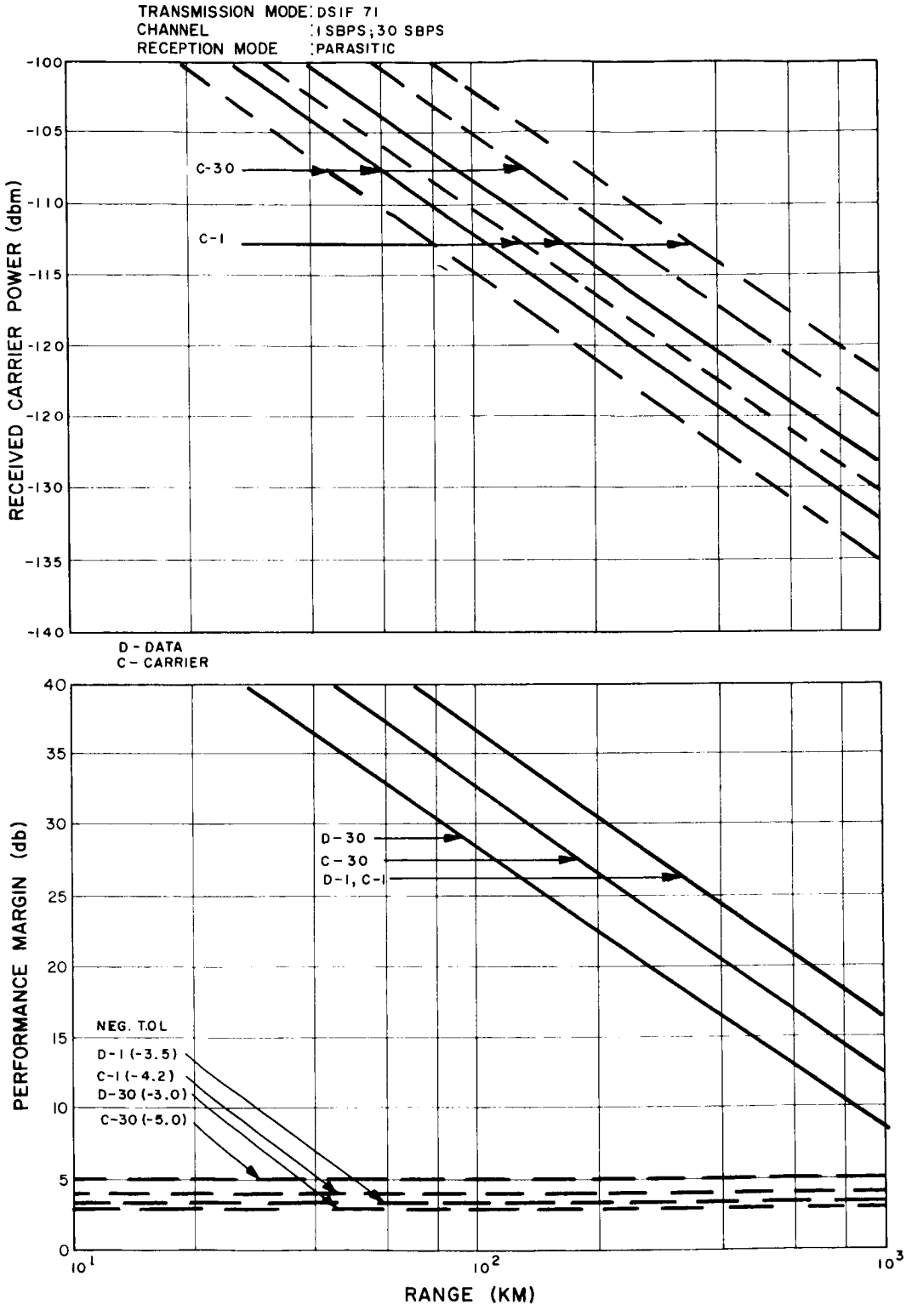


Figure A-17. Link Performance Versus Range (Command)

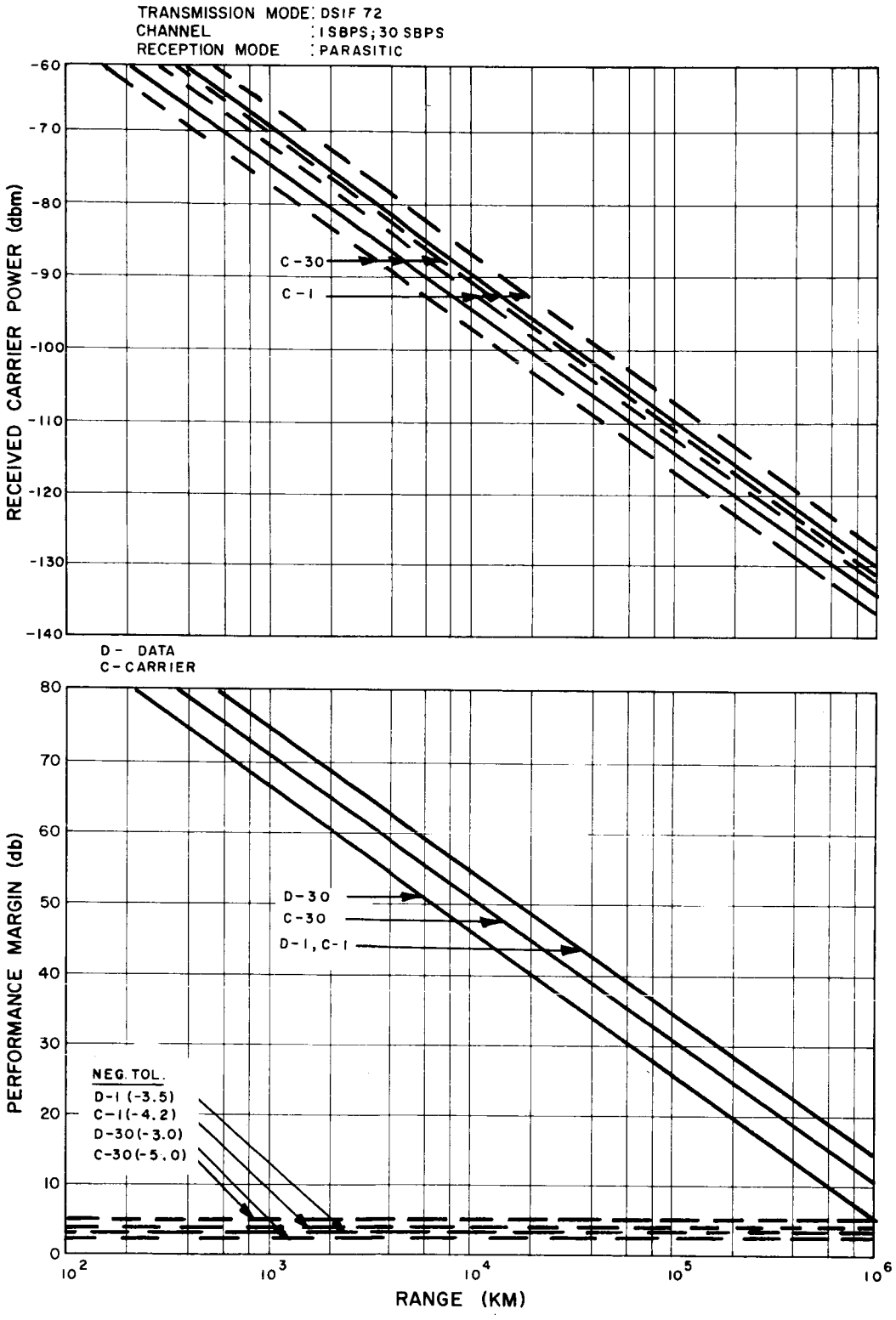


Figure A-18. Link Performance Versus Range (Command)

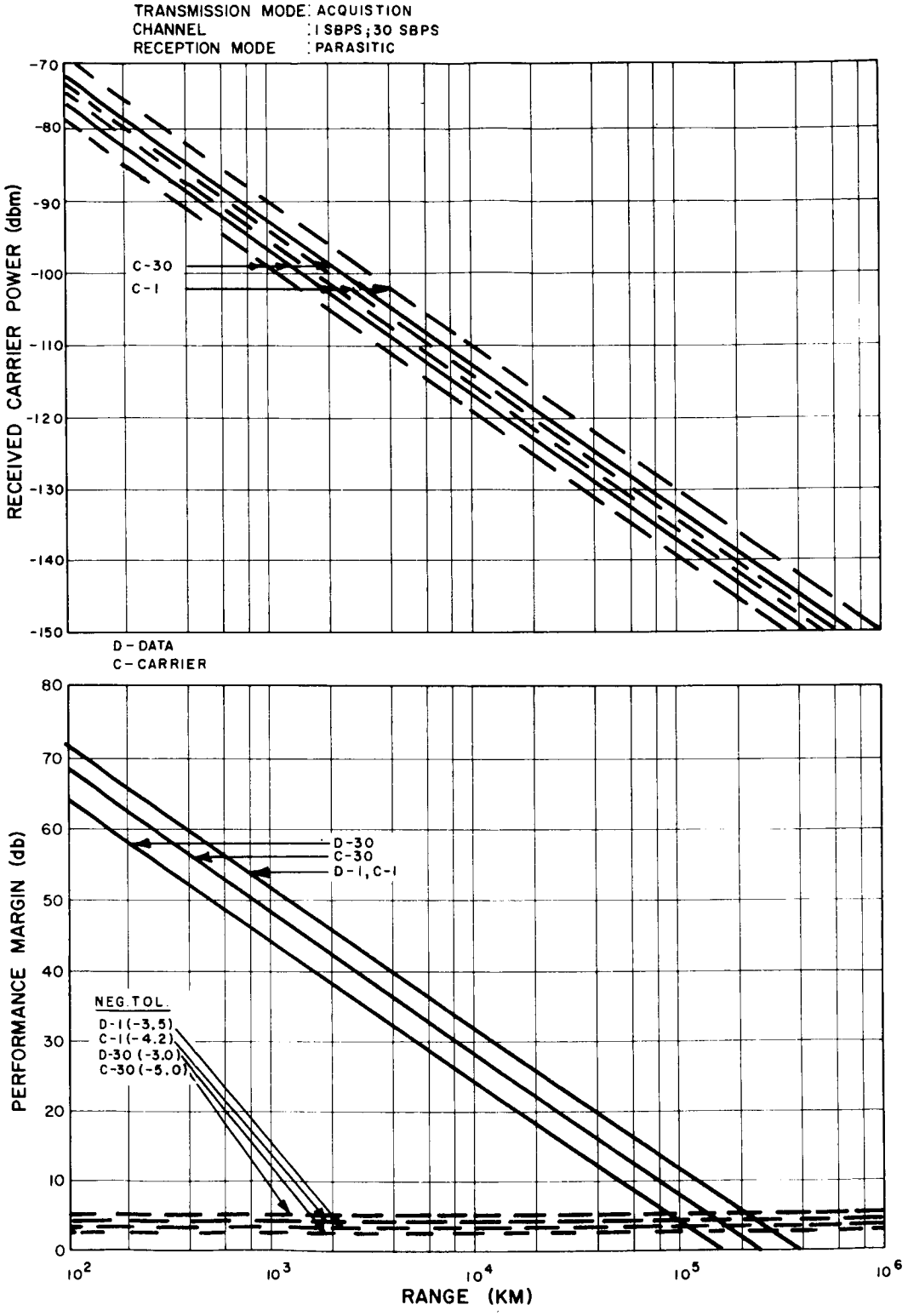


Figure A-19. Link Performance Versus Range (Command)

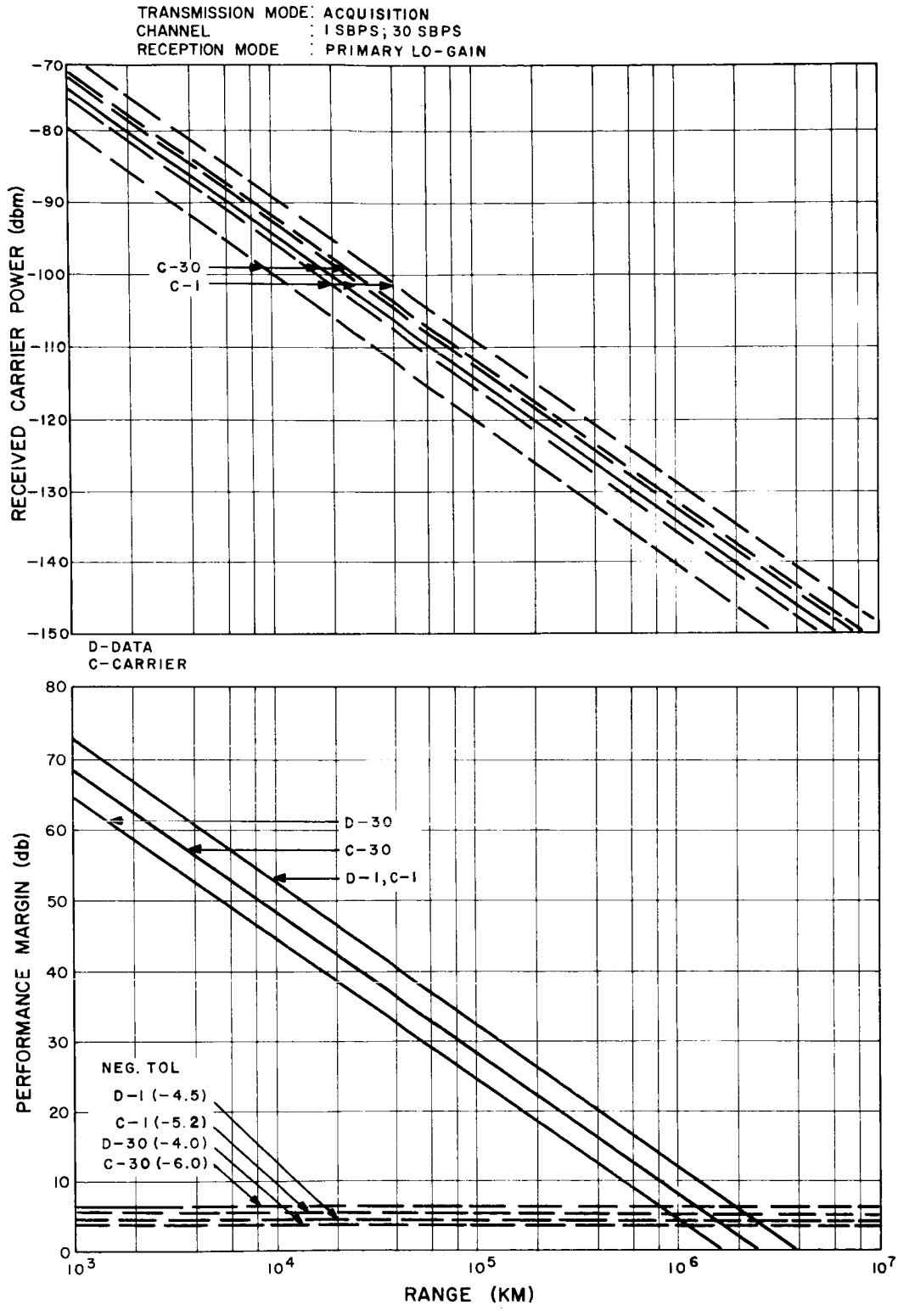


Figure A-20. Link Performance Versus Range (Command)

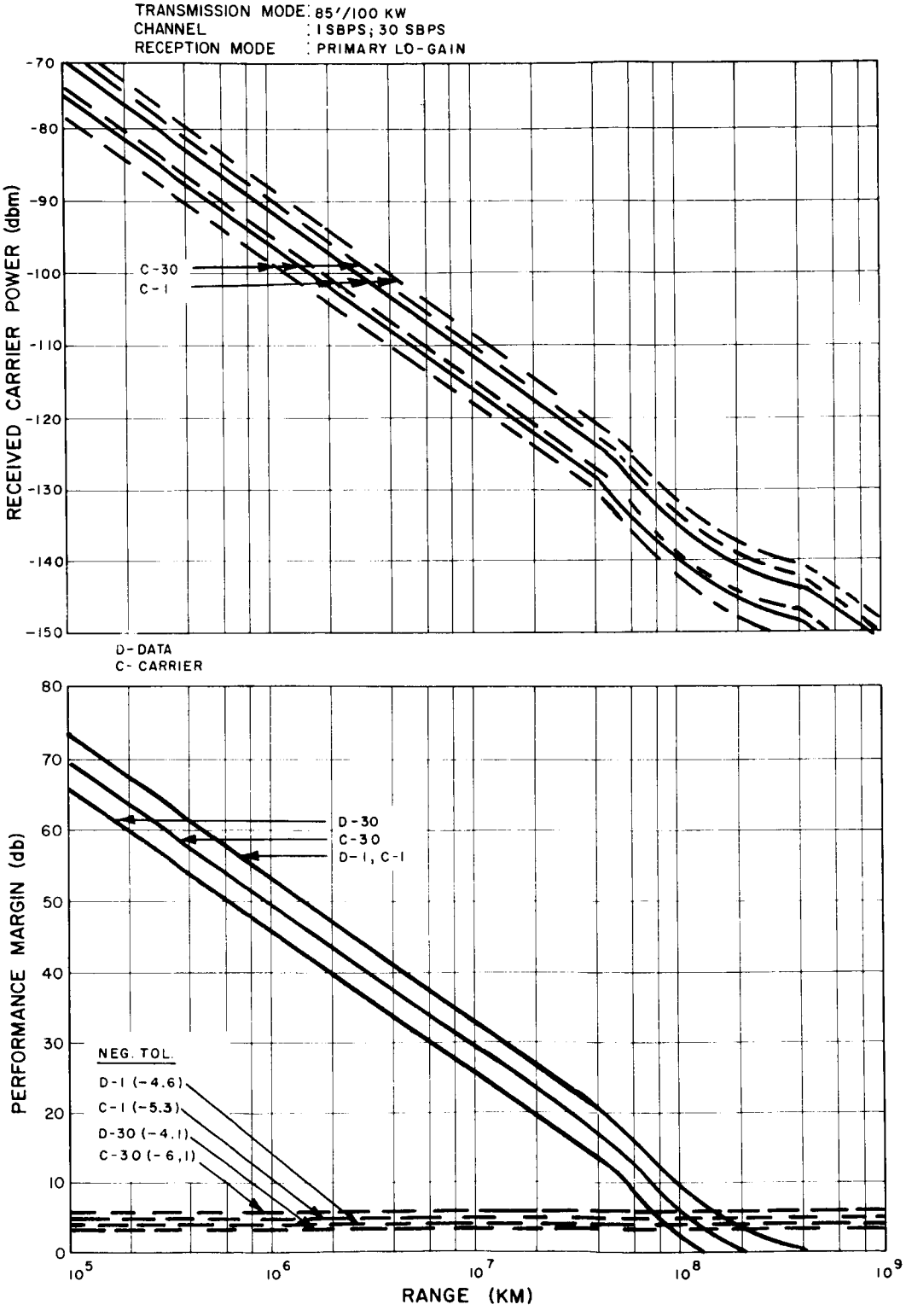


Figure A-21. Link Performance Versus Range (Command)

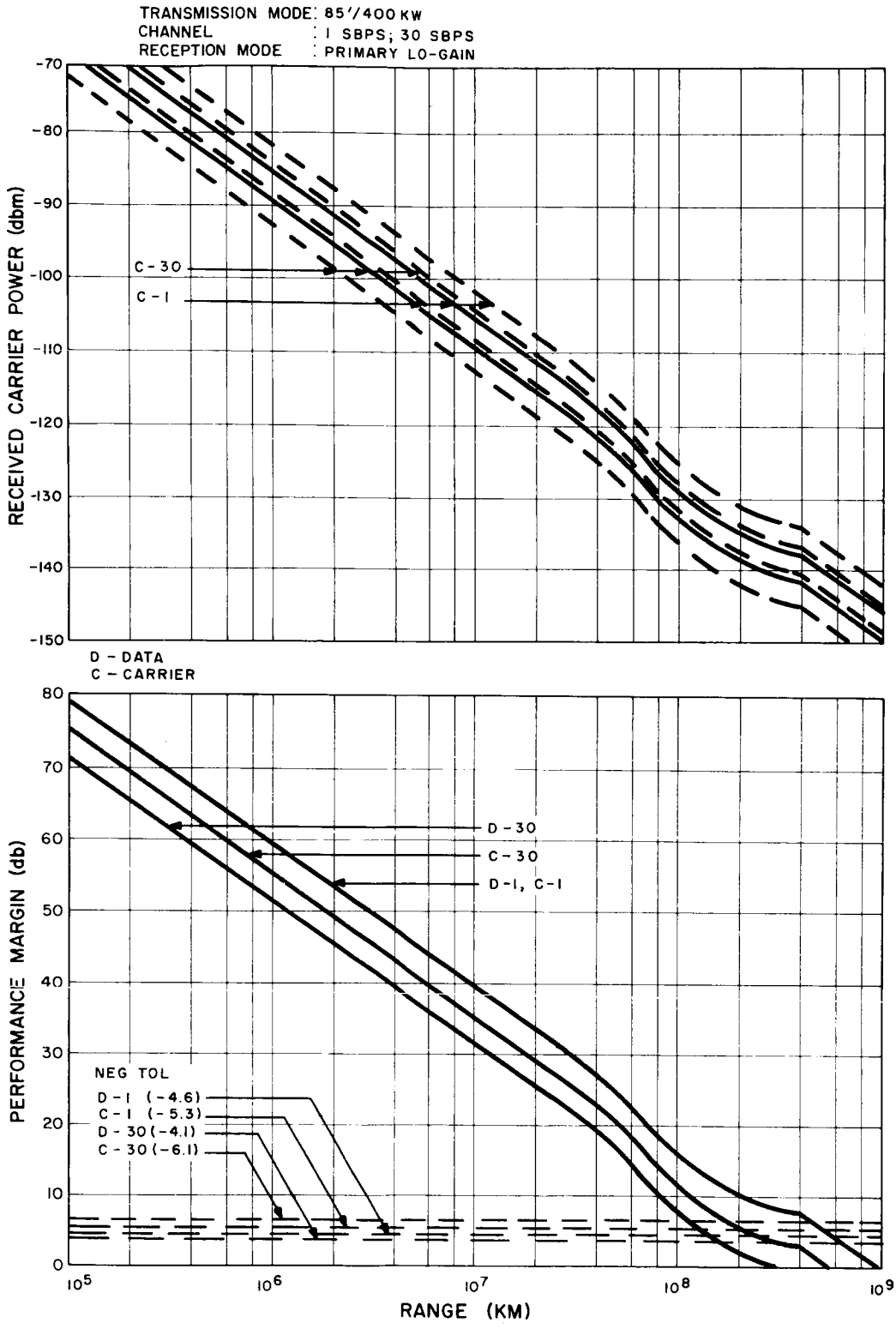


Figure A-22. Link Performance Versus Range (Command)

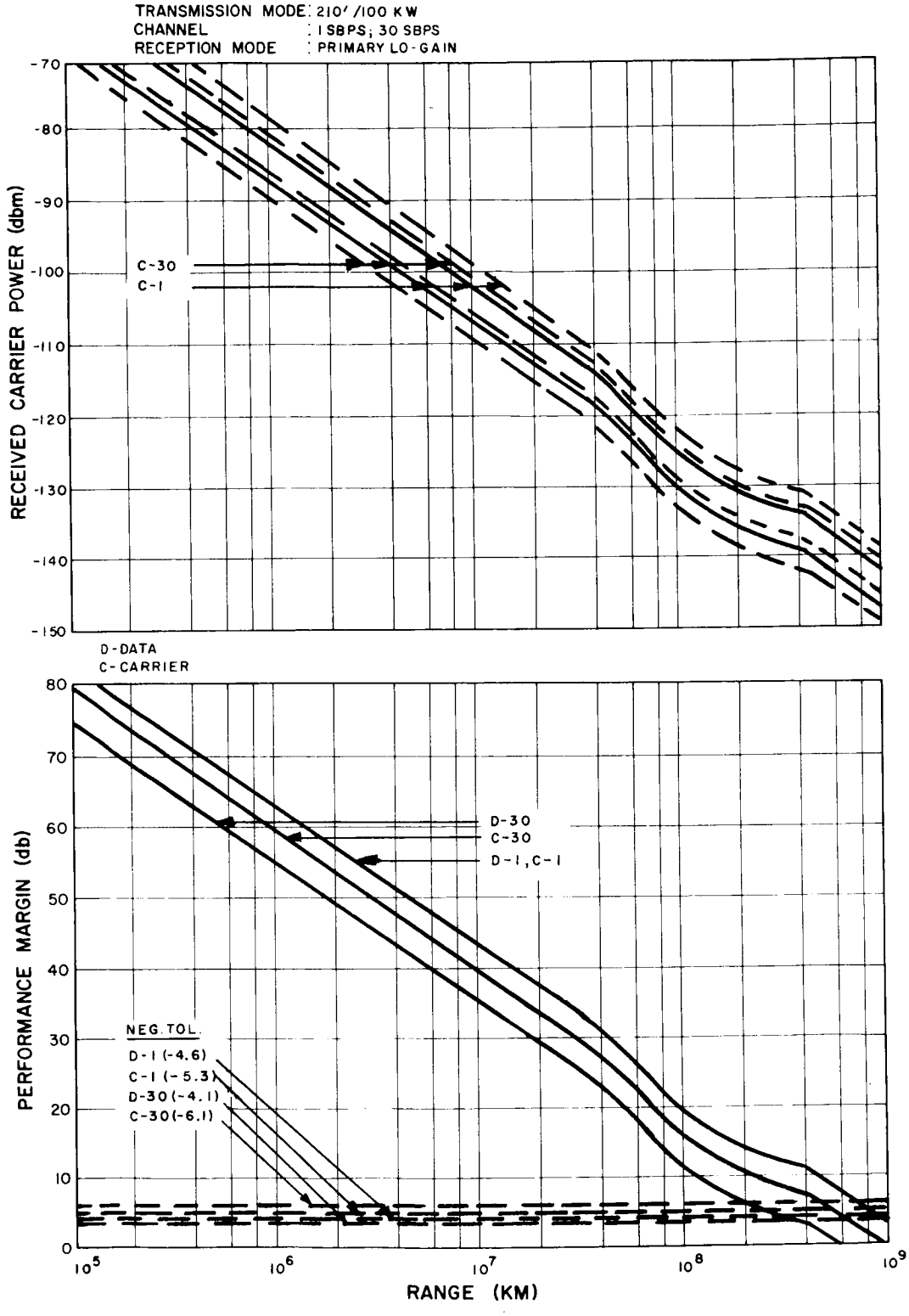


Figure A-23. Link Performance Versus Range (Command)

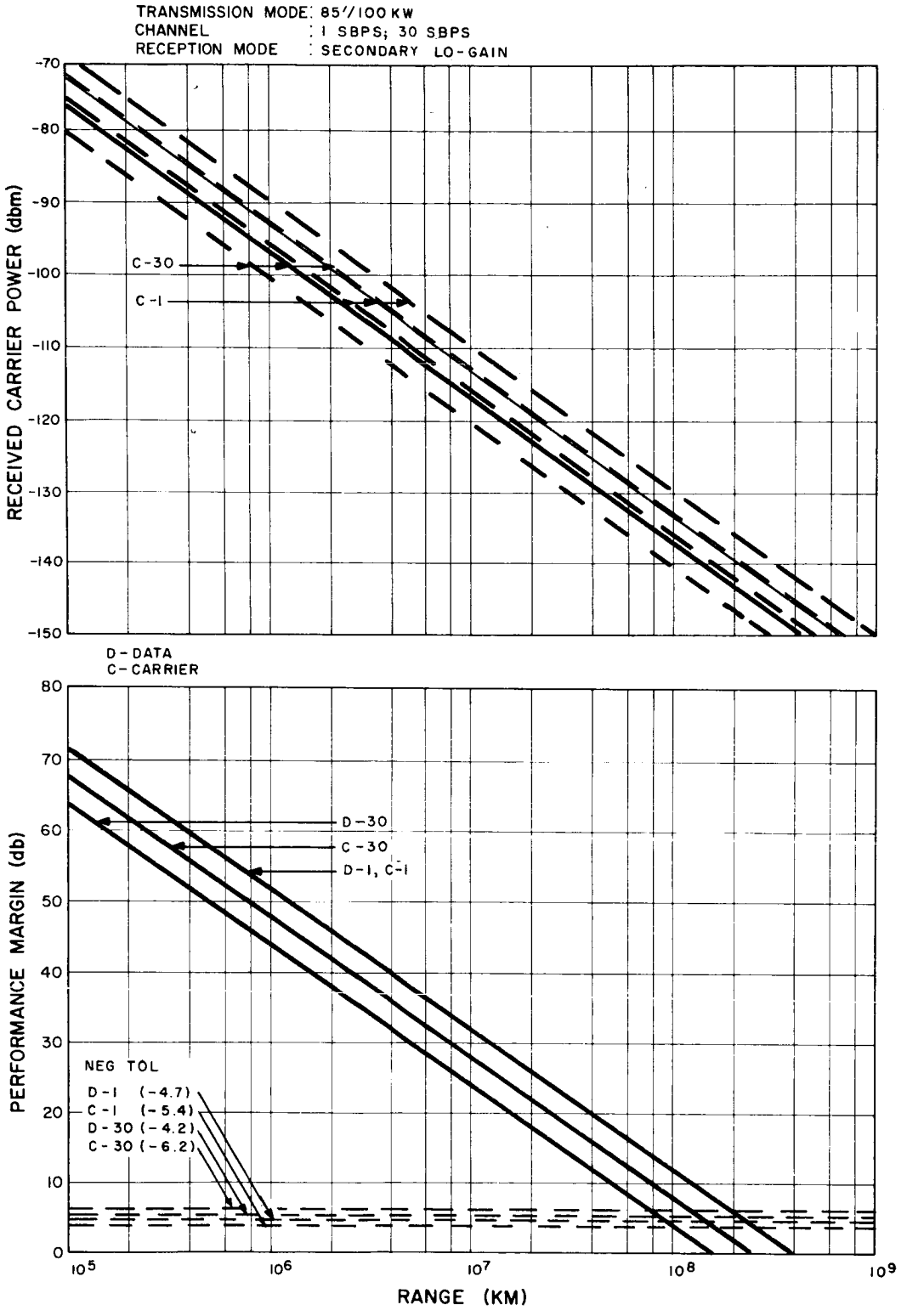


Figure A-24. Link Performance Versus Range (Command)

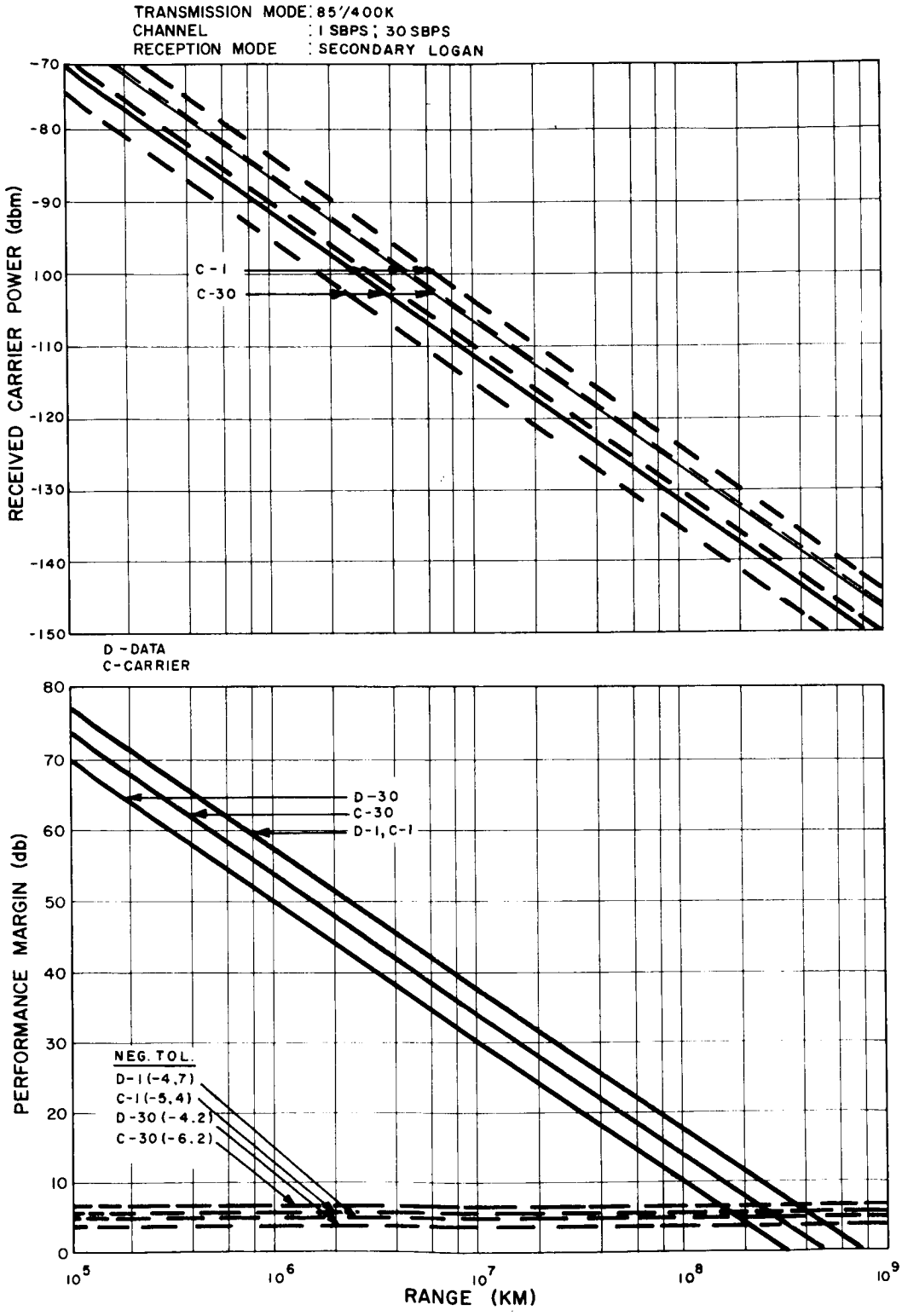


Figure A-25. Link Performance Versus Range (Command)

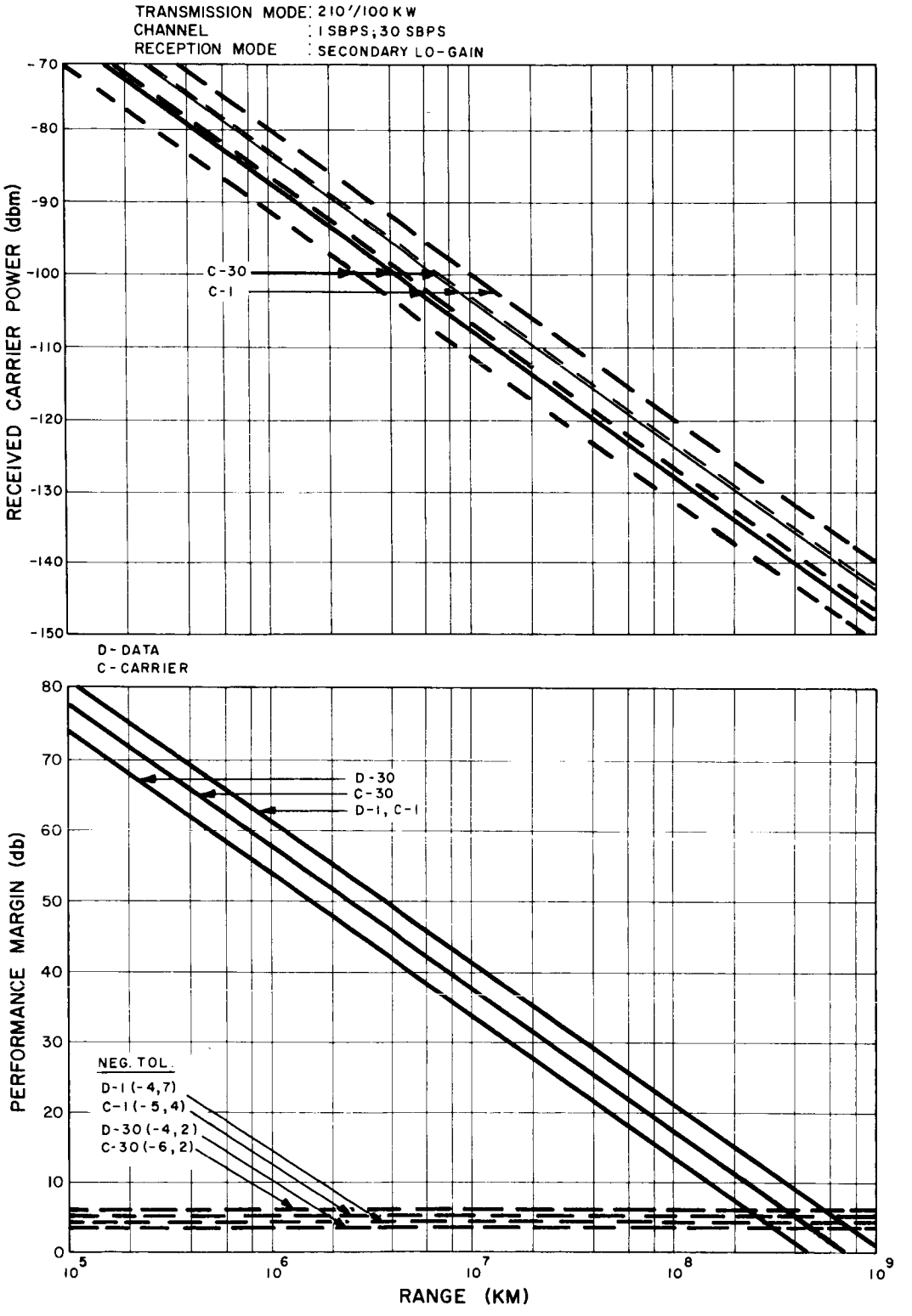


Figure A-26. Link Performance Versus Range (Command)

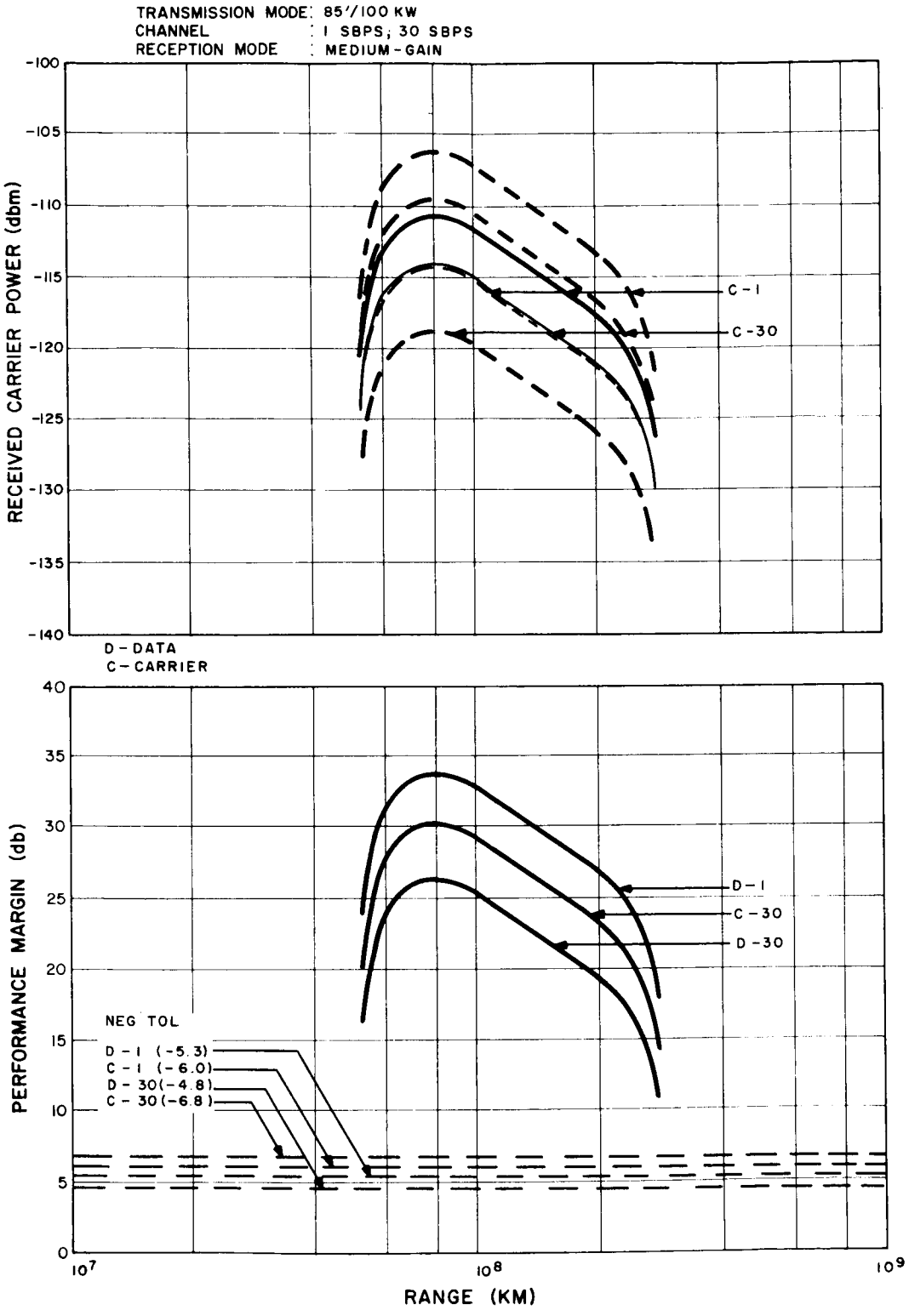


Figure A-27. Link Performance Versus Range (Command)

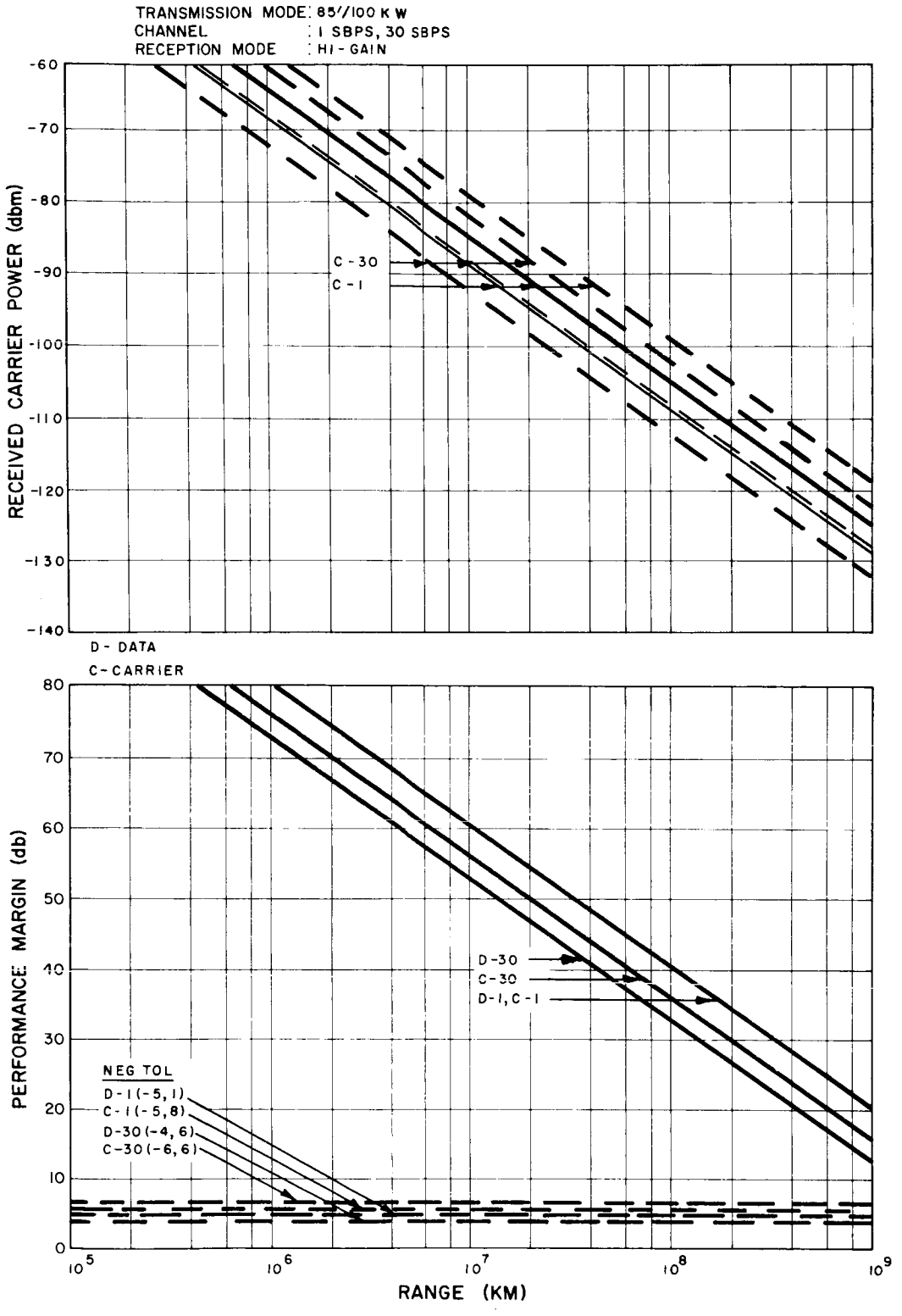


Figure A-28. Link Performance Versus Range (Command)

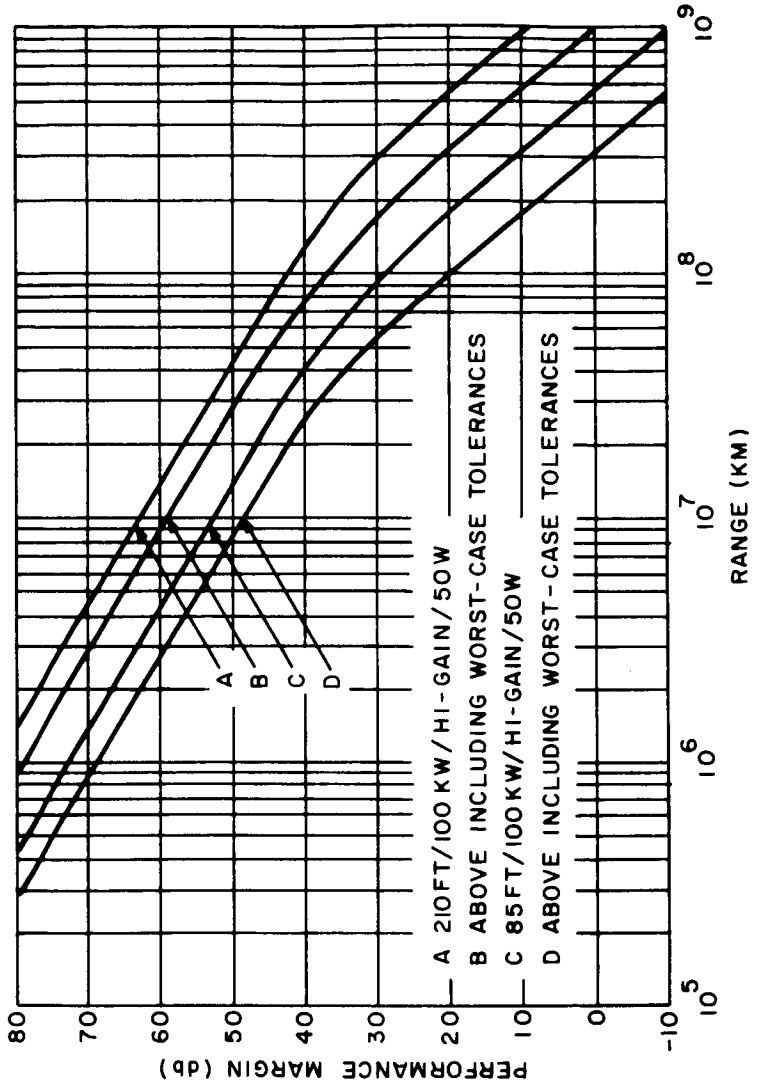


Figure A-29. Performance Margin Versus Range (Ranging)

CII VC233FD102

RADIO SUBSYSTEM

SECTION

1	SCOPE
2	APPLICABLE DOCUMENTS
3	S-BAND RADIO
4	INTERFACE DEFINITIONS
5	PERFORMANCE PARAMETERS
6	PHYSICAL CHARACTERISTICS

RADIO SUBSYSTEM

1.0 SCOPE. This document is a functional description of the 1971 VOYAGER Radio Subsystem and its components. Its purpose is to provide detailed information on the subsystem configuration, indicate the expected performance, and define subsystem interfaces with other spacecraft elements.

2.0 APPLICABLE DOCUMENTS. Reference to the following documents is required for completeness in this description.

VB233FD102 - VOYAGER Radio Subsystem.
VB233AA102 - Alternate Mechanizations Considered, Radio Subsystem.

Final Report (WF2840) S-Band Transponder, Mark I, 20-Cycle Bandwidth, JPL Contract No. 950413, Motorola, Inc., July, 1964.

VC233FD103 - Command Subsystem.
VC220FD109 - Telemetry Criteria

3.0 S-BAND RADIO. This section describes the S-band portion of the radio subsystem. The capsule relay antenna is included.

The proposed Radio Subsystem is designed to satisfy the requirements of the "VOYAGER Performance and Design Requirements Specification" dated 9/17/65 and the "VOYAGER 1971 Preliminary Mission Description" dated 10/15/65. These requirements are summarized here.

The VOYAGER Radio Subsystem is required to perform the following basic functions:

a. Receive the RF signal transmitted to the spacecraft from the DSIF.

b. Coherently translate the frequency and phase of the received RF signal by a fixed ratio (240:221).

c. Demodulate the received RF signal and send a composite command signal to the Command Subsystem.

d. Transmit a modulated RF signal to the DSIF stations, using the translated RF signal (from item b above) or an independent frequency source.

e. Phase modulate the transmitted signal with a composite telemetry signal.

f. Receive and re-transmit a range code signal via a turnaround ranging channel.

In performance of these functions, the subsystem configuration is further constrained by the following additional requirements:

a. The nominal transmitter power level shall be 50 watts.

b. Up-link communications with the spacecraft shall be accommodated from prelaunch through end-of-mission by a low-gain nonsteerable antenna.

c. Capability for downlink communications with the spacecraft from prelaunch through end-of-mission shall be provided. During the cruise phase of the mission, the link shall support a science data rate of not less than 2.5×10^6 bits per day, with a design goal of 5×10^6 bits per day. At the end of the six-month orbital phase of the mission, the link shall support a science data rate not less than 5×10^7 bits per day with a design goal of 10^8 bits per day.

3.1 Subsystem Description. A block diagram of the proposed Radio Subsystem is shown in Figure 3-1. The configuration shown combines three transmitters and three receivers in redundant fashion to ensure reliable performance of subsystem requirements. A condensed list of radio components is given in Table 3-1.

The equipment listed is connected as shown to provide a conservative and uncomplicated approach to the Radio Subsystem design. General considerations of the design are reviewed in the following paragraphs.

No single failure of the Radio Subsystem will result in failure to achieve mission objectives. Multiple backup modes are provided for all required functions.

The antennas selected include a steerable high-gain antenna which provides capability for transmitting the required science data rates when the spacecraft is operating in the stabilized mode. The medium-gain antenna, which is neither steered nor deployed, functions as a backup to the high-gain antenna and will support the required science data rates for several

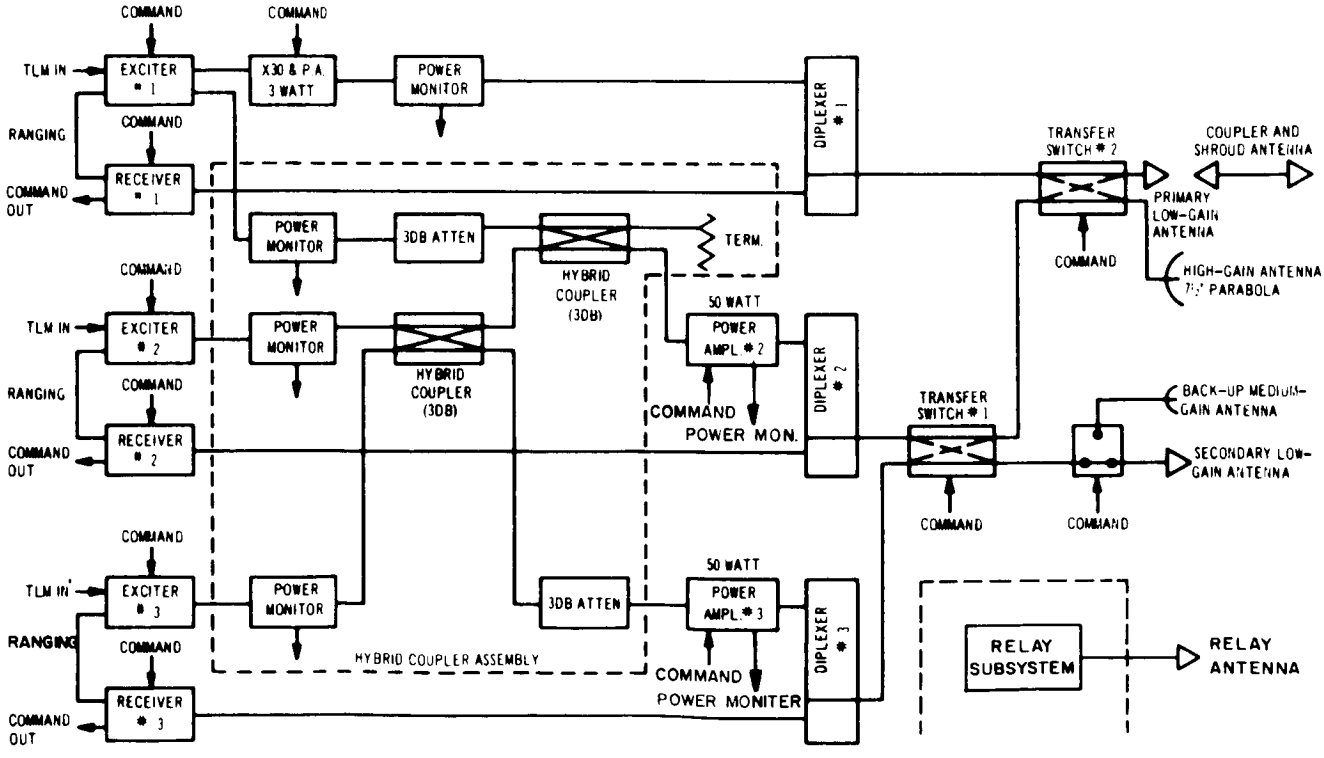


Figure 3-1. VOYAGER Radio Subsystem, Block Diagram

TABLE 3-1. SELECTED LIST OF RADIO COMPONENTS

Component	Quantity
Mark I S-band Transponder	3
50-Watt Power Amplifier	2
3-Watt Solid State Power Amplifier	1
7.5-Foot High-Gain Antenna	1
Primary Low-Gain Antenna	1
Secondary Low-Gain Antenna	1
Medium-Gain Antenna	1
Diplexer	3
Hybrid Coupler Assembly	1
Antenna Switch	3

months in Mars orbit. During early phases of the mission, normal communication is via the primary low-gain antenna which is selected to provide nearly hemispherical coverage, symmetrical about the roll axis. The secondary low-gain antenna provides the greatest angular coverage for maneuvers and emergency conditions. A fixed low-gain antenna is provided for the Relay Subsystem for use during capsule descent from orbit.

Capability for transmitting telemetry is a primary consideration, and multiple backup modes are provided. Each of the three exciters may be used as a source for two of the three power amplifiers. Similarly, the power amplifiers may be connected in multiple combinations to the four antennas shown.

Two of the three power amplifiers operate at the specified level of 50 watts. Two devices, the TWTA (traveling wave tube amplifier) and the ESFK (electrostatically focused klystron), are being considered for this application. A parallel development program will be initiated for these devices and their performance will be evaluated before a selection is made. Possibly, both devices will be used to guard against generic failures.

The third power amplifier is a solid-state unit operating with a minimum output of 3 watts. The development of a reliable device operating at this level is considered to be reasonable for VOYAGER. The 3-watt amplifier will be used from launch until acquisition when the high-gain antenna with a 50-watt amplifier will be used. In the event that both 50-watt amplifiers fail or that a power shortage precludes their operation, considerable science data can be transmitted during the orbit phase by using the 3-watt amplifier and the high-gain antenna.

The performance of the design has been evaluated on the basis of the amount of data which can be transmitted during the orbit operation phase of the mission. During this phase, the primary mode of operation will be with 50-watt amplifier No. 2 and the high-gain antenna. Backup for the high-gain antenna is provided by the medium-gain antenna. Should the 50-watt power amplifier fail, backup is provided by the alternate 50-watt amplifier or the 3-watt solid-state amplifier. Figure 3-2 shows data rate capability as a function of days in orbit for the primary mode of operation and the major backup modes. Note that the required science rate is easily sustained in the primary mode and each of the backup modes will support the lowest data rate of 933-1/3bps for several months in orbit. The data presented is for adverse system tolerances (i.e., the data rates shown are "grey out" rates).

Up-link communication is accommodated by three receivers. These receivers operate on separate frequencies and each remains ON at all times. From prelaunch until separation, communication is restricted to Receiver No. 1 via the primary low-gain antenna and a parasitic shroud antenna. After acquisition of Sun and Canopus references, any of the three receivers may be used for command purposes at any time. During periods when the

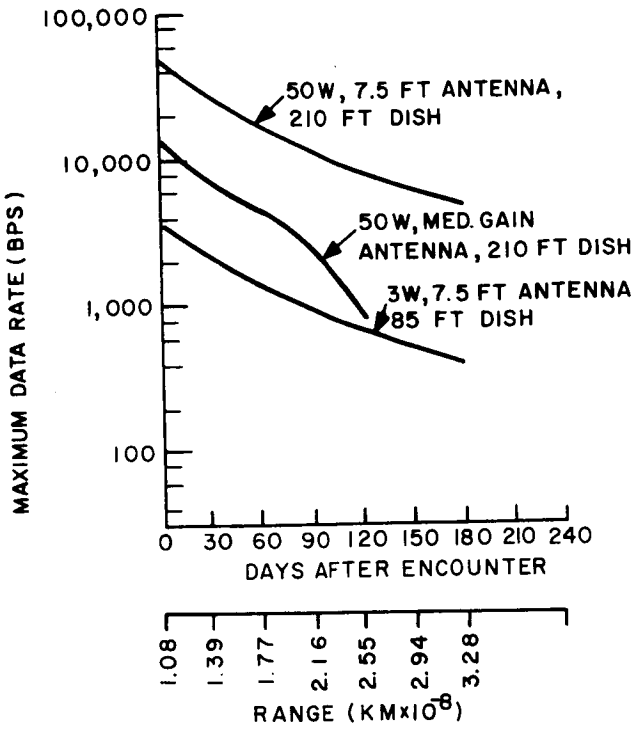


Figure 3-2. Data Rate Capability Versus Days in Mars Orbit

spacecraft is unstabilized, operation is restricted to Receivers 1 and 3 which are normally connected to the primary and secondary low-gain antennas, respectively. Table 3-2 summarizes the performance of these modes for various command rates and ground station configurations. The data presented is based on adverse system tolerances, except that antenna gains for normal spacecraft attitude were used.

Each of the receivers is combined with an exciter in the form of a Mark I S-band transponder. The transponders will be the same design used on Mariner C, with minor modifications directed primarily at achieving greater reliability and improved performance. When operated in the coherent mode for two-way tracking, the transponder translates the frequency and phase of the received signal by the required ratio of 240:221. When the receiver is not phase-locked to a signal from earth, the exciter automatically derives its source from an auxiliary noncoherent oscillator. Each of the transponders is equipped with a turnaround ranging channel which may be turned ON or OFF by command.

The number of RF switches used is minimal when the amount of equipment is considered. There is a maximum of two RF switches in a given transmit path. During a normal mission these switches would never be energized. The use of RF switching for the interface between the exciters and power amplifiers is avoided by using a strip transmission line hybrid-coupler assembly. Whenever possible, switching operations are performed in the component power supplies.

TABLE 3-2. RADIO SUBSYSTEM COMMAND CHANNEL PERFORMANCE

Command Bit (SBPS) Rate	Ground Antenna/Power (Kw)	Spacecraft Low-Gain Antenna	Minimum* Range (km)
1	85'/100	Primary	1.8×10^8
30	85'/100	Primary	0.9×10^8
1	85'/100	Secondary	2.11×10^8
30	85'/100	Secondary	9.9×10^7
1	210'/100	Primary	7.95×10^8
30	210'/100	Primary	3.72×10^8
1	210'/100	Secondary	6.38×10^8
30	210'/100	Secondary	2.98×10^8

* Assumes Adverse System Tolerances

Automatic switching for the radio subsystem is intentionally limited to essential operations. The objective was to maintain a simple and conservative approach yet satisfy the requirements for an automatic spacecraft. The only switching operations are the changeover from the 3-watt power amplifier and primary low-gain antenna combination to the 50-watt amplifier No. 2 and high gain antenna, and the change to the secondary low gain antenna and 50-watt amplifier No. 3 during maneuvers. The choice of receiver and exciter for normal cruise operation is optional. One possibility is to receive via

the primary low-gain antenna and transmit via the high-gain. Another alternative is to receive and transmit via the high-gain. Selected failure mode switching designed to preserve telemetry would also be implemented, but the number of modes would be limited to reduce the complexity of the design. All other failure switching would be performed by command from the DSIF stations.

3.1.1 Antennas

3.1.1.1 High-Gain Antenna. The high-gain antenna is a rigid 7.5-foot diameter parabolic reflector having a 28.8-inch focal length. Studies of various antenna types, both rigid and erectable, have shown that the parabolic reflector meets all electrical and mechanical performance requirements and is the most simple and conservative high-gain antenna approach for this application. A reflector of honeycomb sandwich construction would provide the smallest, lightest, and least complex antenna assembly. However, overall spacecraft systems considerations, including solar pressure, prohibit the use of a solid surface reflector. Accordingly, a mesh type construction is employed to reduce the opaque frontal area of the antenna. The reflector surface is formed of aluminum mesh supported by a framework of six radial ribs and three rings as illustrated in Figure 3-3.

The high-gain antenna feed is a turnstile radiator located at the focus of the parabola. Details of this feed, basically the same as that used for the Mariner C high-gain feed, are shown in Figure 3-4. The antenna has two orthogonal axes of freedom with respect to the spacecraft. The antenna can be rotated 170 degrees about the main gimbal axis which is parallel to the vehicle y-axis. Limited motion (±15 degrees) about the second gimbal axis then permits the high-gain antenna beam to be directed at Earth throughout the life of the mission with the vehicle in the cruise attitude. By providing a capability for 225 degrees rotation about the y-axis, the antenna could also be directed at Earth during maneuvers for any orientation of the thrust axis (z-axis). This would be accomplished by rotation of the antenna about the main gimbal axis, and rolling the vehicle about the thrust axis.

3.1.1.2 Primary Low-Gain Antenna. The primary low-gain antenna is a crossed-slot radiator similar to the Mariner C low-gain antenna as illustrated in Figure 3-5. The slot parameters and other physical details are modified slightly to provide a more nearly hemispherical radiation pattern.

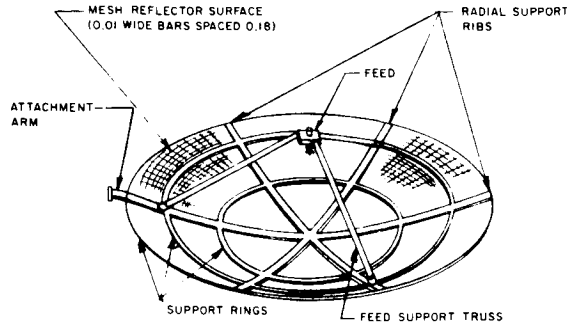


Figure 3-3. High-Gain Antenna

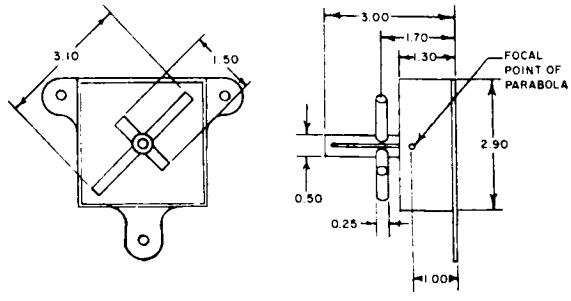


Figure 3-4. High-Gain Antenna Feed Detail

The crossed slots are fed through a low-loss, circular waveguide section which also serves to support the radiator at a sufficient distance from the vehicle to minimize pattern obstruction and distortion within ±110 degrees of the antenna axis. Design and location of the circular waveguide section must take into account the effects of any thermal distortion which might occur during engine firing. The antenna will be installed on the solar panels near the -x axis. It is canted 25 degrees from the -z axis to reduce the effects of reflections from the nozzle, as well as to minimize the portion of the pattern that is blocked by the nozzle. The resulting pattern coverage enables the primary low-gain antenna to be used during acquisition of attitude references and during early cruise phases for the worst case trajectories. A gain of at least 0db will be available in the cruise mode during all but very early mission periods. During prelaunch and launch phases, energy is coupled through the primary low-gain antenna to a parasitic antenna on the shroud.

3.1.1.3 Secondary Low-Gain Antenna. The secondary low-gain antenna consists of four dipole elements spaced 90 degrees apart around a combination feed and support structure as shown in Figure 3-6. The four dipoles are fed in phase and oriented at about 30 degrees with respect to a plane containing their centers. The radiation pattern of this antenna is approximately toroidal in shape and circularity of polarization is excellent over most of the pattern. Installation is such that the toroidal-shaped pattern lies in a plane parallel to the vehicle y-z plane (i.e., the antenna axis of symmetry is parallel to the vehicle x-axis). The antenna is supported at a sufficient distance from the vehicle to provide a clear field of view over ±45 degrees from the plane of the dipoles. Thus, the pattern of the secondary

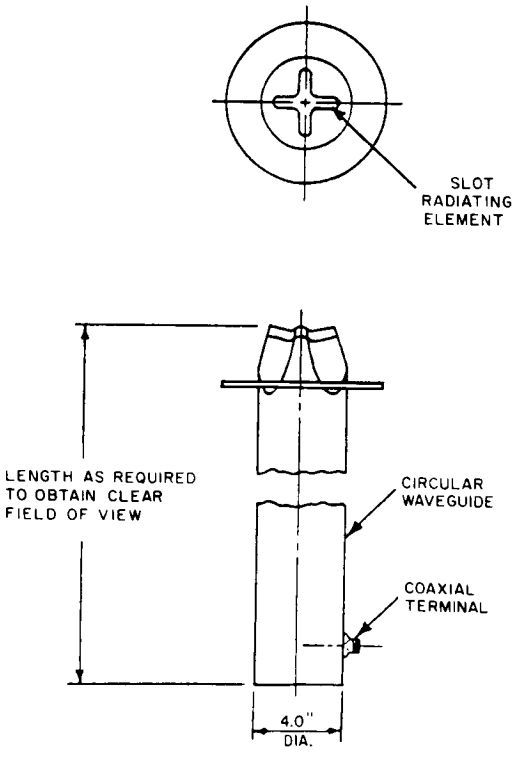


Figure 3-5. Primary Low-Gain Antenna

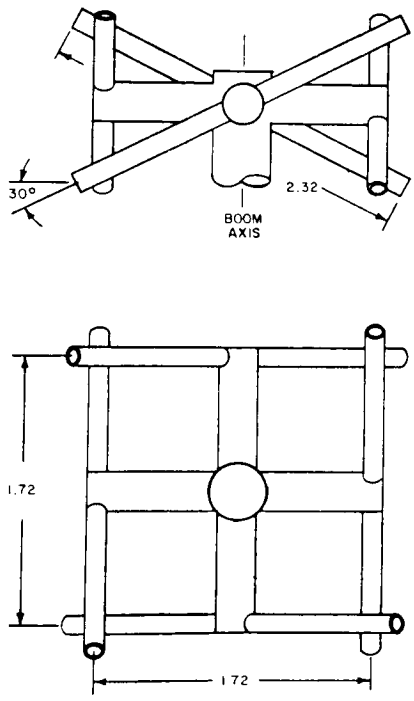


Figure 3-6. Secondary Low-Gain Antenna

low-gain antenna will enable the entire 4π solid angle to be covered during maneuvers if the vehicle may be rolled about the thrust axis. The secondary low-gain antenna provides an excellent pattern for periods of transition between cruise and maneuver attitudes.

3.1.1.4 Medium-Gain Antenna. The medium-gain antenna will provide a backup capability for the high-gain antenna and will support science data for a substantial period in Mars orbit. It is a Mariner-C type fixed parabolic reflector having an elliptical aperture. The major axis of the aperture is 46.0 inches and the minor axis is 21.2 inches. The reflector is constructed as a rigid, lightweight, aluminum honeycomb sandwich. The feed utilizes two turnstile radiators similar to the high-gain antenna feed. These elements are fed through a strip transmission line power-dividing and phase-shifting network. The antenna will provide a fan-shaped beam approximately 15.5 degrees by 7.5 degrees wide at the half-power points, and the peak gain will be 23.5 db. The medium gain antenna will be oriented to maximize the data return for the encounter period of the mission. This antenna will provide 7433-1/3 bps for 20 days after an early encounter, and will support the lowest transmission rate of 933-1/3 bps for 120 days after encounter.

3.1.1.5 Relay Antenna. The design selected for the 400 MC relay antenna is a crossed dipole over a flat groundplane as shown in Figure 3-7. Two crossed, half-wavelength dipoles are fed by a coaxial split balun transformer. One dipole is slightly longer than a half wavelength, the other slightly shorter to obtain circular polarization on axis. A flat groundplane spaced a quarter wavelength provides unidirectional radiation. The antenna provides at least +5 db gain on its axis, tapering off to -0.5 db at ±60 degrees including polarization loss. The antenna assembly is fixed-mounted off the back of the solar array on the + x side, pointing 40 degrees away from the + z axis. The angular clearance to the edge of a typical small capsule is more than 60 degrees off the pattern axis. The antenna is fed by Type RG-142 coaxial transmission line with Type-N terminals. For prelaunch checkout of the complete relay subsystem, an rf test probe will be attached to the spacecraft and will be connected to the spacecraft umbilical by small size coaxial cable (RG-188).

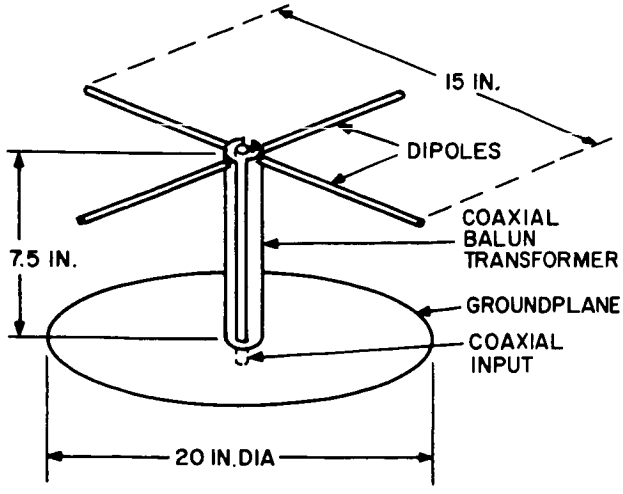


Figure 3-7. Relay Antenna-Turnstile Over Ground Antenna

3.1.1.6 Antenna RF Transmission Lines. The principal rf transmission line used between the electronics package and the antennas is a semi-rigid, aluminum jacketed coaxial cable with a 1/2 inch diameter (Spiroline). For the transitions across antenna deployment axes, RG-142 coaxial cable will be employed. It will also be employed at one of the gimbal axes of the high-gain antenna where the required motion is

relatively small. Wherever the flexible cable is used, it will be kept sufficiently warm to insure that flexibility is maintained. A rotary joint will be used at the main gimbal axis of the high-gain antenna. The rotary joint will be of the choke-coupled variety and will not have metal-to-metal contacting surfaces except for the mechanical bearing. Type N connectors will be used to mate all antenna transmission line components.

3.1.1.7 RF Test Probes. Each of the five antennas will be provided with an RF test probe to accommodate prelaunch checkout of the complete radio subsystem. These will be small coaxially-fed stub elements loosely coupled to the spacecraft antennas. The medium-gain antenna test probe will be permanently mounted to the antenna structure. For the deployable antennas, the test probes can be permanently mounted to the antennas, but in some cases it may be more desirable to mount the probe on the spacecraft structure so that it will be in the field of the stowed antenna. The latter approach eliminates the necessity for routing probe cables across the antenna deployment axes. The RF test probes will be connected through RG-188 coaxial cable to the spacecraft umbilical connector.

3.1.2 Transponders. Three transponders are used in the radio subsystem design of Figure 3-1. Each transponder consists of a phase-lock receiver, solid state exciter, and their associated power supplies and is required to perform the following functions:

a. Receive and demodulate an RF signal from the DSIF via the spacecraft antennas.

b. Provide coherent translation of the frequency and phase of the received signal by a 240:221 ratio for coherent two-way Doppler tracking.

c. Provide a turnaround ranging channel which demodulates the range code to baseband and conditions it for modulation on the transmitted signal.

d. Generate a stable RF carrier at a level suitable for driving the power amplifiers.

e. Modulate the carrier with telemetry and ranging signals.

The proposed transponders have the same basic configuration as the Mariner-C transponder; however, minor modifications directed at obtaining greater reliability and improved performance will be considered. The basic Mariner-C design is selected for its proven reliability and demonstrated performance. A complete description of that design is presented in the "Final Report, S-Band Transponder, Mark I, 20-Cycle Bandwidth", dated July 31, 1964.

A thorough analysis of transponder performance and investigation into known problem areas is planned. This will include a review of performance history available on the transponders for Mariner to determine areas of deficiency. Any modifications found necessary or desirable will be carefully reviewed before they are implemented. A condensed description of transponder operation and brief discussion of modifications under consideration are presented in the following paragraphs. The areas considered are based on Motorola experience with the flight transponders for Mariner and Lunar Orbiter. Figure 3-8 is a block diagram of the transponder for reference during the ensuing discussion. A photograph of the Mariner-C configuration is shown in Figure 3-9.

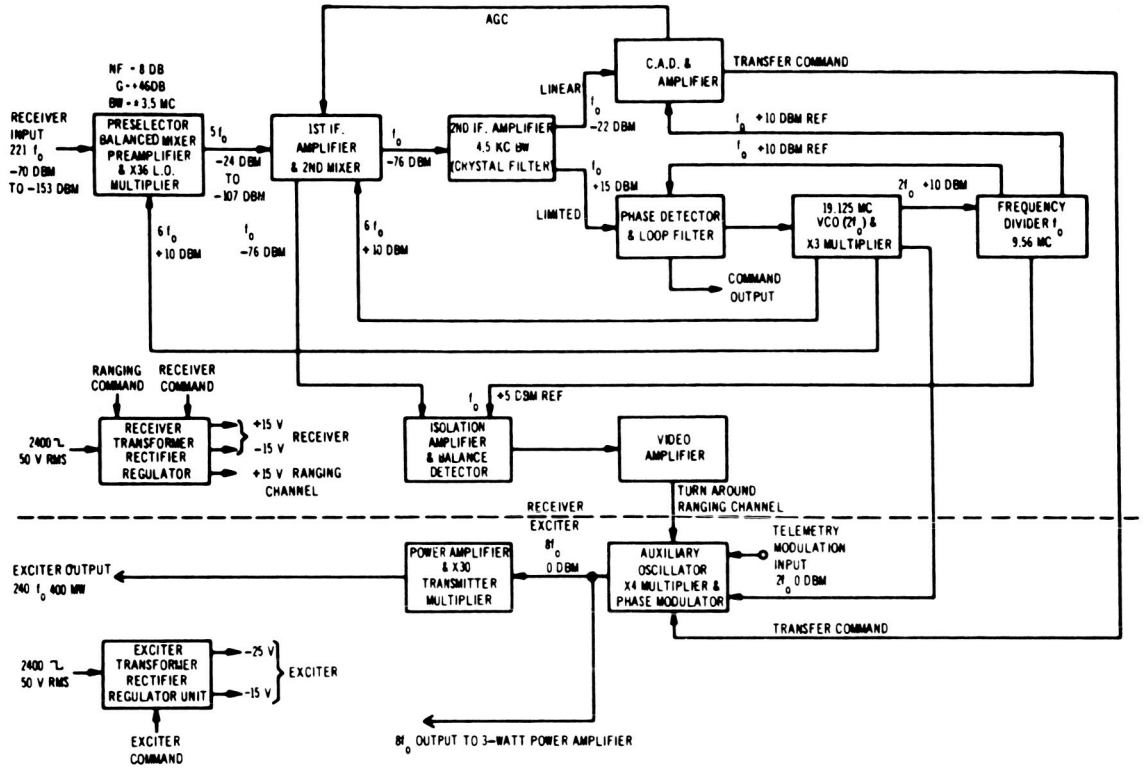


Figure 3-8. VOYAGER Transponder

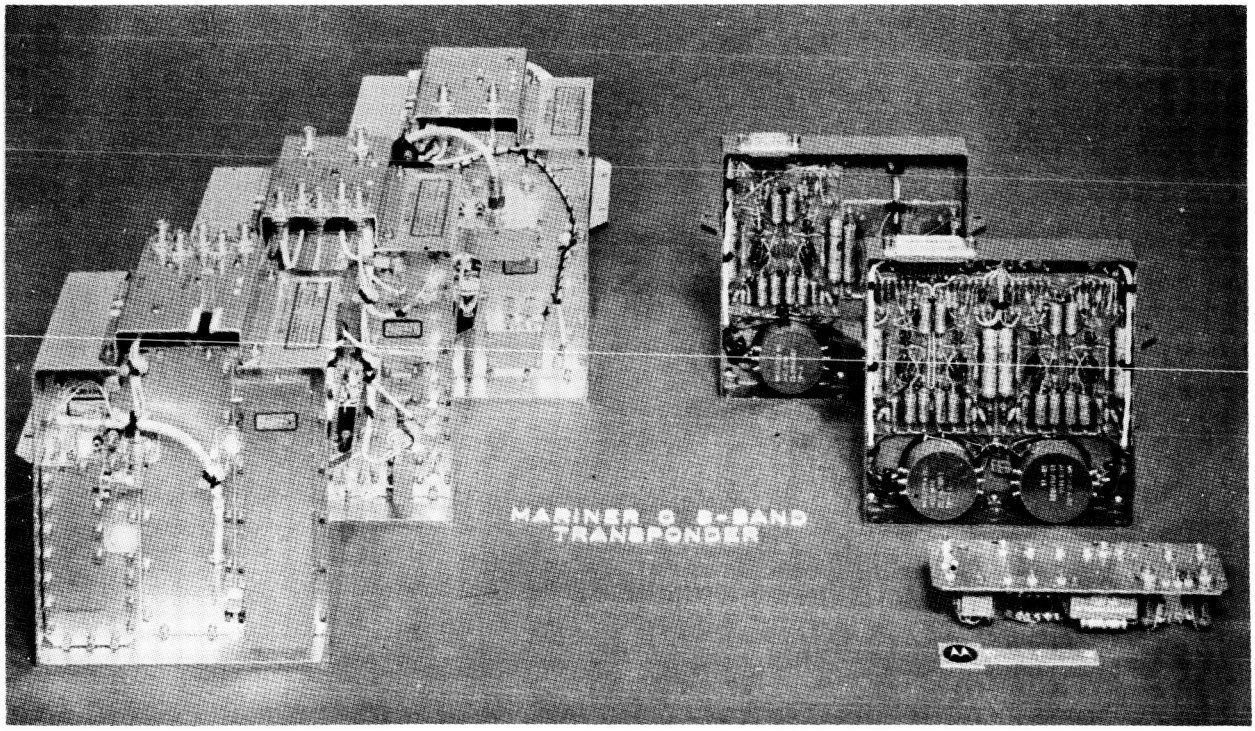


Figure 3-9. Mariner C S-band Transponder

3.1.2.1 Receiver Description. The receiver is the familiar phase-lock design with a nominal noise figure of 8 db and a carrier threshold sensitivity of -153 dbm. As indicated previously, the characteristics are essentially those of the Mariner C receiver. The noise bandwidth of the carrier tracking loop is adaptive to received signal level, and varies from 20 Hz at receiver threshold to 233 Hz for strong signal inputs. This provides capability for tracking high Doppler rates at strong signal strength, and preserves the narrow bandwidth desirable near threshold. The loop transfer characteristics at threshold are patterned after the mathematical model:

$$H(s) = \frac{1 + \frac{3}{4\beta_L} S}{1 + \frac{3}{4\beta_L} S + \frac{9}{32\beta_L^2} S^2}$$

where $2\beta_L$ is the two-sided loop noise bandwidth.

A coherent AGC system which responds only to the received carrier level provides an accurate analog of received signal strength for telemetry purposes. In addition, it serves as an indication of receiver lock and, as such, exercises control over the signal source for the transponder exciter. When the receiver is phase-locked to a signal from DSIF, the exciter derives its source from the coherent receiver Voltage Controlled Oscillator (VCO). Alternately, when the receiver is out of lock, as indicated by the absence of receiver AGC, the exciter is automatically switched to derive its source from a more stable auxiliary crystal oscillator.

Demodulation of command information on the received signal is an auxiliary function of the phase detector in the carrier tracking loop. By virtue of the phase relationships necessary for receiver lock and the bandwidth established, the command subcarrier appears at the carrier loop error point. After suitable conditioning, this information is passed on to the command subsystem.

Because of the position of the command spectrum and the adaptive characteristic of the transponder carrier loop, some filtering of the command signal can occur when the received signal strength is high. The effect of this filtering has been analyzed and the results are presented in "Command Subsystem," CII-VC233FD103. The analysis indicates that distortion of the command spectrum which might be introduced by the proposed carrier loop design would not adversely affect the performance of the Command Subsystem. Also, analysis has shown the command spectrum will not adversely affect the transponder performance or the performance of the DSIF receiver, Doppler, or ranging subsystems.

3.1.2.2 Receiver Modifications. The most significant modification under consideration for the receiver is the development of a low noise RF mixer with a nominal noise figure of 8 db. Advances in the state-of-the-art since completion of the Mariner design indicate this goal can be obtained along with a substantial improvement in reliability. The diode contacts used in the present mixer package are recognized as a weak area. The X36 Local Oscillator (LO)

multiplier would be redesigned as part of the mixer package in a configuration which reduces LO spurious outputs. Other minor modifications being considered for the receiver include:

a. Modification of the first I-F amplifier to extend its dynamic range and reduce its noise figure.

b. Modification of its frequency divider to eliminate potential instabilities in the current design.

c. Modification of the AGE dc amplifier to improve the temperature stability of the current design.

Investigation of known deficiencies in the following areas is also planned:

a. The receiver out-of-lock frequency drifts considerably with time and temperature. The source of drift will be determined and corrected, if possible.

b. The time delay of the turnaround ranging channel has been known to vary with temperature and is not reproducible from unit to unit. The channel will be analyzed to determine the source of instability.

c. The monitoring point lead filtering and power lead decoupling will be examined to determine whether low frequency susceptibility and rf leakage can be further reduced.

3.1.2.3 Exciter Description. The exciter portion of the transponder generates a stable S-band modulated carrier at a level which is suitable for driving the power amplifiers. The signal source for the carrier may be either the coherent receiver vco or the stable self-contained auxiliary crystal oscillator. Figure 3-8 shows the physical as well as functional breakdown of the exciter. Two modules, the auxiliary oscillator and the X30 multiplier, are used. The auxiliary oscillator module contains the alternate crystal oscillator, a X4 multiplier, and the exciter phase modulator. The modulator accepts preconditioned telemetry and ranging signals and modulates them on the carrier at indices up to 4.0 radians peak when converted to S-band. The modulator bandwidth extends from dc to 2 MHz. The X30 multiplier module amplifies the modulated signal and multiplies it by a factor of 30 to provide the S-band output.

3.1.2.4 Exciter Modifications. The development of a new X30 multiplier for the exciter is considered essential. The current design is known to exhibit excessive nonharmonic spurious outputs under certain conditions of temperature and supply voltage. These spurious outputs can cause false lock when the turnaround ranging channel is open. An alternate approach which does not exhibit these instabilities has been under development at Motorola for some time. Its operation is essentially as follows.

The X30 multiplier is required to convert a 0 dbm signal at 76.5 MHz to a 26 dbm signal at 2295 MHz. Figure 3-10 is a block diagram of the alternate design being considered. The input signal is coupled through an isolation amplifier to a X2 transistor frequency multiplier. Both of these stages provide gain; however, a two-stage transistor power amplifier at 153 MHz provides the major amount of power to drive the X15 varactor multiplier chain. The varactor multiplier chain requires a nominal input of 2 watts at 153 MHz to produce 0.5 watt of output

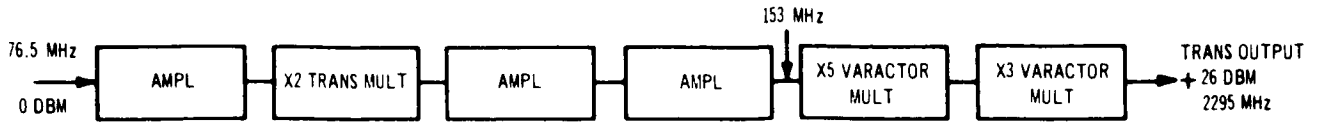


Figure 3-10. Block Diagram of the X30 Module of the Transmitter-Exciter

power at 2295 MHz. The X5 varactor multiplier is a lumped constant circuit with a three-section helical resonator filter at the output. The X3 varactor multiplier is a distributed constant strip transmission line circuit which contains a three-section interdigital bandpass output filter. This basic configuration has been successfully employed in the LEM Transponder to produce 1.4 watts at S-band, and in the Apollo Block II Transponder to deliver 0.6 watt. A similar design produces 0.2 watt in the FM transmitter of the Apollo Block II system. This design has demonstrated reliable, stable, and efficient operation over extended temperature ranges. A 3-db bandwidth of 90 MHz at the output frequency is being realized on the Apollo hardware with a dc to rf efficiency of nearly 15%.

All spurious harmonic outputs are down 60 db at the transmitter output terminals with no evidence of the parametric instabilities which can cause "ring-around" or "false-lock" problems in the transponder. All components have been well derated to comply with Apollo reliability design goals. With a 50°C heat sink temperature, no semiconductor has an operating junction temperature greater than 75°C. The components are plotted in polyurethane foam for maximum resistance to mechanical stresses.

Additional modifications to the exciter would include changes in the auxiliary oscillator module to obtain improved oscillator stability and to reduce the variations in sensitivity of the phase modulator. This transponder module has already been redesigned for the Lunar Orbiter transponder and the improvement verified. The development of low-noise oscillators for both the auxiliary oscillator and the vco is also planned. These oscillators would allow the use of narrower tracking bandwidths in both ground and flight receivers. Finally, an additional output from the auxiliary oscillator module at 76 MHz will be required for driving the 3-watt solid state power amplifier.

3.1.2.5 Receiver and Exciter Power Supplies

The power supplies for the transponder are proposed as shown in Figure 3-11. They are required to perform the following functions:

a. Furnish regulated and filtered +15 vdc and -15 vdc to the receiver
b. Furnish regulated and filtered -15 vdc and -25 vdc to the transmitter
c. Permit remote switching of dc power to the turnaround ranging channel
d. Permit remote switching of power to the receiver and the exciter.

The Mariner C transformer-rectifier unit will be used as a basis for this design. Series regulators will be used to provide filtering and regulation for each output. Overall power supply efficiency will be approximately 75%. The filtering now provided in the transponder is effective primarily at radio frequencies. As a result, the power supply must be well regulated to reduce the receiver and exciter susceptibility to low frequency ripple and transients.

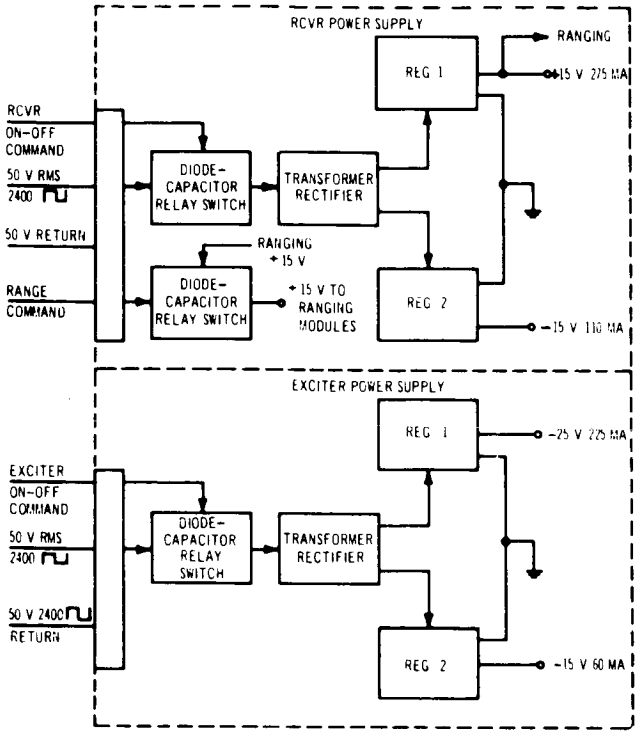


Figure 3-11. VOYAGER Receiver and Exciter Power Supplies

The undesirable effects of insufficient regulation and filtering are distortion of the receiver command output due to receiver vco frequency modulation and modulation of the down-link carrier because of the high gain in the video section of the turnaround ranging channel. The low frequency susceptibility problem is most economically solved by the addition of regulation in the power supply.

3.1.3 Power Amplifiers. The proposed VOYAGER radio subsystem uses three power amplifiers. Two of these amplifiers operate at the specified output level of 50 watts. The third amplifier is a 3-watt solid-state device which satisfies the requirements of early mission phases and serves as a backup during the orbit phase.

3.1.3.1 50-Watt Power Amplifier. Two devices are being considered for the 50-watt application, the TWTA (traveling wave tube amplifier) and the ESFK (electrostatically focused klystron). A survey of the 50-watt devices available indicates these are most suitable for VOYAGER. The nominal gains of the ESFK and TWTA are 26 db and 30 db respectively. This maintains exciter drive requirements at a reasonable level. Both operate at relatively high efficiencies near 35%. Prototype models of these tubes have already been built and operated at power levels in the 50- to 100-watt range. The most significant argument in favor of the TWTA is the fact that it is presently being used in many of the major space programs and has been flight proven. The ESFK, although not yet flight proven, offers potentially the highest efficiency. Also, it does not have an external magnetic field.

Both the TWTA and the ESFK will require development efforts. Although prototypes have been built, these models do not yet satisfy the requirements for VOYAGER. The power amplifier for VOYAGER must operate efficiently to conserve spacecraft prime power and to minimize thermal dissipation. This calls for improvements in the tube design such as depressed collectors, greater thermal dissipation from the collector, and higher beam efficiencies. The power supply must be improved to more efficiently convert dc power to usable power for the tube. Other areas in the amplifier design requiring development effort include size and weight reduction, temperature stability, and external magnetic field reduction. The development program for a 50-watt power amplifier for VOYAGER will be a parallel effort between a TWTA manufacturer and an ESFK manufacturer. The parallel development called for is to insure against failure of one type of device to meet the VOYAGER schedule. The final selection of a specific power amplifier will not be made until a valid comparison of the devices is complete.

3.1.3.2 Three-Watt Solid State Power Amplifier. The 3-watt solid state amplifier will also be a development effort; however, the goal is considered practical and can be achieved well within the constraints of the VOYAGER schedule. Some of the factors which led to the selection of this device for the third power amplifier are:

a. The solid-state device can be safely operated during the launch phase of the mission eliminating the need for a separate launch beacon for telemetry.

b. The use of a single device from the prelaunch phase into the cruise phase eliminates the need for switching operations and allows convenient diplexing with a receiver to accommodate up-link communications during this period of the mission.

c. Operation at a power output level of 3 watts, when used with the high gain antenna, will provide a good backup for the transmission of science data during the orbit phase (See Figure 3-2).

d. Three watts is a reasonable level for advanced solid-state amplifier-multipliers operating at S-band.

Motorola is currently working on S-band power amplifier - multipliers operating at these levels and above. The proposed device is a X30 multiplier which would be used in place of the standard X30 multiplier in the transponder exciter. The transponder design would be modified to provide a suitable output for driving the new multiplier. General considerations of the 3-watt power amplifier design are presented in the following paragraphs.

A block diagram of the proposed configuration is shown in Figure 3-12. The required frequency multiplication (X30) is the same as for the exciter X30 module; however, the multiplication order of the individual stages must be altered to accommodate the higher output power of +35 dbm. A X5 frequency multiplier operating between 153 MHz and 765 MHz cannot reliably handle more than 10 watts of input power. To overcome this limitation, it is necessary to put X3 and X2 multiplier stages at the high power levels and to perform the basic transistor power amplification at 383 MHz. The required input power for the varactor multiplier chain is 12.5 watts. Recent investigations have shown that reliable and efficient transistor amplifiers can be built for this application.

As shown in Figure 3-12, the X5 varactor frequency multiplier follows a buffer amplifier and operates at a relatively low power level. The output of the X5 multiplier is carefully filtered to minimize spurious outputs of the transmitter. The basic power amplification is then performed at 383 MHz prior to the X3 and X2 varactor multiplier stages.

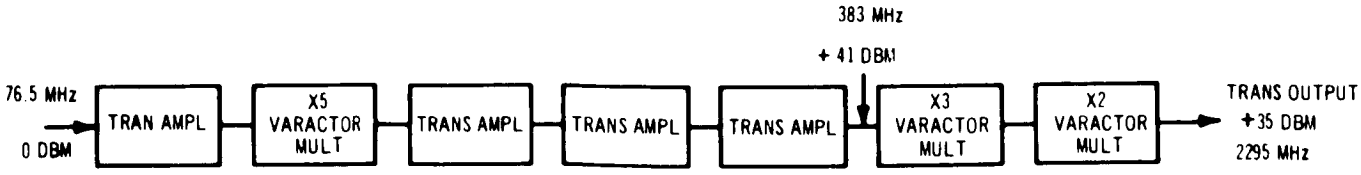


Figure 3-12. Three-Watt Solid-State Power Amplifier

The power amplifiers, the X3 multiplier, and the X2 multiplier will be built in dielectric loaded strip transmission line in order to reduce size, maximize efficiency and to allow reliable reproduction of the design. Conventional lumped constant circuits will be used in the buffer amplifier stage and X5 frequency multiplier stage.

A similar design is currently under development under a company sponsored program. As part of this effort, a 375 MHz power amplifier is being designed to deliver 40 watts of power to a X6 multiplier chain. A 10-watt output at 2250 MHz is the design goal of this transmitter. This effort is scheduled to be completed by April 1966. The power supply for the 3-watt power amplifier will be similar to the transponder power supplies described in Section 3.1.2.5. A design goal of the proposed power supply will be an efficiency of 80%. When combined with the efficiency of the amplifier, this results in a maximum power drain of 50 watts.

3.1.4 Diplexer. The principal function of the diplexer is to provide low-loss coupling of a transmitter and receiver to a single antenna. It also performs essential filtering of the received and transmitted signals. Three diplexers are used in the proposed radio subsystem to perform these operations in a manner which minimizes circuit losses and simplifies switching requirements. The specifications established for these diplexers are shown in Table 3-3.

The factors of this specification which control the diplexer design are those which specify rejection of unwanted signals. The approach taken was to minimize the passband insertion loss within these constraints. The insertion loss specified assumes the use of resonators with an unloaded Q of 4000. This will require a coaxial resonator having an inside diameter of 1.5 inches. The center conductor of the resonator will be about 1.2 inches long, and if 0.7 inch of clearance is allowed between the free end of the conductor and the enclosure, the total outside length will be approximately 2 inches.

The transmit arm of the diplexer uses five of these resonators to meet the specified requirements. The approach to the receiver arm is modified slightly so that part of the filter may be located in a fixed relationship to the receiver. The purpose is to provide a controlled point of reflection for image signals from the receiver mixer so that the phase of this reflection can be adjusted for optimum noise figure. The resulting filter is divided into two pieces. The required specifications are satisfied with a broadband three-resonator filter as part of the diplexer and a relatively narrow-band preselector assembled as part of the transponder.

TABLE 3-3. DIPLEXER SPECIFICATIONS

Parameter	Receive Arm	Transmit Arm
Center Frequency (f_o)	2113 MHz	2295 MHz
Insertion Loss in the Band, $f_o \pm 3$ MHz	0.8 db maximum	0.4 db maximum
VSWR in the Band, $f_o \pm 3$ MHz	1.2:1 maximum	1.2:1 maximum
LO Rejection	60 db minimum at $f_o \pm 45$ MHz	- - - - -
Image Rejection	60 db minimum at $f_o \pm 90$ MHz	- - - - -
Rejection at Transmit Freq.	100 db minimum at $f_o \pm 180$ MHz	- - - - -
Rejection at Receive Freq.	- - - - - -	100 db minimum at $f_o \pm 180$ MHz
Harmonic Rejection	100 db min. at $2f_o$ and $3f_o$	- - - - -
Operating Power Level	- - - - - -	50 watts

3.1.5 RF Switching. The RF switching for the Radio Subsystem is accomplished by ground command and a limited amount of on-board sequencing. In the nominal mission modes no RF switching is required.

Wherever possible, switching functions are performed at the component power supply level, that is, the exciters and power amplifiers are switched ON and OFF via their respective power supply switches (see Figure 3-1). In the event of component failures, the radio subsystem design allows for operational switching in the RF path. This is provided between the RF diplexers and the antenna system by two RF transfer switches and a coaxial single-pole double-throw switch. It is the purpose of these switches to permit antenna selection in order to preserve near nominal communication links between DSIF and the spacecraft. They are used only in the event of a subsystem failure.

3.1.5.1 Transfer Switch. The mechanical rf transfer switch was selected for the proposed subsystem because it allows a simple connection of multiple receivers, transmitters, and antennas. Other switching techniques considered generally resulted in a sacrifice of a capability, reliability, or a significant increase in circuit losses. Transfer switches of the type proposed are now under development for the Apollo program. Two companies, Transco Products, Inc. and the Electronic Specialty Co. are building prototypes of transfer switches for Apollo. It should be noted that the switches are activated only in the event of a subsystem failure. A major consideration of the proposed subsystem design was to achieve a simple configuration with a minimum amount of rf switching. The use of the transfer switch, as indicated in the design of Figure 3-1, is intended to provide maximum versatility in case of failure yet maintain a simple conservative connection for the nominal mission.

The proposed switch is a mechanical latching device which would weigh approximately 7 ounces and have the dimensions 1.2 x 1.2 x 1.8 inches. The insertion loss of the switch will be less than 0.2 db and the isolation between outputs greater than 45 db. The VSWR of the switch will be less than 1.15:1.

3.1.5.2 Coaxial Switch. The proposed coaxial switch is a mechanical single-pole double-throw switch. A typical coaxial switch would weigh approximately 6 ounces and would have the dimensions 2.5 x 2 x 1 inches. The switch action will be make-before-break, thereby permitting switching with rf power applied.

3.1.5.3 Hybrid RF Coupler Package. To eliminate operational switches in the rf path of the Radio Subsystem, hybrid couplers were used to provide the interface between the exciters and power amplifiers. A block diagram of this interface is shown in Figure 3-13. RF coupled power monitors are utilized at the output of the exciters and the power amplifiers. The output from each power monitor is conditioned for telemetry transmission to assess the performance of a particular exciter or power amplifier. These outputs are also used for failure mode sensing. To reduce the number of connectors and individual components, the exciter power monitors, the hybrid couplers, and the 3-db attenuators were combined in a strip transmission line package as shown in Figure 3-14. The weight of the package will be approximately 6 ounces.

4.0 INTERFACE DEFINITIONS. This section of the report is a tabulation of Radio Subsystem signal interfaces.

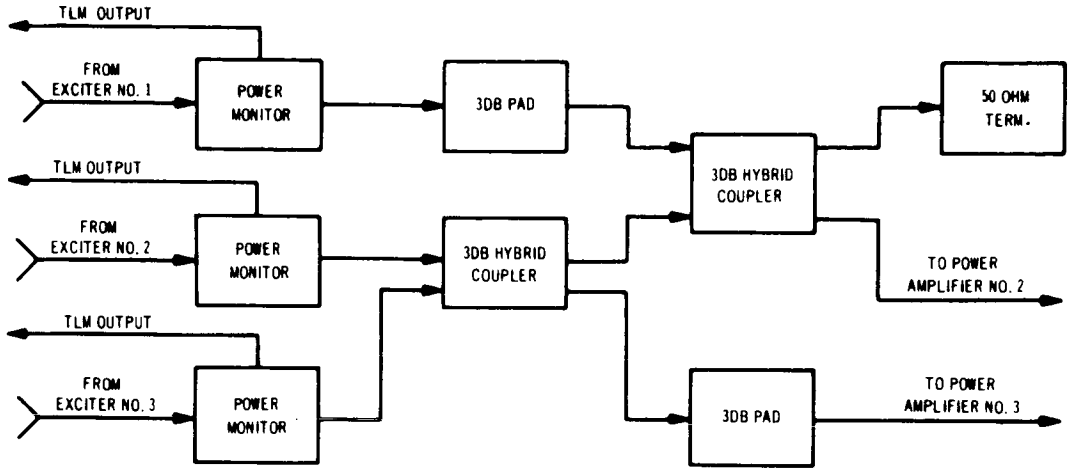


Figure 3-13. Exciter-Power Amplifier Interface

4.1 Input Signals

4.1.1 RF Input. The Radio Subsystem is designed to receive and demodulate an rf signal from the DSIF. Tentative receive frequencies for the three receivers used are:

Receiver	Spacecraft A	Spacecraft B
No. 1	2117.405092 MHz	2110.243056 MHz
No. 2	2117.064034 MHz	2110.584105 MHz
No. 3	2116.722994 MHz	2110.924154 MHz

An additional receiver operating on a fourth frequency would serve as a spare for both spacecraft.

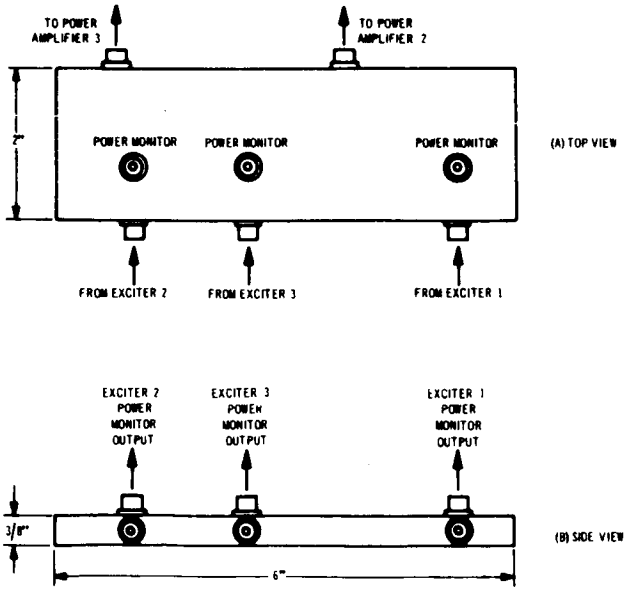


Figure 3-14. Hybrid Coupler Assembly

4.1.2 Telemetry. The Telemetry Subsystem provides a composite telemetry signal to the phase modulator input of each exciter (three exciters are used). The composite signal is the linear sum of two subcarriers used for transmission of engineering data and science data. The exciter phase modulator input impedance is 1000 ohms resistive. The telemetry rates used consist of the following combinations.

Science Data Rate (bps)	Engineering Data Rate (bps)
14933.33	116.66
7466.66	116.66
3733.33	116.66
933.33	29.16

Emergency Rate 7.29

4.1.3 Command. Changes of the Radio Subsystem mode of operation may be achieved by command from DSIF. This action is performed via the Command Subsystem which provides a pulse to initiate change of state of the following functions:

1.	Exciter No. 1	on/off
2.	Exciter No. 2	on/off
3.	Exciter No. 3	on/off
4.	Power Amplifier No. 1	on/off
5.	Power Amplifier No. 2	on/off
6.	Power Amplifier No. 3	on/off
7.	Receiver No. 1	on/off
8.	Receiver No. 2	on/off
9.	Receiver No. 3	on/off
10.	Antenna Transfer Switch No. 1	Norm/Rev
11.	Antenna Transfer Switch No. 2	Norm/Rev
12.	Backup Antenna Switch No. 3	Norm/Backup
13.	Ranging	on/off

4.1.4 Computer and Sequencer. During the normal operations, the C&S automatically sequences the Radio Subsystem through three modes: launch mode, exciter No. 1, power amplifier No. 1; cruise mode, exciter No. 2, power amplifier No. 2; maneuver mode, exciter No. 3, power amplifier No. 3

4.1.5 Power. The spacecraft power subsystem provides the following inputs to the radio subsystem:

1. A 50-VRMS 2400 Hz square wave from a source regulated ±2% or better. The maximum power consumption is 30 watts.
2. Unregulated power from a 34 to 62-volt dc source. The maximum power consumption is 147 watts.

4.2 Output Signals

4.2.1 RF Output. The Radio Subsystem is designed to transmit a modulated rf signal to DSIF. Tentative transmit frequencies assigned to the three exciters used are:

	Spacecraft A	Spacecraft B
Exciter No. 1	2299.444444 MHz	2291.666666 MHz
Exciter No. 2	2299.074074 MHz	2292.037037 MHz
Exciter No. 3	2298.703704 MHz	2292.407407 MHz

An additional exciter operating on a fourth frequency will serve as a spare for both spacecraft.

4.2.2 Telemetry. Telemetry points of the Radio Subsystem are tabulated in "Telemetry Criteria", VC220FD109 and, therefore, are not repeated here. These signals are conditioned

dc data outputs of the Radio Subsystem. The output impedance for all telemetry points is 1000 ohms resistive.

4.2.3 Command. The Radio Subsystem provides a composite signal to the Command Subsystem from each of the three receivers used. The command channel output impedance is 100 ohms resistive.

4.2.4 Umbilical Functions. RF signals are transferred through the umbilical connector via rf probes located near each antenna.

4.2.5 Direct Access Functions. The Radio Subsystem provides the direct-access test points for checkout with the OSE as shown in Table 4-1. These points are provided in addition to telemetered outputs identified in Section 4.2.2.

TABLE 4-1. DIRECT ACCESS TEST POINTS

Test Point	Signal Characteristics	Test Point	Signal Characteristics
Receiver No. 1 AGC	dc	Receiver No. 2 -15v	dc
Receiver No. 2 AGC	dc	Receiver No. 3 +15v	dc
Receiver No. 3 AGC	dc	Receiver No. 3 -15v	dc
Receiver No. 1 SPE (static phase error)	dc	Exciter No. 1 -15v	dc
Receiver No. 2 SPE	dc	Exciter No. 1 -25v	dc
Receiver No. 3 SPE	dc	Exciter No. 2 -15v	dc
Receiver No. 1 DPE (Dynamic phase error)	Signal + Noise	Exciter No. 2 -25v	dc
Receiver No. 2 DPE	Signal + Noise	Exciter No. 3 -15v	dc
Receiver No. 3 DPE	Signal + Noise	Exciter No. 3 -25v	dc
Receiver No. 1 +15v	dc	Power Amplifier No. 1 -15v	dc
Receiver No. 1 -15v	dc	Power Amplifier No. 1 -25v	dc
Receiver No. 2 +15v	dc	Power Amplifier No. 2, all d-c voltages	
		Power Amplifier No. 3, all d-c voltages	

5.0 PERFORMANCE PARAMETERS. Performance parameters of the various Radio Subsystem components are tabulated in this section of the report.

5.1 Antenna Parameters. The four S-band antennas of the Radio Subsystem are designated as the high-gain antenna, the medium-gain antenna, the primary low-gain antenna, and the secondary low-gain antenna. The characteristics of these antennas and their associated cables are summarized in Tables 5-1 and 5-2. The gain patterns of these antennas are shown in Figures 5-1, 5-2, 5-3, and 5-4, respectively. The characteristics of the relay antenna are also given in Table 5-1, and its gain pattern in Figure 5-5.

5.2 Receiver Parameters. The proposed design uses three receivers which are identical, except for operating frequency. Each is integrated with an exciter to form a Mark I S-band transponder. Their characteristics are summarized in Table 5-3; Figure 5-6 shows the output characteristics of the receiver command channel as a function of received signal level.

5.3 Exciter Parameters. Three exciters, identical except for operating frequency, are used in the proposed configuration. The performance parameters for these exciters are tabulated in Table 5-4.

TABLE 5-1. ANTENNA PERFORMANCE PARAMETERS

Parameter	Hi-Gain	Primary Lo-Gain	Secondary Lo-Gain	Medium-Gain	Relay
Type	7.5-ft Diameter paraboloid	See Note 1	Quad dipoles canted 30°	See Note 2	Turnstile over-ground plane
Gain - relative to circular isotropic (db)	$32.5^{+0.4}_{-0.6}$ @ 2295 MHz	2.0 ±0.5 @ 2295 MHz	$0^{+1.0}_{-0.5}$ @ 2295 MHz	$23.5^{+0.25}_{-0.50}$ @ 2295 MHz	5.0 ±0.5 @ 400 mc
	30.3 ±1 @ 2113 MHz	1.3 ±0.5 @ 2113 MHz	$-0.5^{+0.5}_{-1.0}$ @ 2113 MHz	$20.75^{+1.3}_{-1.5}$ @ 2113 MHz	
Polarization Ellipticity - on axis (db)	RHC (Note 3)	RCH	RHC	RHC	RHC
	1.0 ±1 @ 2295 MHz	1.0 ±1.0 @ 2295 MHz	1.0 ±1.0 @ 2295 MHz	1.0 ±1.0 @ 2295 MHz	1.0 ±1.0
	4.0 ±2 @ 2113 MHz	3.0 ±3.0 @ 2113 MHz	1.5 ±1.0 @ 2113 MHz	4.0 ±3.0 @ 2113 MHz	
Ellipticity - 3db pts (db)	$1.0^{+2.5}_{-0.5}$ @ 2295 MHz	2.5 ±1.0 @ 2295 MHz	0.5 ±0.5 @ 2295 MHz		6.0 ±1.0
	$4.0^{+2.5}_{-1.5}$ @ 2113 MHz	4.5 ±3.0 @ 2113 MHz	1.0 ±1 @ 2113 MHz		
VSWR (max)	1.2 @ 2295 MHz	1.2 @ 2295 MHz	1.2 @ 2295 MHz	1.2 @ 2295 MHz	1.2
	1.5 @ 2113 MHz	1.4 @ 2113 MHz	1.4 @ 2113 MHz	1.4 @ 2113 MHz	
Beamwidth - 3db (deg)	4.0	----	----		90
Beamshape	See Figure 5-1	See Figure 5-3	See Figure 5-4	See Figure 5-2	See Figure 5-5
Boresight Error	$.15^{+0.2}_{-0.15}$ degrees	----	----		
Weight (lb)	45.0 ±2	1.5 ±0.25	0.12 ±0.02 excluding mast	4.4 ±0.5	2.0 ±0.2 excluding support
Antenna Cables					
Weight (lb)	2.73 ±0.1	2.43 ±0.1	3.72 ±0.1	1.8 ±.1	0.55 ±.10
VSWR (Max)	1.2:1	1.2:1	1.2:1	1.2:1	1.2:1
Insertion Loss (db)	1.45 ±0.1	1.17 ±0.1	1.24 ±0.1	.36 ±.1	0.8 ±0.2
Impedance (ohms)	50	50	50	50	50

Notes

1. Modified Marimer C Low-Gain (Crossed Slots)
2. Marimer-C Type High-Gain (46.0" x 21.2" parabola)
3. Right Hand Circular

TABLE 5-2. ANTENNA TRANSMISSION LINE PERFORMANCE PARAMETERS

Parameter	Hi-Gain	Primary-Lo-Gain	Secondary Lo-Gain	Medium-Gain	Relay
R-F Test Probes and Cables					
Weight (lb)	0.19 ±.01	0.32 ±.01	0.32 ±.01	0.19 ±0.01	.30 ±0.05
VSWR (max)	2:1	2:1	2:1	2:1	2:1
Insertion Loss (db)	30 ±5.0	30 ±5.0	30 ±5.0	30 ±5.0	30 ±5
Impedance (ohms)	50	50	50	50	50
Rotary Joint					
Weight (lb)	0.35 ±0.05				
VSWR (max)	1.1 @ 2295 MHz				
	1.2 @ 2113 MHz				
VSWR $\frac{\text{max VSWR}}{\text{min VSWR}}$	1.02 (max)				
Insertion Loss - max (db)	0.2 @ 2295 MHz				
	0.2 @ 2113 MHz				
Transmit Ckt Losses (db)					
PA No. 1	2.72 ±0.47	2.09 ±0.37	----	----	
PA No. 2	2.97 ±0.47	2.34 ±0.37	2.46 ±0.37	1.58 ±0.37	
PA No. 3	2.97 ±0.47	2.34 ±0.37	2.47 ±0.37	1.58 ±0.37	
Receiver Ckt Losses (db)					
Rcvr No. 1	3.15 ±0.75	2.52 ±0.65	----	----	
Rcvr No. 2	3.85 ±0.85	3.22 ±0.75	3.34 ±0.75	2.45 ±0.75	
Rcvr No. 3	3.85 ±0.85	3.22 ±0.75	3.34 ±0.75	2.51 ±0.75	

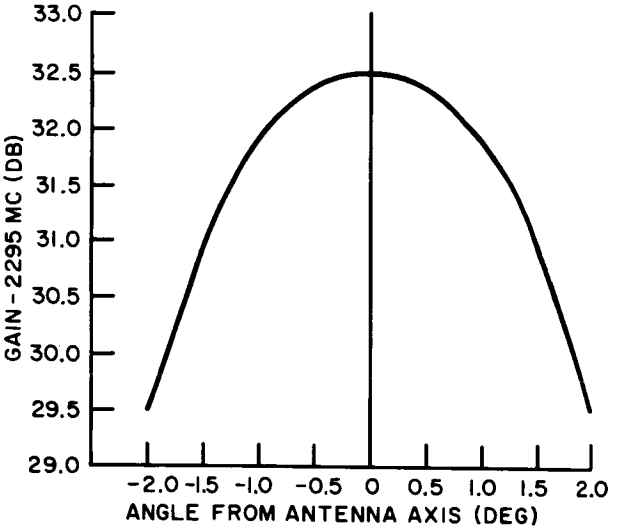


Figure 5-1. High-Gain Antenna Patterns

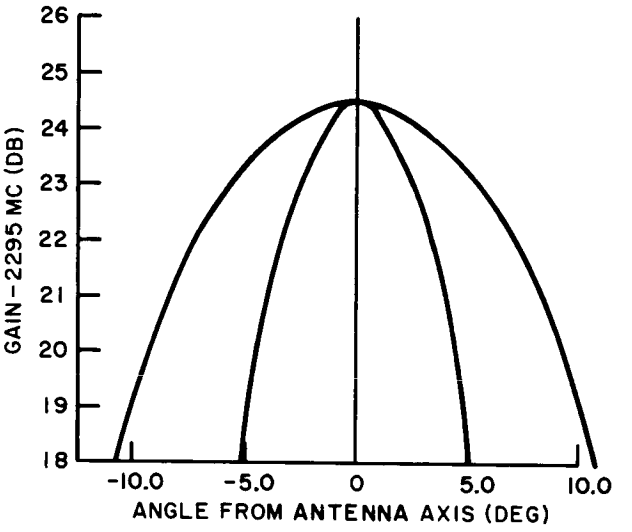


Figure 5-2. Medium-Gain Antenna Patterns

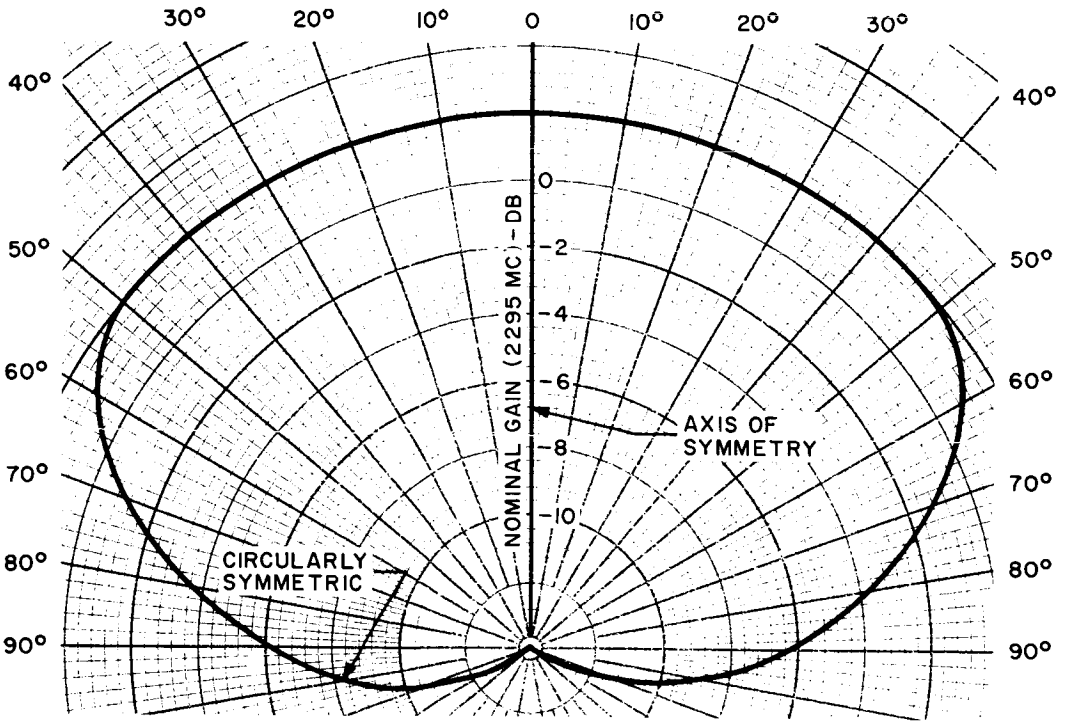


Figure 5-3. Primary Low-Gain Antenna Pattern

5.4 Power Amplifier Parameters. Each of the three power amplifiers of the Radio Subsystem will require development efforts. Tentative specifications for the amplifiers under consideration are presented in Table 5-5.

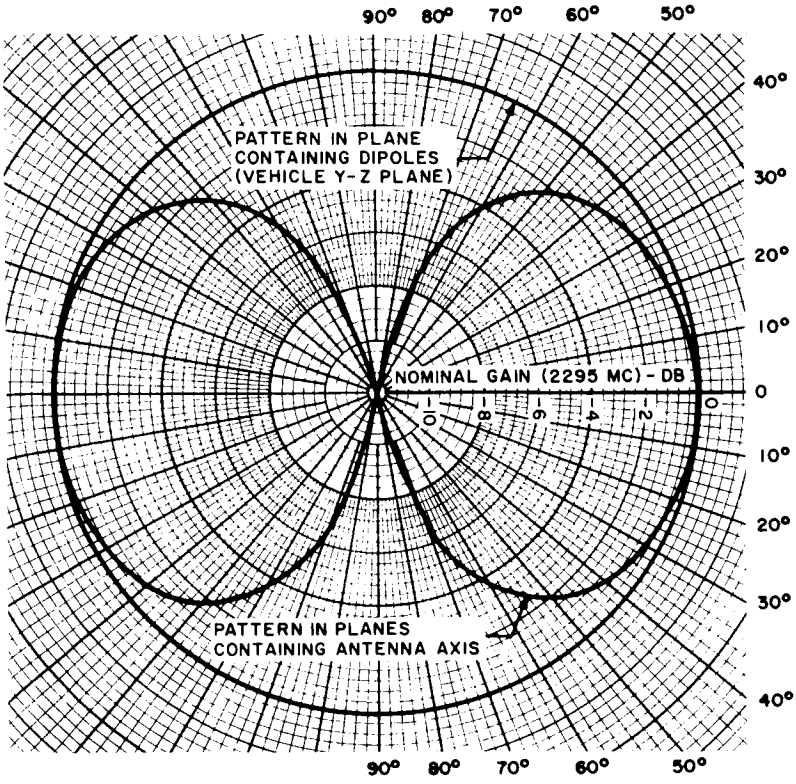


Figure 5-4. Secondary Low-Gain Antenna Pattern

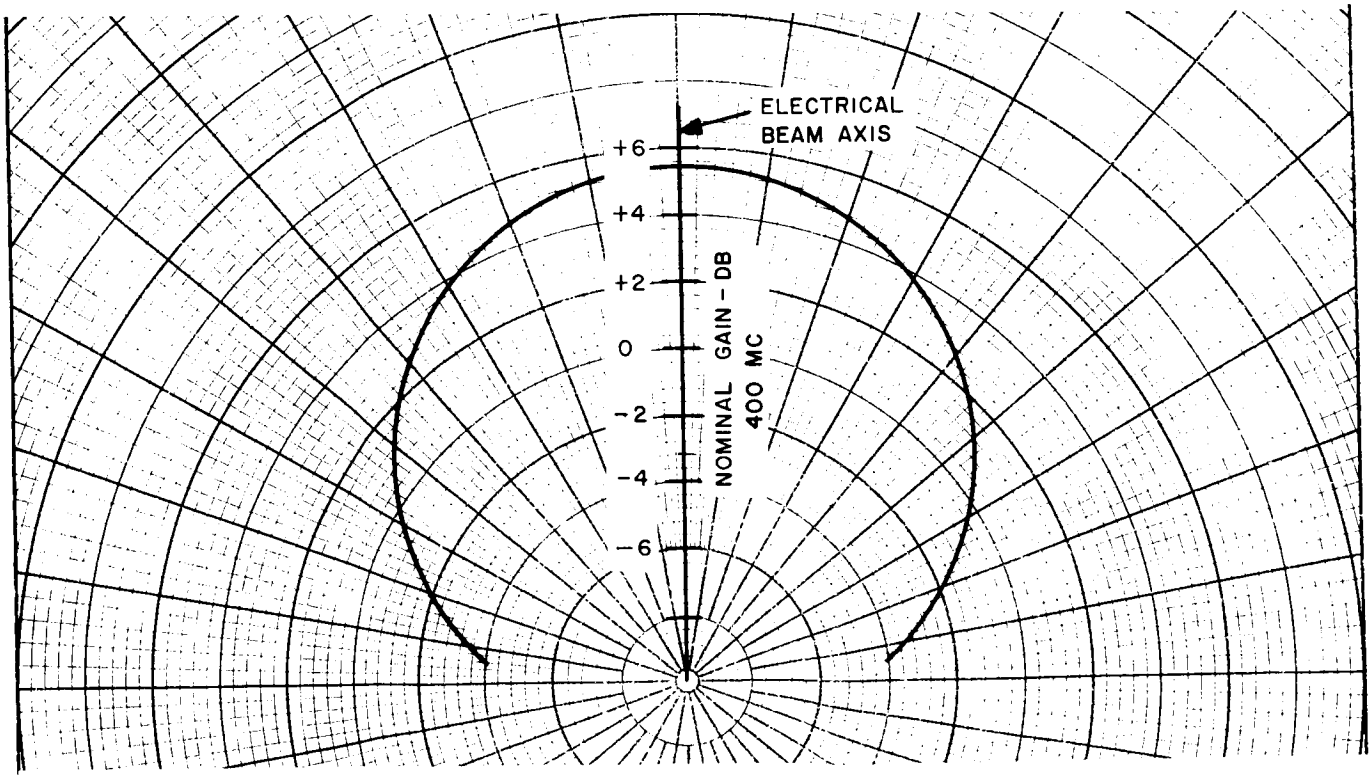


Figure 5-5. Relay Antenna Pattern (400 mc)

TABLE 5-3. RECEIVER PERFORMANCE PARAMETERS

Parameter	Value
Center Frequency	2113 MHz nominal (See Section 4.1.1)
Noise Figure	8 db ±1 db
Strong Signal Carrier Tracking Bandwidth	233 cps ($2\beta_{LSS}$)
Threshold Carrier Tracking Bandwidth	20 cps ($2\beta_{Lo}$)
Threshold Sensitivity	-153 dbm ±1 db
Dynamic Range	-70 dbm to threshold
Tracking Range	±3.0 parts in 10^5 (for R-F signals > -120 dbm)
Carrier Tracking Loop Threshold Transfer Function (model)	$H_{(s)} = \frac{1 + \frac{3}{4\beta_{Lo}} S}{1 + \frac{3}{4\beta_{Lo}} S + \frac{9}{32\beta_{Lo}^2} S^2}$
Carrier Tracking Loop Predetection Filter Bandwidth	4.5 kHz
AGC Loop Bandwidth	0.33 Hz to 0.85 Hz
Ranging Channel I-F Bandwidth (3 db)	3.3 MHz
Video Limiter Rise and Fall Time	70 ns
Ranging Channel Video Bandwidth (3 db)	100 Hz to 2 MHz
Input VSWR	1.3:1 maximum

TABLE 5-4. EXCITER PERFORMANCE PARAMETERS

Parameter	Value
Output Frequency	2295 MHz nominal (see Section 4.2.1)
Output Power	+26 dbm ±0.5 db
Output VSWR	1.3:1 maximum
Auxiliary Osc. Freq. Stability	1 part in 10^5 per year
Phase Stability	Residual PM less than 9 deg peak in a 20 Hz phase coherent receiver
PM Modulator Dynamic Range	0 to 4 radians peak
PM Modulator Linearity	within ±7% of straight line
PM Modulator Sensitivity	1 radian per volt ±5%
PM Modulator Bandwidth	0.5 db BW dc to 1 MHz 3.0 db BW 1.8 MHz min
PM Modulator Input Impedance	1000 ohms resistive

5.5 Diplexer Parameters. Performance characteristics of the three diplexers used in the Radio Subsystem are given in Table 5-6. Characteristics of the preselectors which are assembled in the receivers are also included.

5.6 RF Switch and Coupler Parameters. The characteristics of the rf switches used in the radio subsystem are summarized in Table 5-7. Hybrid coupler parameters are given on the schematic diagram shown in Figure 5-7.

TABLE 5-5. POWER AMPLIFIER PERFORMANCE PARAMETERS

Parameter	50-Watt TWTA or ESFK	3-Watt Solid State P.A.
Operating Frequency	2.29 to 2.30 gHz	2.29 to 2.30 gHz
RF Power Output	50 watts min	3 watts min
RF Power Input	TWTA – 50 mw max ESFK – 150 mw max	0 dbm ±1 db
Gain (saturated)	TWTA – 30 db min ESFK – 25 db min	
Efficiency	33-1/3% min	8% min
DC Power Input	147 watts max	50 watts max
Bandwidth (0.5 db)	TWTA – 5 MHz min ESFK – 3 MHz min	5 MHz min
Noise Figure	28 db max	
Spurious Output		Greater than 50 db below full output
VSWR (Input and Output)	1.4:1 max	1.4:1 max
Absolute Time Delay	10 ns max	10 ns max
Variation in Time	0.5 ns max	0.5 ns max

TABLE 5-6. DIPLEXER PERFORMANCE PARAMETERS

Parameter	Diplexer		Preselector
	Receiver	Transmit	
Center Frequency (nom)	2113 MHz	2295 MHz	2113 MHz
Insertion Loss (max)	0.3 db	0.4 db	0.5 db
Bandwidth (3 db)	45 MHz	45 MHz	34 MHz
VSWR (max)	1.2:1	1.2:1	1.2:1
LO Rejection (min)	20 db		40 db
Image Rejection (min)	35 db		64 db
Rejection at Transmit Frequency (min)	55 db		85 db
Rejection at Receive Frequency		100 db min	
Rejection at Harmonics of Receive Frequency (min)	100 db		50 db

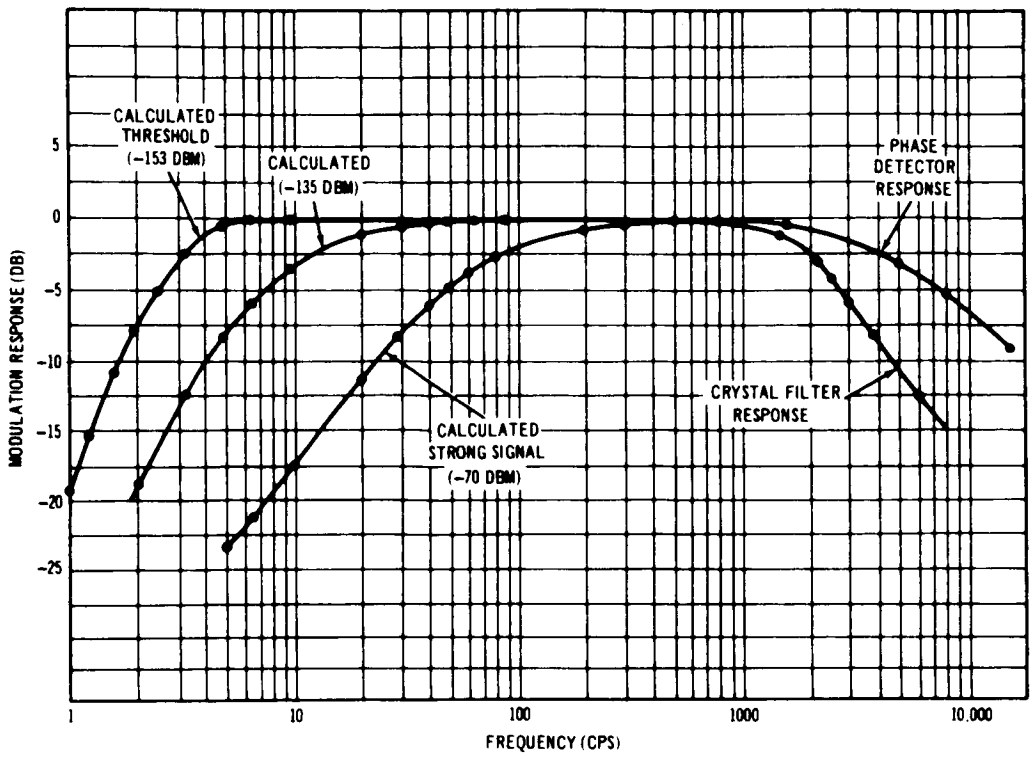


Figure 5-6. Receiver Modulation Response (Command Output)

TABLE 5-7. RF SWITCH PARAMETERS

Parameter	Transfer Switch	Coaxial Switch
Insertion Loss (max)	0.20 db	0.20 db
VSWR (max)	1.15:1	1.15:1
Isolation (min)	45 db	35 db
Type	Latching	Latching
Size (inches)	1.8 x 1.2 x 1.2	2.5 x 2 x 1
Weight (oz)	7	6

6.0 PHYSICAL CHARACTERISTICS

6.1 Packaging. The Radio Subsystem is divided into seven subassemblies, each of which has a rigid aluminum housing designed to fit within the standard 6-inch dimension of the spacecraft equipment bay. Electrical connectors are external to this dimension. Each subassembly chassis is a rigid aluminum housing designed to furnish the required strength and stiffness to withstand the shock and vibration inputs from the spacecraft. Each chassis also serves as a conductive path for the power dissipated within the subassemblies. A good surface finish is provided on those faces of the chassis which are required to transfer the dissipated power to the spacecraft thermal plate.

Wherever possible, spacecraft subassemblies are packaged in a standard modular form so that the equipment may be adaptable to any bay. This approach is not entirely practical for the Radio Subsystem because coaxial lead lengths must be minimized to insure low power losses. Connector locations and subassembly mounting hole patterns also limit complete standardization. Short coaxial lead lengths are maintained on the power amplifier outputs, and the output connections from the subsystem are placed as close to the -y axis of the spacecraft as possible. Figures 6-1 and 6-2 show isometric views of proposed configurations for bay 12 and bay 11 respectively.

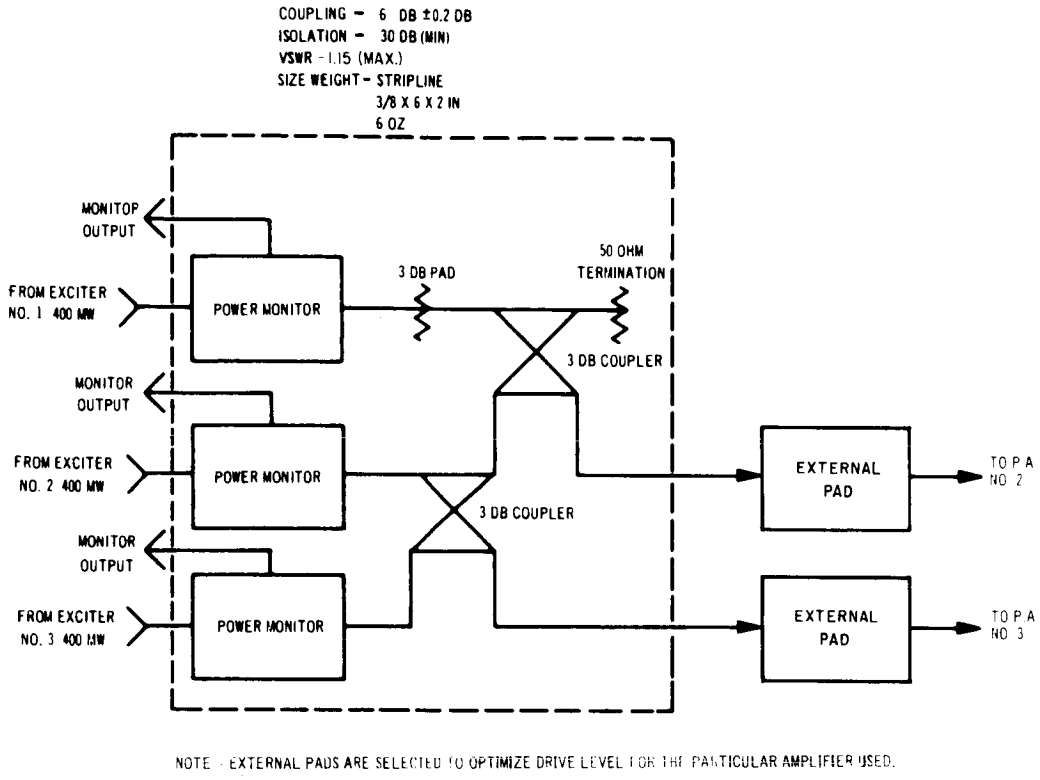


Figure 5-7. Hybrid Coupler Assembly

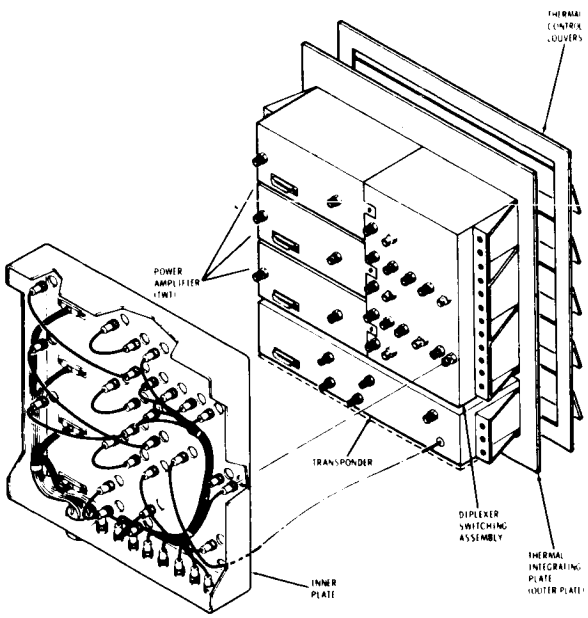


Figure 6-1. Bay 12, Isometric View

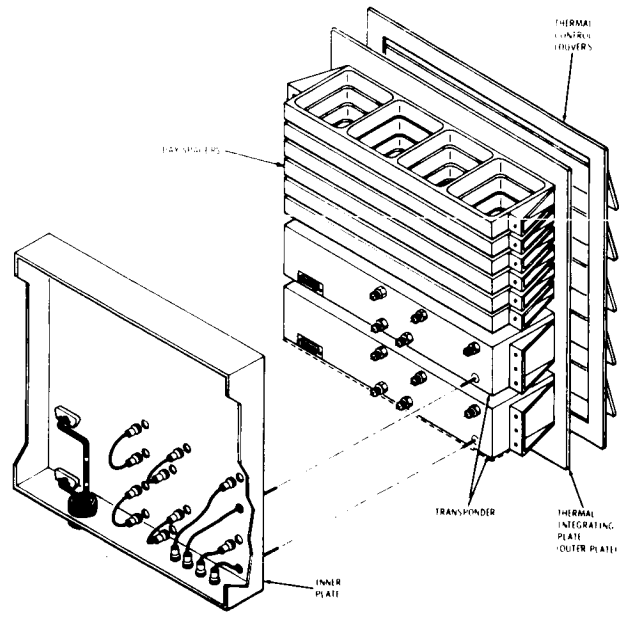


Figure 6-2. Bay 11, Isometric View

6.2 Weight, Volume, and Power Dissipation. A listing of the weight, volume, and power dissipation of each subassembly in the radio subsystem is given in Table 6-1. The total subsystem weight is 78 lb (bay 12 = 49 lb, Bay 11 = 28.6 lb) and the volume is 2929 cu in. (bay 12 = 1885 cu in., Bay 11 = 1044 cu in.). Power dissipation is a variable dependent upon the electrical duty cycle and the particular mission phase. Table 6-2 shows the power dissipation for the various modes of operation.

TABLE 6-1. PHYSICAL CHARACTERISTICS RADIO SUBSYSTEM

Component	Volume (in.^{3})	Weight (lb)	Power (watts)		Failure Rate (% 1000 hr)
			Drain	Diss.	
1.0 Transponder No. 1	522	13.3	15.46	15.46	
1.1 Receiver & P.S.			7.14	7.14	1.7169
1.2 Exciter & P.S.			8.32	8.32	0.9266
2.0 Transponder No. 2	522	13.3	15.46	15.46	
2.1 Receiver & P.S.			7.14	7.14	1.7169
2.2 Exciter & P. S.			8.32	8.32	0.9266
3.0 Transponder No. 3	522	13.3	15.46	15.46	
3.1 Receiver & P.S.			7.14	7.14	1.7169
3.2 Exciter & P.S.			8.32	8.32	0.9266
4.0 Power Amplifier No. 1	162	3.0	50.0	46.0	1.05
5.0 Power Amplifier No. 2	162	7.5	147	97	1.05
6.0 Power Amplifier No. 3	162	7.5	147	97	1.05
7.0 Diplexer Switching Assembly	877	13.35			
7.1 Chassis		4.5			
7.2 Hybrid Coupler Assembly	8	0.5			0.05/conn.
7.3 Diplexer No. 1	49	0.5			0.05/conn.
7.4 Diplexer No. 2	49	1.9			0.30
7.5 Diplexer No. 3	49	1.9			0.30
7.6 Transfer Switch No. 1	3	0.45	15 (20ms)		0.020 (quies) 0.200 (active)
7.7 Transfer Switch No. 2	3	0.45	10 (10ms)		0.020 (quies) 0.200 (active)
7.8 Antenna Switch	5	0.35	10 (10ms)		0.0250 (quies) 0.250 (active)
8.0 Cables		6.5			

TABLE 6-2. POWER DISSIPATION ALTERNATES - RADIO SUBSYSTEM

Component	Mission or Prelaunch Checkout					
	Case 1 Diss. (watts)		Case 2 Diss. (watts)		Case 3 Diss. (watts)	
	Bay 12	Bay 11	Bay 12	Bay 11	Bay 12	Bay 11
1.0 Transponder No. 1						
1.1 Receiver & P.S.	7.14		7.14		7.14	
1.2 Exciter & P.S.	8.32		8.32			
2.0 Transponder No. 2						
2.1 Receiver & P.S.		7.14		7.14		7.14
2.2 Exciter & P.S.						8.32
3.0 Transponder No. 3						
3.1 Receiver P.S.		7.14		7.14		7.14
3.2 Exciter & P.S.						
4.0 Power Amplifier No. 1	46					
5.0 Power Amplifier No. 2			97		97	
6.0 Power Amplifier No. 3						
Totals	61.46	14.28	112.46	14.28	104.14	22.60

6.3 Subassemblies. The subsystem is packaged in the subassemblies shown in Table 6-1. The following paragraphs describe the physical characteristics of these subassemblies.

6.3.1 Transponders. There are three transponders, each containing a receiver, exciter, and their associated power supplies. The transponders utilize the same modular configuration as the Mark S-Band Transponder used on Mariner C. The basic functional blocks are in separate compartments, and the components are mounted to a "T-frame". This provides good RFI shielding, excellent thermal conduction paths, and a structurally sound housing. An assembly drawing of the transponder is shown in Figure 6-3.

6.3.2 Diplexers and RF Switching. These components are located in one enclosure. Since there is a need for minimum cabling, many of the interconnections are made internally. Each diplexer is located so that the output from the power amplifier is in close proximity.

6.3.3 Power Amplifiers. The power amplifiers take three forms. Power amplifier No. 1 is a strip transmission line multiplier similar in design to the Apollo Block II X30 multiplier. The design is structurally and thermally compatible with the VOYAGER environments. Power amplifiers No. 2 and No. 3 may be either traveling wave tube amplifiers or electrostatically focused klystrons. Since both of these devices dissipate a large amount of power in a concentrated location, they will be located so that the major heat source (the collector) is as near the center of the thermal plate as possible. This will provide optimum effective fin area for dissipation of the heat. This allows the plate to distribute this power over a large area so that the temperature gradients remain small, and the power amplifiers

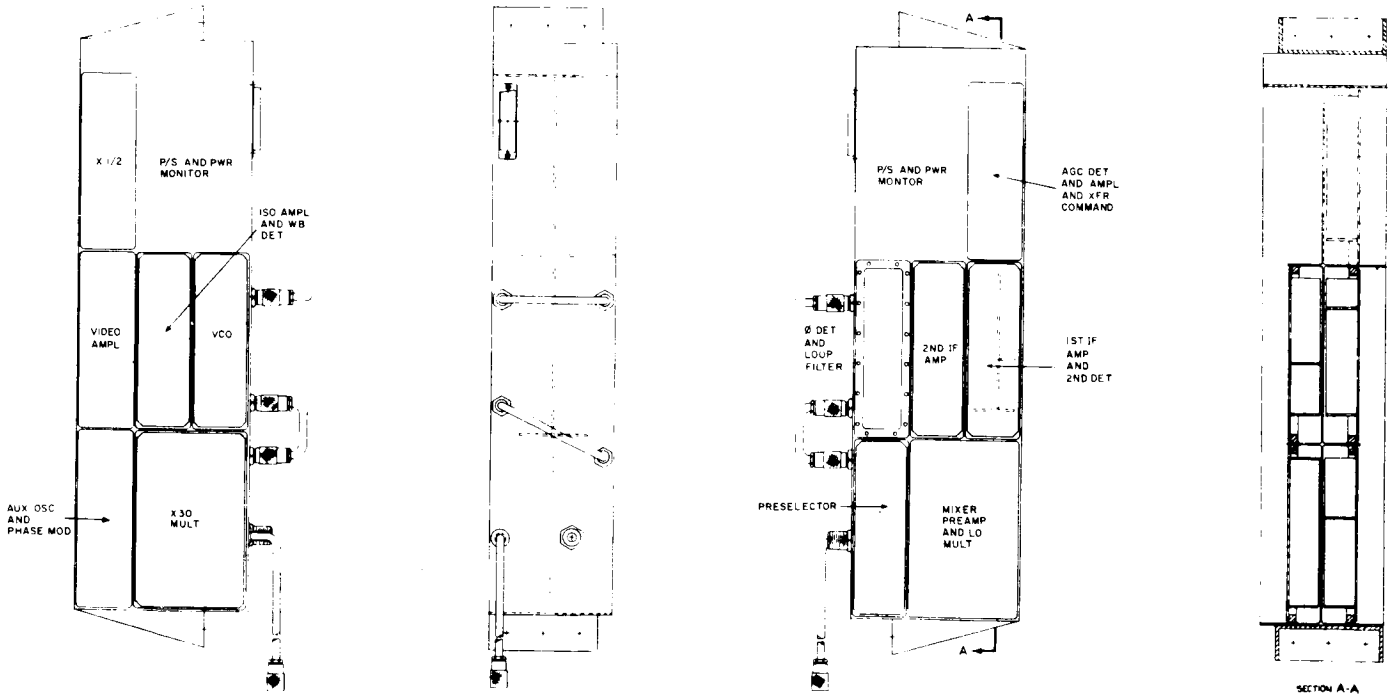


Figure 6-3. Transponder Assembly

operate within the required temperature limits. The thermal plate to which the power amplifiers mount must be maintained between 50 to 60°C for proper operation. It should be noted that only one power amplifier will be dissipating heat at any one time.

6.3.4 Thermal Design. The Radio Subsystem is designed for conduction cooling with the heat sink provided by the spacecraft thermal mounting plates. Subassemblies are located to provide an optimized heat transfer path from component parts to the spacecraft thermal mounting plate.

Table 6-3 presents the maximum allowable thermal mounting plate temperatures for the various subassemblies. These limits must be observed if long system life and reliability are to be achieved.

6.3.5 Shock and Vibration

6.3.5.1 Shock. The subsystem subassemblies and their attachments are designed to withstand the shock input of a 200g terminal peak sawtooth of 0.7 to 1.0 millisecond rise time. Calculations show the subsystem will meet this shock environment with no structural degradation. The equipment used on Mariner C, which is structurally similar, successfully passed equivalent tests and flight environments.

6.3.5.2 Vibration. Interpretation of mission and test requirements shows that the random vibration input to the Radio Subsystem input will result in an average acceleration level of 13.4g rms at the subassembly mounting locations with a sigma level of 40g. A worst case study shows that the components may be subjected to 60g rms. The Mariner C equipment, which was similar in design, successfully passed equivalent vibration tests. The VOYAGER equipment will be designed to have resonant frequencies sufficiently low to yield internal g loads of minimum values.

TABLE 6-3. MAXIMUM ALLOWABLE SUBASSEMBLY MOUNTING TEMPERATURES

Subassembly	Thermal Mounting Plate Temperature (°C)			
	Recommended Prelaunch, Launch and Mission	Resulting Flight Acceptance Test	Resulting Type Approval Test	Resulting Breadboard Test
Transponder	+20 to +30	0 to +50	-10 to +70	-23 to +83
Power Amplifier (TWTA & ESFK)	+50 to +60 *	+30 to +80	+20 to +100	+ 2 to +118
Power Amplifier (3-watt)	+20 to +30	0 to +50	-10 to +70	-23 to +83
Diplexer-SW Assembly	+20 to +30	0 to +50	-10 to +70	-23 to +83

* Thermal considerations on the spacecraft require high temperatures here for proper heat dissipation.

CII VC233FD103

FLIGHT COMMAND SUBSYSTEM

SECTION

1	SCOPE
2	APPLICABLE DOCUMENTS
3	FUNCTIONAL DESCRIPTION
4	INTERFACE DEFINITIONS
5	PERFORMANCE PARAMETERS
6	PHYSICAL CHARACTERISTICS AND RESTRAINTS

FLIGHT COMMAND SUBSYSTEM

The Flight Command Subsystem is presented in the classified supplement of this report.

CII VC233FD106

TELEMETRY SUBSYSTEM

SECTION

1	SCOPE
2	APPLICABLE DOCUMENTS
3	FUNCTIONAL DESCRIPTION
4	INTERFACE CHARACTERISTICS
5	PERFORMANCE PARAMETERS
6	PHYSICAL CHARACTERISTICS
7	SAFETY CONSIDERATIONS

TELEMETRY SUBSYSTEM

1.0 SCOPE. This functional description covers the 1971 VOYAGER Spacecraft telemetry subsystem which performs the commutation and encoding of various spacecraft engineering and scientific parameters for transmission to earth.

2.0 APPLICABLE DOCUMENTS. The following documents pertain to this functional description:

CII VC220SR101 - Design Characteristics and Restraints
CII VC220FD109 - Telemetry Criteria
CII VC233FD101 - Telecommunication Subsystem

3.0 FUNCTIONAL DESCRIPTION

3.1 General. This section contains a functional description of the VOYAGER telemetry subsystem. The functions of the telemetry subsystem and a summary of the basic operation are followed by a more detailed description of the major functional elements.

3.1.1 Functions

a. Analog Signal Inputs. The telemetry subsystem accepts analog signals from the VOYAGER spacecraft subsystems. The signals are conditioned by the subsystems to three standard ranges; 0 to 100 mv, ± 1.6 volts, and 0 to 3.2 volts.

b. Serial Digital Inputs. The telemetry subsystem accepts serial NRZ data from the Data Automation Equipment (DAE), Capsule, and Data Storage Subsystems (DSS).

c. Parallel Digital Inputs. The telemetry subsystem accepts parallel NRZ digital data words from the VOYAGER Spacecraft Subsystems.

d. Event Signal Inputs. The telemetry subsystem accepts and keeps a cumulative count of spacecraft events.

e. Signal Conditioning. The telemetry subsystem conditions analog signals to a standard 0 to 3.2 volt range for digitizing.

f. Encoding. The digitized analog signals, paralled digital signals, and event signals are encoded into a 7-bit binary word format.

g. Commutation. The telemetry subsystem time division multiplexes real-time data, including the digitized analog signals, accumulated event signals, parallel digital signals, and serial digital signals, into a serial NRZ-M format for transmission to Earth.

h. Synchronization. The telemetry subsystem generates a 63-bit length pseudo-noise synchronization code, and provides bit, word, and frame synchronization.

i. Modulation. Two square wave subcarriers are frequency multiplexed to provide the telemetry signal which modulates the RF carrier of the S-band link to Earth.

One subcarrier is modulated with real-time digital data and synchronization information and the other modulated with stored digital data and synchronization information.

j. Control and Timing. The telemetry subsystem provides suitable control and timing signals to execute these functions in accordance with a set of operational modes. The following transmission modes can be selected by either ground commands or stored commands.

1. MODE 1A - Maneuver Mode

   116-2/3 bps engineering and cruise science data stored on maneuver tape recorder; 7-7/24 bps maneuver engineering data transmitted.

2. MODE 1B - Capsule Separation Maneuver Mode

   116-2/3 bps engineering data stored on maneuver tape recorder; 7-7/24 bps maneuver engineering and capsule data transmitted.

3. MODE 2 - Normal Cruise Mode

   116-2/3 bps engineering and cruise science data transmitted.

4. MODE 3A - Normal Orbit Mode

   116-2/3 bps engineering and DAE orbit data; 7466-2/3 bps stored science data transmitted.

5. MODE 3B - Earth Occultation Mode

   116-2/3 bps engineering and DAE orbit data transmitted and stored on maneuver tape recorder. Science playback inhibited.

6. MODE 4 - Cruise Recorder Readout MODE

   116-2/3 bps engineering and cruise science data; 3733-1/3 bps stored data transmitted.

7. MODE 5 - Capsule Checkout Mode

   116-2/3 bps engineering and capsule data; 7466-2/3 bps stored science data transmitted.

3.1.2 Summary Description. The basic operation of the telemetry subsystem is described below and is shown in Figure 3-1. The proposed subsystem independently encodes real-time and stored data and frequency multiplexes their respective modulated subcarriers to form the transmitted signal. The proposed configuration for the real-time data encoder will be described first followed by a description of the encoding of stored data.

The proposed real-time configuration is a dual channel system which time-shares a single commutator. Channel A performs sampling and digitizing operations in the first half of the word time, while Channel B performs the same kind of operations in the second half of the word time. This configuration allows storage of one data format while the same or a different format is being transmitted as well as providing cooperative multichannel redundancy

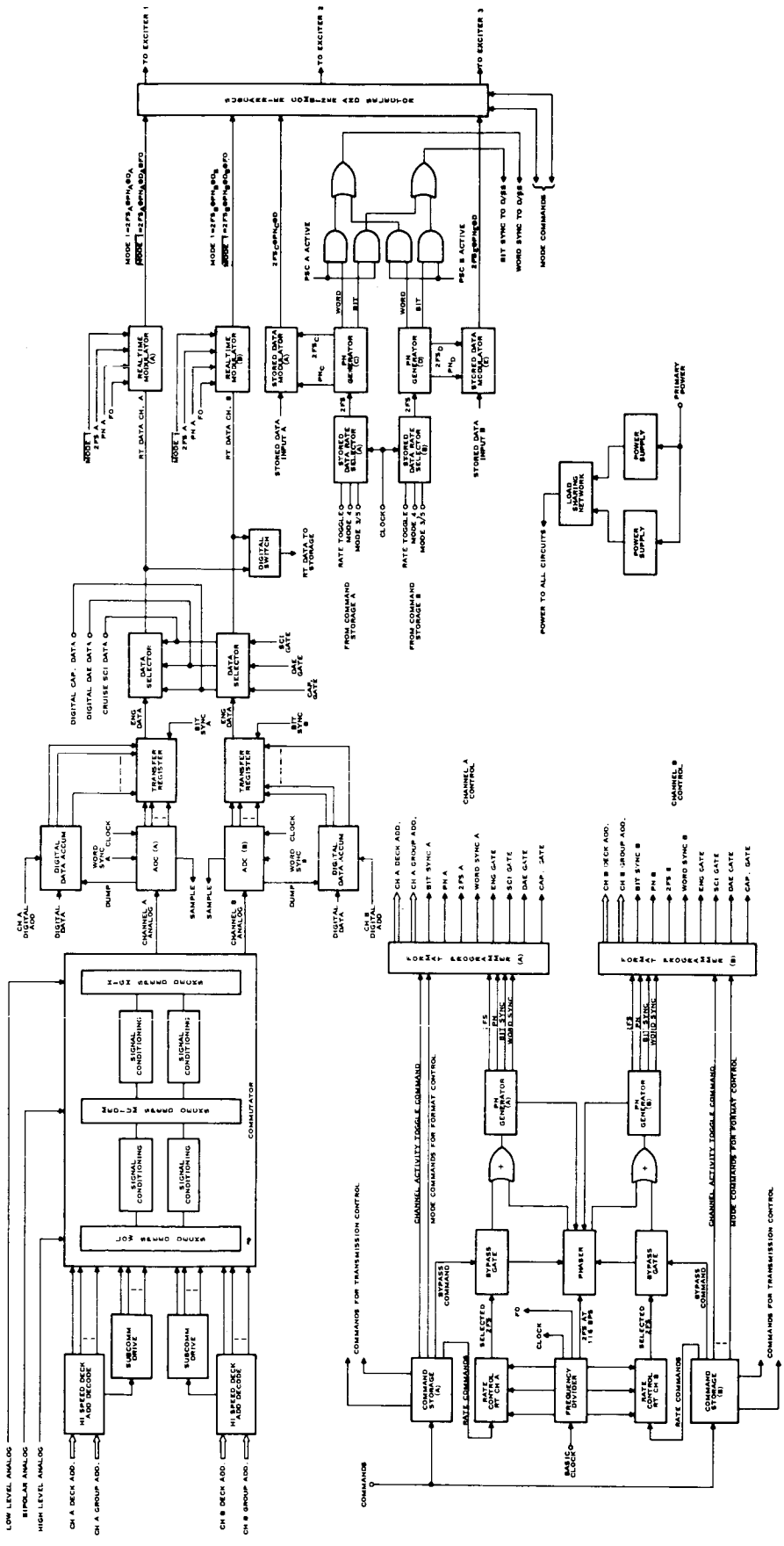


Figure 3-1. Telemetry Subsystem Block Diagram

for enhancement of the reliability of this basic telemetry function. The operation of each of the dual channels is identical; therefore, in the interest of clarity, only one channel is described.

The frequency divider receives a 268.8-kc clock signal from the power subsystem. This signal is divided down to give the appropriate telemetry subcarrier frequencies corresponding to various commanded real-time bit rates of 116-2/3, 29-1/6, and 7-7/24 bps.

The selected 2fs output from the frequency divider drives a pseudo-noise (PN) generator which generates a continuously repeating 63-bit psuedo random code. The 63-bit code is equal in time duration to a 7-bit telemetry word, giving nine PN bits to one data bit. In normal operating conditions, the PN generator is externally synchronized by the phaser. The phaser ensures that the channel sampling period is in the correct half of the word interval. Telemetry timing signals, bit sync, and word sync are also derived from the PN generator.

The format programmer generates and/or distributes the timing and control signals which, in accordance with a commanded mode, determines the format of the real-time data. The format programmer controls the commutator by generating the high speed deck addresses and the commutator group addresses, thereby determining what portion of the commutator will be used, and hence establishing the engineering data format.

The commutator is a multispeed, multiposition device which time division multiplexes analog engineering measurements into the analog-to-digital (A/D) converter. It consists of a 48-position high deck, eleven 10-position medium speed decks sampled at 1/10 the high speed deck rate, and thirteen 20-position low speed decks, sampled at 1/200 the high speed deck rate. For those deck positions reserved for digital data, the commutator deck drive generates the address of the appropriate accumulator register. The content of this register is dumped into the transfer register by the dump pulse generated in the A/D converter.

The A/D converter converts each commutated analog input into a 7-bit binary word. The conversion process is driven by the power subsystem clock signal input divided by two. The digitizing sequence is initiated by word sync and is completed in less than one-half of the word time at the fastest bit rate(116-2/3 bps). After conversion, the 7-bit word is parallel dumped into the transfer register.

The transfer register is a parallel input, serial output device. The 7-bit input words are received from the A/D converter digital data accumulators and from registers in other subsystems. The 7-bit word is shifted out serially, by bit sync, into the data selector.

The data selector receives the following inputs:

a. Engineering data from the transfer register
b. Digital capsule data from the Capsule System
c. Digital real-time orbit data from the DAE subsystem
d. Digital real-time cruise science data from the DAE subsystem

The various gate signals received from the format programmer are used by the data selector to select the sequences and combinations of data required by the various spacecraft modes. The output of the data selector is sent to the real-time modulator. In the real-time modulator, the data is converted to NRZ-M and together with synchronization information modulates the square wave subcarrier. The real-time modulator output is sent to the subcarrier combiner and selector.

Stored data is received from the Data Storage Subsystem on either of two redundant channels. For each channel the encoding process is as follows. The 268.8-kc clock signal from the Power Subsystem is divided down to give the appropriate subcarrier frequencies corresponding to various commanded stored data rates of 14,933-1/3, 7466-2/3, 3733-1/3, and 933-1/3 bps. The selected 2fs output from the stored data rate selector drives a PN generator (PNG C or PNG D) which generates an identical psuedo random code as previously described for the real-time data encoder. Data storage timing signals, bit, and word sync are also derived from the PN generator. The data subcarrier and the PN code are sent to the stored data modulator. In the stored data modulator, the stored data together with the synchronization code modulates the square wave subcarrier. The stored data modulator output is sent to the the subcarrier combiner and selector. In the subcarrier combiner and selector, mode commands are used to select the appropriate combination of real time and stored modulated subcarriers and outputs three identical composite telemetry signals for modulation of the exciters.

Each of the major elements shown in the block diagram are described in detail in the following sections.

3.2 Commutator Arrangement
3.3 Commutator Switch
3.4 Signal Conditioning
3.5 Address Decoding Matrix
3.6 Subcomm Configuration
3.7 Phaser
3.8 PN Generator
3.9 Format Programmer
3.10 A/D Converter
3.11 Data Transfer Register
3.12 Digital Data Accumulator
3.13 Data Selector
3.14 Frequency Divider
3.15 Rate Control
3.16 Real-Time Data Modulator
3.17 Stored Data Subcarrier Modulator
3.18 Subcarrier Combiner and Selector
3.19 Power Supply

3.2 Commutator Arrangement. A block diagram of the commutator arrangement is shown in Figure 3-2. The commutator is arranged in six groups. Group A contains eight high deck positions, one medium deck of length 10 and two low decks each of length 20. Group B contains eight high deck positions, three medium decks each of length 10, and three low decks each of length 20. Group C contains eight high deck positions. Group D contains eight high deck positions and one medium deck of length 10. Group E contains eight high deck positions, three medium decks each of length 10, and three low decks each of length 20. Group F contains eight high deck positions, three medium decks each of length 10, and five low decks each of length 20. The medium decks are sampled at 1/10 the high speed deck rate and the low decks are sampled at 1/200 the high speed deck rate. The commutator groups are selected by the format programmer. This allows only the groups pertinent to a particular mission phase to be sampled. In addition, by grouping the channels, not all channels are

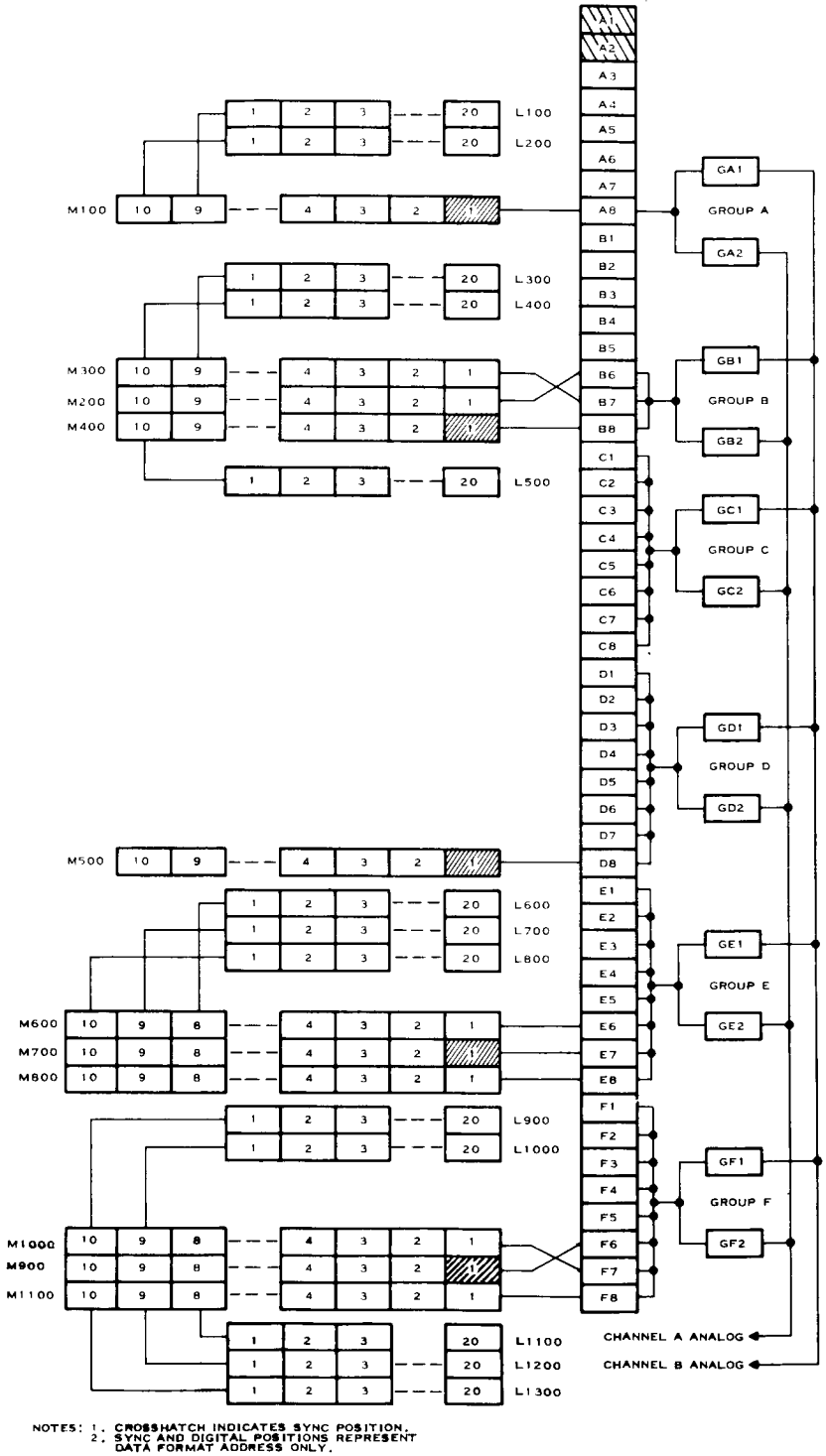


Figure 3-2. Commutator Arrangement

lost in case of a shorted switch. The sampling rate for each real-time data source is shown for each mode in Table 3-1.

TABLE 3-1. DATA COLLECTION RATES

Mode	Bit Rate	Group Format	High Deck		Medium Deck		Low Deck		Capsule		DAE		Cruise Science	
			Channels	Period	Channels	Period	Channels	Period	Channels	Period	Channels	Period	Channels	Period
Maneuver (1A)														
Transmitted RT	7-7/24	A, B	16	15.36	40	153.6	100	3072						
Stored	116-2/3	A, B, C, D	32	3.84	50	38.4	100	768					32	3.84
Capsule Separation Maneuver (1B)														
Transmitted RT	7-7/24	A, B	16	30.72	40	307.2	100	6144	16	30.72				
Stored	116-2/3	A, B, C, D	32	1.92	50	19.2	100	384						
Normal Cruise (2)	116-2/3	A, B, E, F	32	3.84	100	38.4	260	768					32	3.84
Normal Orbit (3A)	116-2/3	A, B, E, F	32	3.84	100	38.4	260	768			32	3.84		
Earth Occultation (3B) Stored	116-2/3	A, B, E, F	32	3.84	100	38.4	260	768			32	3.84		
Cruise Recorder Readout (4)	116-2/3	A, B, E, F	32	3.84	100	38.4	260	768					32	3.84
Capsule Checkout (5)	116-2/3	A, B	16	7.68	40	76.8	100	1536	112	7.68				

NOTE: All Periods are in Seconds

3.3 Commutator Switch. A commutator analog switch schematic is shown in Figure 3-3. During the detailed design phase other analog switches should be evaluated. This switch can be used for both high and low level applications. The switch consists of a P-channel junction FET and redundant inverter drivers. When the control gate voltage is low the control transistors are off and +V is applied to the gate (G) of the FET, cutting the FET off. When the switch is to be turned on, the control gate input goes high saturating the control transistors. This removes the +V from the FET gate, allowing it to conduct. Capacitor C_1 speeds up the turn-on ± time of the FET.

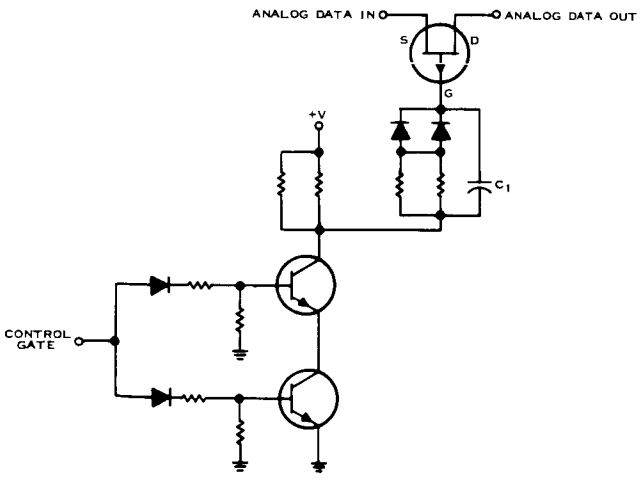


Figure 3-3. Redundant Drive and FET Analog Switch

The redundant diodes prevent forward biasing of the FET, allowing the gate to float at the source potential. The saturation resistance of the FET is the ohmic path of the P channel, which is approximately 200 ohms. The FET has zero offset voltage.

3.4 Signal Conditioning

3.4.1 Temperature Measurements. The temperature measurements are mechanized as shown in Figure 3-4 (Mariner C approach). The constant current generator output is switched to the various temperature transducers, one at a time. This current generates a voltage across the transducer which is proportional to the transducer impedance

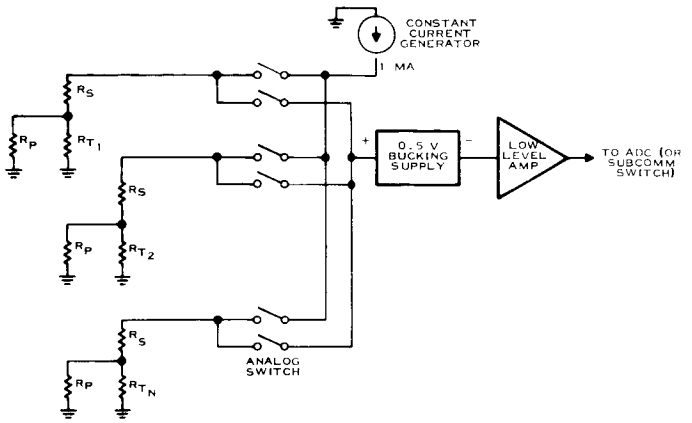


Figure 3-4. Temperature Measurement Technique

and thus temperature. A parallel resistor (Rp) shunts the transducer resistance change to a standard 100-ohm change for all ranges. A series resistor (Rs) is added to the total network resistance to 500 ohms at the low temperature end. At the high temperature end, the total resistance of the network is 600 ohms. Since a 1-milliampere constant current is fed to the network, the voltage across the network varies from 0.5 volt to 0.6 volt from low-band to high-band temperatures. This voltage is commutated through a second switch and bucked down by a series of 0.5-volt bucking supply so that 0- to 100-millivolt signals are presented to the low-level amplifier.

3.4.2 Low Level Signals. Low level signals are amplified by the low level amplifier to the standard range of the ADC.

3.4.3 Bipolar Signals. Bipolar signals are routed through a series bucking supply. These supplies are dc-isolated from the encoder ground and do not lower input impedance on the commutator channel. After being bucked, the signals are treated as the standard 0- to 3.2-volt range.

3.5 Address Decoding Matrix. The high speed deck address decoding matrix is shown in Figure 3-5. An address decoding matrix is required for each of the two systems (channels) of the real-time data encoder. The coded address inputs for the channel A decoding matrix are received from format programmer A and the coded address inputs for the channel B decoding matrix are received from format programmer B. The address is decoded and used to select the correct commutator group and sequentially drives the eight switches in the selected group. This selection technique protects against critical failures which could result if more than one high deck switch was on and a group switch failed shorted.

3.6 Subcomm Configuration. To prevent the need for deck synchronizers and to improve reliability, each commutator group contains independent subcomm drive circuits. Figure 3-6 shows the channel A and channel B subcomm drive circuits and the required signal conditioning for commutator group A. The M100 deck is shown as a ±1.6-volt deck, the L100 as a digital deck, and the L200 as a 3.2-volt deck.

3.7 Phaser. The phaser (Figure 3-7) is the external synchronization unit for the PN generators. The length 63 shift register counter is clocked by 1050 bps. States 1 and 32 are decoded from the register and used to control the start time of the word periods for Channel A and Channel B, respectively. This ensures that the sampling interval of Channels A and B are separated by a minimum of one-half the word interval at the highest bit rate (1 16-2/3 bps). In case of a failure in the phaser, the bypass command is sent and the $2f_s$ needed to clock the PN generator is taken directly from the rate selector. The same command places the other channel in a standby condition.

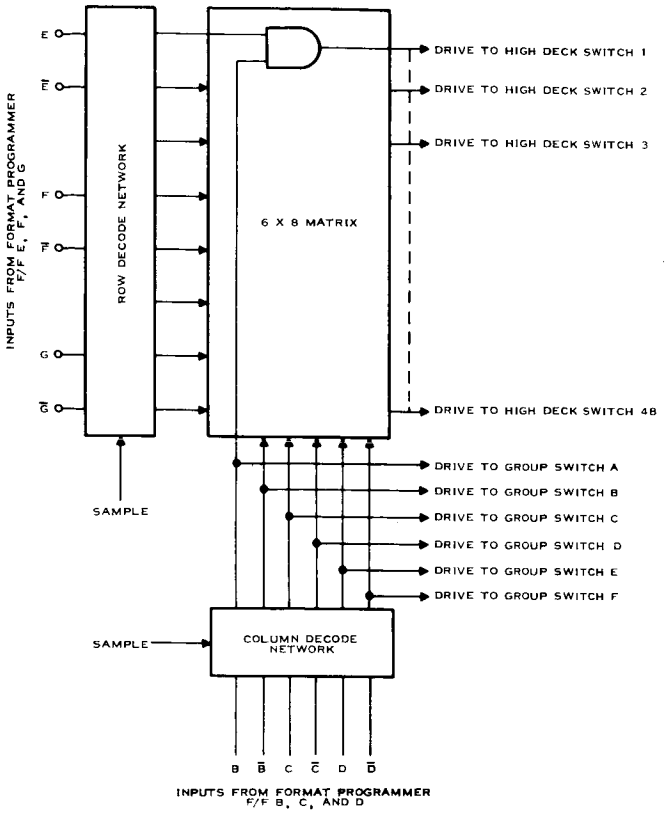


Figure 3-5. High Speed Deck Decoding Matrix

3.8 PN Generator. The PN generator (Figure 3-8) is a shift register counter that is based on the maximum length sequence generator principle. The PN generator generates a 63-bit pseudo-random code which is synchronous with the subcarrier. The timing pulses, word sync, and bit sync are derived by decoding distinct states of the generator. Four PN generators are required, one for each of the real-time data channels, and one for each of the redundant stored data channels.

3.9 Format Programmer. Figure 3-9 is a logic diagram of the format programmer. This circuit controls the formatting of all real-time data. Flip-flops E through G are connected as a length 8 synchronous counter which counts the clock pulse starting at the all "ones" condition and counting to the all "zero" condition. This counter controls the number of words to be read into the data format and generates the fast deck address for the engineering commutator. Flip-flops A through D generate the address of the data source. The decoding of ABCD is as follows:

State A B C D	Data Source
0 0 0 0	Engineering Commutator Group A
0 0 0 1	Engineering Commutator Group B
0 0 1 0	Engineering Commutator Group C
0 0 1 1	Engineering Commutator Group D
0 1 0 0	Engineering Commutator Group E
0 1 0 1	Engineering Commutator Group F
0 1 1 0	Cruise Science
0 1 1 1	Digital DAE
1 0 0 0	Capsule

Registers 1 through 8 contain the data source sequencing instructions. The length of each register is determined by the number of data sources in the format and the number of words to be read from each source. The register outputs, when decoded, indicate which of stages A through D are to be reset thereby determining the address of the data source. The instructions contained in each register are as follows:

Register 1 - 4 States

State 1 8 words from Commutator Group A
State 2 8 words from Commutator Group B
State 3 8 words from Commutator Group E
State 4 8 words from Commutator Group F

Total 32 words Eng. 1

Register 2 - 4 States

State 1 8 words from Commutator Group A
State 2 8 words from Commutator Group B
State 3 8 words from Commutator Group C
State 4 8 words from Commutator Group D

Total 32 words Eng. 2

Register 3 - 2 States

State 1 8 words from Commutator Group A
State 2 8 words from Commutator Group B

Total 16 words Eng. 3

Register 4 - 4 States

State 1 8 words from Cruise Science
State 2 8 words from Cruise Science
State 3 8 words from Cruise Science
State 4 8 words from Cruise Science

Total 32 words Cruise Science

Register 5 - 4 States

State 1 8 words orbital data from DAE
State 2 8 words orbital data from DAE
State 3 8 words orbital data from DAE
State 4 8 words orbital data from DAE

Total 32 words orbital data DAE

Register 6 - 2 States

State 1 8 words from Capsule
State 2 8 words from Capsule

Total 16 words from Capsule

Register 7 - 14 States

State 1 8 words from Capsule
State 2 8 words from Capsule
State 3 8 words from Capsule
State 4 8 words from Capsule
State 5 8 words from Capsule
State 6 8 words from Capsule
State 7 8 words from Capsule
State 8 8 words from Capsule
State 9 8 words from Capsule
State 10 8 words from Capsule
State 11 8 words from Capsule
State 12 8 words from Capsule
State 13 8 words from Capsule
State 14 8 words from Capsule

Total 112 words Capsule Checkout Data

The decoding gates decode the register outputs in accordance with a mode command and a command which indicates whether the format is to be transmitted, or stored on the maneuver (MTR). The data formats for each mode are shown in Figure 3-10a, 3-10b, and 3-10c.

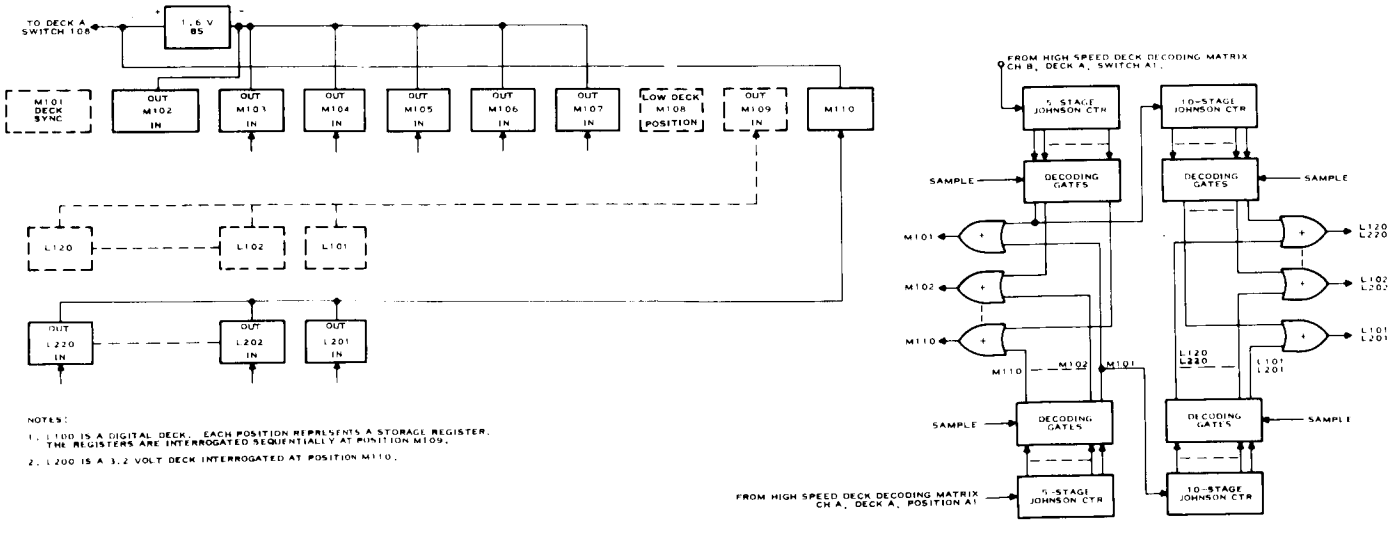


Figure 3-6. Group A - Subcommutator Configuration

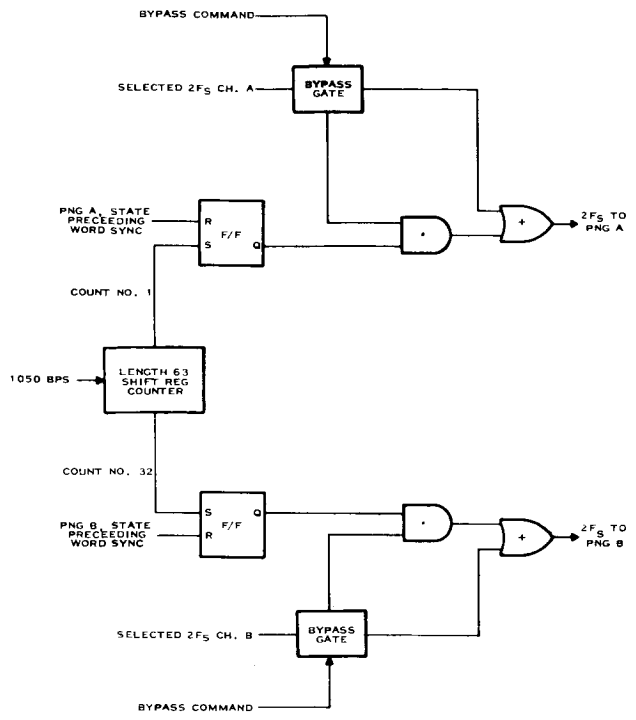


Figure 3-7. Phaser

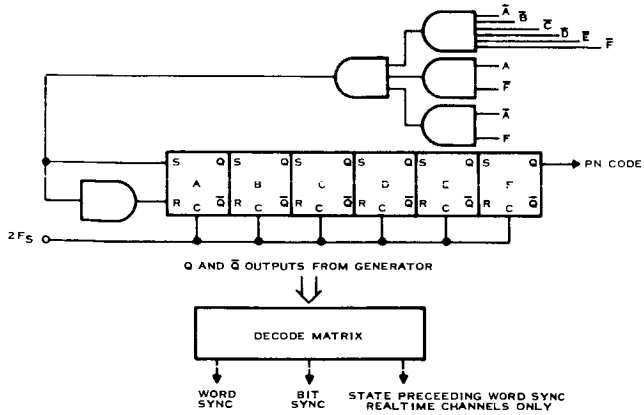


Figure 3-8. Pseudo Noise Generator

3.10 Analog-To-Digital Converter. Figure 3-11 is a block diagram of the analog-to-digital converter (ADC). The ADC uses the successive approximation technique of 7-bit resolution. Figure 3-12, which is a more detailed diagram of the digitizing sequence generator, is presented to aid in the operational discussion. The timing diagram of Figure 3-12 is also presented for clarity. When word sync is received from the PN generator, the flip-flop is set, and the Q output goes high providing the sample pulse to the address decoding matrix and enabling the 1050-bps clock to shift register A. State 8 of shift register A enables the 134.4-kc clock to shift register B. A digital "one" is shifted through shift register B, which sets a "one" into succeeding bits of the storage register causing succeeding legs of the ladder network to be closed to the reference voltage. The bit of the storage register either remains set or is reset depending on the result of the comparison. After shift register B has advanced to the seventh state, a 7-bit digital word, representing the analog input voltage level, is stored in the storage register. On the eighth state of shift register B, the digital word is dumped in parallel to the data transfer register.

The digitized word is then clocked serially into the data selector by the next seven bit-sync pulses.

3.11 Data Transfer Register. The data transfer register (Figure 3-13) is a parallel input, serial output 7-bit data storage register. Data is dumped in parallel form into the register by the dump pulse. The data is then stored in the register until arrival of bit sync which clocks the data out of the register in serial form into the data selector.

3.12 Digital Data Accumulator. The digital data accumulator consists of the necessary logic circuits to perform the collection of miscellaneous bits and words of nonstandard digital signals and the conversion of these signals into the standard NRZ format. The digital data accumulator includes the event counters, the command detector monitors, antenna A and B gimbal angle positions, and science instruments scan platform gimbal angle positions A, B, and C.

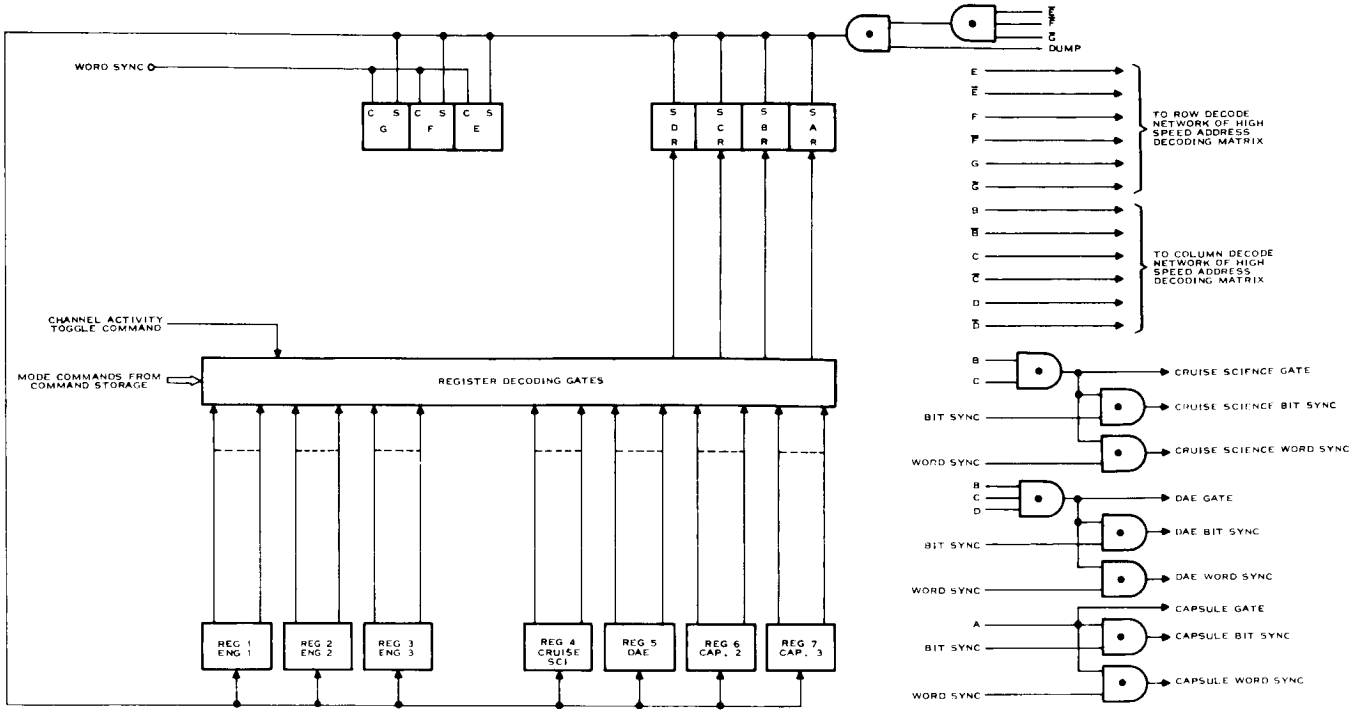


Figure 3-9. Format Programmer

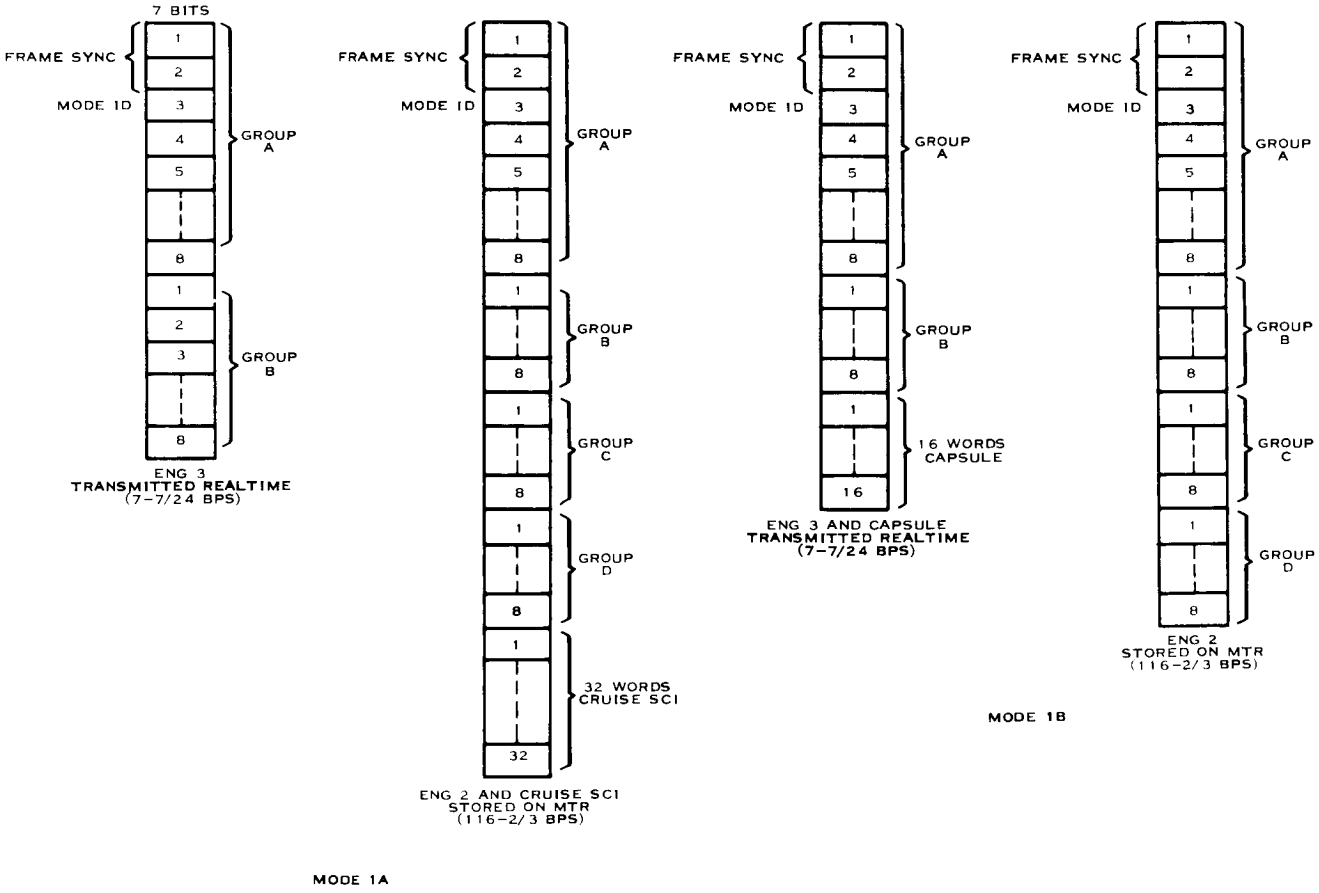


Figure 3-10a. Data Formats

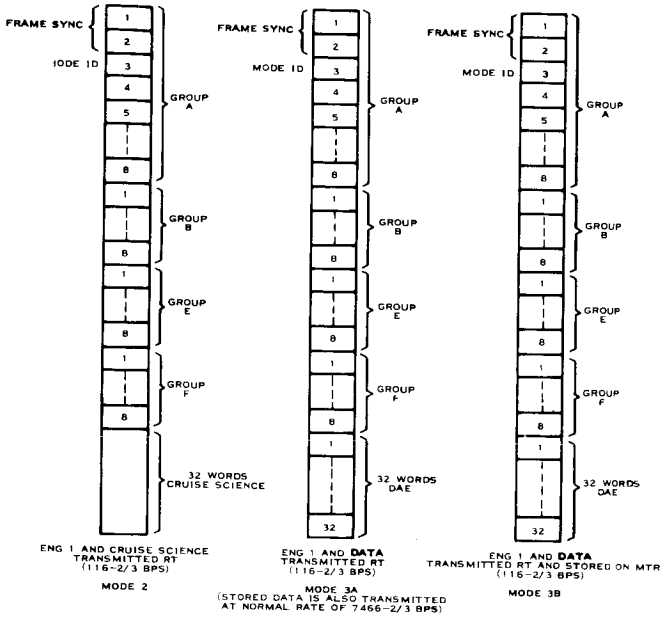


Figure 3-10b. Data Formats

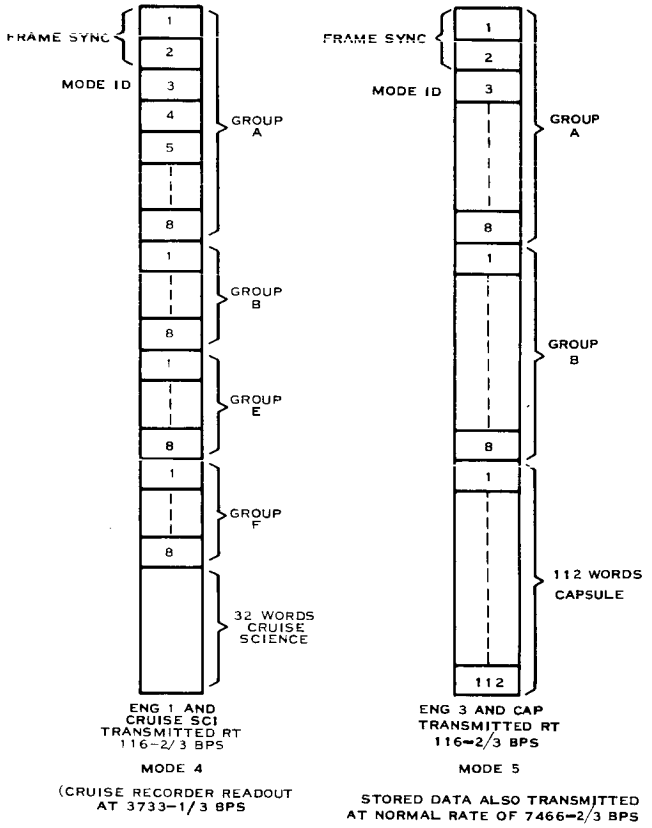


Figure 3-10c. Data Formats

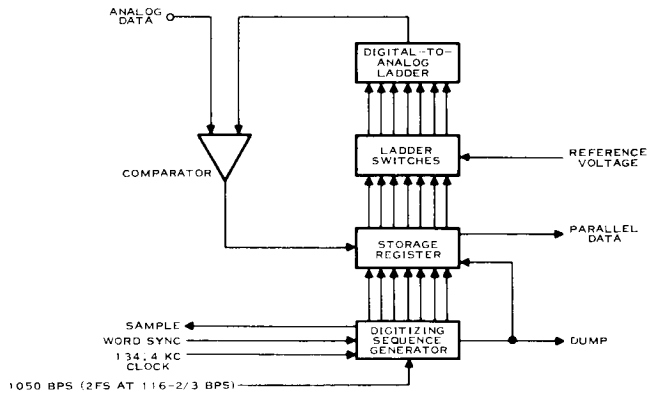


Figure 3-11. Successive Approximations ADC

3.12.1 Event Counters. The event counters consist of four 3-bit counters for the accumulation of spacecraft events. The counters will be read out into two words. Each word will consist of the data contained in two of the counters.

3.12.2 Command Detector Monitor. Three 7-bit words are included, one for each VCO. The words indicate lock and VCO lock and VCO frequency variation. The mechanization of these monitors will be similar to those used in Mariner C. A 7-bit word will also be included to indicate reception and action upon a command plus computer and sequencer (C&S) parity check. The first four bits of the word will be read from a 4-bit counter (16-count capacity) in which an increment will indicate that a command was accepted. The following two bits will be read from a counter which indicates that a command was rejected. The last bit indicates if parity has failed in the C&S.

3.12.3 Gimbal Angle Position Counters. Two antenna gimbal angle position counters and three science instruments gimbal angle position counters will be provided. These gimbal angle position indicators will be mechanized as shown in Figure 3-14. Two inputs will be received by each counter. The first input will be a dc level change to indicate left or right angle change (count up-count down). The second input will be a pulse train which will be accumulated in a η bit counter to indicate the gimbal angle. Two additional

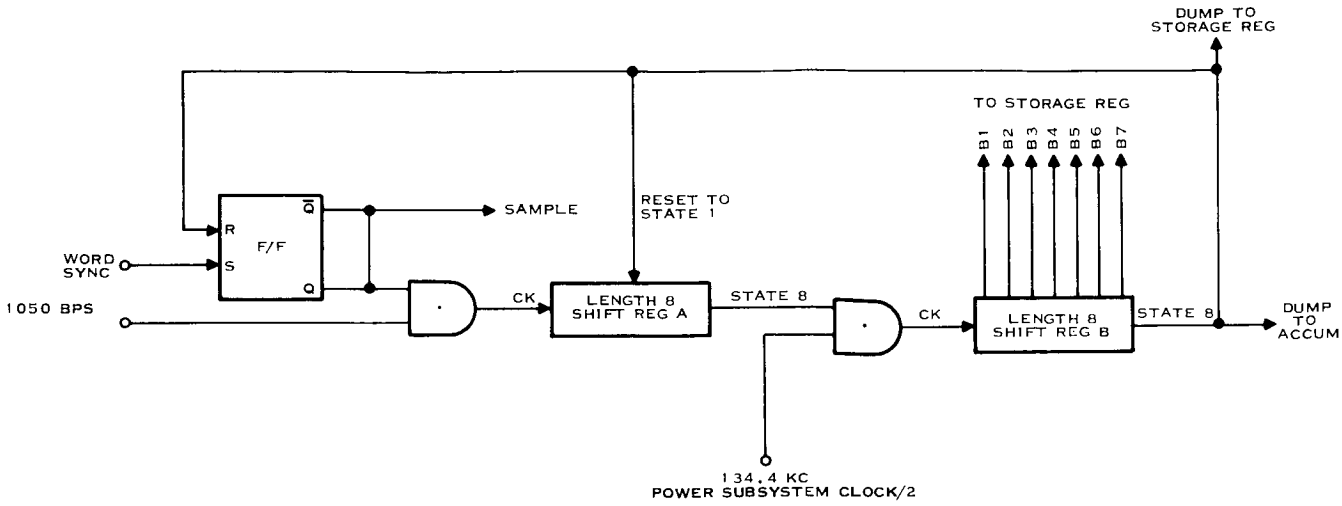


Figure 3-12a. Digitizing Sequence Generator

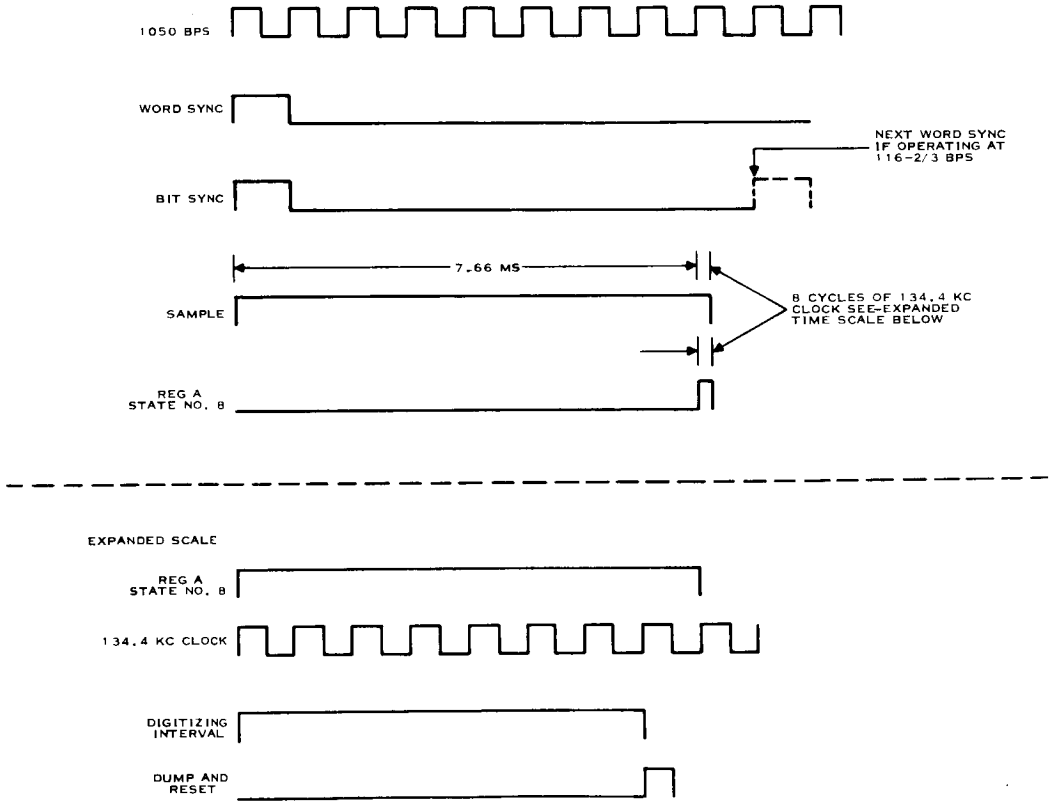


Figure 3-12b. Digitizing Sequence Generator Timing

bits are included to indicate right and left stop. The length (η) of each counter is shown below.

Word	η
Antenna Gimbal Angle Position A	10
Antenna Gimbal Angle Position B	7
Science Instrument Package Gimbal Angle A	9
Science Instrument Package Gimbal Angle B	9
Science Instrument Package Gimbal Angle C	10

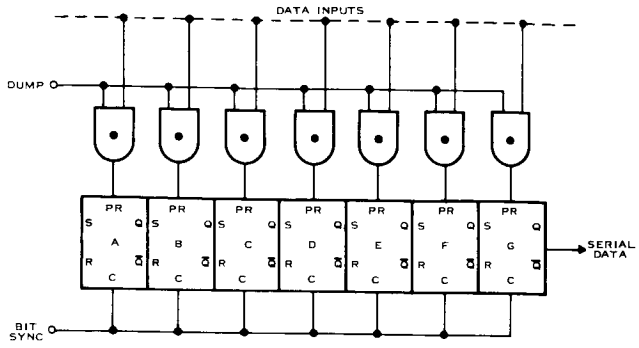


Figure 3-13. Data Transfer Register

3.13 Data Selector. The data selector consists of logic gates which in the presence of the proper control signal gates the data source output to the modulator. The data formats are as shown in Figure 3-10.

3.14 Frequency Divider. The frequency divider consists of the binary stages required to divide down the Power Subsystem clock to give the telemetry subcarriers for the various bit rates. The Power Subsystem clock signal is counted down in parallel paths such that a failure will at worst case cause loss of one rate.

3.15 Rate Control. The rate control consists of the logic required to select the appropriate telemetry subcarrier for the selected bit rate.

3.16 Real-Time Data Modulator. Figure 3-15 shows a logic diagram of the real-time data modulator; two are provided, one each for Channel A and Channel B. Incoming NRZ data is converted to modified NRZ data (NRZ-M) by toggling a flip-flop with each data "one". The NRZ-M data is MOD 2 added to the synchronization pseudonoise code (from PN generator A for Channel A and PN generator B for Channel B). The output is then MOD 2 added to the $2f_s$ subcarrier. Finally, the resultant ($D \oplus PN \oplus 2f_s$) is MOD 2 added in all modes but mode I to a high frequency square wave subcarrier fo (fo = 268.8 KC). The output is then sent to the subcarrier combiner and selector.

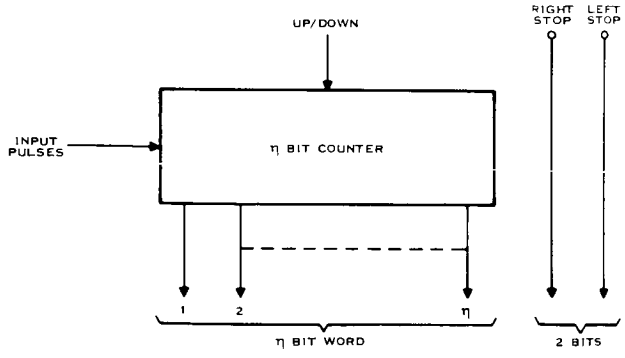


Figure 3-14. Gimbal Angle Indicator Mechanization

3.17 Stored Data Subcarrier Modulator. Figure 3-16 shows a logic diagram of the subcarrier modulator used for modulation of data stored by the DSS. Two stored data modulators are provided for redundancy. An incoming clock signal is counted down by the stored data rate selector to generate a square wave subcarrier $2f_s$ appropriate to the stored data transmission rate. The $2f_s$ also drives a PN generator resulting in bit sync, word sync, and a PN sequence. Incoming serial NRZ data from the DSS, synchronous with these bit and word sync signals, is MOD 2 added to $2f_s$ and the result MOD 2 added to the PN sequence. The output to the combiner and selector is ($D \oplus 2f_s \oplus PN$).

3.18 Subcarrier Combiner and Selector. Figure 3-17 shows a logic diagram of the circuitry used to combine and select the appropriate real-time and/or stored data subcarriers and output three identical composite telemetry signals for modulation of the exciters.

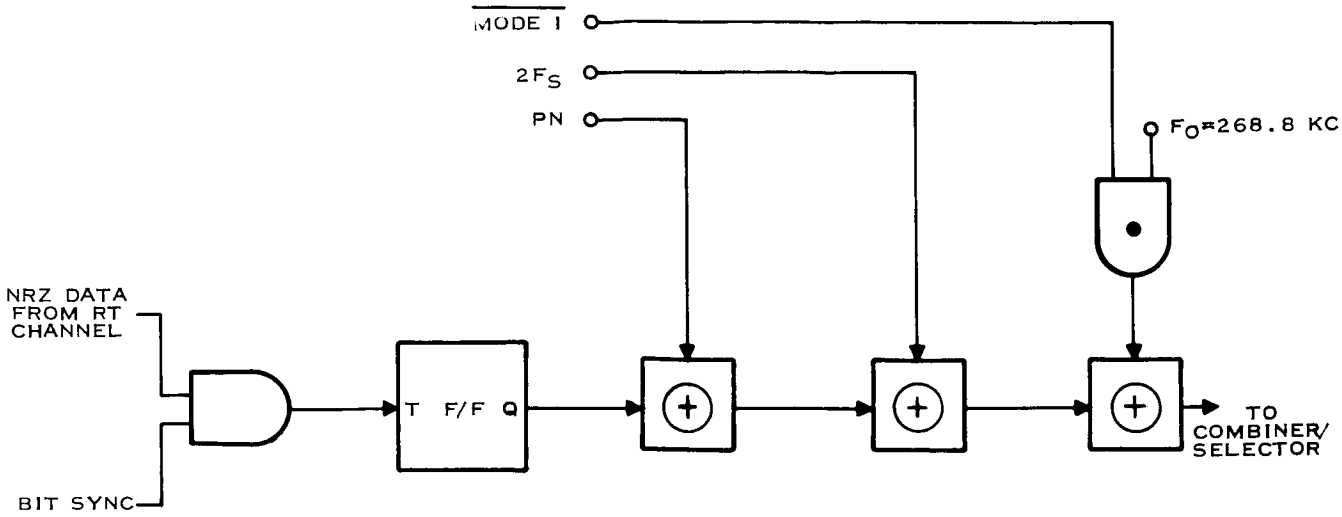


Figure 3-15. Real Time Data Modulator

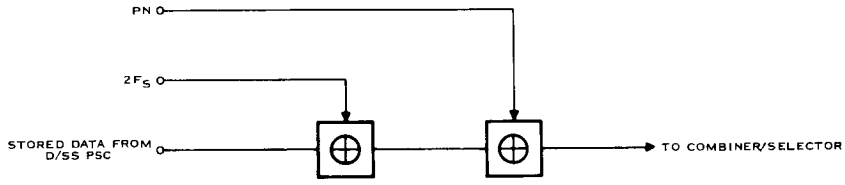


Figure 3-16. Stored Data Modulator

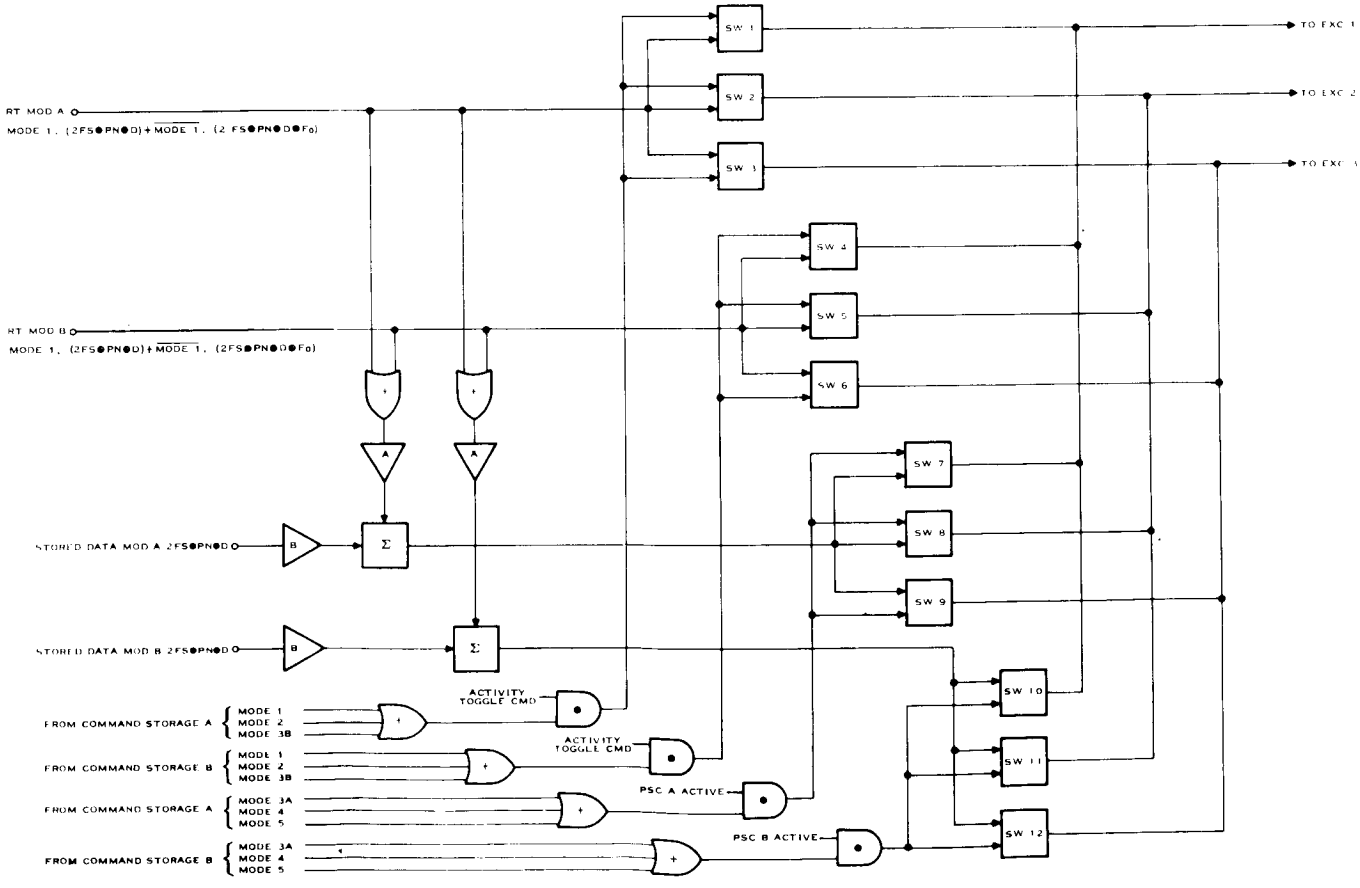


Figure 3-17. Subcarrier Combiner and Selector

In modes 1, 2, and 3B, only real-time data is transmitted from either Channel A or B. An AND gate is used to select the appropriate real-time subcarrier and output it to the three exciters through parallel linear switches. In modes 3A, 4, and 5, stored data and real-time data are frequency multiplexed for transmission. The real-time subcarrier and stored data subcarrier are linearly summed to give:

$$A\,(D_R \oplus (2f_s)_R \oplus PN_R \oplus fo) + B\,(D_s \oplus (2f_s)_S \oplus PN_s)$$

3.19 Power Supply. The telemetry subsystem power supply will transform the 2.4-kc primary power into the following voltages:

+ 20 vdc - analog voltage	+ 3.2 vdc-ADC reference
- 20 vdc - analog voltage	+ 3.5 vdc-logic voltage

The ± 20-volt supplies will be used to power the ADC comparator, the low level amplifiers, and the constant current generators. Circuits can be designed for these applications which will allow ± 5% variations in the supply voltages and stay within the accuracy requirements of the system. The ± 5% variation in the ± 20-volt supplies can be met with no additional regulation other than the specified ± 2% primary power input regulation. The 3.5-volt logic supply will also require no additional regulation. The 3.2-volt ADC reference supply will definitely require regulation to minimize ADC error. For this application a series regulator will be used.

4.0 INTERFACE CHARACTERISTICS

4.1 Performance Data. The number and type of channels shall be adequate to handle all signals listed in the telemetering channel assignment. The following signals will be accepted by the telemetry subsystem.

a. High level analog

Voltage - 0 to 3.2 volts dc
Impedance - less than 10k ohms

b. Low level analog

Voltage - 0 to 100 millivolts dc
Impedance - less than 10k ohms

c. Bipolar analog

Voltage - ± 1.6 volts dc
Impedance - less than 10k ohms

d. Digital pulses (Events)

Voltage - "0" = 0 volts dc; "1" = 3.5 volts dc
Time Duration > 3 milliseconds

e. Serial digital data

Voltage - "0" = 0 volts dc: 1 = 3.5 volts dc
Type NRZ; synchronous with TLM bit sync

f. Parallel digital data

Voltage - "0" = 0 volts dc; 1 - 3.5 volts dc
Type - Pulse data dumped in parallel on receipt of the dump pulse.

4.2 Interface. Tables 4-1 through 4-3 list the interfaces required for the telemetry subsystem as follows:

a. Table 4-1 Input Requirements
b. Table 4-2 Output Requirements
c. Table 4-3 Direct Access Functions, Umbilical Interface, and Command List.

TABLE 4-1. INPUT INTERFACE CHARACTERISTIC TABLE

Input	Source	D. E Input Characteristics	Signal Characteristics	Notes
Serial NRZ data	DAE	Input to logic gate in data selector	NRZ data synchronous with TLM bit sync	Cruise Science
Serial NRZ data	DAE	Input to logic gate in data selector	NRZ data synchronous with TLM bit sync	Orbital RT
Primary power	Power	TR unit	2.4 kc: 50v Rms. ±2%	Telemetry Subsystem will require approximately 9 watts of primary power
Clock	Power	Input to frequency divider	268.8-kc square wave	Basic timing signal
Commands	C&S	Storage logic	Positive going 3.5-volt pulse minimum duration of 3 milliseconds	See Table 4-5 for command list
Serial NRZ data	Data storage	Input to subcarrier modulator	NRZ data synchronous with TLM bit sync	Transmitted in modes 3, 4, and 5
Serial NRZ data	Data storage	Input to subcarrier modulator	NRZ data synchronous with TLM bit sync	Same as above
Commands	Command	Storage logic	Positive going 3.5-volt pulse minimum duration of 3.2 milliseconds	See command list in Table 4-5
Serial NRZ data	Capsule	Input to logic gate in data selector	NRZ data synchronous with TLM bit sync	Multiplexed with cruise or orbital engineering data
Performance data includes: a) Command accept event b) Command reject event c) VCO frequency & lock d) Gimbal angle events e) C&S parity check	All Subsystems Command Command Command G&C C&S	Analog data to commutator switch digital data to accumulator		

5.0 PERFORMANCE PARAMETERS

5.1 Reliability. Three telemetry subsystem configurations were considered in Task B. The first configuration was a triple standby redundant subsystem similar to the configuration proposed in Task A. The second configuration considered was a subsystem employing two independent encoders. The third subsystem considered (the proposed system) time shares a single commutator. A trade off analysis which considered reliability, size, weight, and power indicated that the proposed configuration was the best choice.

Figure 5-1 shows the reliability model for modes 2 through 5. The model for modes 1A and 1B is different in that it requires both real-time data channels to be operative. The mode reliability is defined as the probability of presenting the required modulated subcarrier to at

TABLE 4-2. OUTPUT INTERFACE CHARACTERISTIC TABLE

Output	Destination	D/E Output Characteristic	Signal Characteristics	Notes
Word sync	Data storage PSC	Logic gate output	Positive going 3.5-volt pulse	Playback word sync
Bit sync	Data storage PSC	Logic gate output	Positive going 3.5-volt pulse	Playback bit sync
Speed-range	Data storage MTR	Logic gate output	Logic level on 2 lines to indicate playback speed	Indicates speed range of MTR
Serial NRZ data	Data storage maneuver MTR	Data output from channel A or B	NRZ data synchronous with TLM bit sync	Maneuver mode
Bit sync	Data storage maneuver MTR	Logic gate output	Positive going 3.5-volt pulse	Bit sync for MTR read out
Word sync	Data storage maneuver MTR	Logic gate output	Positive going 3.5-volt pulse	Word sync for MTR read out
Bit sync	Capsule	Logic gate output	Positive going 3.5-volt pulse	During transmission of capsule digital data
Capsule gate	Capsule	Logic gate output	Logic level	High during transmission of capsule digital data
Bit sync	DAE	Logic gate output	Positive going 3.5-volt pulse	During transmission of non-scanned science data
Science gate	DAE	Logic gate output	Logic level	High during transmission of nonscanned data
Modulated subcarrier	Radio exciter 1	Logic gate output	Four level composite signal	Amplitude adjusted to characteristics of exciter
Modulated subcarrier	Radio exciter 2	Logic gate output	Four level composite signal	Amplitude adjusted to characteristics of exciter
Modulated subcarrier	Radio exciter 3	Logic gate output	Four level composite signal	Amplitude adjusted to characteristics of exciter

TABLE 4-3. TELEMETRY SUBSYSTEM DIRECT ACCESS FUNCTIONS, UMBILICAL INTERFACE, AND COMMAND LIST

Direct Access Functions	Umbilical Interface	Command List
1. Command Mode 1A	1. Modulated subcarrier	1. Mode 1A
2. Command Mode 1B	2. Return	2. Mode 1B
3. Command Mode 2		3. Mode 2
4. Commadn Mode 3A		4. Mode 3A
5. Command Mode 3B		5. Mode 3B
6. Command Mode 4		6. Mode 4
7. Command Mode 5		7. Mode 5
8. Command Phaser Bypass		8. Toggle high data rate
9. Command Activity Toggle		9. Toggle low data rate
10. Command Toggle Low Data Rate		10. Phaser bypass
11. Command Toggle High Data Rate		11. Toggle real-time channel activity*
12. -20 V TR Monitor Power Supply A		12. Toggle stored data channel activity
13. -20 V TR Monitor Power Supply B		
14. +3.5 V TR Monitor Power Supply A		
15. +3.5 V TR Monitor Power Supply B		
16. Return		

*Normally the mode automatically selects channel A as the stored data, channel and Channel B as the RT transmission channel. Command 11 reverses the roles of the two channels.

least one of three exciters. It is calculated for the case of (1) 100% engineering data and (2) 80% of the engineering data. These calculations are shown for a mission duration of 5520 hours in Table 5-1 (orbit plus 30 days).

5.2 Transmission Rates. The transmission rates are as follows:

a. 14,933-1/3
b. 7466-2/3
c. 3733-1/3
d. 933-1/3
e. 116-2/3
f. 29-1/6
g. 7-7/24

5.3 Transmission Modes. The data formats for each transmission mode are shown in Figure 3-10 and Table 5-2.

5.4 Analog Signal Inputs. The accuracy of a measurement as read from the input to the data encoder to the ADC output shall be maintained at ± 3% of full scale for 3.2 and ± 1.6-volt signals, and ± 5% of full scale for 0 to 100 millivolts and all temperature measurements. The accuracy shall be maintained for the mission lifetime requirements and under all specified environmental conditions. The linearity of the encoder as read from the measurement voltage input to the ADC output shall be within ± 0.5% of the full scale to the nearest straight line.

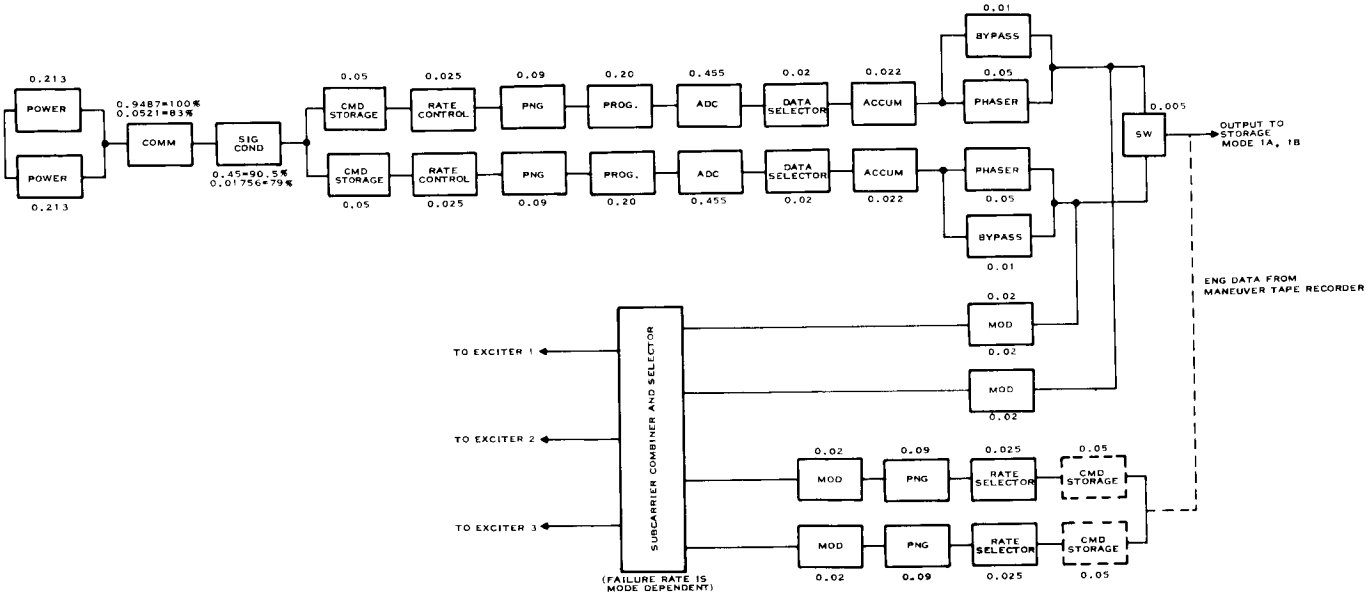


Figure 5-1. Reliability Model

TABLE 5-1. MODE RELIABILITY

	Reliability (100%)	Reliability (80%)
Modes 1A, 1B	85.8%	90.2%
Modes 2, 3B	94.3%	99.0%
Modes 3A, 4, 5	94.3%	99.0%
Mission Duration 5520 Hr Orbit plus 30 days		

5.5 Commutation

5.5.1 Sampling Rate. The real time collection rates are shown in Table 3-2.

5.5.2 Frame Sync. To establish frame sync, two unique words of seven "ones" are provided at the beginning of each cycle of the high speed deck. Full scale (all "ones") is prohibited from occurring in the engineering data.

5.5.3 Medium Deck Sync. To establish medium deck sync, a word of seven "ones" is included at the beginning of one medium deck in each commutator group.

5.5.4 Low Deck Position. A digital word is included in one medium deck of each commutator group to indicate the low deck position.

5.5.5 Mode Identification. A word is included in the high deck which indicates the mode being transmitted.

5.5.6 Spacecraft Time. Three words are included in the high deck which indicates spacecraft time.

5.6 Synchronization

5.6.1 PN Code. The synchronization code generated by all PN generators is as follows:

1-0-0-0-0-0-1-1-1-1-1-1-0-1-0-1-0-1-1-0-0-
1-1-0-1-1-1-0-1-1-0-1-0-0-1-0-0-1-1-1-0-0-0
1-0-1-1-1-1-0-0-1-0-1-0-0-0-1-1-0-0-0-0-

TABLE 5-2. TRANSMISSION FORMAT

Data Type	Mode 1A	Mode 1B	Mode 2	Mode 3A	Mode 3B	Mode 4	Mode 5
Eng. 1 Commutator Groups A B E F (includes 30 analog channels from capsule)			58-1/3 Transmitted Real Time	58-1/3 Transmitted Real Time	58-1/3 bps Transmitted Real Time & Stored on MTR	58-1/3 bps Transmitted Real Time	
Eng. 2 Commutator Groups A B C D	58-1/3 bps Stored on Maneuver MTR	116-2/3 bps Stored on Maneuver MTR					
Eng. 3 Commutator Groups A B	7-7/24 bps Transmitted Real Time	3-31/48 bps Transmitted Real Time					14-7 12 bps Transmitted Real Time
Science 32 Words Cruise	58-1/3 bps Stored on Maneuver MTR		58-1/3 bps Transmitted Real Time			58-1/3 bps Transmitted Real Time	
DAE Data 32 Words Orbital				58-1/3 bps Transmitted Real Time	58-1/3 bps Transmitted Real Time & Stored on MTR		
Capsule Digital Data 16 Words		3-31/48 bps Transmitted Real Time					
Capsule Digital Data 112 Words							102-1 12 bps Transmitted Real Time
Stored Data Transmitted on Stored Data Sub carrier				7466-2/3 Transmitted on Stored Data Sub-carrier		3733-1/3 bps Transmitted on Stored Data Sub-carrier	7466-2/3 bps Transmitted on Stored Data Sub-carrier

5.6.2 Word Sync. Word sync is derived from the PN code, and is coincident with a unique state of the PN generator. Word sync for real-time Channel A is taken from PNG A, and word sync for real-time Channel B is taken from PNG B. The stored data word sync is taken from PNG C or PNG D.

5.6.3 Bit Sync. Bit sync is derived from the PN code and is coincident with every ninth PN bit starting with word sync. Bit sync is taken from the same PNG as its respective word sync.

5.7 Modulator - Demodulator Performance - A detailed discussion of the time versus frequency multiplexing tradeoffs is given in CII VC233FD101 Telecommunications. In summary, the loss in efficiency was more than offset by the savings in data handling hardware and the simplification of the DAE/DSS interface.

5.7.1 Power Division. For the two subcarrier case the modulated carrier can be expressed as

$$m(t) = \cos(w_2 t \pm \alpha_r \pm \alpha_s)$$

α_r = phase deviation by real time data = 21.7°

α_s = phase deviation by stored data = 57.6°

The resultant power division is given by

$$1 = \cos^2 \alpha_r \cos^2 \alpha_s + \cos^2 \alpha_r \sin^2 \alpha_s + \cos^2 \alpha_s \sin^2 \alpha_r + \sin^2 \alpha_r \sin^2 \alpha_s$$

$\cos^2 \alpha_r \cos^2 \alpha_s$ = carrier power = $0.25\ P_t$

$\cos^2 \alpha_r \sin^2 \alpha_s$ = stored data power = $0.61\ P_t$

$\cos^2 \alpha_s \sin^2 \alpha_r$ = real-time data power = $0.04\ P_t$

$\cos^2 \alpha_r \sin^2 \alpha_s$ = intermodulation power = $0.10\ P_t$

The power division was optimized for the 3733-1/3/116-2/3 bps case.

For the two single subcarrier cases the power division is given by

$$1 = \cos^2 \alpha + \sin^2 \alpha$$

$\cos^2 \alpha$ = carrier power = { 0.425 for 7-7/24 bps ; 0.25 for 116-2/3 bps }

$\sin^2 \alpha$ = data power = { 0.575 for 7-7/24 bps ; 0.75 for 116-2/3 bps }

5.7.2 ST/N/B Selections. The ST/N/B selections are given in Table 5-3.

MNRZ was required due to the data ambiguity resulting in demodulating the suppressed RT data subcarrier (f_o). Recovering only the fundamental term of f_o results in a 0.9-db loss. A 0.3 db loss is taken for baseband filtering with cutoff at 8 fs. There is 10 db assumed in the carrier and subcarrier loops. This results in a 0.2-db loss due to phase jitter. The exception to this being the 7-7/24 bps case where 7 db was assumed in the carrier loop with the resulting 0.8-db loss.

TABLE 5-3. ST/N/B SELECTIONS

	Stored	28-1/6 and 116-2/3 bps RT	7-7/24 and bps RT
Theoretical (PSK) 5×10^{-3}	5.2	5.2	5.2
MNRZ	0.0	0.8	0.0
RF Filter Loss (Fundamental f_0)	0.0	0.9	0.0
Baseband Filter (8 f_s)	0.3	0.3	0.3
Carrier RMS and Static Phase Error	0.2	0.2	0.8
Subcarrier RMS and Static Phase Error (f_0)	0.0	0.4	0.0
Subcarrier RMS and Static Phase Error ($2f_s$)	0.2	0.2	0.2
Total Losses	5.9	8.0	6.5

5.7.3 Threshold Signal-to-Noise Ratio. The threshold signal-to-noise ratio in a cps noise bandwidth that must be present at the demodulator data detector is given in Table 5-4 for the different bit rates.

5.7.4 Clock Tracking Phase Locked Loop Threshold Signal-to-Noise Ratio. The clock tracking phase locked loop threshold signal-to-noise ratio in the threshold noise bandwidth, a_L, is given in Table 5-5.

5.7.5 Average Time Required to Sync. The mean time to acquire bit sync at the

TABLE 5-4. THRESHOLD SIGNAL-TO-NOISE RATIO

Bit Rate (bps)	$(S/N_o = (E/N_o)R$ (db)
14.933-1/3	47.6
7466-2/3	44.6
3733-1/3	41.6
933-1/3	35.6
116-2/3	28.67
29-1/6	22.64
7-7/24	15.12

TABLE 5-5. CLOCK TRACKING PHASE LOCKED LOOP THRESHOLD SIGNAL-TO-NOISE RATIO

Data Rate (bps)	a_L db
14.933-1/3	26.9
7466-2/3	26.1
3733-1/3	25.4
933-1/3	23.9
116-2/3	21.6
29-1/6	20.1
7-7/24	18.6

TABLE 5-6. AVERAGE TIME REQUIRED TO SYNC

Data Rate (bps)	Average Time to Sync (No. Decisions Error) (sec)
14933-1/3	0.148
7466-2/3	0.296
3733-1/3	0.590
933-1/3	2.36
166-2.3	18.9
29-1/6	75.8
7-7/24	181

TABLE 6-1. TELEMETRY SUBSYSTEM SIZE AND WEIGHT

Circuit	No. Req'd	Size (in.^{3})	Weight (lb)
1. Commutator	1	287	7.0
2. Signal Conditioning	1	22	0.67
3. Command Storage	2	27	0.81
4. ADC	2	24	0.7
5. Frequency Divider	1	4	0.13
6. Rate Control	2	0.3	0.03
7. Bypass Logic	2	2.5	0.08
8. Phaser	1	1.8	0.06
9. PN Generator	4	6.0	0.20
10. Format Programmer	2	25	0.81
11. Decoding Matrix	2	5	0.16
12. Subcomm Drive	2	31	1.0
13. Digital Accum.	2	35	1.2
14. Transfer Reg.	2	1.8	0.05
15. Data Selector	2	0.40	0.03
16. Modulator	4	15	0.5
17. Power Supply	2	187	2.75
Subtotal		674.8	16.18
Add for Packaging		200.2	1.82
Total		875	18

threshold signal-to-noise ratio based on integrating five code lengths for all but the 7-7/24 bps case; three code lengths are assumed for 7-7/24 bps.

6.0 PHYSICAL CHARACTERISTICS. The telemetry subsystem is packaged in Bay 9 of the spacecraft. The packaging configuration for Bay 9 and locations of each section of the telemetry subsystem electronics are shown in Figure 6-1. Table 6-1 itemizes the weight and volume of data encoder equipment. Magnesium trays are used to house the data encoder electronics. One edge of each tray is fastened to a thermal integrating plate. Thermal control louvers are used to regulate the temperature of the integrating plate. This will allow the operating temperature of each tray to be stabilized within controlled limits. The electronics trays are mounted between the thermal integrating plate and the inner plate as shown in Figure 6-1. The inner plate contains the interconnect wiring and connectors. Intertray connectors are Cannon 50-pin D series; input-output connectors are Bendix Type PT07.

Each tray contains three or more pairs of component carrier boards. The circuit boards in each tray are mounted face to face. Conventional components are packaged in "cordwood" modules and integrated circuits are welded directly to the circuit card. Many cards employ a combination of the two packaging methods to achieve maximum component density.

7.0 SAFETY CONSIDERATIONS. All interface between the ground equipment and the data encoder is protected by isolation amplifiers.

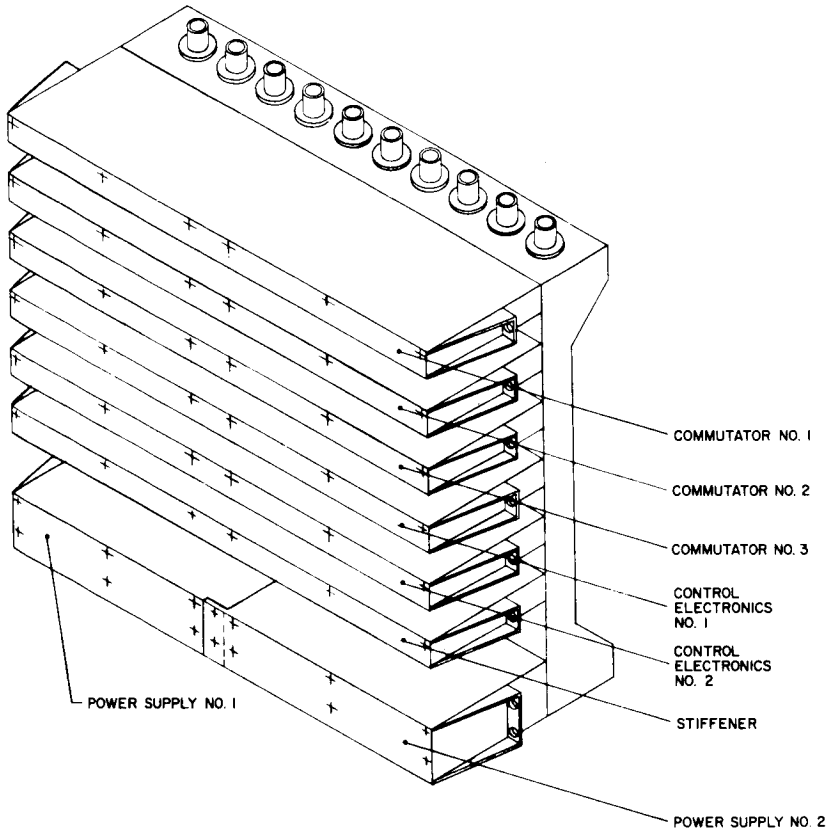


Figure 6-1. Bay 9 Packaging Configuration

CII VC233FD107

DATA STORAGE SUBSYSTEM

SECTION

1	INTRODUCTION AND SCOPE
2	APPLICABLE DOCUMENTS
3	FUNCTIONAL DESCRIPTION
4	INTERFACE CHARACTERISTICS
5	PERFORMANCE PARAMETERS
6	PHYSICAL CHARACTERISTICS AND CONSTRAINTS

DATA STORAGE SUBSYSTEM

1.0 INTRODUCTION AND SCOPE. This document describes the preferred design of the VOYAGER Data Storage Subsystem (DSS). The operation of the control and magnetic tape storage units is described and their specifications tabulated.

2.0 APPLICABLE DOCUMENTS

VC233FD106 - Telemetry
VC220SR101 - Design Characteristics and Restraints
VC220FD108 - Science Interface
VC233FD101 - Telecommunication Subsystem

3.0 FUNCTIONAL DESCRIPTION

3.1 General. The DSS provides for storage of digital binary data as required by mission data handling requirements. The system is composed of six magnetic tape recorders and the control and power supply units required for their operation. The recorders are all physically identical peripheral drive, parallel-recording types, with identical tape pack sizes. The units differ only in having one or two motors for the tape drives.

Each recorder is primarily associated with one data input line, and recording may proceed independently on any or all units. Playback is sequential, one recorder at a time, but individual units may be command selected for fast information return.

No standby redundancy is provided for the recorder units, but functional redundancy is achieved by allowing units to exchange input functions in case of recorder failure. Both standby and operational redundancy is provided for the control and power supply functions.

3.1.1 Functions. The DSS performs the following functions:

a. Storage of combined bus engineering, capsule, and cruise science data during spacecraft maneuvers ($\sim 2 \times 10^6$ bit capacity required).

b. Storage of fields and particles data over an orbit period for delayed transmission ($\sim 2 \times 10^6$ bit capacity required for a seven hour orbit $\sim 10^8$ bit capacity provided).

c. Storage of data from an IR scanner during orbital operations (10^8 bit capacity provided).

d. Storage of data from an IR and/or UV spectrometer during orbital operations (10^8 bit capacity provided).

e. Storage of data from two video instruments during orbital operations (10^8 bit capacity provided per instrument).

f. Storage of high-rate science data during periods of high experimental activity (fields and particles recorder used -10^8 bit capacity)

g. Automatic or commanded sequencing of recorder playback.

h. Execution of recorder function exchange switching as a commanded repair function.

i. Exercise of recorders during launch to prevent possible damage to mechanical components.

3.1.2 Block Diagram and Summary Description. A simplified block diagram of the DSS (Figure 3-1) shows the basic functional elements and external interfaces.

Each Magnetic Tape Recorder (MTR) unit interfaces with its data source and functions to record input data and identifying information at the appropriate rate. Data is replayed in turn from each recorder in bit synchronism with the 15, 7.5, 3.75, or 0.933 kbps transmission rate. Data may be recorded at any time except while the unit is playing back. The Playback Sequence Control (PSC) interfaces with the Telemetry, Computer and Sequencer (C&S), and Command Subsystems; and functions to distribute commands and to control the playback of stored data. The DSS Power Supply supplies power for all DSS logic and executes a commanded power switching function for PSC fault correction.

Table 3-1 is a summary of the operation of the DSS. It is organized chronologically on the basis of mission events that affect DSS operational requirements.

Figure 3-2 is a detailed block diagram of the DSS which shows the major physical elements and the complete external and internal interface connections. In addition, the functional redundancy provisions are shown by the alternate inputs supplied to each MTR unit and the power supply load sharing. The standby redundancy provided for the PSC is also shown.

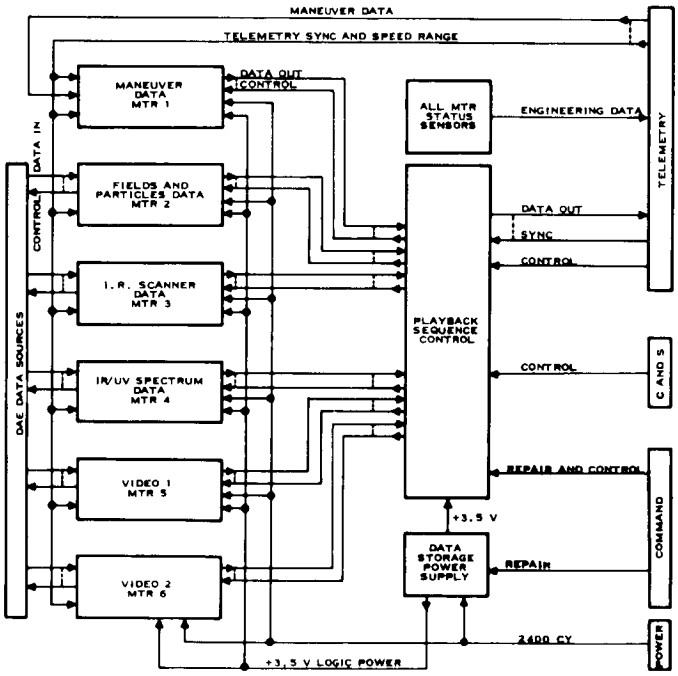


Figure 3-1. Simplified Data Storage System Functional Block Diagram

All MTR units have identical interfaces with the dual PSC units and the telemetry subsystem; except that MTR 1 and MTR 2 have Telemetry data inputs. All MTR Data Automation Equipment (DAE) interface line groups for MTR 3 through MTR 6 are as shown for MTR 3. MTR 1 and MTR 2 are both two motor, low record rate types, and either one may select the Telemetry or Fields and Particles data input. MTR 3 through MTR 6 are able to select the UV/IR spectrometer, scanner, video 1, or video 2 lines; and are single motor types in the preferred design.

The PSC unit standby redundancy is accomplished by switching power between the two units. The outputs are combined in "OR" fashion before routing to Telemetry. Power supply redundancy is accomplished by the use of a passive load sharing network.

TABLE 3-1. DATA STORAGE SYSTEM OPERATIONS

Mission Phase	Requirements on DSS	Description of DSS Operation
Prelaunch	Checkout of all DSS operation (go/no go). Prelaunch preparation	DSS exercised through Telemetry, C&S, and Command to verify operation. Recorders set to launch mode by umbilical command.
Launch	Recorders run to prevent mechanical damage.	All recorders run in record direction until launch completed.
Post Launch	Recorders return to ready state.	One Playback sequence is executed on C&S command to return recorders to prerecord condition.
Science Flare in Cruise	Fields and Particles data recorded at high rate on DAE request.	MTR 2 records at maximum rate of 15 kbps while DAE level "up".
Spacecraft Maneuvers	Store Telemetry data for duration of maneuver	MTR 1 records at 116 bps while Telemetry "record" level is up
Maneuver or Flare Data Replay	Flare or Maneuver automatically replayed for transmission.	On Telemetry command, a playback sequence is executed.
Normal Orbit Recording	All recorders except the Maneuver unit record science data as requested by DAE	Each recorder accepts data from its selected source at the sources request. The record rate adjusts to the data input rate. All recorders operate independently.
Normal Playback	All data is played back over high rate telemetry link.	On Telemetry command, playback sequence begins with MTR 1 and proceeds automatically to play all recorders in sequence. All recorders may be recording at any time except for the unit playing back.
Commanded Playback	Selected recorders are played back.	Command may select any recorder(s) to play back out of sequence
Reduced Capability Operation	If one or more recorders fail, surviving units may be used to obtain data from all sources on time shared basis.	Command may direct recorder(s) to select different input sources at any time.
Earth Occultation	Recording proceeds on any active channels. Maneuver telemetry data is stored.	Same as maneuver except that science data is stored as required.

Detailed descriptions of the major physical elements and their function are given in the succeeding sections.

3.2 Magnetic Tape Recorder Units. All of the proposed VOYAGER MTR units are identical in size and have identical tape pack sizes. The advantages of this approach are discussed in Section 3.2.2. Each MTR unit is composed of two basic sections, the control logic module (CLM) and the tape transport module (TTM), as shown in Figure 3.3. Each MTR unit is capable of accepting data from a data source channel at record rates which may vary continuously over a limited range. The record rate is automatically derived from the incoming bit sync rate. The rate selection of the input channel is a commanded function, and is employed to implement operational redundancy by allowing the substitution of an MTR unit for a defective unit of similar characteristics. Each of the high rate (MTR 3, 4, 5 and 6) units may select any of the four high rate data channels; while MTR 1 and 2 may select either of the low rate inputs. This capability means that all of the high and low rate inputs may be obtained on a time shared basis if only one high rate MTR and one low rate MTR remain operative.

Data is recorded in a word-organized format, with both bit sync and word sync being supplied by the data source. Blocks of data may be of any length. Recording is done in only one tape travel direction. Data playback proceeds, upon command from the PSC, in the reverse order to that in which it was recorded. Once playback is initiated, it proceeds until halted by either a tape end signal or another PSC command. Recording is inhibited during playback. Playback is bit and word synchronous with the telemetry system for the nominal 15, 7.5, 3.75, and 0.933 kbps transmission rates. The playback speed range is commanded by the Telemetry subsystem.

3.2.1 MTR Control Logic Module. The MTR CLM is composed entirely of Silicon Integrated Circuits (SIC) logic and has no mechanical function. A functional block diagram of a CLM is shown in Figure 3-4. The basic functions of a CLM are:

a. Performance of all interface functions for the MTR, except for power input and engineering data output functions. Conversion of external signals to transport operating commands.

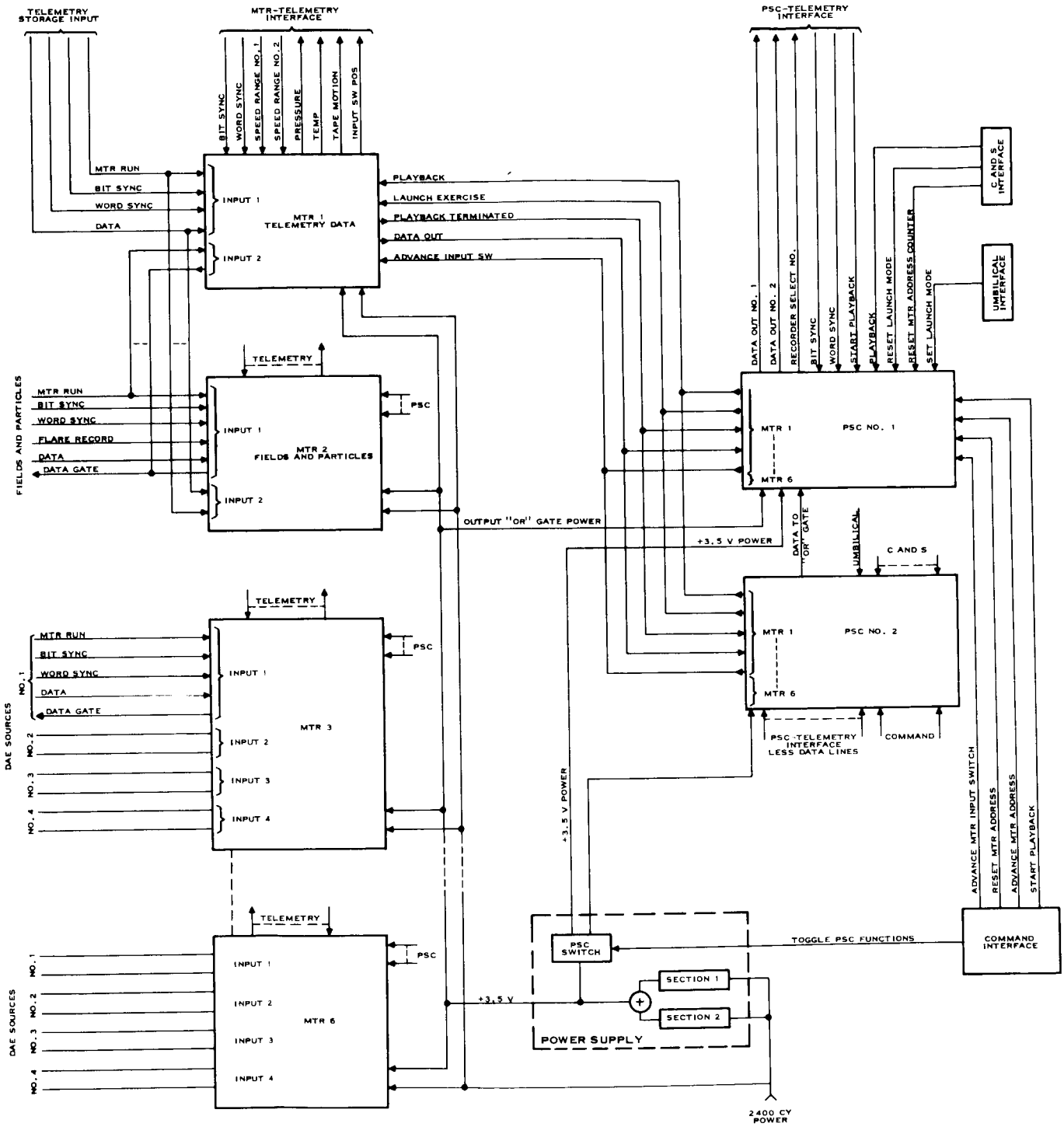


Figure 3-2. Detailed Data Storage Subsystem Functional Block Diagram

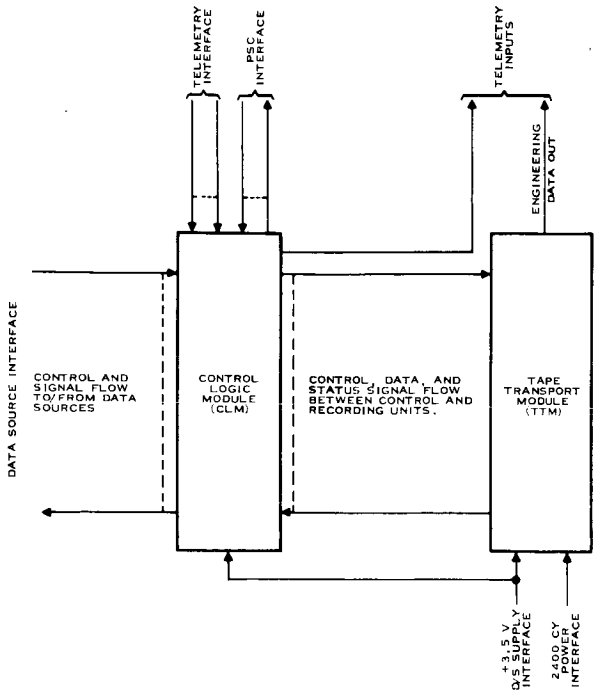


Figure 3-3. Major Magnetic Tape Recorder Functional Elements

b. Conversion of transport internal signals into externally available signals; e.g., tape end signals into "record filled" or "playback terminated" signals.

c. Data input control during transport starting intervals.

d. Switching of input functions between data source channels upon receipt of a command.

e. Generation of input selection switch position signals for output to telemetry.

The major functional elements of a CLM are the Playback Control, the Record Control, and the Input Selection Switch.

3.2.1.1 Playback Control. The Playback Control initiates and terminates playback operation in response to a "Playback" level

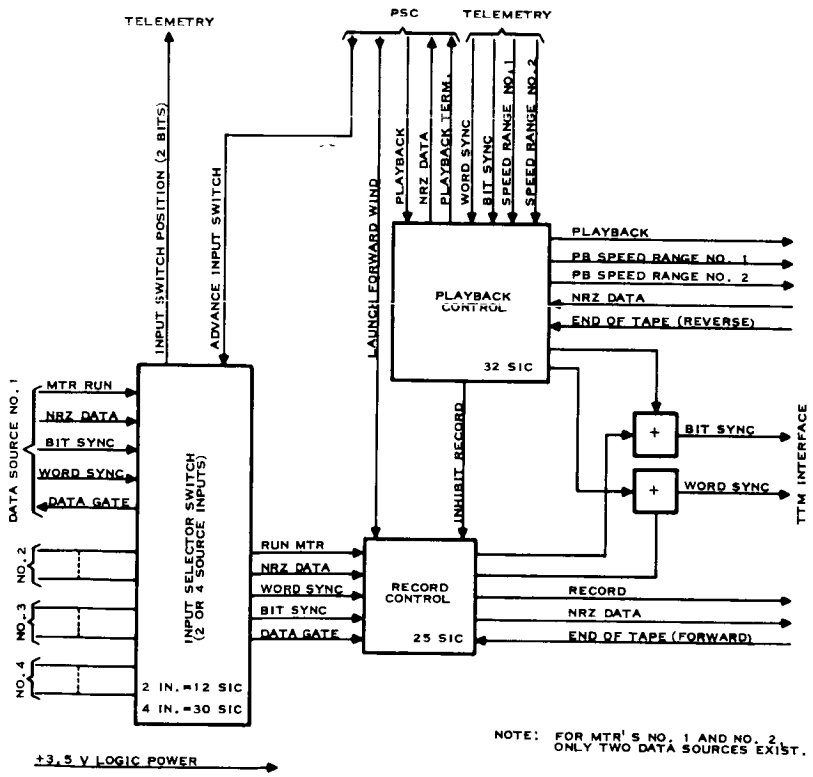


Figure 3-4. Control Logic Module Functional Block Diagram

signal from the PSC. If the TTM is at the end of tape, indicating no more playback possible, the playback control generates a "playback terminated" signal for output to the PSC. During playback, the playback control inhibits recording, and gates word and bit sync to the TTM.

3.2.1.2 Record Control. The Record Control initiates and terminates recording operations in response to an "MTR run" level signal from the data source. In addition, it acts by time delay to inhibit recording until the appropriate tape speed is reached. The clock track is recorded past a data block end, as shown in Figure 3-5, to allow speed synchronization prior to data output in the playback mode.

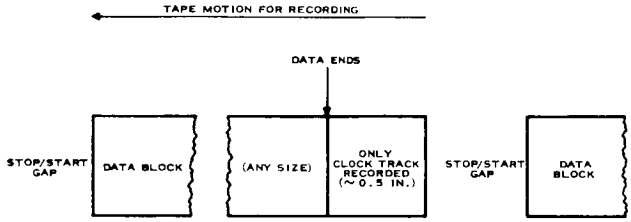


Figure 3-5. Data Block Tape Format

3.2.1.3 Input Selection Switch. The Input Selection Switch allows the MTR unit to select one of the two or four inputs. The selection switch position is advanced by command input, routed through the PSC. The switch position is indicated by a two bit digital engineering data output for each MTR.

3.2.2 MTR Tape Transport Module. The VOYAGER TTM consists of a peripheral drive, 14 data track, plus one clock track, parallel NRZ recording tape transport, and the power supply, electronic, and logic functions closely associated with the recording and playback processes. Peripheral drive was selected over the negator spring approach mainly due to the decreased mechanical complexity. Parallel recording was chosen over series recording, as discussed in the Task A design, mainly because of the resulting slower speeds and fewer head passes. Each TTM is housed in an hermetically sealed, pressurized container. All modules are identical in volume, and all have identical tape pack sizes.

The standardization of TTM size and tape footage was done for economic and mechanical reasons. In spite of the varying capacity requirements, the amount of "waste" tape implied by the standard pack size was less than 0.5 lb per TTM, and the corresponding "waste" volume was estimated to be about 100 in^3. These costs associated with TTM standardization were more than offset by the following advantages:

a. The estimated dollar and time savings for development, production, and spares stock if only one basic design is employed.

b. Standardization of capacity allows functional redundancy interchange to be employed.

c. Electronics packaging can be standardized for the single TTM case design.

d. Mechanically, the transport design can be made most reliable if only one tape pack size is required. This particularly true for the bearing load design for launch survival.

Two motors are used in MTR 1 and MTR 2; one for record and one for playback. This was required due to the high playback-to-record rate ratio, approximately 15,000 bps/100 bps = 150. The preferred two-motor approach is to couple the separate motors through antifeedback clutches to a mylar belt differential which, in turn, drives the tape capstans.

A single motor is used in MTR 3, 4, 5, and 6. The single motor approach was chosen over the two motor with differential because of the obvious reliability improvement. The required speed range ratio is nominally 30:1, assuming a nominal 30 kbps record rate and the back-up playback rate of 1 kbps (50:1 for the 50 kbps maximum record rate). A 12-pole hysteresis synchronous motor with 24:1 speed ratio has been developed by Raymond Engineering. Present indications by Raymond are that a 32:1 speed ratio can readily be achieved and possibly 50:1 with a single motor. Studies are presently being pursued to achieved the 50:1 speed ratio.

The physical characteristics of the transport are summarized in Table 3-2. A functional block diagram of an MTR Tape Transport Module is shown in Figure 3-6. The basic functions of a TTM are constant density recording of incoming NRZ data blocks at various rates (i.e., from different sources), and bit and word synchronous playback of recorded data at four designated speeds.

The major physical elements of a two-motor TTM are shown schematically in Figure 3-7, where they are related to the function blocks of Figure 3-6. The functions of the elements are described in the following paragraphs.

The record electronics chain converts the serial data stream to 14-bit parallel words for storage on the tape. The 14 bits, together with a clock track bit, then generate waveforms which are amplified to the level necessary to drive the record heads. All of the record electronics are implemented in integrated circuitry with the exception of the output stages of the record amplifiers, which employ conventional semiconductor circuitry.

The playback electronics chain is composed of the playback head, which generates waveforms corresponding to the magnetic patterns on the moving tape, the playback amplifiers, which increase the amplitude of the waveforms to a level suitable for detection; the signal detectors, which convert the waveforms to binary information; and the output register, which converts the parallel data to an NRZ serial string in synchronism with externally supplied sync.

The playback amplifiers have first stages composed of integrated circuits, which are physically located near the head assembly to minimize low level signal path lengths. The gain of the playback amplifiers is compensated, for speed related signal level variations, by commands from the speed range control.

The signal detector supplies the output shift register with data at logic levels; and in addition provides a clock track output to the phase locked speed control. The output shift register converts the parallel data to serial form for output to the CLM.

TABLE 3-2. TAPE TRANSPORT MODULE-PHYSICAL CHARACTERISTICS

Size:	550 in^3 including 100 in^3 electronics
Weight:	18 lb
Transport Type:	Dual capstan pheripheral mylar belt drive
Tape:	1 in. tape
Tracks:	15 parallel tracks
Packing Density:	1000 bits/in.
Motors:	1 or 2 hysteresis synchronous motors, depending on speed range requirements.
Record Speed Control:	Open loop voltage/frequency control of record motor
Playback Speed Control:	Wide range by electronic countdown of motor drive frequency. Narrow range by phase locked servo loop and voltage controlled oscillator.
Drive Coupling:	Straight mylar belt/pulley drive for single motor type; belt differential coupling for two motor type.

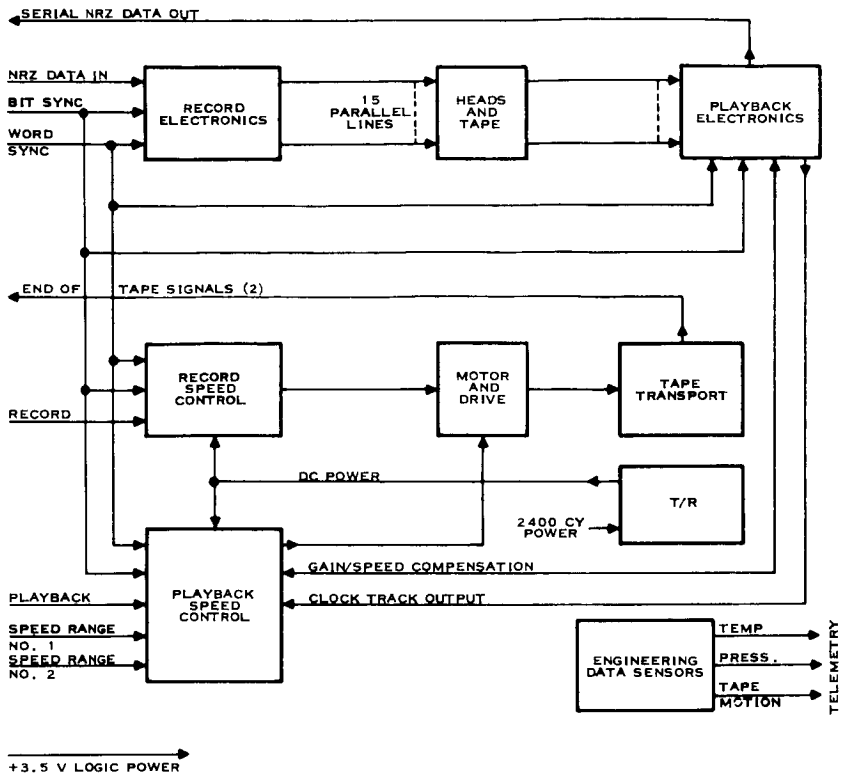


Figure 3-6. Tape Transport Module Functional Block Diagram

The playback synchronization control is a phase locked loop which compares the recorded data clock output to an external pulse train with a period equal to two telemetry word times, and acts to lock the phase of the two signals. This control is accomplished by driving a synchronous motor from a voltage controlled oscillator (VCO), whose frequency is varied by the phase error in the loop. The bit timing stability obtained is high enough to permit the use of the one word dejitter buffer inherent in the output parallel-to-serial conversion.

The four required playback rates are obtained by counting down the VCO output by binary stages and suitably altering the power amplifier output voltage level to obtain proper playback motor operation. The alteration of the output level is accomplished by varying the output voltage of the amplifier power supply. The voltage control is done by a pulse frequency modulation technique. Presently available techniques require that the speed range be selected by external command. Techniques for automatic selection of speed range analogous to the record speed selection should be investigated to minimize the interface requirements and allow more design flexibility.

The record speed control drives the power amplifier directly with the counted down bit sync pulse train. In the single motor TTM's, motor input phase reversal is employed to move the tape alternately in the record and playback directions. For the two-motor configuration, dual power amplifiers are employed to avoid the need for motor lead switching. Frequency/voltage ratio is maintained by the same type of power supply employed in the playback control.

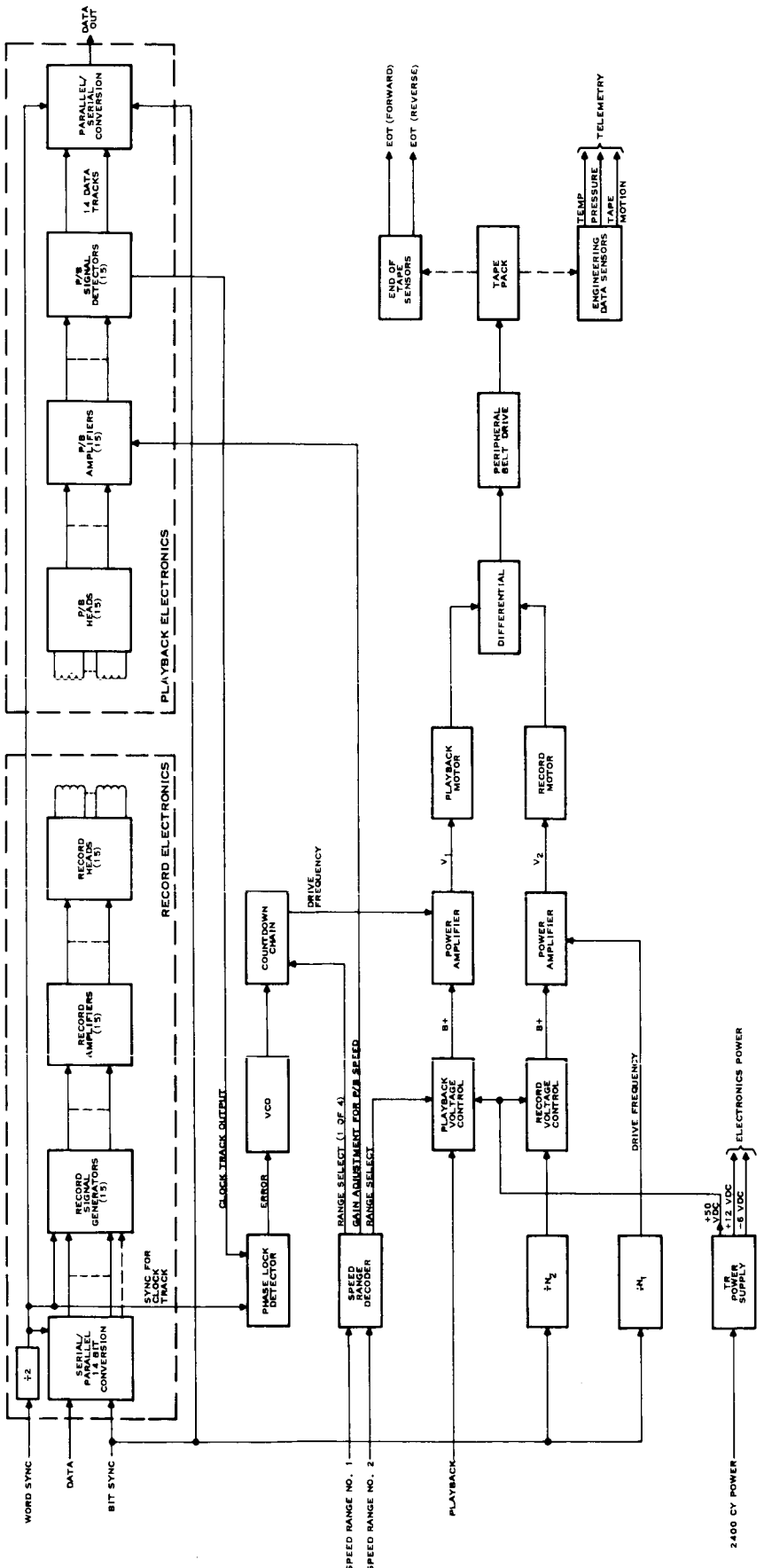


Figure 3-7. Tape Transport Module Major Physical Elements

Two unique engineering data outputs are required by the TTM, in addition to the usual voltages and temperatures associated with electronic equipment. These are an indication of the atmospheric pressure in the recorder case, and a tape motion indication. The pressure measurement is necessary because of the dependence of proper mechanical operation on the presence of a minimum atmospheric pressure. The measurement of case pressure is done by a standard potentiometric pressure transducer. The tape motion indication allows differentiation between mechanical and electronic failures and serves a basically diagnostic function. It is done by means of a magnetic pickup located on a peripheral belt idler.

The DC Power Supply contained in each TTM consists of a transformer, rectifier, and filter combination operating from the 2400 cps distribution. It provides separate dc voltage levels for the electronic circuitry and the power amplifier voltage regulators in the record and playback controls. All TTM logic receives 3.5v power from the DSS Power Supply.

The end-of-tape sensor, signals the approach of either end of the tape pack, thus enabling the CLM to halt the record or playback function. The signal is generated in the record mode when sufficient tape remains to execute a normal stop. In the playback mode, the signal is generated after the last data block. End-of-tape signals are generated optically and are backed up by motor overcurrent actuated reversal switches and solid tapereel anchorage. Two light sources are recommended for further evaluation; a redundant incandescent filament and a solid state light source.

3.3 Playback Sequence Control. Two identical PSC units are included in the DSS to provide standby redundancy. Commanded power switching is employed to operate only one at a time, and the interface lines are combined in "OR" fashion.

The PSC units are composed entirely of SIC logic networks and receive their power from the DSS Power Supply, which also executes the power switching function. Figure 3-8 is a functional block diagram of the PSC. The basic functions of the PSC are:

a. Provide all DSS output interface functions.

b. Automatically select MTR units for playback in rotation when C&S "Playback" level is "up".

c. Begin playback sequence with a particular MTR unit upon command.

d. Route "Input Switch Position Advance" commands to selected MTR units.

e. Identify recorder presently playing back as an engineering output.

f. In addition, PSC1 contains the OR gating employed to combine the PSC outputs. It is separately powered by an unswitched 3.5v supply.

The address generator sequentially directs the playback of the MTR units. It normally initiates playback, when the C&S "Playback" signal goes up, by sending MTR 1 a "playback" level; which remains "up" until a "Playback Terminated" signal is received from the MTR unit. Upon receipt of this signal, the address counter advances to the next MTR address. During a playback interval, data is gated from the chosen MTR to the PSC output. If an MTR

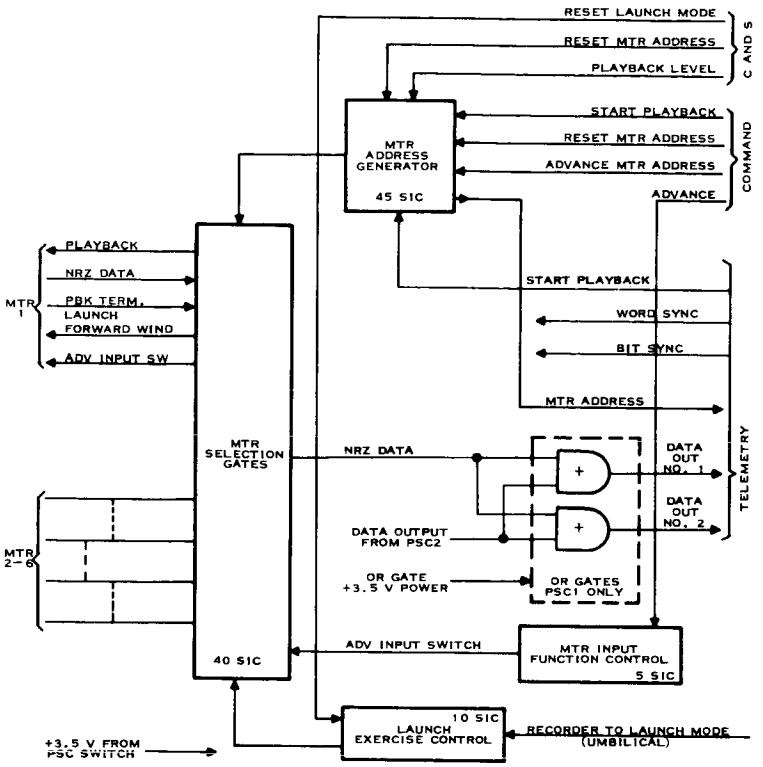


Figure 3-8. Playback Sequence Control Functional Block Diagram

contains no data, the "playback terminated" signal will be detected simultaneously with the selection of the unit, and MTR address will increment on the next logic clock cycle. The playback sequence is automatically terminated after all MTR unit have been addressed, or if a "reset" command intervenes to return the register to a prestart conditions. The sequence is suspended without reset if the C&S "Playback" level goes "down" and resumes at the same point when it again goes "up".

Command playback of any unit may be accomplished by setting the address generator to the desired state by "reset" and successive "advance" commands, and then starting the sequence. Unless a "reset" intervenes, the playback sequence then continues as usual through all the MTR units remaining in the sequence.

The MTR selection gates direct the data and signals to and from the MTR unit addressed. The launch exercise control operates during launch to cause all MTR units to forward wind. It is reset by a C&S signal. The input function control allows the commanding of the input toggling function in any MTR unit. The addressing of the MTR unit is done through the address generator as for playback, then successive "input switch advance" commands are routed to the MTR unit.

An optional feature in the PSC would be a "forward wind" command capability, which could be employed to rewind tapes for replay of stored data. Its function could be combined with the launch exercise control, and would require the routing of a "record inhibit" line to each

MTR through the MTR selection gates. The forward wind could be timed by a command-initialized down counter; or could simply proceed for the whole tape reel of the selected MTR. The relative increase in PSC and MTR complexity would be slight in either case.

3.4 DSS Power Supply. The DSS Power Supply is composed of two identical, fully independent units that supply dc logic voltage from the 2400 cps power line. The voltage supply is filtered but unregulated. Each supply normally carries half the total power load, although it is capable of full load operation without high component stress. Load switching in case of failure is done passively by diode network. The efficiency exceeds 80%. The DSS Power Supply has two basic functions: (1) to supply +3.5 volts to all SIC logic in the DSS and to command switching of power from one PSC unit to the other.

Figure 3-9 is a block diagram of the DSS Power Supply, which also shows the circuit details of the important physical elements. Each of the two sections contains one transformer with center-tapped secondary windings. The transformer core is of the E-I lamination type, lending itself to high reliability construction techniques.

Each rectifier is a full-wave type, operating from a center-tapped winding. The rectifier bridge is an 8-diode serial/parallel redundant type. The filter sections are of the simple single-section RC type with series/parallel part redundancy. The load sharing networks are identical in form to the rectifier network, and function to shift the full load to the surviving

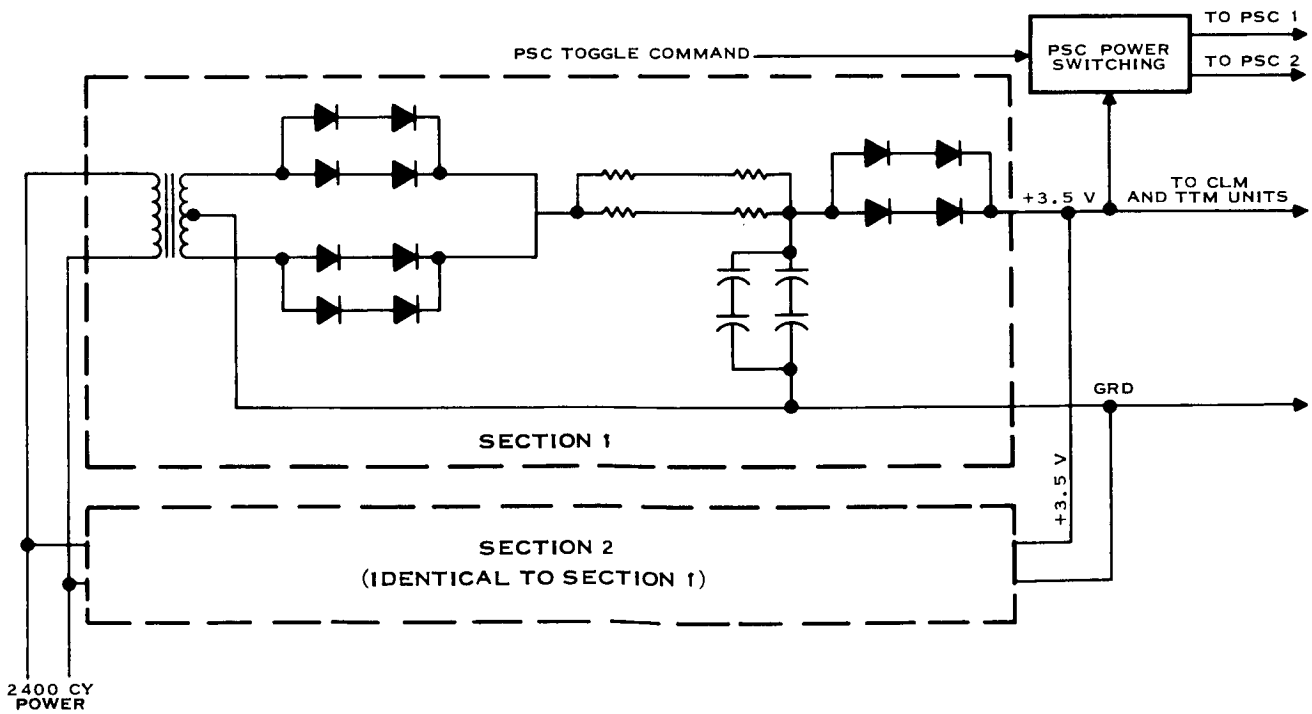


Figure 3-9. Data Storage Subsystem Power Supply Physical Elements

section if one supply fails. The commanded PSC power switch is of the latching relay type, and serves to direct the power to either, but not both, of the PSCs.

4.0 INTERFACE CHARACTERISTICS

4.1 Electrical Interfaces. The DSS interfaces electrically with Telemetry, DAE, Command, C&S, Capsule Relay, and Power Subsystem points. In addition, it has outputs to direct access test points, and inputs from the Launch Vehicle umbilical line. Interface lines, with the exception of direct access connections, are shown for the DSS in Figure 3-2, where they are grouped and identified by interfaces. Table 4-1 lists the DSS inputs. The DSS input characteristics are SIC logic gate inputs unless otherwise specified.

Similarly, the signal characteristics are the standard 3.5-volt SIC logic levels unless otherwise indicated. Table 4-2 lists the DSS signal outputs. The DSS output characteristics and signal characteristics are SIC gates and 3.5-volt NRZ levels unless otherwise indicated. Figure 4-1 is a power profile for the DSS.

TABLE 4-1. DSS SIGNAL INTERFACES-INPUT

Input	Source	D/S Input Characteristics	Signal Type	Notes
Telemetry word sync	Telemetry		RZ	For playback
Telemetry bit sync	Telemetry		RZ	For playback
Telemetry bit rate	Telemetry		Level	2 lines whose state decodes to 1 out of 4 bit rates
Begin Playback	Telemetry		RZ pulse	Starts flare or maneuver data playback
Run MTR (1)	Telemetry	2 parallel SIC	Level	For maneuver data
Maneuver Data	Telemetry		NRZ	storage - two sets
Bit sync	Telemetry		RZ	of lines are re-
Word sync	Telemetry		RZ	quired for the redundant function inputs on the two MTR units
Run MTR (N)	DAE	4 parallel SIC	Level	Five sets of these
Data	DAE	4 parallel SIC	NRZ	lines are required,
Bit sync	DAE	4 parallel SIC	NRZ	in duplicate, from
Word sync	DAE	4 parallel SIC	NRZ	the five DAE data sources
Flare store	DAE	2 parallel SIC	Level	Causes the storage of flare data at high rate in MTR 1 or 2
Playback	C&S		Level	
Reset playback control	C&S		RZ pulse	
Reset launch exercise	C&S		RZ pulse	
Reset playback control	Command		RZ pulse	
Advance MTR address	Command		RZ pulse	
Advance MTR input switch	Command		RZ pulse	
Begin playback	Command		RZ pulse	
PSC exchange command	Command		Pulse	Causes power supply to switch PSC unit power
MTR launch mode	Umbilical		Pulse	Puts PSC launch exercise control into launch mode

TABLE 4-2. DSS INTERFACE-OUTPUT

Output	Destination	D/S Output Characteristics	Signal Type	Notes
Playback Data 1	Telemetry		NRZ	One line to each modulator unit.
Playback Data 2	Telemetry		NRZ	
MTR ID	Telemetry		3 Bits	Engineering data to identify MTR playing back.
MTR Pressure	Telemetry		Analog	Each MTR unit-engr. data
MTR Temp	Telemetry		Analog	Each MTR unit-engr. data
MTR Tape motion	Telemetry		Analog	Each MTR unit-engr. data
MTR Input Switch Position	Telemetry		2 bits	Identifies data source input to MTR.
Data Gate	DAE		Level	Individual lines from 5 science MTR units to data sources.

4.2 Mechanical Interfaces. The DSS is located in Bays 7 and 8.

4.3 Thermal Interfaces. The DSS will require the dissipation of 36 watts of power during launch. During orbital operations, the peak dissipation will be 25 watts while simultaneously recording and playing back data. Standby dissipation is 3 watts. The maximum dissipation in the DSS Power Supply is 0.5 watts.

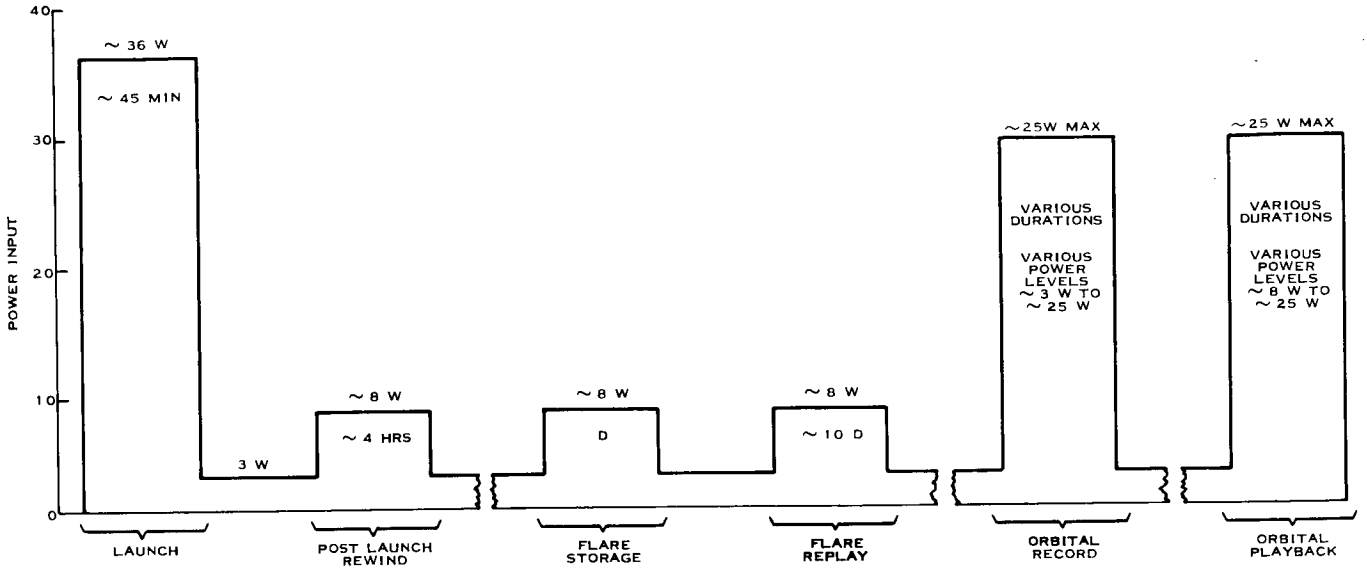


Figure 4-1. Data Storage Subsystem Power Profile

4.4 Umbilical Interface. The DSS will have one direct umbilical connection: Recorder to Launch Mode

4.5 Direct Access Interface. The DSS is provided with direct access points to facilitate system test. The ac voltage waveform from each motor (8) is brought out on direct access lines.

5.0 PERFORMANCE PARAMETERS

5.1 Element Performance Parameters. The performance parameters for the MTR units are given in Table 5-1. The DSS Power Supply performance parameters are given in Table 5-2.

5.2 Reliability

5.2.1 Component Failure Rates. The failure rates for the major DSS components are shown in Table 5-3. The failure rates for the CLM and PSC units were computed on the basis of the number of SIC packages in their construction. The SIC failure rate was taken to be $0.005\%/10^3$ hours per package in either the operating or nonoperating state. Projected vendor estimates indicate that a MTBF of 10,000 hours may be expected for the VOYAGER TTM. This is a failure rate of 10% per 10^3 hours, only while operating.

TABLE 5-1. MTR PERFORMANCE PARAMETERS

Capacity:	1×10^8 bits of data
Bit Packing Density:	1000 bit/inch (parallel)
Number of Tracks	15 tracks/1 inch (parallel)
Data Input:	Various rates from 60 bps to 50 kbps
Data Output:	(kb/sec) 14.933 1/3 7.166 2/3 3.733 1/3 0.933 1/3 Serial NRZ with externally supplied sync
Output timing stability:	Synchronization to external signal to ±0.01 percent
Signal Levels:	Binary zero 0.v ± 0.5v Binary one 3.5v ± 0.5v
Tape Start Time:	1.0 second at 1 ips
Tape Stop Time:	1.0 second at 1 ips
Stop/Start length (X):	1 inch
Maximum Signal dropout:	1×10^5 bits in 1×10^8 bits
Lifetime:	14 months, 2000 tape passes in 2200 hours of operation
Reliability:	MTBF 10^4 hours (operating)

TABLE 5-2. DSS POWER SUPPLY SECTION PERFORMANCE PARAMETERS

Input:	50v peak-to-peak 2400 cps 1-phase square wave
Outputs:	+ 3.5 vdc 600 ma (max)
Filtering:	RC Filtering to ± 1% ripple
Regulation:	No active regulation - 5% (max) regulation between half and full load
Reliability:	The MTBF exceeds 50,000 hours for full load operation.

TABLE 5-3. FAILURE RATES

Component	Failure Rate
PSC Section (100 SIC)	0.500% / 10^3 hours
CLM (77 SIC)	0.385% / 10^3 hours
TTM	10.7% / 10^3 hours
Power Supply Section	0.1% / 10^3 hours
PSC Power Switch	0.000392 per 500 operations

The failure rate of each power supply is essentially that of the power transformer and RC filters. Since the rectifier network and the load-sharing networks consist of series parallel diodes, their failure rate is comparatively negligible. Using the recommended VOYAGER part failure rates, the power supply total is 0.1% per 10^3 hours for one unit. The type of latching relay chosen for the PSC Power Switch has a failure rate of 0.734 per million operations. A baseline value of 500 operations was taken for the mission lifetime.

5.2.2 Reliability Model. The reliability model for the chosen DSS configuration is shown in Figure 5-1 (a). All the elements in the Power and Control section are assumed to operate for a 5520 hour mission duration (orbit plus 30 days). The MTR units are assumed to operate 360 hours, corresponding to a 50% duty cycle for the 30 days of orbital operations.

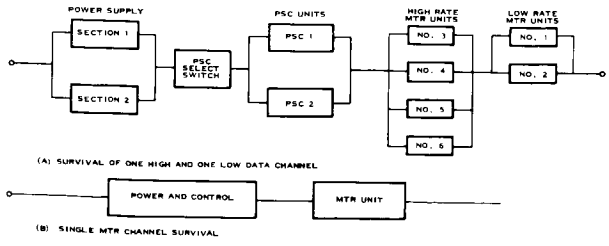


Figure 5-1. Data Storage Subsystem Reliability Models

The model reflects the four way input selection capability of the high record rate MTR units and the two way input selection of the low rate units. This particular organization of the redundancy was chosen because it matched the recording capabilities of the MTR units.

MTR channel survival means the survival of the series CLM, TTM, power, PSC, and PSC switch blocks (Figure 5-1 (b)). Subsystem survival is defined as the survival of one high rate and one low rate data channel, as well as the Power and Control

block functions. This means that data from all sources can be obtained, although necessarily on a time shared basis. The probability of this survival is 0.934 for the end of mission.

The choice of the functional redundancy method of reliability enhancement was made on the basis of comparison of performance with a simplex system. Such a system would have each MTR associated with only one data source. In this case, survival of one MTR channel means the survival of only one data channel. Comparison of the two systems is summarized in Table 5-4.

TABLE 5-4. RELIABILITY RESULTS

	Nonredundant	Redundant
(1) P (Survival of all MTR Channels)	0.727	0.698
(2) P (Survival of a particular high data channel)*	0.773	0.967
(3) P (Survival of a particular low rate data channel)*	0.873	0.964

*all data could be recorded on a time shared basis.

Line (1) indicates the relatively small reliability increase in a single MTR channel due to the elimination of the CLM input selector switch in the simplex system. Line (2) shows the superiority of the redundant system in maintaining a particular high data channel operative (all on a time shared basis). Line (3) indicates the advantages of the system in maintaining a particular low rate data channel.

Because of the large size and weight penalties implied by MTR standby redundancy; and because of the relatively high reliability obtainable with function redundancy, no MTR standby redundancy was employed.

6.0 PHYSICAL CHARACTERISTICS AND CONSTRAINTS

6.1 Basic Characteristics

6.1.1 Size, Weight and Location. The MTR section of DSS is contained in all of Bays 7 and 8. The packaging configuration for these two bays are shown in Figures 6-1 and 6-2. The weight and volume of each component of the DSS is listed in Table 6-1.

The volume of the Data Storage equipment in Bay 7 is 1988 cubic inches and the total weight is 68.6 pounds. Data Storage equipment in Bay 8 has a volume of 1988 cubic inches and a weight of 68.6 pounds.

6.1.2 Packaging. Each of the magnetic tape recorders is enclosed in a cast magnesium housing. Each casting is pressurized with dry nitrogen to prevent sublimation of lubricants in the recorder mechanism..

Tape recorder castings and the MTR control enclosure are bolted directly to the thermal integrating plate of Bays 7 and 8. Thermal control louvers are used to regulate the temperature of the integrating plate. This allows the temperature of the data storage units to be stabilized within controlled limits.

Integral fittings on the tape recorder housing provide structural support and the inner plate, shown in Figures 6-1 and 6-2, contain the interconnect wiring and connectors. Intertray connectors are Cannon 50-pin D series; input-output connectors are Bendix type PT07.

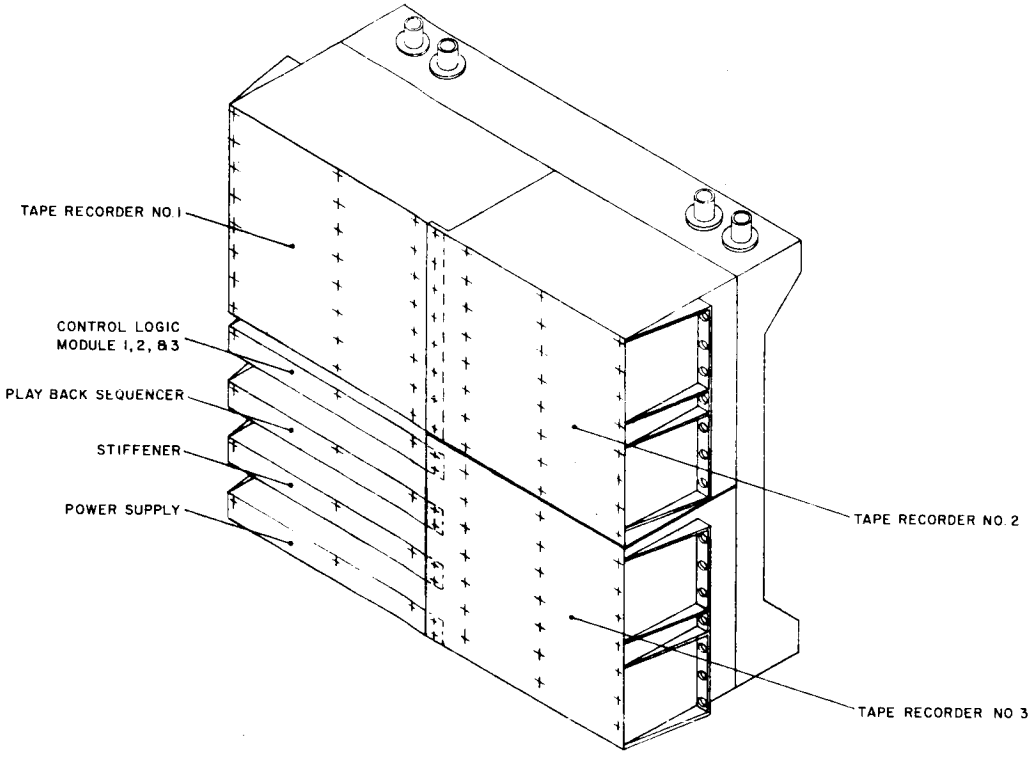


Figure 6-1. Electronic Assembly Data Storage, Bay 7

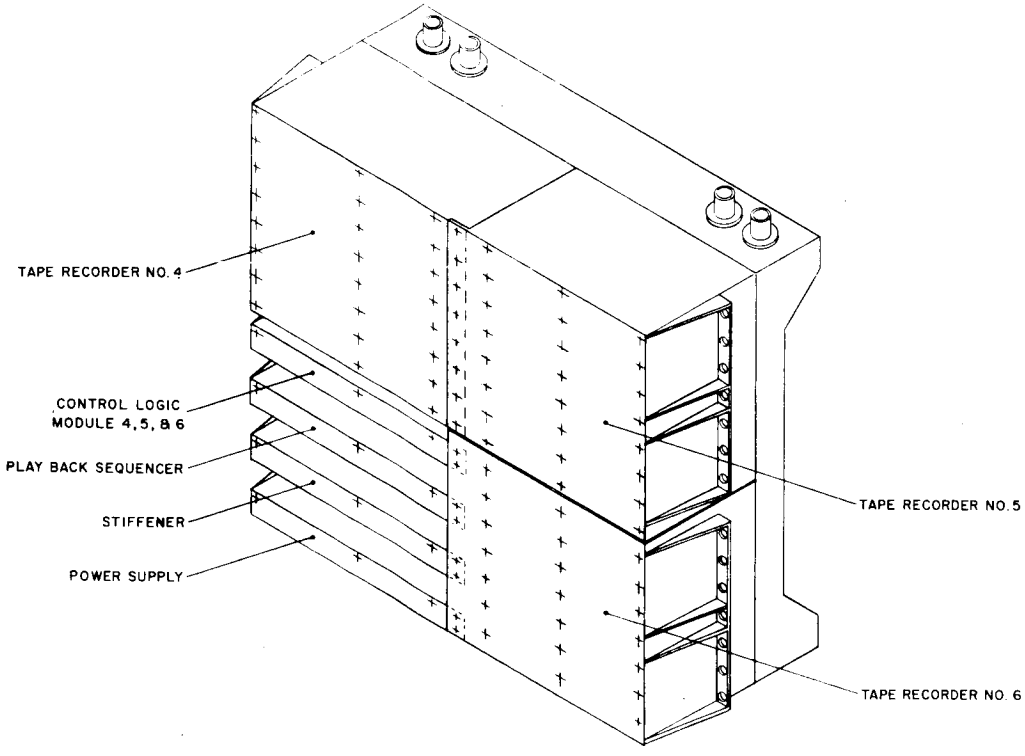


Figure 6-2. Electronic Assembly Data Storage, Bay 8

TABLE 6-1. DSS COMPONENTS WEIGHT/VOLUME

	Volume ($in.^3$)	Weight (lb)
2 - PSC units	60	1.2
6 - CLM units	90	2.2
1 - Redundant power supply	100	4
6 - TTM units	3300	108
DSS Total	3550	115.4

Integrated electronics used in the DSS are packaged on high density printed circuit cards. Integrated circuits are attached to cards with the parallel-gap welding technique.

6.2 Operational Characteristics

6.2.1 Magnetic Field. The configurations and materials employed in all DSS components are chosen to minimize external magnetic fields, particularly those of low frequency.

6.2.2 Angular Momentum. The total angular momentum of the DSS never exceeds 0.35 inch-lb-second with all units operating at fastest speed.

6.3 Environmental Tolerances

6.3.1 Temperature. All components of the DSS conform to the type acceptance temperature test except the MTR units. They are limited to a maximum temperature of 70°C.

6.3.2 General. All DSS components meet all environmental requirements set forth in CII VC220FD103 Component Design Parameters.